THE SEDIMENTOLOGY, PALAEONTOLOGY AND STRATIGRAPHY OF COASTAL-PLAIN DEPOSITS AT HONDEKLIP BAY, NAMAQUALAND, SOUTH AFRICA

JOHN PETHER

Thesis Presented for the Degree of

MASTER OF SCIENCE

in the Department of Geology

UNIVERSITY OF CAPE TOWN

February 1994

John Pether

Supervisor

Dr John Rogers

ABSTRACT

The exposures in diamond mines on the Namaqualand west coast of South Africa provide a rare opportunity to examine a record that is normally inaccessible beneath a thick cover of aeolian sands. This study presents the main results of fieldwork in mine excavations on the farms Hondeklip and Avontuur-A, near Hondeklip Bay. Sections in the deposits were described in detail and the vertebrate and invertebrate faunas were sampled. The buried topography of the gneiss bedrock, obtained by prospecting, is complex, with the main feature consisting of a coast-parallel ridge flanking a wide palaeochannel on its landward side. Advanced kaolinitic weathering affected both the bedrock and a diamondiferous, basal kaolinitic sediment patchily preserved in the channel. The incision of the channel is related to the Oligocene regression and the basal kaolinitic sediment is interpreted as a fluvial arkose deposited in the channel. Both the bedrock and the deposit in the channel were then kaolinized during humid climatic conditions in the late Oligocene and early Miocene. Weathering-profile silcrete also developed in the basal kaolinitic sediment. It is tentatively proposed that this weathering period may be represented in the Namib Desert by the thick laterite capping Eocene sediments at Kakaoberg. Subsequently, the palaeochannel was exhumed and was ultimately filled by late Tertiary marine deposits.

The marine deposits were laid down in shallowing-upwards sequences of the shoreface environment. Two regressive, progradational packages (alloformations) are recognized. The older extends seawards from at least ~50 m asl. and is the "45-50 m Complex" of Carrington and Kensley (1969), now called the 50 m Package. East of the channel, on the exposed coast, high-wave-energy storm-deposition in the lower shoreface dominates the preserved record. With lowering of sea-level, the bedrock ridge emerged to the seaward of the prograding palaeoshoreline, reduced the level of incident wave energy and profoundly influenced the development of sub-environments within the progradational regime. Ultimately, low-energy bay deposits filled the palaeochannel in the bedrock. On the basis of vertebrate evidence and correlation with global sea-level trends, the age of the 50 m Package is middle Pliocene. The upper facies of the 50 m Package (foreshore and upper shoreface) have been extensively removed by later subaerial erosion. The subsequent transgression truncated the seaward extent of the 50 m Package, reached ~30 m asl. and prograded seaward from that elevation. It is called the 30 m Package and combines the "29-34 m Beach" and "17-21 m Complex" of Carrington and Kensley (1969). A late Pliocene age is envisaged. The upper-shoreface facies of the 30 m Package is usually preserved, but may be disguised by pedogenesis.

The diamondiferous marine gravels mined in the area are mainly lower-shoreface storm deposits and pre-existing transgressive lags and shelf deposits have generaly been reworked during regression. Enigmatic, muddy and/or phosphatic units, previously called "E-stage," are patchily preserved in the base of the 50 m Package and are revealed to be distal storm deposits laid down in the transitional shoreface to offshore environment. They are part of the overlying regressive sequence, but may include a fragmentary , petrified, mixed, vertebrate remanié. Nevertheless, eroded remnants of older deposits must also occur in places.

ACKNOWLEDGEMENTS

I am indebted to Mr F. Hoffman of Trans Hex Group Ltd., for unlimited access to the Hondeklip mine exposures. To Mr M. Mittelmeyer and Mr H. Bruwer, mine geologists, for their assistance and hospitality at Hondeklip. To the people of the Hondeklip mine, present and past, from mine managers to workers, for their friendliness and willlingness to help. To Mr R.G. Molyneux, of De Beers Namaqualand Mines, for his assistance and hospitality during field visits to neighbouring areas. To my field assistants at various times, M. Pether, S. Cloete and V. Bartnick, for their patience.

To Dr John Rogers, for his guidance as my supervisor. To Drs Q.B. Hendey R.V. Dingle and B. Kensley, for their encouragement during various stages of this project. To Dr I.K. Macmillan, for analysis of the foraminifera. To Autodesk, via the AfraCAD dealership, for the provision of AutoCAD at a significant discount. To M. Joubert for kindly volunteering to photograph the fossil shells. To C. Booth for his photographic assistance. To J. Boltman, for last-minute binding. To my mother-in-law, without whose toddler-sitting help, I would not have had the assistance of my wife. To my wife, Marilyn, for still being my wife and for her invaluable assistance in this project. To the Director and Trustees of the South African Museum. To those many people here unmentioned who have contributed.

TABLE OF CONTENTS

CHAPTER 1

INTRODUCTION

1.1 OBJECTIVES

The aim of this thesis is to contribute to the knowledge of the stratigraphy, sedimentology and palaeontology of the Cenozoic coastal-plain deposits of the western margin of southern Africa.

The coastal-plain deposits of the Atlantic coast of southwestern Africa have been exploited for diamonds for most of this century. Although some literature has accumulated over this period, there have been few recent contributions examining the deposits from the point of view of modern sedimentological perspectives. With the provision of access to the diamond mine at Hondeklip Bay by the Trans Hex Group Limited, it has become possible to describe and interpret a portion of the coastal-plain record in more detail than has been available in previous reports.

1.2 LOCATION OF THE STUDY AREA

The study area is centrally located on the Namaqualand coastal plain of southwestern Africa (Fig. 1.1), that stretch of coast between the Olifants River in the south and the Orange River in the north. It is near the village of Hondeklip Bay and the deposits examined are situated on the farms Hondeklip and Avontuur-A. The coastal plain is mantled by Quaternary aeolian sands and exposures of the underlying deposits are only available in the "windows" provided by open-cast trenches and pits made in the process of mining marine basal gravels for their diamond content. The exposures are situated at distances of ~1.5 km to ~5 km from the present-day shoreline. The elevations of the Precambrian gneiss bedrock uncovered in these exposures extends from ~10 m asl. (metres above sea-level), up to ~50 m asl.

1.3 SCOPE OF THE STUDY

The scope of the present study is twofold and comprises:

a) Description of the kaolinitic terrestrial deposits and associated silcretes basal to the coastal-plain succession, interpretation of their origin and discussion of their age, regional correlations and palaeoclimatic significance.

b) Description of the overlying marine deposits (lithologies and sedimentary structures), interpretation of the depositional environments represented and description of the palaeontology of the deposits (trace fossils, macro-invertebrates and vertebrates). On the basis of sedimentary facies geometry and fossil content, two marine stratigraphic units are recognized in the study

area. Evidence for their age is presented and correlations with the late Tertiary global sea-level curves are proposed. Regional correlations are presented.

Figure 1.1 Location of the study area. In the left inset, the stars mark the sites of observations presented in this report.

Notably, a classic, step-like succession of wave-cut, marine terraces does not occur in the study area. Instead, a more rugged local relief characterises the bedrock topography. The development of this relief, deposition of the basal terrestrial deposits, subsequent deep weathering and the development of silcrete are associated aspects of the early geological history preserved on the Namaqualand coastal plain. These features are therefore described and discussed in some detail due to the important palaeoclimatic implications of these early events and the control that the antecedent topography had on subsequent marine deposition. Furthermore, this period of the coastal-plain history has significant economic aspects.

By placing emphasis primarily on the sedimentology of the marine deposits, this study differs from previous accounts of the Namaqualand coastal plain between Kleinzee and Alexander Bay (Fig. 1.1), in which emphasis was placed on the occurrence of step-like, marine terraces and cliffs incised in the bedrock (e.g. De Villiers and Söhnge, 1959; Hallam, 1964; Keyser, 1972).

Although only two marine stratigraphic units of formation status are recognized in the study area, these units are extensive. They are the formations most commonly encountered in artificial exposures created by coastal diamond mining on the Namaqualand coastal plain, as well as in the few natural exposures along cliffed coast. Volumetrically, these two formations together probably comprise the bulk of preserved, emerged marine sediment on the Namaqualand coastal plain.

Marine deposits on the Namaqualand coastal plain are known to extend from the present shoreline up to 80-90 m asl. Exposures above ~50 m asl. are not available in the study area and therefore the higher and older portion of the coastal plain deposits, where at least one major marine unit resides, is not described herein. The marine record at these higher elevations is residual, due to erosion and deflation, and has also been longer subjected to pedogenic alteration (Keyser, 1972; personal observations). Close to the coast, below ~10 m asl., are younger, Quaternary "raised beaches." These are also not extensively exposed in the study area and are not dealt with.

The remainder of this chapter explains the types of data and analytical methods employed in this study. The regional physiographic, climatological, oceanographic and continental-shelf settings in which the study area is situated are summarised in Chapter 2 (Regional Setting). A brief history of the development of the stratigraphy of the Namaqualand coastal plain is provided in Chapter 3 (Previous Research). In Chapter 4 (General Geology of the Study Area), detailed description of the study area is commenced, with attention to the surface topography and geology, the offshore bathymetry and geology, the topography of the bedrock buried beneath the coastal-plain deposits, groundwater, the occurrence of dolerite dykes and faulting and the state of weathering of the buried bedrock. Chapter 5 (The Basal Kaolinitic Deposits) summarises previous observations on basal kaolinitic sediments between the Olifants and Orange rivers, describes the field occurrence of the basal kaolinitic sediments in the study area and presents the results of textural, petrographic, SEM and geochemical investigations, concluding with a discussion of the observations. Chapter 6 (The Silcrete) summarises previous observations on silcrete between the Olifants and Orange rivers, describes the field occurrence of silcrete in the study area and discusses the observations. In Chapter 7, the petrography of the silcrete is described and the results of mineralogical and geochemical analyses are presented (Silcrete Petrography and Composition). The classification of the Hondeklip silcrete, in terms of recent contributions to that topic, is discussed, as well as aspects of silcrete fabric, genesis and silica mineralization. Chapter 8 (Age and Correlation of the Basal Deposits and Silcrete) presents the evidence for the age of this portion of coastal-plain history and discusses correlations.

The second part of the thesis (Chapters 9-16) comprises the description of sedimentary, ichnological and palaeontological features of the marine sections in mine excavations, leading to the identification of depositional environments. Chapter 9 (Introduction to the Marine Deposits) prepares the reader for the section descriptions by explaining their presentation in the context of a very brief overview of the stratigraphy. The basic compositions of the deposits are described. In Chapter 10, Trace Fossils, the ichnotaxonomy employed for the trace fossils mentioned in section descriptions is elaborated in detail. Chapter 11 describes the exposures at AV T2/T3 on Avontuur-A (The Avontuur-A T2/T3 Exposures).

In Chapter 12 (Depositional Environments on Avontuur-A and the 50 m Package) the observations are interpreted. Exposures on Hondeklip are presented in chapters 13 and 14. Zone 4A is described and interpreted in Chapter 13, Zone 4A and the context of Phosphorite Deposition. A Block is described and interpreted in Chapter 14 (The A Block Exposures and the 30 m Package). Chapter 15 discusses the palaeontology of the marine deposits and the evidence for their age (The Palaeontology and Age of the Marine Deposits). Chapter 16 is a concluding summary and discussion. An illustrated catalogue of selected invertebrate fossils from the study area is provided in Appendix A.

1.4 DATA AND METHODS

FIELDWORK

Survey and mapping

Maps of the study area, edited to remove data on ore grades and ore thicknesses, were kindly provided by Trans Hex Group Limited. These included large-scale prospecting maps of the surface topography and the topography of the sub-surface bedrock, as well as smaller-scale, mining control maps of the various open-cast excavations.

The data for the map of surface topography was gathered mainly during the setting out of prospecting grids for drilling sites. The gross topography of the bedrock sub-surface was obtained from this drilling, mainly by numerous, small-diameter, percussion-drill holes employing bit and bailer. The holes were spaced ~100 m apart on an approximately uniform grid covering the area. More closely-spaced determination of the bedrock topography, at borehole intervals of ~50 m and ~25 m, was carried out in areas of interest, the more complete coverage also involving large-diameter holes (pits, Benoto piling holes and trenches). This activity continues at the present. The most detailed (micro-topographic) mapping is done during mining control in targeted areas extensively stripped of overburden.

Provision of these maps greatly reduced the burden of surveying. Nevertheless, it was often necessary to "carry" elevations from mine beacons into excavations, using the stadia system of tacheometry and a Dumpy level, in order to establish bedrock elevations at the sites of individual measured sections. Levelling around the walls of excavations was also carried out, in order to record sedimentary geometry with reasonable accuracy. In large excavations the Dumpy level was employed, in small sections the Brunton compass was used.

Section descriptions

The thicknesses of units was measured using a surveying staff or tape measure, depending on the scale of the interval. Accumulated thicknesses were checked against elevations "carried" onto the higher levels of the excavation walls and the surface elevation at the site.

Description was aided by the use of a "Checklist for describing Sedimentary Sequences," compiled from various sources by J. McPherson, Dept. of Geology, University of Cape Town. As work progressed, this aid was further expanded into a small field manual of terminology and classifications. When estimating grain size in the field, a grain-size comparator was used in conjunction with a 10X magnification hand lens, usually enabling estimations of mean size to 0.5 ϕ. Grain size is described in terms of the basic Wentworth classes, subdivided at 0.5 ϕ intervals. Note that Wentworth's terms "granules" and "pebbles" are used for the -1 to -2 ϕ and -2 to -6 ϕ ranges, respectively (Table 1). The descriptors "small, medium, large, very large" are used to refer to whole ϕ classes in the pebble size range. This is preferred to the usage of "fine" or "coarse" pebbles, because "small" and "large" are more generally used when referring to pebbles. Abbreviations used in the text when referring to grain sizes are provided in Table 1.1.

Table 1.1 Sand grain and gravel clast size descriptors. Essentially Wentworth's terms (Wentworth, 1922).

Class	Abbrev.	Size interval	PHI interval
very large pebbles (Upper)	vlpU	45.3–64.0 mm	-5.5– -6.0 ϕ
very large pebbles (Lower)	vlpL	32.0–45.3 mm	-5.0– -5.5 ϕ
large pebbles (Upper)	lpU	22.6–32.0 mm	-4.5– -5.0 ϕ
large pebbles (Lower)	lpL	16.0–22.6 mm	-4.0– -4.5 ϕ
medium pebbles (Upper)	mpU	11.3–16.0 mm	-3.5– -4.0 ϕ
medium pebbles (Lower)	mpL	8.0–11.3 mm	-3.0– -3.5 ϕ
small pebbles (Upper)	spU	5.7–8.0 mm	-2.5– -3.0 ϕ
small pebbles (Lower)	spL	4.0–5.7 mm	-2– -2.5 ϕ
granules (Upper)	gU	2.8–4.0 mm	-1.5– -2 ϕ
granules (Lower)	gL	2.0–2.8 mm	-1– -1.5 ϕ
very coarse sand (Upper)	vcU	1410–2000 µm	-0.5– -1.0 ϕ
very coarse sand (Lower)	vcL	1000–1410 µm	0.0– -0.5 ϕ
coarse sand (Upper)	cU	710–1000 µm	0.5–0.0 ϕ
coarse sand (Lower)	cL	500–710 µm	1.0–0.5 ϕ
medium sand (Upper)	mU	350–500 µm	1.5–1.0 ϕ
medium sand (Lower)	mL	250–350 µm	2.0–1.5 ϕ
fine sand (Upper)	fU	177–250 µm	2.5–2.0 ϕ
fine sand (Lower)	fL	125–177 µm	3.0–2.5 ϕ
very fine sand (Upper)	vfU	88–125 µm	3.5–3.0 ϕ
very fine sand (Lower)	vfL	63–88 µm	4.0–3.5 ϕ

Grain roundness, based on the classes of Powers (1953), was also estimated from a visual image provided on the size comparator. Bedding descriptors used are after Ingram (1954). Descriptors used for the degree of bioturbation are after Reineck and Singh (1973). Colour of sediments is in terms of Munsell colours, estimated by reference to the colour chips in Munsell Soil Color Charts (1975 Edition).

Palaeocurrent azimuths were estimated using a Brunton compass. Recesses were cut into the face in order to obtain 3-dimensional views of foreset orientations. Particular effort was given to obtaining the strike of the foresets from horizontal cuts. Unfortunately, the preponderance of cross-bedding is in coarse sand and at a low angle, representing the tangential toepoints of the foresets. In these cases the strike of foresets in horizontal cuts is not clearly defined and the estimates had to be made from two vertical cuts (face-parallel and face-perpendicular). Furthermore, unless the cross-bedding is well-defined by alternating coarse and fine-sandy foresets, the structure disappears on fresh cuts. These problems account for many palaeocurrent estimations being only a general indication of the direction, in terms of intercardinal (e.g. NW) and intermediate points (e.g. NNE).

Sedimentary structures were recorded by field sketches and by photography. Photo-mosaics of exposures were made in several instances, to record large-scale sedimentary geometry. Lacquer peels were made, some for representative purposes and others targeting interesting sedimentary and biogenic features. The technique used is based on details provided by Bouma (1969). "Duco-type" clear lacquer, diluted with an equal volume of thinners, was applied by spray-gun. After drying for several days, a thin backing of polyester resin, reinforced with net-curtaining, is applied. After several hours the peel is dug out and laid flat in a made-up box for transport and further curing. Loose and weakly-adhering sediment is removed by gentle sand-blasting using the well-sorted, fine, marine sand from the study area. The finished surface of the peel is then stabilized with a light spray of lacquer.

Sediment sampling

Samples of unconsolidated sediment were collected using a cleaned trowel to make a recess in the exposure. A "Minigrip" sealing plastic bag was then positioned in the recess and the sediment was collapsed directly into it, using the trowel point. Sample size was dependent upon the grain size. For fine sand, 100-200 g was taken, for pebbly sediment, 1-2 kg was taken. Cobble to boulder-size pieces of lithified material were collected for thin-sectioning and, in the case of carbonate-cemented lithologies, dissolution.

Palaeontological description and sampling

The species of fossil molluscs present in the sections were recorded during section description. An initial priority of the project was the collection of fossils for taxonomic study by B. Kensley (Smithsonian Institution). Due to his guidance, the writer was familiar with the identity of commonly occurring taxa from an early stage. The abundances of taxa were recorded by general descriptors

(e.g. abundant, common, rare). Basic taphonomic observations on shell orientations and condition were made.

In beds with abundant shell, bulk samples were taken for later assemblage and taphonomic analysis. These were usually between 20-40 kg. Some initial bulk samples were shovelled into large plastic bags, but later the preferred method was to undercut the bed and collapse the material into a box, in an attempt to minimise breakage. For the purpose of the taxonomic examination, individual specimens were carefully excavated using dental picks and small brushes. Friable shells were consolidated using polyvinylbutyrol (PVB) dissolved in acetone, dripped onto the specimen or applied by brush.

Considerable effort was spent in the search for vertebrate material, in order to obtain age constraints for the deposits. This involved lengthy, systematic scrutiny of the exposures and was rewarded by the eventual accumulation of a small, but significant, assemblage. The bones found were excavated and consolidated in the same manner as shells, with field sketches and photographic recording. In some cases an air-hammer was required to expose bones in semi-cemented lithologies. Mine personnel also donated mineralised, remanié vertebrate material from the basal marine gravels, which they had collected from the gravel screening plant (grizzly).

Trace fossils were "captured" in the lacquer peels. Additional sampling involved spraying individual examples with lacquer and removing them when dry. Cemented burrows falling from the eroding faces could be simply collected.

LABORATORY WORK

Grain size analysis

Samples were split and weighed. Gravel, if present, was separated by dry sieving at 2 mm. Calcium carbonate was determined by acetic acid dissolution of the combined sand and mud fraction. For gravel, $CaCO_3$ was estimated by manually separating and weighing shell fragments. Terrigenous mud contents (non-carbonate) were determined by weight loss after wet sieving at 63 µm. The sand fraction was passed through a nest of sieves (-1 to 4 ϕ), at half-phi intervals, on a mechanical shaker for 15 minutes. The gravel fraction was passed through a sieve nest (-4 to -1 ϕ) at half-phi intervals, on a mechanical shaker for 10 minutes. Adjustments for pan contents after sieving the sand and gravel fractions were made.

Some very muddy samples were initially wet-sieved at 2 mm to free mud and sand adhering to gravel, the mud and sand being retained. A few lithologies with $CaCO_3$ cements were placed in acetic acid to provide samples for components and grain size determinations.

Weights were determined on an electronic balance. Calculation of gravel, sand, mud and $CaCO_3$ percentages, the weight percentage frequency distributions and moment statistics, were done using a spreadsheet (Lotus). Histograms were drawn using AutoCAD.

Sediment compositions

The mineral compositions of a selected, representative set of samples from the study area were examined. Quartz and feldspar contents of coarse sand fraction separates (cU) were determined by etching the grains briefly (~1 min) in hydrofluoric acid (HF). The etched feldspar grains could be easily distinguished from the unaffected quartz grains. Quantification was by ribbon count of at least 200 grains per sample, under the binocular microscope. Heavy minerals in weighed fine sand fraction separates were isolated using bromoform. The minerals were identified using standard optical techniques.

Petrography

Thin sections were prepared by the Technical Workshop, Department of Geological Sciences, University of Cape Town (UCT). The main subjects for petrographic study were the silcrete and phosphorite rocks encountered in the study area. Additional semi-consolidated lithologies were also examined petrographically. These included kaolinitic sediments, marine sediments subjected to local cementation, clasts of sedimentary rock and calcrete. With the exception of the silcrete specimens, epoxy-impregnation of the samples was required. Abundances of constituents were estimated using the visual aid of Terry and Chilingar (1955). Sorting was estimated using the comparators modelled by Longiaru (1987). In petrographic descriptions, PPL refers to plane-polarized light, XPL to crossed polars and RL to reflected light.

Scanning electron microscopy

The basal kaolinitic sediments, silcrete and phosphorite were examined at high magnifications using the Jeol JSM-5200 scanning electron microscope (SEM) at the South African Museum. Small fragments of these lithologies were selected under binocular microscope and then photographed using a Zeiss Tessovar photographic microscope. The low-power, light-microscope photographs of specimens were for "navigational" purposes under the high magnifications. Specimens were gold-coated.

X-ray diffraction and X-ray fluorescence analyses

Bulk rock mineralogical analyses by X-ray diffraction (XRD) was performed on samples of silcrete and phosphorite. Due to the dominance of quartz in the silcrete, the mineralogy of resistates was obtained by dissolution of the powdered rock in HF acid, thereby concentrating the minor minerals to produce improved definition of their reflection peaks. Phosphorite rock was finely crushed and wet-sieved, retaining the 63-125 μm fraction. This was separated in bromoform to concentrate the phosphatic mineral. Some selected heavy mineral separates from the sediments were also subjected to XRD analysis, to confirm optical mineral identifications. The samples were run using Cu k-alpha radiation on the Philips XRD equipment in the Department of Geological Sciences, UCT. Reflections were obtained at 0.1°2Θ intervals and graphed using MS Excel 4 spreadsheet software.

X-ray fluorescence analyses were performed on bulk-rock samples of kaolinitic basal sediments, the silcretes and the phosphorite, to obtain element compositional data. The analyses were supervised by Dr D.L. Reid of the Department of Geological Sciences, UCT. The analytical techniques employed are described in Duncan *et al.* (1984).

CHAPTER 2

REGIONAL SETTING

2.1 CLIMATE

The Namaqualand coastal plain, between the Orange and Olifants rivers (Fig. 2.1), is the southern part of the Namib Desert which receives some rain in winter (Ward, Seely and Lancaster, 1983) and has been termed the Namaqualand Sandy Namib (Logan, 1972; Rogers, 1977). The aridity onshore is juxtaposed against high marine biological productivity offshore. Both stem from the dominance of the atmospheric circulation by the subtropical, marine South Atlantic Anticyclone (SAA), with its dry, subsiding air and strong southerly winds (Fig. 2.1).

During the austral summer, the SAA is displaced southwards to ~31°S and is intensified by the strong heating over the continent, causing strong equatorward winds to dominate the entire west coast. The diurnal modulation of the coastal wind of Namaqualand is marked. Daytime heating and thermal low formation on the coastal plain draws cool air inland across the coast. This late morning/afternoon sea-breeze is deflected equatorwards by Coriolis force, amplifying the longshore wind (Jury, 1985a). The acceleration of this southerly wind towards afternoon is a source of chagrin to the fieldworker, the driven sand in excavations sometimes rendering continued observation impractical.

During winter, when the SAA has shifted northwards about 5 degrees, cyclonic lows travelling in the Westerlies encroach more directly upon the west coast, with periods of three to six days, bringing rain and northwesterly winds. Their influence is marked in the south, but rapidly diminishes northwards. Cape Town receives 500-750 mm of winter rain annually, but this decreases to about 125 mm around the Olifants River and to 50-60 mm around Alexander Bay (Schulze, 1972). However, the passage of disturbances in the Westerlies weakens the southerly wind regime and the relaxation of atmospheric pressure gradients allows local thermal contrasts (between air over cold sea and heated land) to control the coastal winds to a greater extent (Jury, 1985b). The climatology of the west coast is also influenced by warm, offshore winds ("berg" or East Wind) and the passage of coastal low-pressure cells. The katabatic "berg" wind occurs most commonly during autumn and spring (Nelson and Hutchings, 1983), when air descends anticyclonically off the interior plateau due to the establishment of a large high-pressure system over or just south of the subcontinent. This adiabatically-warmed flow entrains large quantities of dust that represent a significant sediment contribution to the shelf. Dust plumes may extend up to 150 km offshore, as seen on satellite images (Shannon and Anderson, 1982). Coastal lows form between Lüderitz and Alexander Bay at the approach of a Westerlies cyclonic system and travel down the coast, rounding the Cape just ahead of the cold front (Kamstra, 1985). They are confined by the escarpment and subsidence inversion. Warm offshore flow occurs ahead of the low, whilst cool, onshore flow and foggy conditions follow the passage of the calm centre. The coastal fog, a common occurrence due to the strong land/sea thermal contrast, is an

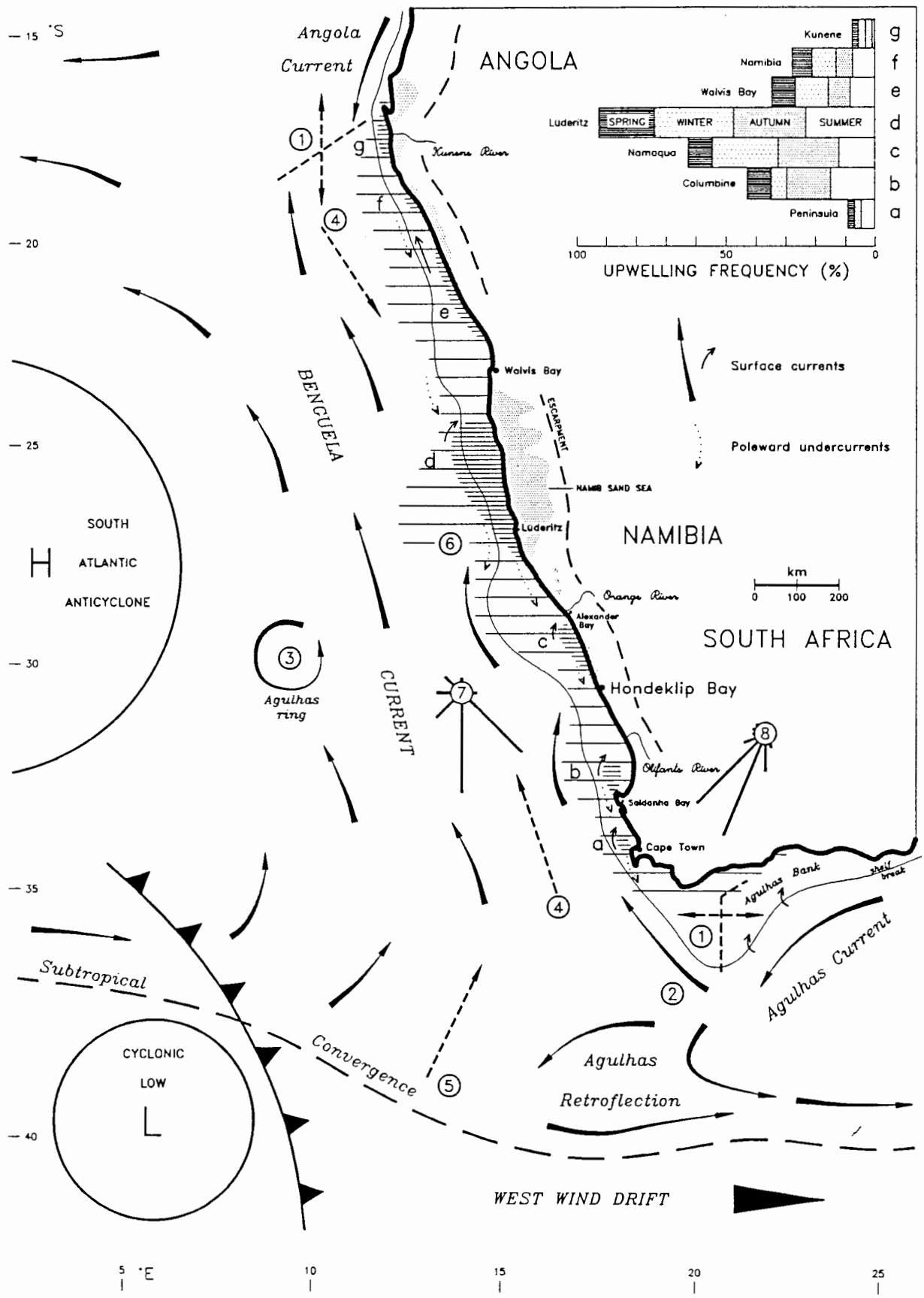

Figure 2.1 The Benguela System. (explanatory notes on facing page)

important source of moisture for plants in the Namib, including the Namaqualand coastal plain.

The aridity of the west coast is primarily due to the SAA limiting northward penetration of the Westerly cyclones and the subsidence inversion associated with the SAA, which limits convectional cloud formation (Preston-Whyte *et al.*, 1977). The cold, upwelled coastal water cools the overlying air, limiting its moisture capacity and enhancing the stability of the inversion. The arid climate of the Namaqualand coastal plain is reflected in the low, undulating topography of ancient linear dunes, stabilised by xerophytic scrub cover (strandveld), that attest to the persistence of strong southerly winds and suggest greater aridity in the recent geological past. Active and semi-active dune plumes occur north of the mouths of ephemeral rivers or south-facing bays (Tankard and Rogers, 1978). The ephemeral rivers (e.g. Buffels River) (Fig. 2.2), rise in the dissected escarpment and traverse the coastal plain in entrenched courses, apparently formed in wetter climates. Other than these rivers, the sandy coastal plain lacks significant drainage.

2.2 OCEANOGRAPHY

The oceanographic regime is an eastern-boundary current, the Benguela, characterized by upwelling of cold, nutrient-rich water that supports an abundant biota (Shannon, 1985). The Benguela Current is a general, but ill-defined, equatorward movement of water forming part of the South Atlantic Gyre. The surface waters, driven by the southerly wind, are deflected offshore (Ekman Drift) due to Coriolis force and cool Central Water from depths of -200 to -500 m upwells across the shelf to compensate. Isotherms slope up over the shelf to intersect the surface. Temperatures close to the coast are thus 8-12°C and a strong thermocline is prevented from forming. A complex front is developed between the cold, upwelled water adjacent to the coast and warm, oceanic surface water offshore (Fig. 2.1) and accelerated currents (frontal jets) occur. The intensity of upwelling varies in time and space, mainly as a function of the seasonality of the wind regime, but also due to modification of the latter by the coastal topography and thermal regime, whilst shelf bathymetry influences the movement of upwelling water across it (Shannon, 1985). These effects result in distinct zones or cells of upwelling along the coast (Fig. 2.1, a–g). Below the surface currents of the Benguela, a general, poleward compensatory flow of oxygen-depleted bottom water is present (Shannon, 1985; Dingle and Nelson, 1993).

Seasonal variation in upwelling is most marked south of the Olifants River, where the modulation of the SAA circulation by the Westerlies is greatest, thus suppressing upwelling-favourable winds in winter (Shannon, 1985) (Fig. 2.1, a, b). Farther north, southerly wind and upwelling are more perennial, reaching a maximum off Lüderitz, the principal Benguela upwelling centre. Off Namaqualand, the Namaqua upwelling cell is present for about 60% of the time (Lutjeharms and Meeuwis, 1987) (Fig. 2.1, c). The narrower and deeper shelf southwest of Hondeklip Bay (Fig. 2.2) increases the availability of cold water inshore (Taunton-Clark, 1985). Upwelling along Namaqualand is also influenced by the effects of the thermal regime and valleys on the southerly wind. The Namaqua cell off Hondeklip Bay is associated with the wind maximum in the zone of wind

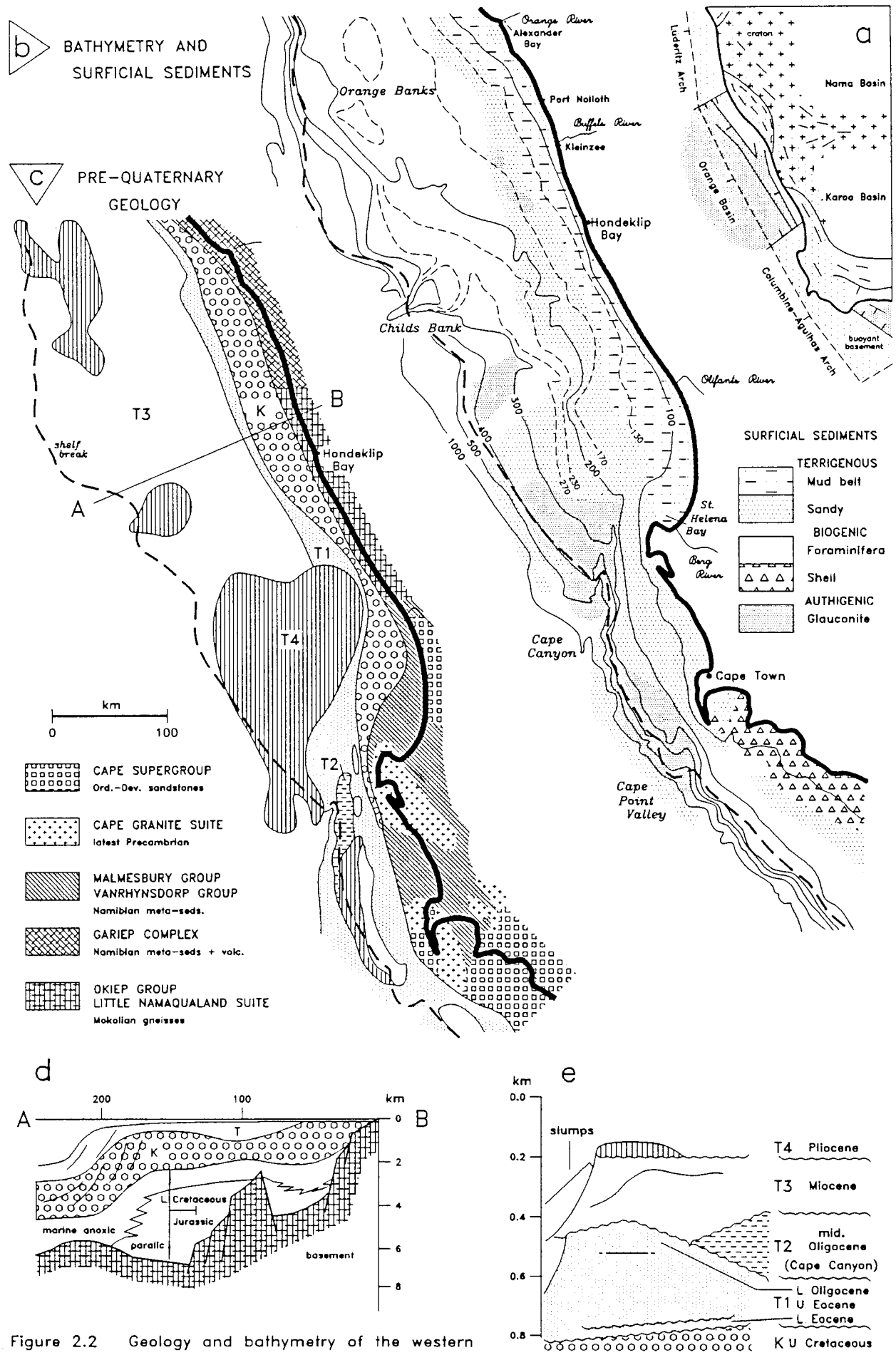

Figure 2.2 Geology and bathymetry of the western continental shelf, South Africa (explanatory notes on facing page)

"overspeeding" towards the Orange River valley and thermal augmentation by warm air entrained down the Buffels River valley (Kamstra, 1985; Jury and Taunton-Clark, 1986).

At its northern boundary, the equatorward-flowing Benguela Current interacts with tropical waters of the poleward-flowing Angola Current (Fig. 2.1), resulting in a permanent, east-west orientated front between 15-17°S, defined by marked temperature and salinity gradients . The front shifts seasonally through ~2° of latitude, being farthest south in summer and farthest north in winter (Shannon *et al.*, 1987, Meeuwis and Lutjeharms, 1990). Occasionally, at an interannual frequency of approximately 10 years, warm tropical water invades the northern Benguela, penetrating as far as 25°S. These episodic events have been termed Benguela *Niños*, due to their similarity with the *El Niño* phenomenon in the eastern Pacific off Peru (Shannon *et al.*, 1986). Tropical fauna is entrained in this flow and the Benguela cool-water fauna is displaced southwards at such times.

In the south, the western-boundary, poleward-flowing Agulhas Current and the West Wind Drift (Antarctic Circumpolar Current) south of the Subtropical Convergence (STC) interact with the Benguela System in the area of complex and highly variable circulation termed the Agulhas Retroflection Zone (Fig. 2.1). Rings, filaments and tongues of Agulhas Water shed in the Retroflection Zone are advected northwards. Much of this warm water dissipates into the northwest and this Agulhas contribution of heat and salt to the surface waters of the Atlantic is considered to be partly compensatory, in the thermohaline circulation, for the export of heat and salt from the Atlantic via production of North Atlantic Deep Water (Gordon, 1985). Water from the Agulhas Bank, a mixture of Agulhas Current and South Atlantic subtropical water, leaks continuously into the Benguela (Nelson and Hutchings, 1983; Shannon, 1985). Warm-water intrusions affect the southern Benguela, particularly during anomalously reduced southerly wind and the occurrence of Westerlies (Walker *et al.*, 1984a,b). Continued upwelling usually keeps warm water offshore off Namaqualand. However, a major perturbation of the Agulhas Retroflection took place during late 1985 and 1986, when Agulhas water penetrated up the west coast as far north as Lüderitz and suppressed upwelling (Shannon and Agenbag, 1987). These events were associated with large-scale atmospheric anomalies such as the abatement of trade winds in the Indian Ocean and a southerly shift of the anticyclonic circulation south of Africa (Shannon *et al.*, 1990).

The abnormal input of Agulhas water into the Atlantic during 1985/86 was terminated by an equally remarkable intrusion of Subantarctic water extending from the STC into the southern Benguela (Shannon *et al.*, 1989b). This was probably caused by enhanced flow of the Antarctic Circumpolar Current due to stronger zonal Westerlies during the summer of 1986/87 and was evidently not an isolated event (an analogous event seems to have occurred in 1950) (Shannon *et al.*, 1989b).

These anomalous conditions suggest that the Benguela upwelling regime, as presently known, could be changed by a relatively minor, but persistent, alteration of the general atmospheric circulation around the subcontinent. Large-scale changes in the warm-water influences at the northern and

southern Benguela boundaries, and the Subantarctic influence in the south, would have accompanied the dramatic climatic fluctuations of glacial and interglacial periods during the late Cenozoic.

2.3 TIDAL AND WAVE REGIME

The tidal regime is simple semi-diurnal with a spring tide range of ~2,0 m and a neap range of ~1 m, the mean range of ~1,5 m falling within the microtidal (<2 m) category of Davies (1964). Tidal currents are significant where back-barrier environments are developed. However, the combination of the arid hinterland and small, narrow, infilled estuaries with limited tidal prisms, together with strong longshore drift tending to close estuary mouths, results in tidal-inlet systems not being significantly developed along the west coast at present. High wave-energy dominates sediment transport on the inner shelf, the effect of tidal currents evidently being negligible (De Decker, 1988). Nevertheless, tidal and inertial currents are significant in the water column over the shelf (Schumann and Perrins, 1982) and play a role in the transport of fine-grained material.

Waves originating in the "Roaring Forties" of the Southern Ocean impinge obliquely on the coast from the southwest (Fig. 2.1), producing strong, northward longshore drift. Median wave heights decrease from ~2,5 m off Cape Town to ~1,75 m off Oranjemund. These long-period waves occur ~25% of the time (Rossouw, 1984; Van Heerden, 1986), except in winter when they dominate ~40% of the time (Rossouw, 1984). Waves from the northwest occur relatively seldom (~1% occurrence), mainly in winter and spring (Rossouw, 1984). Van Heerden (1986) states that locally-generated, short-period, waves impinge from the south upon the coast at Oranjemund for ~40% of the time.

De Decker (1988) provides wave data, supplied by the Fisheries Development Corporation, from a "Waverider" buoy deployed at -15 m depth off Alexander Bay, which would be broadly applicable to the northern Namaqualand coast, barring the influences of shoaling over the Orange River delta. Median values for the period of the highest wave-amplitude (maximum-energy wave period) range from 10.5 s in summer to 12,5 s in winter. Mean wave periods for summer and winter are 5,5 s and 7,5 s, respectively. Significant wave heights (average of the highest 1/3 of the waves) between 0,5 to 3,5 m occur 90% of the time with a median value of 1,5 m except for winter when it is 1,9 m. Waves 5 m high with 20 s periods occasionally occur throughout the year, but only ~1% of the time. De Decker (1988) calculated that average wave conditions could transport very coarse sand down to 30 m and medium pebbles at 15 m, whilst during storms medium pebbles (~1 cm diam.) could be mobile at 30 m and small cobbles at 15 m.

The effect of the wave and current regime of the inner to middle shelf is best evidenced in the fate of sediment provided by the Orange River, described in detail by Rogers (1977), Bremner et al. (1990), Shillington *et al.* (1990) and Rogers and Bremner (1991). Bedload sediment input from the Orange River is dispersed northwards from the river mouth bar to the beaches nourishing the Namib Sand Sea (Rogers, 1977). The delta is entirely submarine and is constructed of very fine sand to clay (Rogers and Bremner, 1991). It exhibits a clear seaward-fining trend and occupies the wave-

dominated extreme of the deltaic spectrum (Wright and Coleman, 1973). Very fine sand characterises the delta front, whilst seaward of the -40 m isobath silt and clay comprise the prodelta, a fractionation generally consistent with the wave regime. Its elongate, northward asymmetry reflects the northward transport, by wind-induced currents, of very fine sand and coarse silt suspended by wave action. Theoretical studies indicate that, in the absence of strong equatorward wind, discharge from a west coast river mouth will turn poleward (south) (Shillington *et al.*, 1990). The plume of low density, sediment-laden fresh water discharging from the Orange River mouth during the 1988 floods was observed to flow poleward and close to the coast (Shillington *et al.* 1990). By this means the finest silt and clay, maintained in suspension longer, is dispersed southwards. Southward dispersal of suspended material (and mud re-suspended during storms) is also effected by the ambient poleward undercurrent, to be deposited mainly in a long, coast-parallel mud belt extending to St. Helena Bay (Rogers, 1977; Birch *et al.*, 1986; Rogers and Bremner, 1991).

2.4 THE CONTINENTAL SHELF

The shoreline of Namaqualand lacks major embayments and is generally rocky, with interspersed pocket beaches of thin, sandy, gravelly and shelly sediment that comprise about one third of the coastline. The shoreline is mainly backed by dune deposits, but cliffs in bedrock, capped by truncated Pliocene marine deposits, are present on either side of the Olifants River mouth and north of Port Nolloth (Fig. 2.2). The Namaqualand littoral is sediment-starved, the scanty rain being absorbed by the sandy hinterland (Rogers, 1977). The Olifants River does not appear to be contributing significant quantities of coarse, terrigenous detritus, as is evident in the negligible sediment cover north of it (O'Shea, 1971). The cover of aeolian sand on the coastal plain attests to the removal of much sediment from the littoral. Although sea-level has fallen 2-3 m in the last 4-5 millennia (Yates *et al.*, 1986; Miller *et al.*, 1993), the Namaqualand shoreline is effectively in a state of transgressive stillstand. This contrasts with the situation north of the Orange River where the submarine Orange River delta merges with a progradational, regressive sandy beach stretching 100 km northwards, nourished by the powerful, northward longshore drift (Rogers, 1977; Bremner *et al.*, 1990; Rogers and Bremner, 1991).

The bathymetry and surficial cover of the western continental shelf are described in detail in a trilogy of theses (Birch, 1975; Rogers, 1977; Bremner, 1981) and have recently been reviewed by Rogers and Bremner (1991). Sets of maps detailing bathymetry and the composition and texture of the surficial sediments mantling the continental shelves of South Africa and Namibia have been published by Birch *et al.* (1986) and by Bremner *et al.* (1986). O'Shea (1971) and Birch *et al.* (1991) have provided regional perspectives on the Quaternary deposits mantling the pre-Quaternary bedrock, whilst De Decker (1987) and Woodborne (1987) have presented the results of detailed surveys of the Quaternary cover on the inner shelf between Alexander Bay and Kleinzee. Dingle and Siesser (1977) have provided a map of the pre-Quaternary geology of the continental margin from Walvis Bay to Mozambique. Dingle *et al.* (1987) have provided both maps and a description of the sedimentary

environments and bathymetry around the southern Africa margin. Dingle *et al.* (1983) have also presented a valuable synthesis of the structure and pre-Quaternary history of this margin. Some salient features only are briefly mentioned and illustrated here (Fig. 2.2).

The inner shelf off Namaqualand is narrow and rocky and is comprised mainly of outcropping late Precambrian bedrock with thin, patchy sediment cover (O'Shea, 1971; Birch *et al.*, 1991). Patches of nearshore sediment are generally only a few metres thick, but thicknesses exceeding 12 m occur in palaeochannels (O'Shea, 1971). Just south of the Orange River delta, inner-shelf sediment thicknesses of up to 14 m have been recorded by De Decker (1987). Palaeochannels incised in the inner shelf are common and many are associated with river mouths, the largest occurring off the Olifants, Buffels and Orange rivers (O'Shea, 1971; Birch *et al.*, 1991). Other inner-shelf palaeochannels occur that are not associated with the modern onshore drainage, but correspond with positions of palaeochannels onshore. Micro-topographic mapping of the inner shelf between Alexander Bay and Kleinzee (De Decker, 1987; Woodborne, 1987) reveals a bedrock topography characterized by many palaeochannels, as well as terraces (slope breaks) at several depths.

Along its outer edge the inner-shelf bedrock slopes relatively steeply (1,1-1,9°, De Decker, 1987) and disappears beneath the elongate lens of terrigenous sediment on the shelf between -70 to -120 m (the "mud belt") (Fig. 2.2). Recent acoustic work off northern Namaqualand reveals that the "mud belt" is up to ~25 m thick and consists of sandy aeolian and transgressive shoreface deposits of Last Glacial to earliest Holocene age, overlain by ~10 m of latest Pleistocene and Holocene mud (Woodborne, 1987; Birch *et al.*, 1991). At each end of the lens are the deltas of the Orange and Olifants rivers, which deflect bathymetric contours offshore (Fig. 2.2) and are the main latest Pleistocene to Holocene depocentres.

The middle shelf lies seaward of the late Precambrian outcrop, the "mud belt" forming the transition to a low-gradient seaward slope of ~0,1° (Rogers, 1977), underlain successively seawards by Cretaceous, Palaeogene and Neogene rocks in coast-parallel zones with negligible Quaternary sediment cover (Dingle and Siesser, 1977) (Fig. 2.2). The contact between Cretaceous and Precambrian rocks is beneath the mud belt at -100 to -110 m. Seawards over the middle shelf, biogenic (foraminiferal) sandy ooze, rich in authigenic glauconite, replaces the inshore terrigenous facies.

The outer shelf, generally seaward of ~200 m, is marked by two bathymetric highs, the Orange Banks and Childs Bank, with depths of 160 and 200 m, respectively (Fig. 2.2). These are formed of limestones deposited on the shelf during the Pliocene (Unit T4, Dingle *et al.*, 1983) (Fig. 2.2). The largest outcrop of Unit T4 is on the middle shelf off St. Helena Bay. Its patchy distribution suggests extensive Quaternary erosion, although original localised deposition may partly account for this distribution. West of Saldanha, the shelf break is interrupted by a major erosional feature, the Cape Canyon, cut by the combined Orange/Vaal/Olifants/Berg river systems during the Oligocene (Dingle, 1973; Dingle and Hendey, 1984). A similar, but smaller feature, the Cape Point Valley, occurs off

Cape Point. Massive slumping, that probably occurred mainly during the Pleistocene glacials, characterises the outer margin (Fig. 2.2) (Dingle, 1980b).

Overall, relative to the Cretaceous, the supply of terrigenous sediments to the margin and its rate of subsidence has decreased during the Tertiary (Fig. 2.2), with a concomitant increase in the importance of biogenic sedimentation and authigenic mineralization (Dingle *et al.*, 1983; Dingle, 1992/93). Weak upwelling developed during the middle Tertiary and intensified from the late Miocene as global climatic deterioration progressed (Siesser, 1978). The effect of late Cenozoic upwelling has been the widespread occurrence of phosphatic and glauconitic authigenic mineralization on the shelf and extensive phosphatization of Tertiary limestones exposed at the sea-bed (T3 and T4) (Parker, 1971; Parker and Siesser, 1972). Authigenic phosphatization extended across the present coastline during Cenozoic transgressions, as is evidenced in phosphatic sands occurring up to 80 m asl. in the early Pliocene Varswater Formation near Saldanha Bay (Elandsfontein, Fig. 3.1) (Rogers, 1980). Similarly, phosphorite occurs in the study area and the analysis presented herein sheds further light on the context of Pliocene phosphorite formation.

CHAPTER 3

PREVIOUS RESEARCH

3.1 INTRODUCTION

The object of this chapter is to provide a brief summary of the development of the stratigraphy of the coastal-plain of Namaqualand. Particular aspects of the previous work will be elaborated further when relevant to topics in subsequent chapters. Recent publications stemming from the writer's research at Hondeklip, such as summaries of main results, are mentioned. Correlations previously suggested between the Namaqualand coastal stratigraphy and farther afield will be discussed in the chapter on stratigraphic correlations (Chapter 29) which will include the correlations suggested in recent works that cite the already published results from the study area. A brief summary of the previous work on the coastal plains of Namibia and the Southwestern Cape will form part of the chapter on regional correlations (Chapter 29).

The earlier work along the Namaqualand coast (pre- World War II), spurred by the initial flurry of diamond prospecting, is presented in chronological order. The later work is presented mainly by area, first the areas north and south of the study area, then the work from the central Namaqualand coast. The chapter is concluded with a brief overview of regional syntheses.

3.2 THE EARLIER WORK

The first recorded references to the raised beaches of Namaqualand (and probably also the first recorded mention of fossils in South Africa) are in the journals of the explorers R.J. Gordon (Raper and Boucher, 1988) and W. Paterson (Forbes and Rourke, 1980). *En route* to the "Great River" in 1779 (to be named the Orange River by Gordon, after the Dutch House of Orange), they headed towards the Holgat River (Fig. 3.1) in search of water. There they noted the presence of fossil marine shells in marine deposits on top of the cliffed shoreline (Forbes and Rourke, 1980; Raper and Boucher, 1988). They also made the distinction between raised beach deposits and shell middens of anthropogenic origin.

One and a quarter centuries after Gordon and Paterson's explorations, Rogers (1904, 1905) made observations on marine gravels and sands on the cliffs at ~25 m asl. between the Olifants River and Doring Bay (Fig. 3.1). He noted their apparent geomorphological association with the occurrence of siliceous and ferruginous duricrusts in the area. Krige, during his survey of raised beaches around South Africa, published in 1927, made observations on the occurrence of low-elevation (<20 m asl.) marine terraces and deposits along the Namaqualand coast, his "Major Emergence" (15-18 m asl.) and "Minor Emergence" (5-8 m asl.) (Krige, 1927). He provided Haughton with fossil shells from the cliffs at Doring Bay, which resulted in the first descriptions of Tertiary fossil molluscs from Namaqualand (e.g. *Donax rogersi* Haughton, 1926; *Chamelea krigei*, Haughton, 1926).

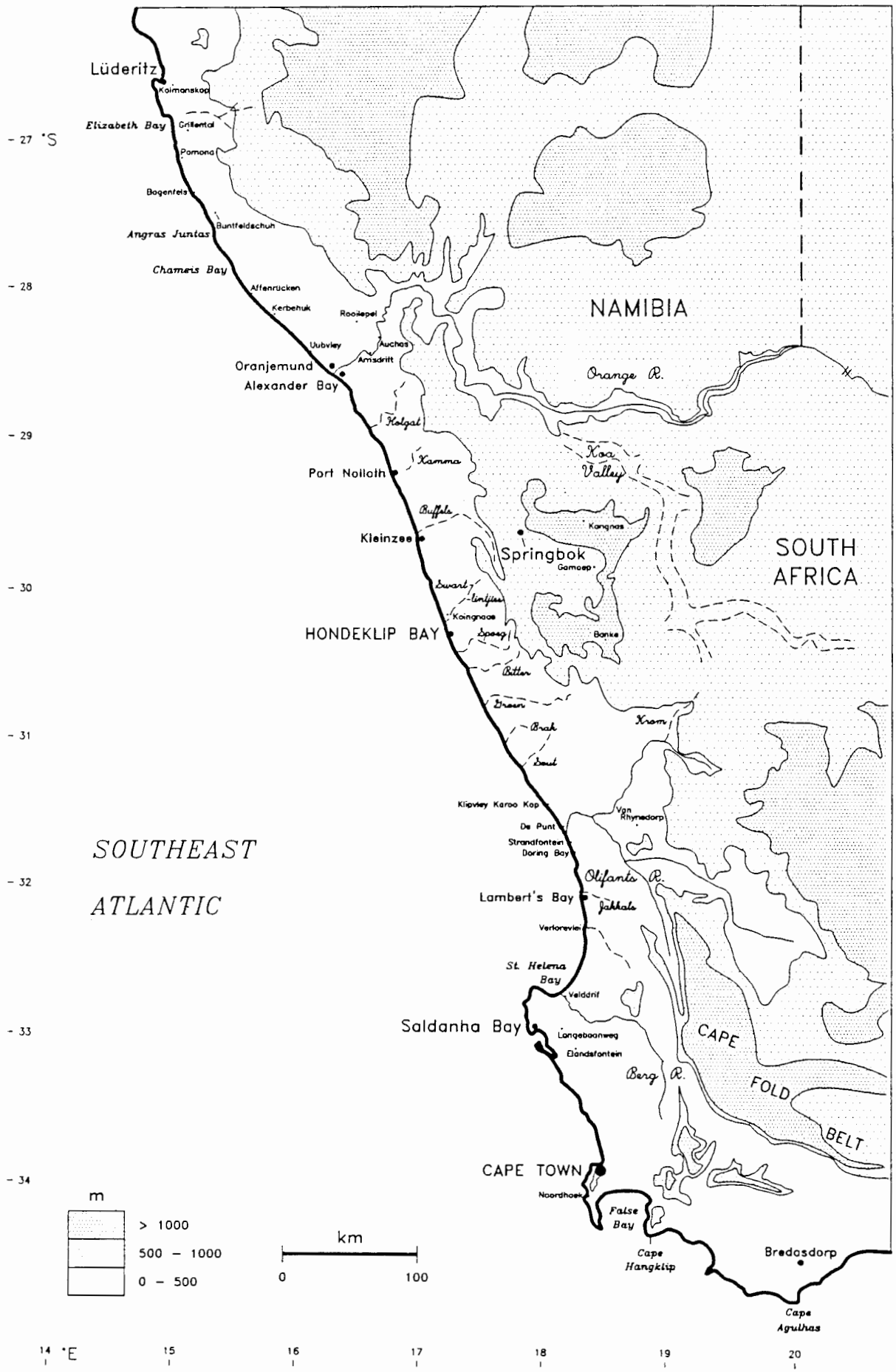

Figure 3.1 Regional physiography and locations of sites mentioned in the text.

Subsequent to the major diamond finds between the Orange River and Kleinzee and at the Groen River mouth, Wagner and Merensky (1928) described the geology of the deposits exposed in the early prospects. In an appendix to this work, Haughton described the fossils they collected (Haughton, 1928). Wagner and Merensky (1928) recognized that "surface quartzites" or silcretes are the oldest stratigraphic unit on the Namaqualand coastal plain. On the basis of the molluscan fossils, Haughton (1928) recognized that the raised beaches are late Tertiary (Mio-Pliocene) to Pleistocene in age and identified three biostratigraphic units: the "*Ostrea* Bed" or "Oyster Line," the "Operculum Bed" and the "Lowest terrace." The oysters in the "*Ostrea* Bed," identified as the living east coast species (*Crassostrea margaritacea*), then called *Ostrea prismatica*, indicated sea temperatures higher than those now occurring on the west coast. Extinct species (e.g. *Donax rogersi*, *Chamelea krigei*) implied a Mio-Pliocene age (Haughton, 1928). The "Lowest terrace" enclosed an extant fauna and a younger, Pleistocene age with sea temperatures similar to the present was implied. The "Operculum Bed" was regarded as an intermediate unit between the "*Ostrea* Bed" and "Lowest terrace."

From fluvial deposits at ~35 m asl. near Kleinzee, Stromer (1931) described a small vertebrate assemblage that included extinct hyaena, otter and mongoose. Reuning (1931) described a section overlying the cliffs at De Punt, just north of the Olifants River, (Fig. 3.1), part of which was interpreted as a silcrete correlated with the "Pomona Quartzite" (Beetz, in Kaiser, 1926) in southern Namibia. Haughton (1932) made observations from Bogenfels, Namibia, to Saldanha Bay. From his further collecting of fossils, he refined his initial biostratigraphy for west-coast deposits, erecting five faunal zones, from "Zone E" (oldest) to "Zone A" (youngest with extant fauna) (Haughton, 1932). Instead of being entirely superseded, Haughton's early biostratigraphic zonations (1928, 1932) are enlarged upon from observations at Hondeklip Bay.

3.3 THE LATER WORK

Hallam (1964) wrote an account, wide-ranging in areal coverage (from northern Namibia to Kleinzee) and subject matter, of the west coast, its raised beach deposits and its diamonds. As a synthesis of west coast economic geology of the 1950s, after a period during which little published information was forthcoming, this remains a useful resource.

THE STATE ALLUVIAL DIGGINGS

De Villiers and Söhnge (1959) provided a valuable description of the marine terraces and deposits of the State Alluvial Diggings (Alexander Bay to Port Nolloth, Fig. 3.1), as seen in 1944. The significance of their observations on sedimentary geometry in relation to cliffed bedrock is revitalised by observations from Hondeklip Bay. Keyser (1972) provided the most detailed, extant description of the terraces in the State Alluvial Diggings (SAD) area (Alexander Bay to Port Nolloth). Marine deposits are present to high elevations and four terraces were recognized.

In order of descending elevation, these are the Grobler Terrace (64-84 m asl.), SAD Upper (34-47 m asl.), SAD Middle (17-26 m asl.) and SAD Lower (0-9 m asl.). The three higher terraces rise gently in elevation to the south. These marine deposits have been named the Alexander Bay Formation (Kent and Davies, 1980). Recently (Hill, in Rogers *et al.*, 1990), the altimetric definitions of the terrace elevations have been altered: 75-90 m asl. (Grobler), 30-60 m asl. (SAD Upper), 15-30 m asl. (SAD Middle) and 0-15 m asl. (SAD Lower). Extinct taxa occur in the older, higher terraces, whereas the SAD Lower Terrace deposits enclose extant molluscan fauna. Gresse (1988) has described sections and listed fauna from the terrace deposits, suggesting correlations with the Hondeklip sequence.

KLEINZEE

From the Kleinzee area, an interesting development is the discovery of a deep channel north of Kleinzee that is infilled with carbonaceous, fluvial sediments, dated palynologically as Lower Cretaceous (Molyneux, in Rogers *et al.*, 1990). Elevations of platforms, stormbeach ridges and cliffs in the Kleinzee area were provided by Hallam (1964) and Davies (1973). The sequence of terraces currently recognized is provided by Molyneux (in Rogers *et al.*, 1990). Notably, although the terrace nomenclature at Kleinzee also employs Upper, Middle and Lower appellations, the terraces to which these apply are at elevations different from those at the State Alluvial Diggings. The Kleinzee Upper Terrace at 75-95 m asl. (corresponding altimetrically with the SAD Grobler Terrace) terminates landward in a marked cliff cut into silcrete-capped hills. The Kleinzee Middle Terrace (≈SAD Upper) is at 30-65 m asl. and is subdivided into upper and lower parts. The Kleinzee Upper Middle Terrace (K-UMT) terminates landward in another well-developed cliff at 65 m asl., whilst a break in bedrock gradient at ~45 m asl. generally marks the boundary between the K-UMT and Kleinzee Lower Middle Terrace (K-LMT). The 65 m asl. cliff is considered to have been produced at the transgressive maximum, whilst the K-LMT represents a stillstand at ~45 m asl. during the subsequent regression. This stillstand was succeeded by renewed transgression that overlapped the seaward edge of the K-UMT sediments (Molyneux, in Rogers *et al.*, 1990). The separation of the K-LMT and the Kleinzee Lower Terrace (≈SAD Middle) is not clearly defined by bedrock topography, but an extent between 10-30 m asl. is indicated and is supported by inflexions of bedrock gradient at ~30 m asl. in some profiles (Molyneux, in Rogers *et al.*, 1990). Late Quaternary beach deposits occur below ~10 m asl. and three units at ~8, ~5 and ~2 m asl. are recognized (≈SAD Lower) and enclose an extant, cold-water fauna.

THE OLIFANTS RIVER AREA

Visser and Toerien (1971) made detailed observations from St. Helena Bay to just north of the Olifants River. They noted a marine erosion surface at 90-120 m asl. and terraces at ~45, ~27, ~18, ~6 and ~3,5 m asl. Davies (1973) made sundry observations in the area.

THE HONDEKLIP BAY AREA

Little information was forthcoming from the Hondeklip area of central coastal Namaqualand until Tankard (1966) described aspects of the succession revealed by prospecting. At that stage, the sequence was seen in terms of the preliminary biostratigraphy erected by Haughton (1932) (Zones E to A). Significantly, Tankard (1966) reported the presence of channel-infilling, kaolinitic, non-marine sediments overlying kaolinized gneiss and the occurrence of phosphatic nodules. He also encountered difficulties in the application of Haughton's (1932) biostratigraphic zones to the more extensive prospecting exposures.

An important advance for the stratigraphy of Namaqualand coastal deposits was Carrington and Kensley's (1969) article describing new molluscan fossils from the central Namaqualand area in which a summary stratigraphic column was presented. Channel-infilling, unfossiliferous, fluviatile clays and clayey sands, considered Mio-Pliocene in age, were recognized as the oldest unit, which was succeeded by remnants of phosphatic beds with abundant shell moulds, considered Pliocene in age. In contrast to the earlier suggestions of a Mio-Pliocene age for the higher elevation coastal-plain deposits (Wagner and Merensky, 1928; Haughton, 1932), Carrington and Kensley (1969) considered the bulk of the succession to be Pleistocene in age. They identified "transgression complexes" at 75-90, 45-50, 17-21, 7-8, ~5 and ~2 m asl. and a 29-34 m Beach. Importantly, they found that the bivalve *Donax rogersi* Haughton, 1926, actually subsumed two species; the thick-shelled, robust *D. rogersi* "proper" and a thin-shelled, generally smaller species (thought by Haughton to be juveniles), which they named *Donax haughtoni*. The latter species occurred only in the fine-grained, usually laminated, sands of the "45-50 m complex," whilst *D. rogersi* occurred only in the coarse, usually cross-bedded, sediments of the younger "17-21 m complex." This finding constituted a major advance in the biostratigraphic subdivision of the older coastal-plain marine deposits. Additionally, species obtained from the "45-50 m complex" suggested a fauna of warm-water affinity.

Further notes on the deposits of central Namaqualand were provided by Davies (1973) and by Tankard (1975a, 1975b). Tankard (1975a) differed from Carrington and Kensley (1969) in regarding the phosphatic beds in the Hondeklip area as older than the "channel clays." As will be shown in a later section (Chapter 5), Carrington and Kensley (1969) were correct and the "channel clays" are older than the phosphatic beds. He provided some information on the phosphatic beds that infill hollows in the bedrock and which had come to be known as "E stage," presumably from Haughton's oldest biostratigraphic unit, "E Zone." Tankard (1975a, 1975b) proposed correlations of lower, middle and upper "E stage" sub-units with the succession in the Varswater Quarry near Langebaanweg. Kent and Davies (1980) informally named the coastal-plain deposits between the Olifants River and Kleinzee the "Hondeklipbaai sandy gravels."

The results of initial work on the "Hondeklipbaai sandy gravels" were presented by Pether (1983). Pether (1986a) provided a summary of the main findings of his research on the succession at Hondeklip Bay, including suggested correlations farther afield. Information was also disseminated at a number of conferences (Pether, 1986b, 1986c, 1987; Pether, in Rogers *et al.*, 1990). More intensive

faunal sampling carried out during this study has led to considerable additions to the marine molluscan fauna of Namaqualand coastal deposits (Kensley and Pether, 1986). The first extinct Tertiary barnacle recorded from South Africa was described from Hondeklip by Pether (1990). Brunton and Hiller (1990) have described the fossil brachiopods collected by the writer in the Hondeklip study area.

Table 3.1 Carrington's summary stratigraphic column for the Namaqualand coastal plain, from Carrington and Kensley (1969). The nomenclature of the marine "transgression complexes" refers to the altimetric maxima of the associated transgressions of relative sea-level.

SUCCESSION	*Thickness*	*Suggested age*
Loose surface sand	0 – 4 m	
—unconformity—		Recent
2 m Transgression complex Highly fossiliferous sands and gravels; berm sands.	2 – 7+ m	
—unconformity—		
5 m Transgression complex Slightly calcareous sands and shelly granule gravels.	2 –3 m	
—unconformity—		Upper Pleistocene
7 – 8 m Transgression complex Stabilised berms; calcareous, often highly garnetiferous marine sands over well-developed boulder gravels.	3 – 5+ m	
—unconformity—		
Terrestrial sands Sheet wash deposits.	2 – 7 m	(to Recent in part)
—unconformity—		
17 – 21 m Transgression complex Coarse sands and grits over massive, basal boulder gravels.	10 – 15 m	Middle Pleistocene
—unconformity—		
29 – 34 m Beach Thin, discontinuous, shelly gravel beach.	uncertain	
—unconformity—		
45 – 50 m Transgression complex Aeolianite and coarse regressive facies overlying locally fossiliferous, fine-grained, transgressive sands.	5 – 25+ m	Lower Pleistocene
—unconformity—		
75 – 90 m Transgression complex Regressive aeolianite overlying coarse marine sands and thin gravels.	35+ m	Basal Pleistocene
—unconformity—		
Fossiliferous phosphatic siltstones	0 – 1 m	Pliocene
—unconformity—		
Fluviatile beds Linear deposits of clays and clayey sands. Unfossiliferous.	up to 20 m	Mio-Pliocene?
—unconformity—		
Basement gneiss		Archaean Complex

3.4 REGIONAL SYNTHESES

The growth of data during the 1970s prompted a number of syntheses emphasising Cenozoic palaeoclimates, biogeography and sea-level history (Tankard and Rogers, 1978; Siesser and Dingle, 1981; Hendey, 1983a, 1983b, 1983c; Dingle *et al.*, 1983), the latter work including offshore data and thus dealing with the evolution of the continental margin as a whole. Previous work describing the nature and evolution of the western continental margin is of fundamental relevance to the coastal plain, the latter being the "feather edge" of the margin depository . Evidence for transgression and regression on the coastal plain should be matched in the submerged record. The coastal-plain record also includes a tectonic component, forming part of the crustal responses to the thermal and sediment loading history of the margin since continental breakup. Furthermore, the development of the coastal plain is not divorced from the geomorphological development of the continental interior; a recent synthesis of the geomorphic evolution of southern Africa emphasizes the links between interior surfaces, coastal-plain surfaces and deposits and the record of offshore sedimentation (Partridge and Maud, 1987), with episodic uplift postulated as the major driving force. However, current data do not yet allow correlation and integration of the emerged and submerged-margin and continental records other than on a general scale (e.g. the general sea-level curve of Siesser and Dingle (1981) and the broad linking of episodic uplifts and offshore sedimentation indicated by Partridge and Maud (1987)). The respective roles of tectonics and eustatic sea-level changes in the genesis of the geological and geomorphological record remains necessarily controversial. The improved knowledge of the coastal-plain record, embodied in this thesis, is one small contribution toward that much larger problem.

CHAPTER 4

GENERAL GEOLOGY OF THE STUDY AREA

4.1 SURFACE GEOLOGY AND TOPOGRAPHY

Bedrock Geology

The study area, on the farms Hondeklip and Avontuur-A, occupies a position between two ephemeral rivers, the Swartlintjies (~6 km to the north) and the Spoeg (~18 km to the south) (Fig. 4.1). The bedrock on which the coastal-plain sediments were deposited consists of Precambrian gneisses. Outcrops of these basement gneisses are rare below elevations of ~100 m asl. on the coastal-plain and they are mainly exposed along the shoreline and in the river courses (Fig. 4.1). The gneisses are Mokolian in age (middle Precambrian) (Visser *et al.*, 1984). Two types alternate along the Hondeklip coastline (Fig. 4.2): meta-sedimentary gneisses of the Garies Subgroup (Okiep Group) (Joubert *et al.*, 1980) and meta-igneous gneisses of the Nababeep-type (Little Namaqualand Suite) (Marais and Joubert, 1980).

The Garies Subgroup gneisses are represented at Hondeklip Bay by the "Quartzo-feldspathic gneisses" of the Kookfontein metamorphic suite (Jack, 1980). These gneisses are grey in colour and more foliated than the younger Nababeep-type gneisses. The latter are augen gneisses that are reddish-pink in colour and, being less foliated and lithologically more uniform than the Garies Gneiss, form large boulders and domes. Contacts between the two are usually sharp, but, in the lower reaches of the Swartlintjies River, the intrusive relationship of the Nababeep Gneiss is seen and migmatites are developed (Jack, 1980). Along the Hondeklip shoreline the foliation of both gneisses generally dips quite steeply into the northwest quadrant (Fig. 4.2). Overall, along the central stretch of the coast of Namaqualand, the foliation in the gneisses strikes north-south and dips to the west (Jack, 1980).

Surficial Sediments

Immediately inland of the littoral, the bedrock is covered by late Quaternary shelly beach sands, gravels and aeolian sands. A small plume of active foredunes is present on the promontory just north of Hondeklip Bay (Fig. 4.2) and is nourished by deflation of the sandy beach in the cove. This is underlain by older, compacted aeolian sand exposed between the active dunes. On the seaward side, the older, compacted aeolian sands are overlain by a beach conglomerate at 2-3 m asl. This latest addition to the coastal-plain succession represents the middle Holocene high sea-level recorded from the Namaqualand coast by Carrington and Kensley (1969), from the Saldanha area by Flemming (1977) and from Verlorevlei by Yates *et al.* (1986) and Miller *et al.* (1993).

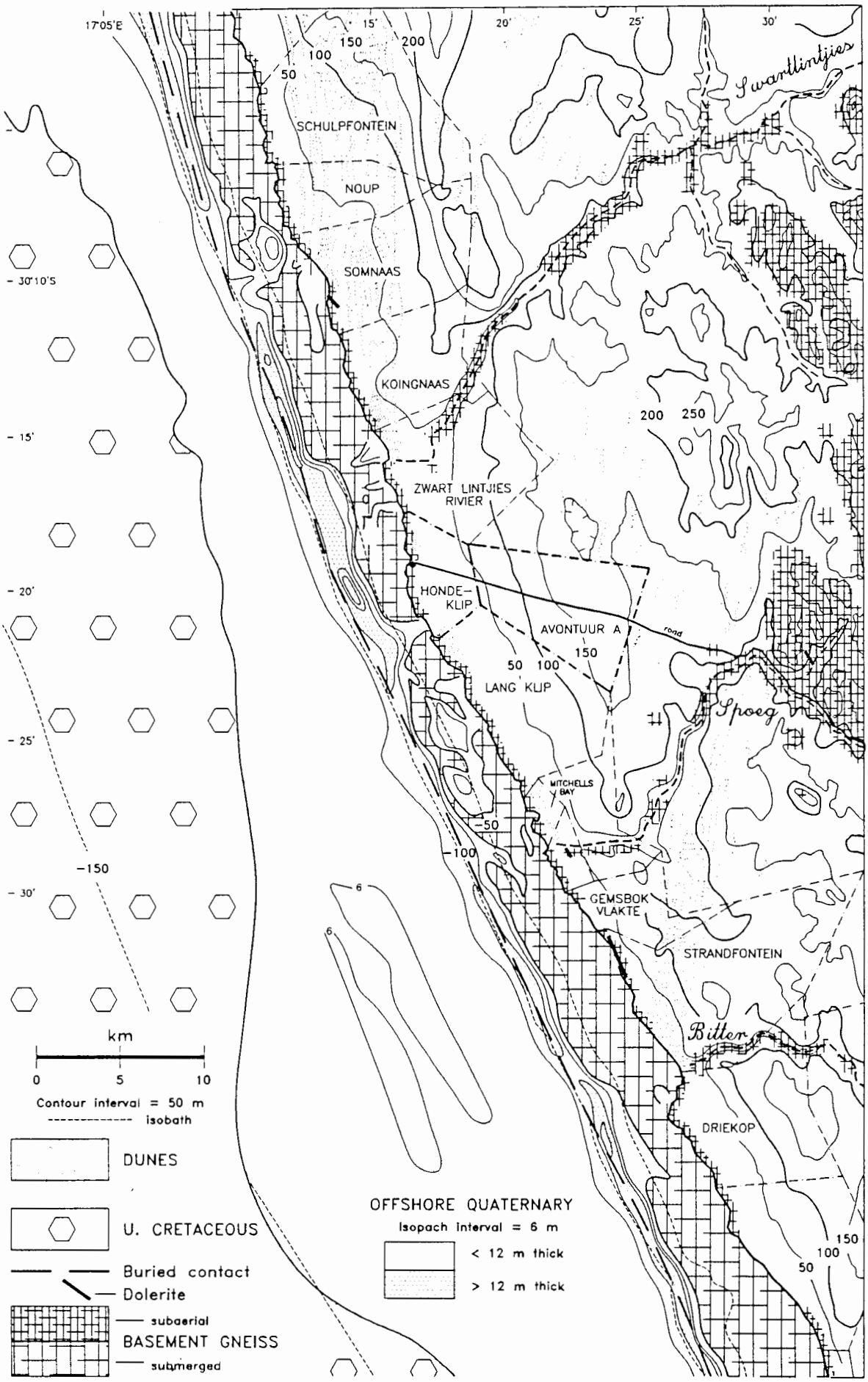

Figure 4.1 Local setting of the study area. Compiled from aerial photographs, O'Shea (1971) and Jack (1980).

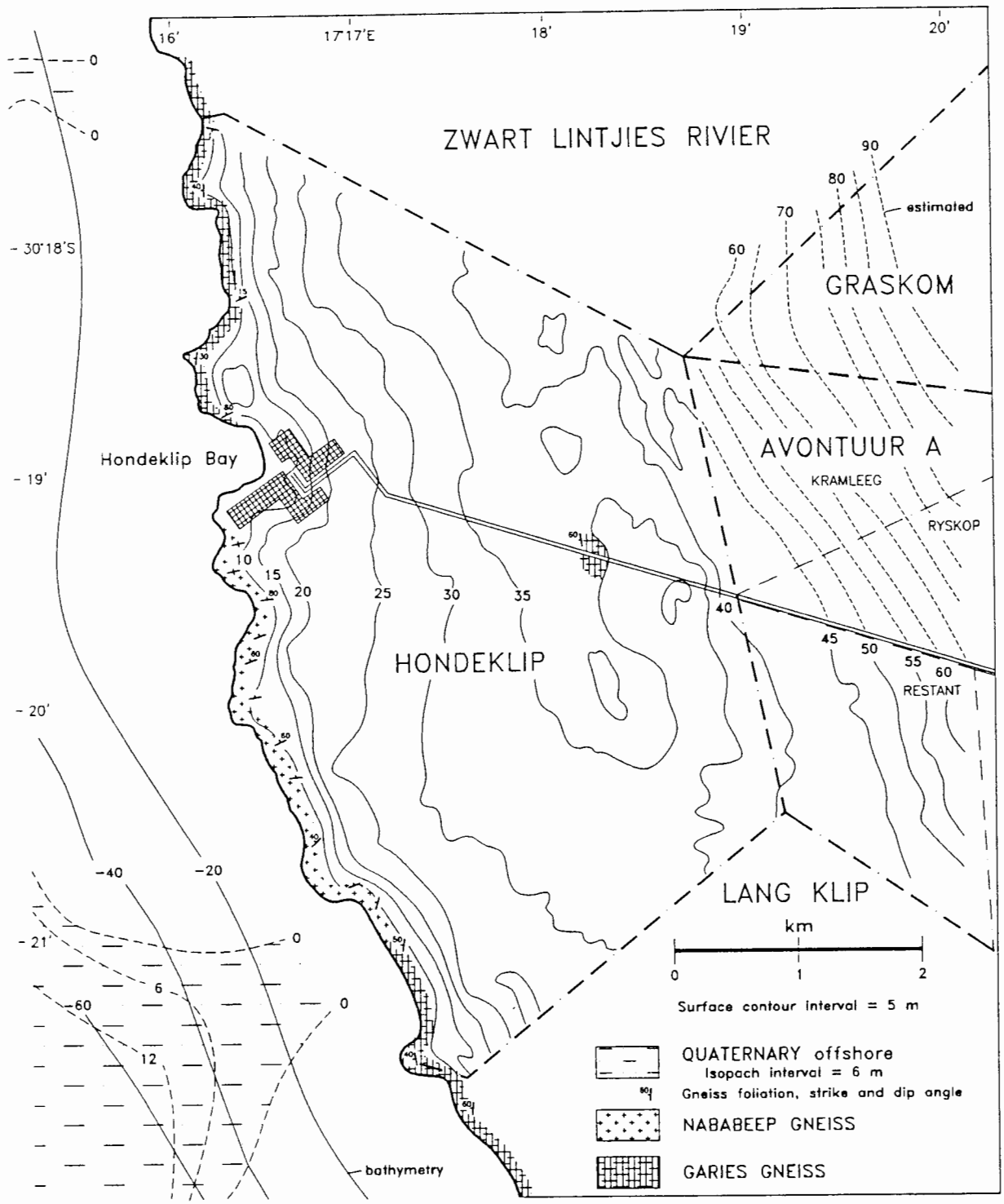

Figure 4.2 The study area. Surface topography and geology of the exposed gneissic bedrock, offshore bathymetry and offshore sediment thickness. Topography courtesy of the Trans Hex Group Ltd. Bedrock geology from Jack (1980). Offshore data from O'Shea (1971).

Within ~300 m inland from the shore, surface elevations increase rapidly to ~20 m asl. (Fig. 4.2) and the colour of the surface sands changes from pale grey to a pale orange-brown hue. Thereafter the surface rises more gently (~10 m per km) to about 45 m asl., where the gradient gently steepens up to the more complex topography above ~120 m asl. The coastal plain is overall broadly concave, with a narrow convexity along its seaward edge (Fig. 4.3). A low, undulating relief is superimposed on the overall profile.

The pale orange-brown, clean, loose, medium-grained sands mantle the coastal plain as an aeolian sandsheet. Destruction of stabilising xerophytic vegetation results in immediate remobilization and the formation of wind ripples. This loose surface sand is about a metre thick, but locally thickens into elongate lenses (up to 5 m thick) representing stabilised, degraded ancient dunes, which contribute to the low relief of the plain. An example, resolved in Fig. 4.2, occurs in the northeastern corner of the Hondeklip property where a linear NNW trend is seen. The loose sands rest on a hard, compact surface formed on similar, older sands in which has developed a pedogenic mud content.

More recent additions to the surficial sand sheet are betrayed by the presence of swaths of pale sand quite far inland. Their origin is clear from the examination of aerial photographs that show linear bands of contrasting vegetation patterns extending NNE from the coast or from the lower reaches of rivers. The youngest of these is further distinguished from the surrounding older sands by relatively well-preserved parabolic dune morphology and patches of active barchanoid dunes, particularly closer to the coast, where the plumes extend from the beaches immediately north of the presently ephemeral river mouths (Fig. 4.1).

The example north of the Swartlintjies River has been discussed in detail by Rogers (1977) and Tankard and Rogers (1978), who relate its origin to the changes of coastal configuration, rainfall and sediment supply during the late Pleistocene/Holocene (Flandrian) transgression. Sand delivered by increased winter run-off to the Last Glacial river mouth, at the -130 m isobath, was blown northwards onland from the adjacent beaches by summer southerly winds. Sand masses in the form of unvegetated barchanoid dunes advanced onto the coastal plain and, under the influence of the higher rainfall of the Last Glacial, trailed linear ridges stabilised by vegetation, leading to the parabolic form. Rainfall and sediment supply decreased during the deglacial with the poleward shift of the Westerlies, but erosion of the seaward end of the plume during the transgression became increasingly important in supplying sand to the plume and active masses of Holocene barchanoid dunes are now superimposed on the earlier parabolic dunes. A regional study of the grain-sizes, shapes and heavy mineral contents of the surface sands of the Namaqualand coastal plain (Harmse and Swanevelder, 1987) shows variations associated with river mouths that supports the importance of fluvial input to the littoral as an aeolian sediment source. The extent of older plumes is more readily distinguished by vegetation patterns seen on aerial photographs than by observation on the ground. Evidently, much of the surficial sand sheet has formed by the degradation and amalgamation of plumes throughout the Pleistocene.

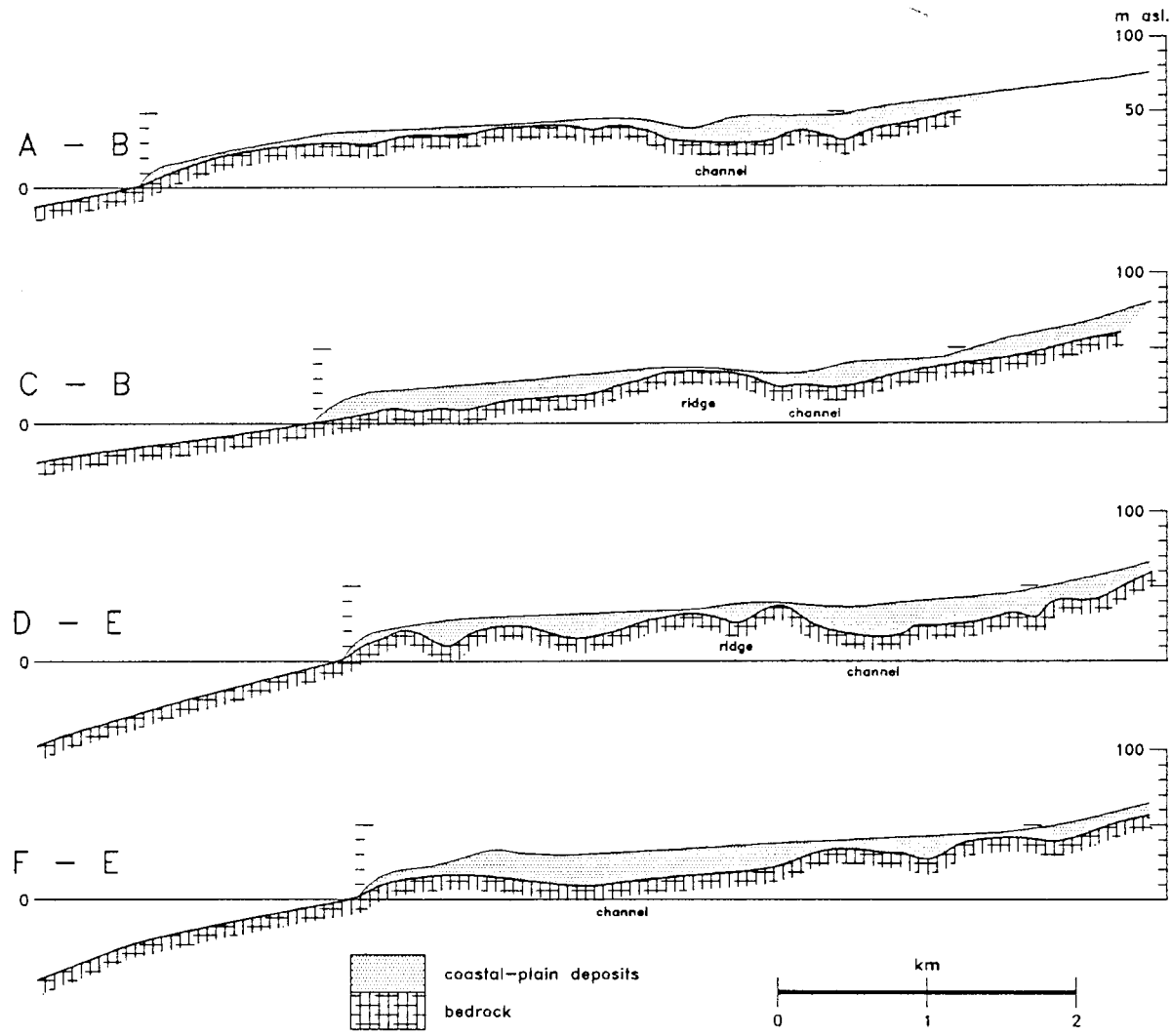

Figure 4.3 The study area. Cross-sections showing sediment thicknesses in relation to surface and bedrock topography. Locations of sections shown in Fig. 4.4.

4.2 BATHYMETRY AND OFFSHORE GEOLOGY

Information on the offshore bathymetry and geology is provided by O'Shea (1971). Below sea-level the gneissic basement descends steeply with a convex surface to -90 to -120 m (Figs. 4.1, 4.2, 4.3), where it is overlain by Upper Cretaceous bedrock (Dingle, 1973) and the offshore bedrock gradient becomes very gentle (Fig. 4.1). Generally, the bedrock inshore off Hondeklip Bay has thin, patchy sediment cover and cobble and boulder fields occur (prospecting observations). Seaward of the ~-60 m isobath, the bedrock is overlain by the late Quaternary sediment wedge, reflected in the decreased bathymetric gradient and the sediment isopachs (Fig. 4.1). The latter indicate a general thickness of ~15 m of late Quaternary sediment, but the thickness exceeds ~24 m in a patch west of Hondeklip (Fig. 4.1). The presence of a palaeochannel extending towards the southwestern corner of Hondeklip is indicated by the shoreward excursion of isopachs (Figs. 4.1 and 4.2). Palaeochannels also occur off the Spoeg River, Swartlintjies River and Somnaas, whilst more basin-like features are present off Lang Klip and Somnaas (Fig. 4.1).

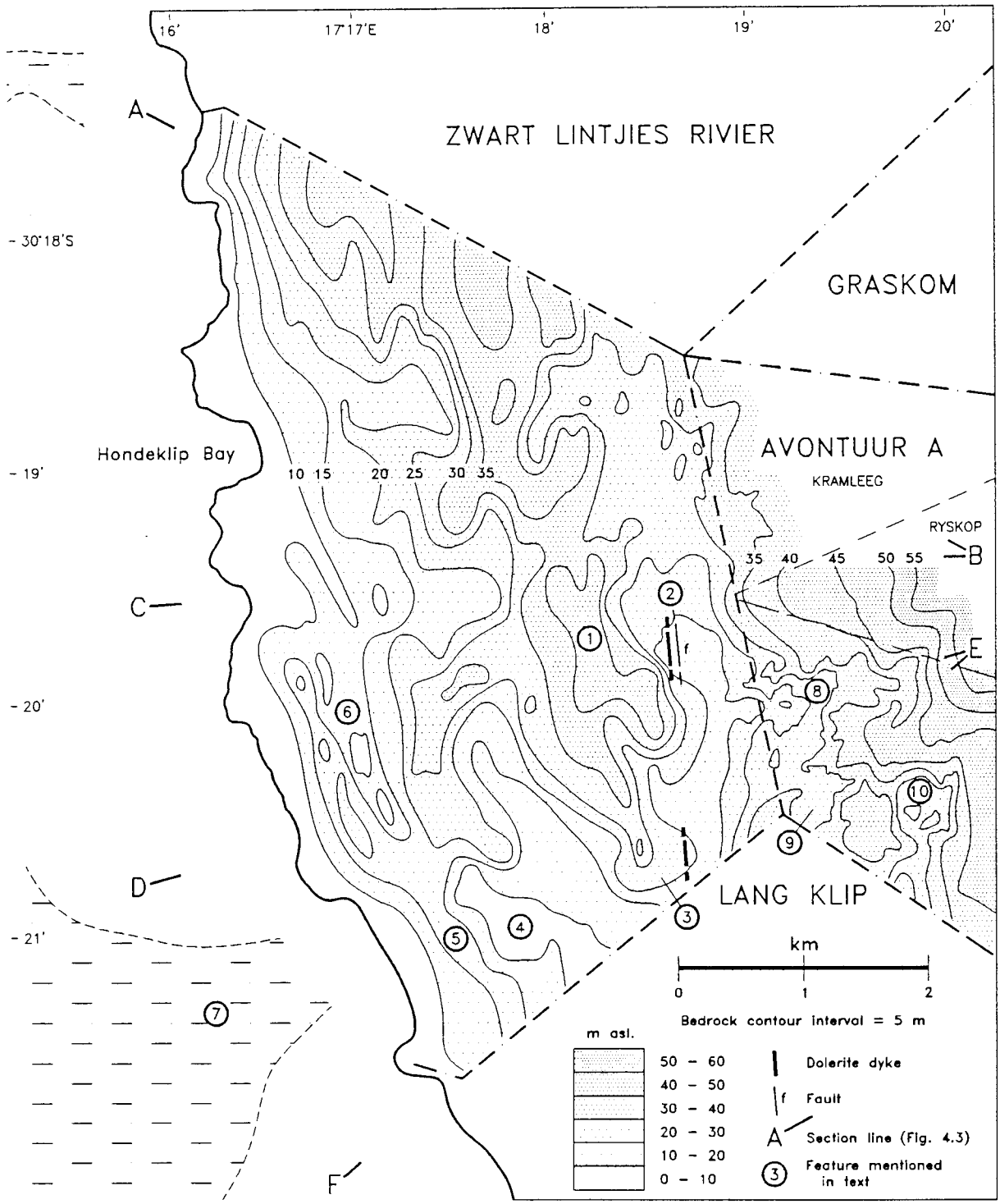

Figure 4.4 The study area. Topography of the buried gneissic bedrock. Encircled numbers refer to features mentioned in the text. Bedrock topography courtesy of the Trans Hex Group Ltd. Offshore data from O'Shea (1971).

4.3 THE BURIED BEDROCK

BEDROCK TOPOGRAPHY

The topography of the buried gneiss bedrock (Fig. 4.4) was established during the process of prospecting by the mining concern. The striking characteristic of the topography is its significant relief (up to 15 m) and complexity, as opposed to the development of classic marine terraces separated by steeper gradients, rising step-like from the coast (cf. Kleinzee, Alexander Bay). Although a regular succession of wave-cut platforms is absent, the drill line and hole spacing is such that narrow platforms and low cliffs "notching" the general topography would not be easily resolved. This comment applies to bedrock topographic mapping on diamond prospects in general, when the borehole spacing exceeds ~25 m. Accumulations of unweathered boulders or single very large boulders overlying the bedrock will also obscure its topography as derived by drilling. The contours around the basinal areas on Avontuur-A are more convoluted than elsewhere on the map. This reflects greater resolution due to closer-spaced drilling in that area. It is expected that similar complexity would be revealed by finer sampling grids in other areas.

In the following description, numbers mentioned in brackets in the text refer to features thus marked in Figure 4.4.

Hondeklip

The main feature is a NNW/SSE-striking, coast-parallel ridge (1) running the length of Hondeklip and extending from relatively high bedrock in the north to low bedrock in the south. The ridge flanks are embayed and the channel-like feature on its eastern side (2) connects with the low bedrock elevations in the south (3) where the ridge terminates. An elongate basin below 10 m asl. (4) is in the southwestern portion of Hondeklip and extends onto Lang Klip. It is flanked in the west by a minor ridge (5). The northward continuation of that ridge next to the coast flanks a minor bedrock channel (6), which trends towards Hondeklip Bay village. Notably, the palaeochannel offshore (7), inferred from the sediment isopachs (Figs. 4.1 and 4.2), is evidently the submarine extension of the onshore channel. However, bedrock of relatively low elevation obviously extends onto the adjoining property Lang Klip, but published data are not available to reveal its extent and morphology. It is therefore not clear whether the channel on Hondeklip (2) is the main channel, which then turns west on Lang Klip around the "nose" of the ridge (3) to join with the offshore channel (7), or whether it is a tributary of a another channel on Lang Klip. The low ridge (6) appears to separate the onshore and offshore channels, but drilling coverage in the area of (6) is widely spaced and may have missed local bedrock lows. The embayment opposite the offshore channel (7) has a sandy beach, indicative of low bedrock and consistent with the onshore trend of the channel crossing the coastline.

Avontuur-A

The 30-40 m asl. bedrock contours on the eastern side of the channel (2) run approximately parallel to the coast on the northwestern part of Avontuur-A (portion Kramleeg), but farther south (portion

Restant) the contours swing eastwards and outline a basinal area of low bedrock-gradient (8). A second, smaller basin (9) occurs right in the southwestern corner of Avontuur-A, partially enclosed by a hook-like promontory defined by the 30 m asl. contour under the Hondeklip/Avontuur-A/Lang Klip boundaries intersection. East of this little basin, a third basin is present (10), separated from the former by bedrock above 35 m asl., outlined by the 30 m asl. contour and opening and descending southwards beneath the Lang Klip boundary.

GROUNDWATER

Saline groundwater is encountered in and over the local bedrock lows in the study area. The thickness of waterlogged sediment is not solely determined by topography as it domes over the low areas. There is no obvious lithological control, such as less permeable strata, to account for doming by the "perched" water-table phenomenon. Presumably the doming of water tables is controlled by pore-pressure/hydraulic gradients over the catchment areas. Delivery of groundwater continues to the accumulation zones during dewatering.

DOLERITE DYKE AND FAULTING

A dolerite dyke was exposed in excavations along the main channel on Hondeklip (Fig. 4.4, (2)). It has positive relief and although weathered, is not deeply decomposed. Clasts eroded from it, showing typical concentric "onion" weathering, are common in the gravels in its vicinity. Its weathering has contributed Fe-oxides to nearby sediments, as is evident in local iron-staining and iron-cementation.

A shallow excavation into the decomposed bedrock near the northern exposure of the dyke (Fig. 4.4) revealed a fault breccia, ~6 m wide, indicating the presence of a substantial fault line. A trend could not be ascertained from the single exposure on the muddied footwall, but it is not improbable that the bedrock foliation influenced the fault orientation. Curious pebbles of laminated, grey, quartz druse with angular cavities, formed by the dissolution of calcite crystals, are found in the overlying marine gravels and are derived from the hydrothermal precipitates interstitial to the brecciated country rock.

WEATHERING OF THE BEDROCK

The state of weathering of the bedrock varies dramatically in the area, from fresh on the bedrock highs (e.g. the main ridge) to deeply weathered in the lows (e.g. the main channel), where advanced kaolinization is encountered. Intermediate weathering states tend to be encountered on the intervening slopes. The mining excavations are situated over the topographic lows and thus clayey, deeply weathered to kaolinized bedrock underlies most of the sections to be described. On the Avontuur-A gradient, small-scale, reef-like islands of relatively unweathered bedrock locally jut above the surrounding decomposed bedrock. Their variable, foliated character suggests that they are composed of Garies Gneiss.

4.4 DISCUSSION

Bedrock Topographic Influences

The influence of the bedrock topography on the coastal-plain sedimentary record is evident in the surface topography. The 35 m asl. surface contour (Fig. 4.2) outlines the underlying ridge and adjacent channel. The ridge and the relatively high bedrock the north has thin sediment cover and in places the gneiss crops out (Figs. 4.2, 4.3). The cross-sections (Fig. 4.3), show that the variation in thickness of the coastal-plain sediments in this area has been determined primarily by the bedrock topography. Local aeolian accumulation has had much less influence. It will be shown that the bedrock topography profoundly influenced marine deposition in the area.

Context of Coastal Dolerites and Faults

Dolerite dykes of similar strike to the one at Hondeklip occur both north and south of the area (Somnaas and Spoeg River mouth, Fig. 4.1). Petrographically they are normal dolerites (Jack, 1980). It is not known to the writer whether the Namaqualand coastal dolerites have been dated. No dates were available to Jack (1980) and he speculated that they were of Karoo age. De Villiers and Sõhnge (1959) reported that the youngest intrusions in the Richtersveld (northernmost western Namaqualand) are dolerite dykes that occur at the coast. These are generally coast-parallel, relatively thin (~1-2 m) and only a few kilometres in length (1-3 km). Notably, they are fine-grained, verging on lava (De Villiers and Sõhnge, 1959) and, although admitting that with the evidence available the dykes could be of Karoo age, De Villiers and Sõhnge (1959) preferred to assume a post-Karoo age for these intrusions.

The majority of faults, exposed landward of the sand-covered coastal lowland to the Escarpment, trend approximately coast-parallel and are downthrown to the west (Jack, 1980). For example, small outliers of Nama Group rocks occur in the foothills of the Escarpment. The faults are marked by breccias and quartz veins, the latter sometimes being crushed and suggesting reactivation (Jack, 1980). Rare east-west faults cutting the previous set also occur.

The main coast-parallel faults and coastal dolerites are considered by the writer to date from the phase of taphrogenesis associated with continental breakup and margin development in the Jurassic and Lower Cretaceous. Pre-existing basement structure influenced the taphrogenic basin development associated with continental breakup (Dingle *et al.*, 1983). Subsequently, Cretaceous sediment loading and subsidence offshore was accompanied by upwarping of the margin periphery in response, with scarp retreat giving rise to the Escarpment (Scrutton and Dingle, 1974). This differential vertical movement was probably partially accommodated by the north-south faults of the coastal zone. The lack of subsided basins extending onshore is at least partly due to this well-developed fault system coincident with the pre-existing grain of the basement (Scrutton and Dingle, 1974). The rare, cross-cutting east/west faults are consistent with the probability that some flexuring perpendicular to the coast or differential uplift has occurred. Continuing neotectonic adjustment

through the Cenozoic has probably occurred by reactivation of the faults. Historical records of seismicity in Namibia are concentrated in the Escarpment and suggest continued, slow upwarping (Korn and Martin, 1951) and this activity may be implicated in the generation of offshore slumps on the continental slope off Namaqualand (Dingle, 1980b).

Although the Namaqualand coastal dolerite dykes may be of Jurassic age, coeval with the Karoo dolerites and the rifting phase of Atlantic development, Day (1987) has argued that the dyke swarms in the southwestern Cape, south of the study area, are associated with the early to middle Cretaceous onset of sea-floor spreading in the South Atlantic. This has been confirmed by four K-Ar dates with a mean age of 132 ±6 Ma (Reid *et al.*, 1991), indicating that the dykes are coeval with the Early Cretaceous Etendeka lavas of northern Namibia. The Namaqualand coastal dolerite dykes may be of similar age, or possibly coeval with the lavas interbedded with Barremian-Aptian continental red beds and sands offshore in the Orange Basin (Dingle *et al.* (1983). Day (1987) suggests that emplacement of the early Cretaceous dykes is related to the crustal flexure accompanying rapid subsidence of the margin.

Origin of the Bedrock Topography

The main topographic features of Hondeklip, namely the ridge and channel (Fig. 4.4, (1) and (2)), are generally parallel to the gneissic foliation, to the dolerite dyke and, very probably, to a substantial fault. The regional trend of the gneissic foliation evidently influenced both faulting and dolerite intrusion. A dolerite dyke occurring together with a fault could constitute a significant control on the locus of erosion, unless overpowered by significantly lowered base-level. Notably, the north-south faulting in the region has resulted in many valleys of westward-flowing rivers having zigzag deviations in their courses (e.g. the Spoeg River) (Jack, 1980).

The topography also corresponds with the state of weathering of the bedrock, the most advanced decomposition (kaolinization) being encountered in the main channel. In contrast, the denudation of an "idealised" old, mature, land surface, subjected to prolonged weathering, should result in topographically high areas of weathered bedrock preserved on local watersheds, separated by fresher, more recently exposed bedrock in the valleys. This situation is observed along the Garies-Hondeklip road, where fresh bedrock outcrops in the bed of the Spoeg River, whilst borrow pits in the surrounding slopes reveal weathered profiles. The situation at Hondeklip, with the most advanced weathering in the channel, is quite the contrary. This would support an argument that marked differential weathering of the bedrock has occurred.

Differential weathering depth, controlled by jointing, is a feature of saprolitic terrains and is well illustrated by the weathering of the Cape Granite exposed in cuttings in the southwestern Cape (Hartnady and Rogers, 1990). Denudation has exposed islands of unweathered rock (tors or corestones) surrounded by weathered material. Similarly, hyperbolic reflectors on seismic profiles offshore in False Bay and Saldanha Bay betray the marked subsurface relief of unweathered granite within the saprolite (Glass, 1977; Du Plessis and Glass, 1991). A faulted, brecciated zone, as is

probably present along the weathered channel on Hondeklip, could have been the locus of more intense weathering. A dolerite dyke may function as a subterranean "dam" or conduit to groundwater passage and subjacent rocks could also be preferentially weathered. Subsequent fluvial denudation of the differentially weathered land surface is likely to excavate the deeper portions of the weathered profile. Similarly, marine erosion during a transgression, lapping around unweathered portions, could produce bays, headlands and reefs, as opposed to planation terraces.

At present, the accumulation and passage of groundwater in the study area is mainly controlled by topography and thus the existing bedrock lows should be preferentially weathered. This process would have commenced from the inception of the topography and continued to the present. It is therefore also feasible that pre-existing, fluvially eroded topography could have contributed to preferential weathering.

The above considerations generate a variety of permutations for the development of the bedrock topography. All commence with the bedrock structure and end with the marine erosional episode immediately preceding the marine deposition in the area, with the possibility of continued, subsurface weathering. The overlying sedimentary record provides some constraints for these considerations.

CHAPTER 5

THE BASAL KAOLINITIC DEPOSITS

5.1 INTRODUCTION

Over practically the entire study area, the marine sediments rest directly on gneissic bedrock. Where the gneiss has been decomposed and kaolinized, its original gneissic nature can be discerned by the presence of relict gneissic banding or foliation. This is defined by lineated "flecks" of yellow staining considered to be the "ghosts" of weathered biotite mica, or by thin, fractured, quartz-rich zones or larger veins. However, in a limited area around the "nose" of the bedrock ridge (Fig. 5.1), an extremely cryptic sedimentary deposit occurs beneath the marine basal gravel. Its cryptic nature is due to its thinness and the fact that it also consists, like the underlying and surrounding decomposed bedrock, mainly of kaolin and quartz. Its sedimentary origin is revealed, on closer inspection, by the presence of rounded clasts and sedimentary structures such as cross-bedding. As a result of the thinness and poor exposure of this deposit in the study area, observations on the nature of its sedimentary structures are limited. Due to its composition and position at the base of the stratigraphy, it is called the basal kaolinitic deposit.

Previous Observations on Basal Kaolinitic Deposits

Rogers (1911) noted the occurrence of kaolinitic, sandy and gravelly, quartz pebble deposits in a tributary of the Groen River (Fig. 3.1). Associated with the deposit was a capping "surface quartzite" and a ferricrete was locally developed. A quartz pebble deposit with an associated "surface quartzite" was also noted in the Sout River drainage.

In the most well-known, published article of relevance to the study area, the summary stratigraphy of Carrington and Kensley (1969) (Table 3.1), it is reported that the oldest sediments present are fluviatile clays, silts and sands, up to 20 m thick, occupying a system of partly confluent channels deeply incised in the gneissic bedrock. These fluviatile beds were recorded as unfossiliferous, possibly of Mio-Pliocene age and separated by unconformities from the underlying basement gneiss and the overlying fossiliferous, phosphatic siltstones.

In unpublished reports, Tankard (1966, 1975a) provided considerably more information which will be quoted at length here because these are the most detailed, public-domain descriptions available. Tankard (1966, p. 20) described "channel sediments" from the Hondeklip area that he regarded as fluvial deposits laid down in an old channel of the Swartlintjies River. In Figure 5.2a (modified from Tankard, 1966, 1975a) the positions of bedrock channels infilled with basal deposit on properties north of Hondeklip are shown. A section from Zwart Lintjies Rivier (SL3, section 252) (Fig. 5.2b) (Tankard, 1966) comprised a basal deposit (Sub-zone A) of massive, white to grey, very fine sandy clay with

organic-stained (presumably carbonaceous staining) angular gravel directly overlying bedrock (kaolinized gneiss).

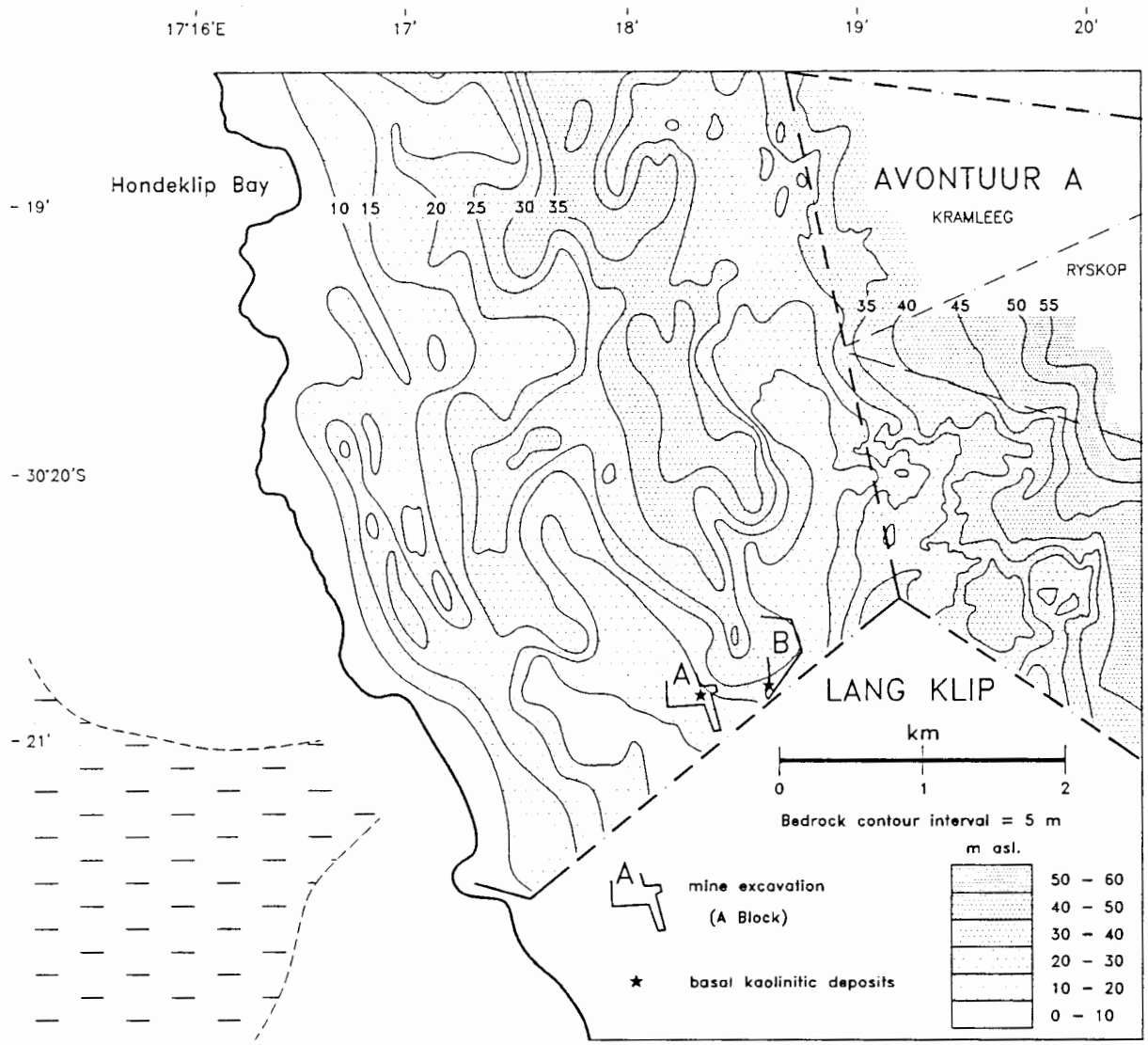

Figure 5.1 Location of the basal kaolinitic deposits exposed in A and B blocks and intersected between by drilling.

The overlying material (Sub-zone B) was described as fine to medium, occasionally coarse, sandy bedded clay. Interestingly, Tankard (1966, p. 22) mentioned that Sub-zone B is absent in some localities due to marine erosion and that "in its place a swamp or lagoon is formed which would produce the organic acids necessary to decompose the felspars (*sic*) of the lower horizon. Decomposition has taken place from the top downwards. Zero decomposition actually occurs below bedrock level, i.e. some of the gneiss has been decomposed to kaolin." Tankard (1966, p. 22) clearly suggested that "the deposits were decomposed *in situ*."

Figure 5.2 Bedrock palaeochannels and associated basal kaolinitic deposits north of Hondeklip Bay. **a**, positions of palaeochannels (from Tankard, 1966), including the palaeochannel on Hondeklip and showing basins and palaeochannels on the inner shelf cf. Fig. 5.1 (from O'Shea, 1971). **b**, log of large-diameter borehole just south of the Swartlintjies River (Line SL3, Section 252) (datum not supplied) (from Tankard, 1966). **c**, log of large-diameter borehole just north of the Swartlintjies River (Line KN1A, Section 158/9) (from Tankard, 1975a).

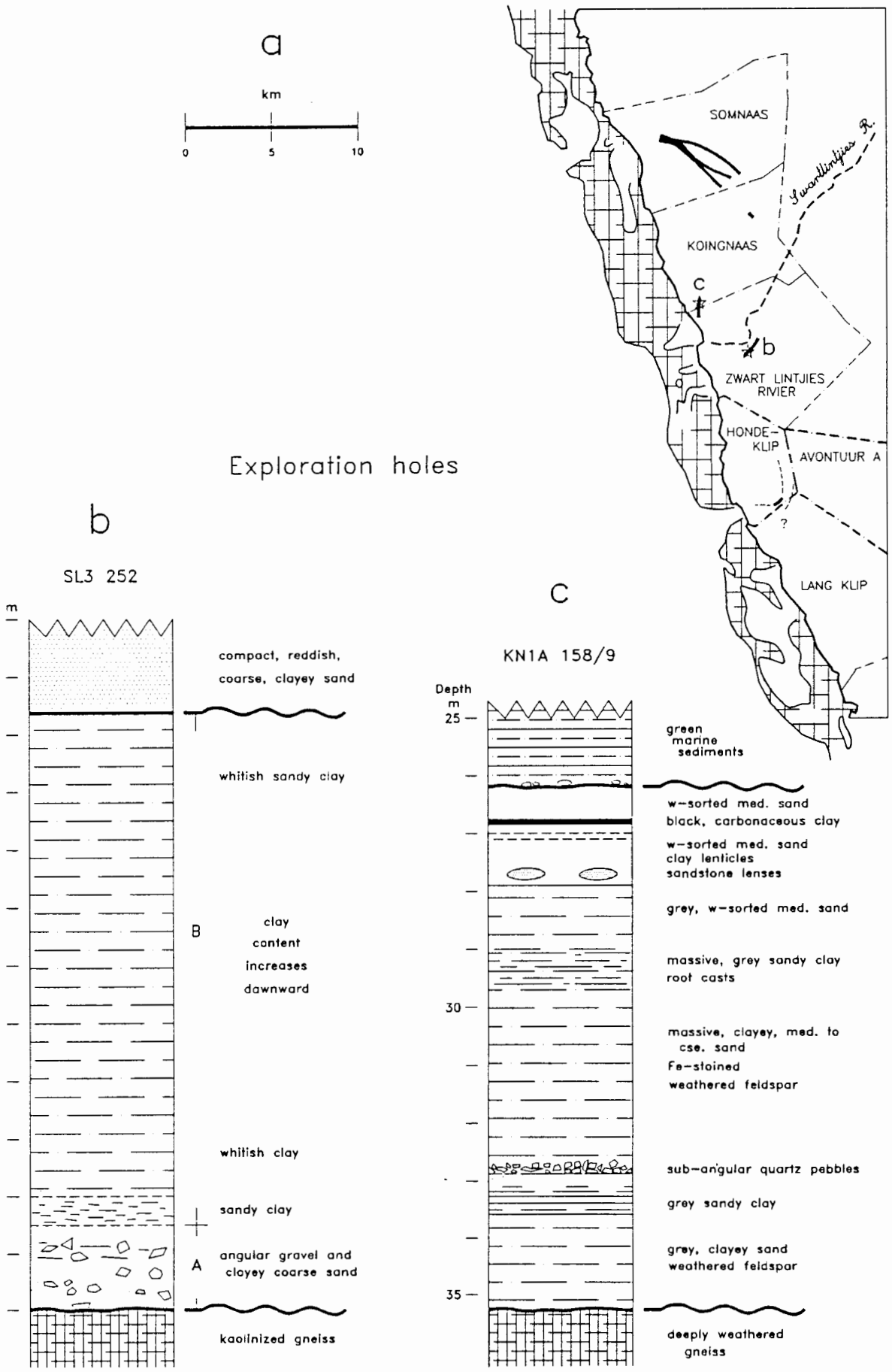

Figure 5.2 Bedrock palaeochannels and basal kaolinitic deposits north of Hondeklip.
(explanatory notes on facing page)

In Tankard (1975a, p. 278), a downcore section is described from a large-diameter borehole in a channel near the coast on Koingnaas (KN1A/hole 158/9) (Fig. 5.2c). "The fluvial bed on Koingnaas is characterized by medium to fine quartzose sands with appreciable clay, broken by horizons which have a more clayey nature. At a depth of 28 m an horizon of blocks of brown, medium sandstone was encountered. The blocks gave the impression of a once continuous sandstone bed. From about 30 m massive, grey "channel clays" were encountered. Towards the base of this test hole proximity to the bedrock was first shown by very weathered felspar (*sic*). At this point heavy minerals were not encountered. With increasing depth weathered biotite and finally fresh biotite were found."

Similar sediments were also recorded from Driekop, ~35 km south of Hondeklip (Fig. 4.1), by Tankard (1975a, p. 279). "The basal unit is a carbonaceous sand composed of black and brown fine to coarse sandy clay. It contains pebble- and cobble-size quartz. The colouration is due to the high carbon content. Well-preserved wood and leaf impressions have been found in this horizon. When freshly excavated it has the smell of marsh sediments. Overlying the carbonaceous sands is a complex horizon of interbedded clay, sandy clay and sand. The clay beds overlie the carbonaceous sand and are light grey to purple in colour. The topmost unit is a coarse, angular clayey quartz sand. It is generally a grey colour, but in places is red and contains ferruginous concretions."

Tankard (1966, 1975a) had no evidence on the age of the "channel sediments," but tentatively suggested a Pliocene or younger age (1975a). This was due to his incorrect impression (Tankard, 1974a, 1975b) that Miocene phosphatic marine deposits, equivalent to his "Saldanha Formation," were basal to the Namaqualand coastal-plain succession. Observations on the "channel sediments" at the Hondeklip mine firmly establish that they are the oldest deposits encountered in the study area and provide additional detail on their nature and origin.

5.2 THE BASAL DEPOSITS AT THE HONDEKLIP MINE

Field Observations

Localities

The basal deposits were partially exposed at the seaward edge of the tip of the bedrock ridge in the excavation called A Block at ~15 m asl. (Fig. 5.1). They have since been removed. The deposits were also found in B Block at the southern tip of the ridge at ~17 m asl. and were intersected during drilling in the intervening area between A and B blocks. They may also be locally present in other patches northwards along the bedrock channel, but these indications from prospecting have not been confirmed. The description below is from the exposure of the basal deposits in A Block where the bed is Unit 1 of Section 11.

Description

Poorly-bedded, poorly-sorted, angular and sub-angular, oligomictic, grey quartz paraconglomerate in a white, poorly-sorted, sandy, kaolinitic matrix, interbedded with poorly to moderately-sorted, kaolinitic, quartz sands.

The basal deposits in A Block are up to a metre thick, but pinch out laterally over ~30 m. The deposit is mainly conglomeratic, with interbedded sandy beds and lenses. Bedding in the unit is poorly defined and the structure is indicated by the density of gravel clast distribution. The clasts are exclusively grey quartz. The largest quartz clasts (cobbles and small boulders) are concentrated at the base of the unit (Plate 5.1), but the majority of the clasts are pebble-size. The angularity of the quartz clasts is immediately noticeable, but close inspection reveals that many clasts (~50%) are sub-angular, with their edges narrowly rounded off. Sub-rounded clasts can be found without difficulty and a minority of clasts (~1-2%) are well-rounded. The quartz clasts verge on being supported in the matrix, with local areas, several cm across, that are mainly supported in the matrix and local areas that are clast-supported.

The matrix is sandy, white to very pale grey in hue and kaolinitic, with flecks and mottles of yellow staining (~5Y 7/8). In the conglomeratic parts of the deposit, the sand portion of the matrix is poorly-sorted with readily visible, coarse and very coarse, angular and sub-angular, quartz grains. The matrix is also inhomogeneous, with "clots" of kaolin clay, that lack included coarse sand grains, occurring between pebbles and within the coarse-sandy matrix. Sandy, kaolinitic parts of the deposit include poorly sorted, coarse-sandy portions, as well as moderately-sorted, fine-sandy portions. Coarse-sandy beds also contain "clots" of clay. These are not readily seen in fine-sandy clay.

The vestigial bedding present in the conglomerate is illustrated in Plate 5.1. A layer of cobbles and pebbles overlying the kaolinized bedrock is overlain by a sandy zone with few pebbles. A pale zone, in which pebbles are more concentrated, occurs in the middle of the unit and is overlain by coarse-sandy material in which inclined, thin bedding or lamination is present. Manual excavation into the unit revealed further information on its bedding. Steep cross-bedding in trough-based sets is defined by layers richer in quartz clasts, which are separated by sandy cross-beds with streaks of coarse grains (Plate 5.2). These lensoid beds are up to 0.5 m thick and are estimated to be 3-4m in lateral extent. A large lens of compact, homogeneous kaolin clay was noticed in the exposure (Plate 5.3). It is slightly sandy, has well-defined, steep edges and a crudely conchoidal fracture pattern. It is rather atypical of the bulk of the material in the exposure.

A feature noticed when digging into the conglomeratic beds is that the clay "clots" sometimes break along distinct planes, suggestive of a cleavage. Another feature observed in the field are shiny, clear "films," sub-millimetre in thickness, in places within lumps of the deposit. These fragile films shatter when probed with a dissecting needle and appear to be quartz, locally precipitated in narrow fissures. These features were confirmed during preparation of samples of the deposit for analysis (e.g. Plate 5.4).

Plate 5.1 Basal kaolinitic deposits in A Block, showing conglomeratic nature. Contact with kaolinized gneiss at base of tool handle. Tool is 42 cm long.

Plate 5.2 Basal kaolinitic deposits in A Block, showing trough cross-bedding.

Plate 5.3 Basal kaolintic deposits in A Block, showing atypical, steep-sided lens of slightly sandy, compact kaolin clay resting on kaolinized bedrock.

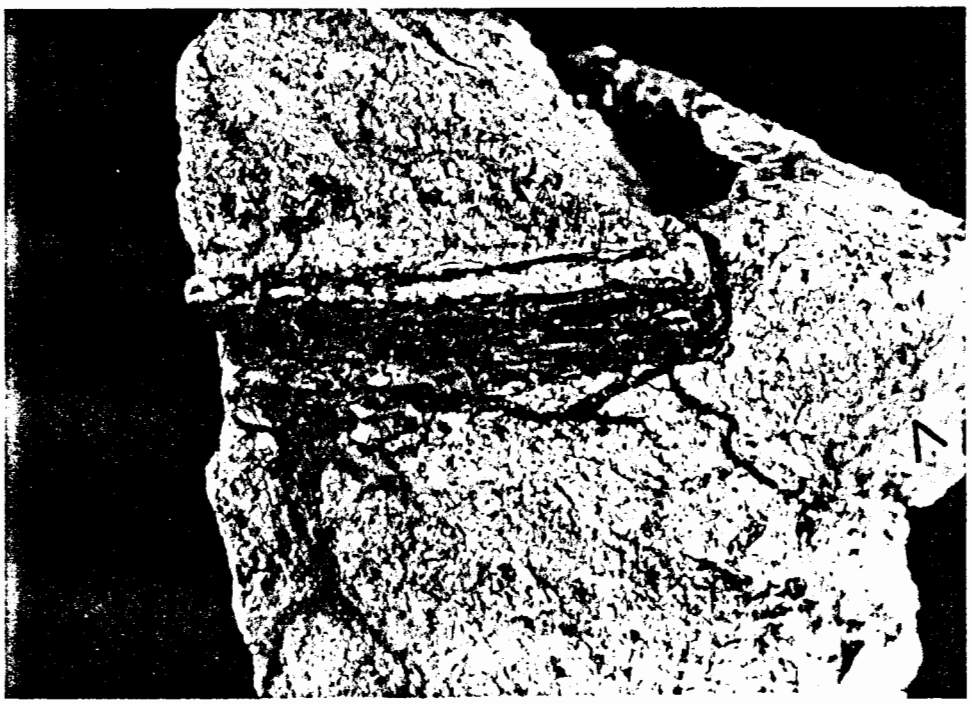

Plate 5.4 Basal kaolinitic deposits in A Block. Vestigial plant fossil from cross-bedded, clayey coarse sand. Stem is ~1 cm long. Note shiny film of quartz on fracture surface (arrowed, right).

Notably, the disaggregation, using a small chisel, of boulder-size samples of thoroughly dry conglomerate, produced some clay "clots" with rounded pebble morphologies. Similarly, rounded kaolinitic grains were found under the binocular microscope whilst examining coarse-sandy material. The investigations in the laboratory provide more information on these aspects.

Palaeontology

A small-boulder-size sample, collected from the cross-bedded facies of the deposit, fortuitously broke to reveal branching, plant-like structures defined by yellow, Fe-oxide-stained clay with surrounding, parallel, black lines (Plate 5.4). The feature is ~1.0 cm in length and ~3 mm wide and has a side-branch ~0.5 mm in diameter which, in turn branches dichotomously and decreases in diameter. The feature itself originates from a larger ill-defined, concave groove in the fractured surface, ~1 cm in diameter, that appears to be the vestige of a larger stem.

The yellow clay of the feature has a fibrous texture orientated longitudinally and the surrounding black lines are made up of small spheres, ≤50 μm in diameter, of carbon. Although cellular structure is absent, the resemblance to plant material is striking. The clay evidently infiltrated the cavities produced on decay of the plant material, preserving some of its texture. The carbon spheres are presumably the vestiges of the plant carbon.

LABORATORY OBSERVATIONS

Grain size analysis

Grain size analysis (Fig. 5.3) was performed on four samples: (a) pebbly cross-bed, (b) coarse sandy bed, (c) fine-sandy cross-bed, (d) the atypical lens of fine-sandy kaolin (Plate 5.3). The sieves were cleaned and stained prior to sieving, to mark contaminant grains. The compact material was disaggregated using ~15% H_2O_2 and gentle heating. Notably, on addition of the peroxide, the sample lumps rapidly collapsed and small islands (1-2 cm diameter) of fizzing (oxidising) grey material appeared at the centre of the liquid surface of samples a, b and c. This reaction was most noticeable for sample c, a sediment that is pale grey in hue. The reaction indicates a very minor carbon content, reflected in the pale grey hue of the kaolinitic sediment.

The sampled pebbly cross-bed consists of ~57% gravel, ~23% sand and ~20% kaolinitic matrix (Fig. 5.3a). It is a paraconglomerate (>15% matrix), with a muddy sand matrix. The grain size distribution is very poorly sorted, very positively skewed (fine skewed) and is truncated at the coarse end, suggesting that the sample size is too small for capture of the complete gravel size range. The modal size class is medium pebbles. The secondary peak in the coarse sand class indicates a bimodal sediment. The muddy, coarse-sandy bed (~71% sand) (Fig. 5.3b) contains some minor gravel (~7%) and ~22% kaolinitic matrix. The sand fraction is a poorly-sorted, medium to coarse sand. The fine-sandy cross-bed (Fig. 5.3c) consists of ~45% sand and ~55% kaolinitic matrix (a sandy mud). The sand fraction is moderately sorted and negatively skewed (coarse skewed), with the modal size class being fine sand (fU). The grain size distribution appears to be truncated at the fine end. The atypical,

fine-grained lens consists of ~88% kaolinitic mud and ~12% sand (a slightly sandy mud) and the grain size distribution is clearly truncated at the fine end.

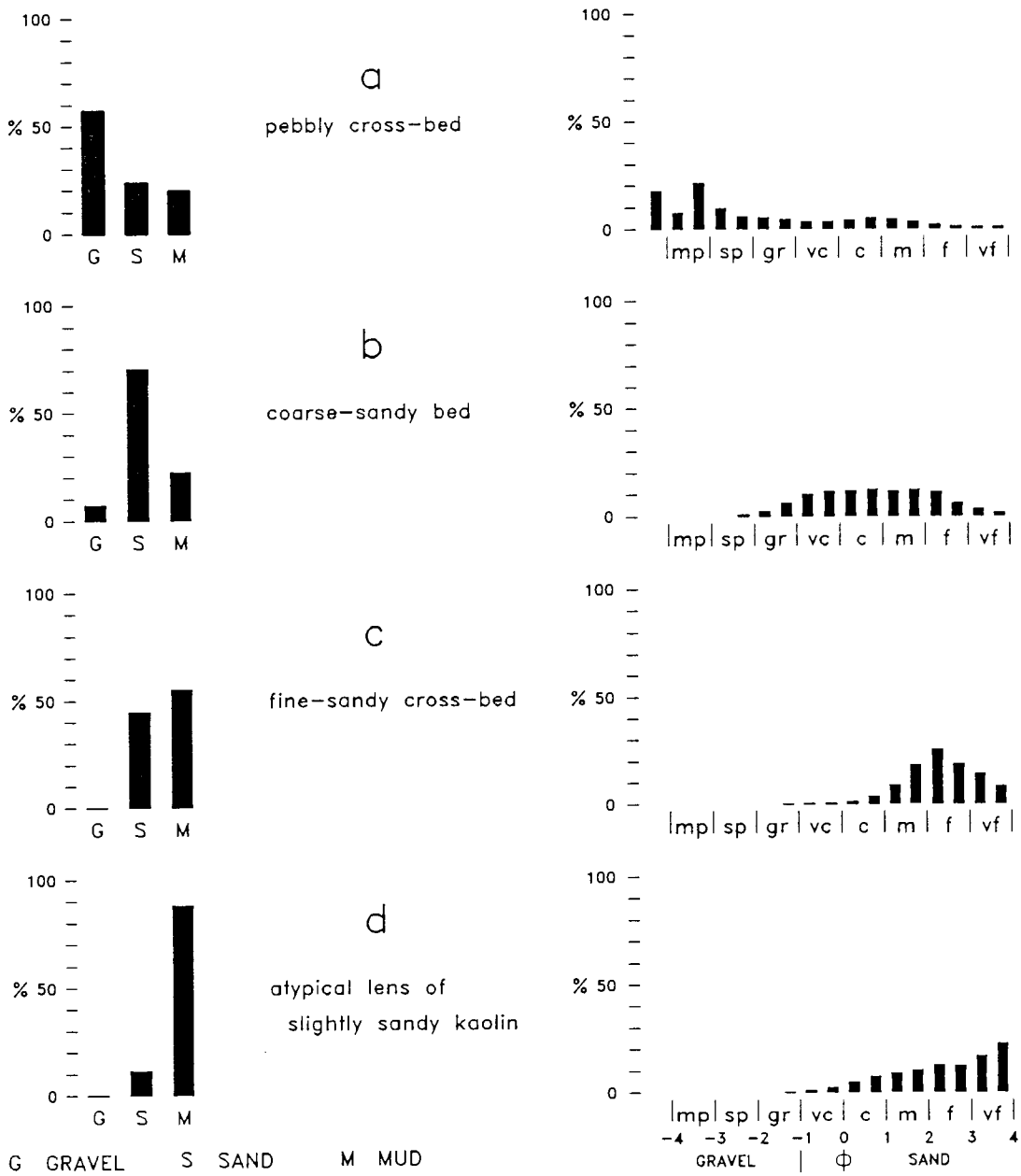

Figure 5.3 Basal kaolinitic deposits. Grain size analyses.

Composition

The washed gravel (sample a) confirms field observations that many angular quartz clasts have narrowly rounded edges, that sub-angular clasts are common and that sub-rounded clasts are present. Opaque, white or Fe-oxide-stained, weathered feldspar is present in all gravel size classes and becomes increasingly common with decreasing clast size, comprising up to 5-10% of granules. Some of the weathered feldspar forms parts of composite clasts with quartz. Similarly, quartz clasts with complex shapes, particularly blocky pits, were also part of quartzo-feldspathic clasts. Cleavage

faces are present in some examples of weathered feldspar and rare feldspar fragments from disintegrated rounded clasts also occur. Aggregates of coarse sand, cemented by Fe-oxide derived from weathered ore minerals, are a minor component of the gravel fraction.

The poorly-sorted sand fraction from the pebbly cross-bed (a) is angular quartz in which the coarser grains are mainly polycrystalline. The majority of the quartz grains are clear, but a proportion (~10%) is milky and slightly opalescent in appearance, indicative of a probable vein-quartz origin. Sub-rounded to well-rounded quartz grains, although minor, can easily be found in the medium and fine sand fractions. Sparse, white, opaque grains, usually rounded (artificially, during disaggregation?), but sometimes blocky, are a very minor component and are relict feldspar fragments. Yellow-brown, opaque grains, apparently kaolinitic matrix cemented by Fe-oxide, become increasingly abundant with decreasing grain size, until they form ~5% of the vfL fraction. Heavy minerals are minor (<1%) in the vc and c sand fractions and comprise black ore grains, some red garnet and rare, bluish to grey (slightly altered?), kyanite laths. The heavy mineral fraction is most abundant in the mL and fU fractions where it comprises 10-15%. In the fU fraction of extracted heavy minerals, black, opaque ore grains are dominant (~70%) and often have adhering yellow-brown material (kaolin plus Fe-oxide), but some have adherent red haematite. Many exhibit response to a hand magnet, but very weakly magnetic and non-magnetic grains indicate heterogeneity and the probable presence of ilmenite. Jack (1980) recorded that the opaques in the country rocks are complex, showing exsolution of magnetite, haematite and rutile from ilmenite. Rounding of the black ore grains is common. Very pale pink, lustrous grains are next in abundance and usually occur in prismatic habit with rounded ends, but some well-rounded examples occur. These are zircon and comprise 20-30% of the heavy mineral fraction. Only a few grains of sub-rounded red garnet were observed and some rutile is also present. Pleochroic, honey-coloured grains of staurolite are present, but are extremely rare.

The compositions of the coarse-sandy bed (b) and the fine-sandy cross-bed (c) are essentially similar to that of (a) above, except that ferruginous kaolin grains are much less common. The heavy mineral fraction of (b) is identical, but is most concentrated (~5%) in the fL fraction. The heavy minerals in the fine-sandy cross-bed (c) are mainly in the vf fraction (~3%) and are also overwhelmingly magnetite/ilmenite and zircon. The atypical, fine-grained lens of slightly sandy kaolin differs from the other samples in that the quartz grain population of the vcU to mL fractions is homogeneous, consisting nearly exclusively of very angular, uniformly polycrystalline, "sugary" quartz grains. Opaque, white blocky grains with well-developed cleavage and pearly flakes are increasingly abundant in the fractions finer than fU and comprise ~90% of the VfL fraction. This is evidently well-crystallized kaolinite. Heavy minerals are absent.

Petrography

An oversize thin section of epoxy-impregnated kaolinitic gravel reveals that the very poorly sorted quartz grains have mainly undulose extinction and are dominantly polycrystalline, with sheared, metamorphic grains being common. Disintegrating, composite quartz grains are ubiquitous. Notably, 10-20% of the section consists of recognizable feldspar (microcline and orthoclase, with minor perthite

and plagioclase). The feldspar is extensively disintegrated, with fretted edges and cracks filled with cloudy alteration products (Plates 5.5, 5.6). Some feldspar can be seen to have been part of a quartzo-feldspathic clast (Plate 5.5). In other instances, masses of small "islands" of feldspar are in optical continuity (Plate 5.6), indicating that they are the relicts of a larger feldspar clast. Compaction of the sediment is indicated by disintegrating feldspar squeezed between surrounding quartz grains, with rotations of the relict fragments. Some feldspar grains with clearly rounded edges are present (Plate 5.7). Opaque ore grains and highly birefringent, sub-euhedral zircon grains were the only additional minerals recognized in thin section.

The matrix is very pale yellow (PPL), with finely-divided "dust" and is fine-grained kaolinite (<50 μm), darkly speckled under XPL due to its low birefringence, superficially resembling chert. Scattered in the fine-grained kaolinite are well-formed blocks of columnar kaolinite (books) (Plate 5.7), up to 1 mm in length. The kaolinitic matrix is extensively clouded by irregular mottles of dark, fine-grained, grey-brown (PPL) alteration product. Under XPL, the dark material loses its granular texture and appears as smooth, olive-grey clouds obscuring the kaolinite. It is very pale pinkish brown under RL. It may be very finely disseminated Fe-oxide contaminating the kaolinite. In places the dark material is concentrated against grain boundaries. It is also locally concentrated in arcuate features that may be migration fronts associated with the boundaries of pre-existing grains and pores. In some cases, the distribution of alteration products defines distinct, rounded areas in the matrix which are evidently the vestiges of completely decomposed feldspar grains.

The dark material grades into clouds of yellow-brown Fe-hydroxide (limonite) that are present locally and which intensify around opaque ore grains that are the source. Some of the ore grains have been markedly corroded along cleavage and reduced to a number of parallel plates. Black (opaque), isotropic haematite (red in RL) is commonly precipitated in pore spaces as fillings and linings. A notable feature is the presence of authigenic silica precipitated in fine fissures narrower than ~100 μm (Plates 5.5, 5.7). The fissures apparently formed by shrinking and swelling of the matrix concomitant with moisture fluctuations. Individual crystals are not clearly defined in the fissure fills and the fibrous characteristic of chalcedony is not present. However, locally the fills have a type of sweeping, ray-like extinction and may therefore be a type of chalcedonic quartz. The fissure fills are the shiny films seen on fracture surfaces in hand specimen.

An impregnated thin section of the atypical lens of compact, slightly sandy kaolin reveals a low quartz content (~10%) of polycrystalline grains with undulose extinction. Notably, the quartz grains occur in linear streaks with common orientations, with a tendency for elongate grains to be similarly aligned (Plate 5.8). The texture is suggestive of a foliated fabric. Vestigial feldspar (orthoclase?) is present, but not common. No rounded grains are present. The kaolinitic matrix is noticeably more coarse-grained than in the previous thin section, with many well-formed kaolinite "books." Also in the matrix are stellate (radial) aggregates, up to ~0.5 mm in diameter, of a colourless (PPL), non-pleochroic, second-order-birefringent, micaceous mineral, provisionally identified as sericite, or possibly talc.

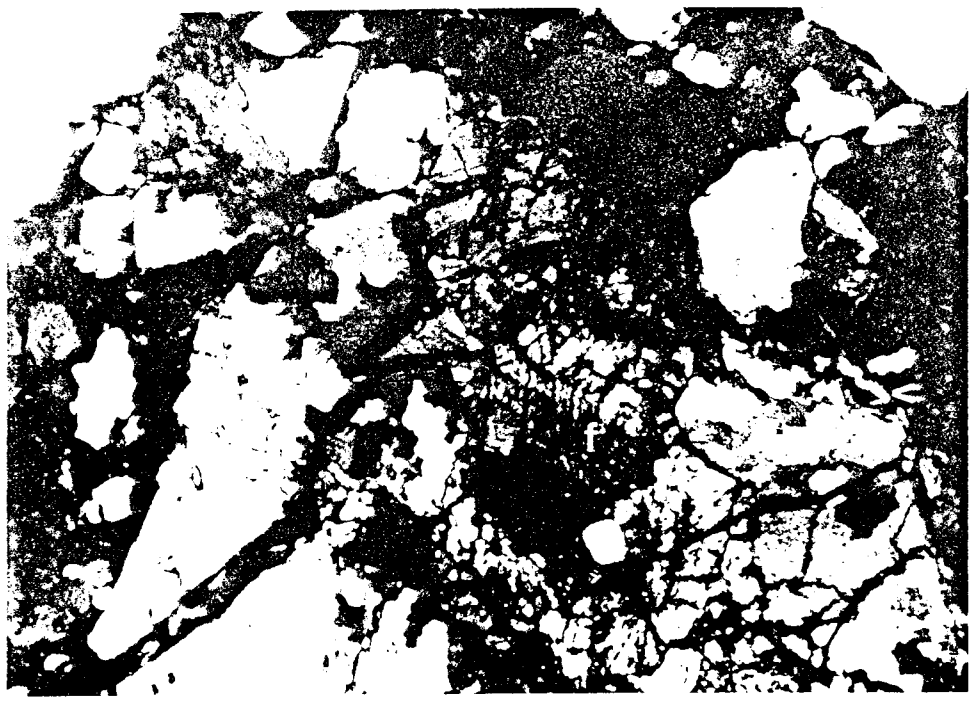

Plate 5.5 Thin section (epoxy-impregnated) of basal kaolinitic deposits, showing weathered feldspar (f) in a disintegrating quartzo-feldspathic clast. Note fissure-filling quartz (arrowed). Field of view = 2.5 mm, XPL.

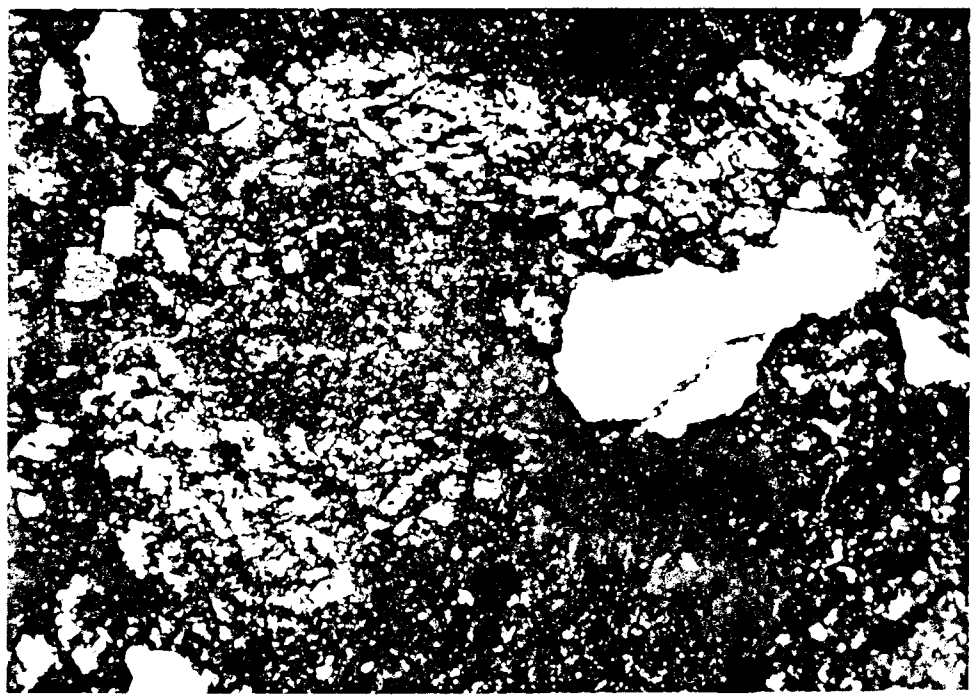

Plate 5.6 Thin section (epoxy-impregnated) of basal kaolinitic deposits, showing remnants of weathered feldspar in the kaolinitic matrix. Field of view = 2.5 mm, XPL.

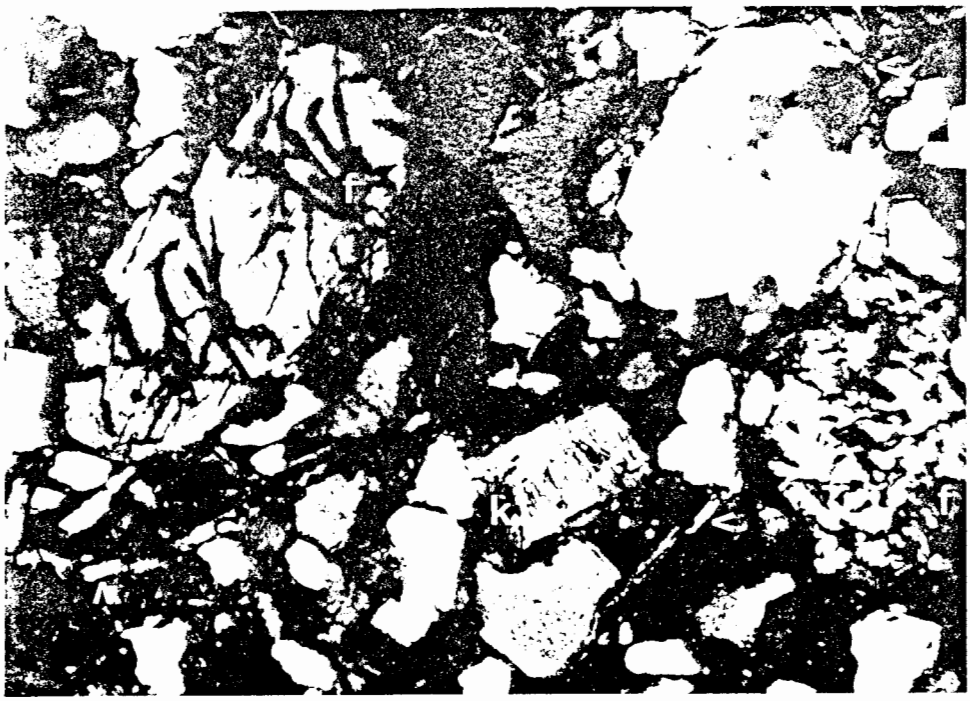

Plate 5.7 Thin section (epoxy-impregnated) of basal kaolinitic deposits, showing weathered feldspar (f), including rounded grain (left), well-developed kaolinite "book" (k) and quartz precipitated in fissures (arrowed). Field of view = 2.5 mm, XPL.

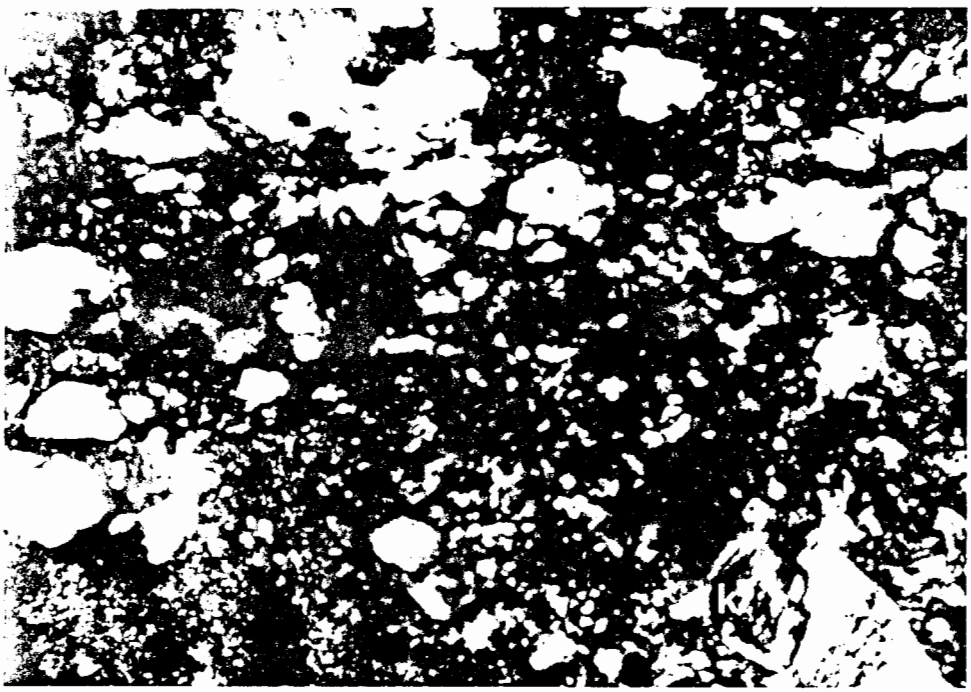

Plate 5.8 Thin section (epoxy-impregnated) of atypical, slightly sandy kaolin lens (Plate 5.3), showing metamorphic texture of polycrystalline quartz and large kaolinite "book" (k). Field of view = 2.5 mm, XPL.

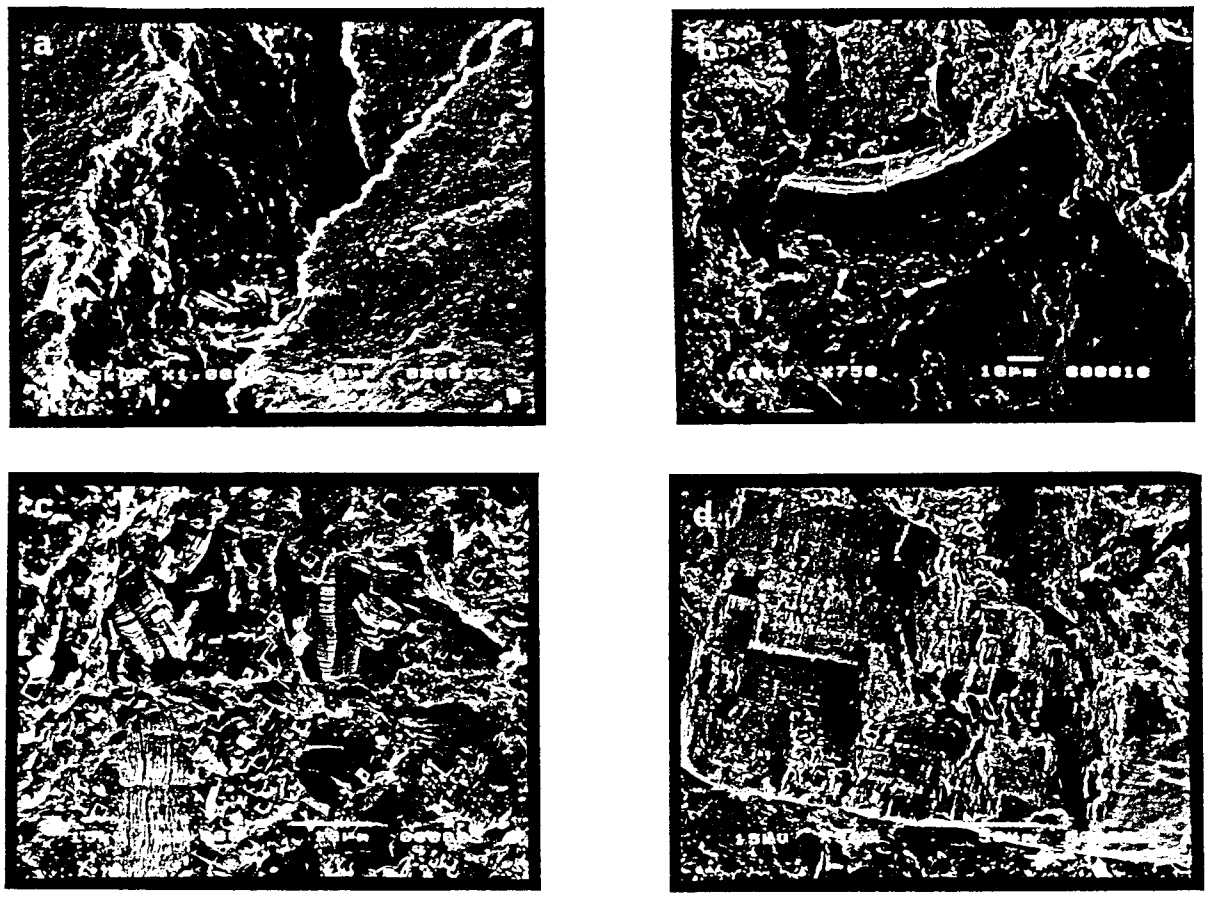

Plate 5.9 Scanning electron photomicrographs of matrix of the basal kaolinitic deposit. **a**, masses of crudely orientated kaolinite "books" beneath planar fracture surface that may represent relict feldspar crystal cleavage. X1000. **b**, large kaolinite "book." X750. **c**, authigenic kaolinite "books" of various sizes and small, cubic crystals, probably the remnants of feldspar. X2000. **d**, corroded feldspar crystal. X500.

Scanning electron microscope observations

Examination of a fragment from a clayey sand cross-bed under the SEM reveals the presence of abundant authigenic kaolinite (Plate 5.9a,b,c). The kaolinite occurs mainly in small stacks 5–20 μm in length (Plate 5.9a), with much larger, curving stacks present locally (Plate 5.9b). Examples of corroded feldspar crystals are present (Plate 5.9d). Small crystals of cubic appearance and with common orientation also occur in some places in the kaolinitic matrix (Plate 5.9c). Their common orientation suggests they are mineral "relicts," probably of feldspar (cf. Plate 5.6), rather than being a nucleated, authigenic mineral. More detailed investigation using X-ray microanalysis to identify element compositions is envisaged for follow-up study.

5.3 INTERPRETATION

The presence of a minority of well-rounded, quartz gravel clasts, a minority of rounded quartz sand grains, depositional bedding, plant fossils, carbon and a detrital heavy mineral component, leaves no doubt as to the sedimentary nature of the basal kaolinitic deposit.

Field observations of the occurrence of kaolin clay with apparent relict feldspar cleavage, suggesting that the kaolinitic composition of the deposit is due to the decomposition of a feldspathic component, were confirmed in the laboratory on disaggregation of sediment samples, when the relict "cores" of weathered feldspar crystals were also revealed. Some clay lumps with rounded clast morphology, varying from both small pebble to coarse sand size, were also liberated from the deposit. The presence of weathered feldspar grains, including rounded examples, disintegrating composite quartz grains and authigenic kaolinite "books," is evident in thin section. Similarly, SEM observations confirm the alteration of feldspar to kaolin. Pronounced weathering is also evident in the oxidation of opaque ore grains and redistribution of the Fe-oxides, as well as the mobility of silica and its precipitation in small fissures.

It is therefore proposed that the kaolinitic quartz gravel deposit was originally a conglomeratic arkose, locally with sandy beds, that has been extensively decomposed *in situ*. The original mud content of the deposit was probably negligible. The grain size distributions of the resistant quartz fraction, due to the disintegration of composite grains, cannot accurately reflect the size distributions of the original sediments. The coarser size classes must now be diminished to a degree, with concomitant increase of the finer size classes and a worsening of sorting. Nevertheless, size distributions of samples a, b and c (Fig. 5.3) appear to retain basic features of the original sediment. For instance, the pebbly cross-bed (a) was probably a clast-supported, medium to large pebble gravel with an interstitial coarse sand component. The coarse-sandy bed (b) may have had its mode in the very coarse to coarse sand range. The fine-sandy cross-bed (c) very likely originally lacked as pronounced a very fine sand content. The original size distribution of gravel samples could be obtained by selecting only the quartz clasts with encompassing evidence of abrasion for measurement.

The quartz sand fraction of the atypical lens of slightly sandy, compact, kaolinitic clay contrasts with the other samples in that the grains are entirely polycrystalline, metamorphic quartz. The epoxy thin section confirms the absence of clastic grains and reveals a presence of polycrystalline quartz "stringers," rather than a sedimentary fabric. The size distribution of the extracted quartz sand merely reflects the truncated distribution of particle sizes produced from disintegration of the "stringers." The curious lens is therefore considered to be a kaolinized boulder that, from the low quartz content, consisted mainly of feldspar.

In view of the alteration of the deposit, the absence of marine fossils and authigenic marine minerals does not disprove a marine origin. However, a marine origin is unlikely due to the lack of pervasive rounding of quartz clasts. Furthermore, nearshore marine gravels are disposed in well-segregated beds that are laterally persistent (Clifton, 1973), as is evident in the marine beds overlying the basal deposits. A colluvial origin for the deposit, involving the local redistribution of material from the deeply weathered profile on the surrounding gneissic terrain, is also unlikely. Instead, the occurrence of cross-bedding in large trough-sets indicates sub-aqueous processes. The heavy-mineral components, magnetite/ilmenite and zircon, are locally available from the surrounding gneisses, but their degree of rounding is incompatible with very local derivation and the zircon is clearly recycled.

Detrital kyanite is a very minor component in the samples of basal deposit examined, but it constitutes a significant portion of the heavy mineral concentrate in the coarse sand to fine gravel size range from marine gravels. It is likely that the kyanite has been derived from the aluminous gneisses and schists of high metamorphic grade that occur elsewhere on the coastal plain (Jack, 1980).

Notably, very high grades of diamond content are encountered in the basal kaolinitic deposits (G. Bonaccorsi, personal communication, 1980; Molyneux, in Rogers *et al.*, 1990). The concentration of this exotic component is incompatible with a locally-derived, colluvial origin for the basal deposits.

It is concluded that the basal kaolinitic deposit in the study area was laid down as a conglomeratic quartzo-feldspathic sediment in a fluvial environment. The fluvial environment represented was of high energy, as is evident in the occurrence of boulders, trough cross-bedding and placer mineralization. However, it is clear from the fining-upward sections recorded by Tankard (1966, 1975a) from other palaeochannels nearby (Fig. 5.2) that the conglomeratic kaolinitic deposit at Hondeklip is the basal remnant of a more extensive sedimentary sequence and only one facies in a larger suite that also involves lower-energy deposition. The deposit confirms that the major channel-like feature of the bedrock topography of Hondeklip represents fluvial erosion and not marine erosion of a differentially-developed weathering profile in the gneiss. The locus of the fluvial channel was controlled by bedrock structure, in view of the coincidence of the gneissic foliation, faulting and dolerite dyke intrusion.

Subsequently, both the channel-filling, arkosic sediments and the underlying gneiss bedrock were deeply weathered, with extensive alteration of feldspar to kaolinite. Humid climatic conditions and high rates of leaching are implicated in the kaolinitic weathering (Singer, 1980). The leaching reached its greatest development in the channel, the porous infill of the topographic low being the preferential accumulation zone and conduit of groundwater. The presence of carbonaceous material and plant fossils (Tankard, 1966, 1975a), confirmed from the study area, are supportive of humid, vegetated conditions.

This interpretation does not exclude the probability that the erosion of the channel was influenced by prior weathering and that the arkosic fluvial sediments were "grus" produced by denudation of a weathered landscape. On the contrary, this is to be expected, in view of the global and local evidence that Cretaceous and Palaeogene climates were, overall, more humid and warmer than the later Cenozoic (Frakes, 1979; Dingle *et al.*, 1983) and these conditions persisted into the lower Neogene (Coetzee & Rogers, 1982; Coetzee *et al.*, 1983). Thus it is possible that a portion of the basal terrestrial sediments might have consisted of saprosand or alterite (*sensu* Johnsson, 1990), these being lithic fragments that have maintained physical integrity although intensely weathered, clay-sand composites. Some (uncommon) petrographic features could be interpreted as such. However, vigourous fluvial transport and subsequent pronounced weathering is likely to have destroyed most evidence of the existence of "preweathered" clasts.

After the period of deep weathering, the fluvial channel was exhumed by erosion of the weathered infill. The preservation of remnants of the infill indicates that the channel still retains its basic original form. The relief of the channel must have been reduced by the removal of the weathering mantle from the surrounding high areas of bedrock. Additionally, decomposed gneiss has probably been eroded from within the channel, accounting, for instance, for features such as the basin (4) in Fig. 4.4.

5.4 DISCUSSION

It is reasonable to assume that the "linear, clayey, fluviatile beds" recorded by Carrington and Kensley (1969) at the base of their stratigraphic column referred to the basal deposit described herein, although the kaolinitic composition was not specifically mentioned. Tankard's (1966, 1975a) more detailed observations are sufficiently in accordance with the features of the basal deposit at A Block in Hondeklip mine to be certain of the equivalence of the deposits. Exposures of the kaolinitic basal deposits on Koingnaas and Zwart Lintjies Rivier were shown to the writer in 1985 by Messrs R. Molyneux and K. Elford (De Beers Namaqualand Mines) and the equivalence with that on Hondeklip confirmed. This work therefore endorses the opinions of previous workers (Carrington and Kensley, 1969; Tankard, 1966, 1975a) for a fluvial origin of the basal kaolinitic deposits and for subsequent *in situ* kaolinization (Tankard, 1966).

The remnant of kaolinitic, quartz-clast-rich sediment associated with silcrete in the Groen Rivier drainage (Fig. 3.1), reported by Rogers (1911), is an apparently rare instance where the basal kaolinitic deposits of the coastal plain are exposed naturally (personal observations) and also shows that these deposits occur inland of the immediate coastal tract. Together with the example Tankard (1975a) described near the Bitter River (Driekop) (Fig. 5.1) and the possible correlate farther south in the Sout River valley (Rogers, 1911), the occurrence of kaolinitic basal deposits extends from just north of the Hondeklip area southwards almost to the Olifants River. To the writer's knowledge, similar kaolinitic, quartz conglomerates and sands have not been identified in the intensely prospected and mined area north of Kleinzee, nor south of the Olifants River and are, at this stage, apparently mainly associated with the Namaqualand gneissic bedrock terrain.

Although now volumetrically small relative to the overlying marine deposits, due to their remnant, channel-associated nature, these kaolinitic gravels and sands are of considerable economic significance due to their diamond content. The channel deposits are actively mined and represent the richest deposits in the area (Molyneux, in Rogers *et al.*, 1990). The active mining of these deposits, at mines in the Hondeklip area, may have revealed information on rare constituents possibly present, of which the writer is not aware. In the Hondeklip samples examined, there is no indication that the lithology of the basal deposit includes significant quantities of material other than that which could have been derived from the regional gneisses. The catchment must also have been largely denuded of Nama Group and Dwyka Formation rocks at the time of deposition, as resistant clasts (quartzites, indurated mudstones, jaspers, banded ironstones) are not readily evident in the basal fluvial deposit. The diamond content, revealed by prospecting, is the main incongruity, but the diamonds must also

have been available within the drainage systems associated with the generation of the basal deposit. As such, these deposits represent an important phase of diamond transport to the western shelf, perhaps the most important.

It is worth noting that banded ironstone pebbles, usually associated with gravels of the Orange River and pebbles recycled from Dwyka rocks, were transported to the Hondeklip area at some stage. The banded ironstone pebbles were found in concentrate from a limited "patch" of basal gravel from within the kaolinized bedrock channel. These "exotic" clasts are not generally recognized in heavy mineral concentrate from the marine gravels at Hondeklip, although the nature of small, cherty clasts in the concentrates requires investigation, as some of these may be the remnants of banded ironstone pebbles

The erosion of the kaolinized, fluvial diamond depositories during subsequent marine transgressions must have provided a local, secondary source for many of the diamonds in the overlying marine gravels. At least some of the abundant detrital kyanite in the marine placer concentrate is derived from the basal kaolinitic deposits. Data on the size frequencies of diamonds from the basal deposits and those from the marine gravels, within particular palaeo-coastal compartments, could be compared in order to test whether the respective size distributions are compatible with local derivation of the "marine" diamonds from the basal deposits. The evidence for the age of the deposits will be discussed in Chapter 8.

CHAPTER 6

THE SILCRETE

6.1 INTRODUCTION

Silcrete (Lamplugh, 1902) is a rock produced by siliceous induration at or near the land surface and is usually readily recognized in hand specimen and by its geomorphological context. Early investigations referred to silcrete as "surface quartzite" and this term is retained in the brief summary of previous work presented below. The occurrence of silcrete on the Namaqualand coastal plain, both *in situ* as a duricrust and as derived clasts in marine gravels, was recognized from the outset of serious investigations. The Hondeklip Bay study area is no exception and silcrete occurs both as large, exhumed slabs not far from their primary context and as pebbles and cobbles derived by their erosion.

PREVIOUS OBSERVATIONS ON NAMAQUALAND SILCRETES

As noted in Chapter 5, Rogers (1911) recorded "surface quartzites" from the drainages of the Groen and Sout rivers (Fig. 3.1), where the occurrences are associated with kaolinitic, sandy and gravelly, quartz pebble deposits.

Wagner and Merensky (1928) recorded "surface quartzites" as the oldest unit in the coastal plain stratigraphy of Namaqualand and mentioned that they occur at various distances from the coast and various elevations above sea-level. Typically the "surface quartzites" are found as outcrops capping bedrock inland of the coastal-plain marine prism and Wagner and Merensky (1928) mentioned occurrences east of Alexander Bay, Port Nolloth and the Buffels River Mouth (Fig. 3.1). They described the "surface quartzites" as mainly breccias comprising angular quartz, quartzite and other rocks in a grey or yellowish-brown, ferruginous matrix of chalcedonic silica. An origin by the silicification of surface detritus and scree on old erosion surfaces under arid conditions was suggested. They also mentioned the occurrence of "big waterworn blocks" in the highest marine deposits known at that time near Kleinzee (~64 m asl.). Pebbles of "surface quartzite" were also noted in marine gravels at Alexander Bay at 23-34 m asl., Groen River at 9-14 m asl. and Klip Vlei at 18-21 m asl. (now Klipvley Karoo Kop, ~25 km north of Olifants River) (Fig. 3.1).

Wagner and Merensky (1928) were cautious in assigning the same age to all "surface quartzites," due to the observations of Rogers (1904) of silicification of marine coastal plain deposits near the Olifants River. Thus, on the assumption that the oldest Namaqualand coastal silcretes may correlate with the Pomona silcrete of southern Namibia, they uncertainly ascribed an Upper Cretaceous? to Recent age to the "surface quartzites" of Namaqualand.

Reuning (1931) described sections in marine deposits on the cliffs at De Punt, just north of the Olifants River (Fig. 3.1), in which he recognized a silicified horizon that he correlated with the pre-Middle-Eocene "Pomona Quartzite" of southern Namibia. The writer can confirm that silcrete caps

deeply weathered, Late Precambrian, Vanrhynsdorp Group phyllites along the coastal cliff-tops in the De Punt area.

The occurrence of silcrete clasts in the (subsequently discovered) highest elevation, oldest marine deposits was later confirmed on Annex Kleinzee by Hallam (1964), who reported that marine deposits are at the foot of a cliff cut into a silcrete at ~88 m asl. and that all marine deposits are post-silcrete in age. Hallam (1964) mentioned correlation with the Pomona silcrete, but also quoted Du Toit's (1954) opinion of a Pliocene age for coastal silcretes.

Keyser (1972) noted the presence of silcrete clasts in the gravels of the highest terrace at Alexander Bay (Grobler terrace, 64-84 m asl.). North of the Olifants River (Fig. 3.3), Visser and Toerien (1971) were not able to confirm the presence of silcrete clasts in marine gravels. However, the writer can confirm the earlier observations of Wagner and Merensky (1928) and Haughton (1932) that clasts of silcrete are present in marine gravels on Klipvley Karoo Kop (personal observations).

6.2 SILCRETE AT THE HONDEKLIP MINE

FIELD OBSERVATIONS

Localities

Large slabs and boulders of silcrete (Plate 6.1) occur in the mining excavations in which the basal deposits are preserved (A and B blocks, Fig. 5.1). Although none of these slabs could be observed in primary context, because they had been bulldozed into heaps during mining, their surface features (see below) indicate that some were *in situ* prior to mining disturbance. Rounded boulders, cobbles and pebbles of silcrete are present in the marine basal gravels throughout the study area, but are particularly common in the excavations around the "nose" of the bedrock ridge (A and B blocks), where the largest slabs and boulders of silcrete occur.

Description

The silcrete is yellow-brown (buff) in colour (about Munsell Hue 2.5Y 6/2) and is a profoundly cemented rock which rings to the hammer stroke, exhibits conchoidal fracture and releases a pungent odour when struck. The large slabs in A Block are up to 1 m thick, but are usually ~0,5 m thick and most have clearly distinguished upper and lower surfaces. The upper surfaces have been smoothed by abrasion and are of a darker hue than the rough-textured, pale undersides (Plate 6.2). On the sides a clear boundary separates the waterworn and unworn surfaces. Shattered surfaces reveal that the rough, pale undersides reflect an outer layer ~1 cm thick surrounding the densely silicified, darker, interior portions of slabs with conchoidal fracture. This outer layer represents either incomplete silicification, or possibly a degree of exterior leaching, or both, but it is nevertheless hard and evidently well-cemented.

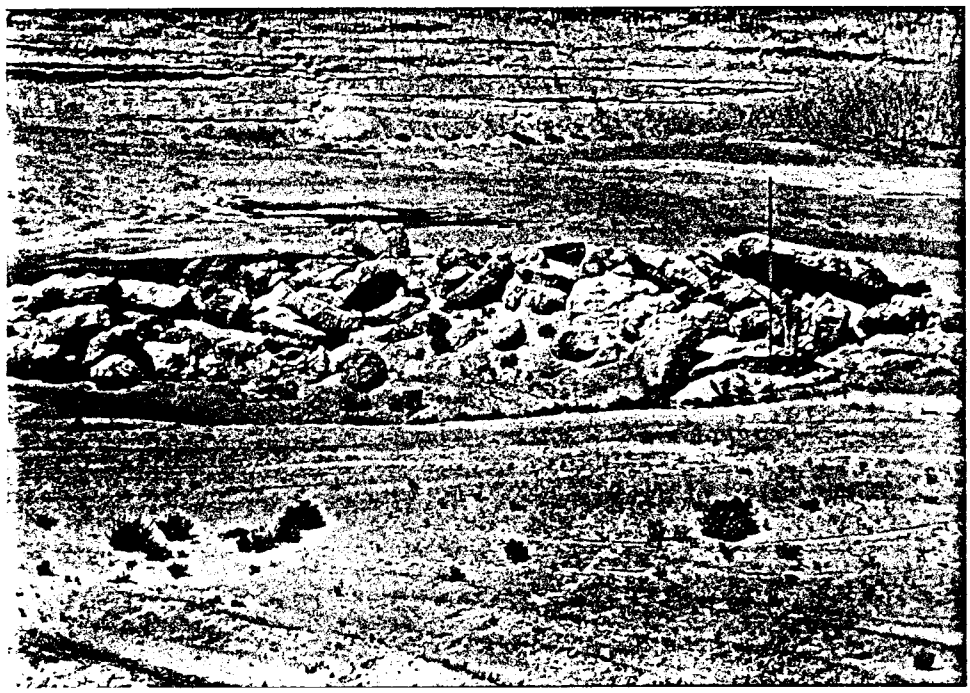

Plate 6.1 Silcrete slabs in A Block, pushed into a heap during mining. Person with 4 m surveying staff for scale. Note area of swept kaolinized gneiss bedrock in background to right of staff.

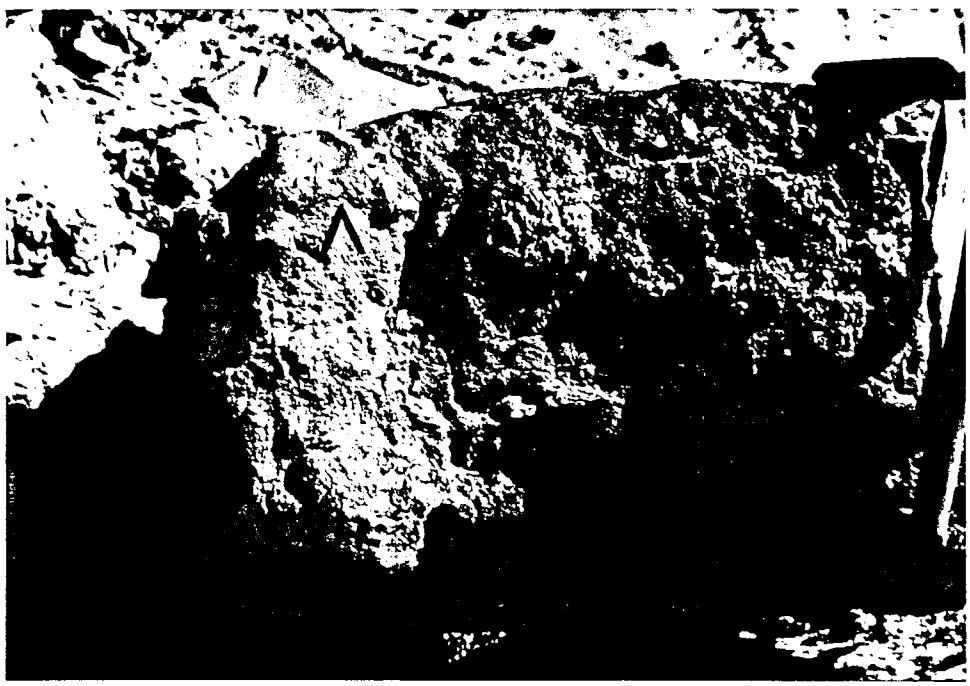

Plate 6.2 Silcrete slab in A Block with dark, abraded top and rough, pale, unworn undersides. Note dark phosphorite (arrowed) along boundary. Tool is 42 cm long.

Both tops and bottoms of slabs have numerous pits and large, crack-like sutures (Plates 6.3 and 6.4). On the worn slab-tops the pits are often infilled with chocolate-brown phosphorite cement enclosing rounded coarse sand and gravel and this material is sometimes preserved as a rind along the boundary of the surfaces (Plate 6.2). The phosphorite infillings and coatings have also been abraded and smoothed. The sutures are widely spaced and do not result in a columnar or prismatic aspect to the silcrete slabs. Curious, patchy areas of high, varnish-like gloss occur on the silcrete. These tend to be best developed on protuberances, but are not strictly confined to the worn, upper surfaces. This varnish also "overlies" some of the patches of adhering phosphorite.

On the sides of some slabs occur thin pipes, ~0,5 cm in diameter and several centimetres in length, that are partially infilled with dark yellow Fe-oxides or clay. Many walls of these pipes are fluted or striated. Dark brown stains, more typical of Fe-oxide, occur in the pipes and in patches on the sides of slabs. Some shattered silcrete slabs reveal that the pipes are not confined to their sides, but are generally evenly distributed through the rock (Plate 6.5). However, one example showed a concentration of empty pipes along a sutural feature (Plate 6.6). The internal piping has obviously contributed to the pitted appearance of the tops and bottoms of the slabs.

Fresh breakage surfaces also reveal pipe-like voids on smaller scales, down to a sub-millimetre scale (Plate 6.7). These are lined or partially infilled with Fe-oxide and some have surrounding dark-brown haloes indicating penetration of oxide into the adjacent matrix. They are more varied in orientation than the large, vertical pipes and root-like branching is present. Some of the Fe-oxide infills are fibrous in appearance. Other examples of pipes observed have no infilling Fe-oxides, but instead have bleached surrounds. Still others are infilled with siliceous material resembling the matrix and fibrous textures are again present (Plate 6.8). Other voids visible in the silcrete are sparsely distributed and irregular in dimensions and include mere sub-millimetre-size, angular holes to more obvious, crack-like, interconnected cavity systems several millimetres in diameter. They are lined with yellow Fe-oxide or clay, but in a few cases the presence of scintillation indicates minutely crystalline coatings, probably of quartz. The visible voids are widely spaced, comprising a very minor portion of the rock (<<1%).

Small, irregular areas free of visible quartz grains also occur in the silcrete and resemble irregular mud clots. On some silcrete cobbles these were observed to occur in irregular streaks several centimetres in length with a general common orientation, but generally no common orientation is readily discernible. A notable feature, evidently uncommonly preserved, is the occurrence of meniscoid lamination defined by dark Fe-oxide, strongly resembling a spreite produced by burrowing (Plate 6.9).

Except for the features mentioned, the silcrete examples in A Block are overall massive in aspect, but on one up-ended silcrete slab probable relict thin bedding to lamination was found (Plate 6.10).

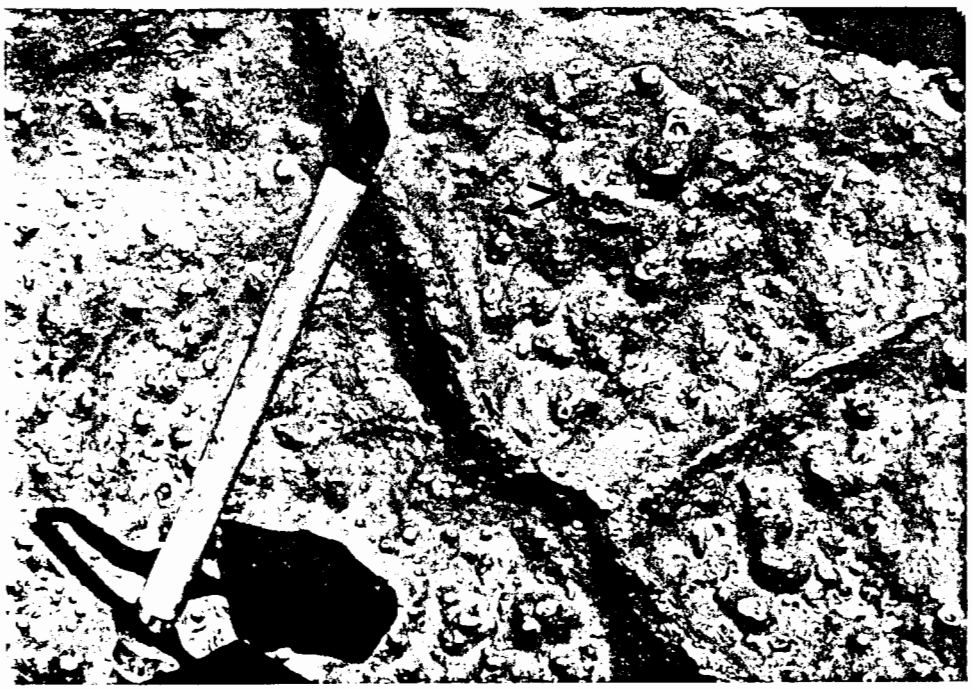

Plate 6.3 Silcrete slab in A Block showing abraded top with sutures and numerous pits. Remnant of phosphorite coating arrowed.

Plate 6.4 Silcrete slab in A Block showing underside with suture and deep pits.

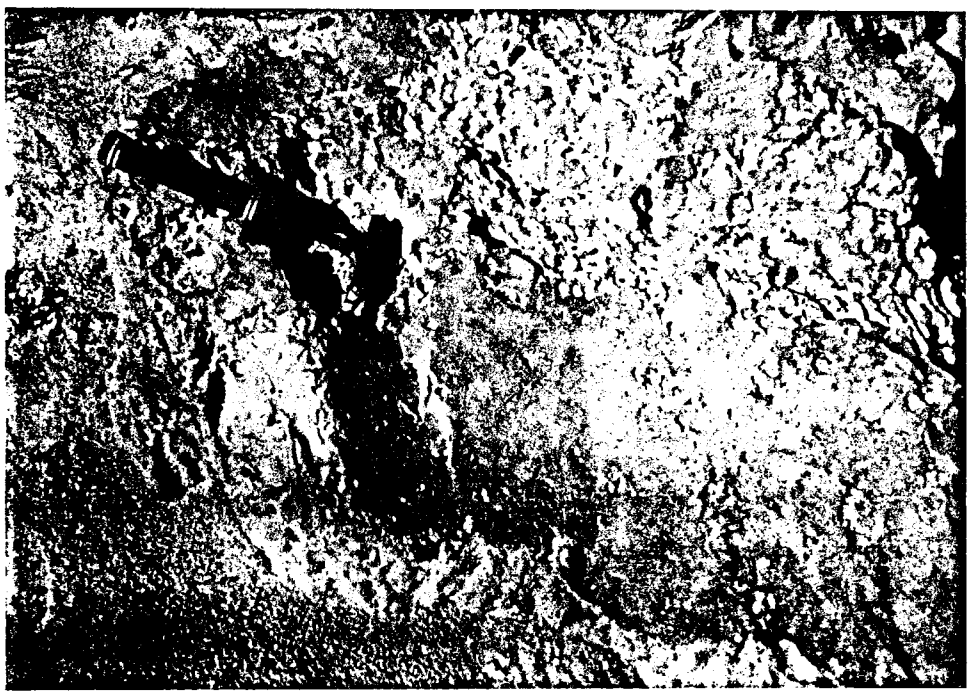

Plate 6.5 Silcrete slab in A Block. Shattered underside shows that pits may extend as pipes through slab.

Plate 6.6. Silcrete slab in A Block. Underside showing linear concentration of pipe-like voids.

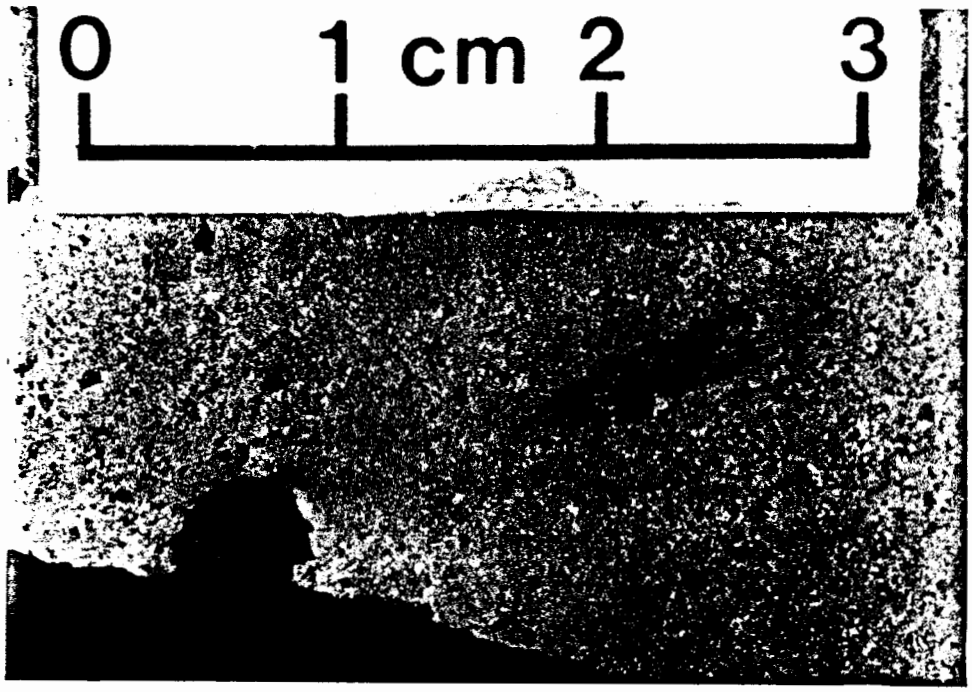

Plate 6.7 Silcrete from A Block. Pipe-like voids with Fe-oxide coatings.

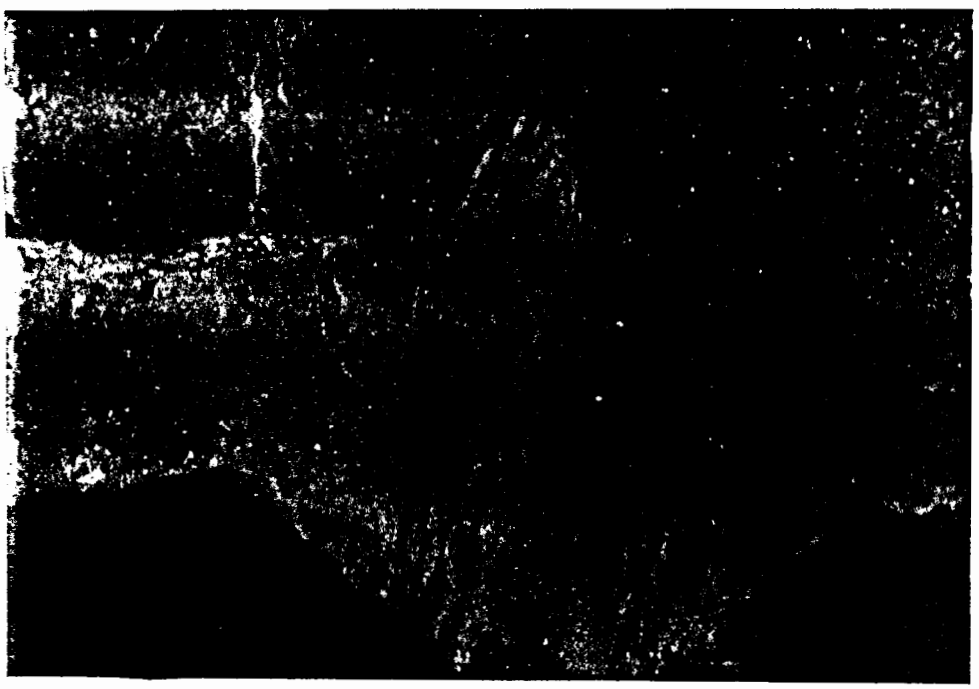

Plate 6.8 Silcrete from A Block. Fibrous structure in matrix (~1 cm long).

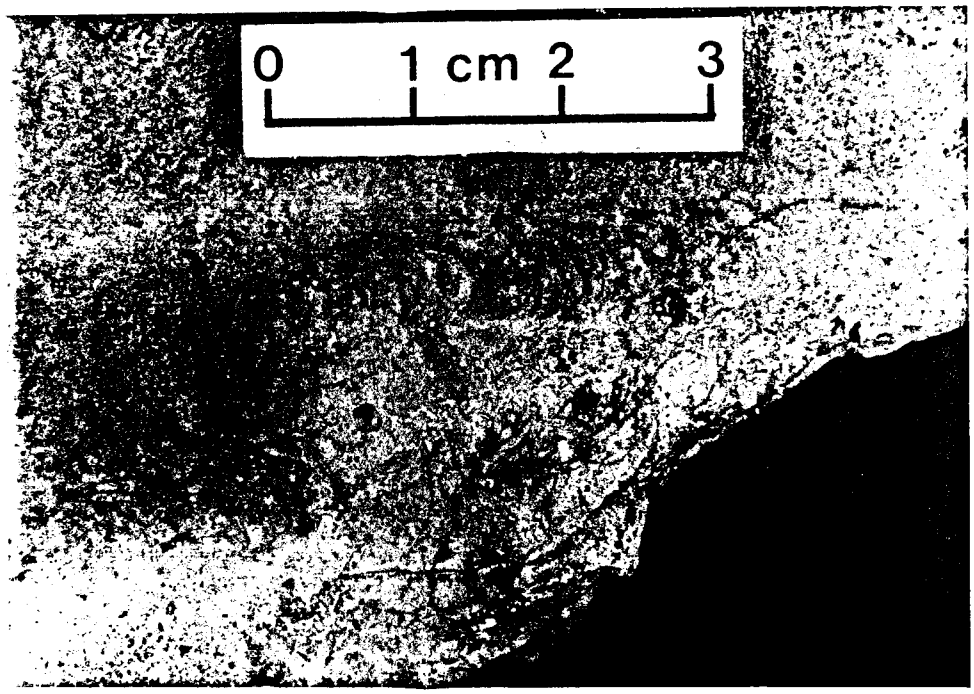

Plate 6.9 Silcrete from A Block. Meniscate structures resembling burrows.

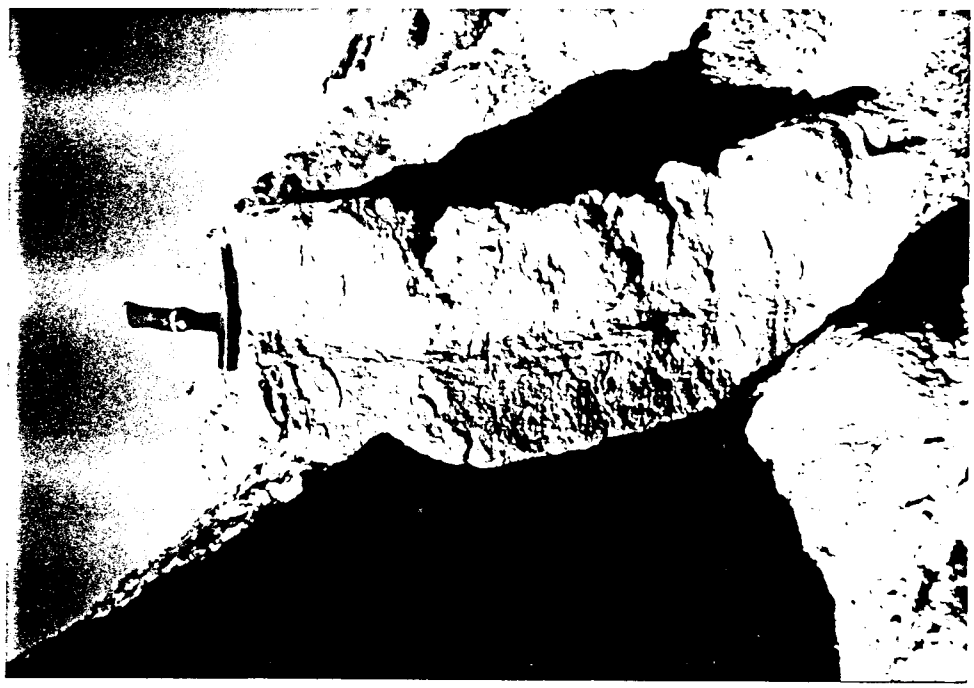

Plate 6.10 Silcrete slab in A Block with probable relict bedding. The photograph is rotated from the vertical.

In contrast to the pitted silcrete slabs and boulders in A Block, those in B Block farther landward (Fig. 5.1) are more heterogeneous in size and shape (Plate 6.11) (cf. Plate 6.1). The B Block silcrete was seen to contain abundant clasts of sub-angular quartz gravel, a feature absent in A Block silcrete examples. Rounded quartz clasts also occur (Plate 6.12) and embedded, elongate kyanite grains and black ore grains are present. Furthermore, silcrete slabs and boulders in B Block commonly possess relict sedimentary layering and both thin bedding (Plate 6.13) and trough-shaped sets occur (Plate 6.14). No fine-scale features, possibly reflecting relict sedimentary lamination, could be discerned here. The presence of pipe-like features is also not ubiquitous; they were not observed on fresh silcrete surfaces in B Block and the associated pitting is more strikingly a feature of the slabs in A Block, a few hundred metres to the west.

The more pronounced knobs and cavities of the B Block silcrete are due to the influence of sedimentary structures, but also appear to have been influenced by other inhomogeneities in the matrix. Although internal piping is not a feature of B Block silcrete examples, nevertheless some pitting is present and therefore the pitted appearance is not exclusively due to piping, but also reflects uneven silicification at the outer margins of silicifying masses. The "tougher" portions of the matrix standing in relief are slightly darker in hue, superficially resembling pebbles of silcrete within silcrete. However, some of these areas occur with an irregular outline, inconsistent with clast origin and even in hand specimen grains can be seen across boundaries. No indication of more silicified and resistant nodules are present in the seemingly partially silicified material in B Block.

In other respects (worn upper surfaces, abraded phosphorite coatings, large suture-like features, crack-like voids, irregular "mud clots"), the largest slabs of silcrete in B Block resemble those in A Block. However many large boulders have been entirely exhumed, overturned and waterworn. These are often encrusted with oysters (*Crassostrea margaritacea*, Plate 6.15) and barnacles (*Austromegabalanus kensleyi*, Plate 6.16). Another feature, exclusive to B Block, is the occurrence of what appears to be very localised leaching of the silcrete surfaces, manifested as pale bands branching root-like over and affecting the surfaces of both silcrete and phosphorite coatings (Plate 6.17). A patchy glossy or varnish-like effect, like that seen in A Block, is also locally present and preferentially occurs on projections (e.g. Plate 6.16).

In one area in B Block, fragments of angular, quartz conglomerate occur that are not profoundly silicified. This material is light pinkish-grey in colour (10YR 7/2) and, being crumbly, sheds grains. Very sparse kyanite grains can be found. The rock differs in appearance and hardness from the pale yellow, hard, outer layer of silcrete-slab undersides. The material was present in significant quantities and the uniformity of the matrix with respect to hardness and colour tends to suggest that partial silicification, rather than desilicification, accounts for the nature of this lithology. Under hand-lens magnification, concavo-convex microlamination is visible in some of the muddy clots in the matrix and in association with pore spaces. Yellow, clay-like material occurs in cracks and lines larger cavities. As will be shown in Chapter 7, the material resembles the silcrete petrographically and is regarded as incompletely indurated silcrete.

Plate 6.11 Silcrete boulders in B Block. Person with 1.5 m staff.

Plate 6.12 Conglomeratic silcrete in B Block. Shattered boulder showing quartz pebbles in coarse sandy matrix. Note presence of some rounded clasts. Scale bar ~1 cm long.

Plate 6.13 Silcrete in B Block showing thin bedding.

Plate 6.14 Conglomeratic silcrete in B Block showing curved bedding planes indicating trough-sets. Scale in cm.

Plate 6.15 Silcrete in B Block with worn phosphorite coating and encrusting oysters.

Plate 6.16. Silcrete in B Block with encrusting barnacles and "varnish." on protuberances

Plate 6.17 Silcrete in B Block with leached zones branching root-like over upper surface. Scale in cm.

6.3 DISCUSSION

The widespread occurrence of silcrete clasts in the overlying marine basal gravels indicates that significant quantities of this rock were reduced to gravel. Although no longer in primary context, the abrasion on the upper surfaces of the large silcrete slabs in A Block clearly indicates that they were embedded, whilst their exposed surfaces were subjected to erosion. It is evident that these large slabs in A Block with upper-surface wear were the only remaining *in situ* remnants of a more widespread (but not necessarily continuous) horizon of silcrete.

The presence of angular to rounded clasts of quartz, visible detrital heavy minerals and sedimentary layering in the silcrete boulders of B Block shows that the silcrete there has developed in basal, kaolinitic, quartz-gravel deposits such as those described from A Block (Chapter 5). This indicates a pre-existing, more widespread occurrence of the basal kaolinitic deposit in B Block than is now preserved there. The rarity of quartz clasts in the silcrete slabs of A Block may suggest that the slabs remaining there are mainly silicified bedrock. However, at least one slab in A Block possesses relict bedding. The kaolinized Garies Gneiss bedrock in A Block is quartz-rich with steeply dipping foliation. Relict bedrock texture should be present if the silcrete there had formed in the bedrock, but this was not observed. Thus it seems that the silcrete in A Block developed in basal kaolinitic sediments that were finer-grained and more homogeneous relative to those now remaining there and relative to those

that were silicified in B Block. This fine-grained lithology must have closely overlain the conglomeratic, basal deposits described in Chapter 5.

The large-scale sutures observed on silcrete slabs in A Block probably reflect an aspect of the late-stages in the spatial development of silicification. Columnar, polygon silcrete facies are suggested to result from the volume reduction associated with dehydration (Wopfner, 1978). This is supported by one example from the study area where open pipes are associated sutures, the pipes in the intersutural area having been infilled to a greater extent (Plate 6.6). Alternatively, it is possible that the pipes functioned as conduits for siliceous solutions during the later stages of silicification, limiting volume losses by dehydration. In noting that the Hondeklip silcretes do not have an overtly columnar aspect similar to that reported by , it must be remembered that the existing silcrete slabs must reflect the portions of the silcrete horizon with the greatest physical integrity. It is possible that more open sutures characterized the eroded portions, although the preserved spacing of sutures suggests blocky rather than columnar "jointing."

The pipe-like voids may be the relict expression of plant stems or reeds. The root-like branching of smaller voids in A Block silcrete is similarly suggestive of vegetation, but an unequivocal relationship between "pipes" and "roots" has not been observed. The fibrous, siliceous features (Plate 6.8) are very likely the silicified equivalents of the moulds of relict plant material observed in the basal kaolinitic deposits, supporting the possibility that the other features may also be of fossil plant origin. The occurrence of features resembling burrow spreiten suggests bioturbation.

It is significant that sedimentary structures dominate the silcrete boulders of B Block, whilst the slabs in A Block are massive, with only one found showing thin bedding. There is no reason to regard the A Block silcretes as being any less faithful than those of the nearby B Block in preserving the gross features of the host lithology. Thus the more massive, "piped" aspect of the silcrete in A Block is considered to reflect the original characteristics of the sediment prior to lithification. The contrast between silcrete boulders of the two sites reflects different facies of the basal deposits that became indurated. In B Block, gravelly, high-energy sediments with primary sedimentary structures were silicified, similar to the basal facies of the patch of unconsolidated kaolinitic gravel preserved in A Block. In A Block, silicification affected a lower-energy, probably bioturbated and vegetated facies of the basal kaolinitic sediments.

The last events to affect the exhumed, abraded silcrete slabs were the deposition of gravelly, marine phosphorite on their exposed surfaces, subsequent abrasion of that cover to remnant patches and infillings of pits (Plates 6.5, 6.6, 6.15), encrustation by shelly fauna (Plates 6.15, 6.16) and, finally, burial under the basal gravels of the overlying marine sequence. As will be shown at a further point in this thesis, the overlying, basal marine gravels were deposited in the lower-shoreface environment, i.e. whilst the silcrete slabs and clasts were fully submerged. They were not again subaerially exposed until artificially exhumed by diamond-mining. Thus any superficial effects superimposed on the smooth, but basically matt surface, produced by nearshore submarine abrasion, such as patchy

varnish and leaching, reflect early diagenetic processes that occurred within the sediment pile, or subsequent to artificial subaerial exposure. Significantly, both localised leaching and gloss effects overlie abraded phosphorite veneers.

The branching, localised surface leaching of some B Block silcrete examples (Plate 6.17) is rather enigmatic, in view of a lack of evidence of penetration of the ~12 m thickness of overburden by large root systems and the absence of obvious pedogenic features in the immediately overlying material. Another possibility is that the leaching may have been controlled by fabric variation in the overlying sands. For instance, large-scale thalassinoidean burrow systems ramify over the bedrock and the "armoured" tops of basal marine gravel beds. (They are seen in this plan view in the period intervening between overburden stripping and gravel mining, subsequent to some wind deflation.) The burrow infills are usually poorly sorted and preferentially reddened. Thalassinoidean burrow systems, produced by crustaceans, influence the local geochemical environment in the sediments from their inception (ventilation) on to diagenesis. By operating as preferential conduits for groundwater, they may have caused localised leaching. It may also be significant that the overlying marine basal gravels in B Block are lithified by calcite cement, whilst those in A Block are unlithified. This implies strong lateral gradients in diagenetic processes and the more "active" geochemical environment implied by the calcareous cementing in B Block could have involved some local silica leaching.

Very glossy, rounded, granule to small pebble gravel is locally encountered in the overlying, basal marine gravels, but also occurs in gravel lenses in the marine (overburden) sands higher in vertical sections. This gloss is present in fresh exposures. Opaline silica nodules are present at a locality in terrestrial sands immediately overlying marine sediments. The latter occurrence is unusual and is associated with the rim of a carbonate pan. Nevertheless, these occurrences indicate mobility and precipitation of silica in both the marine gravels and the overlying terrestrial deposits.

The development of patchy gloss is not confined to silcrete slabs, but it is also encountered on other exposed cobbles and boulders of fresh gneiss in the older excavations (e.g. A and B blocks). Pebbles on the deflated surfaces of old dumps were seen to have gloss developed on their exposed parts, but not where embedded. Glossy surfaces also occur on the surfaces of gneiss bedrock boulders at the present seashore. Thus at least some, if not all, of the patchy gloss on boulders exposed for several years in excavations may be due to contemporary development on exposed surfaces due to wetting and drying by dew and mist, with probable involvement of airborne siliceous dust and salt and microbial activity dissolving and re-precipitating surface silica and dust. Estimates of the rates of desert-varnish development vary enormously (summary in Kukal, 1990), from a few years to many thousands of years. Clearly the former applies to the coastal strip of Namaqualand. The superficial features of sub-millimetre thickness on silcrete surfaces, such as the patchy gloss and localised leaching, are unlikely to have survived the marine abrasion that must clearly have preceded the final interment of the silcrete and cannot be regarded as evidence for preceding subaerial exposure.

SUMMARY

The writer's observations at Hondeklip confirm the conclusions of previous workers that silcrete development and erosion are among the earliest events preserved in the coastal plain record. The presence of silcrete clasts in marine gravels is an ubiquitous feature of the Namaqualand coastal plain. There is little doubt that the silcrete at Hondeklip mine is silicified basal kaolinitic deposit and that the most of the silcrete clasts in the overlying marine gravels are derived from the immediate area.

CHAPTER 7

SILCRETE PETROGRAPHY AND COMPOSITION

7.1 INTRODUCTION

Examples of silcrete from southern Africa have featured prominently in the literature on silcrete (e.g. Frankel and Kent, 1938; Mountain, 1952; Frankel, 1952; Smale, 1978, Summerfield, 1981, 1982, 1983a,b,c,d). The latter author has reviewed previous work on silcretes and has provided a synthesis based on extensive observations of southern African coastal-zone silcretes associated with weathering profiles, as well as arid-zone silcretes from the Kalahari. The Hondeklip silcrete will now be classified in terms of the petrographic and geochemical criteria proposed by Summerfield (1983a,c). The chapter is concluded with a discussion on aspects of silcrete fabric and near-surface silicification.

7.2 SILCRETE PETROGRAPHY

DESCRIPTION

Thin-sections of examples of massive silcrete reveal that the grains present are almost entirely quartz with mainly undulose extinction. Other detrital mineral grains present are sub-angular to sub-rounded, opaque, ore grains and sub-euhedral to rounded, high-relief, zircon grains, each at ~1%. The quartz grains vary in size from very coarse sand to silt (very poorly-sorted), but are mainly medium to fine sand-size (Plates 7.1-7.5). Although the percentage of grains can be quite high (up to ~80% by visual estimation), the grains are mainly floating in the matrix, forming a wackestone (or quartzwacke) (classification according to Pettijohn (1975), p. 211). The massive silcrete has markedly non-uniform distribution of grains (Plates 7.1-7.5), with areas up to several millimetres across containing only a few floating grains (Plate 7.4). These matrix-rich areas correspond to the irregular "mud clots" seen on close inspection in the field and in hand specimen. Furthermore, the distribution of grain-sizes may be non-uniform, with some areas containing mainly fine grains, others larger grains (Plates 7.2-7.5). Some grain clusters originate from larger grains that have been brecciated, with displacement of the fragments (Plate 7.6). In many places there is an expression of "lines" of grains, as if dragged by a viscous flow during some incomplete mixing process (Plates 7.2, 7.3). This effect is more noticeable for the coarser grains, but "swirls" also occur in areas of finer grains and fine quartz particles, generated at diffuse grain boundaries, sometimes trail away into the matrix.

Grain shapes are mainly sub-angular, although very angular and well-rounded grains do occur. Embayed grains and indefinite grain boundaries are ubiquitous. The latter are best described as "spongy" or "hazy" (Plate 7.6, 7.7) rather than "dusty", to avoid possible confusion with "dust lines" commonly found preserving the pre-existing grain boundaries of overgrown quartz grains.

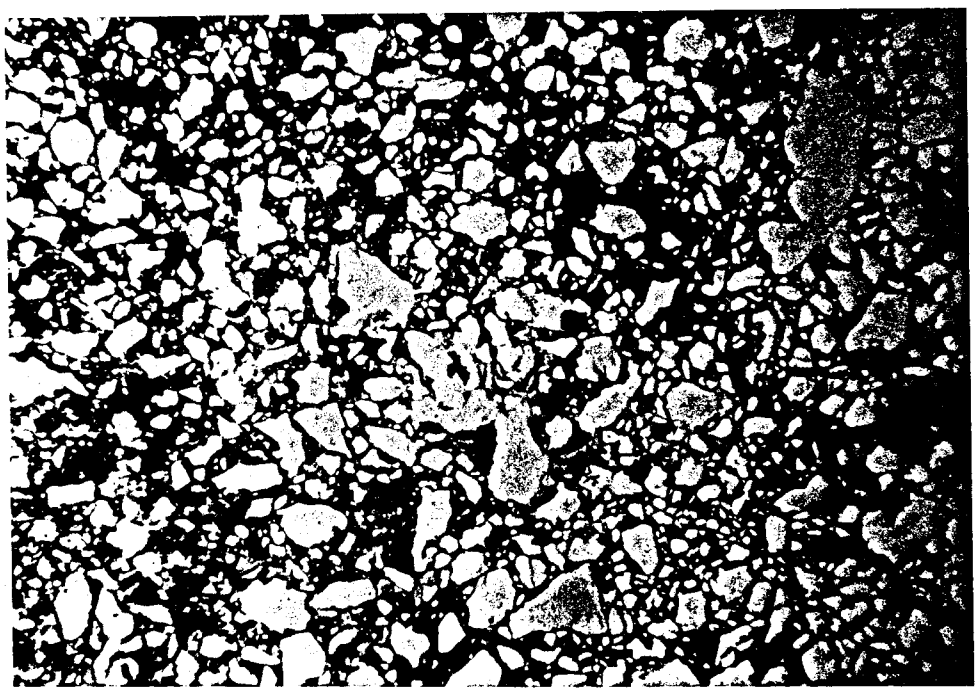

Plate 7.1 Massive silcrete, showing poorly-sorted quartz grain population. PPL, field of view is 6 mm wide.

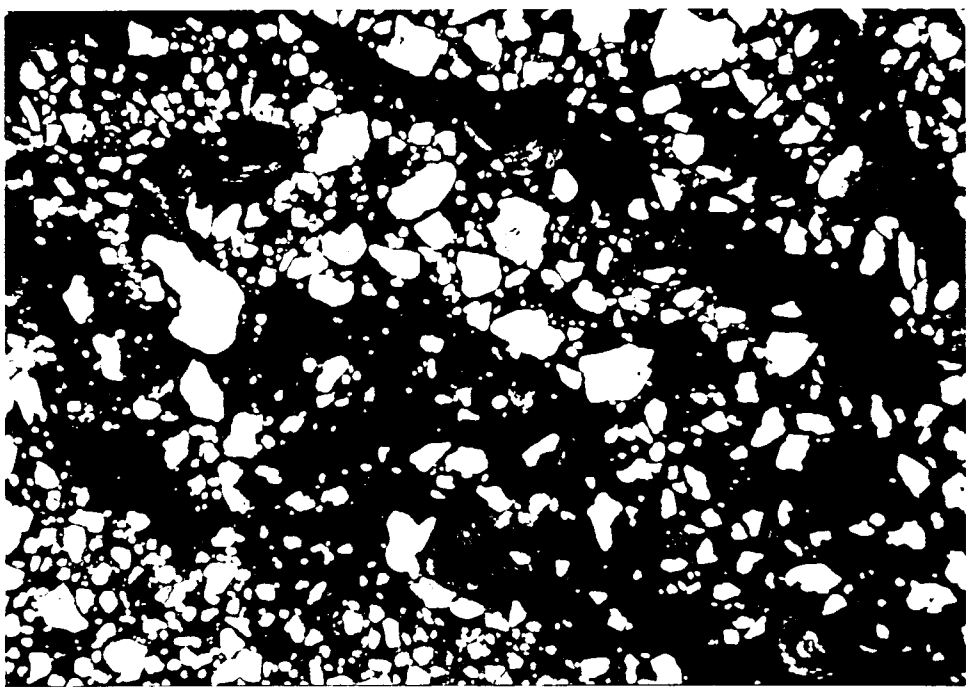

Plate 7.2 Massive silcrete, showing quartz grains arranged in irregular streaks. PPL, field of view is 6 mm wide.

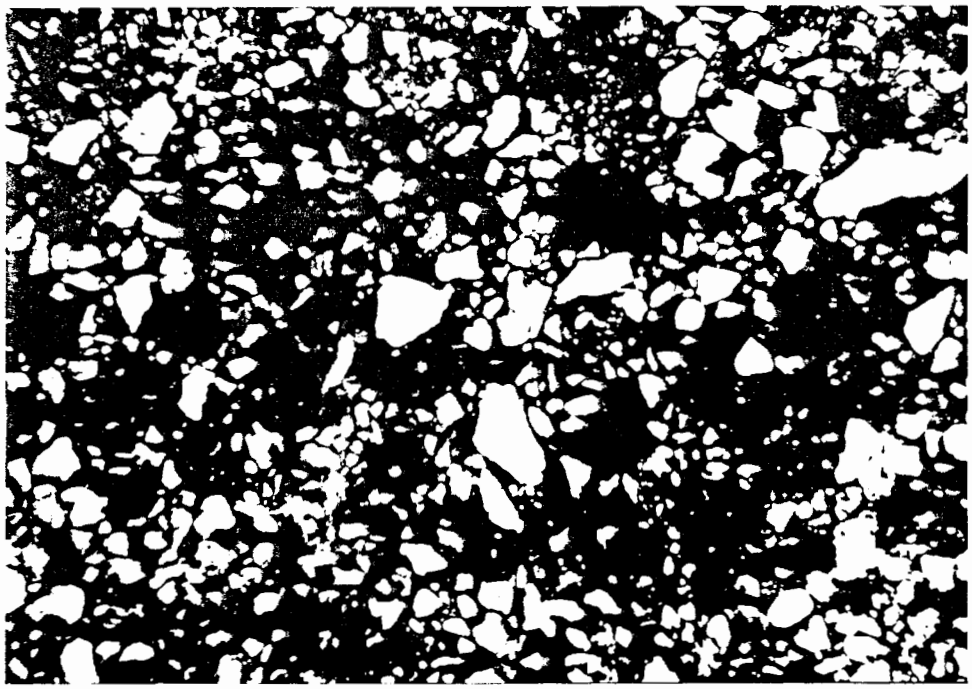

Plate 7.3 Massive silcrete, showing portion with circular areas of matrix. PPL, field of view is 6 mm wide.

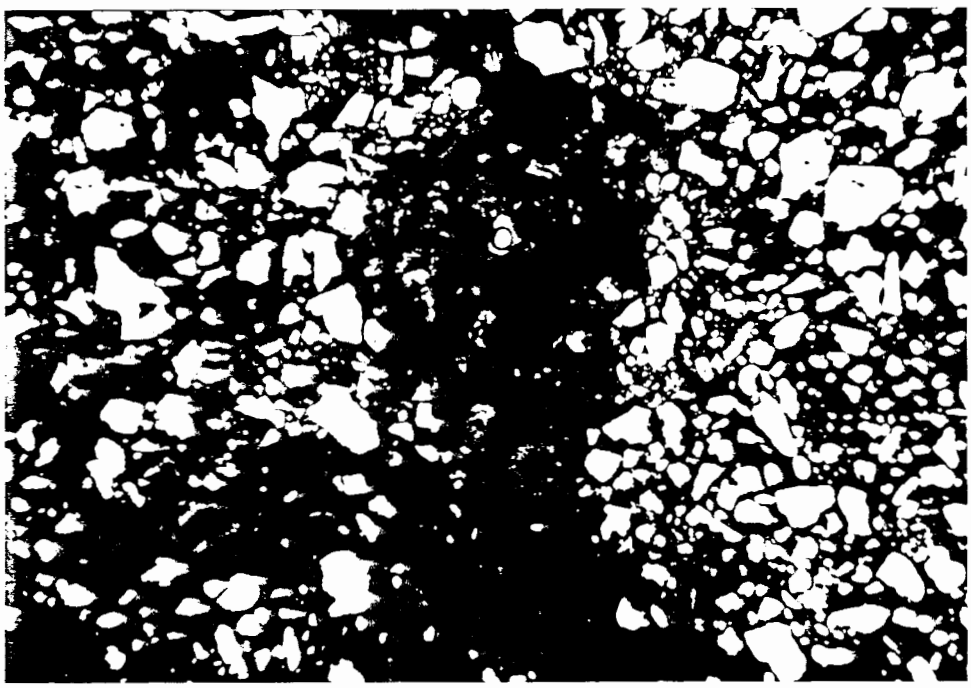

Plate 7.4 Massive silcrete, showing matrix-rich area with colloform features and a void (lower centre, with bubble). PPL, field of view is 6 mm wide.

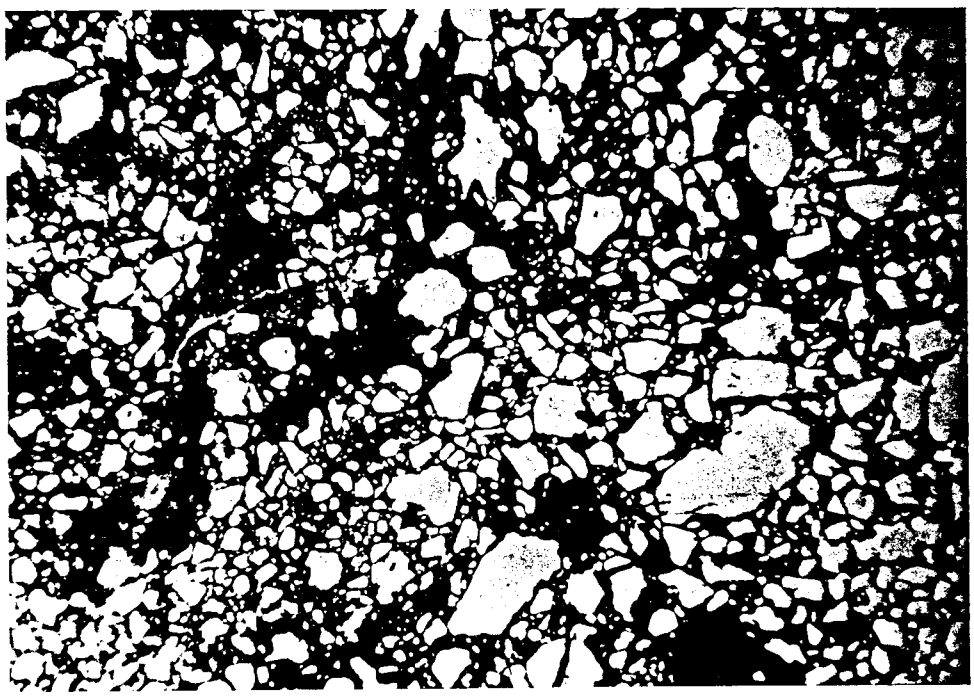

Plate 7.5 Massive silcrete, showing streak of quartz grains with relatively more interstitial quartz silt (lower left) and well-rounded grain (upper right). PPL, field of view is 6 mm wide.

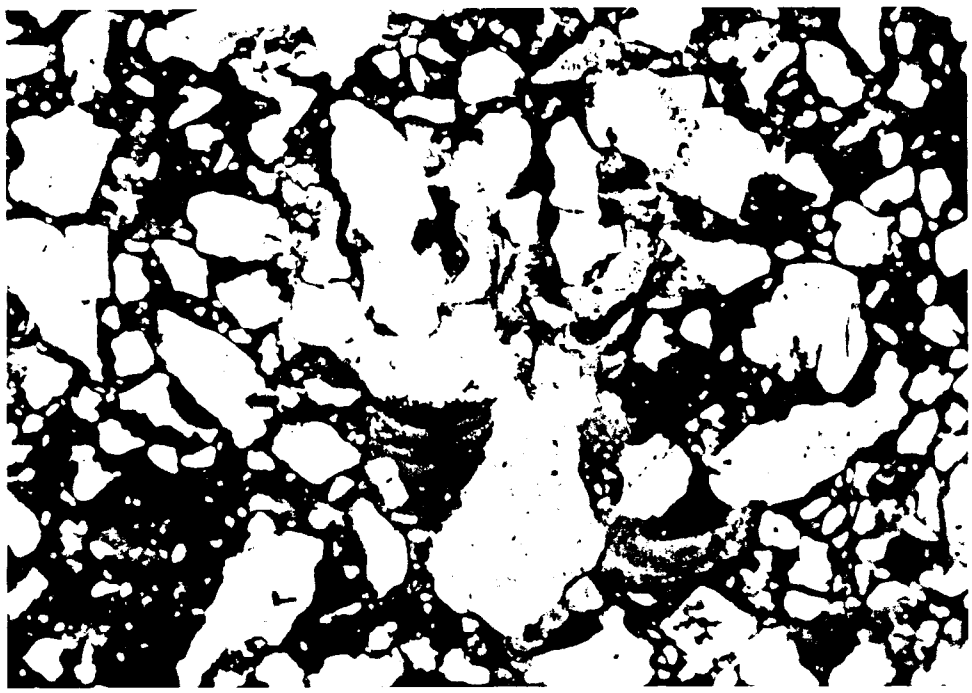

Plate 7.6 Massive silcrete, showing brecciating grain (centre), indefinite grain boundaries and colloform features. PPL, field of view is 2.5 mm wide.

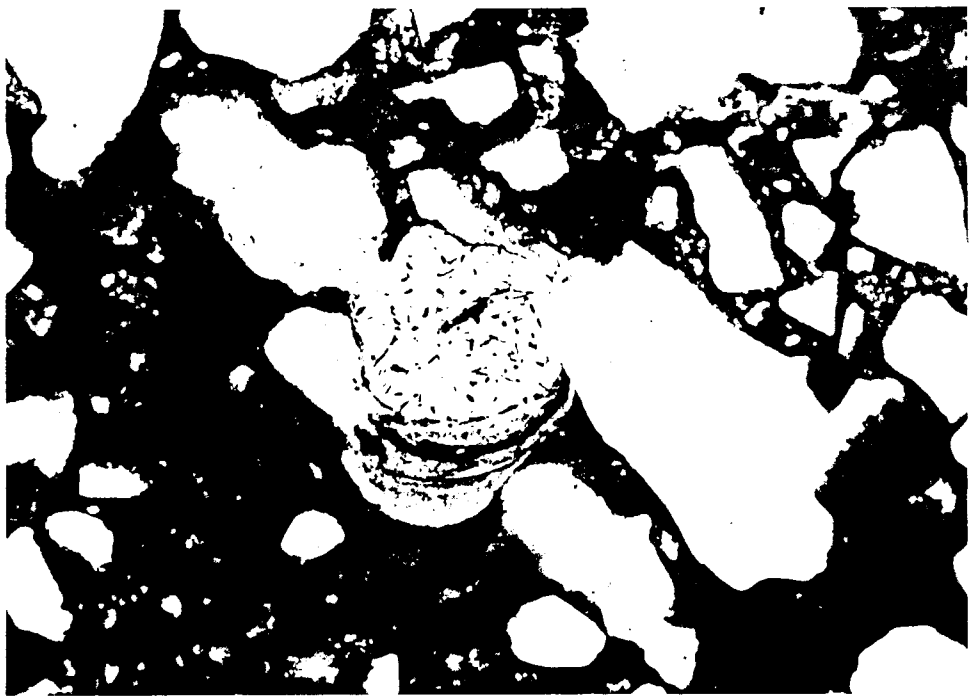

Plate 7.7 Massive silcrete, showing empty void above colloform feature. PPL, field of view is 1 mm wide.

The "spongy" grain boundaries evidently consist of clay-size quartz at the limits of resolution and appear to have been produced by disintegration/dissolution of grain surfaces. Optically continuous overgrowths on quartz grains are completely absent in this silcrete.

Under RL, the sectioned matrix is mainly yellow-brown in colour with clearer, translucent, arc-shaped areas and "cracks" of orange hue (Plate 7.8). Mottles of grey-coloured matrix occur particularly in association with laminated, colloform features in matrix-rich areas (Plate 7.9). However, grey matrix can be generally developed, as evident from entirely grey hand specimens. Grey mottling may have boundaries defined by abrupt colour change, but gradational colour changes also occur. Dark yellow and reddish, Fe-oxide rich matrix is often present around opaque grains, indicating alteration and reaction with the surrounding matrix.

With PPL, the matrix is a mottled dark brown and consists of finely-divided, brown "dust" and speckles between transparent material and silt to clay-size quartz grains (Plate 7.7). Darker areas of more homogeneous texture and reddish-yellow hue occur, these representing greater concentrations of Fe-oxide. Under crossed polarizers the matrix is slightly anisotropic. Together with the results of X-ray diffraction (reported below), indicates that the apparently opaline, amorphous matrix is in fact cryptocrystalline quartz, with the crystallinity beyond the range of standard optical resolution.

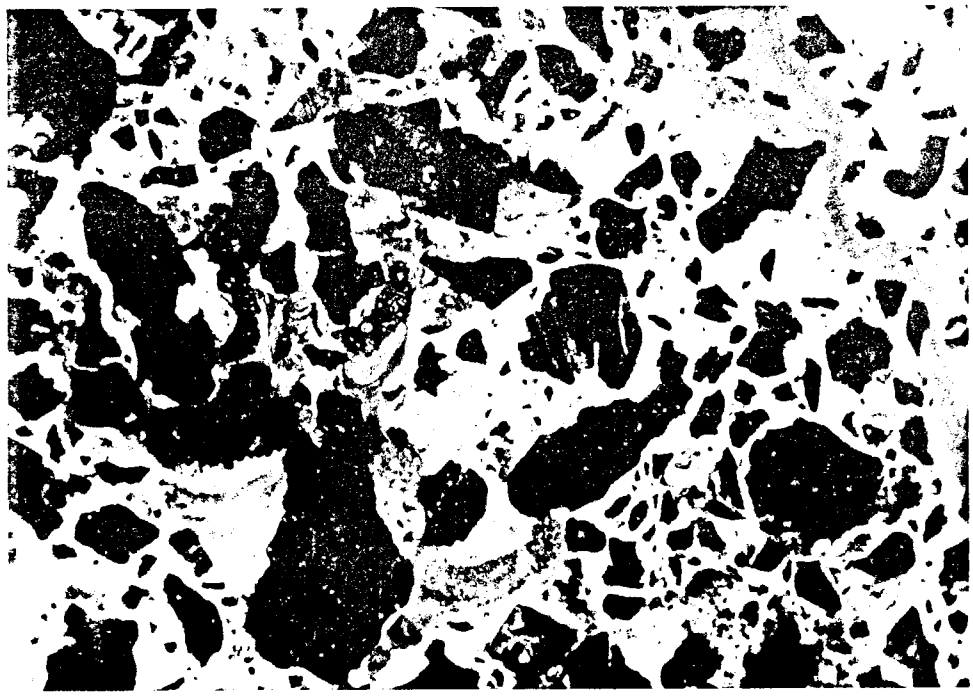

Plate 7.8 Massive silcrete, showing colour of matrix and crack infill (right) in RL. Field of view is 2.5 mm wide.

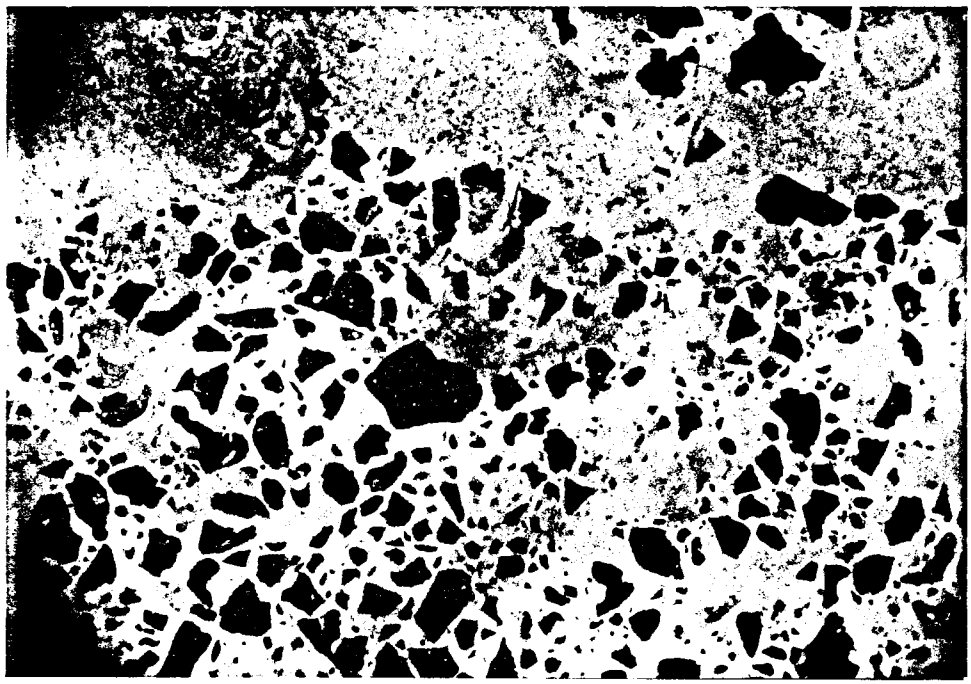

Plate 7.9 Massive silcrete, showing grey-coloured matrix with colloform features (upper half). RL, field of view is 6 mm wide.

In more transparent patches in the matrix (Plates 7.7, 7.10), associated with the colloform features described below, minute crystals of quartz 1-5 µm in size are visible (Plate 7.11) and these are therefore microcrystalline areas (crystals smaller than 20 µm).

The grey mottles (under RL) are very dark brown under PPL (Plate 7.10) and contain tiny, apparently isotropic, black grains generally up to 10 µm in size, as well as black, diffuse patches that represent concentrations of the same material (Plate 7.11). The grains have irregular boundaries and have a finely "fluffy" aspect and appear to be authigenic in origin (Plate 7.12). They are considered to be carbon, due to their resemblance to the carbon spherules observed under magnification in the basal kaolinitic sediments (Plate 5.4) and the presence of grey residue from HF dissolution of silcrete that reacts with H_2O_2 and presumably contains carbon.

Concave-up, nested, micro-lamination occurs abundantly in the matrix between grains and characterizes matrix-rich areas (Plates 7.6-7.13). These features are identical to those called colloform features in silcretes described by Summerfield (1983a). The laminae are defined by alternating lighter and darker hues, indicating episodes of "clean" quartz precipitation as crystals ~3 µm in size, separated by intervals of "dirty" cryptocrystalline quartz with varying concentrations of carbon and Fe-oxides. These features are up to 1 mm in diameter and several millimetres in length. Much smaller versions of such structures ~0,05 mm in diameter are also present outside the grain-poor areas, between the more densely packed grains. They have a generally common orientation (concave-up) and are therefore geopetal features, but occasional examples are more oblique to the overall orientation. The lamination of such "sideways" infills is asymmetric, the longer arms of the concave laminae overlying the floor of the cavity. Episodes of dissolution and subsequently continued precipitation are evident in cross-cutting colloform features (Plate 7.10).

Late-stage voids seen on the scale of thin sections are much less than 1% of the section, occur in both grain-rich and matrix-rich areas and have mainly smooth outlines (e.g. Plate 7.7). Voids often occur at the top of colloform features (Plate 7.7). Cavities may also occasionally occur in the Fe-oxide-filled cracks. Most voids do not have obvious linings or partial fillings. Rare examples are rounded by concentric micro-lamination of Fe-oxide-rich material and a small void observed at the top of a colloform feature was incompletely infilled with dark yellow, Fe-oxide-rich matrix.. It is probable that similar loose fillings were lost during thin-section preparation. The largest authigenic quartz crystals observed were in a "palisade" of megaquartz crystals 30-50 µm in length, completely filling a void at the top of a colloform feature beneath a composite quartz grain (Plate 7.13). In the other, second example, also involving a colloform feature pendant on a closely overlying quartz grain, quartz crystals ~25 µm long had grown down from the overhanging quartz grain.

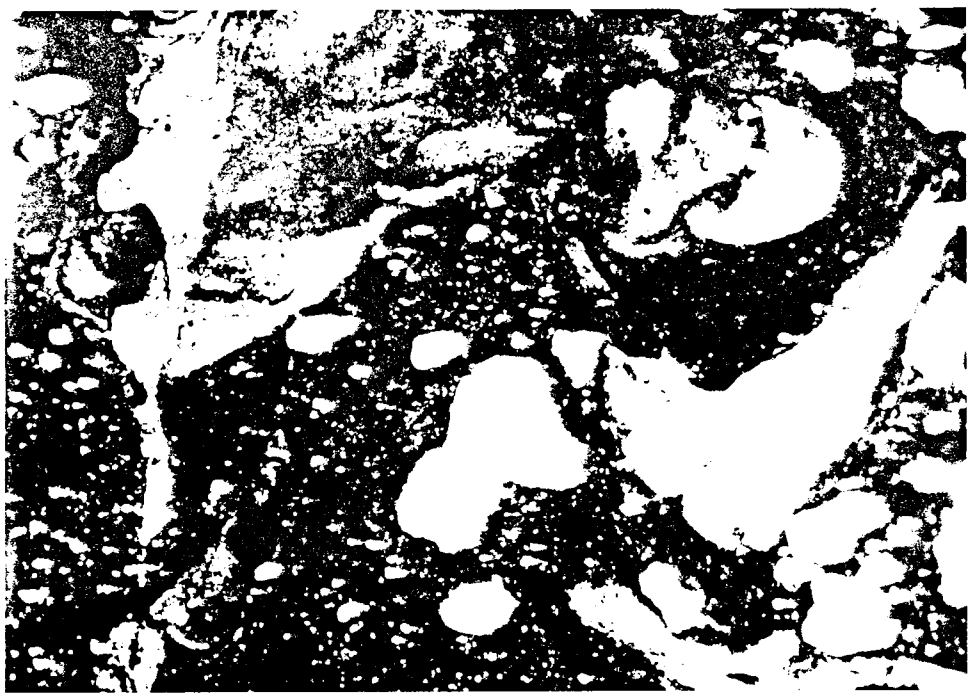

Plate 7.10 Massive silcrete, matrix-rich area with "clean" microquartz colloform features and cross-cutting relationship (left) . PPL. Field of view is 2.5 mm wide.

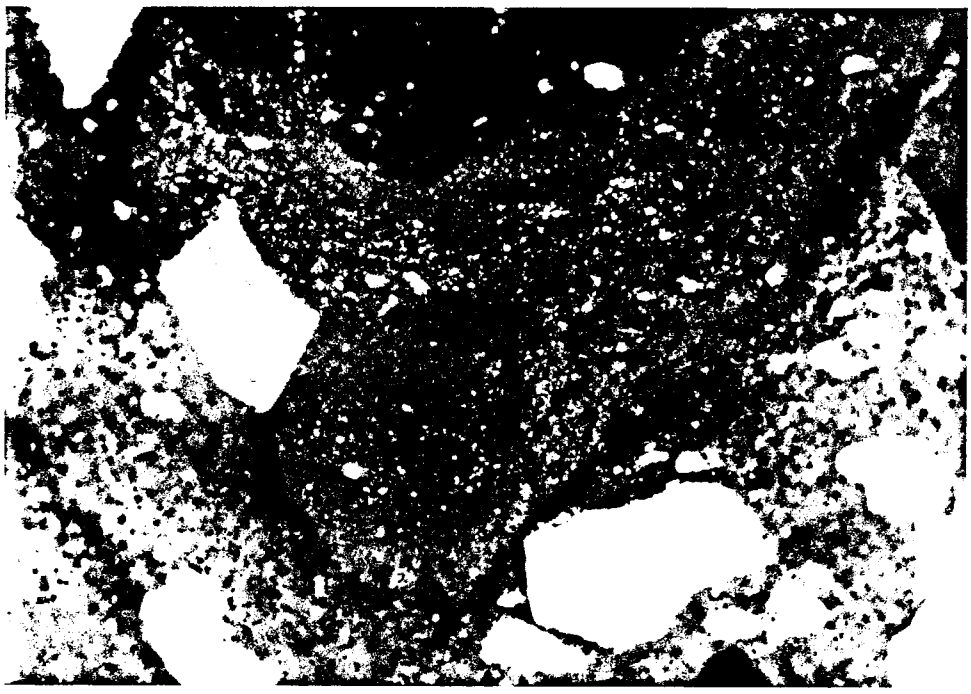

Plate 7.11 Massive silcrete. Detail of previous (lower right), showing "clean" microquartz infill and finely-disseminated Fe-oxides/clay in surrounding matrix. XPL, field of view is 1 mm wide.

Plate 7.12 Massive silcrete. Detail of previous. Black grains are probably carbon. PPL, field of view is 0.25 mm wide.

Plate 7.13 Massive silcrete, showing colloform feature below polycrystalline quartz grain and megaquartz filling of the void. XPL. Field of view is 1 mm wide.

Cracks are up to ~50 µm wide and their dark yellow to reddish hues indicate that Fe-oxides and clays are concentrated along them. The cracks are best observed under a combination of PPL and RL, as the opacity of the matrix under transmitted light alone makes it difficult to follow them (Plate 7.8). Most cracks are defined by the colour of the infill, with wall boundaries that are vague under higher magnification, suggesting welding or annealing with the matrix. These yellow cracks usually terminate by fading away into the matrix as their defining colour becomes diffuse. One example of a crack was filled with matrix and quartz silt that had filtered down it (Plate 7.14), suggesting a pre-lithification origin, with the final infill consisting of Fe-oxide-rich material.

Less common are cracks with microcrystalline linings and one example with a micro-quartz infilling was observed. The cracks skirt grains and only one instance of a cross-cut quartz grain was seen. No preferred orientation could be discerned. The largest crack noticed was infilled with a pale, greenish-brown cement embedding quartz, feldspar and glauconite grains (Plate 7.15), representing the penetration into the crack of the phosphorite coatings noticed in the field.

The suggestion of nodule development, seen megascopically, is not evident in the thin sections. Under the naked eye, in one section, an elliptical feature ~6 mm in length appeared to be a nodule, but under the petrographic microscope it was obscure due to the lack of a definite boundary, being revealed as a general crowd of grains partly with darker matrix and partly defined by the "trails" of roughly segregated grain size mentioned previously.

The thinly-bedded silcrete from B Block, in thin section, has very fine to medium-sized quartz grains that are evenly distributed in the matrix (Plate 7.16). The matrix lacks large grain-poor areas and colloform features. Relict sedimentary fabric is evident in linear concentrations of coarser grains cross-cutting the bedding-normal section, indicating ripple cross-lamination. The partially indurated, coarse-grained material from B Block has abundant colloform features in the matrix and strongly resembles examples of massive silcrete petrographically (Plates 7.17, 7.18), but cracks and voids lacking fillings of Fe-oxides/clays are more common. Importantly, multiple deposition of colloform lamination is very evident, together with indications of sharp "unconformities" and of collapse and rotation of pieces of colloform matrix (Plate 7.17).

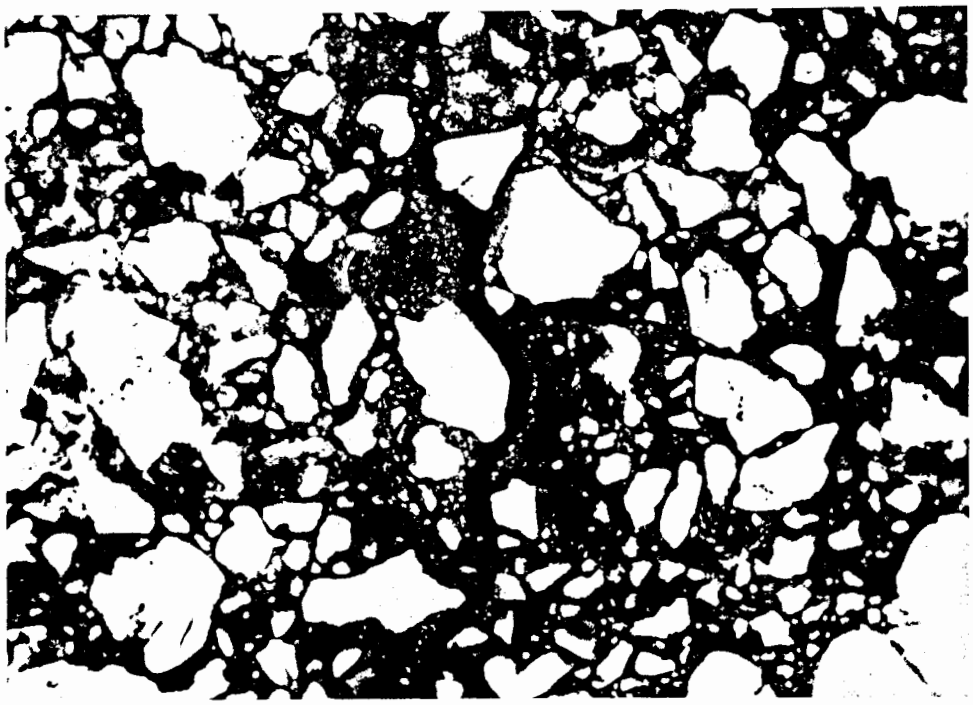

Plate 7.14 Massive silcrete, showing crack with infiltrated, silty matrix and final Fe-oxide-rich infill. PPL, field of view is 2.5 mm wide.

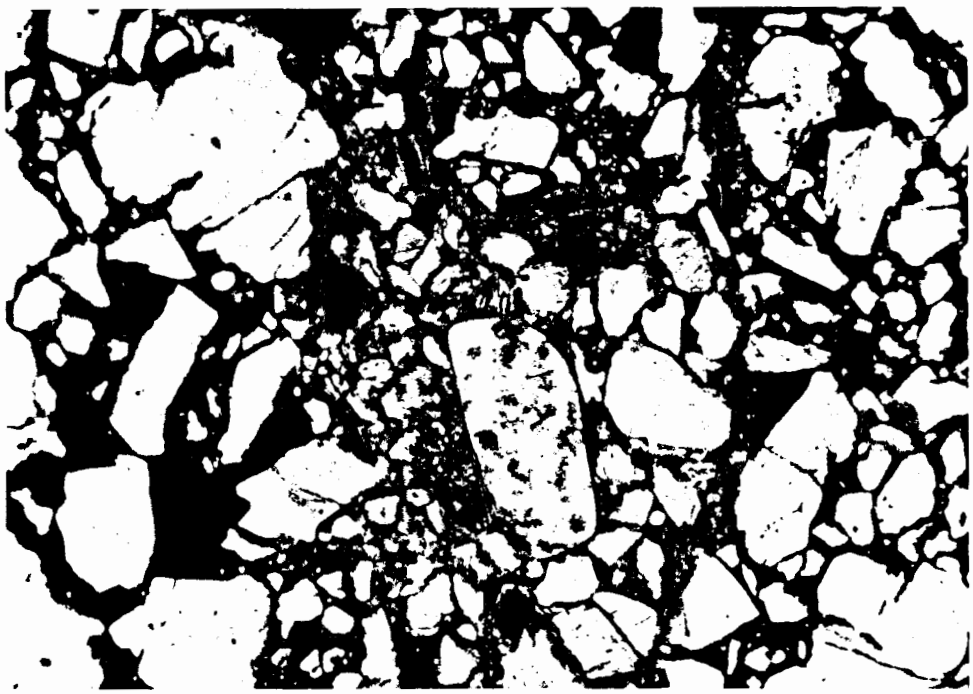

Plate 7.15 Massive silcrete, showing post-lithification crack filled with collophane-cemented marine sediment (phosphorite). PPL. Field of view is 2.5 mm wide.

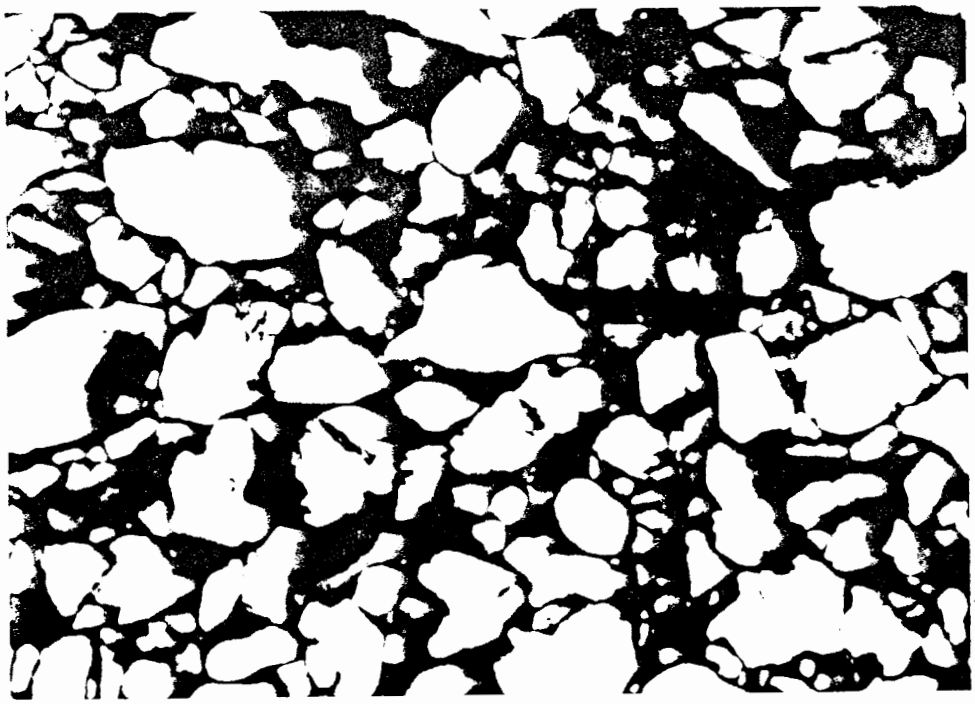

Plate 7.16 Bedded silcrete, showing uniformly-distributed quartz grains and suggestion of sedimentary texture. PPL. Field of view is 2.5 mm wide.

Plate 7.17 Partially-indurated silcrete, showing matrix-rich area with several generations of colloform features. Note unfilled cracks (top and lower right). PPL, field of view is 2.5 mm wide.

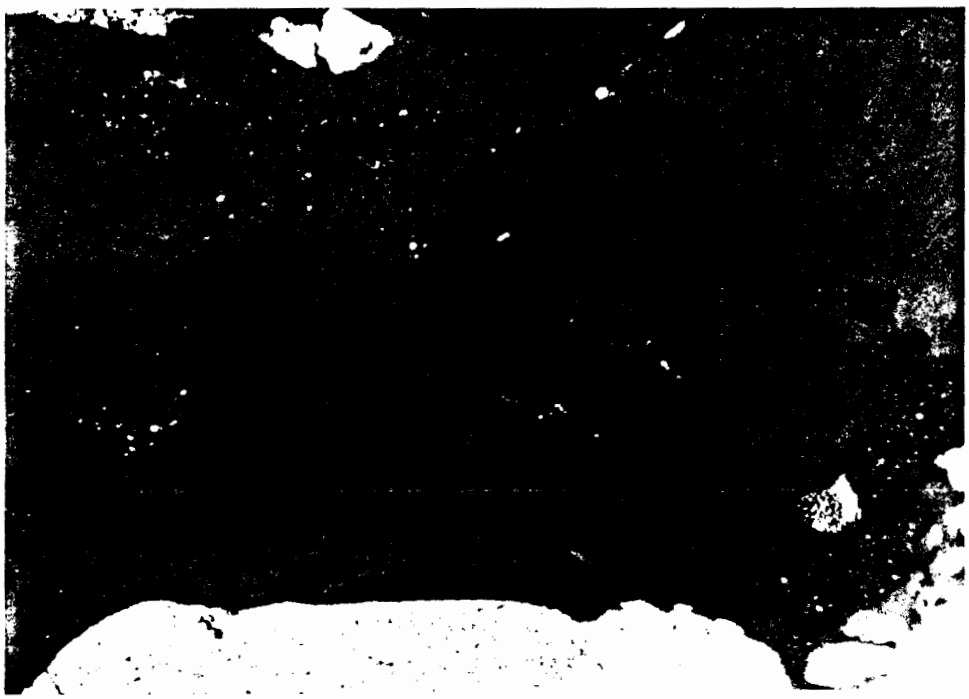

Plate 7.18 Partially-indurated silcrete. Previous view under XPL, field of view is 2.5 mm wide.

Scanning electron microscope observations

High magnification of a fresh chip of Hondeklip silcrete reveals the finely granular nature of the microcrystalline matrix material between the conchoidal surfaces of fractured detrital quartz grains (Plate 7.19a). The microcrystals range in size from less than 1 µm, up to ~5 µm, and their crudely polygonal, interlocking pattern is seen on the surfaces of moulds of dislodged detrital grains(Plate 7.19b). Many silt-size quartz grains in the matrix have irregular surfaces (Plate 7.19b). The microcrystallinity within colloform feaures is markedly smaller than in the general matrix, being ~0.5 µm (Plate 7.19c, d), with some laminae consisting of coarser crystals (Plate 7.19e). Etching of the silcrete chip in concentrated HF for 10 minutes does not appreciably alter the appearance of the micro- to cryptocrystalline matrix (Plates 7.19f,g), but does bring out the micro-lamination within colloform features (Plate 7.19h). The nature of the green pan silcrete is quite different from the Hondeklip silcrete, with a fibrous-looking matrix (Plate 7.19i) composed of "sheaves" of blade-shaped crystals typical of opal-CT (Plate 7.19j).

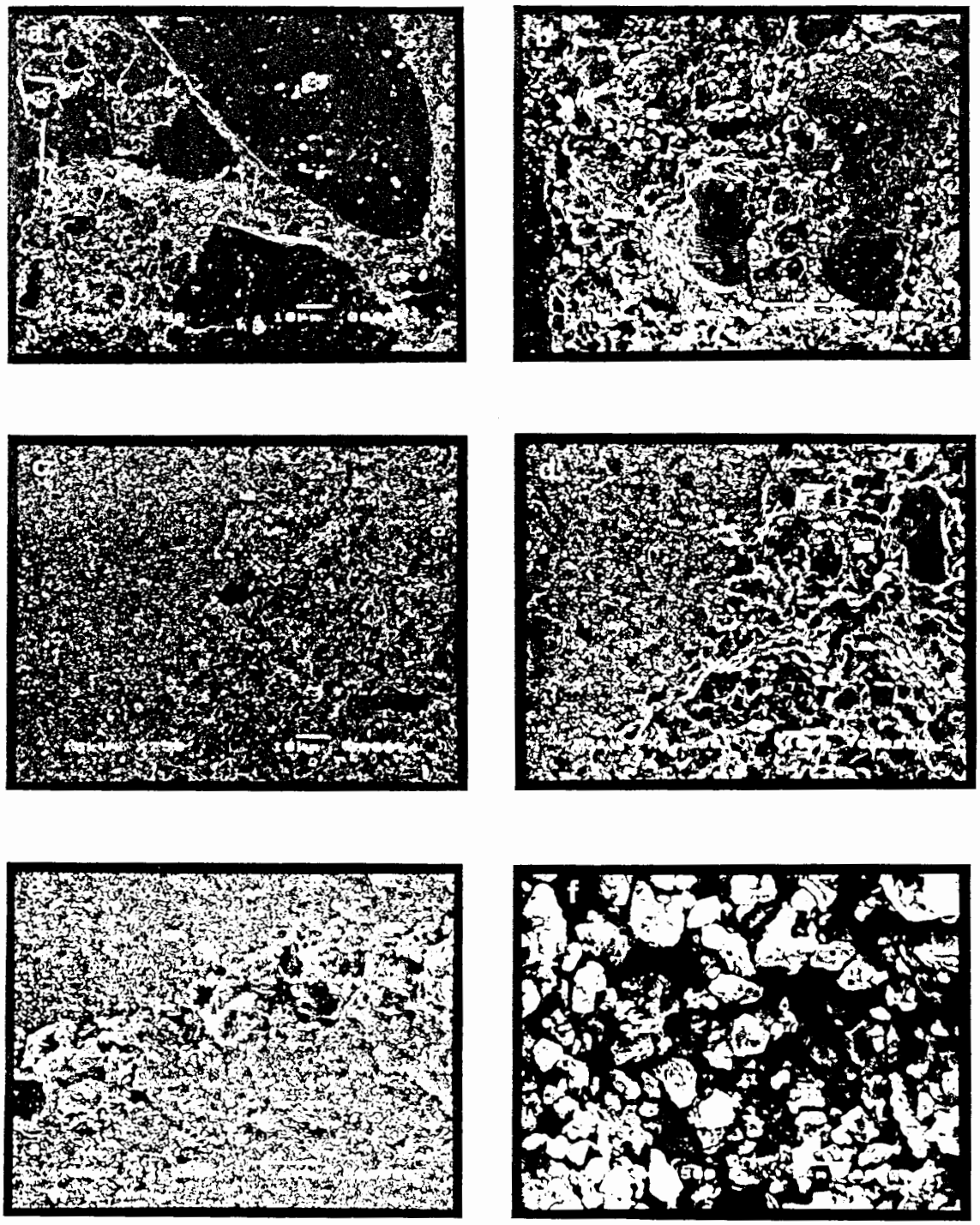

Plate 7.19 SEM photomicrographs of silcrete. **a–h**, Hondeklip massive silcrete. **i–j**, opaline, green pan silcrete, SE of Kleinzee. **a**, general view, showing sand and silt grains in microcrystalline matrix. X750. **b**, detail of matrix. Note triangular grain mould surface (right). X2000. **c**, boundary between general matrix (right) and matrix in colloform feature (left). Note simple voids. X750. **d**, detail of boundary of colloform feature (left), showing contrast in crystallinity. X1500. **e**, more coarsely-crystalline micro-lamination in colloform feature. X2000. **f**, appearance of general matrix after etching in HF. X7500.

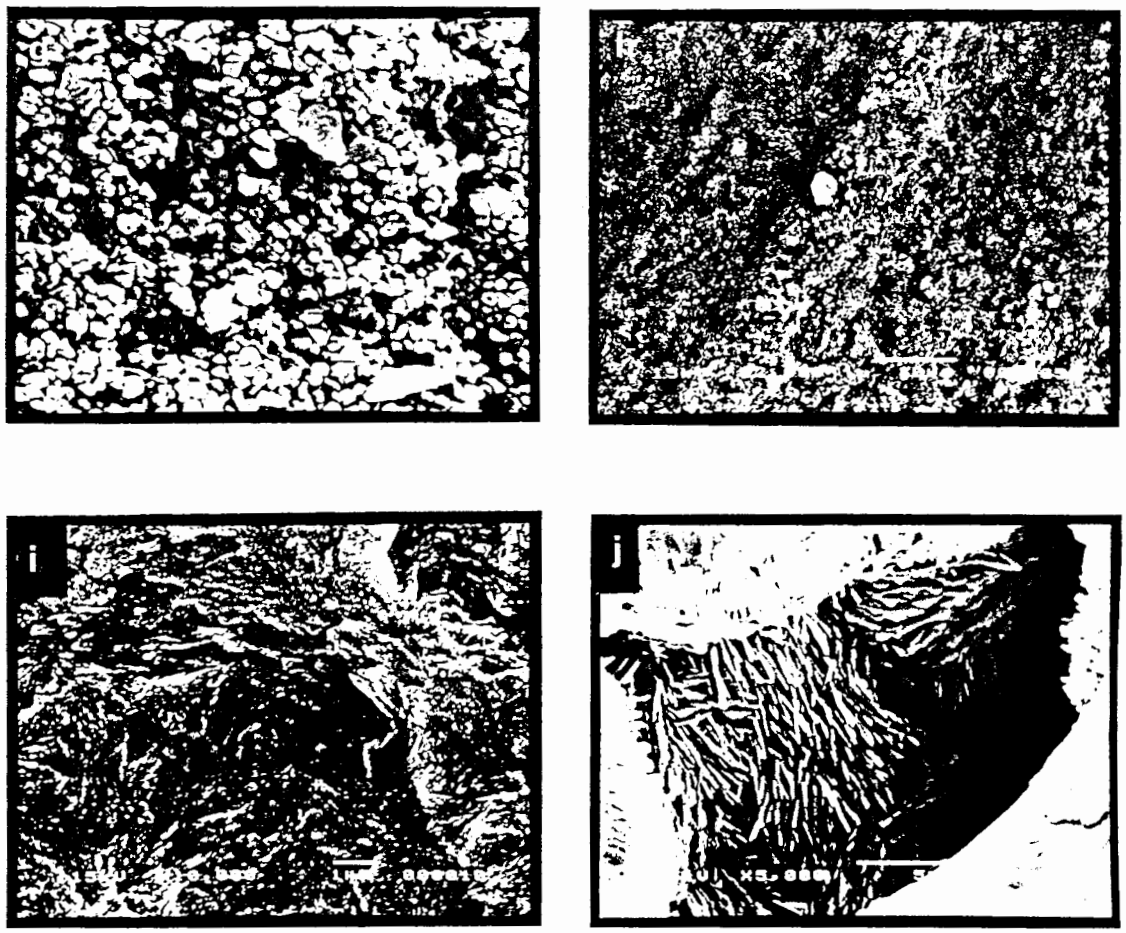

Plate 7.19 cont. **g**, appearance of matrix in colloform feature after etching. X10000. **h**, the micro-lamination in a colloform feature, revealed by etching. X2000. **i**, fracture surface of opaline, green pan silcrete, showing fibrous appearance. X10000. **j**, interior of small, unlined void in green pan silcrete, showing bundles of bladed crystals of opal-CT. X5000.

Discussion

The presence of rounded, detrital grains of quartz, opaques and zircon, indicates that all silcrete thin sections examined consist of silicified, basal kaolinitic sediment. The quartz grains have been modified by dissolution (embaying and small-scale disintegration of grain boundaries) and at least some edge-rounding is attributable to this etching. The "spongy" quartz-grain boundaries suggest that a portion of the fine silt and clay-size quartz in the matrix has been generated by dissolution prior to or during silicification. That these fine quartz particles generated at "spongy" grain boundaries "trail" into the surrounding matrix in some instances favours a dissolution origin rather than that "spongy" boundaries represent nucleation of quartz on skeletal grains. Some coarse grains have undergone brecciation, further indicating grain-modification processes prior to or during silicification. Brecciation indicates displacive processes and this observation is allied to the evidence of small-scale, local

rotation of elongate grains to common orientations, "grain trails" and size segregations (Plates 7.1-7.6). The cross-cutting, colloform pore fills attest to an active matrix in which pore spaces were both being filled and were forming penecontemporaneously.

The variation in the matrix is mostly due to variation in the concentration of finely-divided, optically-indeterminate materials, evidently mainly Fe-oxides and/or clay, whilst carbon apparently accounts for grey mottles. Chalcedony (fibrous, cryptocrystalline quartz) was not observed and megaquartz (crystal width >20 μm; terminology in Summerfield, 1983a, p. 897) is very rarely developed. The most definite boundaries within the matrix are the colloform laminations and in these features the more crystalline, transparent laminae consist of microquartz. Observations by SEM reveal that the smallest crystal sizes(<1 μm) (cryptocrystalline) occur in colloform features. The crystal size in the coarse laminae in colloform features is comparable that of the general matrix. The general matrix is therefore also microquartz, but in thin section this is obscured by the impurities. There are no clear indications of sites of early nucleation or nodule development, but the colloform features are evidence of both interrupted (cross-cutting) and rhythmic development (lamination). Colloform features clearly represent the infillings of voids and their occurrence in the partially indurated silcrete rock suggests that they are not particularly a late-stage development, but are cavities intermittently infilled throughout the silicification process. This infilling may eventually be arrested, as suggested by the voids that were found in indurated silcrete above colloform features. Most crack infilling seen in thin section is a later-stage phenomenon, but the cracks rarely cross-cut detrital quartz grains and their indefinite boundaries indicate that silica was still mobile during and/or subsequent to their formation. The open cracks, such as the example filled with the younger marine phosphorite, are probably very late or post-induration.

7.3 BULK MINERALOGY AND CHEMISTRY

X-Ray Diffraction Analyses

X-ray diffractograms of samples of crushed bulk silcrete (e.g. Fig. 7.1) are dominated by the alpha-quartz peaks and the remaining peaks are of much lower intensity relative to quartz. The quartz d[212] peak at 67,76° 2 is well-developed, indicating well-crystallized quartz (Murata & Norman, 1976). There are no indications of the broad, low peak in the 18-25° 2Ø range attributable to opal-A, or of the cristobalite peak at ~22° 2Θ. For the remaining peaks, the Search Index first generated anatase (TiO_2) as a possibility. In order to confirm the presence of anatase, chips of crushed silcrete were place in HF until they had disintegrated, but not dissolved. The detrital, sand-size quartz grains were separated by filtering using nylon cloth and the mud fraction rinsed, dried and analysed by XRD. The result was improved definition of the main anatase peaks (Fig. 7.1), but considerable quartz is still present in the mud fraction.. The remaining peaks are attributable to zircon and rutile. Curiously, the presence of ilmenite and magnetite is not overt, although in certain runs some "blips" occurred in the background at appropriate positions. This is consistent with the alteration of ore minerals seen in thin section. The rutile and anatase content would have been produced by the breakdown of ilmenite ($FeTiO_3$) to leucoxene, an amorphous aggregate of TiO_2 minerals.

A sample of partially-indurated silcrete also produced the major quartz peaks, but at slightly reduced intensities, whilst anatase is slightly better resolved (Fig. 7.2). For comparative purposes, green silcrete capping a low hill southeast of Kleinzee was also analysed. The outcrop represents topographic inversion of an ancient pan. It yielded an X-ray diffractogram characteristic of opal-CT (Jones and Segnit, 1971) (Figure 7.2), but the presence of detrital quartz exaggerates the maturity of the opal. Opaline nodules associated with the rim of an ancient, buried pan carbonate in the study area yielded a diffractogram indicating a more disordered opal-CT composition (Figure 7.2).

The X-ray-diffraction (XRD) analyses indicate that amorphous opal (opal-A) and opal-CT (cristobalite & tridymite) are not present in the Hondeklip silcrete and that the bulk mineralogical composition is quartz and anatase, although anatase is not obviously optically identifiable. Summerfield (1983c) reports that anatase occurs as microcrystalline, brown, earthy aggregates, concentrations of which are betrayed by darker colour in the matrix.

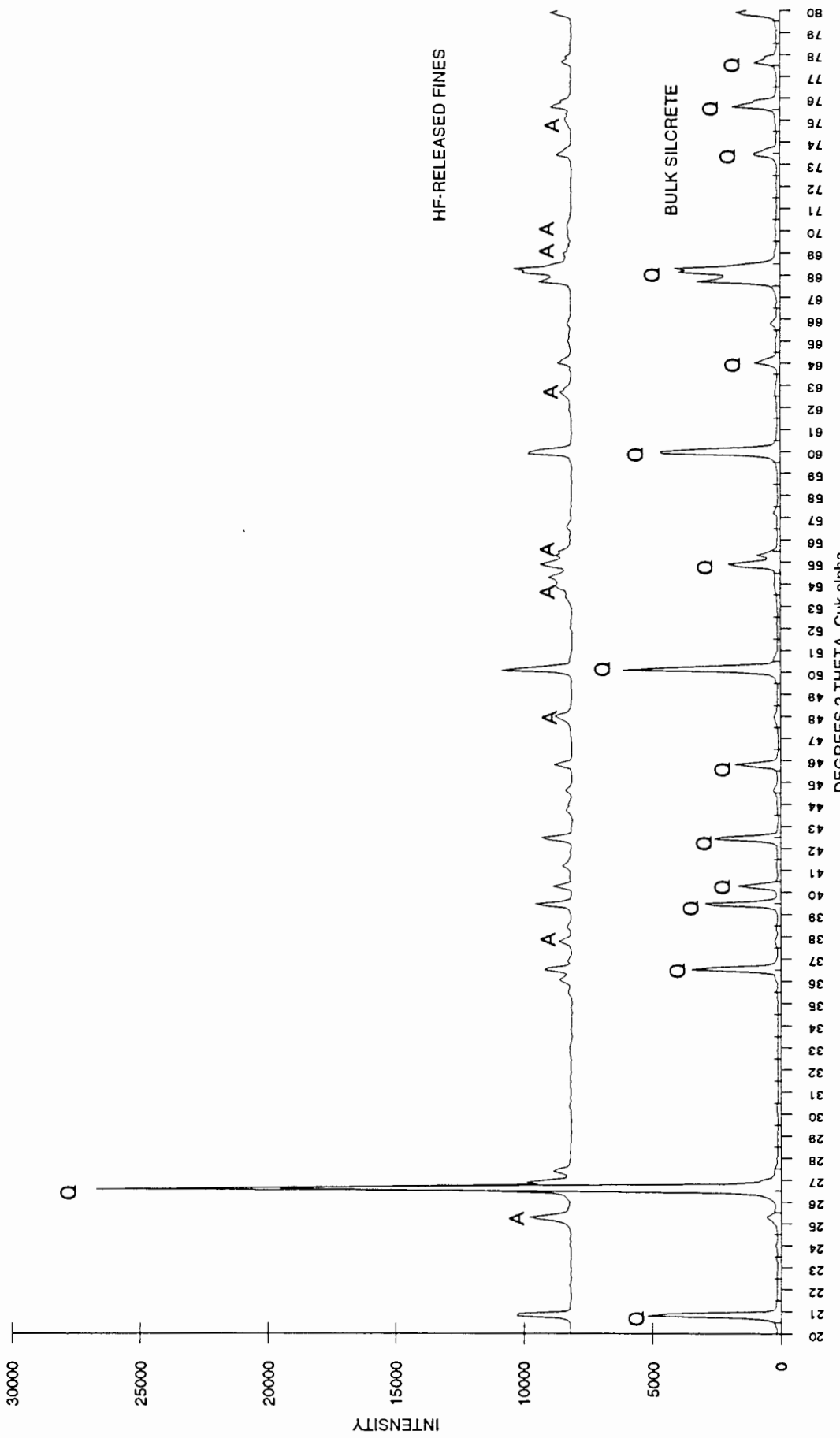

Figure 7.1 X-ray diffractograms of bulk silcrete and fines from HF-disaggregated silcrete. Q=quartz, A=anatase.

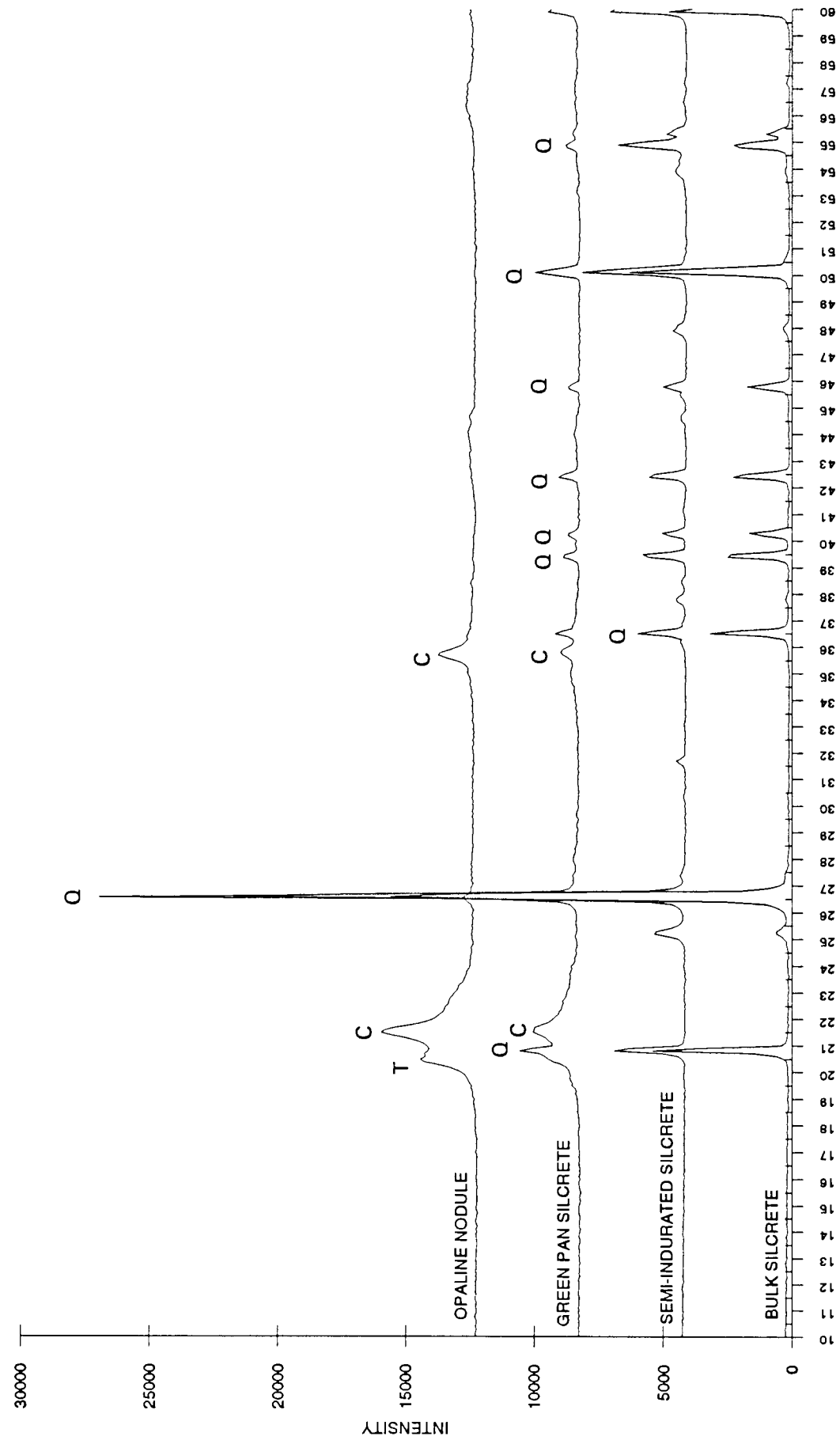

Figure 7.2 Comparative X-ray diffractograms of microcrystalline and opaline silicification. Q=quartz, C=cristobalite, T=tridymite.

X-RAY FLUORESCENCE ANALYSES

Bulk chemical X-Ray fluorescence (XRF) analysis of basal kaolinitic sediment, partially-indurated silcrete and the crushed silcrete yielded the results shown in Table 7.1. Relative to the kaolinitic sediment, SiO_2 and TiO_2 are noticeably enriched in the silcretes and Al_2O_3 is depleted. The higher MgO, Na_2O and K_2O contents of the kaolinitic sediment reflect the relict feldspar, whilst the low CaO content probably reflects its early removal due to the rapid breakdown of plagioclase.

Table 7.1 XRF analyses of basal kaolinitic sediment, semi-indurated silcrete, massive and bedded silcrete.

	1	2	3	4	5
	kaolinitic sed.	semi-indurated	mass. silcrete 1	mass. silcrete 2	bedded silcrete
SiO_2	82.26	90.99	92.49	94.14	90.68
TiO_2	0.97	4.37	2.17	3.29	4.38
Al_2O_3	8.91	0.32	0.26	0.28	0.31
Fe_2O_3	1.14	1.69	2.00	1.07	2.90
MnO	0.02	0.03	0.03	0.01	0.10
MgO	0.32	0.19	0.18	0.05	0.13
CaO	0.07	0.22	0.79	0.03	0.05
Na_2O	1.49	0.48	0.01	0.07	0.15
K_2O	1.49	0.04	0.06	0.04	0.06
P_2O_5	0.04	0.17	0.55	0.11	0.08
H_2O-	0.36	0.39	0.11	0.06	0.13
LOI	3.82	1.22	0.50	0.46	0.69
Zr (ppm)	1553	1137	----	1519	3637

The zirconium content is from detrital zircon. The relatively higher Zr, Fe_2O_3 and MnO content of the bedded silcrete (Col. 5, Table 3.1) reflects a higher concentration of detrital heavy minerals. The elevated presence of calcium and phosphorus in massive silcrete in Column 3 (Table 7.1) is due to contamination from the ingress of phosphorite into cracks in the silcrete.

7.4 SILCRETE CLASSIFICATION

FABRIC TYPE

The silcretes of southern Africa have been classified on the basis of petrography into four main fabric types by Summerfield (1983a):

C - (conglomeratic); detrital component includes pebbles.

GS - (grain-supported); skeletal grains (>30 µm) in self-supporting framework.

F - (floating); skeletal grains floating in matrix and forming more than 5% of rock.

F-fabric glaebular - glaebules present.
F-fabric massive - glaebules absent.

M - (massive); skeletal grains less than 5% of rock.

M-fabric glaebular - glaebules present.
M-fabric massive - glaebules absent.

The F and M fabric types are both subdivided into massive and glaebular subtypes depending on (respectively) the absence or presence of glaebules (nodules).

In terms of sandstone classification (Pettijohn, 1975, p. 211), the grain-supported, floating and massive silcrete types may be termed packstones, wackestones and mudstones, respectively.

The Conglomeratic (C) fabric type would apply to the pebbly portions of the silcreted basal deposit, but this is just a variation of the host lithology and has no separate genetic implication here. With a floating grain content greater than 5%, the Hondeklip silcrete is an F-fabric type or GS-fabric type. Since the dominant impression imparted by thin sections is of separated grains and some displacement, the Hondeklip silcrete should be regarded as basically of the F-fabric type. However, small areas in any one section may have a sufficiently dense grain population so as to verge on being grain-supported. As mentioned above, well-defined, markedly darker glaebules such as those figured by Summerfield (1983a) are absent in the thin-sections examined and larger glaebules are also not evident on freshly fractured silcrete surfaces. Although some of the resistant areas of silcrete on worn surfaces resemble nodules, overall the resistant areas are too vaguely defined and variable in shape to be considered as nodules *sensu stricto*. Thus the Hondeklip silcrete must be considered to be mainly the F-fabric type, massive subtype, with the C-fabric present locally and merely reflecting host lithology.

GENETIC TYPE

Summerfield (1983a,b) has also provided a basic genetic classification of southern African silcretes on the basis of stratigraphic settings, petrographic features and bulk geochemistry. Weathering-pro-

silcretes of the Cape coastal zone occur within or capping kaolinitic pallid zones, typically have colloform features and authigenic glaebules and are F-fabric or M-fabric types with skeletal grains reflecting both inherited characteristics and dissolution features. The matrix usually appears to be cryptocrystalline and XRD indicates that it is, in fact, well-crystallized. Void fills are usually restricted to thin microquartz linings, but when present are simple precipitates of microquartz or clay and sesquioxide accumulations. Geochemically, weathering-profile silcretes are titanium-rich (TiO_2 >1%) (Fig. 7.3), the TiO_2 enrichment occurring as authigenic anatase (Fig. 7.1).

In contrast, non-weathering-profile silcretes of the Kalahari are not associated with pallid zones, but involve silicification of aeolian, alluvial and pan sediments and calcretes. They lack colloform and glaebular features, but have complex vug fills, commonly consisting of sequences of chalcedony, microquartz (crystals <20 µm wide) and megaquartz (>20 µm wide), the occurrence of chalcedony being particularly diagnostic. They are titanium-poor (TiO_2 <0,2%) (Fig. 7.3).

The titanium-rich Hondeklip silcrete clearly resembles other silcretes in southern Africa that are also directly associated with kaolinitic weathering profiles (Fig. 7.3), as characterized by Summerfield's (1983a,b,c) criteria.

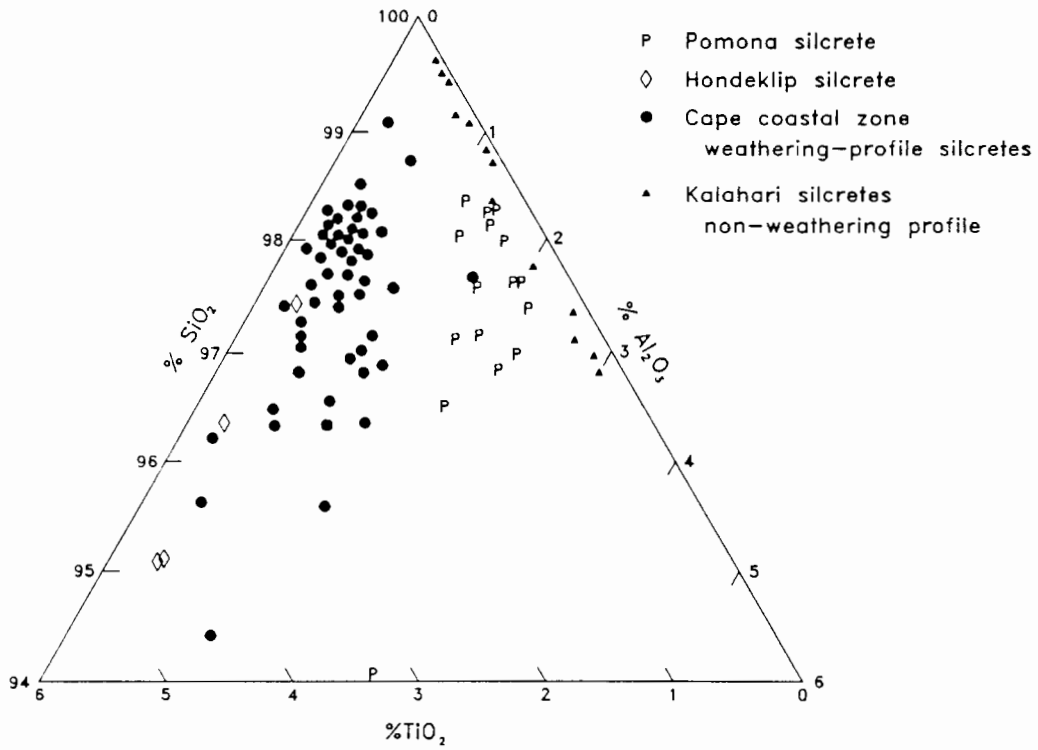

Figure 7.3 The silcrete ternary plot of Summerfield (1983b), with silcrete analyses from Hondeklip included.

7.5 DISCUSSION

Colloform Features

Colloform features, distinguished by their geopetal, nested character (Plates 7.6-7.13), are the main structures in the matrix of the Hondeklip silcrete. Colloform features were first noted in weathering-profile silcrete from Grahamstown by Frankel and Kent (1938). Summerfield (1983c) suggested that they indicate rhythmic precipitation of silica, Ti and Fe-oxides in voids in the developing silcrete, the concave-up laminations possibly arising from gravitational collapse of infilling, dehydrating silica gel. The voids may also be the result of dehydration shrinkage of silica gel, or perhaps are pedotubule features (Summerfield, 1983c). Alternate Ti-rich and Ti-poor zones may reflect fluctuating pH (in the range 3,5 - 4,0), giving rise to alternating Ti mobility and precipitation (Summerfield, 1983b).

Thiry and Millot (1987) have recorded similar colloform features in weathering-profile silcrete developed in Eocene deposits of the Paris Basin. The features they examined occur in fine cracks cutting columnar silcrete blocks and were interpreted as illuviation structures. They differ from those of the Hondeklip silcrete and those described by Summerfield (1983a) in that opaline silica forms the uppermost laminae below the void space. The basal laminae are composed of microcrystalline quartz and granular titania that Thiry and Millot (1987) suggest represents recrystallized opal. The upper, opaline laminae exhibit cracking caused by dehydration of the gel, but these features are lost on recrystallization. Although not specifically remarked upon by Thiry and Millot (1987), it is evident from their figure 2 that colloform features are also present in the microcrystalline matrix between the partially-opaline features in the larger cracks.

It is worth noting that colloform features were not recorded by Thiry and Millot (1987) from other silcretes in the Paris Basin that are not associated with weathering profiles. Silcretes in Kuwait, that formed by silicification of gypsiferous and anhydritic sandstones, calcrete, dolocrete and freshwater limestone (Khalaf, 1988), do not possess colloform features, but exhibit the more complex petrography that Summerfield (1983a,b,c) has associated with arid-zone silicification (e.g. microcrystalline and megaquartz druses and mosaics and void-filling, fibrous and spherulitic chalcedony). Proterozoic silcretes described by Ross and Chiarenzelli (1985) have been interpreted as arid-zone silicification on the basis of associated evaporitic and aeolian sediments, evaporitic mineral pseudomorphs, low Ti content and the petrographic criteria established by Summerfield (1983a,b), including the absence of colloform features. However, Cenozoic analogues might not be applicable in the Precambrian due to (*inter alia*) the lack of vegetated environments (Summerfield, in Ross & Chiarenzelli, 1985).

A chalcedonic, Fe-rich silcrete from Portugal (Bom Sucesso Fm.) possesses colloform features formed of alternating laminae of silica and Fe-oxides (Meyer & Pena Dos Reis, 1985). This silcrete is pervasively developed and marks a hiatus within rubified terrestrial sediments of Eocene to Middle Miocene age. It is easily broken with a hammer and only locally is it "quartz-cemented sandstone". Significantly, the authors report that K-feldspars have been decomposed and that kaolinite is

increasingly developed towards the top of the profile. They infer lateritic-type weathering of a soil under a warm climate with abundant water and suggest that the weathering process had not gone to completion due to subsequent aridification. This represents an example where colloform features are associated with a silcrete that is not unequivocally a microcrystalline-quartz, weathering-profile type. Nevertheless, an association with a weathering profile is present and the interpretation of the authors may suggest initiation of weathering-profile silicification in an immature profile from which Fe and Al has not been mostly flushed.

In summary, colloform features are geopetal structures reflecting illuviation or similar processes involving descending solutions and colloids (Thiry and Millot, 1987), such as occurs in soil profiles. This sounds a cautionary note on the uncritical acceptance of them as diagnostic features of weathering-profile silcretes in particular. Notably, they are apparently absent or rare in the silcrete example with relict thin bedding from the study area. Rather, the colloform features very likely reflect processes characteristic of the weathering profile, or parts thereof, that became host to the silcrete. Their occurrence in the crumbly, partially-indurated silcrete from B Block supports their formation prior to and during the early stages of silicification. However, it is possible that colloform features that are enriched in TiO_2may be diagnostic of weathering-profile silicification.

Fabric Genesis

The general correspondence between the basal kaolinitic deposit and silcrete with respect to (angular) grain shapes and (poor) sorting suggests that, overall, these characters have been inherited from the host material. Larger-scale features such as bedding are preserved in the silcrete. The silcrete with relict thin-bedding reveals a relatively dense, moderately well-sorted grain population, with grains in depositional orientations and a lack of grain-poor "mud clots" and colloform features. Clearly, significant original characteristics of the host sediment can be preserved during weathering-profile silicification.

However, in the gravelly, kaolinitic deposits, quartz-pebbly silcrete and massive silcrete, the occurrence of brecciating, coarser, quartz grains of complex shape indicate that a portion of the quartz grain population consists of disintegrated, larger grains. Significantly, although "pseudomorphs" of kaolinite after feldspar and relict feldspars are present in the kaolinitic matrix of the basal fluvial sediments, no "pseudomorphs" or relict feldspars are obvious in the silcrete. This would be consistent with total decomposition of feldspars in the silicifying horizon and some displacive redistribution of the clay content, with concomitant grain movement. Multiple, cross-cutting colloform features, together with instances of material percolated down cracks, also indicate mobility and displacive processes in the matrix. They suggest infilling of pores by precipitation from descending solutions, as well as creation of pore space by removal of matrix. Smale (in Wopfner, 1978) mentioned evidence, in a thin section from a weathering profile, of movement of kaolin apparent in the "bundling together" of vermicular quartz bodies previously separated by intergrown feldspar. He also suggests that grain brecciation may have occurred in the capping silcrete. From "terrazzo" silcrete equivalent to the F-

fabric type, Smale (1978, p. 262) mentions "occasional flow lines probably related to the direction of movement of solutions."

In view of the above, silcrete examples from the study area with an uneven distribution of quartz grain sizes and matrix, with evidence of grain movement, probably largely reflect the overprint of weathering processes on the original sediment. The basic fabric of the host prior to and during the early stages of silicification has been preserved. Silcrete with relatively well-preserved primary sedimentary structure may have formed below the zone of active soil-forming processes, possibly below the groundwater table. Implicit in this interpretation is that bioturbation, for which there is evidence from plant-roots and possible burrows, could contribute to irregular grain-size distributions and lineations preserved in the silcrete.

These observations endorse the views of Frankel and Kent (1938) and Summerfield (1983a,c) that the grain population of weathering-profile silcretes is mainly derived from the host rock and emphasize that the gross character of the host fabric is preserved. The preserved host fabrics may include original depositional textures in some cases, as well as disturbed textures more typical of weathering or soil profiles. Although the Hondeklip silcrete is evidently dominated by the floating (F) fabric type, with conglomeratic (C) fabric locally present, it also includes variation verging towards grain-supported fabric and, if silt and clay beds were also silicified, would include the massive (M) fabric type.

Summerfield (1983a,c) did not find any evidence of displacive or expansive/contractive processes in weathering-profile silcretes from the Cape coastal zone, thereby speculating that the isovolumetric evaluation of the geochemistry of weathered and silcreted profiles may be valid. It is conceivable that small-scale displacements are primarily a feature of the decomposition and silicification of uncompacted, unlithified sediments, as opposed to the silcretes examined by Summerfield that are developed in weathered, lithified bedrock such as Bokkeveld, Dwyka and Witteberg rocks. As such, abundant evidence of displacive processes may be a useful criterion for the recognition of silcretes developed in previously unlithified, weathered sediments. Nevertheless, colloform features occur in both the Hondeklip silcrete and silcrete developed in lithified host rocks. As evidence of displacive processes involving both erosional and depositional episodes in the matrix, their presence suggests that the assumption of isovolumetric processes in attempts to quantify element transfers during weathering and silicification requires more careful evaluation and is not applicable to all parts of the weathering profile.

Silica Mineralization

In the palaeoenvironmental model for weathering-profile silcrete genesis advanced by Summerfield, the removal of Al_2O_3 and evidence for the mobility of titanium indicates low pH conditions (pH ~4) during silicification of weathering profile clay containing residual grains. The low pHs are developed by humic-acid production, associated with abundant vegetation in a humid tropical or subtropical climate. The silicate weathering and silicification is considered to take place simultaneously in different parts of the weathering profile (Summerfield, 1983a,b,c) and may involve poorly understood

organic complexing. The silica released during kaolinization is retained in the profile and precipitated in zones of low permeability, nucleating on fine quartz particles and replacing the clay, whilst its aluminium is removed. The silicified zones are likely to be controlled by the water-table under conditions of poor drainage, the silcrete forming at depth in the profile (Summerfield, 1983b,c).

In non-weathering-profile silcretes the association with calcretes, pan environments and arid, evaporitic climate suggests that alkaline solutions are dominant in the mobilization and concentration of silica. Silica could be derived from dissolution of aeolian abrasion dust, transport by groundwater from the margins of the Kalahari basin where weathering is more active, or within the profile in the case of the silcrete-calcrete association (Summerfield, 1982). Notably, surface and groundwaters of the Kalahari are usually supersaturated with respect to quartz and precipitation could take place due to pH shifts induced by rainfall or freshwater input, or simply in areas of groundwater accumulation and/or reduced permeability (Summerfield, 1982).

The earlier model of Frankel and Kent (1938) for silcrete formation in Cape coastal zone weathering profiles involved upward migration of the silica released on weathering by capillary rise, with subsequent precipitation taking place when downward diffusing, geochemically contrasting conditions were encountered in the soil profile. They regarded downward percolating NaCl, derived from the nearby sea-shore, as particularly important in promoting silica precipitation. Summerfield (1981) has pointed out that this model is based on the then current, erroneous assumption that the silica is present as a colloid, but since silica concentrations above equilibrium solubility with respect to amorphous silica are exceedingly rare in the pore waters of soils and weathering profiles, the silica is rather present in true ionic solution as monosilicic acid (H_4SiO_4). Salinity appears to have little effect on silica solubility except when it is very high. Moreover, later findings show that pH decrease, rather than the increase invoked by Frankel and Kent, promotes silica precipitation. The capillary rise aspect of the Frankel and Kent model is also inadequate to explain the thicknesses of silcrete developed and occurrence of multiple silcrete profiles; initial silica precipitation will inhibit and eventually prohibit evaporation and further capillary action and the capillary capacity of most host materials is generally restricted to several centimetres (Summerfield, 1983d).

Although Summerfield (1983a,b,c) freely admits that silcretes are still incompletely understood, particularly with respect to the controls of silica precipitation, his central thesis that there are at least two basic associations in its occurrence that can be distinguished geochemically and petrographically is convincing. More recent contributions to the silcrete topic are worth brief consideration at this point, specifically the larger topic of silicification controls.

Summerfield (1983a) enumerated the controlling factors on silica mineralogy and morphology in silcrete as follows: 1) the geochemical environment during initial precipitation, 2) host sediment characteristics, 3) post-silicification diagenesis. These include the pore-water silica concentration, pH, presence of foreign ions and clays that may inhibit crystal growth, the spacing of potential growth nuclei in the host and the rate of pore-water movement.

From a petrographic examination of various forms of silcrete in France, Thiry and Millot (1987) conclude that silica mineralization proceeds by recrystallization from the least ordered, most soluble forms (opal), via chalcedony and microcrystalline quartz, to well-ordered, clear, megaquartz. The controls of this sequence are solubility, determined by degree of disorder reflecting degree of supersaturation (nucleation rate) and amount of foreign ions, together with percolation rate. The effect of percolation rate is to prohibit recrystallization when it is too low, promote dissolution when too high, whereas intermediate rates (and porosities) favour progressive recrystallization. They conclude that the relative interaction between percolation, dissolution and recrystallization controls the distribution of silica minerals in silcretes. Thiry and Millot (1987) therefore primarily place emphasis on the silica sequence dictated by thermodynamic and kinetic controls.

As an example of a mature silcrete profile, Thiry and Millot (1987) present the weathering-profile silcrete developed in Eocene sediments of the Paris Basin (mentioned above). According to their petrographic analysis, it is mainly cemented by microcrystalline quartz considered to represent both replacement of opal and direct replacement of kaolin. The upper zone exhibits dissolution and partial development of coarser quartz, whilst opal dominates in the lower zone. This is considered to be the result of the increasing concentration of dissolved silica and other ions in the descending solution. Thiry and Millot conclude that ultimately silcrete should evolve to stable quartz. They seemingly imply an ongoing process tending to produce a continuum of silcrete types that, if percolation rates remain favourable, converge on an ultimate "mature" quartzitic silcrete. However, in this example of a mature, "silica profile" silcrete, they mention that opal-CT could not be detected by XRD. Thus it appears that this silcrete resembles the Hondeklip (and other weathering-profile examples from southern Africa) in that it is dominated by crypto- and microcrystalline quartz, any pre-existing opaline silica being either recrystallized or not originally present.

Meyer and Pena dos Reis (1985) remark that recrystallization of disordered silica does not seem to alter its optical properties in thin section. It appears inadvisable to identify the presence of amorphous silica on optical properties only, without confirmatory XRD analysis. This preservation of optical appearance is useful. For example, very old, Proterozoic silcretes can be interpreted as arid-zone silcretes by Summerfield's criteria, as originally chalcedonic void fills are identifiable (Ross and Chiarenzelli, 1985). However, a problem is the distinction of finely microcrystalline, recrystallized opal from finely microcrystalline quartz with no disordered precursor. In an important example, the precursor silica mineralogy of finely microcrystalline Ordovician chert nodules can only be identified after etching in HF and examination under SEM, which reveals the relict, precursor opal-CT lepispheres (Gao and Land, 1991). This simple check now seems obligatory for the evaluation of precursor forms of silica in cherts and silcretes.

The transformation rates of silica polymorphs are slow and they persist in metastability. The Miocene, diatomaceous (opal-A) Monterey Formation of California has only undergone transformation to opal-CT and quartz after being buried at sufficient depth to speed up the process. Amorphous opal (opal-A) and opal-CT are known from rocks of Cretaceous age and can persist even longer (Williams

et al., 1985). The Hondeklip silcretes are of Cenozoic age and have remained at the land surface. Examination by XRD indicates that opaline silica is absent, or at least negligible, and chalcedony was not seen in thin section. Etching and SEM examination shows no evidence of crystalline opal-CT precursor. The largest authigenic megaquartz crystals (~50 µm) filled the final void space remaining above a colloform feature (Plate 7.13). These largest crystals are very rare and, rather than being a recrystallization effect, are consistent with the decrease of pore-water movement in the almost complete void-fill promoting larger crystal sizes. The general lack of void-filling silica phases that contrast with the matrix suggests that silica precipitation subsequent to the main formational period of the silcrete was not significant. Thus it appears that the silicification took place by direct replacement of the kaolinitic matrix by microcrystalline quartz, or the precursor opal-A has completely recrystallized.

The discussion of silica diagenesis by Williams *et al.* (1985) and Williams and Crerar (1985) suggests that the key to understanding silcrete genesis and mineralogy lies in the initial controls of silica solubility and precipitation rather than an emphasis on the progressive transformations from disordered to more ordered polymorphs. Based on experimental data and theoretical considerations, they indicate that the silica polymorph transformation sequence can be the consequence of the variation of polymorph solubility with surface area and surface free energy. Particularly significant is the effect of "impurities" in the system. For instance, adsorption of dissolved silica by high-area clay such as kaolinite decreases the silica concentration and suppresses the formation of less-ordered polymorphs, which are bypassed and quartz is slowly precipitated from dilute, monomeric solution.

Unfortunately, Williams *et al.*, (1985) and Williams and Crerar (1985) were primarily concerned with alkaline systems and considered silcrete only very superficially, thus remarking that they had no well-documented evidence from the natural realm to support suppression of silica polymorphs. However, it is probable that this sort of process is involved in the formation of crypto-/microcrystalline quartz in silcrete associated with kaolinitic weathering profiles. Possible polymorph transformations may have been rapid and intrinsic to the period of silicification, as opposed to an ongoing process converging on an ultimate "mature", quartzitic silcrete profile (as Thiry & Millot seemingly imply). Interestingly, abundant, irregular, silt and sand-size grains of quartz have been found in a soil profile formed on quartz-free norite in Georgia state, North America (Robinson, 1980). Opal and chalcedony are absent in the quartz-rich soil horizon and Robinson suggests that silica released from the breakdown of silicates might have precipitated directly as quartz. The quartz grains have Fe-oxide/hydroxide inclusions and Robinson cites experimental evidence that amorphous hydroxides of metals can absorb silica from solution, concentrating it until amorphous silica forms. Subsequently, quartz can crystallize rapidly (within days) if the hydroxide-silica precipitates are in contact with solutions supersaturated with respect to quartz, e.g. in the poorly-drained soil conditions (Robinson, 1980).

Concluding remarks

Petrographically, mineralogically and geochemically the Hondeklip silcrete is a typical weathering-profile silcrete, suggesting that its development was intrinsically associated with the kaolinization of

the host, basal fluvial arkosic sediments and underlying bedrock. Although this detailed examination of the Hondeklip silcrete has placed it properly in the context of the most recent contributions to the topic, it also emphasizes the fact that the genesis of weathering-profile silcretes is still to be more completely elucidated. The petrographic features of most, but not all, examples of silcrete from the study area indicate that comparison with the petrography of soils is required for a more complete evaluation. Similarly, the observations and concepts of soil scientists would be beneficial to more detailed mineraolgical and geochemical evaluation of silcrete.

Whilst basically agreeing on the fundamental controlling factors in silcrete formation, Summerfield (1983a,b,c), placed emphasis on the initial, climatically determined, geochemical environment, whilst Thiry and Millot (1987) emphasized the diagenetic silica sequence. Both perspectives are crucial to the classification and interpretation of silcrete types and the recognition of ongoing silica mobility and alteration effects. Both authors also mention the importance of "impurities" such as clays in the system. The theoretical considerations of silica precipitation represented by the work of Williams *et al.* (1985) and Williams and Crerar (1985), together with observations such as those of Robinson (1980), focus attention on the role, in quartz precipitation, of "impurities" or substrates in the host lithology. The composition of "impurities" would be strongly influenced by climatically-determined weathering-profile mineralogy and their type of geochemical activity will reflect climatically-determined groundwater compositions.

The Hondeklip silcrete is a fossil silcrete in the sense that, unlike many other examples of Cenozoic weathering-profile silcretes, it consists of buried remnants. *In situ* Cenozoic (or older) weathering-profile silcretes at the present-day land surface on interfluves and plateaus have remained within the range of the processes active in the "geomembrane" for an extended period. It is conceivable that some ancient, surficial silcretes could have undergone later modification during climatic fluctuations subsequent to their main period of development (a possible example being the Paris Basin silcrete described by Thiry and Millot, 1987). Other examples may have been "frozen" by consistent aridification. This factor may contribute to different perspectives of weathering-profile silcrete development, depending on the example studied. By implication, further studies of weathering-profile silcretes will result in a more detailed facies taxonomy that must attempt to isolate both the effects of host lithology and subsequent modifications.

CHAPTER 8

AGE AND CORRELATION OF THE BASAL KAOLINITIC DEPOSITS AND SILCRETE

8.1 INTRODUCTION

The topography of the depositional floor for coastal-plain sediments in the study area has not been primarily created by erosion during marine transgressions, but reflects an antecedent fluvial topography modified by minor erosion. The courses of the ancient rivers carving the topography, like the associated channels still maintained by the scant modern rainfall, were influenced by the faulting associated with continental rifting. Although the channel is the preferred locus of groundwater accumulation, the lack of significant weathering of the marine sediments now residing in it for at least the last 2 million years is consistent with the proposition that the deep weathering of the bedrock and basal sediments and silcrete formation occurred under climatic conditions quite unlike those that reigned during the latest Cenozoic. This suggests that a land surface of considerable antiquity is associated with the coastal-plain basal unconformity.

8.2 AGE ESTIMATION OF THE BASAL KAOLINITIC DEPOSITS

Sea-level and Palaeoclimatic History

Previously the writer (Pether, 1983) has suggested that the basal fluviatile sediments are of Miocene age and speculated that the palaeochannel may have originated during the extensive late Oligocene/early Miocene regression, with kaolinization of the bedrock and of channel sediments, together with silcrete formation, taking place during early Miocene times.

The above suggestions were based on the major scale of the late Oligocene/early Miocene regression identified by Dingle (1971) on the basis of the extensive unconformity inferred from continental-shelf seismic records and further discussed by Dingle *et al.* 1983). In addition, deep weathering of the Cape Granite in the Cape Peninsula occurred during pre-Middle-Miocene times, according to Glass (1977). Dingle *et al.* (1983) sketched a basic palaeogeography for late Oligocene/early Miocene times off the west coast. Due to a lowering of sea-level of ~500 m, the coastline would have been up to 200 km west of its present-day position. The present-day shelf would have been a very wide and flat coastal plain crossed by slow, meandering rivers. Dingle *et al.* (1983 p. 313-314) suggested that the large gradient change in the vicinity of the present coast, corresponding to the inner margin of the well-vegetated, middle Tertiary coastal plain, caused rivers to dump their coarse sediments as they debouched onto the low-gradient, Oligocene/early Miocene coastal plain. The Hondeklip area would have been situated well inland of the coastline, in the foot-hill zone fronting the retreating escarpment farther east. During the Oligocene regression, fluvial channels were incised into the bevel of Precambrian gneisses now corresponding to the outer edge of the present-day coastal plain and the

inner shelf. Vigourous flow conditions caused the local concentration of heavy minerals. Renewed transgression in the early Miocene would have resulted in fluvial aggradation within these channels. Under relatively well-watered, subtropical climate, with abundant vegetation providing acidic groundwaters, humid weathering ensued. Kaolinization was best developed in the fluvial channels, where draining meteoric waters facilititated high leaching rates. Locally, silcrete developed in the weathered fluvial sediments. The formation of the silcrete may have been associated with the development of impeded or decreased drainage of groundwater in the channels. As the shoreline approached during the early Miocene transgression, rising base-level may have led to the development of swampy and waterlogged conditions in the valleys. The clay-rich, weathered sediments may have contributed to decreasing groundwater flow rates. Decreasing rainfall may also have favoured the lowering of groundwater flux through the kaolinitic sediments.

Palynological Evidence for the Age of the Basal Kaolinitic Deposits

Samples rich in organic matter from the basal kaolinitic deposit at Zwart Lintjies Rivier were submitted by De Beers Namaqualand Mines to Mr A. Scholtz (previously of the South African Museum) for palynological examination. The results are presented with the permission of De Beers Namaqualand Mines Division. The pollen assemblage is dominated by *Podocarpus falcatus* (yellowwood) and *Olea capensis* (ironwood). Several types of proteaceous pollen are present, asteraceous pollen (Compositae or "daisies") are present in low percentages, but grass pollen are absent. The presence of Proteaceae indicates an age not older than Maastrichtian (end-Cretaceous), whilst Oleaceae and Asteraceae indicate an age not older than Oligocene (Muller, 1981). The assemblage represents yellowwood forest and, together with the minor presence of daisies, this suggests, in terms of the general global pattern and local data, a Lower Miocene age (A. Scholtz, personal communication).

This suggestion must be qualified due to the possibility that the low abundance of angiosperms (flowering plants) and lack of grasses may be a reflection of the lack of more open areas in the forest near the accumulation site, raising the possibility that the deposit may be younger than Lower Miocene (A Scholtz, personal communication). However, by the late Miocene in the southern Cape, plant taxa characteristic of fynbos were becoming prominent in the coastal vegetation (Coetzee *et al.*, 1983). Thus it is improbable that yellowwood forest would have existed north of the southwestern Cape, in the likely more arid Hondeklip area, during and subsequent to late Miocene times.

Discussion

The age indicated by the pollen assemblage does not conflict with the earlier suggestion (Pether, 1983) of palaeochannel incision and fluvial deposition during the late Oligocene/early Miocene, with kaolinization and associated silicification ensuing during the early Miocene transgression. The pollen evidence for forest vegetation supports the case for pene-contemporaneous humid weathering, with infiltration of precipitation dominating over runoff. Nevertheless, accepting the pollen age constraints provides a maximum age for deposition, kaolinization and silcrete formation of not older than Oligocene. Ideally, the suggestion that the latter two processes ensued soon after deposition, in the

early Miocene, requires additional supporting evidence. The local evidence for the minimum age of kaolinization and silcrete consists of the overlying marine deposits. As will be motivated in a subsequent chapter (Chapter 15), these are middle Pliocene in age.

The yellow- and ironwood-dominated assemblage of pollen from the basal kaolinitic deposit is startling in its contrast with the modern, xeric vegetation. Although broadly qualitative, the assessment excluding a younger than Upper Miocene age for forest and kaolinization along the now arid central Namaqualand coast is likely to be sound.

All kaolinitic sediments on the Namaqualand coastal plain are not necessarily coeval with those of the Hondeklip area; sediments older than the basal fluvial deposit of Hondeklip would also have been kaolinized and silcreted during the same deep weathering period. An Early Cretaceous, channel-filling fluvial deposit is present on Kareedoornvlei, north of Kleinzee (Molyneux, in Rogers *et al.*, 1990). Details of the lithology and weathering state of this occurrence are not available to the writer. It is apparently a unique occurrence and may have been preserved due to particular, local tectonic circumstances. Nevertheless, erosion associated with the marked extent of the Oligocene regression would have resulted in persistent fluvial topography, rendering it likely that most channels incised in the bevelled edge of buoyant Precambrian basement, where it abuts the subsided Orange Basin (Fig. 2.2), date from this period.

The palynological results are preliminary and more sampling should provide a larger assemblage, enabling improved characterization of the broader vegetation of the coastal plain during deposition of the basal kaolinitic deposit. Additional work should also more certainly exclude the possibility of contamination of samples by modern pollen. Under the sponsorship of De Beers, further research is currently under way (I. B. Corbett, personal communication). Despite the preliminary nature of the available age constraint, the remainder of this chapter is an exercise founded on the assumption that the age constraint is valid.

8.3 THE GEOMORPHOLOGICAL CONTEXT OF WEATHERING-PROFILE SILCRETES

Silcretes have been widely reported from the southern African coastal zone, from southern Namibia in the northwest, to the Transkei in the southeast. They are developed in the immediate hinterland of the Namaqualand coast, along the edge of the interior plateau (Bushmanland), and on valley flanks in the Cape Fold Mountains in the Cape Province (Fig. 3.1). The broad-scale, geomorphological context of well-developed silcretes associated with deep, advanced weathering of the host lithology has been discussed by Partridge and Maud (1987), in their recent review and synthesis updating the evidence and concepts of the geomorphic evolution of the southern African subcontinent.

Partridge and Maud (1987) regard deep weathering and duricrust development as the main diagnostic feature of the oldest surviving erosion surface formed subsequent to continental break-up. This, the African surface, is the important geomorphic datum in their analysis and is extensively preserved

along the outer rim of the plateau interior to the Great Escarpment, whilst residuals of the equivalent surface occur patchily around the coast below the escarpment. The duricrust developed on the weathered African surface in the southern and western portions of the subcontinent is silcrete. The development of the African surface is considered to be lengthy and polycyclic, extending from rifting (Upper Jurassic–Lower Cretaceous), to the end of the early Miocene (~18 Ma), when it was terminated by uplift (Partridge and Maud, 1987).

Along the Namaqualand coast, Partridge and Maud (1987, fig. 12) identify substantial areas of African surface occuring in a dissected state, with residuals of the original surface sometimes preserved on interfluves. In their topographic cross-section closest to Hondeklip (their fig. 5, section 19), they show the African surface extending beneath the coastal Neogene sediments and passing below sea-level. Thus the coastal-plain bedrock unconformity is closely associated with the African surface and, from a geomorphological viewpoint, the basal fluvial deposit, weathering profile and silcrete at Hondeklip apparently have an origin associated with the African surface. The suggestion of an early Miocene age for kaolinization and silcrete formation at Hondeklip implies that the African cycle continued well into the Miocene along the Namaqualand coast, consistent with Partridge and Maud's (1987) contention that the African cycle persisted into the early Miocene.

However, it is clear from a subsequent paper (Partridge and Maud, 1989) that they regard African surface silcretes associated with deep weathering profiles to be well-constrained to the Palaeocene, citing the Namibian Pomona silcrete (overlain by the early Eocene Buntfeldschuh Formation) (Fig. 3.1), the silicification apparently associated with the end-Cretaceous/Palaeocene Gamoep volcanicity on the edge of the Bushmanland Plateau on the Great Escarpment, east of Hondeklip (Fig. 3.1), and the silcrete clasts in the early Eocene Bathurst Formation in the eastern Cape. Partridge and Maud (1989) suggest that most deep weathering took place in the Cretaceous, with silcrete formation during the Palaeocene when drier climatic conditions ensued. Thus they dismiss a direct genetic relationship between deep, kaolinitic weathering and silcrete formation. In their view silcretes associated with deep weathering profiles are confined to a single period and, although silcretization occurred both earlier and later than the Palaeocene, these lesser silcretes are not extensive and are not associated with deep weathering profiles. In this view, the middle Tertiary Hondeklip basal deposits, deep weathering and silcrete cannot be correlated with the primary African surface features and must represent subsequent, more minor modifications to the surface, such as local weathering and silicification confined to incised channels. Importantly, the regional geomorphological assessment of weathering-profile silcretes in southern Africa does not support a younger than Middle Miocene age for their development.

8.4 CORRELATIONS WITH FLUVIAL DEPOSITS

THE ELANDSFONTYN FORMATION OF THE SOUTHWESTERN CAPE.

Over much of the coastal plain of the southwestern Cape, the deeply weathered, late Precambrian-early Cambrian bedrock is overlain by the fluvial Elandsfontyn Formation (Rogers, 1980, 1982), which attains its greatest thicknesses in bedrock topographic lows and is never exposed. It is distinguished from overlying paralic and marine sediments by the angularity of its sands and the lack of carbonate and phosphate. A number of fining-upward cycles terminating in muddy and peaty layers is usually present. The depositional environments are interpreted to be those of meandering rivers under humid climatic conditions (Rogers, 1980, 1982).

The Elandsfontyn Formation sediments are considered to be derived from the deeply weathered, coastal-plain bedrock as "newly released, first cycle" material (Rogers, 1980, 1982, 1983). For instance, the flanks and base of the Noordhoek valley on the Cape Peninsula (Fig. 3.1) consist of deeply kaolinized Cambrian granite and seismic profiles show the continuation of this bedrock condition offshore. Silcrete was encountered in the S20 borehole below -50 m bsl. (below sea-level) and was also present in other boreholes in the area. In contrast, the Elandsfontyn sediments infilling the valley are angular, feldspar-rich, quartz sands. The strong variations in mud content recorded in the graphic borehole logs in Rogers (1980) are consistent with the mud being primarily depositional.

On the basis that it is overlain by the early Pliocene, paralic and marine Varswater Formation and contains fossil pollen indicative of forest vegetation with palms, the Elandsfontyn Formation is considered to be Miocene in age (Coetzee, 1978; Rogers, 1982; Hendey, 1981a). In a proposed correlation of the succession in the Langebaanweg area (Fig. 3.1) with the cycles of relative, global sea-level change advanced by Vail and Hardenbol (1979), Hendey (1981a,b,) suggested that the Elandsfontyn Formation was laid down by fluvial aggradation during the early to middle Miocene transgression. The overlying Gravel Member of the Varswater Formation was considered to represent the final marine encroachment truncating the aggraded fluvial sequence and, in turn, it was eroded during the late Miocene regression. Pollen from peats of the Elandsfontyn Formation in the Langebaanweg area (S1 borehole) suggested a middle Miocene age (Coetzee and Rogers, 1982). The Elandsfontyn Formation in the Noordhoek S20 borehole has been suggested to be as old as late Oligocene near the base of the sequence (Coetzee, 1978).

Discussion

In terms of the above interpretations (Coetzee, 1978; Hendey, 1981a,b), the Hondeklip basal fluvial deposits and the Elandsfontyn Formation are chronologically equivalent, accepting the age for the former proposed in the preceding part of this chapter. The immediate problem with a correlation between the Elandsfontyn Formation and the Hondeklip basal deposits is that the former have been interpreted as the product of erosion of the weathered landscape, whilst the latter are interpreted as having weathered *in situ* together with the landscape.

Yellowwood and palms are present in the Noordhoek S20 borehole, but the presence of Asteraceae (Compositae) pollen suggests that the the maximum age feasible is Oligocene. The most ancient pollen type present, *Clavatipollenites* cf. *C. hughsii*, is a problematic indicator of age as it is very similar to the extant genus *Ascarina* of Malagasy and the Pacific. Coetzee (1981) suggests that it may have become extinct in southern Africa during terminal Miocene times. Dingle *et al.* (1983) point out that additional evidence is required to establish whether the 33 m of fluvial sediment in the S20 borehole represents ~25 my of accumulation. Conceivably, the pollen assemblage changes could be the result of local changes in the surrounding landscape and in the depositional environments, rather than reflecting large-scale climatic changes. Thus the constraints for late Oligocene/early Miocene antiquity of the Elandsfontyn Formation at Noordhoek seem tenuous.

Accepting that *in situ* decompostion best explains the observations on the Hondeklip basal fluvial deposit and that the presence of Asteraceae renders a pre-Oligocene age unlikely, the most probable alternative is that the age of the Elandsfontyn Formation is younger than early Miocene. Due to the discovery of vertebrate remains of early Pliocene aspect, apparently from beneath the Gravel Member, Hendey (1983a) and Hendey and Dingle (1990) raise the possibility that both the Elandsfontyn and Varswater formations (the Sandveld Group) may be early Pliocene. However, fossil pollen from the Elandsfontyn Formation, that is indicative of subtropical rain forest, contrasts with pollen from the Varswater Formation indicating that sclerophyll (fynbos) vegetation was becoming prominent in the Pliocene (Coetzee, 1986). A pre-latest-Miocene age for at least part of the Elandsfontyn Formation is therefore indicated on palynological grounds.

In summary, the basal deposits of the Hondeklip area and the Elandsfontyn Formation both contain forest pollen types and Asteraceae, indicative of an Oligocene or younger age. However, the fluvial deposits at Hondeklip are kaolinized and silcreted, whilst the Elandsfontyn sediments overlie the weathering profile and were derived from the weathered landscape. On lithological and geomorphic grounds they cannot be regarded as stratigraphic and temporal correlates. In the light of the above discussion, the Elandsfontyn Formation must be middle Miocene and younger, with its top no older than early Pliocene. This is also consistent with the geomorphic interpretation of Partridge and Maud (1987), in which the Elandsfontyn Formation is correlated with the postulated middle Miocene uplift that initiated the Post-African I cycle. The Elandsfontyn sediments were not subjected to intense weathering, a circumstance consistent with the general oceanographic and climatic evolution towards aridity along the western margin concomitant with the acceleration of global cooling and glaciation in the late Miocene.

NAMAQUALAND RIVERS

Published information on the exploited Buffels River terraces and deposits, and other prospects on Namaqualand river terraces (e.g. Spoeg, Groen) (Fig. 3.1), is minimal. Molyneux (in Rogers *et al.*, 1990) describes remnants of a gravel deposit, preserved in deeper bedrock depressions, that consist of basal, indurated, oligomictic gravels comprised of sub-angular to sub-rounded quartz clasts. The

overlying sediments comprise sandstones, siltstones and clays. This description suggests that these remnants may be correlates of the basal fluvial sediments in the Hondeklip area. Molyneux (in Rogers *et al.*, 1990) suggests possible correlation of both the Hondeklip basal fluvial sediments and the old Buffels River gravels with the Elandsfontyn Formation.

Keyser (1976) reported that the diamondiferous terrace gravels of Namaqualand river valleys are lithologically distinct and appear to occupy a single terrace within the terrace sequence preserved. The sediments are "clean-washed to clayey (kaolinitic), reasonably sorted, and sometimes cross-bedded sands incorporating thin, disjunct, lensiform, very well-rounded ("golf-ball") and well-sorted quartz and quartzitic pebble gravels." The basal layer is the main diamondiferous horizon, is best developed in channels incised into the main level of the terrace and is a poorly-sorted, massive gravel with clasts of decomposed bedrock. These "white quartz" gravels are patchily preserved in the rivers south of the Buffels River (Keyser, 1976).

The basal, poorly sorted, vein-quartz gravels in the terrace depressions may either be, as suggested (Molyneux, in Rogers *et al.*, 1990), equivalent to the coastal basal fluvial deposits, or may represent their reworking. Evidence of *in situ* kaolinization or the presence of silcrete clasts might resolve these alternatives. The apparently overlying fluvial terrace deposits with "clean-washed" sands and lenses of very well-rounded, "golfball" gravels are difficult to reconcile with the kaolinitic, angular, basal fluvial conglomerates at the coast and are probably younger. The interpretation of Keyser (1976), who considers the "white quartz" terrace gravels to have been derived from the kaolinized terrain, implies that these deposits post-date the kaolinized channel deposits and are broad correlates of the Elandsfontyn Formation.

The Koa Valley on the Bushmanland Plateau above the escarpment (Fig. 3.1) is considered to be an exhumed, pre-Karoo feature (De Wit, 1990). Abundant gomphothere fossils in the fluvial deposits beneath pan infill indicate that the valley was active during the Miocene. These deposits are considered by Dingle & Hendey (1984) to indicate the palaeocourse of the upper Orange/Vaal drainage when it reconnected with the lower course of the Orange River during the Neogene. The age of the Kao Valley deposits is not well constrained. It is speculated that the Koa drainage was probably active during the early Miocene, although the age of the fluvial deposits preserved in the valley may reflect its abandonment and could therefore be younger than early Miocene, possibly coeval with the "Proto-Orange" deposits and the earliest Elandsfontyn deposition.

THE NAMIB

A suite of alluvial deposits with similar vertebrate faunas occurs in the southern Namib. On the north bank of the Orange River at Arrisdrift (Fig. 3.1), the vertebrate assemblage obtained from the oldest, "Proto-Orange" terrace indicates an age of ~15 Ma (Hendey, 1984; Pickford, 1987). The alluvial deposits in the valleys of the Grillental, Langental, and at the northern end of the Buntfeldschuh escarpment (Fig. 3.1), enclose vertebrate fossils that, on the basis of comparison with the dated East African faunal record, indicate an age of 17 to 17.5 Ma (Pickford, 1981). These deposits are of

slightly differing ages about the Early to Middle Miocene boundary (16.2 Ma), but the faunas are essentially similar in respect of their palaeoenvironmental implications (Hendey, 1984). The palaeoenvironment during the Namibian Mammal Age is inferred to have been more vegetated and wetter than the present (Hopwood, 1929; Hendey, 1978, 1984). Potentially, this wet period in the Namib may correlate with the more humid conditions implicated in the weathering at Hondeklip to the south.

However, Ward *et al.* (1983) point to the "linear oases" provided by the modern rivers that rise in the better-watered hinterland and traverse the narrow, arid tract below the escarpment. In this view, the Miocene vertebrate assemblages are regarded as anomalous and not an accurate reflection of the wider palaeoenvironment, a view supported by Corbett (1989) in his recent interpretation of the "Grillental" depositional environment as arid. The Rooilepel Sandstone, a red aeolianite just north of the Orange River (Fig. 3.1), contains a fossil rodent, *Paraphiomys piggotti* Andrews, 1914, (Corbett, 1989), which also occurrs in the Grillental and Arrisdrift assemblages. Thus the Rooilepel Sandstone is probably penecontemporaneous with Grillental-type and "Proto-Orange" deposition, supporting aridity in the surrounding environment.

The "Proto-Orange" terrace sediments are not profoundly weathered and include feldspathic sands, although the mud content is relatively greater than the younger, "Meso-Orange" terrace sediments (Cooper, in Rogers *et al*, 1990). If it is assumed that the "Proto-Orange" terrace and the basal, kaolinitic deposits at Hondeklip are coeval, it may also be expected that the former would include a relatively well-developed weathering profile, although not necessarily as advanced as at Hondeklip due to the possibility of some climatic gradient with southward-increasing moisture. This is not the case and the "Proto-Orange" terrace is unlikely to correlate with the basal, kaolinitic deposits at Hondeklip. Similarly, although the Grillental Beds represent a wetter phase in the Namib, the similarity in age between the Grillental Beds and Arrisdrift and the overall arid depositional environment inferred by Ward *et al.* (1983) and Corbett (1989), render unfeasible a correlation of the Grillental Beds with deep weathering ~400 km to the south in the Hondeklip area.

Discussion

The latest early Miocene palaeoclimate inferred for the southern Namib therefore provides a vertebrate-based, minimum age constraint for the development of deep weathering profiles 200-400 km to the north of Hondeklip. Excluding a dramatic climatic gradient, advanced weathering at Hondeklip is probably older than ~18 Ma. Cooper, in Rogers *et al.*, (1990), correlates the "Proto-Orange" (Arrisdrift) terrace with the Elandsfontyn Formation. Due to their basically similar ages, only 2-3 my apart, this correlation would include the Grillental Beds. This broad correlation is supported here, with the proviso of the probability that the respective deposits may represent different portions of latest early Miocene, middle and late Miocene sea-level history.

Notably, in their palaeoclimatic reconstructions for the Namib, Ward *et al.* (1983), Ward (1987) and Corbett (1989) recognize that the early to middle Miocene constituted the most humid period in the

Tertiary. However, there are apparently no fluvial deposits known from Namibia that are certainly of Oligocene/earliest Miocene age and that may correlate with the Namaqualand kaolinized basal fluvial deposits. Accepting the existence of a significant Tertiary palaeoclimatic gradient along the west coast, it is nevertheless still difficult to entertain the position that Oligocene/early Miocene deep weathering along the Namaqualand coastal plain would leave no record 200 to 400 km farther north.

However, there is one significant lithology in the Sperrgebiet that has perhaps been somewhat neglected in the recent palaeoclimatic inferences on the Namib. This is the impressive 15-20 m thickness of ferricrete developed in the aeolian Kakaoberg Sandstone at Buntfeldschuh (Fig. 3.1) and which caps Kakaoberg (Plate 8.1). Although this extent is apparently only locally developed, this should be viewed against the nearly complete erosion of Eocene (and Cretaceous) sediments in the area. The Kakaoberg ferricrete is described as a deep brown to red, pisolitic rock containing chalcedonic pedotubules and it is underlain by gleyed and mottled horizons (Corbett, 1989). The latter author notes that similar ferricrete (laterite) presently developes along the humid, tropical coast of Zululand. It is generally regarded that Fe-enriched, lateritic, weathering profiles are produced by humid weathering in tropical climates (McFarlane, 1983). However, other than the acknowledgement of middle Tertiary humidity, the potential implications of the Kakaoberg lateritic profile for palaeo-rainfall in the southern Namib are not taken into account in recent palaeoclimatic reconstructions (e.g. Ward and Corbett, 1990).

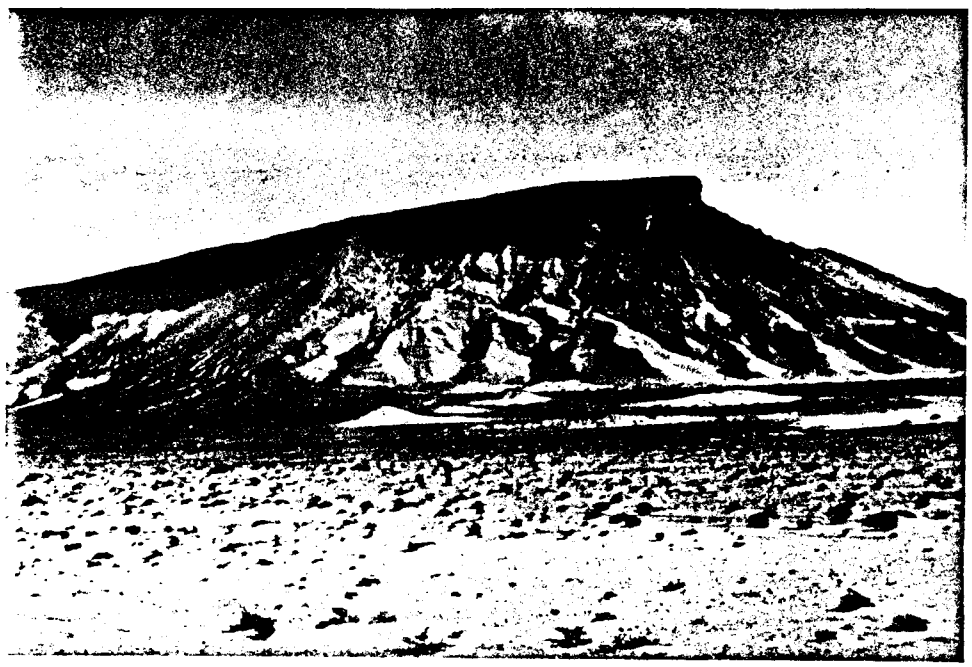

Plate 8.1 The ferricrete capping of Kakaoberg, Buntfeldschuh, southern Namibia. Photograph courtesy of J. Rogers.

The poorly-fossiliferous, marine Buntfeldschuh Formation underlying the Kakaoberg Sandstone has been speculatively considered to be late Palaeocene/early Eocene of age by Siesser and Salmon (1979), due to its elevation higher than the marine deposits at Langental dated by them (calcareous nannoplankton) as late Eocene (Priabonian). The marine Buntfeldschuh beds contain clasts of volcanic phonolite (Corbett, 1989), suggesting that they post-date the Klinghardt volcanism dated to a minimum age of 36-37 Ma (latest Eocene) (Kent and Davies, 1980). They may therefore be coeval with the Priabonian Langental beds. The overlying Kakaoberg aeolianite, which also contains a volcanic component (Corbett, 1989), is therefore Upper Eocene or younger in age.

It is tentatively suggested that the lateritic profile in the Kakaoberg Sandstone may have developed during Oligocene/early Miocene times, coeval with the more advanced weathering along Namaqualand. It is reasonable to assume that the lateritic soil profile developed within the top of Eocene sediments must have more widespread. Otherwise, it must be motivated that the occurrence is indeed a local peculiarity of no regional palaeoclimatic significance. Interestingly, ferruginous horizons and pedotubule horizons are intercalated in the Kakaoberg Sandstone (Corbett, 1989). It is possible that middle Tertiary soil development in the southern Namib would have been most marked in the porous, fresh, Eocene aeolian deposits. In the mature, pre-Eocene, kaolinitic weathering profile of the Plain Namib of southern Namibia, a subsequent and less intense weathering episode might be relatively cryptically recorded.

8.5 CORRELATIONS WITH SILCRETES

THE POMONA SILCRETE OF NAMIBIA

Corbett (1989) reports that the Pomona silcrete caps mesas or "table mountain" hills from the Orange River as far north as Grillental (Fig. 3.1), apparently being absent farther north. It is up to 3 m thick and is associated with an underlying, kaolinized weathering profile. The silcrete capping appears to be remnants of a gently undulating horizon between 100-160 m asl., now topographically inverted.

The Pomona Silcrete varies widely in colour (brown, purple, light grey-green) and in composition (Corbett, 1989). Plotting the bulk chemical analyses of 15 samples tabulated by Corbett (1989) on Summerfield's (1983b) $SiO_2/TiO_2/Al_2O_3$ ternary plot of southern African silcrete compositions (Fig. 8.1) illustrates that Pomona silcrete TiO_2 contents vary from low values typical of non-weathering-profile type to the higher values of weathering- profile type, with one anomalously high, outlying value from an Fe-rich sample. The Al content of the Pomona silcrete is overall higher than weathering profile type, but is comparable to the more Al-rich non-weathering type. The compositions of the Pomona silcrete are atypical of the silcretes examined by Summerfield (1983b) and appear to define a third field in the ternary diagram (Fig. 8.1).

Storz (in Kaiser, 1926) provided some petrographic details of the Pomona silcrete. His illustrations of thin sections are informative and show the presence of chalcedony (interference figures), euhedral

overgrowth of skeletal quartz grains and greater development of crystallinity in the matrix (Fig. 8.2). These features do not occur in the Hondeklip silcrete and are not characteristic of weathering-profile silcretes in general (Summerfield, 1983a). Furthermore, colloform features, prominent in weathering-profile silcrete, were not illustrated. Thus, petrographically, the Pomona silcrete appears to be atypical of weathering-profile silcrete.

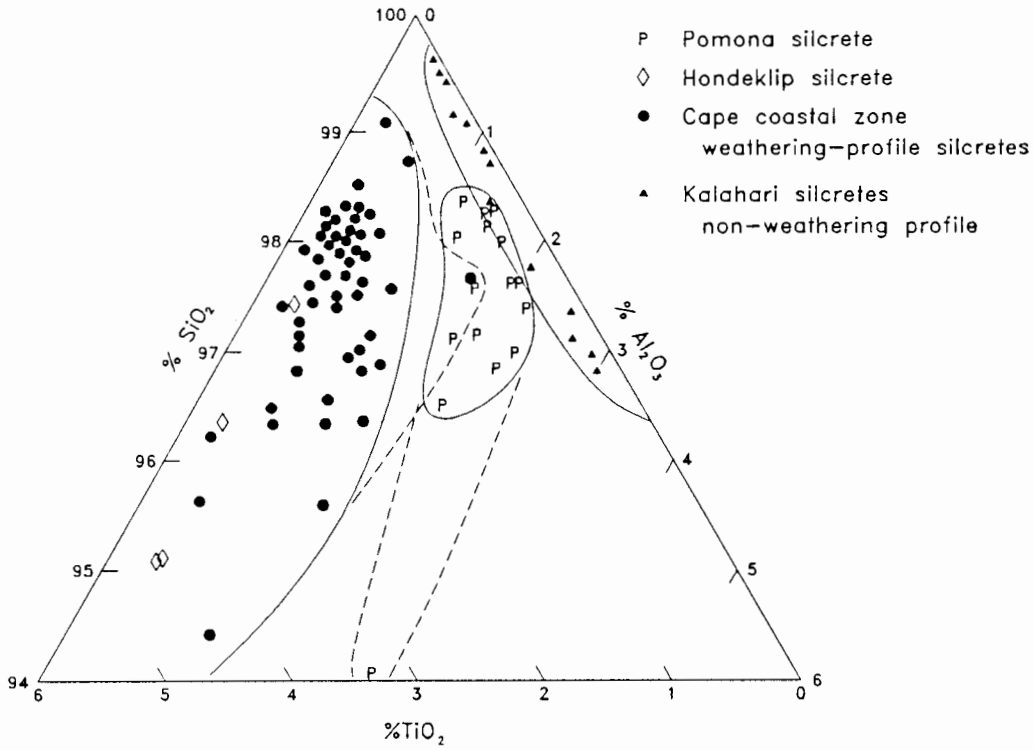

Figure 8.1 Summerfield's ternary plot of silcretes (Summerfield, 1983b), with analyses of the Pomona silcrete included (from Corbett, 1989).

Age control for the Pomona silcrete is provided by its capping by lava of the Klinghardt Phonolite Formation K/Ar dated at 36-37 Ma (latest Eocene) (Kent and Davies, 1980). The Pomona silcrete is therefore Eocene or older in age.

In summary, although the Pomona silcrete is associated with a kaolinized weathering profile, it differs from the Hondeklip and other weathering profile silcretes in colour, composition and petrographically. Moreover, its minimum age is Upper Eocene, whereas the Hondeklip silcrete cannot be older than the Late Oligocene age indicated by the fossil pollen in the host sediments. It is clear that with the available information it is inadvisable to accept the Hondeklip silcrete as a correlate of the Pomona silcrete. Accepting that the Pomona silcrete is a weathering-profile silcrete, its atypical petrography could possibly be explained by subsequent modifications concomitant with its greater age.

Abb. 43. Gelapptes Korn aus einem Pomona-Quarzit von Kaukausib Tafelberg, in einer Gel-Masse von Kieselsäure und Eisenhydroxyd. Ausheilung durch Chalcedon; bei q Quarzin. Vergrößerung 85 fach.

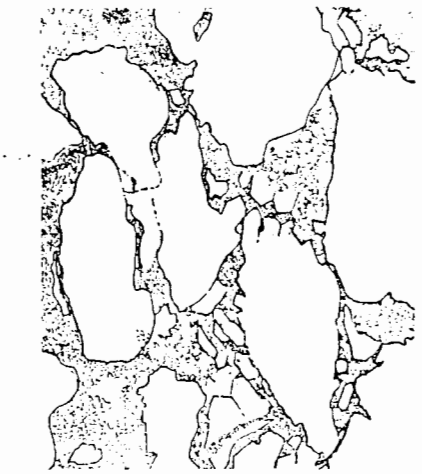

Abb. 44. Einkieselung in einem Pomonaquarzit vom Swartkopp. Weiß klastische Quarze in einem gemischten Gel schwimmend. Neugebildete Kristalle von Quarz, als spitze, sperrige Formen erkennbar. Vergrößerung 60 fach.

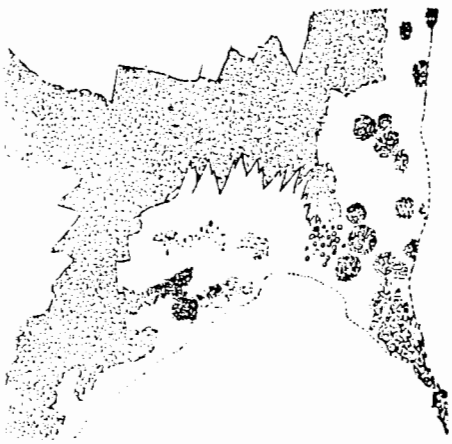

Abb. 57. Umstehungsvorgang der Kieselsäure bei einem Pomonaquarzit. Vergrößerung 450 fach.

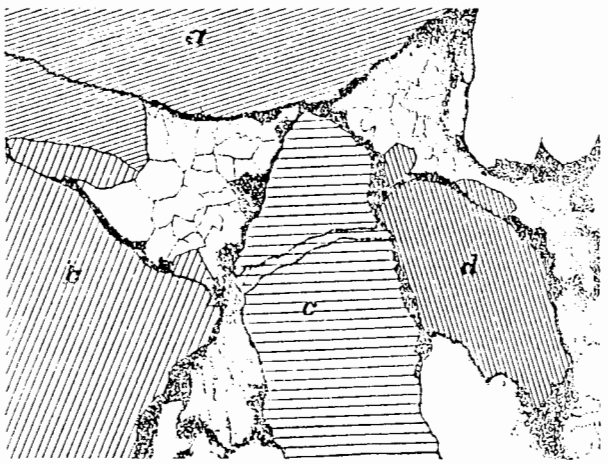

Abb. 54. Eingekieselter Pomonaquarzit. Buntfeldschuhsteilkante, östl. Advokat. Orientiert und nicht orientiert weiter gewachsenes Zement. Vergrößerung 30 fach.

Figure 8.2 Petrographic features of the Pomona silcrete. From Storz, in Kaiser (1926).

Silcrete at De Punt

Reuning (1931) described sections through cliff-top marine deposits at De Punt, just north of the Olifants River (Fig. 3.1), where late Precambrian Vanrhynsdorp Group bedrock phyllites are planed at 21-27 m asl. The sections described were exposed in prospecting shafts. The sections included a silicified horizon that Reuning correlated with the Pomona Quartzite (silcrete) of the coastal plain of southern Namibia. He reported that the silcrete is underlain and overlain by shelly, carbonate-cemented conglomerates and had been eroded prior to deposition of the overlying material.

According to Reuning's (1931) description, the silcrete apparently represents silicification of argillaceous sediments that gradationally overlie the marine basal gravel, this fining-up sequence being subsequently truncated. Reuning's (1931) correlation with the Pomona silcrete of southern Namibia was apparently on the sole basis of the presence of silicification and he did not take into account the association of a weathered profile with the Pomona silcrete.

Reuning's (1931) correlation of the silicified horizon in the De Punt marine exposure with the Pomona silcrete implies that the silicified horizon and the underlying marine deposits should be of pre-Upper-Eocene age. Notably, the "basal grits" beneath the silcrete contained a few marine fossils. Examples were collected by Reuning, some of which are in the collections at the South African Museum. The identity of these exclude a Palaeogene age (discussed in Chapter 16). From the writer's own observations in the area, the deeply weathered phyllites are capped by silcrete. The latter is overlain by Pliocene marine deposits that can be correlated, on the basis of fossil content, with the stratigraphy defined at Hondeklip (Chapter 16). It is probable that the marine "basal grits" apparently underlying the silcrete are the same age as the marine deposits overlying the silcrete and merely represent deposition under undercut and exhumed slabs of silcrete. The possibility that the weathering-profile silcrete capping the cliffs at De Punt may correlate with the Pomona silcrete therefore remains open.

Silcrete in the Olifants River Valley

Rogers (1904) recorded "surface quartzites" formed on river-cut terraces of the Olifants, Berg, Jakkals and Verlorevlei valleys (Fig. 3.1). From his description, which refers to underlying decomposed bedrock, these are apparently weathering-profile duricrusts and not mere silicification. Visser and Toerien (1971) discussed the silcrete on the Olifants River terraces. It is clear from their account and accompanying map that both silicified terrace gravels and underlying silcrete duricrust on weathered bedrock occur, but they did not clearly separate the two in their discussion. Visser and Toerien (1971) did not find any silcrete clasts in the Olifants River terrace gravels and, coupled with their observations of silicified terrace gravels and of "early" stages of silicification, this caused them to regard all the silcretes as younger than the youngest river terrace.

The writer's personal observations in the area confirm that the higher Olifants river terraces are locally formed on weathered bedrock with silcrete capppings and younger terrace conglomerates overlie the water-worn upper surfaces of the silcrete. The silcrete was evidently exhumed during formation of the

overlying terrace deposits. The apparent absence of clasts derived from the underlying silcrete is probably a result of dilution by the voluminous, overlying terrace gravel. The silcretes from this area were part of Summerfield's (1981, 1983a,b,c) sample of weathering-profile types.

Visser and Toerien (1971) noted that the 27 m asl. marine terrace gravels at the Olifant River mouth are contiguous with the second youngest (T2) river terrace. As noted above (and to be elaborated in Chapter 16), the marine deposits are Pliocene in age. Assuming that the river terraces are arranged in descending chronological order with elevation, it would imply that only the lowest (T1) river terrace is possibly Pleistocene, the higher (T2–T6) terraces then being Pliocene and older. Other preliminary evidence pointing to the age of the Olifants terraces is the observation by Visser and Toerien (1971) that river terraces T6, T5, T3 and T2 have locally developed on marine sediments (T4 is locally absent). On the broad basis that the bulk of marine sediments on the coastal plains of the Cape Province are Pliocene and younger, then all the river terraces and gravels may be younger than the Early Pliocene transgression to ~100 m asl. However, the valley, now apparently sequestering a patch of early Pliocene, must then be a pre-Pliocene feature.

The presence of silcrete duricrust within the Olifants valley, pre-dating the terraces and gravels, supports the contention that a "Proto-Olifants" valley was already in existence before the phase of fluvial activity that produced the valley position and extent now evident. That silcrete occurs only in places under the terraces suggests that only locally were the duricrusted, pre-existing valley flanks preserved during the subsequent fluvial activity. Assuming uplift very broadly comparable to southern Namibia and the eastern Cape, the Olifants River area (Van Rhynsdorp embayment) was transgressed (twice?) during the Eocene. Furthermore, during the Palaeogene, the valley was the locus of sub-continental-scale drainage connected to the Orange/Vaal drainage (Dingle and Hendey, 1984). Subsequently, the valley would have been subjected to regressive fluvial erosion during the Oligocene. It is therefore likely that the general land surfaces of area had approximately attained their present elevations towards the end of the Palaeogene, as opposed to Late Cretaceous/Palaeocene surfaces persisting to the present.

On the basis of the above, admittedly broad-brush, argument, the weathering-profle silcrete on the flanks of the Olifants River is unlikely to correlate with Eocene and older deep weathering in southern Namibia. Notably, lignitic material has been obtained from boreholes in the Olifants River area and contains a pollen assemblage closely resembling that from the basal fluvial deposits of the Hondeklip area (A. Scholtz, personal communication). This suggests the presence of equivalent terrestrial deposits. At this stage, a similar age for the Olifants River valley silcretes and those of the Hondeklip area is not improbable.

8.6 DISCUSSION

The age constraints and arguments presented above are summarised in Figure 8.3. The proposed occurrence of a post-Eocene period of weathering on the west coast of southwestern Africa depends entirely on the reliability of the Oligocene maximum age for the basal kaolinitic deposits. This is based on the presence of pollen of Oleaceae (ironwood) and Asteraceae (daisies) in peat from the deposits at Zwart Lintjies Rivier.

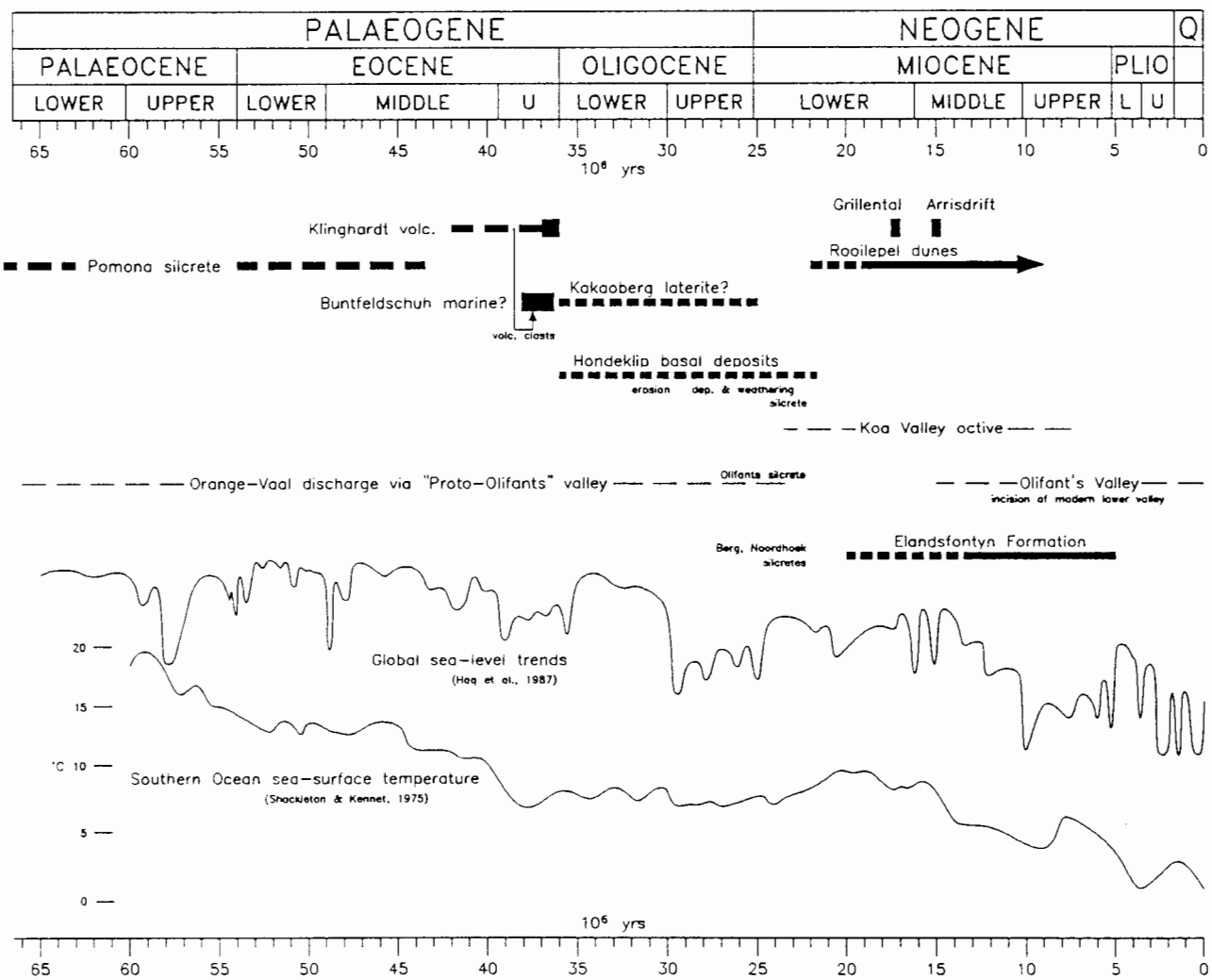

Figure 8.3. Graphic summary of age constraints and correlations discussed in the text.

The aeolian Rooilepel Sandstone has a maximum age of ~22 Ma, from the fossil rodent *Paraphiomys piggotti* which ranges from that time in the East African faunal record (Hendey, 1978). Together with the relatively arid conditions inferred for deposition at Grillental (~17 Ma) and Arrisdrift (~15 Ma) (Ward *et al.*, 1983; Corbett, 1989), this suggests the onset of aridification of the Namib from about the middle Lower Miocene. Contemporaneous weathering along Namaqualand would have been unlikely during the onset of Namib aridification. This suggests that the weathering took place during the Upper Oligocene and early Lower Miocene. The middle to late Lower Miocene was a period of rapid climatic change.

Clasts of late Eocene volcanic phonolite in the marine Buntfeldschuh Formation (Corbett, 1989) are considered critical in constraining it to the Upper Eocene, probably coeval with the dated marine Langental beds (Fig. 8.3). The overlying Kakaoberg aeolianite (and its capping ferricrete) have a maximum age constraint of Upper Eocene. By implication, the Kakaoberg Sandstone accumulated relatively rapidly (in the latest Eocene/early Oligocene) before potentially undergoing erosion during the continuing Oligocene regression and being subjected to laterite-forming soil processes. The interpretation of the Kakaoberg Sandstone as a palaeo-erg (Corbett, 1989) does not conflict with the relatively rapid accumulation, but evidently requires a "dryer to wetter" climatic fluctuation in the Lower Oligocene. This direction of climatic change may be viewed as contrary to global Oligocene cooling relating to the development of the Antarctic circumpolar circulation (Shackleton and Kennet, 1975), when dryer climates would theoretically be expected along the west coast. Similarly, Oligocene kaolinitic weathering along the Namaqualand coast can be cast into doubt.

There are very few observations on southern African middle Tertiary palaeoclimates to compare with global palaeoclimatic trends. Siesser (1978) suggested that weak, spasmodic Benguela upwelling took place from early Oligocene to Middle Miocene times. McMillan (1986) reported that "larger" foraminifera (e.g. *Nummulites*) occur in early Oligocene and Lower Miocene deposits from the Orange Basin. Notably, the "larger" foraminifera are indicative of warm, tropical to subtropical, shallow-marine waters (McMillan, 1986). Curiously, larger foraminifera are apparently absent in the Eocene of the west coast offshore, but *Nummulites* and *Operculina* are abundant in the Lower Oligocene of the Orange Basin (McMillan, 1986). This may suggest that, subsequent to cooling in the Upper Eocene associated with the development of the circum-Antarctic circulation, a warming of sea-surface temperatures occurred in the Lower Oligocene off the west coast. The available data are, therefore, consistent with a "dryer to wetter" climatic trend around the Eocene/Oligocene boundary, corresponding to Kakaoberg aeolianite accumulation and subsequent lateritic weathering. The extensive Upper Oligocene hiatus is succeeded in the Orange Basin by late Aquitanian to late Langhian sediments (~20 to ~15 Ma) that also contain abundant large foraminifera, particularly *Heterostegina* and *Miogypsina (Miogypsina)* (McMillan, 1986). Thus relatively warm shelf sea-surface temperatures evidently persisted off Namaqualand until Middle Miocene times. Siesser (1978) has argued, on the basis of microfossil and geochemical indicators, that intensification of Benguela upwelling and aridification of the adjacent coast extends from Upper Miocene times (~10 Ma).

Warm sea temperatures off Namaqualand and Namibia during the middle Tertiary are certain to have increased the availability of moisture to weather systems. During the late Oligocene/early Miocene, the Hondeklip area was situated ~7° of latitude farther south, at about 37° South (Smith *et al.*, 1981). This southerly latitude suggests a subtropical climate, rather than tropical. Southwesterly to westerly winds blowing across the relatively warm southeastern Atlantic would have delivered rain to the coastal plain. The westerly winds may have been associated with the southern limb of the maritime, subtropical anticyclone. Southern Africa may also have been within range of an expanding, circumpolar, Westerly atmospheric circulation, perhaps seasonally. During the Oligocene regression, the escarpment backing the wide coastal plain rose to ~1500 m asl., probably increasing the

effectiveness of orographic rainfall against it, particularly in the foothills (e.g. in the vicinity of Hondeklip). The rainfall during this period was sufficient to cause kaolinitic weathering, but was insufficient for advanced kaolinization because relict feldspar is still abundantly preserved in the basal fluvial sediments.

The hyperaridity of the Atacama region on the west coast of South America, like the aridity of the Namib region, is associated with a maritime anticyclone, cold upwelling and attenuation of moisture transport from the east. One may predict that there should be similarities in palaeoclimatic history between the regions. Porphyry-copper deposits formed by hydrothermal activity during the early Oligocene 36-31 Ma in the Atacama region subsequently underwent supergene enrichment associated with the extensive formation of kaolinite (Alpers and Brimhall, 1988). Initiation of the supergene enrichment took place during late Oligocene to early Miocene uplift and erosion. Dating by K-Ar techniques of supergene alunite from the La Escondida deposit indicates that the period of supergene enrichment from infiltrating meteoric waters persisted through the Lower Miocene (Alpers and Brimhall, 1988). Severe aridification took place from the Middle Miocene ~15 Ma and was associated with the intensification of upwelling and cooling in the Humboldt Current, in turn associated with the expansion of the Antarctic ice sheet (Alpers and Brimhall, 1988). Although the latter authors suggest that the palaeoclimate during Lower Miocene supergene copper enrichment and kaolinization was probably arid to semi-arid, this must be viewed against the present-day hyperaridity of the region. The evidence for late Oligocene/early Miocene kaolinitic weathering from the Atacama supports the proposal for weathering in the Namib during the same period in the Tertiary.

Detailed comparison of the petrography and geochemistry of the relatively elevated, residual-surface silcretes (e.g. Alexander Bay, Kleinzee and on the Bushmanland plateau) with the Hondeklip "buried channel" silcrete is yet to be carried out. While this may confirm that all are weathering profile silcretes, it will not necessarily provide constraints for relative ages, unless evidence of modification characterizes the older silcretes. The Pomona silcrete is incontrovertible evidence for pre-Upper-Eocene weathering and silcrete formation on the western margin. It could be argued that there is no compelling reason to regard silcreted, weathered bedrock and regolith separately from silcreted fluvial deposits because silcrete formation in a regional weathering profile is unlikely to be confined to either situation. The apparent absence of silcrete clasts in the basal fluvial deposit could also be invoked as evidence for a single period of silcrete development. (Although, being derived from a single stratum in the landscape, they could potentially be rapidly diluted and a deliberate search of a large volume of clasts from the basal deposits has probably not been attempted.)

However, if all the silcretes of the western margin are correlates of the Pomona silcrete, possibly of late Cretaceous/early Tertiary age, then large areas of the present-day landscape are that age and Tertiary uplift, climatic variations and sea-level fluctuations have had remarkably subdued impact on the coastal plains. Accepting the evidence from the Hondeklip area suggests that post-Eocene weathering and silcrete formation took place on the Namaqualand coastal plain. A proposal, arising from the geomorphological assessment of Partridge and Maud (1987), is that the higher elevation

silcrete cappings on interfluves may represent the main, late Cretaceous/early Tertiary African surface. Within-valley weathering-profile silcretes, including those sporadically present on the flanks on modern drainages (e.g Groen, Olifants, Berg valleys) may represent Oligocene/early Miocene dissection and weathering.

This chapter concludes considerations of the origin and age of the basal kaolinitic deposits and silcrete in the Hondeklip study area on the Namaqualand coastal plain. The following chapters describe the overlying marine deposits.

CHAPTER 9

INTRODUCTION TO THE MARINE DEPOSITS

9.1 INTRODUCTION

This chapter provides background information for the following chapters (11-14) in which a selection of measured sections through the mainly unlithified coastal-plain deposits are described and interpreted. The locations of the mine excavations that are mentioned in the text are shown in Fig. 9.1. Figure 9.1 does not reflect the full extent of mining exposures available in the study area over the period of the last decade. For instance, the bedrock embayments on Avontuur-A have been extensively mined. Similarly, the full extent of detailed fieldwork on the marine deposits in the study area, and the analysis thereof, are not presented in this thesis. The excavations from which sections are presented (fig. 9.1) are the key exposures of stratigraphic importance in the study area. The reason for presentation of only a selection of the observations is that it is here intended to motivate general environmental and stratigraphic conclusions, consistent with the more restricted scope of an M.Sc. thesis. Furthermore, the presentation of all the observations in the study area will result in a very lengthy document. The selective presentation of the observations from Hondeklip does not imply incompleteness because the observations not presented are corroborative of the conclusions advanced herein. It is hopefully expected that the interpretations of the key sections, together with the summary of the depositional environments and sedimentary geometry in the study area, will be considered adequate for the conclusions.

The order in which the section descriptions are presented is briefly explained in relation to the stratigraphy. The motivation for the stratigraphy will emerge from the section descriptions (Chapter 11-14). The basic composition of the deposits is described here. Trace fossils are a valuable complement to primary sedimentary structures in the interpretation of depositional environments. The next chapter, Chapter 10, elaborates the nomenclature employed for the trace fossils encountered in the sections. The trace fossils are described and taxonomically assigned, with the assignments qualified where necessary. This enables ichnotaxa to be simply named in the section descriptions, avoiding trace-fossil descriptions being scattered about in the section descriptions, or having to refer to a later chapter or an appendix.

9.2 PRESENTATION OF SECTION DESCRIPTIONS

One or more sections are described from a selection of the excavations examined in the mine (Fig. 9.1). The names used for the excavations (e.g. Zone 4A, A Block) are those used by the geological personnel of the mine. Units are identified in the sections and are numbered upwards from the section bases. There is no intentional correspondence between the unit numbers of sections. With the exception of one section on Hondeklip (Section 11) that overlies the previously described

basal, kaolinitic sediments (Chapter 5), all sections overlie basement gneiss. Every section consists of a lower shallow-marine portion and an upper, terrestrial, mainly aeolian, portion. The marine sediments, which usually have abundant sedimentary and biogenic features preserved, are the prime focus of this study. The overlying terrestrial deposits are mainly medium-grained sands that have an intergranular, brown, pedogenic mud content. The intergranular mud masks much of the sedimentary structure of the terrestrial deposits. Aspects of these terrestrial deposits that are visible in the field will be described. Examination of these sediments and the pedogenic alteration to which they have been subjected will require more specialised field techniques, sampling methods and laboratory work. They are not investigated in detail in this study.

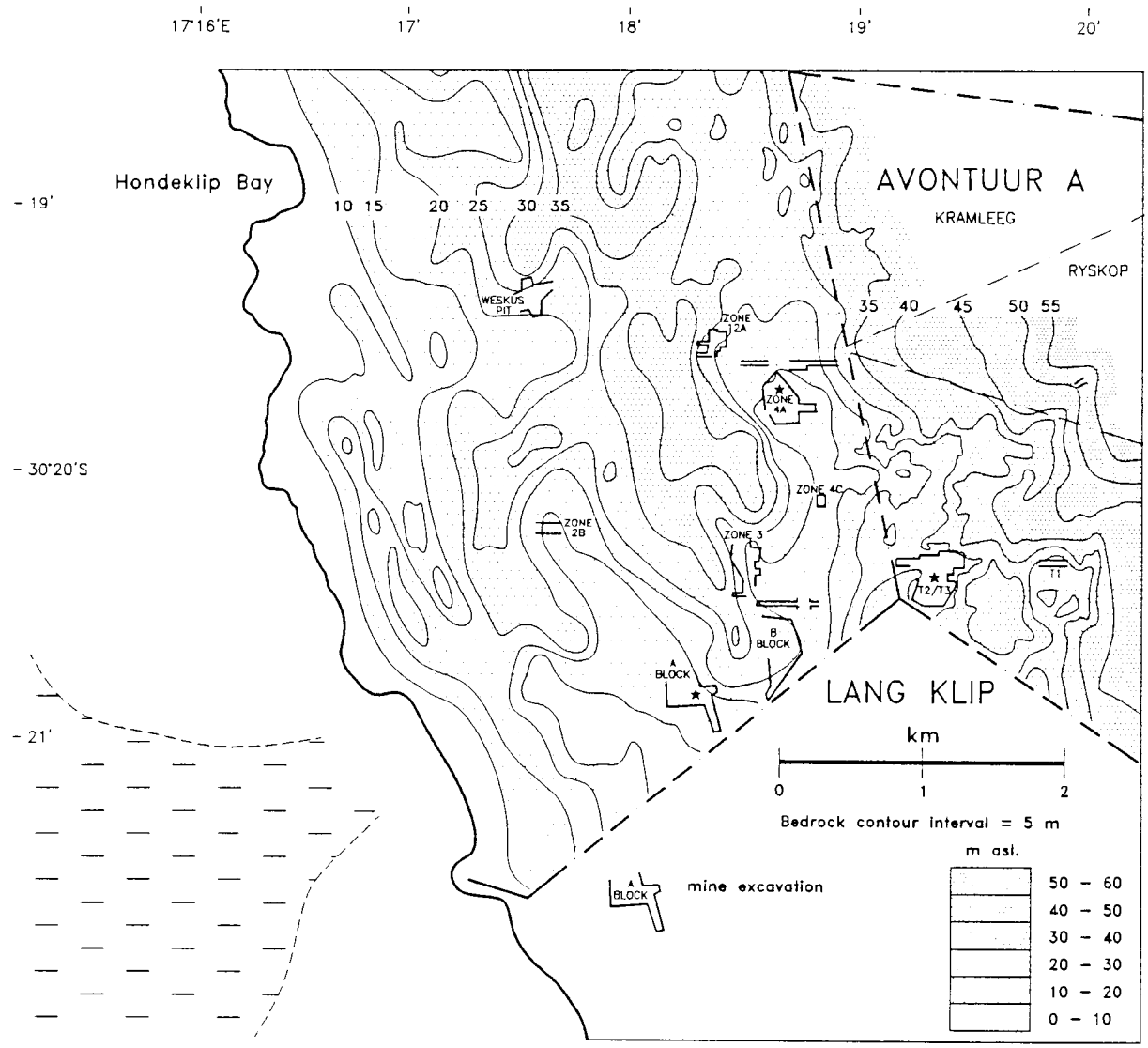

Figure 9.1 Locations of mine excavations described or mentioned in the text. Excavations marked with asterisks are described in detail.

It will be shown that the marine sediments were deposited during seaward (westward) progradation of the coast. Furthermore, on the basis of facies geometry and fossils, it will be shown that only two marine-stratigraphic units of formation status are represented in the mine excavations. The older of

these has been informally named the 50 m Package, the younger the 30 m Package (Pether, 1986a). These informal names refer to the altitudes reached by the transgressions of sea-level associated with each sedimentary package. These altitudes are approximate transgressive maxima, from which the associated marine deposits extend seawards as progradational packages. Inland, on Avontuur-A and the northeastern portion of Hondeklip, only the 50 m Package is represented in the excavations. On the southeastern portion of Hondeklip, marine sections consist of a lower 50 m Package part and an overlying 30 m Package part. The underlying 50 m Package thins westward (seaward) below a seaward-thickening 30 m Package, so that in the westernmost excavations on Hondeklip only the 30 m Package is present.

The descriptions of exposures are followed by the interpretation of the depositional environments represented, with reference to diagnostic sedimentary features and relevant literature. This procedure is a departure from a more conventional format where all observations are presented initially and then followed by the interpretations. The purpose of distributing the section interpretations is to avoid a continuous mass of descriptive detail, with no explicit information on the depositional environments being described. Instead, the instalments of interpretation improve readability, making the "tour" of the exposures easier to follow.

The inland (eastern), altitudinally higher and older 50 m Package exposures on Avontuur-A are described and interpreted first (AV T2/T3) (Fig. 9.1). Thereafter, contrasting exposures within the pronounced embayment, formed by the antecedent fluvial channel landward of the bedrock ridge, are described and interpreted (Zone 4A) (Fig. 9.1). The farther seaward (westerly) and youngest exposures on Hondeklip (30 m Package) are described and interpreted last (A Block) (Fig. 9.1). The descriptions therefore proceed from sections that are entirely composed of 50 m Package deposits (AV T2/T3, Zone 4), to sections that mainly consist of 30 m Package deposits (A Block).

9.3 INTERPRETATIONAL SCOPE

Fundamental to the scope of a stratigraphic study of marine deposits is the determination of the deposits and palaeosurfaces that represent transgression and regression in the record. This is because a marine stratigraphy must be related to the history of relative sea-level movement in order to achieve basin-wide correlations (e.g. dynamic and sequence stratigraphy). In the previous stratigraphic column of Carrington and Kensley (1969), the stratigraphic units are identified as "transgressive complexes" that include "transgressive sands" and "regressive facies." Similarly, in more recent stratigraphic contributions from the Alexander Bay area (Fig. 3.1), both transgressive and regressive deposits are identified within single stratigraphic units (Gresse, 1988). This is problematic for a stratigraphy related to sea-level history, unless the implicit sea-level fluctuations are minor disturbances of a larger sea-level cycle. In mainly arenaceous, shallow-marine sequences, the establishment of the scale of sea-level trends requires accurate diagnosis of the depositional environments and associated palaeodepths by means of sedimentary structures and ichnofabrics.

The interpretation of shallow marine sediments has advanced to the stage where the general spectrum of facies changes over the intertidal to offshore sedimentary interface, for a similarly general range of wave and tidal conditions, is established (e.g. reviews in Heward, 1981: McCubbin, 1982; Elliott, 1986). Interesting challenges are posed by the necessary attempt to forge links between modern studies (instrumental measurements of processes, morphodynamics and hypothetical vertical sections of piled-up, shallow, box-cores) and the long-term depositional record. The intensive study of cores in Holocene barrier islands has contributed much to the knowledge of vertical sequences (e.g. Heron *et al.*, 1984; Howard and Frey, 1985; Moslow and Tye, 1985). Improved clarification on the types of sedimentary structures and their vertical associations must come from the detailed documentation of laterally extensive exposures of shallow-marine sediments from geologically young sequences that can be related to present-day wave climate (late Pleistocene and Holocene progradation) (e.g. Dupré, 1984). In the case of Pliocene deposits such as those of the study area, the present-day wave climate cannot be assumed to be directly applicable, but it probably was not greatly divorced from modern conditions. Many marine sedimentary features in the study area, including broad-scale facies architecture, deserve more detailed discussion in terms of processes and preservation (and nomenclature). Some can provide additional information for palaeoenvironmental reconstruction, for example, the calculation of palaeo-wave conditions from ripple spacings and grain size (e.g. Clifton and Dingler, 1984). However, because the scope of this thesis is primarily limited to the stratigraphic aspects, this detail is not presented.

9.4 SUMMARY OF SHALLOW-MARINE PROCESSES AND DEPOSITS

Clarification of terminology is a necessary preface to the interpretations. Both geomorphic terms (e.g. shoreface) and dynamic terms (e.g. surf zone) are used in the description of shallow-marine environments (Bourgeois and Leithold, 1984). There is also variation in the meanings of the same terms between different authors. The terminology used herein is summarised in graphic form in Fig. 9.2, which also incorporates the main elements of a generalized model of the sedimentary processes and products in the open-coast, shallow-marine environment. The following summary is compiled from various sources, including McCubbin (1982), Bourgeois and Leithhold (1984), Elliott (1986) and Clifton (1988). The summary is presented from shallow water, where the processes are familiar, in the offshore direction to the lower shoreface and offshore environments, where processes are mainly inferred. In this study the term "offshore" is used for the deeper environment seaward of the lower shoreface, where the transition to muddy, bioturbated shelf deposits takes place.

The *backshore* is landward of the crest of the beach and is a narrow to wide (tens to hundreds of metres), flat area that is periodically flooded during storms when the beach crest is breached. During the stormy season, when run-off and the water-table also rise, this area may be flooded for several weeks and densely colonized by burrow-dwelling invertebrates (e.g. Noordhoek beach, Cape Peninsula). The beach crest or berm is a constructional feature that may be eroded entirely during intense storms. It is not a feature of high-wave-energy beaches (Short, 1984). The *foreshore* is the

intertidal seaward slope (the beach as generally understood), where the dominant processes are swash and backwash. Seaward-dipping lamination with low-angle truncations representing the changes in beach slope are the main diagnostic structures.

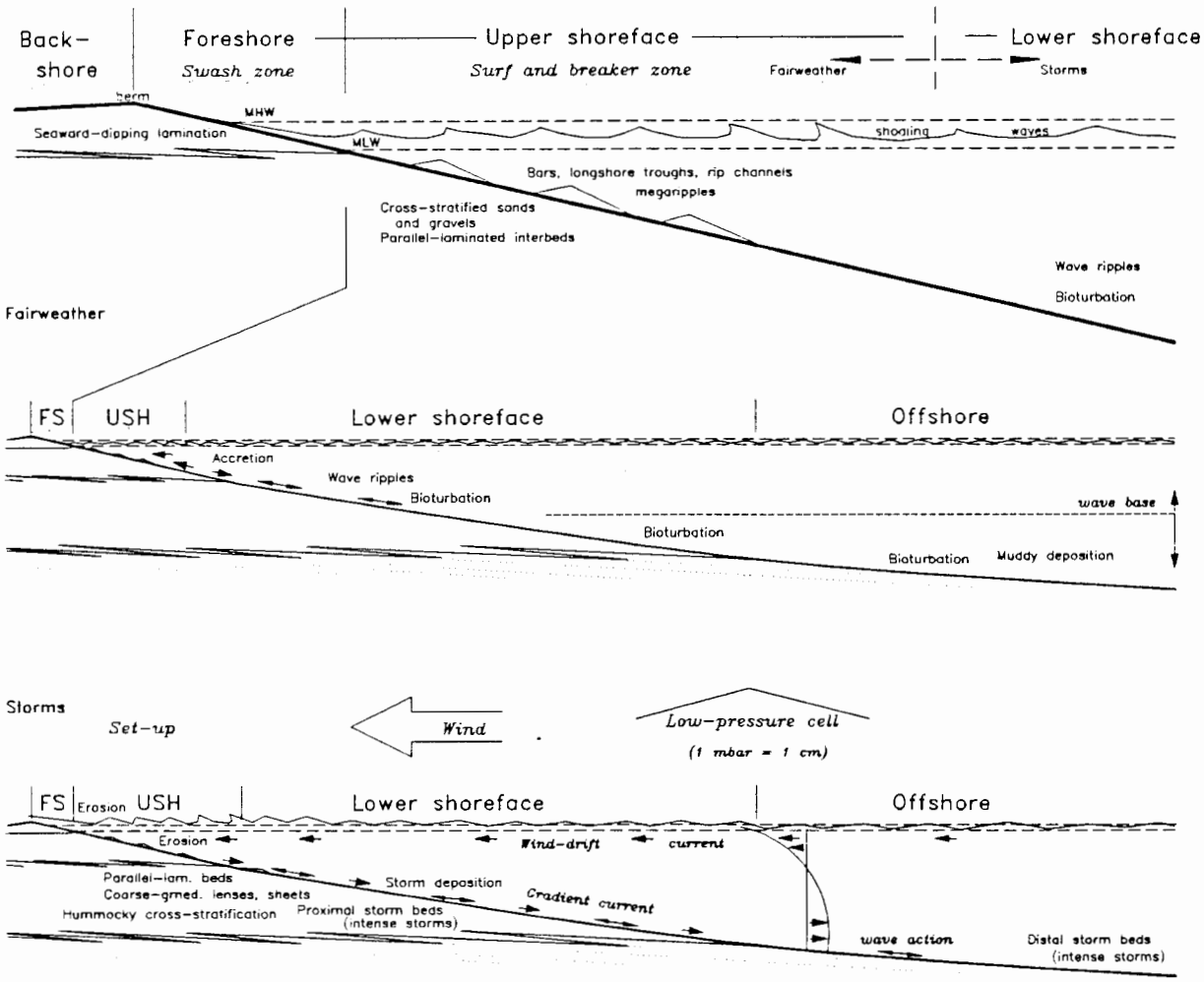

Figure 9.2 Summary of shallow-marine environments and processes. See text for explanation and sources.

The *upper shoreface* is the shallow, subtidal zone extending seawards from the low-tide level. It is the breaker and surf zone, where asymmetric, oscillatory wave currents transport sediment particles onshore, while the return flow seawards forms nearshore circulation cells involving longshore and offshore rip currents. The onshore transport generates 3-dimensional, lunate bedforms (megaripples) from depths just seaward of the breaker zone. Larger, composite bedforms form under a wide variety of wave conditions. These bars are parallel to the shoreline under coast-normal wave approach and oblique to the shoreline under oblique wave approach. Bedforms migrate alongshore in the bar-troughs and offshore in rip channels. Due to the shifting of bars, troughs and rip channels with changing wave conditions, upper shoreface deposits are characterized by an abundance of trough cross-bedding and the coarsest sediment in the shallow-marine sequence is concentrated there. The seaward boundary of the upper shoreface is dependent on the wave conditions, shifting seaward

during storms and landwards during fairweather periods. In marine regressive sequences, the lower contact of upper-shoreface deposits is usually marked by a well-defined facies contrast with underlying, mainly laminated and bioturbated, fine sands.

The *lower shoreface* is seaward of the breaker zone and the associated, larger bedforms. It is subject to oscillatory wave currents during fairweather periods and the less routinely-mobile sediment is colonized by benthic organisms. The processes active in the lower shoreface are to a large extent inferred from the deposits, rather than by direct observation. Essentially, erosion and deposition in the lower shoreface takes place mainly during and immediately after storms. Typical evidence of storm deposition consists of thin to thick beds, each consisting of an erosive base overlain by parallel-laminated sand passing upward into a bioturbated top, sometimes with an intervening wave-rippled interval (laminated-to-burrowed sequences or "lam-scram" beds) (Howard, 1972; Bourgeois, 1980; Howard and Reineck, 1981). Much thicker, but basically similar, storm-deposited sequences are documented by Kumar and Sanders (1976). These consist of a basal lag of coarse gravel, up to 0.5 m thick, overlain by finely-laminated sand, up to 2.0 m thick, with capping bioturbated or wave-rippled sand, up to 0.3 m thick. The basal lag is inferred to have developed during storm erosion, with the thick-laminated interval being deposited rapidly under high turbidity (suspension) and strong currents as the storm waned. The bioturbated/wave-rippled interval represents subsequent fairweather conditions.

Hummocky cross-laminated, fine-sandy beds, consisting of low-angle, undulatory lamination disposed in broad, overlapping troughs and low hummocks, are recognized as the products of storm deposition at lower shoreface to offshore depths (Dott and Bourgeois, 1982). The hummocky cross-laminated beds form part of storm to fairweather sequences. Basal lags may be present, whilst the beds grade upward into wave-rippled and bioturbated intervals. In proximal, lower-shoreface settings, more marked storm-erosion results in removal of the post-storm intervals and amalgamation of successive, hummocky-laminated, storm beds. Relative to the upper shoreface, the lower shoreface contains more bioturbated beds and a greater diversity of trace fossils. The lower shoreface grades seawards to the *offshore* environment of the shallow shelf, where muddy deposition dominates, punctuated by distal deposition from storms and the rare, but intense storm that produces shell lags. In many shelf settings, residue from the preceding transgression may occur along the outer edge of the prograding shoreface wedge. These may be unreworked and therefore truly *relict* sediments (e.g. cobble and boulder lags), or *palimpsest* sediments (e.g. an "abandoned" transgressive sand-sheet infrequently reworked at shelf depths by major storms) (Swift *et al.*, 1971).

During fairweather (low wave-energy) conditions, wave-base intersects the lower shoreface, but moves progressively offshore with increasingly stormy conditions. During fairweather periods, sand eroded from the upper shoreface moves onshore and accretes to the foreshore, forming a berm and a relatively steep, reflective beach. During moderately stormy conditions, the foreshore is eroded and sediment accumulates in the upper shoreface where it contributes to the construction of bars. A proportion of sediment is transported seawards via rip channels to the lower shoreface, to form thin

storm sequences. During rare intense storms, the foreshore, upper shoreface and lower shoreface are eroded and considerable quantities of sediment are deposited on the lower shoreface and farther out in the offshore region The physical aspects of basic storm conditions have been detailed in a model by Allen (1982). As a storm approaches and atmospheric pressure drops, for every millibar decrease the sea-level is raised 1 cm. A typical elevation increase is ~20 cm, with extreme events raising sea-level by up to 60 cm (G. Brundrit, 1994, personal communication). The onshore wind tilts the sea-surface up towards the shore and drives a *wind-drift* current within the surface water, causing a *set-up* of sea-level against the shoreline (Fig. 9.2). The raised sea-level or storm surge results in compensatory, bottom return flow, the *gradient current*. This current transports sediment mobilized in the nearshore to the lower shoreface and farther offshore.

The same basic processes operate through the range of different, incident wave energies. This results in similar facies expression of foreshore, upper and lower shoreface deposits, but wave energy primarily determines the widths and depths of the dynamic zones over which similar processes operate. Progradation of a high wave-energy coast, where wave and storm processes act to considerable depth, results in a thick shoreface deposit of sands and gravels. On a low wave-energy coast, wave-driven shoreface processes are limited to shallow water and progradation will produce a corresponding thin shoreface deposit. The thicknesses of shallow-marine facies are therefore related to the wave energy (Howard and Reineck, 1981; Short, 1984). The sediment supply will also influence facies development, due to the influence of grain size on bedform type.

9.5 GENERAL COMPOSITIONAL ASPECTS OF THE MARINE SEDIMENTS

GRAVELS

The marine gravels are mainly rounded to well-rounded and derived from the local gneissic rocks. Quartzite, amphibolite and epidote-rich clasts, derived from lithologies locally present in the gneisses, are readily noticed. The gneissic foliation results in a tendency for bladed and tabular clasts. Cobbles and pebbles of chocolate-brown phosphorite are an ubiquitous component of the marine gravels. They are most abundant in the basal gravels, where the largest clasts occur, and are particularly concentrated where an *in situ* phosphorite bed is preserved. Included in the phosphorite clasts are quartz pebbles. Abraded remnants of phosphorite on clasts are common. As noted in Chapter 5, silcrete pebbles and cobbles are common in basal gravels in the study area, but are not as abundant as phosphorite clasts. Silcrete clasts are particularly abundant in those excavations where the large boulders of silcrete occur (A and B blocks). Lithoclasts of marine sandstone, cemented by yellow collophane and sometimes calcite, are also present in the gravels as a very minor component. These are fine to coarse-grained quartzose sands, with minor, fine-grained glauconite and phosphatic shell fragments. They are usually pebble-size, but at one site cobbles occurred.

Heavy mineral concentrate from marine gravels, that includes the very coarse sand and granule fractions, has abundant kyanite (~20%) as clouded, grey laths, but some examples still have patches

of more typical blue hue. Black ore grains (ilmenite and magnetite), garnets, epidote, amphibolitic rock fragments, small, rounded, brown to black, cherty granules and, more rarely, diamonds, are present.

Bone pebbles, consisting of brown, mineralized bone and usually rod-shaped, are very common. Large bone clasts, derived mainly from whales, are particularly common in Zone 4A (Fig. 9.1). Shark teeth and various other fish teeth are also found in the heavy concentrate from the gravels.

SANDS

The coarse fractions of the marine sands are rounded and quartzo-feldspathic, with 15-25% feldspar. The coarse sand size feldspar grains vary in colour from opaque white, pale orange and pale pink. Their abundance was estimated by grain counts after brief etching in HF acid. Resinous orange to vitreous white, curving, striated, angular platey grains are abundant and these are fragments of the phosphate-mineralized shells of the inarticulate brachiopod *Pelagodiscus*. Occasionally, intact shells of *Pelagodiscus* are found which are low conical ("chinese hat") in shape, with fine, concentric striae, leaving no doubt as to the origin of most of the phosphatic grains in the coarser sand fractions. Detrital heavy minerals (ore grains , kyanite and garnet) are a very minor part of the coarse sand fractions, except in the instances of enrichment on erosion surfaces (e.g. basal gravels, channel lags).

The fine sand fractions are angular and quartzose, with glauconitic and phosphatic grains comprising the main, secondary components. The glauconite occurs as rounded to discoidal, green, opaque grains and comprises 1-2% of the fine sand fraction. Its appearance ranges from pale green and earthy to very dark green and shiny. Some of the latter are slightly sutured, but deeply-sutured grains are rare. Most of the glauconite does not sink in bromoform (S.G.= 2.89) and that which does is mainly dark green. The glauconite contributes to the green hue (~5Y 7/2) of the marine sands. Under high magnification (x150), fine quartz grains with patches of adhering green material, presumably glauconitic, are seen to be common. These grain coatings also contribute to the green hue of the sand.

Phosphatic grains in the fine sand fractions are platey, often grooved, angular grains varying from resinous orange, to vitreous white, to translucent and clear. As in the coarse sand fractions, these are clearly derived from *Pelagodiscus*. Sub-rounded to well-rounded grains of the same material are also abundant. The occasional translucent, yellow fish tooth and atypical grains with pores indicates that vertebrate skeletal material has also contributed to the sand-size apatite. Rounded, chocolate-brown grains of slightly resinous lustre are common and these are apparently derived from erosion of precipitated phosphorite beds. Light brown, rounded phosphorite grains also occur.

Black ore grains are angular to well-rounded and some are magnetic (magnetite), whilst others have parallel cleavage outlined by white material, the ilmenite alteration product leucoxene. The garnets are angular, pale-pink, pyralspite-group garnets, with a few of pale red hue. They are probably mainly almandine. Plates of biotite mica are bronze to greenish brown and most have rounded corners.

Angular and sub-angular, clear to very pale green grains, often clouded with inclusions, exhibiting etching and with alteration to opaque, white material, are considered to be sphene, with extensive alteration to leucoxene. Rare, grey-green, prismatic cleavage fragments, sometimes of fibrous aspect, are an amphibole, possibly hornblende. Rare, sub-rounded, lime-green grains are probably epidote. Rare, colourless grains, with prismatic to tabular habit and marked cleavage, often causing "steps" on the grain surface, are kyanite. Zircon is very rare in the marine sands.

The proportions of ore grains, garnet, biotite and sphene are variable. In sands that have apparently undergone a degree of heavy-mineral concentration, ore grains and garnets are more abundant than phosphatic grains and biotite is absent. In one sample examined, sphene was the dominant heavy mineral (40-50%) in the bromoform separate.

Preservation of Carbonate

An initial impression of the marine deposits at the Hondeklip mine, imparted by the abundant fossil shells, is that carbonate in the sediments is well-preserved. This initial impression is qualified on more detailed examination when it becomes apparent that a large proportion of the marine sands has only a negligible carbonate content of less than 1 percent. These carbonate-barren sands are yellow in hue (~5Y 7/4) compared with sand with a carbonate content of a few percent that is pale green (~5Y 7/4). The yellow hue is due to a faint coating of yellow mud/clay on the sand grains. Careful examination of freshly exposed, damp faces in barren, yellow-hued, fine sands, producing by collapsing material from the faces, usually reveals vestigial evidence of a pre-existing shell content. Very thin arcs and lines outlined by yellow mud betray the sites of shell fragments and sometimes small cavities containing the delicate traceries of filled microborings are present. These subtle features become less obvious after the surface dries, sheds grains and becomes etched by wind-driven sand. In other examples of leaching, the yellow hue is not developed and the leached sand is darker green (~5Y 6/2) and softer than surrounding sand with carbonate. The darker, soft and usually structureless areas occur as irregular patches on all scales and have sharp boundaries. Thus the marine deposits are extensively leached of carbonate. Where some isolated shell is present in the leached sands, it is almost invariably of oyster or barnacle origin, these shells being of calcitic composition and more stable than the metastable aragonite that composes most marine shell.

It is concluded that, over much of the study area, the original, "average" or "background," mainly sand-size carbonate content of the marine sands has been removed, with only a minor portion remaining as interstitial carbonate mud. This condition is particularly applicable to the marine sands on Avontuur-A, overlying the westward bedrock gradient to the east of the channel on Hondeklip.

The beds with abundant shell gravel have been preserved due to the buffering effect of the significantly greater carbonate content on the corrosive groundwater. Within shelly beds, the transitions between "inner" portions with well-preserved carbonate and "outer" portions in which the carbonate is totally dissolved take place over a few centimetres. It is probable that a requirement for the dissolution of shell concentrations from their outer margins inwards would be relatively slow pore-

water movement and renewal. Basal gravels, with a shell content consisting nearly exclusively of calcitic oysters, probably originally contained a greater variety of shells that have been lost due to enhanced groundwater flow in the gravel aquifer.

CHAPTER 10

THE TRACE FOSSILS

10.1 INTRODUCTION

Bioturbation is a major feature of the marine sediments. A wide variety of trace fossils is present. The most visually obvious are dealt with here, as well as cryptic ichnofabrics revealed by the lacquer peel technique. The majority of trace fossils encountered have been assigned to existing, familiar ichnogenera and in several cases to existing ichnospecies, but not all the traces can be readily identified to ichnospecies level with certainty. In cases of uncertain ichnospecies, *ad hoc*, informal, descriptive terms are used between single quotation marks. This use of descriptive labels is preferred to the use of alphabet letters to label ichnotaxa, because a descriptive term (e.g. *Planolites 'threads'*) has more visualisation value for the reader than, for instance, *Planolites* B. The expression and degree of bioturbation (ichnofabrics) in beds and facies are described in the section descriptions.

A factor contributing to taxonomic uncertainty is the lack of bedding-plane exposures of trace fossils in the unlithified deposits. The enhancements of diagenesis and preferential weathering, that affect the aspect of biogenic structures in lithified rocks, must be taken into account in comparisons of unlithified specimens with figures and descriptions of existing ichnotaxa. Burrows with semi-consolidated infills, that etch into relief, are identified with more certainty than those that break off at the level of the exposure and therefore resemble the traces seen in cores. More extensive collecting by artificial consolidation and study by "dissection", serial sectioning and epoxy-impregnated thin sections, are requirements for resolving taxonomic uncertainties.

Ichnotaxonomic problems are also reflected in the level to which traces can be identified. A conservative approach has been adopted, rather than suggesting that traces, for which precise analogues cannot be found, are new. The approach also follows D'Alessandro and Bromley (1987) in regarding meniscate backfill alone as an unsuitable taxonomic criterion, as it may be produced by any tunnelling involving transfer of material backwards. Furthermore, in compound traces involving more than one taxon, the name of the predominant component is assigned to the entire structure (Bromley and Frey, 1974).

For each established ichnotaxon listed alphabetically in the systematic ichnology below, a diagnosis from the literature is provided verbatim, with additional remarks in some instances. Thereafter the features of the traces from the study area, that are assigned to the particular taxon, are described and discussed.

10.2 SYSTEMATIC ICHNOLOGY

ICHNOGENUS *GRANULARIA* POMEL, 1849

Diagnosis: — Elongated fillings of burrows; long, diameter up to about 15 mm, twig-shaped, with rather regular branching; walls originally lined with clay particles (Häntzschel, 1975).

Remarks: — *Granularia* is an ichnotaxon in need of revision. Häntzschel (1975) regarded *Alcyonidiopsis* Massalongo, 1856, as a synonym. Frey *et al.*, (1978) and Pemberton and Frey (1982) suggested that *Ophiomorpha* is a synonym for *Granularia*, but did not elaborate a formal synonymy. However, *Ophiomorpha* is a large-scale burrow system that usually crosscuts beds, whilst the burrows here referred to *Granularia* occur on a distinctly smaller scale, in localised volumes of bioturbated sediment, within individual beds. Furthermore, the wall pellets in *Ophiomorpha* are themselves comprised of smaller pellets (Frey *et al.*, 1978), whilst those in *Granularia* (as used herein) are discrete. Pemberton and Frey (1982) mentioned *Alcyonidiopsis* as an example of a pellet-filled burrow, obviously regarding it as a valid ichnogenus. However, *Alcyonidiopsis* has been regarded as a *nomen oblitum* (name fallen into disuse) by Pickerill (1989), who, along with others, assign unlined, pellet-filled burrows to *Syncoprulus* Richter and Richter, 1939. Other similar taxa are *Tomaculum* Groom, 1902, which consists of strands of pellets on bedding planes, *Discotomaculum* Chiplonkar and Badwe, 1972, which are zigzag, unlined burrows filled with disc-shaped pellets and *Walpia* White, 1929, which has a lining of disc-shaped pellets (Häntzschel, 1975). *Compaginatichnus* Pickerill, 1989, is an unusual, unlined burrow with an upper, meniscate portion and a lower, pellet-filled portion.

Study area examples: — *Granularia* is used to accommodate burrows that are lined and locally stuffed with small (1.0-1.5 mm), ovoid, mud pellets (Plate 10.1) that are faecal or pseudo-faecal in origin. Whilst the pellets may be referred to the coprolite ichnogenus *Tibikoia* (see below), burrows made up of the pellets are herein assigned to *Granularia*. Well-developed *Granularia* burrows (Plate 10.2) are ~0.5 cm in diameter and sinuous, with pellets forming both the burrow walls and the infills. One example seen exhibited meniscate, active-fill structures in which the laminae, 2-3 mm apart, were constructed of pellets. Branching is present and is dichotomous, with an angle of 70-80° in the Y-shaped fork. *Granularia* burrows occur in association with *Palaeophycus tubularis* burrows, in volumes of totally bioturbated, muddy sediment in which pellets are concentrated (*Granularia-Palaeophycus* clumps) (see Plates 10.8, 11.4). Within the pellet-rich, bioturbated zones, examples of incompletely-formed burrow walls, pellet-clumps representing burrow-stuffing and interpenetrant burrows are abundant. The churned appearance of the pellet-rich, bioturbated zones has evidently resulted from the interpenetrating reprocessing of the pellet-rich sediment.

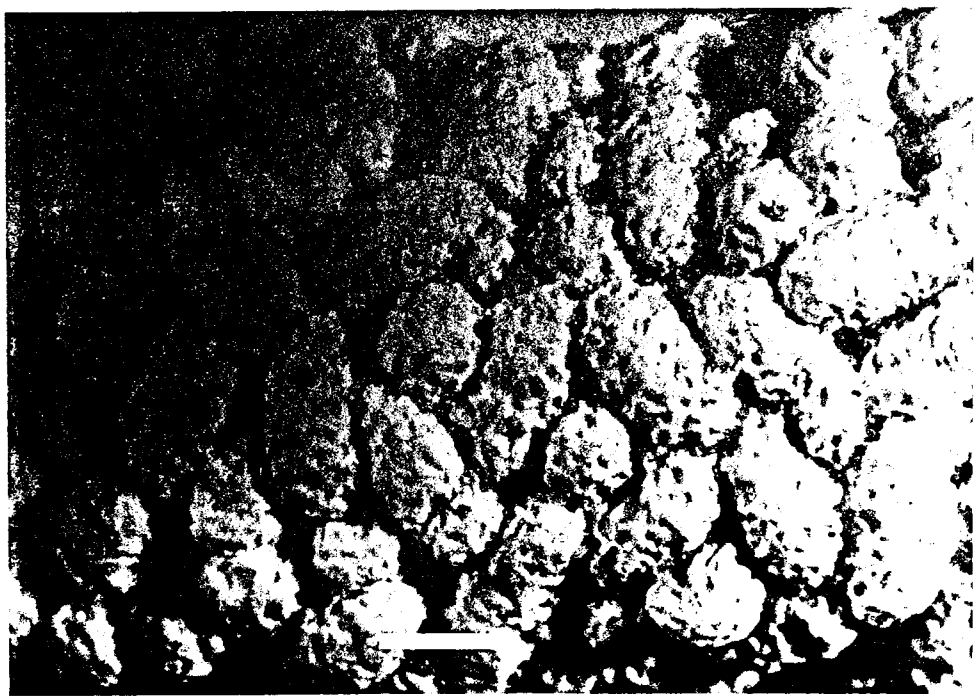

Plate 10.1 Ovoid pellets (*Tibikoia*) of white, calcareous mud forming the wall of a *Granularia* burrow. Scale bar is 1 mm.

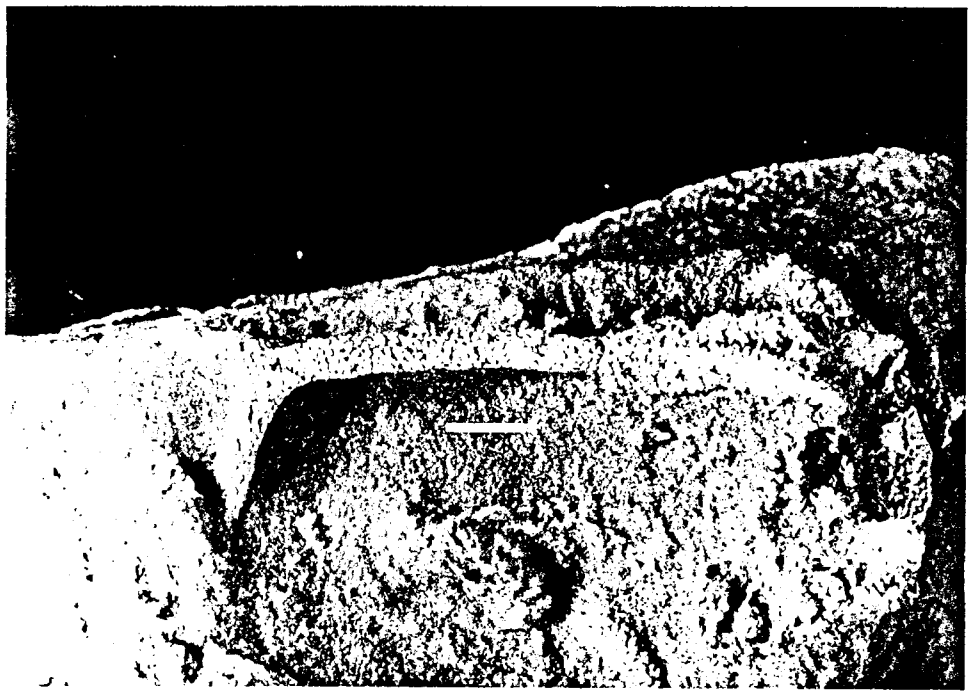

Plate 10.2 Branched *Granularia* burrow. Scale bar is 1 cm.

ICHNOGENUS *GYROLITHES* DE SAPORTA, 1884

Diagnosis: — Burrows more or less describing a dextral or sinistral, circular helix more or less upright in the sediment; surface with or without structure or scratch traces; radius of whorls and diameter of tunnel rather constant; may branch and interconnect with *Thalassinoides* or *Ophiomorpha* networks (Bromley and Frey, 1974).

Remarks: — The type ichnospecies of *Gyrolithes*, *G. davreuxi*, redescribed by Bromley and Frey (1974), consists of irregularly coiled helices, with variable separation of individual coils and frequent reversals of coiling direction. However, the burrow diameters and radii of the coils are relatively constant. The burrows are ~1 cm in diameter and the radii of spiralling 1.2-2.1 cm (average of 1.5 cm). The longest helix measured 12.5 cm.

Study area examples: — Well-developed, helical *Gyrolithes* burrows occur (Plate 10.3), but they are part of *Thalassinoides 'multiplex'* burrow systems. The burrows forming the helices are 1.5-2.0 cm in diameter, with generally smooth exteriors, and are composed of slightly muddy, fine sand with scattered coarse grains. Burrow walls a few mm thick are vaguely defined by the tendency for the infilling to fall out, leaving a slight circumferential rim. Similarly, poorly-defined active backfill can be seen in some wind-etched specimens. The helices are erect, 20-30 cm high, with radii of coiling of 3-4 cm and vertical separation of the coils of 3-7 cm. They coil both clockwise and anticlockwise, branches from off the spiral are sometimes present and the spirals end with branches. Two examples with reversals of the coiling direction below a branch were seen.

The *Gyrolithes* from the study area are about twice as large as the type species, *G. davreuxi.* Moreover, the coiling of most of the helices is more regular in form, with approximately even spacing between coils, although some examples with coiling reversals are tortuously looped (e.g. Plate 10.3, centre). Interestingly, *Gyrolithes* occur at a distinct level within the regressive sequences, in the upper portion of the lower shoreface in open-coast settings, where deposition of 10-20 cm thick, plane-laminated, moderately bioturbated, fine sand beds dominated.

ICHNOGENUS *OPHIOMORPHA* LUNDGREN, 1891

Diagnosis: — Simple to complex burrow systems distinctly lined with agglutinated pelletoidal sediment. Burrow lining more or less smooth interiorly; densely to sparsely mammilated or nodose exteriorly. Individual pellets or pelletal masses may be discoid, ovoid, mastoid, bilobate, or irregular in shape. Characteristics of the lining may vary within a single specimen (Frey *et al.*, 1978).

Remarks: — Four ichnospecies of the knobby-walled burrow *Ophiomorpha* are currently defined on the basis of wall construction; *O. annulata* (Ksiazkiewicz, 1977), *O. borneensis* Keij, 1965, *O. irregulaire* Frey *et al.*, 1978, *O. nodosa* Lundgren, 1891 (Frey *et al.*, 1978; Frey and Howard, 1985). The constructors of *Ophiomorpha* burrows are mainly thalassinidean shrimp (Frey *et al.*, 1978).

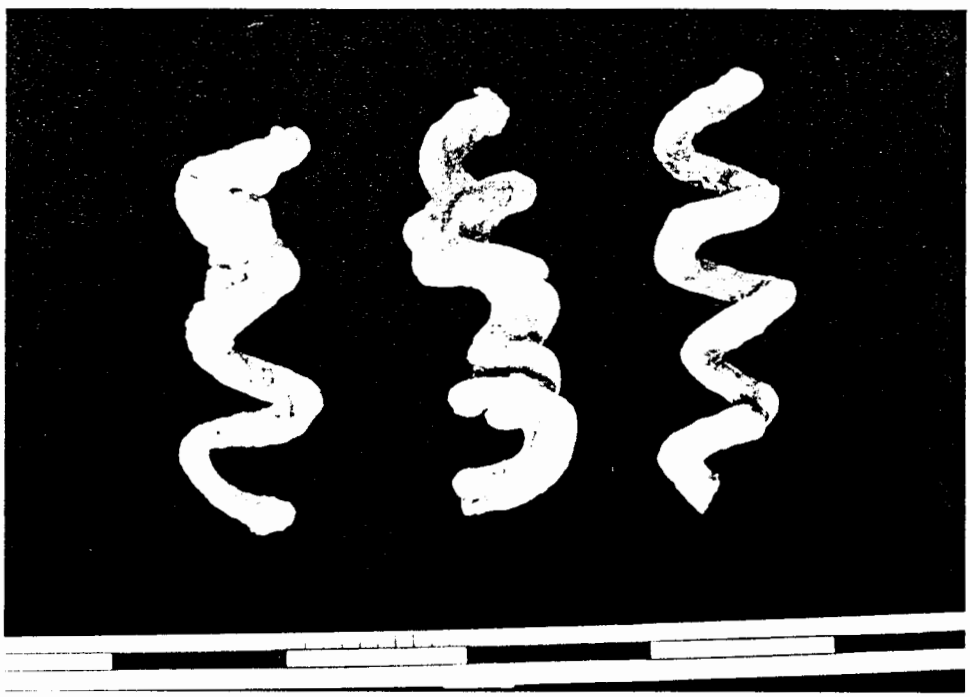

Plate 10.3 *Gyrolithes* burrows. Left, anticlockwise helix; centre, convolute example; right, clockwise helix. Scale in dm.

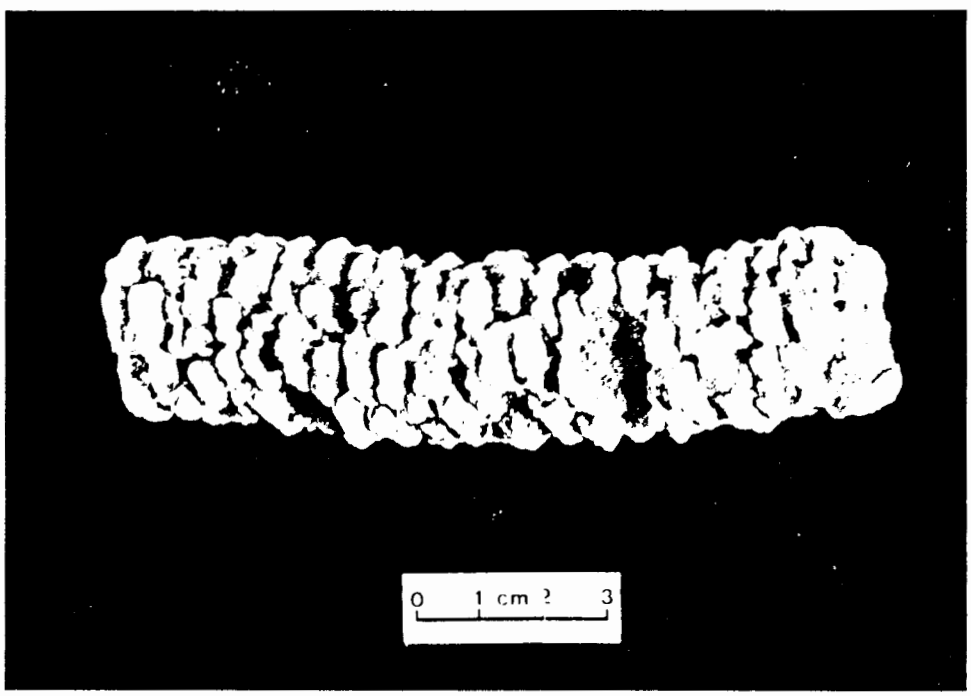

Plate 10.4 *Ophiomorpha borneensis*, showing wall construction of bilobate pellets.

The examples of knobby burrows from the study area can readily be assigned to three ichnospecies of *Ophiomorpha*. *O. nodosa* is abundant, but is not represented by discrete, monospecific burrows. Instead it occurs as a subsidiary part of very large *Thalassinoides 'multiplex'* systems. *O. borneensis* and *O. irregulaire* burrow walls are much less common in the study area, but are consistently developed in the burrow systems where they occur. These systems have a limited vertical extent of ~1 m, in contrast to *Thalassinoides 'multiplex* systems bearing *O. nodosa* that extend over several metres. *O. annulata*, not found in the study area, is characterized by a wall made from elliptical pellets arranged end-to-end, in rings around the burrow circumference (Frey and Howard, 1985).

Ophiomorpha borneensis Keij, 1965

Diagnosis: — Burrow walls consisting predominantly of dense, regularly distributed, bilobate pellets (Frey *et al.*, 1978).

Study area examples: — The burrows walled with paired pellets from the study area vary in size from ~1.5 cm in diameter, with pellets ~2 mm in diameter, to burrows ~3 cm in diameter, with pellets ~4 mm in diameter (Plate 10.4). The pellets consist of sand grains embedded in a hard, slightly calcareous, white mud matrix. The grains are mainly densely packed rather than floating in the matrix, (within grain diameters of each other), although areas with sparse, floating grains do occur. Infills are like the host sediments. The burrows are both steeply oblique and subhorizontal. In steeply oblique examples, smaller burrows about half the diameter of the main burrow, branch upwards from it at ~45°. Some of the branches are *culs de sac*, the end closed with pellets. Where best developed, the steep burrows occur above a horizon, ~10 cm thick, along which transverse sections are exposed, indicating horizontal burrows. This suggests a maze connected to the surface by the steep burrows.

Ophiomorpha irregulaire Frey, Howard and Pryor, 1978

Diagnosis: — Burrow walls consisting predominantly of sparse, irregularly distributed, ovoid to mastoid pellets or pelletal masses. The sparse, pointed pellets or pelletal masses are the main distinguishing characteristics of *O. irregulaire* (Frey *et al.*, 1978).

Study area examples: — These are burrows, 1.5-2.0 cm in diameter, with thin (1-2 mm), but well-defined, hard linings of greenish-white, slightly calcareous mud. The burrows are mainly oblique and subhorizontal, with some steep examples, and branch dichotomously. Scattered apparently randomly about on the exterior of the uppermost, "roof" parts of burrow linings are pointed "nipples", 3-7 mm in diameter and height, 1-3 cm apart, composed of the same material as the linings (Plate 10.5). These tend to be more dense, ~1 cm apart, where branching occurs. Sometimes projections are elongate in the longitudinal direction of the burrows. The linings and their projections are finely granular and consist of small, poorly-defined, amalgamated pellets ~0.5 mm in diameter, made from white mud and embedded fine sand grains. The linings are also enriched in benthic foraminifera, relative to the host sediment. In places, vermiform, convolute ribbons, presumably of faecal origin, have been pressed

relative to the host sediment. In places, vermiform, convolute ribbons, presumably of faecal origin, have been pressed into the linings. These are ~1 mm wide, but are flattened and elliptical in cross-section. They are composed of fine sand and white mud. Taxonomically, they could be referred to the coprolite taxon *Lumbricaria* Münster (in Goldfuss), 1831 (Häntzschel, 1975).

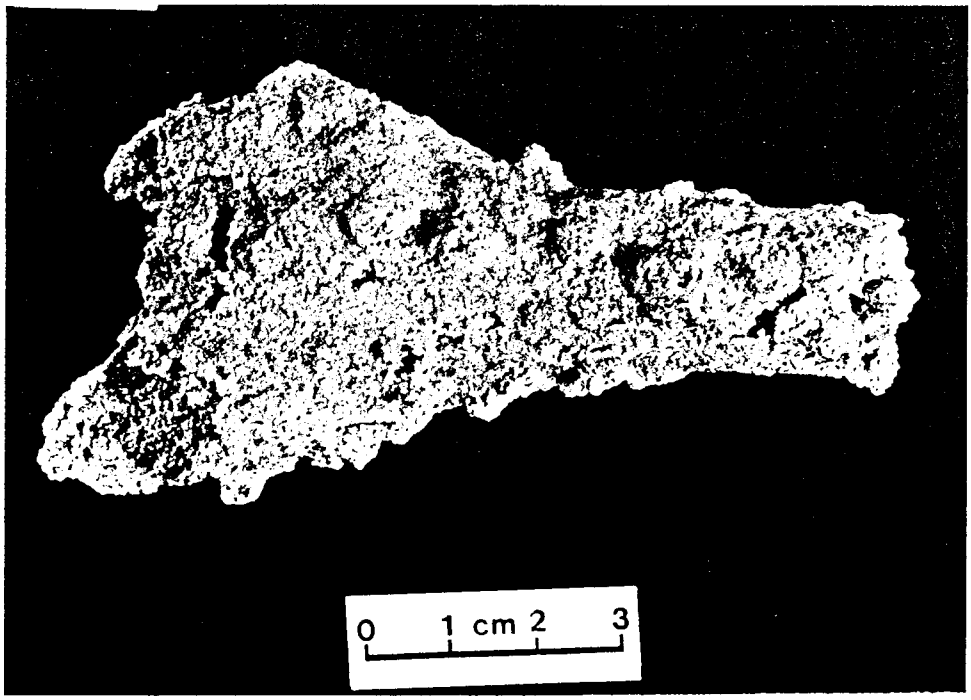

Plate 10.5 *Ophiomorpha irregulaire*. Y-shaped bifurcation with typical, sparsely scattered, pointed pellets embedded in wall.

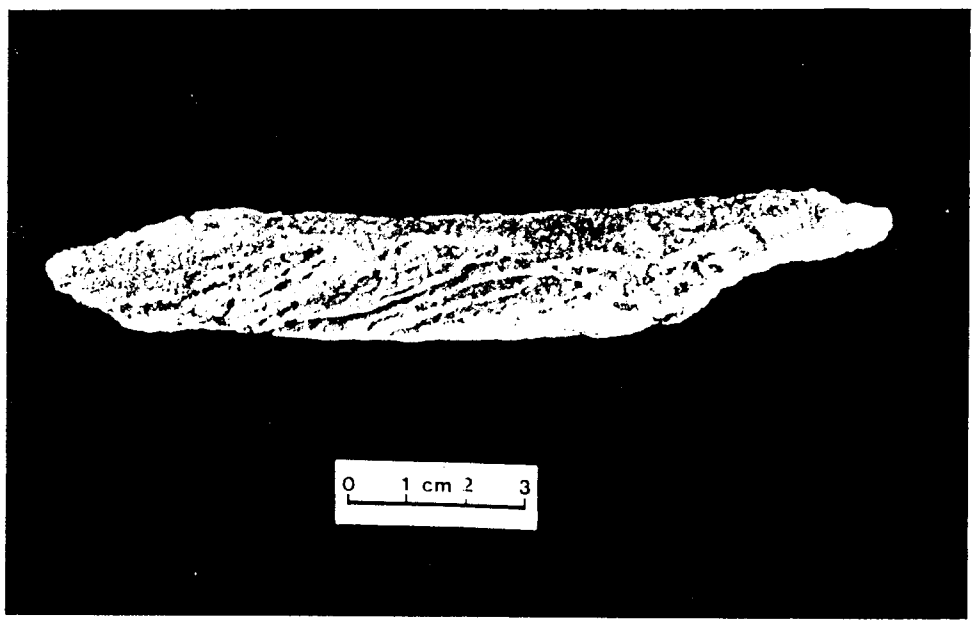

Plate 10.6 Portion of burrow from *O. irregulaire* system with planar cross-laminae, possibly representing passive fill of an oblique burrow.

The burrow infills, seen in transverse section, either resemble the host sediment, indicative of passive infill, or are composed of material resembling the linings, but not as compacted. Some dislodged burrow portions have internal cross-laminae representing planar surfaces at a low angle (20-30°) relative to the burrow walls (Plate 10.6). They are composed of the same material as the linings, to which they are connected at the edges of their elliptical borders. They vary from closely spaced and on top of each other, to up to 5 mm apart and separated by sandy intervals, sometimes with scattered pellets. Faecal ribbons quite commonly lie on the mud-pellet cross-laminae.

The flatness of the burrow cross-laminae suggests that they are geopetal features, representing the successive surfaces of passive, sedimented infill in an oblique burrow. Their composition of pellets and faecal ribbons suggests that the tracemaker (and commensals?) occupied the upper part of the burrow during formation. The sandy intervals probably represent influxes of sand into the burrow, whilst the mud-pellet and ribbon laminae represent deposition of detritus, produced by the animals, in the lowermost part of the filling burrow. Nevertheless, an *in situ* example is required to confirm the horizontal orientation of the cross-laminae.

Ophiomorpha nodosa Lundgren, 1891

Diagnosis: — Burrow walls consisting predominantly of dense, regularly distributed, discoid, ovoid, or irregular polygonal pellets. The morphology of this, the most commonly occurring species of *Ophiomorpha*, overlaps somewhat with *O. borneensis* and *O. irregulaire*, but in most specimens the distinction can be made with ease (Frey *et al.*, 1978).

Study area examples: — As noted, this type of knobby wall occurs as part of *Thalassinoides 'multiplex'* burrows (Plate 10.7). It is typically developed on the walls of composite structures composed of amalgamated burrow masses that resemble "chambers" and "trunks". The pellets are 0.5-1.0 cm in diameter, are well-rounded and are composed of the same reddened, muddy sandy that much of the *Thalassinoides 'multiplex'* burrows systems consist of. They are noticeably larger than the pellets in the other two *Ophiomorpha* ichnospecies present in the study area. The pellets are closely packed and are often paired, but the pairing is not as consistently developed as in *O. borneensis* from the study area, nor are the pairs as regularly arranged.

Plate 10.7 Part of thalassinoidean burrow system with development of *O. nodosa* morphology. Scale in cm.

Plate 10.8 *Granularia-Palaeophycus* burrow clump. *P. tubularis* burrows (Pt), showing thin linings. Large burrow (Th) is *Thalassinoides*. Photograph is rotated, arrow shows top. Scale in cm.

ICHNOGENUS *PALAEOPHYCUS* HALL, 1847

Diagnosis: — Branched or unbranched, smooth or ornamented, lined, essentially cylindrical, predominantly horizontal burrows of variable diameter; infillings typically structureless, of same lithology as host rock (Pemberton and Frey, 1982).

Remarks: — The presence of wall linings, infillings very similar to the ambient sediment, evidence of passive, gravitational infill and collapse of incompletely-filled burrows are features that distinguish *Palaeophycus* from *Planolites*. These are mainly open dwelling burrows (domichnia), probably of suspension feeders, surface detritus collectors and predators (Pemberton and Frey, 1982).

Palaeophycus tubularis Hall, 1847

Diagnosis: — Smooth, unornamented burrows of variable diameter, thinly but distinctly lined (Pemberton and Frey, 1982).

Remarks: — Burrows are straight to slightly curved and rarely branch, but crossovers, interpenetrations and collapse features are common (Pemberton and Frey, 1982).

Study area examples: — The burrows assigned to this ichnospecies are circular to slightly elliptical in section, mainly ~1 cm in diameter (varying between 0.5-1.5 cm), with thin, "papery" linings of slightly calcareous mud, 0.5-1.0 mm thick and infills like the surrounding (fine-sandy) sediment (Plate 10.8). Sometimes faint, internal meniscate lamination is visible. They are interpenetrating and incompletely formed, with missing sections of lining. Distorted, thin lenticles of mud suggest collapsed burrows. Branches were not observed and orientations are variable and mainly oblique. They mainly occur in intensely bioturbated volumes in association with *Granularia* burrows and numerous pellets (Granularia-Palaeophycus clumps) (Plates 10.8, 10.12, 10.4).

Palaeophycus heberti (de Saporta, 1872)

Diagnosis: — Smooth, unornamented, thickly-lined, cylindrical burrows (Pemberton and Frey, 1982).

Remarks: — Similar to *P. tubularis*, but with thick linings making up a large part of the total diameter. Platy grains in the linings typically reveal a concentric structure (Pemberton and Frey, 1982). Pemberton and Frey (1982) note that the linings typically consist of agglutinated sediment, coarser and better sorted than the adjacent rock.

Study area examples: — The simple burrows assigned to this ichnospecies are 0.5-1.5 cm in diameter and have well-defined linings, 1-2 mm thick, of coarse sand grains, with fine-sandy infills like the surrounding sediment. Their orientations are horizontal to shallowly oblique. They are fragile and never project from the face. They occur where coarse sand laminae are interbedded in fine sand and below coarse sand lenses in fine sand. These burrows are not common.

Palaeophycus 'annulatus'

Remarks: — In their revision of *Palaeophycus* and *Planolites*, Pemberton and Frey (1982) anticipated that a sixth species of *Palaeophycus*, *P. annulatus*, will be necessary to accommodate lined burrows with continuous annulations along their length. They did not erect this species at the time of their revision, due to the lack of adequately documented specimens.

Study area examples: — Thinly-lined, annulate burrows, ~0.7 cm in diameter, with infills like the host sediment, are assigned to this informal taxon (Plate 10.9). The linings consist of slightly calcareous mud. The annuli are thin (0.2-0.3 mm) and acuminate. They are paired, with two closely adjacent annuli 0.5-1.0 mm apart separated from adjacent pairs by 2-3 mm. However, less commonly, examples with closely-spaced, more irregularly paired annuli also occur, as well as more widely annulate examples, with single annuli ~5 mm apart. Very rarely, the burrows exhibit a curious constriction or narrowing to about half their diameter, for a short length of ~1.5 cm.

ICHNOGENUS *PLANOLITES* NICHOLSON, 1873

Diagnosis: — Unlined, rarely branched, straight to tortuous, smooth to irregularly-walled or annulated burrows, circular to elliptical in cross-section, of variable dimensions and configurations; infillings essentially structureless, differing in lithology from host rock (Pemberton and Frey, 1982).

Remarks: — The unlined walls and infills that differ in fabric, composition and colour from the surrounding sediment are the main features that distinguish *Planolites* from *Palaeophycus*. The lack of linings and collapse features, altered nature of the infills and presence of backfills and annulations indicate that the burrows are endichnial pascichnia (grazing traces) made by mobile, deposit-feeding endobionts. Burrows tend to be disposed along horizons (horizontal expansion) and often reburrow other traces (Pemberton and Frey, 1982).

Planolites montanus Richter, 1937

Diagnosis: — Relatively small, curved to contorted burrows (Pemberton and Frey, 1982).

Remarks: — The main features of this ichnospecies are small size, tendency for horizontal development and undulatory aspect, the latter resulting in only small sections of burrow being exposed on plane surfaces. The infills tend to consist of cleaner, better-sorted sediments than the host matrix (Pemberton and Frey, 1982).

Study area examples: — Burrows regarded as *Planolites montanus* consist of subtle spots and lenses of generally uniform diameter (4-6 mm) in fine sand (Plate 10.10). These are defined by a minor, but definite colour contrast with the surrounding sediment. Linings and haloes are absent. Branching was not observed on the outcrop face, nor could it be recognized in progressive sections made by scraping the face.

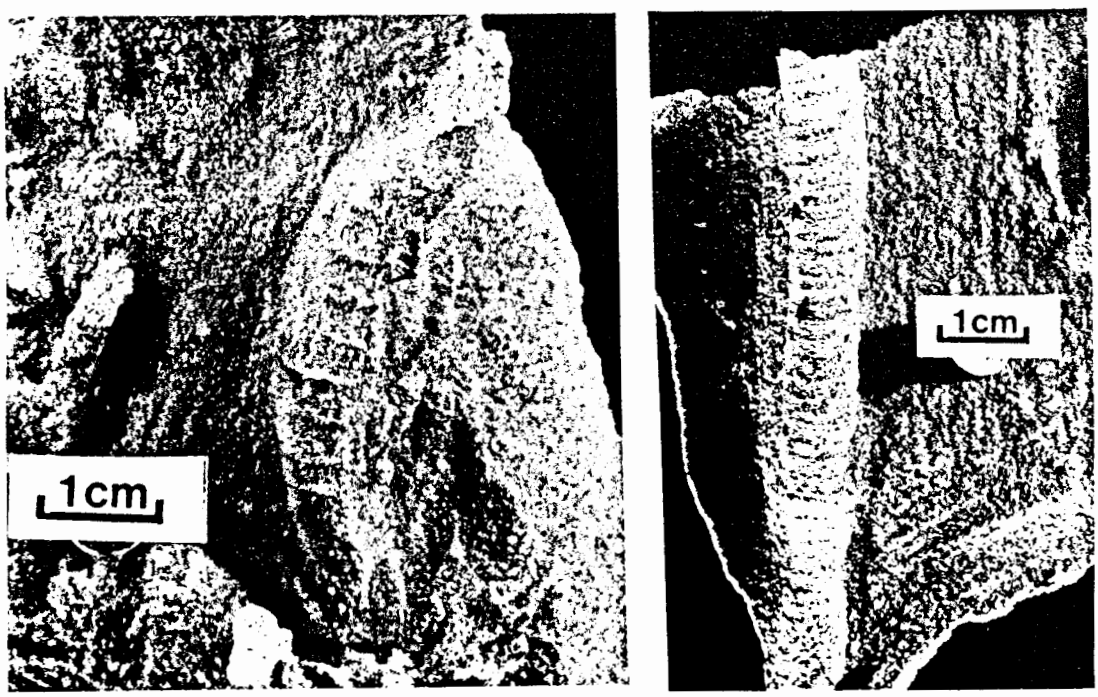

Plate 10.9 *Palaeophycus 'annulatus'* burrows. Scale bar is 1 cm.

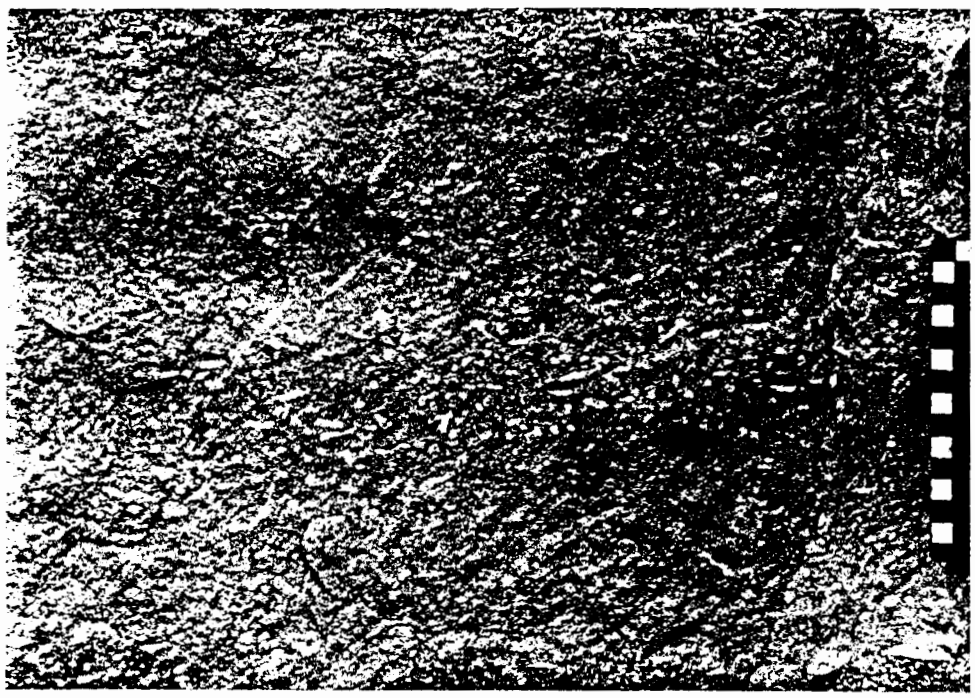

Plate 10.10 *Planolites montanus* burrows (pale spots and streaks). Scale bar is 1 cm.

The lengths of longitudinal burrow sections exposed in any plane rarely exceed ~3 cm and these are usually gently concave or convex, indicating that the burrows are gently sinuous in both the horizontal and vertical planes. They have a horizontal to subhorizontal orientation and tend to occur quite densely and uniformly distributed, usually two to three burrow diameters apart (~1 cm), but both wider spacings and densely interpenetrant patches also occur.

A lacquer peel was made of a near-structureless, fine sandy bed with abundant examples of this burrow type. Under magnification (10X), poorly-developed annulations are sometimes visible in longitudinal sections and are defined by variations in grain packing, as curves with fewer grains and tangential alignments of platy grains. This is consistent with active backfill. The burrows are usually slightly raised, due to enhanced penetration of lacquer within them. Burrows that are slightly more yellow-hued than the surrounding sediment have small, scattered particles of yellow clay adhering to grains and imparting the colour. In those that are more pale, the grains appear more "matt" and this is assumed due to faint coatings of whitish clay.

An important aspect of the lacquer peel is its pervasive, "bumpy" texture (Plate 10.11). Slightly raised bumps on the same scale as the visible, pale, *P. montanus* burrows cover its entire surface. In contrast, peels of thinly laminated, fine sand, with negligible destruction of primary structure, are flat, except for continuous ridges along laminae. The similarity in scale of visible burrows and the bumps suggests that only a minor portion of the *P. montanus* type of burrowing is actually visible to the eye. Visible burrows account for ~30% of the bioturbation, but the peel confirms that the near total destruction of primary structure is due to "invisible" bioturbation. Without the revelation of the peel, the degree of visible bioturbation and lack of primary structure would be difficult to reconcile. Burrows with no linings and an infill identical to the host sediment provide a brief ichnotaxonomic amusement, but have no practical reality. Their manifestation in the lacquer peel is due to heterogeneity in grain fabric. The term 'adelobioturbation' is coined here for bioturbation that is invisible except for revelation by enhancement techniques (see Additional Traces below, Cryptobioturbation and 'adelobioturbation').

The burrows herein assigned to *P. montanus* also strongly resemble the somewhat informally designated trace *Macaronichnus segregatus* Clifton and Thompson (1978). *Macaronichnus segregatus* is described as a cylindrical, smooth-sided, sinuous, intrastratal burrow, 0.3-0.5 mm in diameter, filled with sand slightly lighter in colour than the host sand. Mica flakes or heavy minerals generally are concentrated around the margin. Burrows tend to be more or less horizontal, generally occur in dense concentrations and interpenetrate, but do not branch. They occur in shallow-marine sandstones and sands of Jurassic and younger age (Clifton and Thompson, 1978). Clifton and Thompson (1978) found modern analogues of *Macaronichnus segregatus* in intertidal sediments and identified the tracemaker as the deposit-feeding, marine polychaete *Ophelia limacina*. The burrow is differentiated by selective ingestion of smaller, rough-surfaced grains, the rejected grains (mica plates, certain heavy minerals and coarser grains) being moved to the burrow circumference.

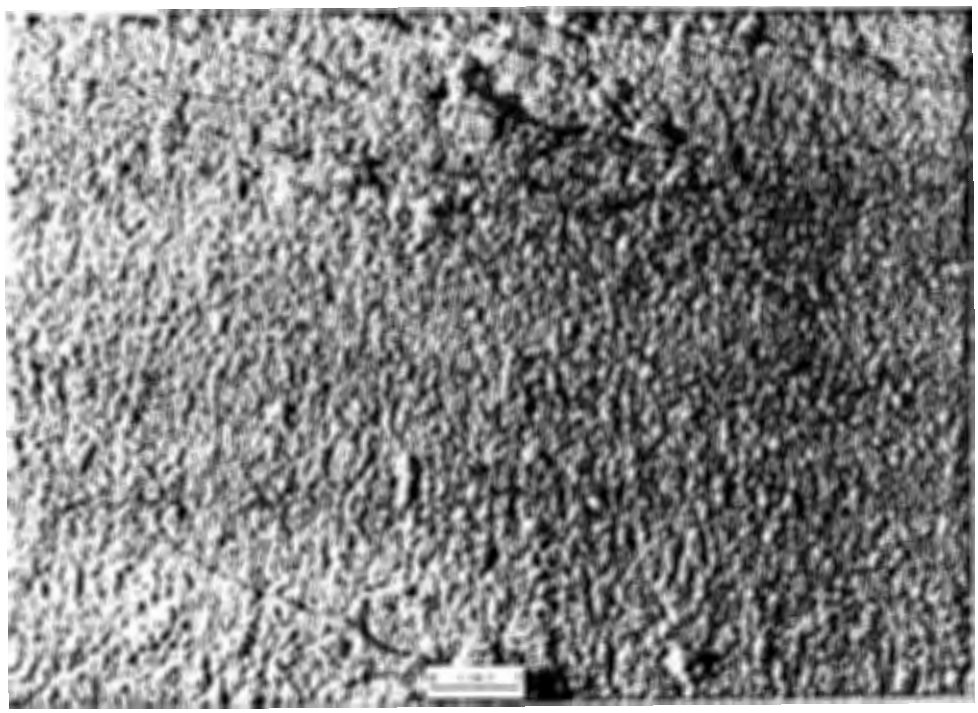

Plate 10.11 Obliquely-illuminated lacquer peel of nearly structureless fine-sandy bed with *Planolites montanus* defined by pale burrow fills. Bumpy texture on scale of visible burrows indicates true intensity of bioturbation.

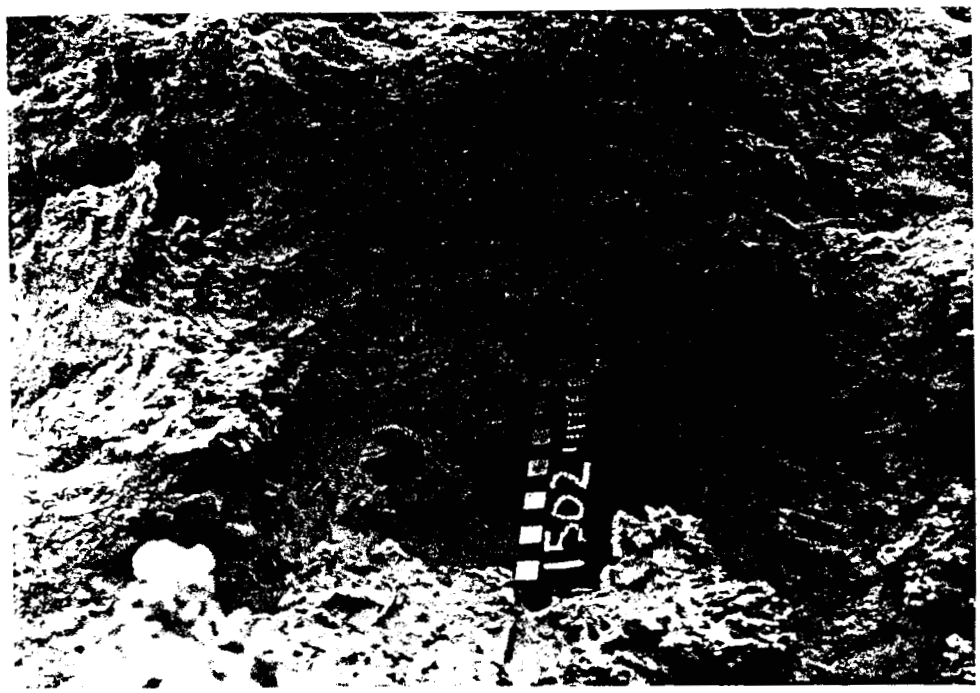

Plate 10.12 Numerous *Planolites 'spaghetti'* burrows in sandy area between intensely bioturbated, slightly muddy *Granularia-Palaeophycus* burrow clumps. Scale in cm.

Close examination of the burrows herein assigned to *P. montanus* in various peels, including one rich in heavy mineral concentrations in wave-ripple laminae, revealed very few with clear segregation of heavy minerals or larger grains. Examples with ilmenite grains concentrated around the outside, along the base and generally within the infill could be found, but these are exceptions rather than the rule. Nevertheless, the basic similarity of the traces with *Macaronichnus segregatus*, in terms of scale, ichnofabric and ethology, is striking. Clifton and Thompson (1978) pointed out that their burrows resemble *Planolites*, but the presence of active backfill structures prevented them from assigning the traces to *Planolites*. In terms of the redefinition of *Planolites* (Pemberton and Frey, 1982), evidence of active backfill is intrinsic to *Planolites* and therefore it could be argued that *Macaronichnus* should be regarded as a junior synonym of *Planolites* .

Planolites 'spaghetti'

Study area examples: — A thin burrow, 1.5-2.0 mm in diameter, gently sinuous and consolidated to a degree sufficient to allow them to project 1-2 cm from the face (Plate 10.12). The infill is slightly calcareous, white to pale yellow mud and is impoverished in sand grains, whilst the exterior is studded with adhering grains. They do not have an obvious preferred orientation. Branching is present, although uncommon, and takes place dichotomously (Y-shaped), at an acute angle.

Planolites 'threads'

Study area examples: — A minute, very thin burrow type, ~0,5 mm in diameter. These threadlike, delicate burrows are gently sinuous and consist of slightly calcareous mud. They are fragilely cemented and project from the wind-eroded faces. Rare dichotomous branching is present. *P. 'threads'* and *P. 'spaghetti'* are very similar in morphology, but represent clearly distinct size classes of small burrows, with no intermediate size intergrades.

ICHNOGENUS *SKOLITHOS* HALDEMAN, 1840

Diagnosis: — "Ordinary pipes"; straight tubes or pipes perpendicular to bedding and parallel to each other, subcylindrical, unbranched; 1 to 15 mm in diameter, constant for each tube; few cm up to 30 cm (max. 100) long; inner walls may be finely annulated; tubes commonly closely crowded, but may also be widely spaced (Häntzschel, 1975).

— Cylindrical to slightly subcylindrical, straight to curved to sinuous, lined or unlined, never branched, vertical to steeply inclined burrows (Pemberton and Jones, 1988).

Remarks: — At least 15 ichnogenera and 64 ichnospecies involving single entrance, vertical shafts have been described and named, resulting in considerable difficulties in assigning specific names (Pemberton and Jones, 1988). A revision of *Skolithos* has been long overdue and is evidently being undertaken by Pemberton and Frey (Frey, *et al.*, 1984). The diagnosis in Häntzschel (1975) reflects

classic *Skolithos* as found in shallow-marine, Palaeozoic "pipe-rocks". In contrast, *Skolithos* "pipe-rock" is not dominant in post-Palaeozoic shallow-marine sediments where *Ophiomorpha* is typical, particularly in Cretaceous and younger rocks (Droser and Bottjer, 1989). A more generalised diagnosis, such as that used by Pemberton and Jones (1988), is usually employed at present. *Skolithos* is considered to represent the dwelling structures of opportunistic, suspension feeders, very probably polychaete worms (Vossler and Pemberton, 1988).

Skolithos 'bundles'

Study area examples: — *Skolithos 'bundles'* is used here for discrete vertical and subvertical burrows, that occur abundantly to very densely along distinct horizons, reflecting successive recolonisations of a vertically aggrading substrate (Plate 10.13). This usage is consistent with the spirit of the definition of the taxon, although the burrows in question are not parallel, but anastomose and interpenetrate. Burrows are 2-5 mm in diameter and 10-30 cm in length and are very fragile. Examination of lacquer-consolidated specimens under magnification reveals that the burrows are defined by slightly muddy sand, the mud present as thinly adhering coatings and bridges binding the ambient fine sand grains. Very obscure meniscate lamination is present in some examples. Burrows along a particular horizon tend to form downward-tapered groups in which closely adjacent burrows converge downwards and interpenetrate (hence *'bundles'*). This may suggest that a single animal often produced a number of adjacent burrows by shifting the surface aperture whilst approximately maintaining its lowermost position. The tendency for clumps of burrows to anastomose convergently downwards imparts a "colonnade" aspect to densely-burrowed horizons. The downward-tapered burrow clumps resemble to a degree the "V-form" burrows illustrated by Bourgeois (1980), that also appear to consist of a group of burrows that converge downwards.

Continuation of the burrows through increments of sedimentation is ubiquitous. Colonnades of *Skolithos 'bundles'* burrows vary in their development. They may occur as horizons of relatively limited lateral extent (several metres), indicating that the producer densely, but ephemerally, inhabited discrete patches on the sea floor. Wide columns composed of stacked colonnades indicate the persistence of patch colonies of the producer through 2-3 m of incremental sedimentation. *Skolithos 'bundles'* burrows are the dominant structures in certain examples of near-totally bioturbated shoreface sands, where the depositional environment is inferred to have been of relatively low energy and sedimentation rate.

Skolithos 'mini'

Study area examples: — *Skolithos 'mini'* burrows are very small, vertical and subvertical, somewhat irregularly formed, tapered "rods", composed of slightly calcareous, white mud, that are ~0.5 mm in diameter and up to 10 mm long. They mainly occur in a single row (Plate 10.14), distributed from 3-10 mm apart to sparsely scattered, along a particular horizon.

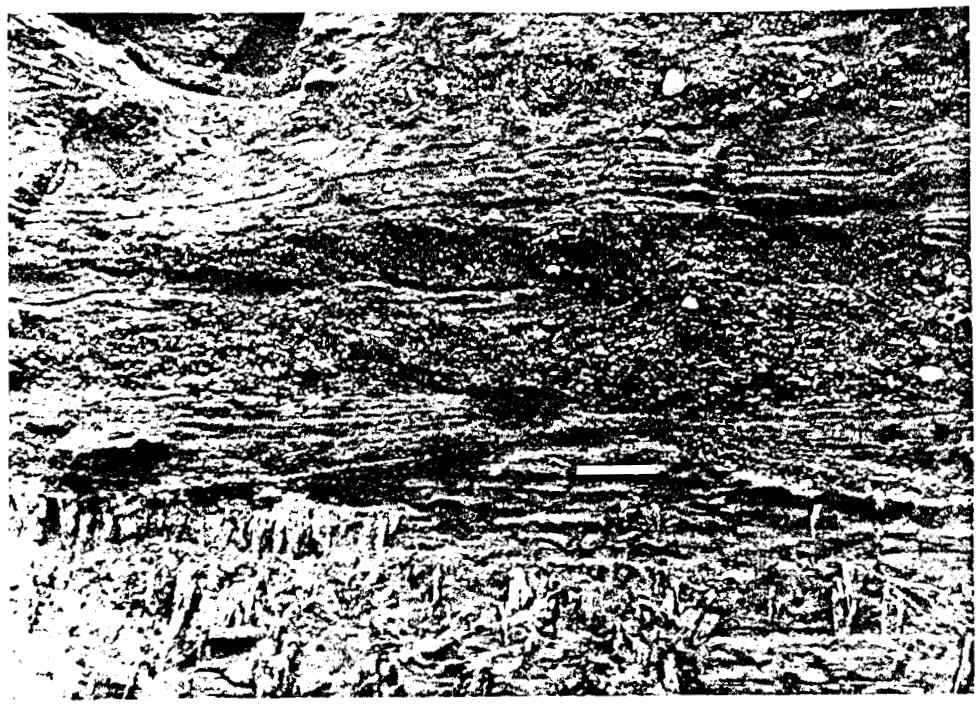

Plate 10.13 V-shaped clumps of vertical burrows, herein called *Skolithos* '*bundles*,' below the sharp contact developed on the lower shoreface facies that is overlain by megaripple trough-cross-bedding of the upper shoreface. Scale bar is 10 cm.

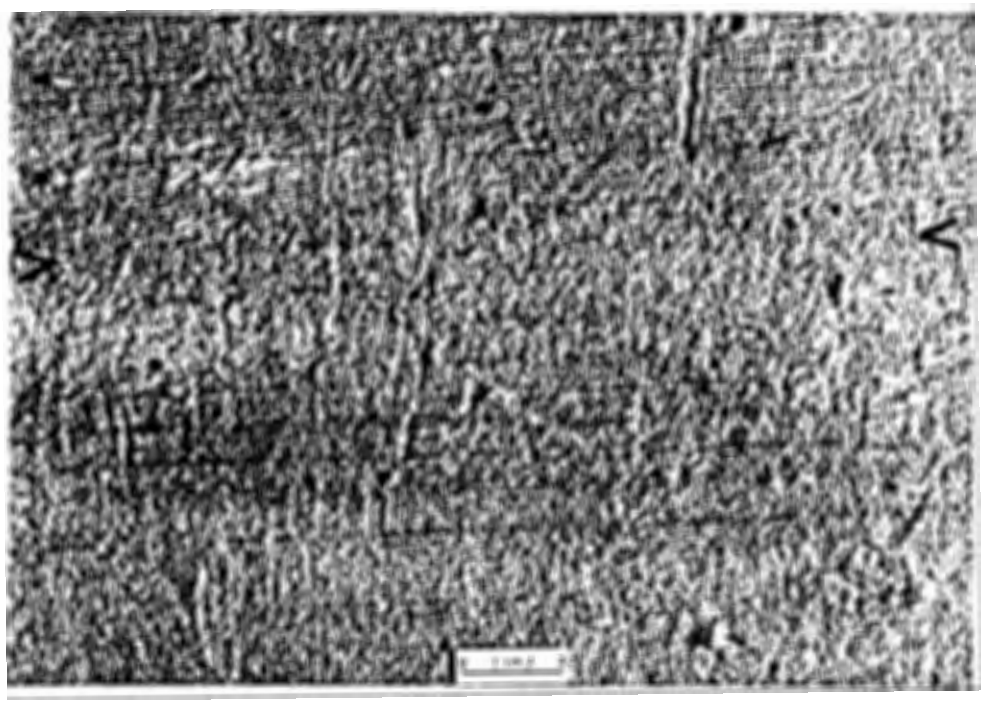

Plate 10.14 *Skolithos* '*mini*' along surface (arrowed) in "parallel/ripple-laminated-to-burrowed" facies. Note numerous "escape structures," including chevron lamination (centre left, extreme right). Photograph of a lacquer peel.

The *Skolithos 'mini'* horizons are in the slightly eroded tops of the bioturbated, upper portions of parallel and ripple-laminated, dm-scale beds of fine sand (parallel/ripple-laminated-to-burrowed sequences). Some examples are very sparsely scattered within the laminated-to-burrowed units.

Ichnogenus *TEICHICHNUS* Seilacher, 1955

Diagnosis: — Bladelike to gently curved, rarely branched spreiten structures consisting of a stack of several closely concentric, longitudinally nested burrows converging to simple, single tunnels. Burrows within a given spreite commonly displaced upward (retrusive), or less commonly downward (protrusive) and oriented at various angles with respect to bedding (Häntzschel, 1975; Frey and Howard, 1985).

Teichichnus rectus Seilacher, 1955

Diagnosis: — Vertical, blade-like spreiten consisting of several closely concentric, horizontal or inclined, longitudinally nested individual burrows (retrusive) (Frey and Howard, 1990).

Study area examples: — Classical teichichnians occur as part of *Thalassinoides 'multiplex'* burrow systems. The component burrows are 1-2 cm in diameter, composed of muddy sand, usually reddened, with scattered coarse grains and poorly defined linings and backfill. The spreiten are usually straight to gently arcuate in the vertical plane. The long axes of the spreiten are inclined (10-30°), sometimes quite steeply (30-50°). The heights of spreiten generally vary from 10-40 cm. All examples examined are retrusive and in many the uppermost burrow has a loose, fine-sandy, passive infill. One particularly spectacular, large teichichnian structure, composite in construction, was encountered (Plate 10.15). This consisted of a sinuous "wall" of burrows, in which the individual burrow components are steeply dipping, with sections composed of burrows with opposite orientations.

Ichnogenus *THALASSINOIDES* Ehrenberg, 1944

Diagnosis: — Extensive burrow systems with both vertical and horizontal elements. Burrows cylindrical, between 2 and 20 cm in diameter. Branching regular, characterized by Y-shaped bifurcations, swollen at point of branching. Horizontal elements joining to form polygons. Burrow dimensions variable within a system. Horizontal systems connecting to surface by vertical or steeply inclined shafts (Kennedy, 1967).

Remarks: — *Thalassinoides* burrows are commonly assigned to two ichnospecies. In *T. suevicus* (Rieth, 1932), the burrows are mainly smooth-walled, with Y-shaped branching, forming a predominantly horizontal, ramified system. *T. paradoxicus* (Woodward, 1830) is characterized by irregular branching, with many T-shaped intersections, the burrow system comprising both vertical and horizontal components, the former typically as shafts joining horizontal networks at several levels (Kennedy, 1967; Fürsich, 1981; Howard and Frey, 1984; Frey and Howard, 1985).

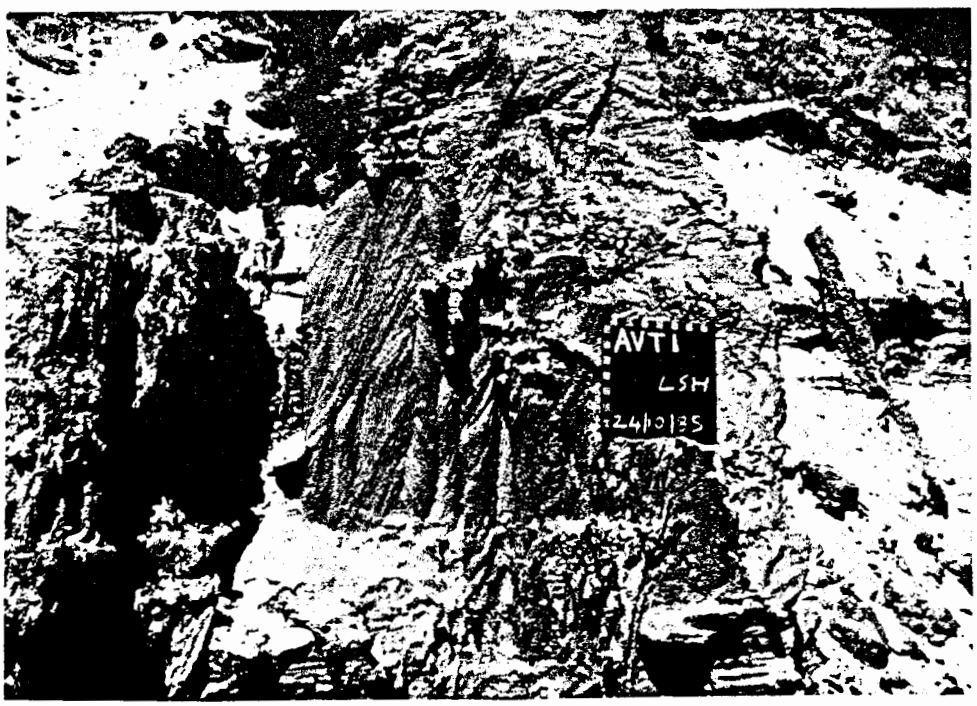

Plate 10.15 Large, composite teichichnian structure in bioturbated, lower shoreface fine sands. Note *Thalassinoides* '*multiplex*' "trunk" in background right with *O. nodosa* external morphology and *Skolithos* '*bundles*' in foreground and left. Scale in cm.

Plate 10.16 Single and amalgamated burrows referred to *Thalassinoides* '*multiplex*', in lower shoreface, fine sands. Note "trunks" with *O. nodosa* morphology. Scale in cm.

It is now recognized that *Thalassinoides* burrows exhibit considerable variation and a single burrow system often includes portions that morphologically intergrade with other ichnogenera such as *Ophiomorpha*, *Spongeliomorpha*, *Gyrolithes* and *Teichichnus* (Bromley and Frey, 1974; Frey *et al.*, 1978; Bromley, 1990). These morphological variations represent different behavioural aspects of the same animal, such as responses to substrate type and cohesiveness, to sedimentation or erosion, production of cumulative structures by deposit-feeding and "permanent" features such as dwelling chambers and ventilation shafts. The burrow systems may be dominated by shafts, may be a mainly horizontal network of tunnels (mazes), or may form three-dimensional, interconnected networks (boxworks) (Frey *et al.*, 1978). Mazes and boxworks usually occur at depth and are connected to the surface by shafts. The main architects of *Thalassinoides* systems are anomuran Crustacea, particularly the fossorial thalassinidean shrimps, e.g. *Callianassa* and *Upogebia* (Bromley, 1990). Notably, the scale of these burrow systems is remarkable. Observations from modern and ancient shore profiles indicate vertical shafts extending down to mazes 3-5 m below the sediment surface (Frey *et al.*, 1978).

Thalassinoides 'multiplex'

Study area examples: — The burrow systems here assigned to *Thalassinoides 'multiplex'* are among the most visually obvious burrows in the exposures, due to their large size and reddish colour. They are semi-consolidated and erode into strong relief on the retreating, wind-etched faces (Plates 10.15, 10.16). Their occurrence is ubiquitous (a facies-breaking trace), but their best development is in open-coast shoreface deposits.

The subcylindrical burrows are mainly 1-2 cm in diameter and typically consist of muddy sand with scattered coarse sand grains. The presence of coarse sand "peppering" the material of the burrow is a ubiquitous feature, regardless of whether the host lithology is well-sorted, fine sand, or coarse sand. The colour of burrows is imparted by the intergranular mud component. Colours vary from light olive-browns (~2.5Y 5/4), to reddish yellow (~7.5YR 6/6). Gradations through these hues may occur in close proximity in same burrow. Burrow construction, as seen in transverse sections of broken burrows, is very variable. The entire burrow may be structureless, with no differentiation of a wall and infill. More usually, a wall, 2-5 mm thick, can be discerned by the fact that the lithologically identical red infill is less compacted and preferentially falls out. Clear passive fills occur, in which the red wall encloses soft, loose green sand like the surrounding sediment. Similarly, longitudinal sections vary from structureless, to those with discernible walls and structureless infill, to those with walls and meniscate backfill.

The predominant orientation of burrows in shoreface deposits is steeply oblique, so that burrows that superficially appear to be isolated *Skolithos* are actually partially exposed lengths of single *Thalassinoides* burrows. Branching is common to abundant and usually Y-shaped downwards, the branched-off burrow also continuing obliquely downwards. Single, long burrows generally have smooth exteriors. The length of individual burrows is considerable. An example, excavated at

Avontuur T2/T3, Section 15, had a vertical extent of ~2.5 m (Plate 10.17). It branched on penetration of the basal gravel (Unit 1) and side branching from a bulbous node occurred at ~1 m from the top of Unit 1. A horizontal, backfilled, thallassinoidean burrow, exposed by deflation on the floor of a prospecting trench, ran in a near-straight line for more than 12 m. An interesting feature of wall construction is the occasional presence of streaks of green, micaceous mud. This mud is derived from the decomposed gneiss bedrock, but it occurs in burrows up to 4 m above the bedrock. Its presence suggests that the tracemaker actively transported decomposed bedrock material and incorporated it in the burrow. One impressive example was a burrow, ~3 m above bedrock, with thick walls composed almost entirely of decomposed bedrock and which still remained unfilled by sediment. This mud transporting activity may possibly reflect an insufficiency of mud available from the host sediments and the water column.

Plate 10.17 *Thalassinoides* burrow, ~2..6 m long, cross-cutting Unit 2, Section 15, Avontuur T2/T3. Scale in cm.

The most striking and characteristic feature of these burrows is their amalgamation into structures much larger than the component burrows (hence *'multiplex'*) (Plates 10.15, 10.16). The amalgamated

features vary from irregularly-shaped, chamber-like masses at the intersections of burrows, to "trunks" consisting of bundles of parallel burrows in three dimensions that together resemble a giant burrow , to teichichnian features consisting of several to many burrows stacked vertically above each other. The chamber-like masses, which may be up to ~0.5 m in diameter, have mottled, mixed textures in which burrow walls and meniscate backfills are present in places. They are volumes of sediment in which activity of the tracemakers was concentrated. Similarly, the "trunks" are likely to be cumulative structures resulting from the shifting of a single burrow. Uncommonly, vertical sections reveal several burrows radiating divergently outward from a "chamber". Such structures are reminiscent of the "brood structures" described by Curran (1976), but they differ in their much larger size. Particularly, the radiating burrows are not small and therefore seem unlikely to represent the burrows of juveniles. Furthermore, in some examples they radiate downwards, deeper into the sediment.

A feature of amalgamated burrow masses, particularly "chambers" and "trunks", is the occurrence of exteriors that are irregularly mammilated by rounded bumps 0.5-1.0 cm in diameter, resembling crude versions of the ichnotaxon *Ophiomorpha nodosa*. The wall-like, vertical stacking of burrows results in spreiten referable to *Teichichnus*. The occurrence of *Teichichnus* suggests deposit-feeding activity (Bromley, 1990). An uncommon, but spectacular, variation is the occurrence of helical burrows, the ichnogenus *Gyrolithes* (Plate 10.3). The remaining burrow type observed in *Thalassinoides* systems, *Spongeliomorpha* de Saporta, 1887, was not observed. Fine, elongate ridges on burrow exteriors, the defining feature of *Spongeliomorpha,* are regarded as a bioglyph produced by the crustacean occupant. These claw (cheliped) sculptings are considered more likely to be a feature of crab burrows, rather than shrimp burrows (Frey *et al.*, 1984). Their absence is consistent with a shrimp or prawn origin for these *Thalassinoides* burrows.

Although these burrows are dominantly of steep aspect, subhorizontal burrows are nevertheless common, but distinct horizons of concentrated subhorizontal burrows, that would indicate mazes or boxworks, are not typical. This observation must be qualified by noting that irregular networks, ramifying over the tops of basal cobble gravels, are sometimes seen when exposed by deflation in excavations prepared for mining. These appear to be only locally developed and do not form well-integrated systems.

Thalassinoides* sp. cf. *paradoxicus (Woodward, 1830)

Diagnosis: — Sparsely to densely, but irregularly branched, subcylindrical to cylindrical burrows oriented at various angles with respect to bedding; T-shaped intersections are more common than Y-shaped bifurcations and offshoots are not necessarily the same diameter as the parent trunk (Howard and Frey, 1984).

Remarks: — Diameters may be inconsistent along a single shaft or tunnel. Some components display bulbous enlargements, especially at points of branching. Burrow components in a given setting may

consist of sparse, rarely branched, essentially vertical or steeply inclined shafts, or of dense, highly branched, essentially horizontal boxworks (Howard and Frey, 1984).

Study area examples: — The burrow systems referred to *T. paradoxicus* are distinctly different in form and lithology from those of the reddened, amalgamated systems of *T. 'multiplex'*. They are whitish in colour and cemented (Plates 10.18, 10.19). The reddened burrows of *T. 'multiplex'* occur intimately between the white, cemented burrows, but do not show interlinks or gradations. Moreover, the white, cemented burrows occur in back-barrier and tidal-inlet environments characterized by high to total bioturbation, where they form irregular boxworks of meshing burrows in varying burrow density, in contrast to the strongly vertical, penetrative aspect of *T. 'multiplex'*.

The burrows are fine-sandy, with sparse coarse grains, vary widely in diameter, from 1-10 cm, are white to very pale green and yellow in colour (5Y 8/1-4), with calcareous matrix and are moderately to strongly cemented. Branching takes place at all angles. In strongly cemented examples, a white, friable rind, 1-3 mm thick, surrounds a dense, grey, crystalline internal portion of pore-filling calcite. The boundary between the friable rind and the hard, internal portion is gradational. Within the densely cemented portions, a cylindrical core, 1-2 cm in diameter and varying from vestigial to well-defined, is usually present. This core presumably represents the final burrow fill. Well-defined cores are defined by pale cream to pink hues reflecting a mud content, as well as visible porosity. The mud content has probably interfered with growth of the cement, preserving porosity. Poorly preserved cores are very faintly defined by arcuate, dark wisps in the dense, grey matrix.

Due to cementation, the burrows project from the exposure and break off in profusion. The *in situ* burrows and the burrow "litter" exhibit a variety of morphologies, including shapes reminiscent of the flint nodules weathered from The Chalk of southern England (Kennedy, 1967). Similarly, there is uncertainty about what exactly of the burrow has been lithified, but many likenesses between the cemented burrows and illustrations of casts of modern shrimp burrows (reviewed in Bromley. 1990), suggest that external burrow forms are mainly present and that it is the sediment that was disturbed by the animals that has been cemented.

One notable exception to the preservation of morphology occurred at a particular exposure in barrier sands. This was easily recognized by the fact that cemented horizontal and vertical burrows in the plane parallel to the depositional strike (shore-parallel) had an exaggerated, pointed, ellipticity in the down-dip direction, the burrow sections having been "drawn out" in a common direction to form "backed blades" (Plate 10.20). The thickest, updip part of the "blades" contains the burrow-fill core. The impression is imparted that cementation extended into the "lee shadows" of the burrows, under the influence of solutions moving seaward through the barrier sand. The effects of the cementation anisotropy on "flow-parallel" burrows are less obvious. The common azimuth of the blade-like extensions imparts a false impression that the projecting burrows have been strongly eroded by sand-laden wind.

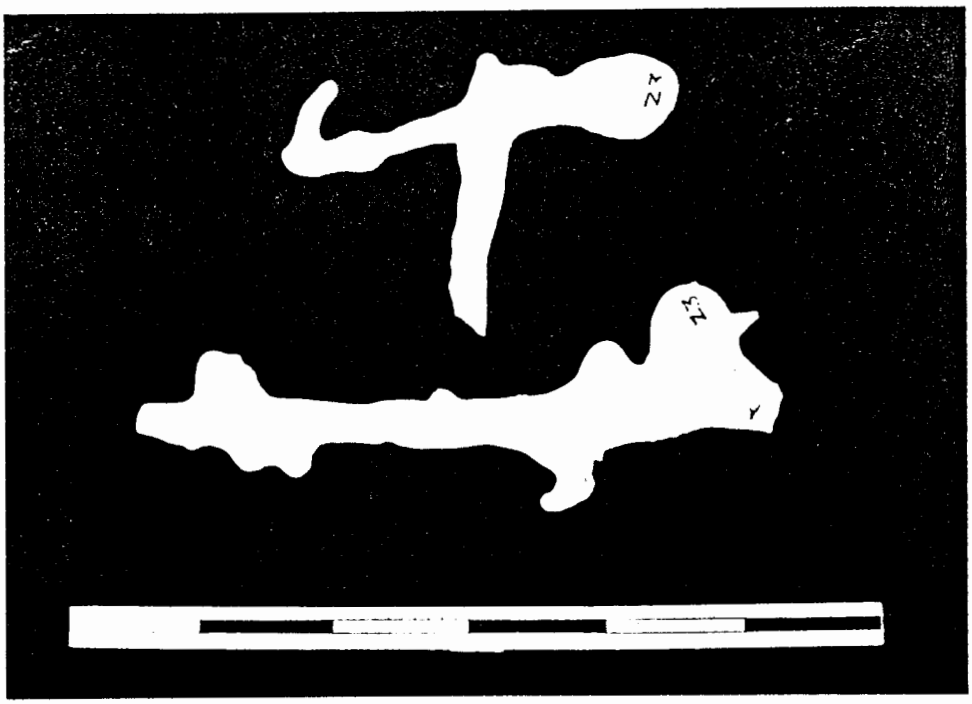

Plate 10.18 Portions of cemented, calcareous burrows assigned to *Thalassinoides* cf. *T. paradoxicus*. Scale in dm.

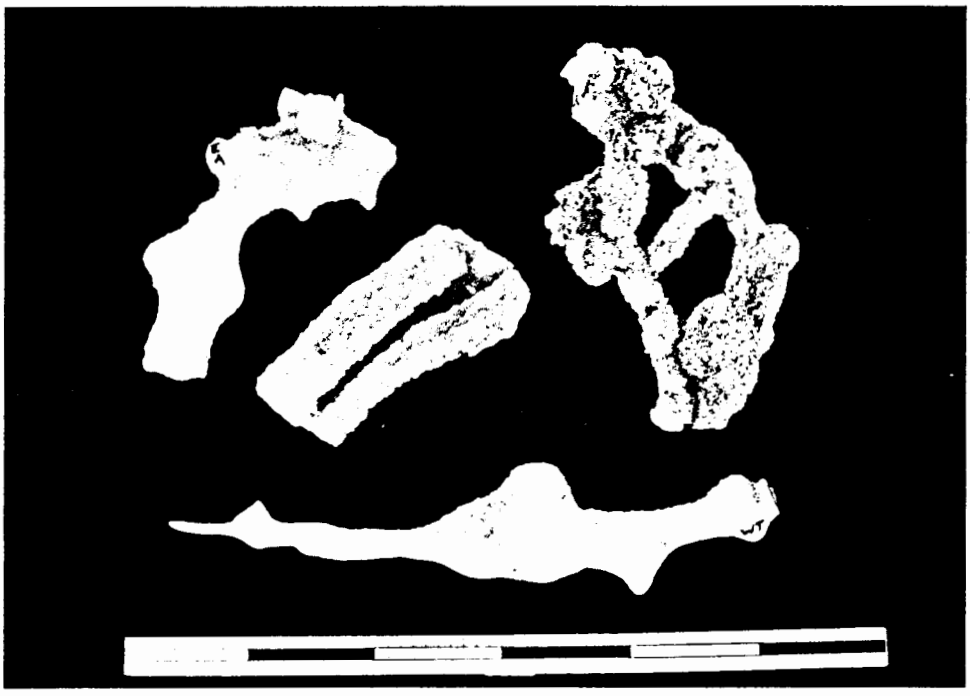

Plate 10.19 Portions of cemented, calcareous burrows assigned to *Thalassinoides* cf. *T. paradoxicus*. Scale in dm.

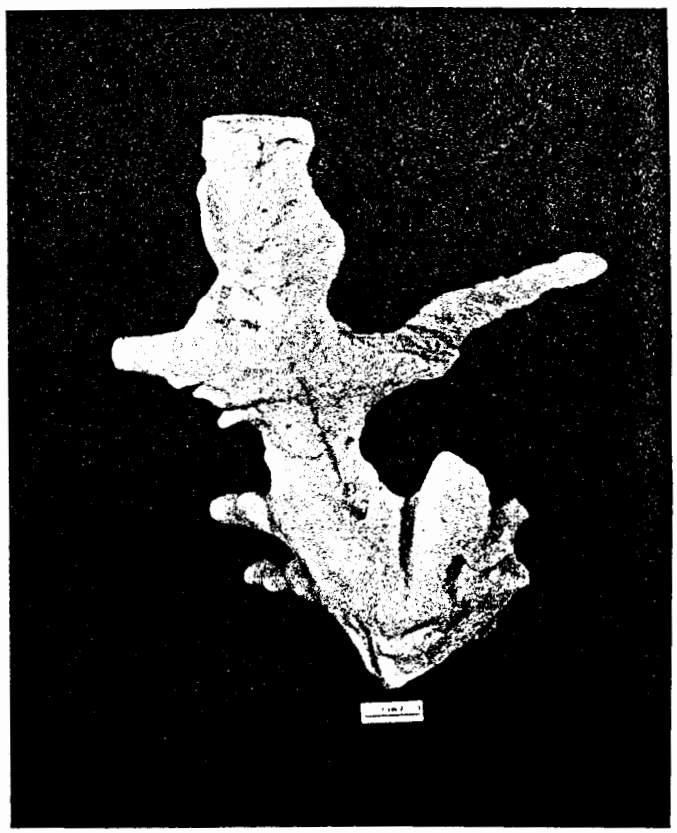

Plate 10.20 *Thalassinoides* burrow with bladed morphology, probably related to a groundwater flow effect.

The larger burrows tend to have surfaces that are either smooth (Plate 10.18) or that are granular (Plate 10.19), with both sometimes in close proximity (e.g. smooth tunnel with granular protuberances). The granular appearance is formed by fine sand that has been "clotted" into small pellets 0.5-2.0 mm in diameter. Burrow diameters vary, with interconnections of various size and bulbous widenings, particularly at intersections (Plates 10.18, 10.19). Both bulbous and pointed *culs de sac* branches occur (Plate 10.18, upper; Plate 10.19, lower), so that the burrow system resembles the morphology of the burrow of the thalassinidean shrimp *Jaxea nocturna*, illustrated by Pervesler and Dworschak (1985). Other exhumed portions are dominated by bulbous chambers linked by short tunnels (Plate 10.19, upper right), as in the burrow system of *Callianassa californiensis* (Bromley. 1990, fig. 5.19). Some very large burrows, ~10 cm in diameter, have thick walls (Plate 10.19, centre), with rugose exteriors crudely resembling *Spongeliomorpha*-type sculpture, surrounding an open tunnel ~3 cm wide. Knobbiness resembling crude *Ophiomorpha* is common on smaller burrows, but does not approach the regular placement of well-defined pellets that characterises proper *Ophiomorpha*. Teichichnian structures were not observed in these systems. Another interesting feature is the occurrence of "double-barrel" burrows, where two straight burrows run side-by-side for considerable lengths (up to 1.5 m).

Larger burrows tend to be mainly horizontal and concentrated along horizons, these horizons separated by intervals dominated by boxworks of smaller burrows (1-2 cm diameter) with a strong vertical component. Along horizons, in association with large burrows, large irregularly-shaped, semi-

cemented masses also occur. Burrow-like projections and the presence of granular and rugose surface textures, similar to those found on *Thalassinoides* burrows, suggests that these masses at least partly represent volumes strongly burrowed by *Thalassinoides*. One curious lens consisted entirely of pellets, 6-9 mm in diameter, themselves composed of smaller pellets or "clots" of fine sand ~0.5 mm in diameter. However, the bioturbation along these horizons probably also involves other small burrows between the *Thalassinoides* burrows. This was particularly obvious at some sites where semi-cemented masses of small burrows (2-3 mm diameter), intricately branching and interconnected, filled the volumes within the *Thalassinoides* boxwork.

The intriguing lithological contrast between the reddened *Thalassinoides 'multiplex'* systems and the semi-cemented to well-cemented, pale *Thalassinoides paradoxicus* systems is due to early diagenetic processes. It appears that the activities of the burrow-makers initiated and influenced the subsequent diagenetic reactions.

Ichnogenus *TIBIKOIA* Hatai, Kotaka and Noda, 1970

Diagnosis: — Oblong faecal pellets, cylindrical, sometimes ovoid or of short, rod-like shape; circular in cross-section; both ends bluntly and flatly rounded; surface smooth; about 1 mm long, diameter 0.5 mm (Häntzschel, 1975).

Study area examples: — The pellets referred to *Tibikoia* are 1-2 mm long, consist of pale, slightly calcareous mud, are ovoids to very short rods, with rounded ends (Plate 10.1). The surfaces are not smooth, however, having encrusting fine sand grains and dents where grains have been dislodged. No internal canals are present and the pellets may be homogenous, white mud, or may incorporate floating grains of fine sand.

Ichnogenus *TRICHICHNUS* Frey, 1970

Diagnosis: — Branched or unbranched, hairlike, cylindrical to sinuous burrows distinctly less than 1 mm in diameter, oriented at various angles with respect to bedding. Burrow walls more or less distinct, commonly lined with diagenetic minerals (Frey, 1970).

Remarks: — *Trichichnus* is intended to include all very small, branched or unbranched, dominantly cylindrical or curvilinear burrows having walls that are at least moderately distinct from both adjacent sediment and the burrow filling. The type species, *Trichichnus linearis* Frey, 1970, is from Upper Cretaceous chalk and most specimens have pyritic and limonitic linings and somewhat hollow, drusy cores (Frey, 1970).

Study area examples: — The burrows assigned to *Trichichnus* are best described as vertical and subvertical, rarely oblique, linear to gently arcuate "scratches" on vertical faces in fine sand (Plate 10.21). There are no discernible infills as the traces are defined by loss of material, presumably loosely arranged, disturbed, sand grains. The traces are 0.2-0.6 mm wide, mainly ~0.3 mm, and 1-5 cm long. Branching was not observed.

In lacquer peels, the "scratches" usually have raised margins (parallel ridges or "levees"), ~1 mm wide. There are no discernible linings. They are not densely distributed, being a few to several cm apart. They occur in dm-scale, parallel/ripple-laminated-to-burrowed fine sand beds, where they are associated with *Skolithos 'mini'* and may be the escape structures of the latter.

Although *Trichichnus* best accommodates these traces, the assignment is tentative due to the lack of a clear lining. They could be confused with thin plant root traces from hairlike root masses, but these occur more densely, in more varied and radiating orientations, with frequent branching.

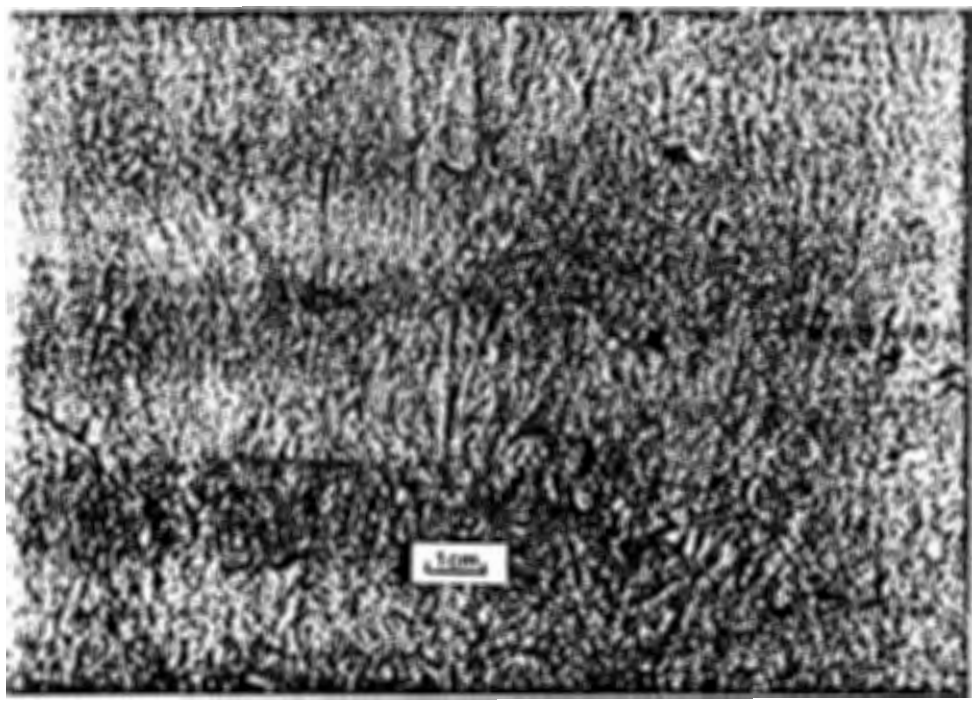

Plate 10.21 Thin, "scratch-like" burrows assigned to *Trichichnus*. Scale bar is 1 cm.

9.3 ADDITIONAL TRACES

Chevron lamination

Vertical structures produced by the deformation of primary lamination into nested chevrons (V-in-V laminae) are usually interpreted as the escape traces (fugichnia) of infaunal bivalves or anemones in response to burial by depositional events (Howard and Frey, 1975; Simpson, 1975). Similar structures may be produced by the burrow occupant modifying its burrow in response to more gradual aggradation and erosion of the substratum i.e. slight up or down adjustments of position. These are now called equilibrium traces (equilibrichnia) (Bromley, 1990). Settling of sediment into collapsing burrows also produces chevron structures and these have been particularly noticed in association with large burrows such as *Ophiomorpha* (Frey *et al.*, 1978). Collapse of overlying sediment into a vertical burrow results in a funnel of nested laminae, whilst furrows result from the collapse of horizontal

burrows (Frey *et al.*, 1978). An upward decrease in the dips of the nested laminae distinguishes collapse structures (Kamola, 1984).

Study area examples: — Chevron structures are particularly noticeable in weak to moderately bioturbated, fine sands with well-preserved lamination (Plate 10.14), especially sands with heavy mineral lamination. The majority are 0.5-2.0 cm in diameter and a few to several cm in length, but they vary in scale from very small features only a few mm in depth, to features several cm across and several dm in vertical extent. They are most commonly recognized in dm-scale, parallel/ripple-laminated-to-burrowed fine sand beds, in the laminated intervals, in association with *Trichichnus*. Their occurrence between the burrowed tops of depositional increments in "lam-scram" bedding (laminated-to-scrambled) suggests that they are mainly fugichnia. They are locally very dense, the contorted, convex-up laminae between chevrons imparting a scalloped appearance to the bed.

The large examples occur in coarse sand where the chevron structures are mainly defined by the rotation of platy shell fragments to steeply inward-dipping, subvertical orientations. The large, deeply infaunal mactrid bivalve *Lutraria* occurs within several of these examples (Plate 10.22). In this case the traces may be fugichnia, the *in situ* bivalves being unsuccessful escapees. A few examples of apparent entrapment of bivalves beneath deposited, loose shells, together with the nature of the overlying deposition (migrating, coarse-grained, megaripples in the upper shoreface), suggests that at least some of the traces are fugichnia. Alternatively, they could be mainly equilibrichnia representing the bivalves' adjustments to a relatively unstable substratum, with the *in situ* bivalves reflecting natural mortality in a less than favourable environment. As most *in situ Lutraria* occur within, rather than at the top of their burrows, the latter alternative is more probable.

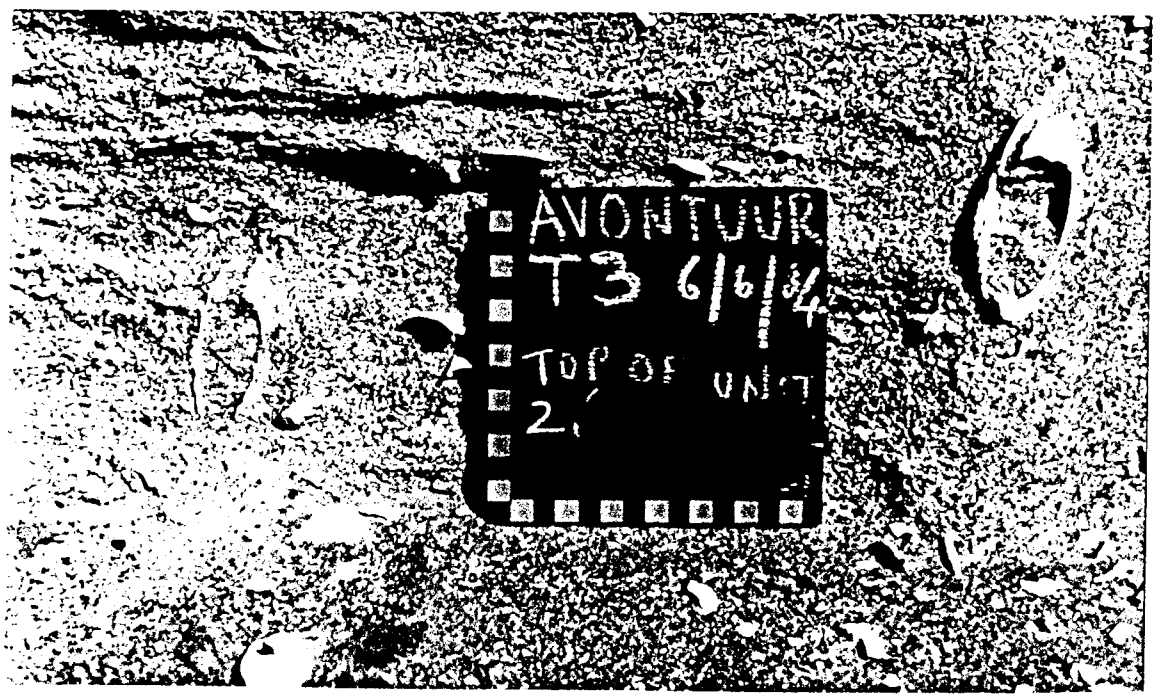

Plate 10.22 Mactrid bivalves *Lutraria* in their chevron-structured traces. Scale in cm.

Cryptobioturbation and 'adelobioturbation'

Cryptobioturbation (Howard and Frey, 1975) refers to subtle, very-small-scale disruption of primary laminae and pre-existing biogenic structures, so that these are "blurred, but not actually obliterated. This microscale bioturbation is the work of the interstitial meiofauna and very tiny crustacea such as amphipods. Because the primary structure is relatively well-preserved, the bioturbation is cryptic. The bioturbate texture associated with *Planolites montanus* burrows (Plate 10.11), that is revealed in nearly structureless sand by the peel technique, has already been discussed. It is another example of cryptic bioturbation, as the full extent of the apparent activity of the *P. montanus* animal is not evident without "development." However, as defined, the term "cryptobioturbation" is not entirely appropriate for this cryptic bioturbation because it refers to "unexpected" bioturbation in sediments with well-preserved primary structure. In contrast, in the massive sand, the bioturbation is "expected," but most of it is invisible. Furthermore, it is on a larger scale than "cryptobioturbation." The term, *adelobioturbation*, is therefore proposed here for cryptic bioturbation in massive sands with insufficient visible burrows to account for the loss of structure (*adel(o)*=concealed, Greek). By definition, it is only revealed by technical means (lacquer peels or X-radiography).

Study area examples: — 'Adelobioturbation' associated with *Planolites montanus* has been discussed. Lacquer peels also reveal smaller-scale 'adelobioturbation' as a bumpy texture with bumps 1-2 mm in diameter. This fine-scale ichnofabric occurs where *P. montanus* is poorly represented, such as the totally bioturbated, structureless areas between *Granularia/Palaeophycus* burrow clumps (Plate 10.12), where it must be regarded as a major contributor to the loss of primary structure. Notably, the identical, fine scale ichnofabric occurs pervasively in peels of heavy-mineral-rich, ripple cross-laminated, fine sands, with well-defined primary structure. In this case it is cryptobioturbation *sensu* Howard and Frey (1975).

Gravel-filled burrows

Study area examples: — This category represents burrows, 1-10 cm in diameter and up to 40 cm long, that occur in fine sand and that are filled with gravel that has been "piped down" from an immediately overlying, coarse-grained bed (Plate 10.23). They lack linings and other differentiation and are merely sharply-defined holes that have been filled. The host sediment must have been reasonably compacted to allow the production of apparently unreinforced burrow walls. The associated erosive contact above the burrows is very irregular, evidently due to the unroofing of burrows and apparent enlargement of the depressions by scour. They are probably crustacean burrows referable to *Thalassinoides sensu latu*.

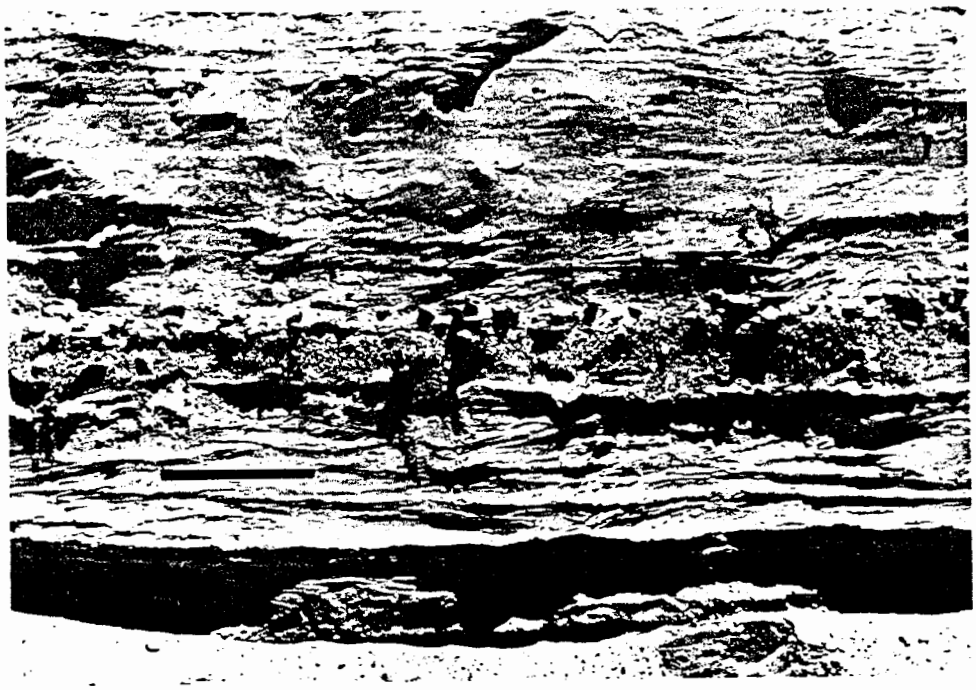

Plate 10.23 Gravel-filled burrows and holes associated with an erosive contact (Zone 3). Scale bar is 0.5 m.

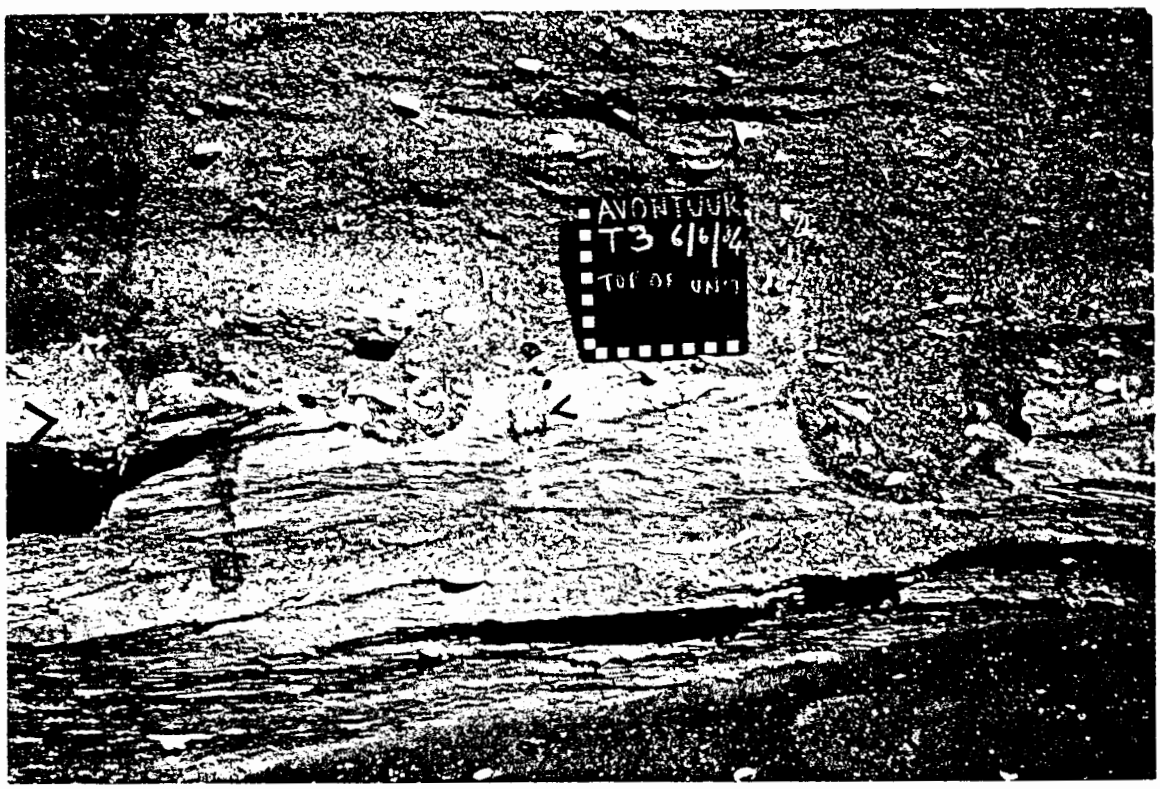

Plate 10.24. Probable ray holes excavated into low-angle, cross-laminated fine sand in upper shoreface. Note burrows of *Lutraria* (arrowed), filled with coarse sediment, along same horizon (extreme left, centre). Scale in cm.

Ray holes

Study area examples: — Occurring in shelly, cross-bedded, coarse sands are steep-sided scours infilled with the sediments from the overlying bed. These are bowl-shaped, 15-30 cm wide and 5-15 cm deep, with sharp, smoothly curving sides. Some are symmetrical "bowls", others are scoop-shaped, with a steep side and a sloped side (Plate 10.24). Sometimes the steep sides may be slightly overhung at the upper margin of the scour. These structures, although not abundant, are not uncommon and often several are found in close spatial association along a particular horizon. A notable association in the same facies are *in situ* bivalves.

The scours strongly resemble the lower portions of holes made by rays during excavatory benthic feeding, as illustrated by Howard *et al.* (1977). The traces described by Howard *et al.* (1977) consist of an upper, wide, shallow depression and a lower, steep-walled, bowl-shaped, circular hole. In the examples from the study area, upper, shallow "craters" are not present, probably due to erosive truncation of the tops of the structures. The asymmetric, scoop-shaped examples may be longitudinal sections of the holes, or they may, similar to gravel-filled burrows, possibly have been produced by erosional modification.

CHAPTER 11

THE AVONTUUR-A T2/T3 EXPOSURES

11.1 SETTING

The Avontuur-A T2/T3 excavation is situated in the southwestern corner of Avontuur-A, near the corner in common with the farms Hondeklip and Langklip (Fig. 9.1). The "overburden" was stripped from a small basin (Fig. 11.1), best defined by the 30 m asl. bedrock contour, which partially encloses a north-south elongate area, ~500 m by ~300 m in size. Most of the floor of the basin is a relatively flat area, ~300 m by ~120 m and between 25 to 26 m asl., developed on fresh to slightly weathered, strongly foliated, quartzitic gneiss. Along the inland (eastern) flank, bedrock rises relatively steeply (~6 m/100 m) to 35 m asl. In the northwest corner the basin is open to the west over a saddle at ~28 m asl. A ridge in the southwest corner, cresting at ~28 m asl., separates a small, subsidiary basin. Bedrock topographic data is incomplete in the south and the extent to which the T2/T3 basin may have opened to the south is not clear.

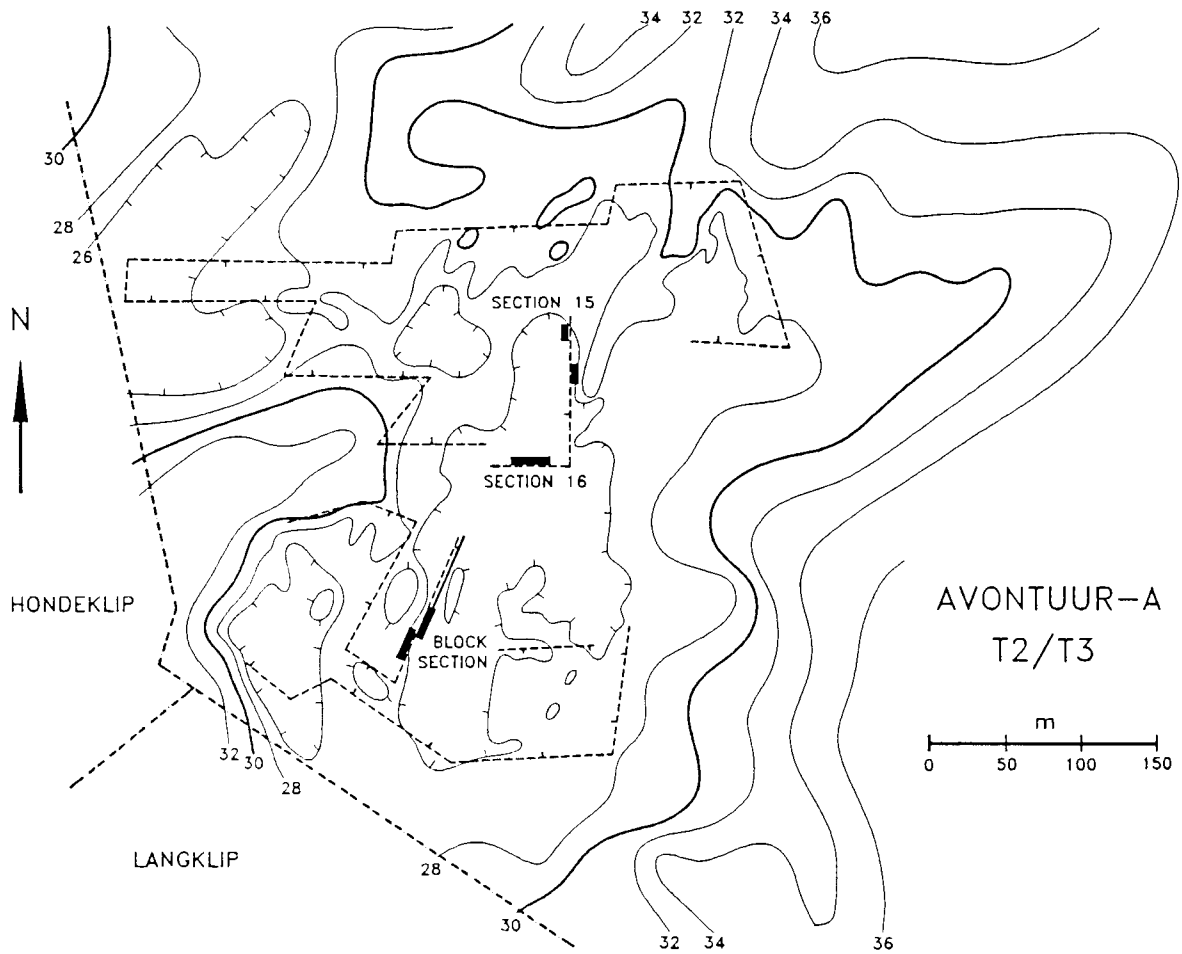

Figure 11.1 The Avontuur-A T2/T3 excavations. Bedrock contours in m asl. Locations of detailed section observations indicated by thick lines.

11.2 SECTION 15

Section 15 (Fig. 11.2) is located in the centre of the northern part of the T2/T3 basin, opposite its opening over a saddle to the west (Fig. 11.1). The upper part of the section was described from exposures ~35 m south of the lower portion. The base of the section is on bedrock at 25.8 m asl. and the faces examined are orientated N–S, approximately parallel to the coast.

UNIT 1

A mainly coarse-sandy bed, 0.5-0.6 m thick, with a basal, thin cobble gravel overlain by coarse sand and scattered pebbles, with interstitial fine sand.

The coarse sand (cL-vcU, Fig. 11.3: 1) is sub-rounded to rounded. It is mainly quartzitic and is therefore overall grey in colour (5Y 7/1), but in outcrop the presence of the minor, pale yellow to orange-coloured feldspar grains imparts a pale brown hue (cf. 10YR 7/4). The interstitial fine sand (fL, angular) is pale yellow (5Y 7/4) and constitutes ~10% of the sand (Fig. 11.3: 1). Bedding planes are poorly defined in the loose, running sand, but on the basis of gravel distribution four sub-units (a–d) are recognized (Plate 11.1). Lateral exposure is limited due to collapse of overlying material, forming a "talus" apron covering the lower 1-2 metres of the excavation wall.

Sub-unit 1a: — The largest clasts present in the section, rounded, large pebbles and cobbles composed mainly of local gneiss, overlie slightly weathered bedrock and form a clast-supported sub-unit ~15 cm thick. A small, rounded silcrete cobble with an abraded, brown phosphorite coating is present, as well as pebbles and small cobbles of dark, chocolate-brown (7.5YR 4/2) phosphorite rock. A few abraded *Crassostrea* valves are present.

Sub-unit 1b: — Ten to 15 cm of coarse to very coarse sand with scattered granules and small pebbles. Primary structure is not discernible and some bioturbation is visible as sporadic mottles 2-4 cm in diameter predominantly composed of fine sand.

Sub-unit 1c: — Ten to 15 cm thick with small to very large pebbles and some cobbles, mainly supported in the very coarse sand matrix. Discoidal and tabular clasts are aligned sub-horizontally. A clast of yellow sandstone is present.

Sub-unit 1d: — Approximately 15 cm of coarse sand with scattered small pebbles and poorly-defined, low-angle cross-bedding dipping southwards. The upper contact of Unit 1 is gradational as the coarse sand content decreases and laminae of fine sand appear over a short interval. A small exposure oriented NE-SW, made by excavation into the face, revealed sedimentary structures that are not apparent on the N-S face (Fig. 11.4). This consists of interbedded, cross-laminated sets of variable form, but mainly with erosional, trough-shaped bases. The cross-lamination is defined by the contrast between coarse and fine-sandy laminae and is poorly defined to indecipherable in the areas without interbedded coarse and fine-sandy laminae.

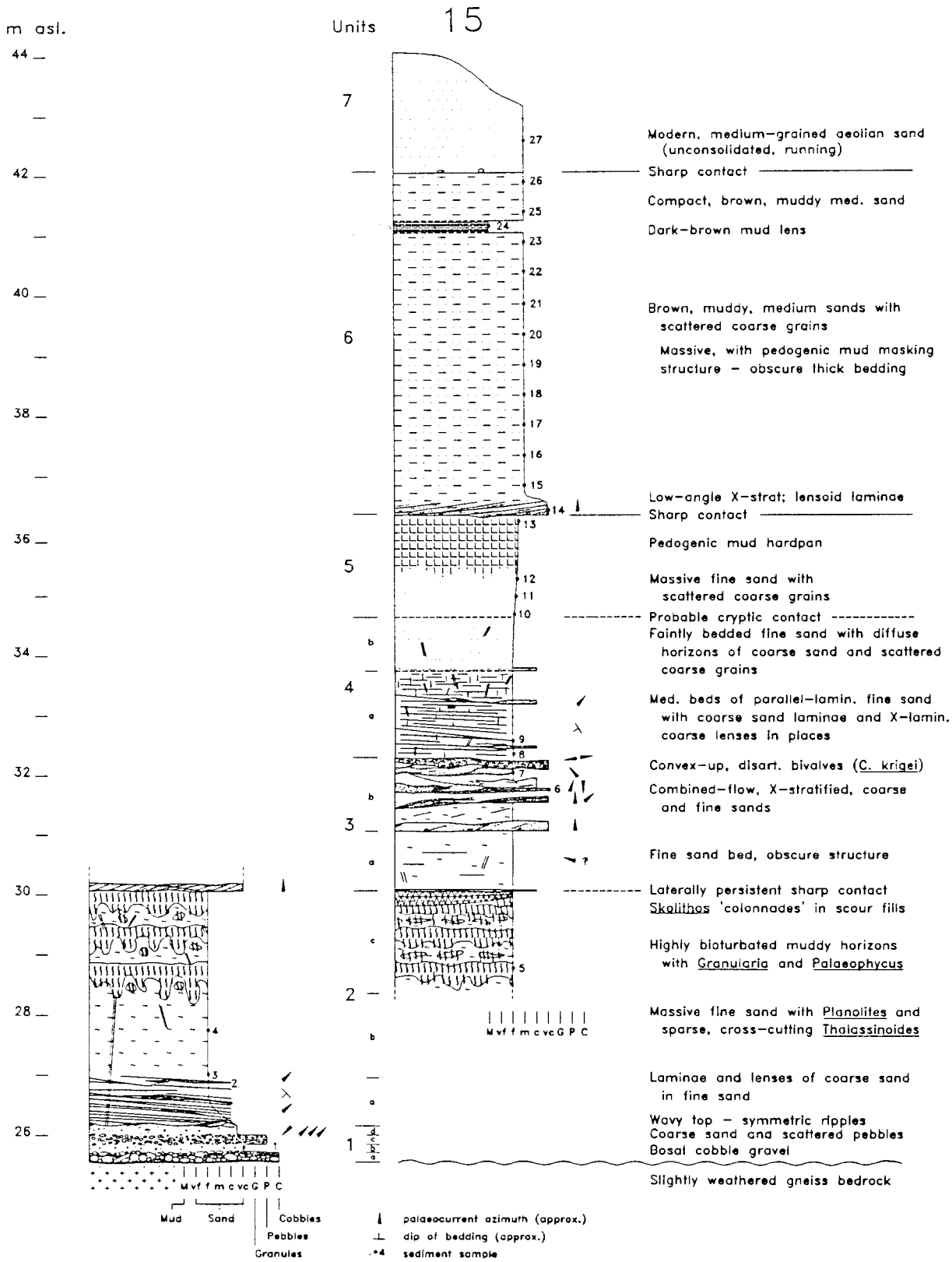

Figure 11.2 Section 15 graphic log.

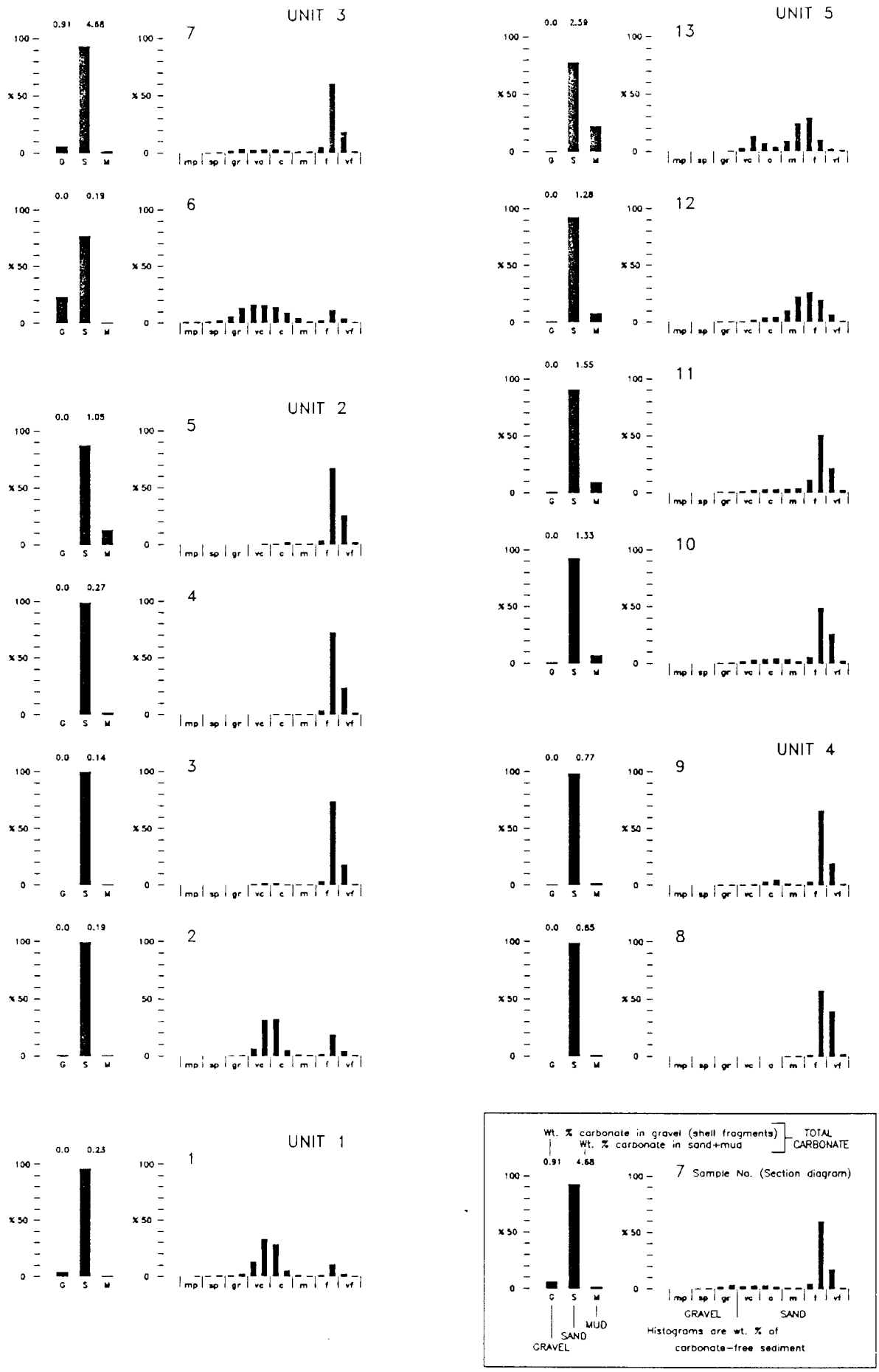

Figure 11.3 Section 15. Grain size analyses ($CaCO_3$ free). Sample positions in Fig. 11.2.

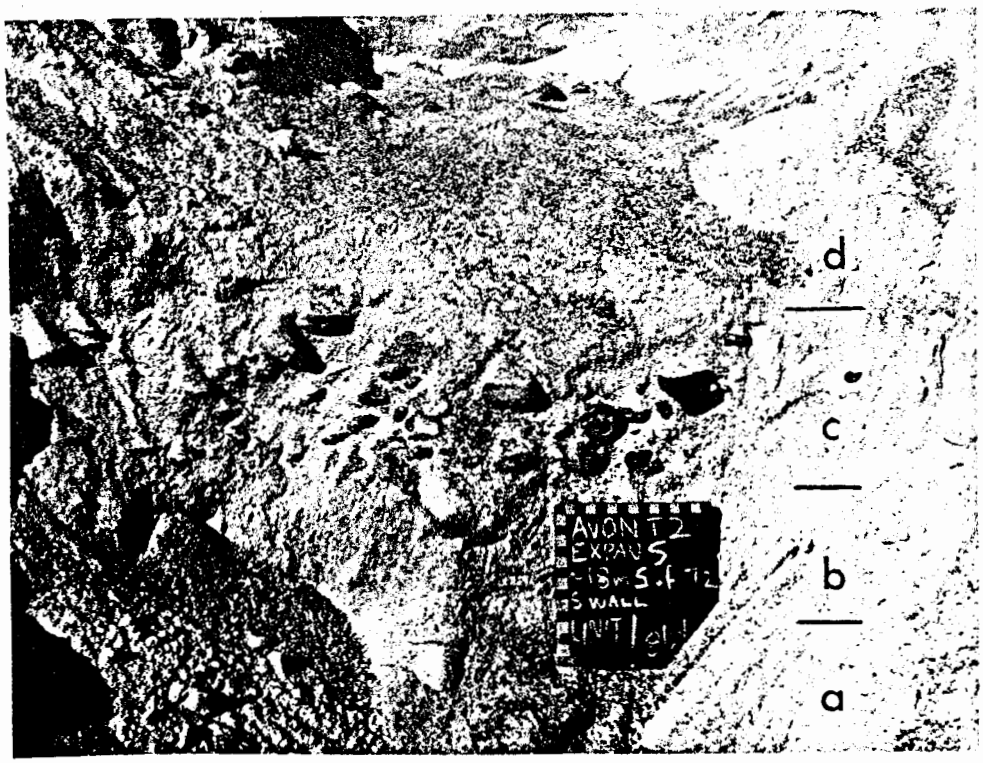

Plate 11.1 Marine basal gravel. Section 15, Unit 1, with sub-units a-d indicated. North is left. Scale in cm.

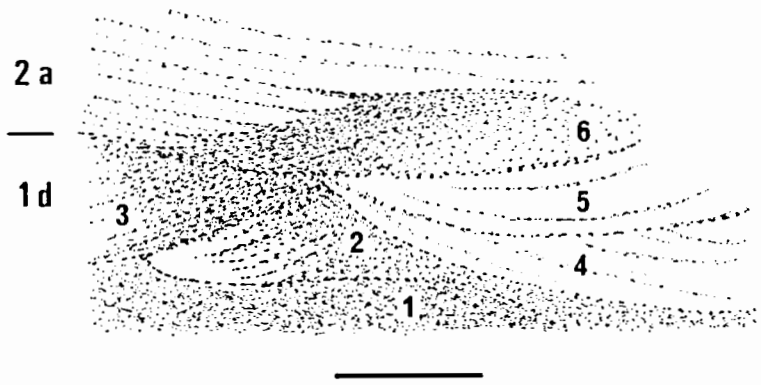

Figure 11.4 Coarse-grained ripple cross-stratification in the upper part of basal Unit 1, Section 15. Face is orientated NE-SW. Density of stipple approximates density of coarse to very coarse sand content. Set numbers are referred to in the text. Note the "feathering" of the landward side of the coarse-grained wave ripple into the coarse interlaminae in the overlying fine sand, indicative of combined-flow conditions. Scale bar is 10 cm.

A coarse-sandy set with poorly-defined cross-bedding dipping to the west (offshore) (Fig. 11.4, set 1) was eroded into a sigmoidal, slightly convex surface. A coarse-grained ripple with tangential-based foresets (set 2) migrated ~NE (landward) onto this surface, but became progressively more fine-sandy, the fine sand accumulating on the lower foresets. Similarly, set 3 suggests a ripple with a coarse-grained crest and fine-sandy lower foresets and trough. The other limb of set 3, exposed on the N-S face, has cross-bedding dipping south at a low angle, indicating a trough orientated approximately NW-SE. Two sets of swaley, cross-laminated fine sand (sets 4, 5), with sparse coarse laminae, then infilled a trough eroded seaward into sets 2 and 3. A ripple (set 6), which caps sub-unit 1d, migrated ~NE (landwards) onto the previous sets and was preserved as a form set with a rounded crest. The coarse laminae sweep down from over the crest and the set exhibits lateral coarsening with migration. The leeward boundary coarse laminae are interdigitated or "feathered out" into the abutting fine, laminated sand of the overlying Unit 2.

The occurrence of the convex-crested ripple form suggests that the top of Unit 1 is undulatory, at least locally. Notably, the lensoid, cross-bedded sets seen in the limited NE-SW exposure (approximately shore-normal) are not present in the N-S exposure (approximately shore-parallel). This suggests that the upper part of Unit 1 represents two-dimensional (straight-crested), approximately symmetrical bedforms, with a crestal orientation oblique to the N-S face and approximately NW-SE.

UNIT 2

A thick unit (~3.8 m thick) of mainly pale yellow (5Y 7/4) fine sand (fL). Bedding is defined by interlaminated coarse sand in the lower, unbioturbated portion. Primary structures dwindle upwards as coarse laminations disappear and bioturbation increases. The central portion is structureless. The uppermost portion is totally bioturbated and slightly muddy, the greenish mud component extensively pelletised and mixed by the bioturbation. Although the unit consists overwhelmingly of fine sand, these features impart a fining-upward aspect to the unit and define three sub-units with gradational boundaries (Plate 11.2, Fig. 11.2).

Sub-unit 2a: — ~O.7 m thick. Sub-parallel, very thinly bedded to laminated fine sand (fL, angular) interbedded with laminae and small lenses of coarse sand (cU–vcL, rounded) (Fig. 11.3: 2,3), with structure defined by grain size contrast (Plate 11.3). Overall, the depositional surfaces dip gently to the southwest at a low angle (2-5°).

The lower portion of the sub-unit is interlaminated fine and coarse sand dipping at ~5° to the SW. The laminae are sub-parallel with very low-angle discordancies due to changes in thickness of individual laminae as they locally split, amalgamate or thin to disappearance. In NE-SW section (Fig. 11.4).the laminae are tangentially-based where they overlie Unit 1. As noted, small-scale interfingering developed as coarse grains on the surface of the convex form set capping Unit 1 were washed onto surfaces of the fine sand that was covering it up.

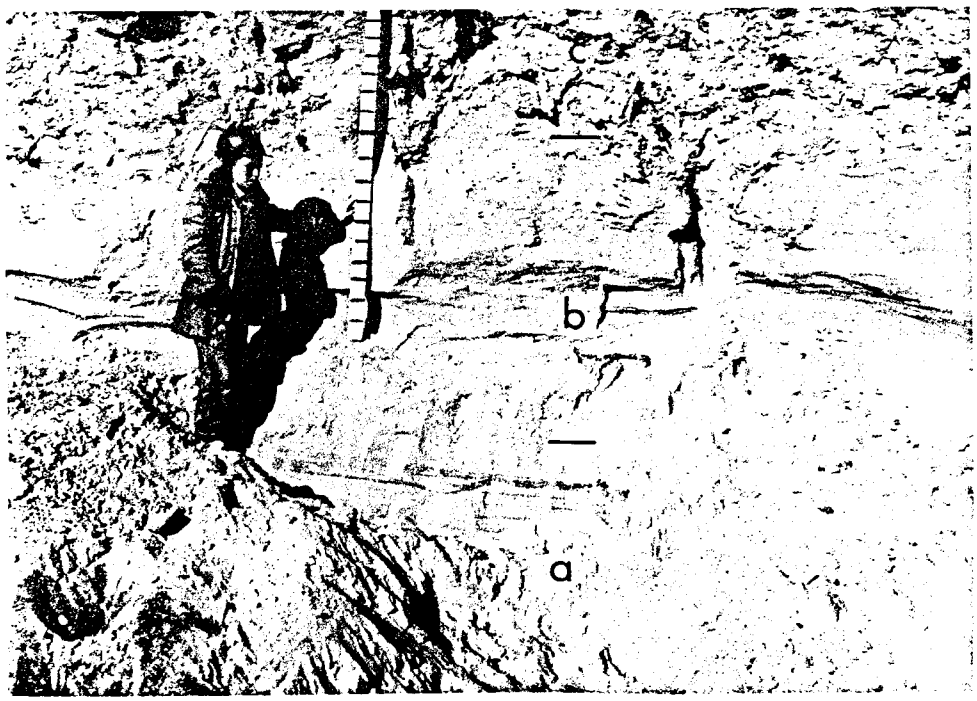

Plate 11.2 Section 15, Unit 2., showing lower portion with coarse sand laminae (2a), massive central portion (2b) and highly bioturbated upper portion (2c). Note thalassinoidean burrows (centre). North is left. Scale in dm.

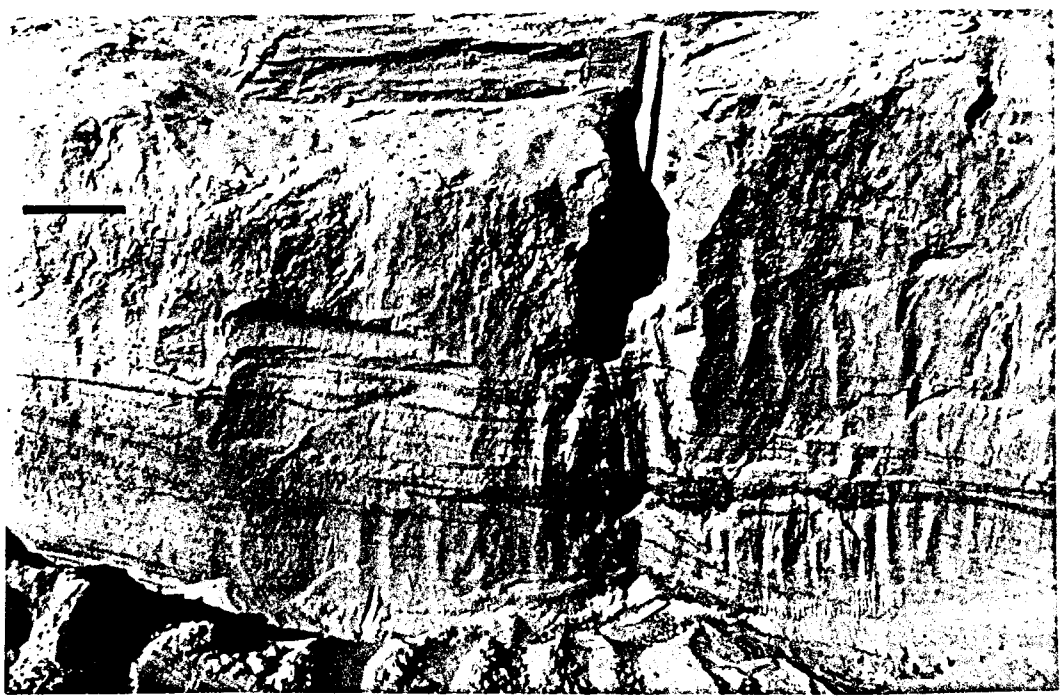

Plate 11.3 Section 15, sub-unit 2a. Low-angle, sub-parallel laminae and ripple cross-laminae of coarse sand in fine sand. Note steepening of lamination (right) and trough-set (centre left). North is left. Scale bar is 2 dm.

The proportion of fine sand increases upwards, the upper portion of the sub-unit being dominated by very thin beds of fine sand with coarse sand interlaminae and lenses (Plate 11.3). The low-angle, sub-parallel lamination locally steepens to become cross-lamination dipping offshore to the SW (Plate 11.3, right). The fine-sandy laminae exhibit lateral thickening and thinning, due to scour associated with the deposition of the coarse laminae and lenses. Many of the coarse laminae in the uppermost portion are only a grain diameter in thickness, but the most marked erosional surfaces underlie the larger accumulations of coarse sand. Coarse sand lenses appear to have been "swept out" prior to and during deposition of the overlying sand. Overlying, fine-sandy laminae locally both abut and sweep over coarse lenses . A small, cross-laminated trough-set is present near the top of the sub-unit (Plate 11.3, left centre). This indicates migration of a coarse-crested ripple NE-wards (landwards), up the depositional slope.

The upper boundary of this sub-unit is gradational and taken where primary structure is no longer visible due to the disappearance of coarse sand laminae and the dominance of bioturbation (Plate 11.3).

Sub-unit 2b: — ~1.4 m thick. This sub-unit of pale yellow (5Y 7/4), fine sand (fL, Fig. 11.3: 4) is massive in appearance (Plate 11.2) and the main features are biogenic in origin. There is only a faint hint of primary layering made visible by the relief produced on etching by the sand-laden wind. This suggests parallel bedding on a scale of a few cm to dm. Tiny black mottles, ~1 mm in diameter, are randomly distributed through this sub-unit at ~1 cm apart. These are soft little aggregates of grains weakly cemented by black material. Application of a drop of 50% H_2O_2 (hydrogen peroxide) to a black aggregate on a glass slide produced a strong, effervescent reaction, confirming that the black material is organic carbon.

The dominant trace fossil is *Planolites montanus*. These burrows are evenly distributed and spaced 1-3 burrow diameters apart (≤1 cm), but locally there are areas where the burrows are more widely spaced (1-3 cm). There is no obvious spatial relationship between the burrows and the tiny, carbonaceous aggregates. This "*Planolites montanus* in massive, fine sand" ichnofabric is consistently developed in Unit 2 around the T2/T3 excavation. A lacquer peel suggests that the structureless character is due to concealed bioturbation (adelobioturbation, Chapter 10) and that only a portion of the burrowing by the producer of *Planolites montanus* is readily visible. Visible burrows account for ~30% of bioturbation, but the destruction of primary structure (lamination) is near total. The minute , sinuous burrow, *Planolites 'threads*,' is evenly distributed at a density of a few cm apart. The large-scale, reddish burrow systems of *Thalassinoides 'multiplex'* occur sporadically (1-2 m apart). These are actually present throughout Unit 2 and some penetrate down to Unit 1. An instructive example, excavated at the section site, extended downwards from the overlying sub-unit 2c in near-vertical orientation over ~2.5 m (Plate 10.17). In addition to single burrows, clumps of amalgamated burrows are also present (Plate 11.2, centre).

The upper boundary of this sub-unit is gradational and is distinguished by a change in lithology, colour and the appearance of a more diverse assemblage of trace fossils (Plate 11.2).

Sub-unit 2c: — ~1.3 m thick. The massive sub-unit 2b is overlain by a slightly muddy, greenish (5Y 7/2), completely bioturbated, irregular horizon ~10-15 cm thick. Similar churned, bioturbated areas extend irregularly down from the main, muddy horizon into the top of 2b (Plate 11.4). These pendant zones are spaced 20-50 cm apart and generally extend 0.5-1.0 m into 2b. Overlying the main muddy horizon is a ~0.5 m interval of pale yellow, structureless, bioturbated, fine sand resembling the upper part of 2b, in turn overlain by another green, muddy, completely burrowed horizon with irregular pendants (Fig. 11.2). Similarly, a further interval of yellow fine sand is succeeded by a third muddy, green burrowed horizon. Due to the mud content, the green horizons and pendants stand out in relief on the wind-eroded exposure. The green, muddy horizons contain small, irregular mud lenses a few mm thick and 0.5-3 cm long and in places there is a suggestion of relict contorted lamination. Grains of coarse sand sparsely "pepper" the muddy horizons and their pendant zones. Analysis of a sample indicates a mud content of 10-15% in well-sorted fine (fL) sand with 2–3% coarse sand (Fig. 11.3: 5).

All three ichnospecies described from sub-unit 2b are present in the structureless sands surrounding the muddy horizons and pendant burrow clumps. *Planolites 'threads'* also occur within the pelleted, muddy zones and *Thalassinoides 'multiplex'* burrows cross-cut them. The *Thalassinoides* burrows are mainly sub-vertical and are sporadic in occurrence, but they are more numerous and smaller in diameter (0.5-1.0 cm) relative to the few, larger, cross-cutting examples in the underlying sub-unit 2b.

The muddy horizons and pendant zones have a porous, granular appearance and are predominantly composed of aggregated, ovoid muddy pellets ~1 mm in long dimension (*Tibikoia*). Some well-defined, pellet-lined and pellet-stuffed *Granularia* burrows are present, but the pellets are mainly concentrated into small clumps, thin, irregular "sheets" and incomplete tubes (Plate 11.8). Thinly-lined *Palaeophycus tubularis* burrows are common, both within the pelleted, muddy zones (*Granularia-Palaeophycus* clumps) and in the surrounding sand. *Planolites 'spaghetti'* occurs locally in some of the areas between the pendant *Granularia-Palaeophycus* clumps where they are relatively dense (1–3 cm apart) (Plate 11.12).

The uppermost, bioturbated, muddy, fine-sandy horizon is sharply truncated and overlain by cross-bedded, very coarse sand with sparse small pebbles. This sharp contact and overlying coarse sand defines the base of Unit 3. Nearby exposures at this level show that this sharp, gently undulatory, erosive lower contact separating Units 2 and 3 is laterally persistent. In fact, around the entire T2/T3 excavation, a major facies change occurs at this level, which consists of a sharp contact separating underlying, eroded, bioturbated and laminated, fine sands from overlying, cross-bedded, locally shelly, coarse sands.

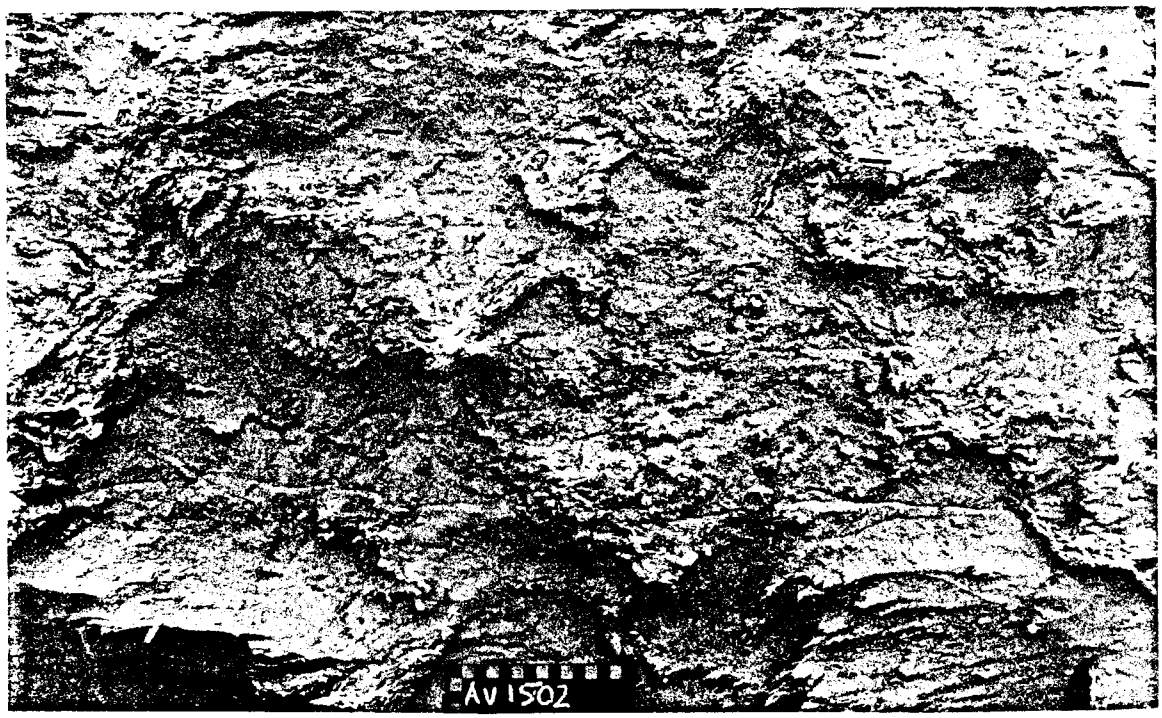

Plate 11.4 Section 15, sub-unit 2c. Totally bioturbated (*Granularia-Palaeophycus*), muddy sand volumes in positive relief. Note vestigial thin bed of muddy sand (top, outlined), with "pendant" bioturbated zones (left and right) North is left. Scale in cm.

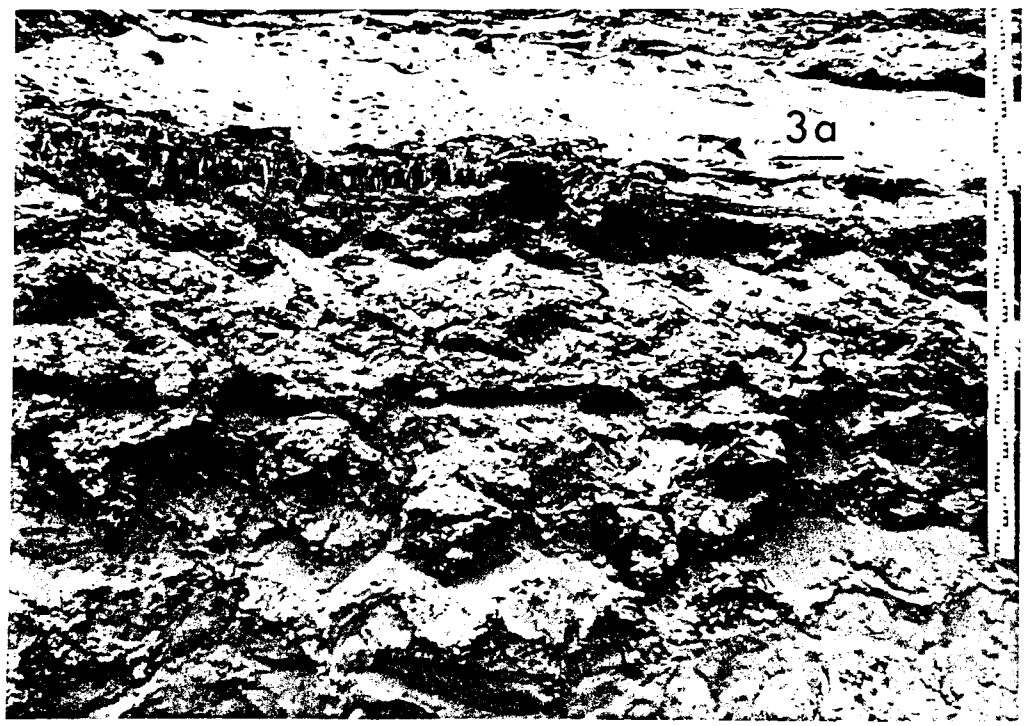

Plate 11.5 Section 15, sub-units 2c and 3a. Note *Skolithos 'bundles'* in shallow troughs capping 2c. North is left. Survey staff for scale (cm and dm).

At this particular site, a bench was cut into the excavation wall just above the level of the contact between Units 2 and 3. Collapse of material onto the bench obscured Unit 3, except for its lowermost ~20 cm. The description of the Section 15 was therefore continued at a position ~35 m to the south (Fig. 11.1), where face collapse was less, enabling manual excavation of exposure. This was permissible as the essential characteristics of facies were constant around the excavation walls. Levelling with the Brunton compass confirmed that the top of 2c maintained its elevation to the new site. However, sub-unit 2c exhibited some differences, noted below.

Lateral variation in sub-unit 2c: — At the new site the occurrence of three distinct, green, muddy horizons in 2c, separated by two intervals of non-muddy, yellow sand, is not as clear as at the previous location. The two lower muddy horizons are discernible (Plate 11.5), but are more disrupted by the "clumping" of the muddy sediment into pendants and islands. The upper portion of 2c consists of at least another three intensely bioturbated, extensively disrupted, "clumped" muddy horizons, with little intervening yellow sand. Very shallow, gently concave scours 2-3 m wide are developed in the uppermost part of 2c (Plate 11.5). The infill consists of very thin beds of fine yellow sand with interlaminated, green, muddy sand, subsequently disrupted by bioturbation. Numerous vertical burrows occur within the scour infills and are referred to *Skolithos 'bundles'*. A contorted, very thin bed of bioturbated muddy sand overlies the uppermost *Skolithos* horizon

UNIT 3

A unit, ~2.3 m thick, consisting of low-angle, inclined, parallel-laminated fine sands and cross-bedded coarse and fine sands. Two sub-units are defined. A thick bed of yellow, fine sand, with obscure internal structure, is at the base of the unit. This is succeeded by an interval characterized by interbedded sets of cross-stratified coarse and fine sand. This cross-bedded interval also contains the only significant skeletal carbonate in the section, as shells in the coarse sand sets and comminuted shell debris in the fine-sandy sets.

At the initial site, as mentioned, sub-unit 2c is sharply overlain by cross-bedded, coarse to very coarse sand with sparse small pebbles basal to Unit 3. The foresets are very low angle and tangential to the bases of sets that are 10-15 cm thick. Cross-bed azimuths are directed northward. Due to collapse, only these lowermost cross-beds are exposed. At the site where the section was continued, the muddy surface exposed on top of the *Skolithos* "colonnades" developed in the wide, shallow scours in sub-unit 2c is sharply overlain by a very thin bed (1-2 cm thick) of coarse sand with scattered, small pebbles. Although not appearing as a major feature, this thin, coarse bed is on the same level as the major facies contrast present around the excavation and is therefore regarded as the base of Unit 3 at this location (Fig. 11.2).

Sub-unit 3a: — The thin, coarse "lag" is basal to a bed of pale yellow (5Y 7/4), well-sorted, fine sand (fL) ~1 m thick (Plate 11.5). Internal structure is poorly defined, with only a hint of horizontal thin bedding which disappears on freshly-made, vertical surfaces. Laminae of coarse sand appear in the uppermost 10 cm of the bed. *Planolites montanus* is the main biogenic trace, suggesting moderate to

strong bioturbation. Sub-vertical *Thalassinoides 'multiplex'* burrows occur sporadically. Although lateral exposure at this level of the face was poor due to the presence of collapsed material on the bench, this fine sand bed was estimated to be 10-15 m in lateral extent.

Sub-unit 3b: — Sub-unit 3a is sharply overlain by a coarse to very coarse sand bed ~15 cm thick, with scattered, small to medium-size pebbles (Fig. 11.2). Internal structure is obscure, but northward-dipping cross-bedding can be discerned in places. The top of the bed is gently undulating, with a smooth relief of ~2 cm over ~1 m. This was succeeded by a fine-sandy bed ~30 cm thick which resembles sub-unit 3a in its obscure internal structure and *Planolites montanus* traces, but a faint north-dipping texture is visible.

The previous bed was eroded, producing gentle relief of up to ~10 cm (Plate 11.6). An abrupt colour change in the fine sands occurs upwards across this surface, from pale yellow (5Y 7/4) to very pale green (5Y 8/1). The upward change to very pale green colour correlates with the preservation of comminuted shell. The erosion surface is overlain by a discontinuous, cross-laminated, very coarse-sandy, thin bed with northward cross-bed azimuths (Fig. 11.5). The coarse sand in this thin bed is disposed in flat-based lenses, up to ~10 cm thick, with convex tops that result in lateral thickening and thinning. These are overlain by cross-laminated, fine sand, 5-15 cm thick, with cross-bed azimuths directed to the NNE. Notably, local interfingering of the fine sand cross-lamination with the underlying lamination in the coarse lenses indicates that deposition of the coarse lenses and overlying fine sand took place penecontemporaneously, i.e. they form a coarse-fine composite unit or couplet. The upper surfaces of the coarse lenses are generally sharp, but their up-current ends are "ragged" and interfingered with fine sand cross-laminae at places where fine sand deposition dominated during the migration of the composite bedform. In this particular example (Fig. 11.5, bed 1), it appears that the coarse lenses were formed intermittently in the vanguard of a fine-sandy, small, subaqueous dune. A possible mechanism is temporary flow reversal over the dune, eroding it backwards and producing a sharp contact on coarse sand deposited on the toes of foresets. The coarse lens so produced is then covered when migration resumes.

A shallow trough eroded into the previous couplet bed (Fig. 11.5, bed 1) is infilled by a more complex example of a coarse-fine, couplet bed (bed 2), but with similar basic features (basal coarse lenses to thin beds, at places separated from overlying, fine-sandy laminations by sharp, convex to undulatory contacts, at other places interfingering). Direction of migration is similar to the underlying couplet (N to NE). An overlying, more pronounced erosional trough is infilled by another coarse-fine, couplet bed (bed 3). Structure in the basal coarse portion is indistinctly sub-horizontal to swaley and a few convex-up bivalves are present. Interfingering with overlying fine sand occurs only in the northern side of the trough and the top of the coarse sand is smoothly undulatory, with a wavelength of ~0.5 m. Very low-angle lamination in the upper, fine-sandy portion dips southward.

Plate 11.6 Section 15, sub-unit 3b, Unit 4 and lowermost sub-unit 5a. Note cross-stratified, coarse-fine sand couplet beds in 3b and uppermost, shell-rich trough-lag. Low-angle, parallel-lamination characterizes Unit 4. Unit 5 exhibits loss of primary structure and is relatively more massive in aspect. Survey staff for scale.

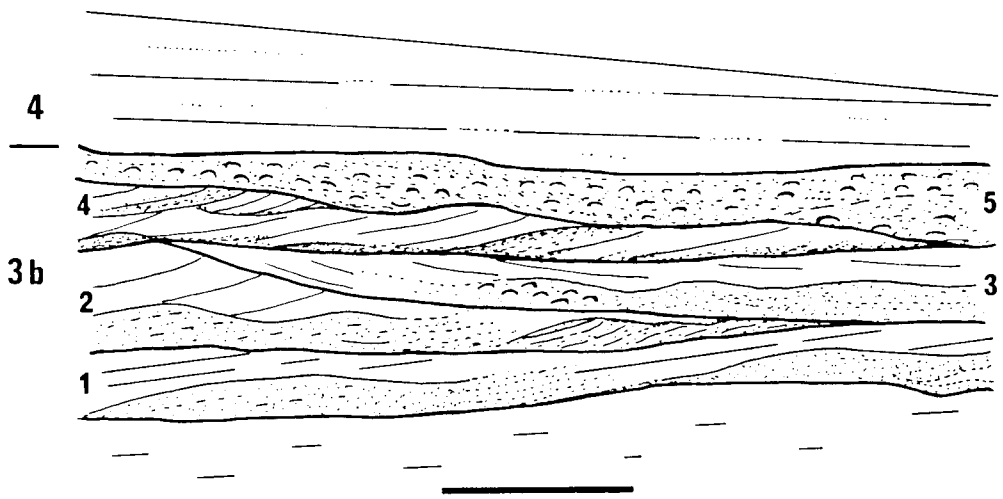

Figure 11.5 Detail of cross-stratified, coarse-fine sandy couplet beds of sub-unit 3b. Stipple approximates coarse sand distribution. From field sketch of exposure shown in Plate 11.6. North is left.. Scale bar is 0.5 m.

A further, very gently undulatory erosion surface is overlain by a bed consisting of several sets of cross-laminated, fine sand (Fig. 11.5, bed 4), with coarse sand deposited on foreset toes defining the lower set boundaries. Cross-bed azimuths are directed north to northwest. The local presence of small, convex lenses of coarse sand indicates that this bed is an incipient coarse-fine couplet. This is erosively overlain by shelly, very coarse sand to granule gravel (bed 5), with small pebbles, in a bed with indistinct sub-horizontal to swaley cross-stratification suggestive of deposition in troughs. Clear cross-stratification azimuths were not obtainable, due to low angles, but stratification appears to dip very gently both into and out of the face, suggestive of bipolar transport in eastward and westward directions. The grain-size distributions in samples of coarse-sandy and fine-sandy, cross-laminated sets (Fig. 11.3: 6,7) provide examples of the respective proportions of the two grain populations in the Coarse-fine couplets.

Bioturbation in sub-unit 3b is weak and practically confined to the sporadic occurrence of *Thalassinoides 'multiplex'* burrows and small volumes of *Planolites montanus* in fine sand beds. The macrofauna in the uppermost shelly bed is dominated by the orbicular valves of the extinct, shallow infaunal venerid, *Chamelea krigei*. These are disarticulated, abraded and fragmented and the more complete valves occur predominantly in convex-up orientations. Abraded right valves ("lids") of the oyster *Crassostrea margaritacea* are common. Worn, disarticulated valves of *Tivela compressa* are also present. Among the gastropods present, limpets are common (patellids and fissurelids), particularly the keyhole limpets *Fissurella robusta* and *Diodora elevata*, whilst the herbivorous snails *Oxystele sinensis* and *Turbo cidaris* are well represented.

UNIT 4

A unit, ~2.4 m thick, with a lower portion (sub-unit 4a, ~1.4 m thick) of gently inclined, medium beds of parallel-laminated fine sand, with some coarse sand laminae and interbedded, thin, cross-bedded, coarse-sandy lenses in places. The upper sub-unit (4b, ~1 m thick) is faintly bedded with diffuse horizons of coarse sand in pale green, fine sand.

Sub-unit 4a: — The lower boundary is the top of the shelly bed capping Unit 3, above which parallel-laminated, pale green (5Y 7/2), fine sand (fL) dominates (Fig. 11.3: 8,9). The lamination is 0.5-1.0 cm thick and disposed in beds 15-30 cm thick that mainly dip gently at 2-4°S on the N-S face (Plate 11.6). Apparent bed contacts are difficult to trace completely as a well-defined plane at one location becomes indistinct laterally from the general lamination. Bedding planes are clearest where they dip more steeply than the underlying lamination, which is erosionally truncated. The overlying lamination is less inclined and laps onto the bedding plane updip (Plate 11.7). These contacts are locally overlain by coarse sand laminae with scattered granules. Lenses of cross-bedded, slightly shelly, coarse sand also occur on major bedding planes. These are flat-based or in very shallow troughs and are up to 10 cm thick, but their undulatory, rounded tops result in lateral thickening and thinning. They are laterally discontinuous, thinning to "stringers" and eventually to laminae. The truncation of cross-laminae indicates that the form of the lenses developed during erosion. The cross-bedding in these coarse

lenses is directed into the northeast quadrant. The lenses of coarse sand are not pervasively developed laterally in this unit. They were absent at the immediate section site except in the lowermost part. Where present, they appear to become thinner and less common upwards in the unit.

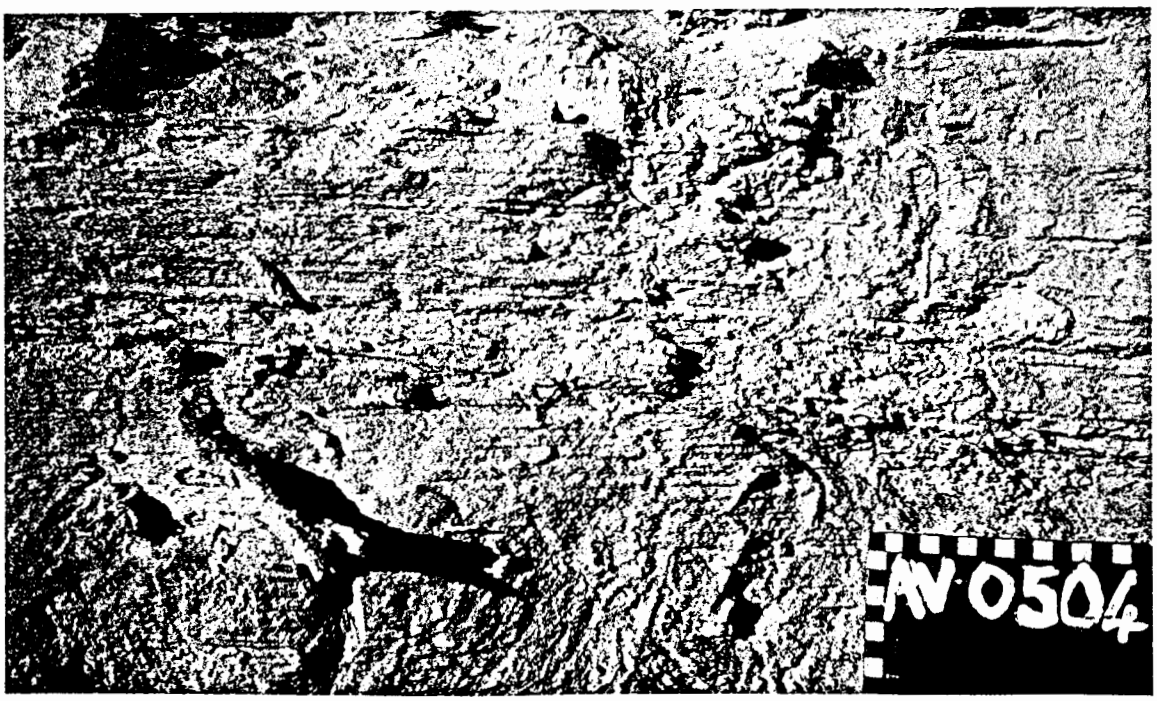

Plate 11.7 Section 15, Unit 4. Detail of parallel lamination and truncating bedding plane. North is left. Scale in cm.

Within apparent beds, laminae of coarse sand from one to several grains thick may be present, but are not pervasively developed. The laminated appearance is also present where the material is exclusively fine sand. In this case, grain size contrasts or heavy mineral segregation could not clearly be established as the origin of the lamination. Oblique sections through laminae were unhelpful as the definition of laminae disappears on fresh cuts, being revealed only by wind-etching. Very locally, lamination defined by finely comminuted shell is present.

In contrast to sub-unit 3b, trace fossils are abundant in this sub-unit. The visually dominant traces are large-scale *Thalassinoides 'multiplex'* burrows (0.5-2.0 cm in diameter) and related large burrow mottles and amalgamations. Orientations are dominantly vertical to steeply oblique. In addition to the reddish hues more common in underlying units, *Thalassinoides* burrows of greenish hue occur and colour intergrades are present. The size range of these systems appears more variable than in underlying units, smaller diameters being more common. Large-scale, amalgamated, *Thalassinoides*-type burrows are more common in the upper part of the sub-unit. *Planolites montanus* affects small volumes and *Planolites 'threads'* are present, although uncommon and mainly commensal to larger burrows. *Palaeophycus 'spaghetti'* burrows are very sparsely present. The degree of destruction of primary lamination increases upward in this sub-unit, from ~10% in the lowermost portion, to ~50% in

the uppermost portion. However, distinct burrow structures to which this destruction could be ascribed are not clear and it may represent cryptobioturbation by small organisms.

Sub-unit 4b: — A distinct horizon occurs above the vestigial lamination in the uppermost part of sub-unit 4a, above which primary structure is near absent and the outcrop appearance becomes more massive (Plate 11.6). A diffuse, discontinuous, thin bed of coarse sand occurs along this horizon, but a clearly-defined, sharp contact is not present. Similar, horizontal, thin beds of coarse sand, with diffuse upper and lower contacts, characterize the sub-unit. These are not very persistent laterally and disappear over several metres. Degraded (powdery) comminuted shell occurs in diffuse patches. Reddish, thalassinoidean burrows are present.

UNIT 5

A unit, ~1.7 m thick, of structureless fine sand, with scattered coarse grains. The unit is capped by a hardpan consisting of pinkish-white, slightly calcareous, mud.

The diffuse horizons of coarse sand in sub-unit 4b disappear upwards and the overlying material is massive, compact and has a slightly darker green hue (5Y 7/3) than the underlying fine sand. Coarse sand grains and the occasional granule are scattered throughout the fine sand. The size analyses of samples from the unit show a subtle, upward shift of the modal size class, from fL to fU, concomitant with an increase in the proportion of medium sand (Fig. 11.3: 10-12). Towards the top, the unit gradationally but rapidly becomes hard and pinkish-white (7.5Y 8/2) and developed in the upper metre is material that strongly resembles a crudely laminar, hardpan calcrete with blocky fracture (Plate 11.8). However, acid digestion analysis revealed that the soluble carbonate content is only ~3% and that the material is actually a pale, muddy sand (Fig. 11.3: 13). Notably, the bimodal size distribution resembles that of the immediately overlying sand (Fig. 11.6: 14). Mottles of reddish sediment occur very sporadically in the unit and bear a superficial resemblance to *Thalassinoides* burrows. They are not well-exposed as they etch into negative relief in the compact material.

UNIT 6

A unit, ~5,7 m thick, of muddy, brown, thickly-bedded, medium-grained, massive sands. The colour is due to the mud content that occurs as grain coatings and interstitial mud.

The pale mud capping Unit 5 has a sharp upper contact. Sparsely scattered on this contact and in the immediately overlying brown sands are small, rounded quartz pebbles. Clasts derived from the pale, mud "hardpan" capping Unit 5 also occur in the lowermost 20 cm of Unit 6 (Plate 11.9), indicating exposure and erosion of the underlying "hardpan."

Only the lowermost 40 cm of Unit 6 exhibits readily discernible primary structure and is anomalously coarse relative to the bulk of the unit, being mainly coarse to very coarse sand (Fig. 11.6: 14). The gross structure is lamination to very thin bedding dipping northwards at a low angle (~5°)

Plate 11.8 Section 15, Unit 5. Faint bedding in sub-unit 5a, with gradational change to structureless, slightly darker-coloured sub-unit 5b. Calcrete-like capping is actually a slightly calcareous, pedogenic mud hardpan. North is left. Scale board is 15 by 15 cm.

Plate 11.9 Section 15, lower contact of Unit 6. Note pale clasts eroded from underlying pedogenic hardpan and low-angle. locally distorted, thinly lensoid lamination dipping northwards. North is left. Scale in cm.

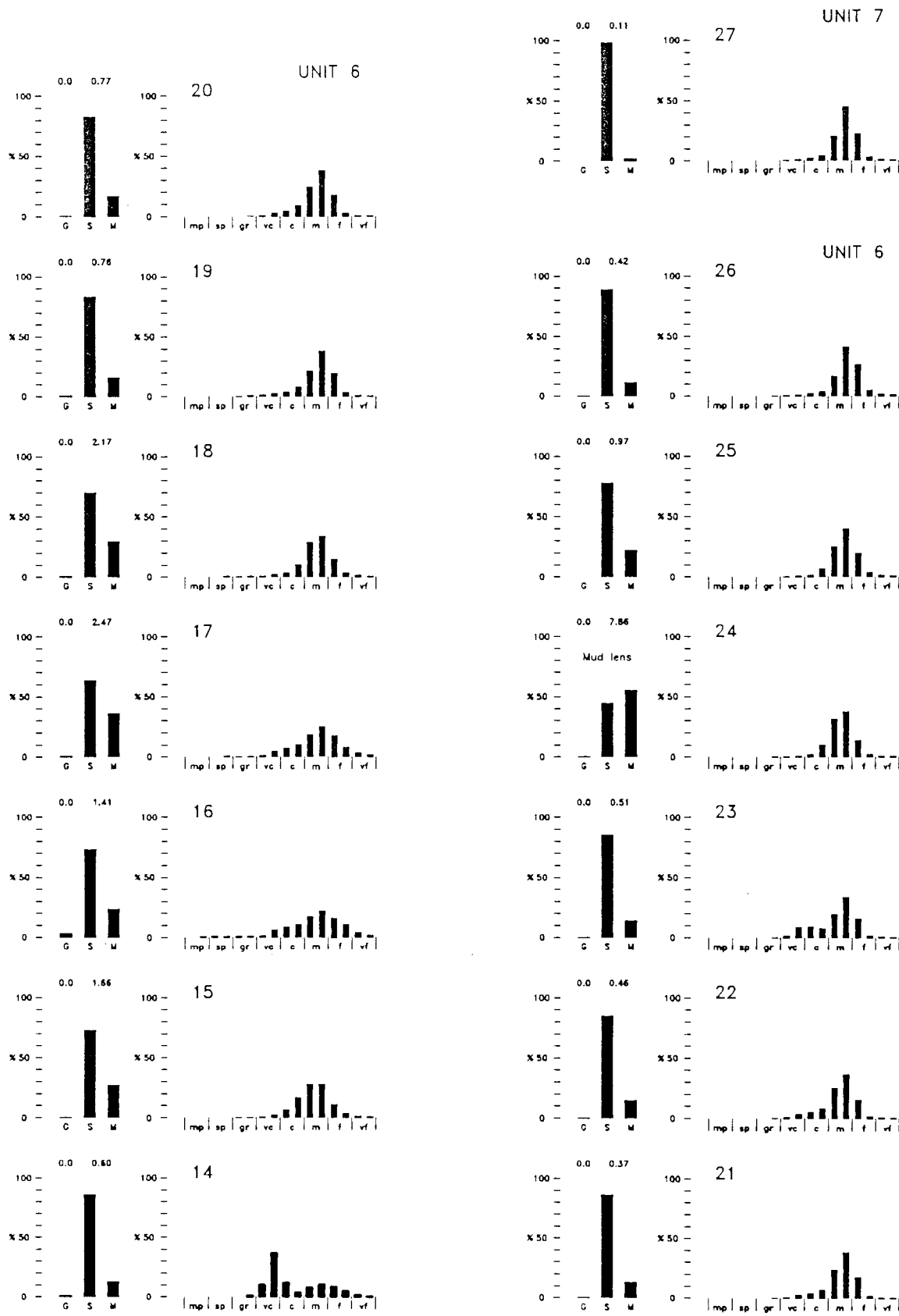

Figure 11.6 Section 15. Grain size analyses ($CaCO_3$ free). Sample positions in Fig. 11.2.

Plate 11.10 Layering defined by subtle colour contrasts in equivalent of Unit 6 (Section 15) (in trench T1, Avontuur-A. Face is ~5 m high.

The structure is defined by the size contrast between interbedded coarse and medium sand laminae and very thin beds. Close inspection reveals that the lamination/very thin bedding is not continuous, but appears to consist of thin "stringers" of coarse or medium sand that wedge out over 0.3-1.0 m. In some thicker, less elongate examples of the very thin lenses (~1 cm thick, 10-30 cm in length), faint internal cross-lamination can sometimes be discerned, dipping very shallowly northwards. In places the lamination is wavy and this appears to be the result of soft-sediment deformation (Plate 11.9). Bioturbation is indicated by the presence of indistinct mottles interrupting lamination.

Above this lowermost portion, the unit is homogeneous, medium-grained sand with sparsely scattered coarse grains (Fig. 11.6: 15-26). The basic colour is brownish yellow ~10YR 6/6. Bedding is not visible due to the freshness of the exposure at the time of examination, but older faces exhibit layering on the scale of 0.3-1.5 m, defined by faint colour contrasts from variation of the basic yellow-brown by tints of more reddish or greenish hue. (Plate 11.10). Some of the layering is clearly depositional and primary, such as dark, muddy beds, but soil-profile development has also have contributed to the layering defined by subtle colour contrasts.

The grain size analyses (Fig. 11.6) suggest that there is an overall an upwards decrease in pedogenic mud content in Unit 6. At a level 1 m below the surface of the unit is a dark brown (10YR 4/4), muddy lens, 20-30 cm thick, with gradational upper and lower boundaries (Fig. 11.2). This lens is ~20 m in lateral extent, thinning to pinch-out laterally. Such lenses are common in the equivalents of this unit in

all the Avontuur-A excavations and vary from a few cm thick and several m in lateral extent, to ~0.5 m thick and several tens of metres in extent. They seem to occur at any level within the unit.

UNIT 7

Structureless, pale yellow-brown, loose, medium sands, 1-4 m thick, with sparse coarse grains.

This unit sharply overlies the compact, hard surface of the previous unit. It is the modern cover, consisting of loose, running, pale yellow-brown (2.5Y 7/4), aeolian sand and was deposited as sandsheets and dunes. Over large areas it is ~1 m thick, but thickens up to ~4 m where stabilised dunes are present. Plant roots and shells of the extant terrestrial snail *Trigonephrus* are the main "potential fossil" constituents.

11.3 SECTION 16

Section 16, at 26.1 m asl., is approximately centrally situated in the T2/T3 exposures, ~50 m south of Section 15 (Fig. 11.1). Its vertical sequence of facies (Fig. 11.7) is very similar to that of Section 15, but a thick bed of inclined. parallel-laminated sand, equivalent to Unit 4 at Section 15 (Fig. 11.2), is not present. The exposure examined is orientated east-west (north-facing), approximately perpendicular to the coast, revealing additional aspects of facies architecture.

UNIT 1

Basal large pebbles and small cobbles overlain gradationally by very coarse sand to small pebble gravel, in a normally-graded bed 0.6-0.8 m thick, with large, symmetrical, ripple form sets preserved at the top of the bed.

Rounded pebbles and small cobbles, with scattered small to medium boulders, overlie bedrock. These larger clasts dwindle upwards so that the upper portion consists mainly of the matrix material of coarse sand to granules, with scattered small pebbles and interstitial fine sand. The basal gravel at this section therefore differs from that of Section 15 in being more uniformly normally graded. Dark-brown phosphorite and bone pebbles are present, as well as a medium-sized boulder of silcrete and some rounded pebbles (lithoclasts) of marine sandstone. Notably, abraded coatings of *in situ* phosphorite adhere to the bedrock. Included in the phosphorite coatings are coarse sand and small pebbles and moulds of shell fragments.

On the approximately shore-normal (E-W) faces of the sampling trench, the surface of the unit is revealed to have been formed into rounded, near-symmetrical bedforms, with wavelengths of 2,2-2,4 m and amplitudes of 15-20 cm (Plate 11.11). This confirms the presence of straight-crested (2-dimensional), coarse-grained ripples, as inferred at Section 15. Similarly, the landward flanks of the ripples are "feathered" into the abutting, southwest-dipping lamination of the overlying sands.

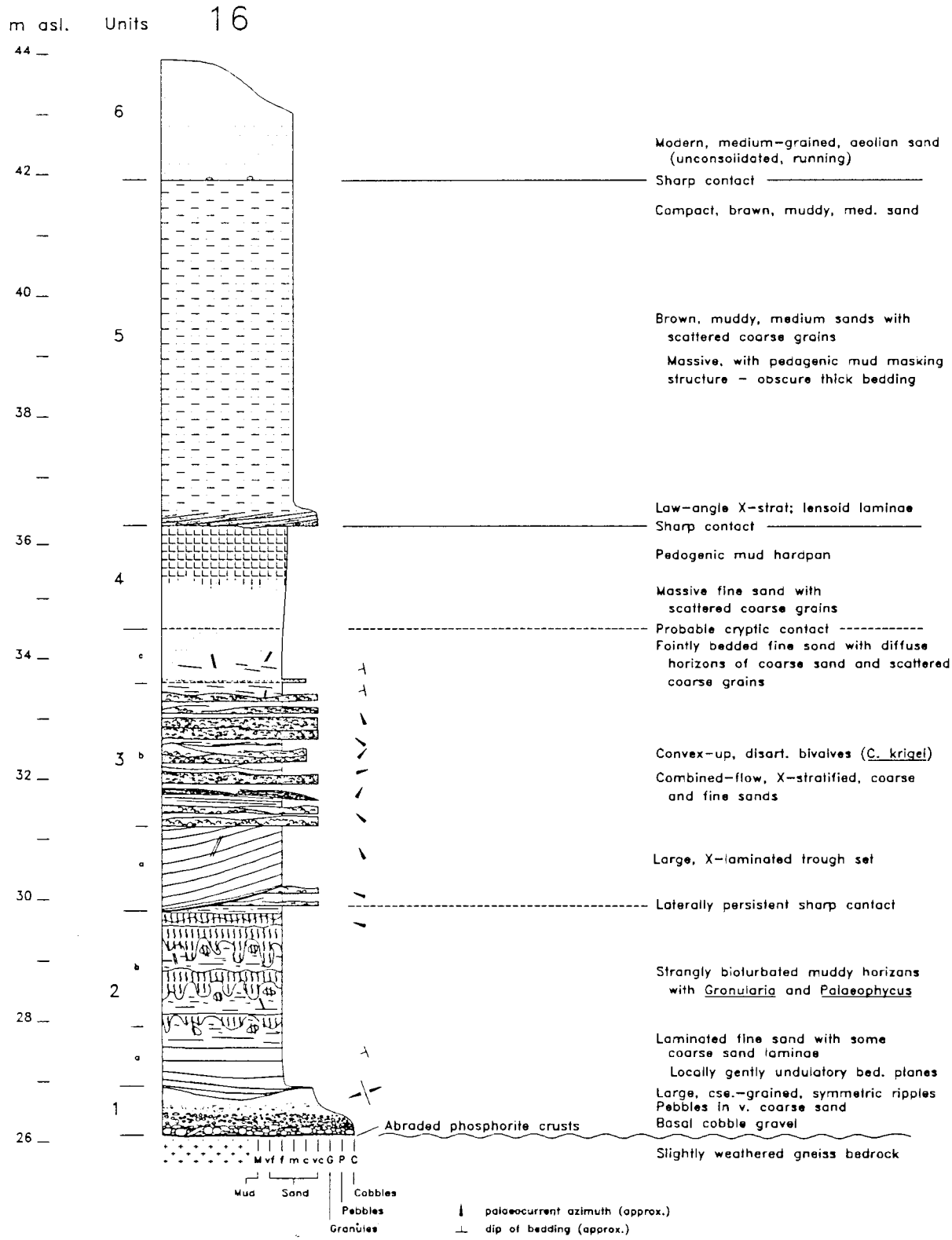

Figure 11.7 Section 16 graphic log.

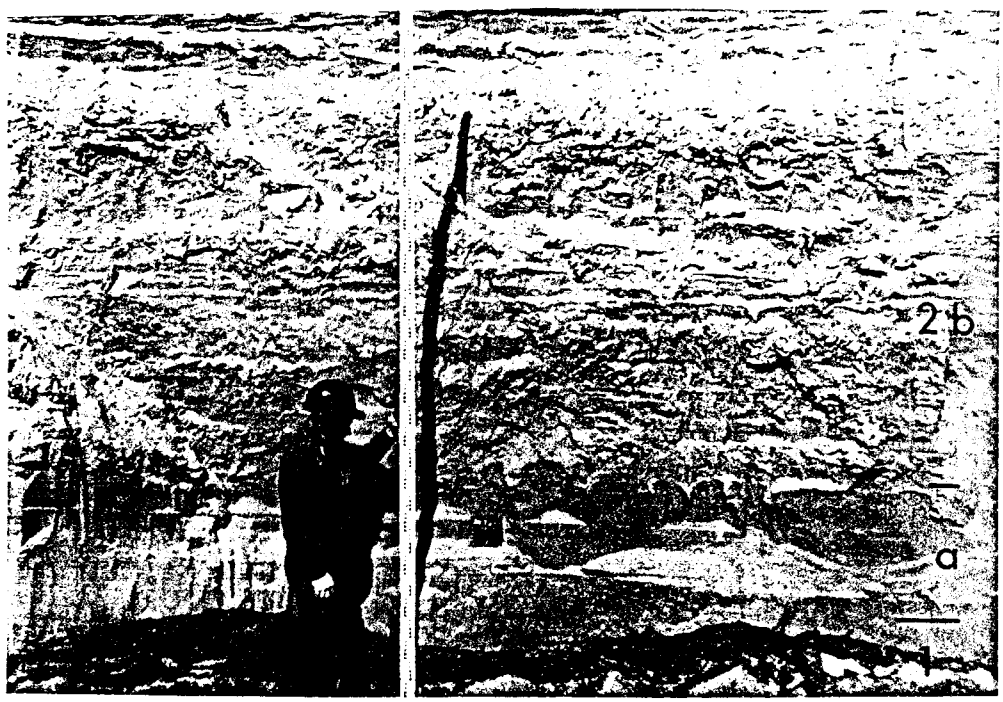

Plate 11.11 Section 16. Large, symmetrical, very coarse-grained ripples capping Unit 1. Note gently undulatory bedding in laminated sands (sub-unit 2a) and upward increase in bioturbation (sub-unit 2b). East is left. Survey staff for scale.

The internal structure of the ripples is obscure, but both landward and seaward-dipping cross-stratification can be discerned in places. The short, N-S oriented face in the eastern end of the trench showed a north-dipping bed surface extending from a ripple crest in the SE corner. The lamination in the overlying sands abuts the "feathered out" coarse sand, indicating the landward flank of the ripple. The approximate strike of the coarse-grained ripple crests is therefore about 330 to 340° (NNE-SSW).

UNIT 2

Mainly laminated, pale yellow (5Y 7/4) fine sand (fL), ~3 m thick, with laminae of coarse sand in the lower metre and a rapid upward increase in bioturbation associated with slightly muddy, thin beds (Plate 11.11).

Unit 2 is divisible into two sub-units as an equivalent of sub-unit 2b at Section 15 (massive, burrowed sand dominated by *Planolites montanus*) is not developed.

Sub-unit 2a: — ~1.0 m thick. The lower contact is gradational as the southwestward-younging lamination in fine sand, with coarse sand laminae, laps onto the "feathered-out" landward flanks of the underlying, coarse-grained ripples. Laminae are 1-5 mm thick and medium bedding, defined by coarse laminae and local low-angle truncations, is on the scale of 10-20 cm in thickness. As at

Section 15, gently undulatory bedding planes are present (Plate 11.11) and apparent bedding planes tend to obscurity laterally, where lamination across the bedding plane becomes parallel.

Sub-unit 2b: — ~2.0 m thick. The unit rapidly becomes strongly bioturbated, the primary structure being disrupted by churned, slightly muddy, *Granularia-Palaeophycus* burrow clumps formed along general horizons, as at Section 15. In contrast to Section 15, this upper, bioturbated part occupies a greater portion of the unit and primary structure has been preserved between the churned volumes to a greater extent. This is disrupted lamination to thin bedding, including slightly muddy, greenish (5Y 7/2) thin beds. The ichnotaxa noted at Section 15, sub-unit 2c, are also present here. The extent of the bioturbated, churned zones and slightly muddy sediment increases upwards (Plate 11.11).

Near the section site, the articulated rib-cage of a small whale occupied a swale in the middle of sub-unit 2b. The ribs are vertical and bioturbation of the swale infill is markedly less than in the adjacent sediments. The swale was eroded to a depth of ~20 cm and the initial infill lapping around the bones consists of thinly laminated, slightly muddy, fine sand. This laminated infill is laterally contiguous with a highly bioturbated horizon, confirming that the latter were originally finely laminated. The more thickly-laminated fine sand filling the swale developed upwards into a hummock over the bones. This hummock was capped by a lens of shelly fine sand with coarse sand grains. Although the sedimentary structure around the bones resulted from their influence on local deposition, the "anomaly" suggests that erosion preceded deposition of the slightly muddy, bioturbated (finely - laminated) intervals. During deposition of the less-bioturbated, fine-sandy intervals, coarse sand and shells may have been by-passing the depositional area (being trapped only at the site of the whale bones). This might suggest relatively strong bottom currents and high turbidity (suspended fine sand) during deposition of the laminated fine sands.

UNIT 3

A unit, ~4.7 m thick, consisting mainly of cross-stratified, shelly, interbedded, coarse and fine sands, with low-angle, parallel-laminated, fine-sandy interbeds in places (sub-unit 3b). Locally, large-scale, cross-bedded troughs (10-15 m wide, up to ~1.4 m thick) occur in the lower part (sub-unit 3a). The uppermost metre (sub-unit 3c) is nearly structureless fine sand, with diffuse horizons of coarse sand

Sub-unit 3a: — The lower contact of Unit 3 is sharp on the bioturbated fine sand of Unit 2. A large-scale trough infill is present at the immediate section site (sub-unit 3a) (Plate 11.12). This single, isolated set is ~12 m wide and ~1,4 m thick at its centre. The trough was eroded after at least ~1.4 m of the intercalated coarse and fine sands typical of this facies had accumulated and the maximum erosion extended slightly into the underlying Unit 2, to the level of the uppermost churned, bioturbate horizon. This trough is symmetrically infilled by a subaqueous dune. The foreset lamination is 3-15 mm thick and inclined at ~20°, decreasing to ~8° near the trough base where the foresets become tangential. Migration direction, measured from a horizontal cut through foresets in the centre of the bed, is ~340°.

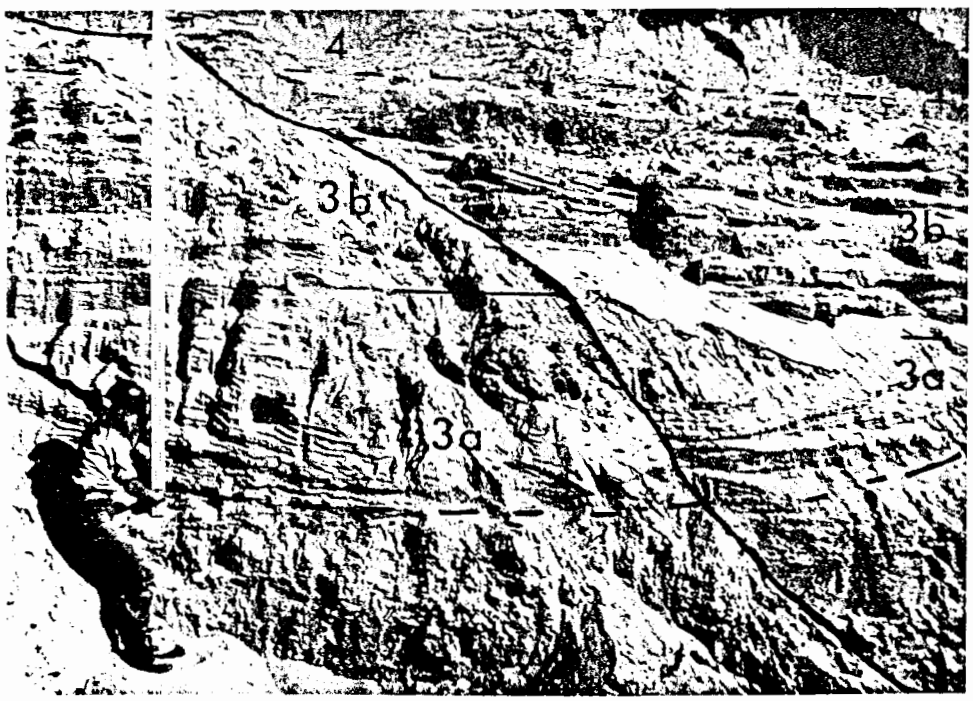

Plate 11.12 Section 16, Unit 3. Large trough (sub-unit 3a) overlain by shelly, cross-stratified, coarse and fine sand (sub-unit 3b). Note that exposure faces are staggered across an offset (outlined). East is left. Survey staff for scale.

The foreset laminae are mainly fine sand, but some foreset laminae are of medium sand with scattered coarse grains. Bioturbation is absent, with the exception of some large-scale burrows and mottles attributable to cross-cutting *Thalassinoides 'multiplex'*. The foreset toepoints and underlying, slightly muddy, bottomset laminae are enriched in finely comminuted shell. Muddy laminae in the bottom sets are undulatory and are drapes on small ripples (< 1.0 cm high, wavelengths of 3-4 cm) composed of comminuted shell and developed in the leeside trough.

Sub-unit 3b: — The upper foresets of sub-unit 3a are sharply truncated by a laterally persistent erosion surface, overlain by low-angle, cross-stratified, coarse sand (Plate 11.13). Similar, laterally persistent, flat to gently undulating erosion surfaces, overlain by coarse, shelly sands, typify the remainder of the unit (Plates 11.12, 11.13). The surfaces are 10-30 m in lateral extent and the local undulations represent deeper-scoured troughs. Cross-stratification in the coarse sands varies from very low angle (nearly flat), to low-angle, tangential foreset stratification. The coarse sands are typically shelly (Plate 11.13) and dominated by disarticulated, convex-up valves of the shallow-infaunal venerid *Chamelea krigei*. The coarse sediment and low-angle, cross-stratification indicate that these beds represent accumulation in the troughs of relatively large, migrating ripples (trough lags).

As described at Section 15, sub-unit 3b, the tops of the trough-lags are ubiquitously formed into rounded, convex ripple forms. Locally, the coarse-ripple forms interfinger with overlying fine sands

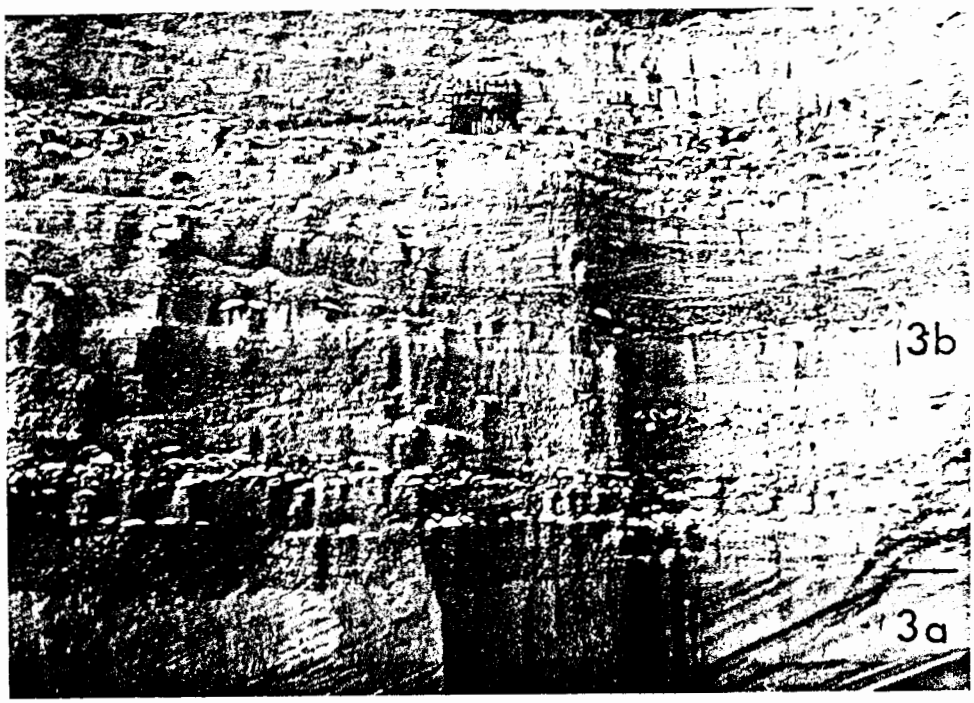

Plate 11.13 Section 16. Truncated top of sub-unit 3a, overlain by shelly, coarse-sandy, trough-lags and interbedded fine sand beds. Note "interbraiding" of fine sand with trough-lag cross-stratification (centre right). North is left. Scale in cm.

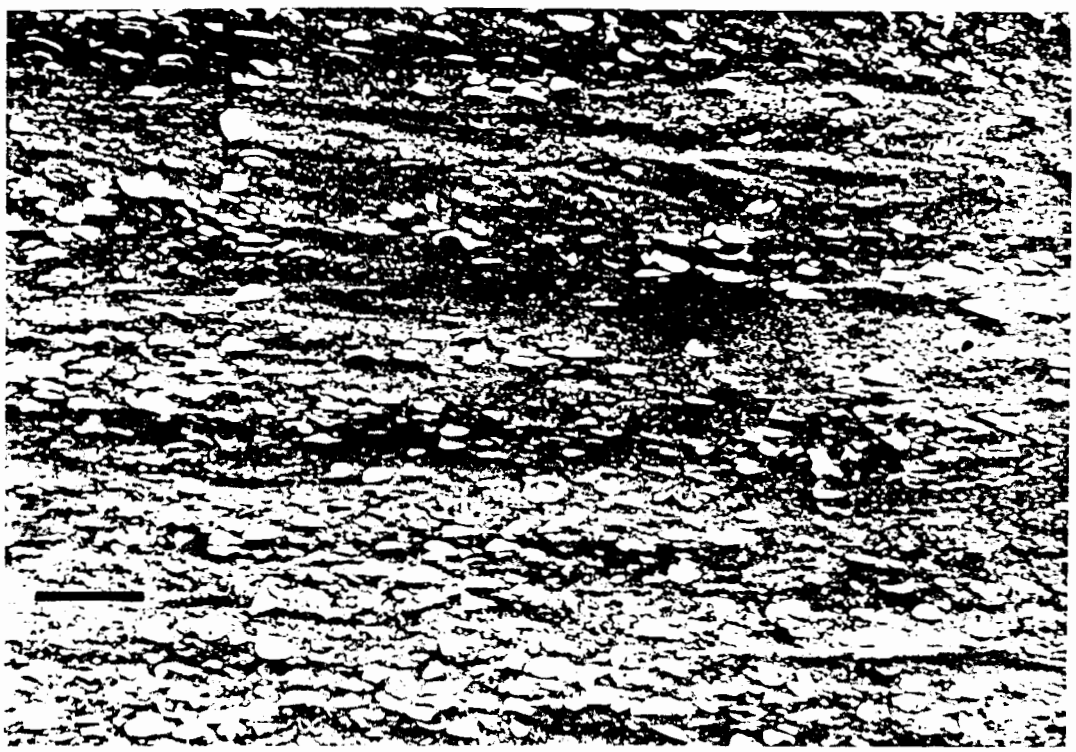

Plate 11.14 Section 16. Amalgamation of shelly trough-lags in Unit 3. East is left. Scale bar is 10 cm.

that are low-angle, cross-laminated or trough cross-laminated, resulting in coarse-fine couplet beds (e.g. Plate 11.13, centre right). Coarse laminae are often interbedded in the fine-sandy part of couplet beds. Laterally, the coarse trough-lag part of a couplet bed may become increasingly discontinuous and lensoid, the bed then being dominated by fine sand. Similarly, the fine-sandy portion may thin to disappearance. The coarse trough-lags are also amalgamated into thick, coarse, shelly beds, often with thin, interbedded "stringers" of fine sand. Such amalgamation of trough-lags may dominate considerable thicknesses in the unit (Plate 11.14). All permutations between well-defined coarse-fine couplets and amalgamation of coarse trough-lags seem to occur. Palaeocurrent azimuths in fine-sandy beds are predominantly westwards (offshore). Both onshore and offshore transport directions (W-wards and NE-wards) are indicated in the coarse-sandy cross-stratification.

As at Section 15, bioturbation in sub-unit 3b is sporadic, with cross-cutting *Thalassinoides 'multiplex'* and patches of *Planolites montanus* in fine-sandy intervals. Similarly, the shell assemblage is comparable in faunal composition and taphonomic state, occurring as worn shells in trough lags and being dominated by *Chamelea krigei*, with oyster valves, patellids, fissurellids and the herbivorous snails *Oxystele sinensis* and *Turbo cidaris*.

Sub-unit 3c: — The top of sub-unit 3b is gradational and sub-unit 3c is distinguished from the underlying deposits by a marked decrease in primary structure and preserved shell. The lower contact is positioned along the base of a diffuse, coarse-sandy horizon underlying the near-structureless, fine-sandy interval. Its main feature is the development of a clotted texture on wind-etched portions of the face. This texture probably reflects the scale of bioturbatory sediment disturbance responsible for the loss of structure. Thin, diffuse, coarse-sandy horizons occur ~0.8 m above the lowermost example. Some low-angle (~2°) vestigial lamination dipping to the west is present on the wind-etched surfaces. Thalassinoidean burrows occur sporadically

UNIT 4

A unit, ~1.7 m thick, of mainly structureless, fine sand, with scattered coarse grains. The unit is capped by a hardpan consisting of pinkish-white, slightly calcareous, mud.

Unit 4 is very similar to Unit 5 at Section 15. The material overlying the uppermost, diffuse, coarse-sandy horizons of sub-unit 3c is massive fine sand, with scattered coarse grains, and unequivocal marine trace fossils are absent. Similarly, a pale, pedogenic mud hardpan is developed in the top of the unit.

UNIT 5

A unit, 5-6 m thick, of muddy, brown, thickly-bedded, medium-grained, massive sands. The colour is due to the mud content that occurs as grain coatings and interstitial mud.

Overlying the sharp contact developed on the "hardpan" capping Unit 4 is a thick unit identical to Unit 6 of Section 15.

UNIT 6

Structureless, pale yellow-brown, loose, medium sands, 1-4 m thick, with sparse coarse grains.

The loose, modern sand cover overlying the sharp contact developed on the compact, muddy sands of Unit 5.

11.4 BLOCK SECTION

The T2/T3 Block Section, at 25.4 m asl., is situated in the southern part of the T2/T3 excavation, adjacent to the ridge separating the subsidiary basin in the southwestern corner (Fig. 11.1). It is a land-facing exposure oriented at 30°E of N. The vertical sequence is basically similar to the previous sections in facies development, but includes an additional facies not encountered elsewhere in the T2/T3 exposures, as well as other notable variations in the lower, mainly fine-sandy half of the section (Fig. 11.8). The lower portion (~4 m) of the section was described from the central part of the exposure and the upper portion from the bench just farther south (Fig. 11.1). The section graphic log (Fig. 11.8) is not drawn staggered because lateral variation across the "step" is not marked. Note that the lowermost portion of the section is situated along a wide, shallow channel in the bedrock, between a small, low reef to the east (~1 m high) and the flank of the wider ridge in the west (Fig. 11.1).

UNIT 1

A very thin (~0.2 m thick), pebble to small cobble, basal gravel with coarse sand is present at the section site. Nearby, rounded, cobble to small boulder, basal gravel was 0.3-0.4 m thick and had a winnowed aspect, with flat-lying, tabular clasts armouring its surface.

At the section site, the basal gravel is a poorly-exposed, thin (~0.2 m), pebbly unit with scattered cobbles. To the east of the section site, quartzose gneiss bedrock, swept of its diamondiferous gravel, is abundantly encrusted with abraded crusts of dark-brown phosphorite (Plate 11.15). The crusts are 1-3 cm thick and, as at Section 16, contain rounded quartz grains and moulds of shell fragments. To the south of the section site, basal gravel stripped of its "overburden," with the remaining sand removed by deflation, consists mainly of rounded, large pebbles to small boulders. Discoidal and tabular clasts are predominantly sub-horizontal and the unit has a coarsening-up aspect imparted by larger clasts that armour the top of the unit (Plate 11.16). This suggests that the basal gravel was subjected to very high-energy depositional or winnowing conditions.

UNIT 2

Unit 2 consists mainly of medium beds of pale green (~5Y 7/1), fine sand that are parallel-laminated or small-scale, ripple, trough cross-laminated. Mud drapes occur locally on rounded, slightly asymmetric to symmetric, ripple form-set crests. The tops of beds are bioturbated. The unit is up to ~1.2 m thick, but is of limited lateral extent due to strong erosion.

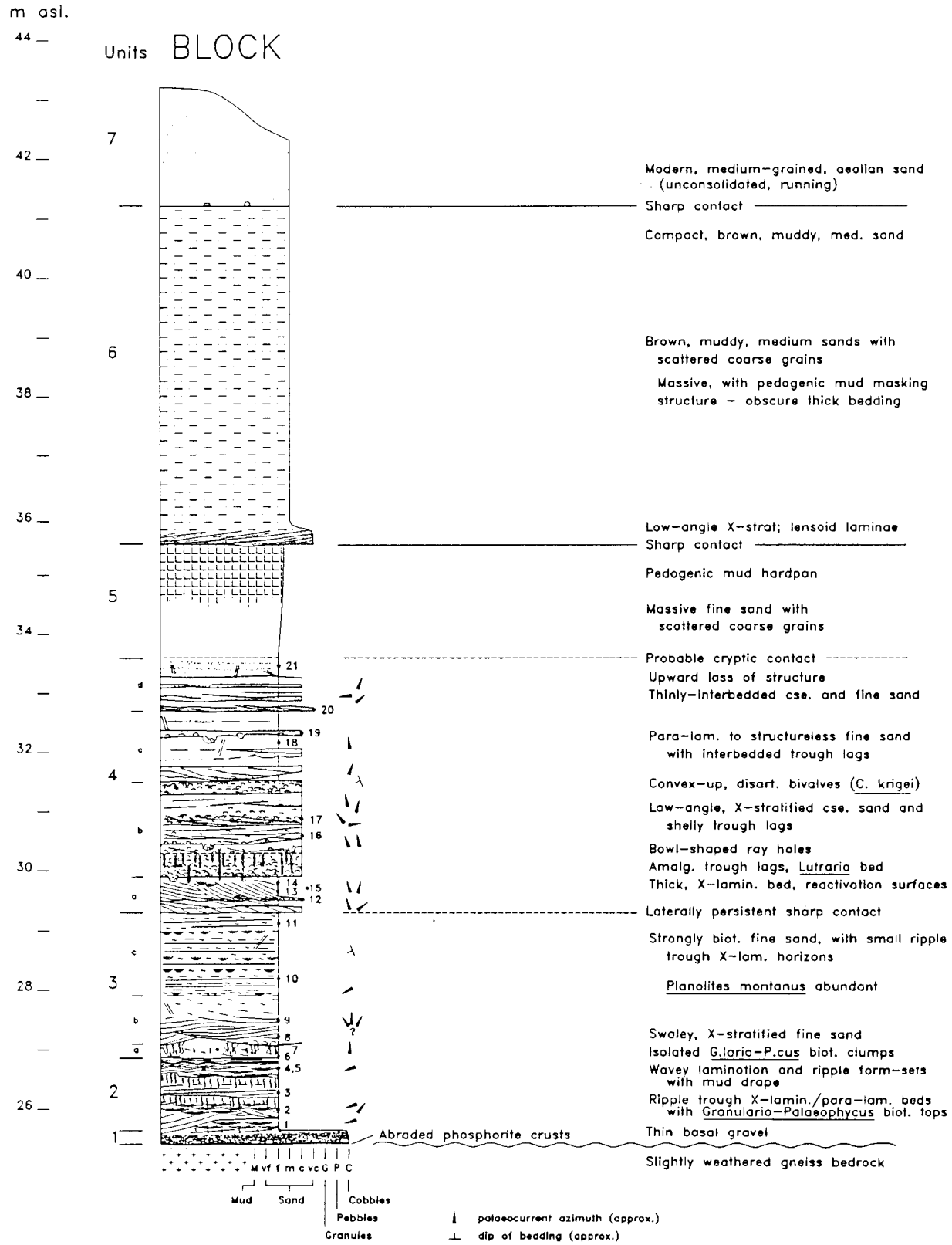

Figure 11.8 Block Section graphic log.

Plate 11.15 Abraded crusts of phosphorite (dark) adhering to quartzose gneiss (pale). Location is east of Block Section. Tool is 42 cm long.

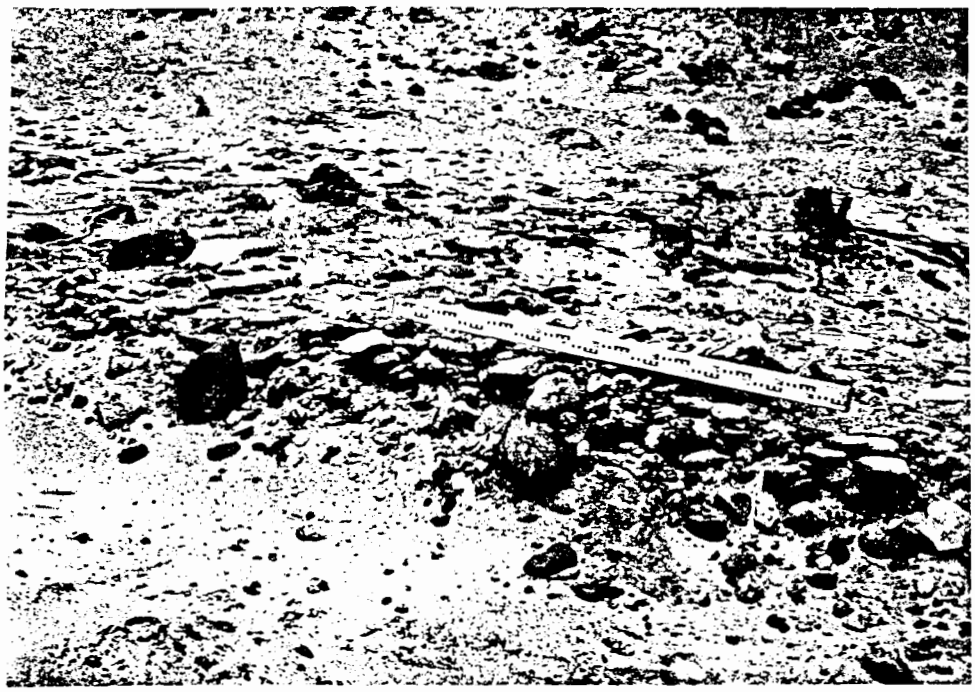

Plate 11.16 Basal gravel with large, flat-lying clasts armouring top. Thalassinoidean burrow system ramifies over top of the unit. Location is south of Block Section. Survey staff for scale.

Small-scale, trough cross-lamination in fine sand (fL, Fig. 11.9: 2,4,5), representing ripple migration, is the main primary feature of Unit 2. The cross-laminated trough-sets are 2-6 cm thick and 10-30 cm in length, with tangential-based laminae 2-3 mm thick. Perpendicular cuts into the face show similar-scale troughs, rather than more elongate sets, indicating that the ripples are 3-dimensional. The predominant palaeocurrent direction, defined by the steepest laminae, is into the southwestern quadrant. This offshore transport direction is applicable to the entire Unit 2. The ripple cross-lamination is noticeably more calcareous and resistant than the softer, interbedded, parallel-laminated, fine sands that are recessed in the exposure (Plate 11.17)

The vertical sequence of Unit 2 commences with low-angle, cross-laminated, fine sand immediately overlying the basal gravel. This passes upward into small-scale, trough cross-lamination (Fig. 11.10: bed 1). Bed 1 was deeply eroded and overlain by cross-laminated, fine sand infilling scours and swaley cross-laminated sets (bed 2) that pass upward into trough cross-lamination (bed 3). An interbedded swale in bed 3 shows that the deposition of the rippled interval was interrupted (Fig. 11.10, right). The top of bed 3 is very strongly bioturbated, with a pelletised *Granularia-Palaeophycus* ichnofacies similar to that developed in the upper part of units 2 at sections 15 and 16 (Plate 11.17). The bioturbated horizon is succeeded by a fine-sandy interval with poorly-defined, sub-horizontal lamination, that passes upwards into a similar, but completely bioturbated top (bed 4). Some *Palaeophycus* burrows connect the two bioturbated horizons. With some erosion, producing relief around the slightly muddy, calcareous, burrow clumps, bed 4 is overlain by a rippled interval (bed 5). Notably, trough cross-lamination in bed 5 passes laterally southwards in gently undulating (wavey) lamination (Plate 11.17). The wavey lamination is capped by rounded, ripple form-sets, on which was deposited an undulating, muddy drape 1-3 cm thick. The ripple form-sets are slightly asymmetric, with steeper lee-sides on their southern limbs. The mud drape is overlain by more wavey lamination, locally with interbedded ripple troughs. The top of the unit is eroded and overlain by nearly structureless, fine sand comprising Unit 3.

The grain-size distributions of samples of ripple cross-laminated sands (Fig. 11.9: 2,4,5) and low-angle, parallel-laminated sands (Fig. 11.9: 1,3) are essentially similar, but the former may have a larger proportion of the vfU fraction. Interestingly, the sample of wavey-laminated sand had the highest mud content (~10%) and was relatively rich in finely comminuted shell.

Lateral exposures confirm that medium beds of ripple-trough cross-lamination, with offshore (SW) palaeocurrent azimuths and bioturbated tops, are characteristic of Unit 2. Lateral transitions to wavey lamination and mud drapes capping ripple form-sets are common (Plate 11.18). Notably, rounded, symmetric, ripple form-sets also occur (Plate 11.18). Excavation into the exposure, to reveal the palaeosurface of the drapes, showed that the underlying form-sets are straight-crested ripples, with crestal strikes of ~330°. This contrasts with the inferred 3-dimensional bedform nature of most ripple cross-lamination. Some grooves in a drape surface are 10-20 cm in length, with v-shaped cross-sections and pointed ends. The orientation of these probable tool marks is ~230°. Some sinuous grooves may represent fish trails.

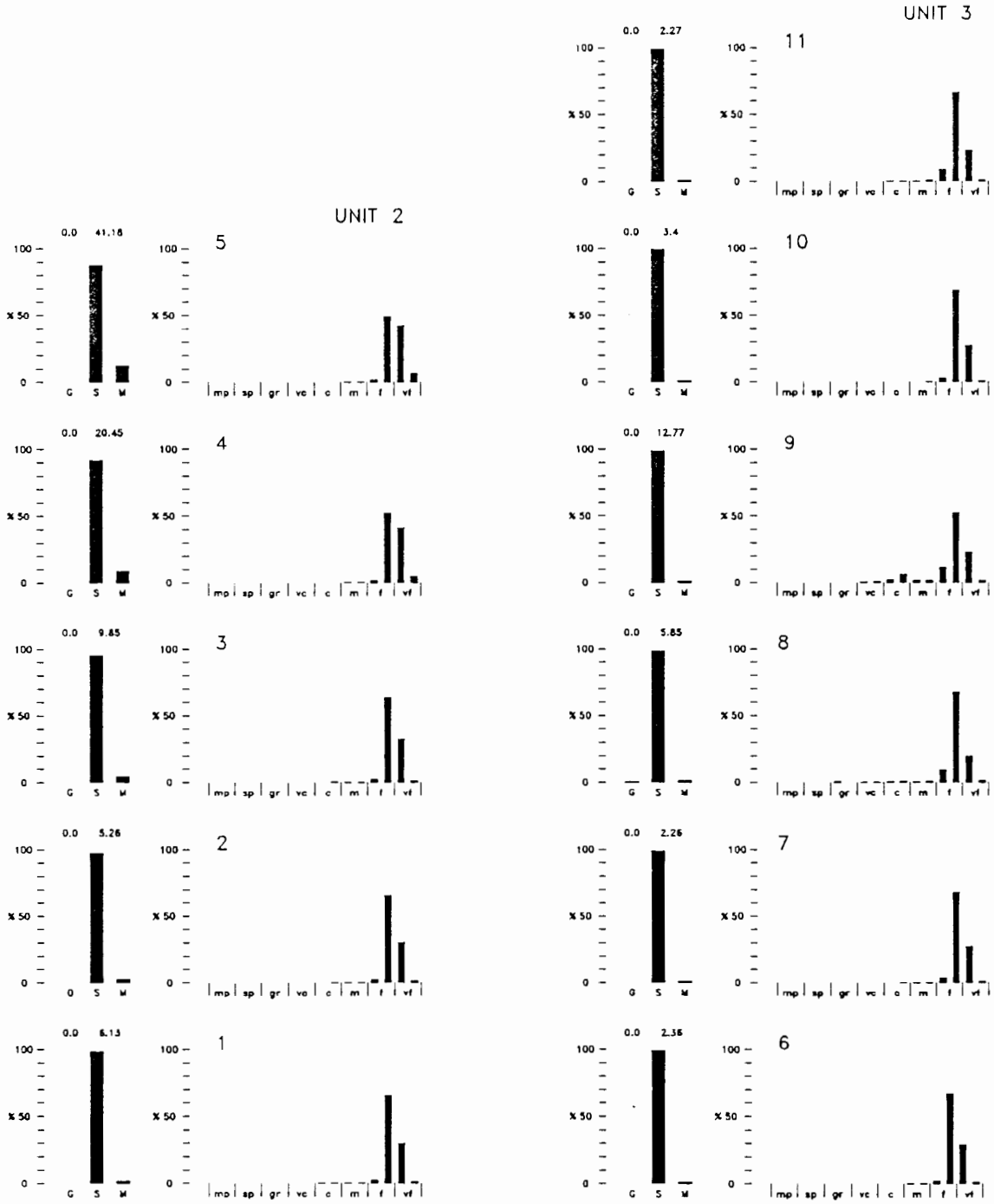

Figure 11.9 Block Section, units 2 and 3. Grain size analyses ($CaCO_3$ free). Sample positions in Fig. 11.8.

Plate 11.17 Block Section, Unit 2, Ripple trough cross-laminated and parallel-laminated beds with bioturbated tops. Note wavey lamination, overlying form-sets and mud drape in sub-unit 5. North is right. Scale in cm.

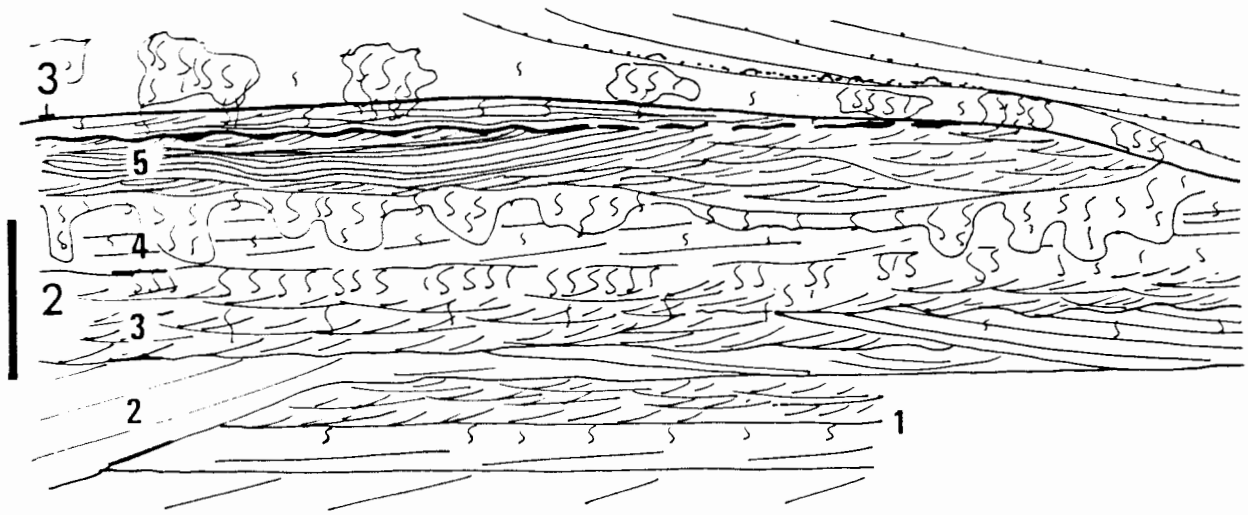

Figure 11.10 Block Section. Sketch of Unit 2. Left part of sketch detailed in Plate 11.17. North is right. Scale bar is ~0.5 m.

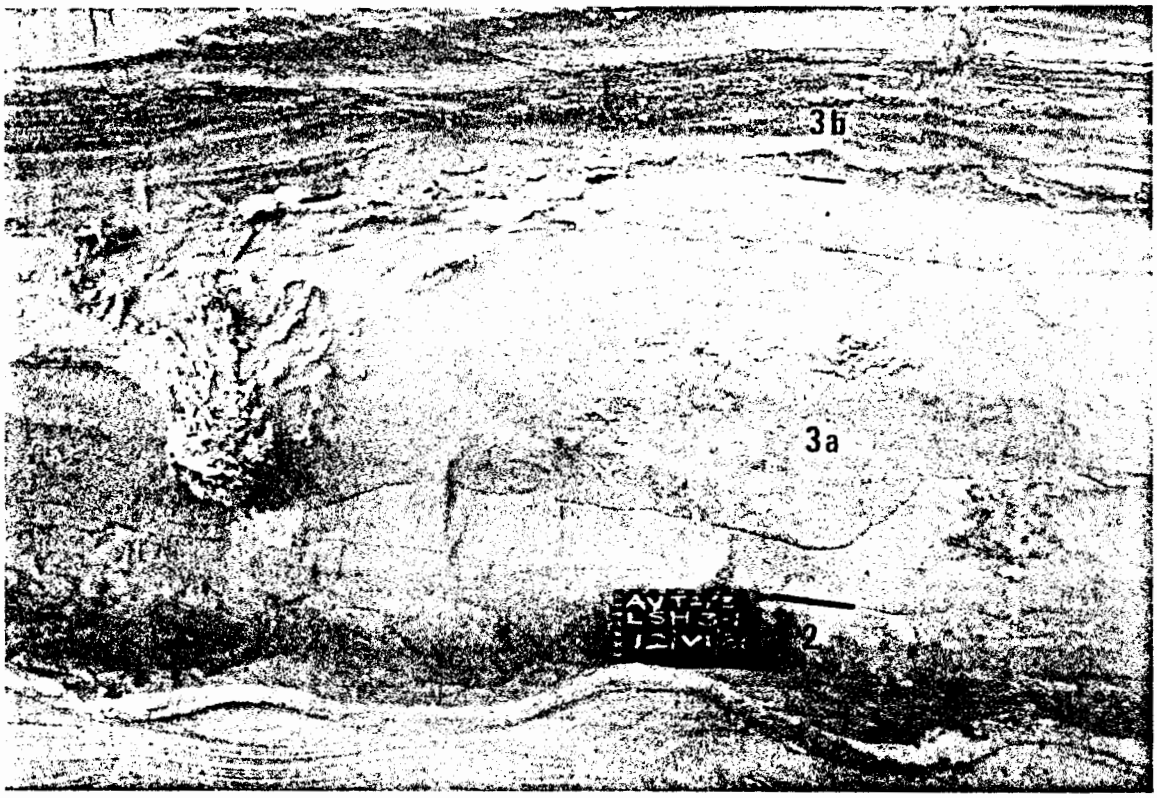

Plate 11.18 Block Section. Mud drape on straight-crested, symmetric, ripple form-sets overlying wavey lamination (Unit 2). Sub-unit 3a is bioturbated and nearly structureless, with isolated *Granularia-Palaeophycus* burrow clumps. It is sharply eroded and overlain by swaley cross-lamination (3b). North is right. Scale in cm.

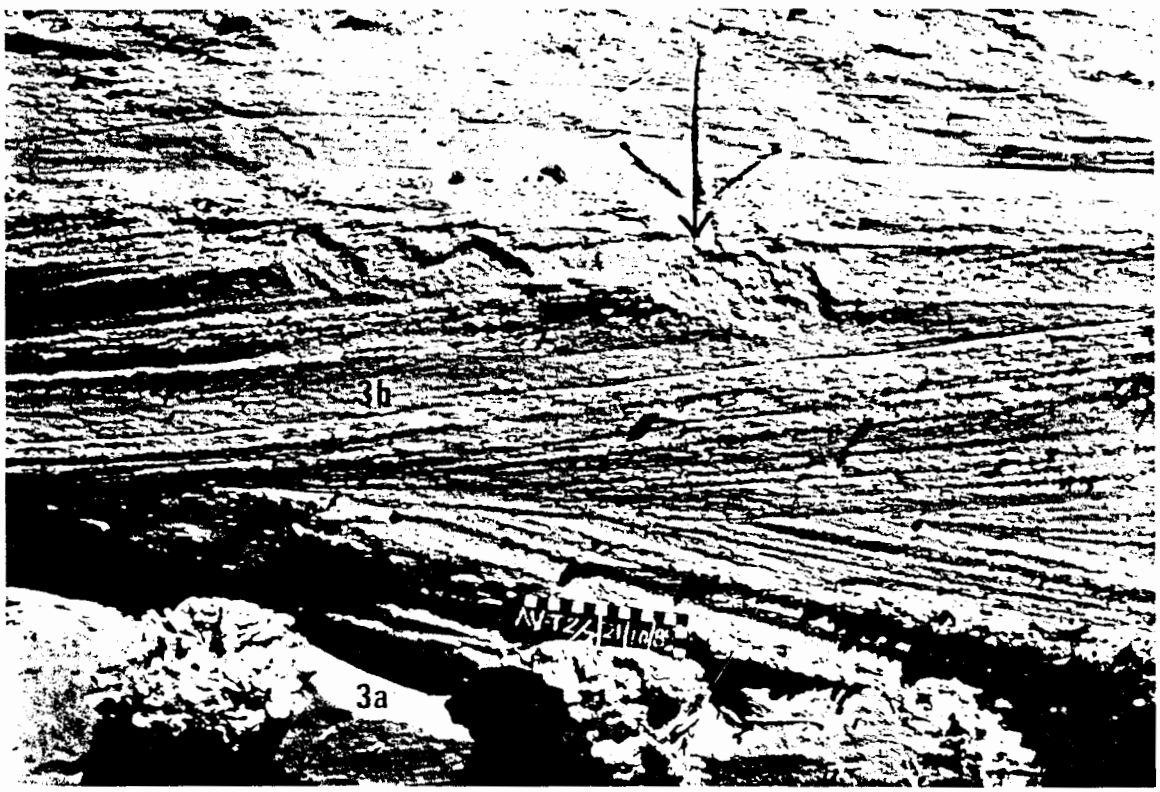

Plate 11.19 Block Section. Swaley cross-stratification (sub-unit 3b) sharply overlying sub-unit 3a. Note false bedding trace (arrowed), with cross-cutting lamination to left of arrow. North is right. Scale in cm.

Although the *Granularia-Palaeophycus* bioturbation in Unit 2 is very similar to that at sections 15 and 16, some notable differences are that well-defined *Granularia* burrows are more abundant and burrows attributable to *Palaeophycus* '*annulatus*' are common (in addition to *P. tubularis* burrows). *Planolites montanus* occurs in small volumes in the weakly bioturbated intervals of ripple cross-laminated sand. Chevron structures (downbent lamination) are common. *Skolithos* '*mini*' occurs in intervals with poorly-defined parallel lamination (e.g. bed 4). Sub-vertical, reddened, *Thalassinoides* '*multiplex*' burrows sporadically cross-cut the unit.

Unit 2 was strongly eroded, producing a sharp contact with local, irregularly undulating relief of up to ~30 cm. To the north of the section site, the unit thins beneath a north-dipping erosion surface. The unit is clearly only locally preserved, as similar ripple-trough, cross-laminated sediments occurred at no other site in the T2/T3 excavation.

UNIT 3

Unit 3 is ~2.5 m thick and mainly fine-sandy. It is divided into three sub-units Sub-unit 3a is an irregular bed of nearly structureless, bioturbated fine sand, with sharply-defined, isolated clumps of intense Granularia-Palaeophycus bioturbation in muddy, calcareous sediment. Sub-unit 3b consists of trough cross-stratified to swaley cross-stratified, laminated fine sand, in sets 1-2 m wide. Coarse sand laminae and shelly lags in troughs are present. Locally, lamination is built up into low hummocky forms. Sub-unit 3c consists mainly of near-structureless, parallel-laminated and locally ripple cross-laminated, fine sand, with bioturbation dominated by Planolites montanus burrows.

Sub-unit 3a: — This sub-unit is of irregular thickness due to the relief of its underlying erosive contact and the relatively large (1-2 m wide) erosive troughs, basal to sub-unit 3b, that "scallop" its surface. It is thickest where the top of Unit 2 is deeply eroded (e.g. ~0.5 m thick, Plate 11.18). It pinches out northwards along the exposure where erosion preceding sub-unit 3b extends deeply into Unit 2. In the fine sand (Fig. 11.9: 6,7), vestigial, low-angle, north-dipping lamination is faintly visible, mainly in the lower portion. In places there are hints of internal erosion surfaces of moderate relief, partly indicated by the truncated tops of *Granularia-Palaeophycus* burrow clumps (Plate 11.18).

A striking feature of the sub-unit is that large *Granularia-Palaeophycus* burrow clumps occur as isolated "islands", rather than as burrowed horizons (Plates 11.18, 11.19). The dominant *Palaeophycus* ichnospecies is *P. tubularis* (smooth-walled), with relatively few *P* '*annulatus*' burrows present (in contrast to Unit 2). *Palaeophycus* burrows are also scattered within the sub-unit and *Planolites montanus* and *Planolites* '*spaghetti*' burrows occur in places.

Sub-unit 3b: — Shallow, wide troughs eroded into Sub-unit 3a (1-2 m wide, ~20-30 cm thick) are infilled by pale yellow (~5Y 7/4) laminated fine sand, with some coarse sand laminae (Fig. 11.9: 8,9). The laminae are up to ~1 cm thick and are rich in relatively coarse-grained, comminuted shell consisting mainly of barnacle fragments. The laminations are nearly concordant with the trough bases in some examples (swaley lamination), but generally lap onto one trough limb at a very low angle

(Plates 11.18, 11.19). The toesets of laminae are often shell rich, resulting in bedded lenses of shell in the troughs.

Sub-unit 3b exhibits marked lateral variation northwards along the exposure, from the position where erosion has removed sub-unit 3a and cuts deeply into Unit 2 (Fig 11.11). A large set overlying the sigmoidal-shaped basal contact exhibits upbuilding, with some low-angle discordancies, into a low hummock form (Fig. 11.11, upper panel, centre) (Plate 11.20). The lamination in overlying, offset, swales sweeps over this hummock. Subsequently, accumulation of sub--unit 3b took place by lateral accretion resembling the intermittent migration of a large, subaqueous dune (Fig. 11.11, lower panel) (Plate 11.20). North-dipping erosion surfaces, marked by truncation of laminae, cross-cut the entire sub-unit. The lamination within the accretion increments is at a lower angle than the "reactivation surfaces" and very low-angle discordancies are present in places. Locally, the lamination is built up into low hummocks. At the northern end of the exposure, a markedly high-angle scour with an overhang was cut into the underlying bed (3a) (Fig. 11.11) (Plate 11.21, arrowed). Excavation into the face revealed that the upper edge of the scour was orientated at ~250° at that point.

Notably, a few pebbles occur amongst the concentrations of shell in the lower parts of troughs and in two examples, isolated cobbles are present. Isolated small cobbles and large oyster shells also occur on laminae in the "lateral accretion" sets in the northern part of the exposure. These indicate high-energy conditions during the accumulation of sub-unit 3b. Some laminae in the "lateral accretion" sets are rich in small-pebble-size mud clasts, suggesting possible contemporaneous erosion of nearby mud-containing facies such as Unit 2.

Bioturbation is practically absent in the trough infills and "lateral accretion" sets, except for very sporadic, superimposed *Thalassinoides* burrows. However, burrows with linings of coarse sand grains, here referred to *Palaeophycus heberti*, occur amongst the shells in the trough bases. In the uppermost ~20 cm of the sub-unit the primary structures become poorly-defined and the top of the sub-unit is marked by a distinct horizon of weak to strong bioturbation (Plate 11.20). This horizon is ~10 cm thick, is laterally extensive and dips gently southwards, so that sub-unit 3b thickens to the north (Fig. 11.11). For the most part, few burrows except for *Planolites montanus* are visible in the bioturbated horizon. However, at one spot, a patch of *Skolithos* '*bundles*' penetrates the top of 3b, in association with *Planolites* '*spaghetti*' and *Planolites* '*threads*'. In places in the bioturbated horizon, very-small-scale, ripple trough cross-lamination is visible, outlined by heavy mineral concentrations in the foreset laminae. The cross-laminated sets are less than 10 cm in length and usually do not exceed ~1 cm in thickness. They represent ripples that are markedly smaller than those characteristic of Unit 2. The dominant transport direction is southwestwards (offshore).

The shelly fauna deposited at the bases of foresets in the troughs is markedly different from the abraded, *Chamelea krigei*-dominated assemblage that occurs in the cross-stratified coarse sands higher in the vertical sequence. The assemblage is of high diversity and characterized by abundant, unabraded, well-preserved shells and a profusion of small, delicate species, particularly gastropods.

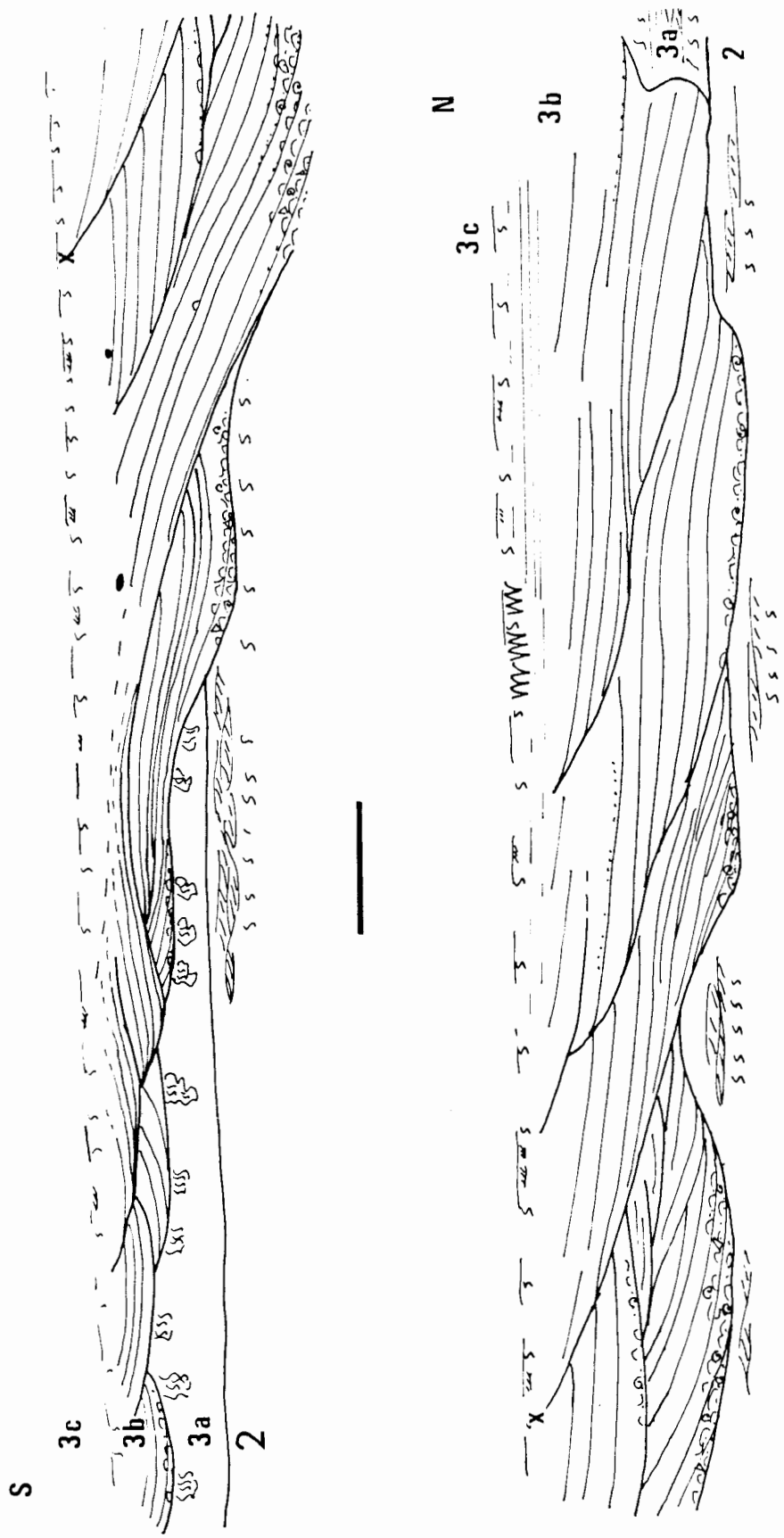

Figure 11.11 Block Section. Sketch of lateral variation in sub-unit 3b, showing thickening of the sub-unit northwards and the marked erosion surface on underlying beds. Note swaley to locally hummocky nature of lamination in the large-scale "lateral accretion" sets. Scale bar ~1 m.

Plate 11.20 Block Section. View of units 2 and 3, c.f. Fig. 11.11, upper panel centre. Bioturbated horizon separating sub-units 3b and 3c outlined. Although sub-unit 3c is clearly bedded, much internal lamination has been destroyed by fine-scale bioturbation. North is right. Scale in cm/dm.

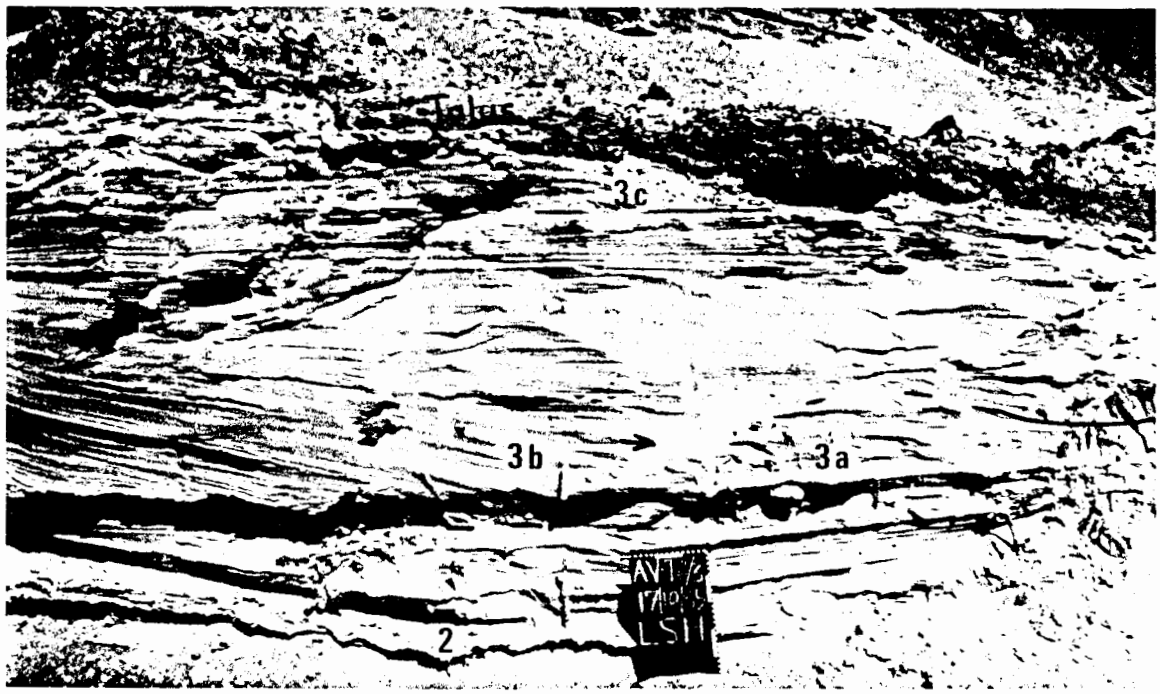

Plate 11.21 Block Section. High-angle scour with overhang cut into sub-unit 3a (immediate right of arrow). North is right. Scale in cm/dm.

Some articulated (but transported) bivalves are present and these are the thin-shelled razor clam *Phaxas decipiens* and small (juvenile) mytilids (*Aulacomya ater* and *Perna perna*). Notably, detached clusters of the small barnacle, *Notomegabalanus kensleyi*, occur. The dislodgement of the barnacles from their attachments indicates high-energy conditions, but the individual specimens forming the delicate clusters did not separate during transport, indicating short transport paths and rapid deposition. A notable inclusion in the assemblage in sub-unit 3b are intact valves of *Donax haughtoni*, a species of biostratigraphic importance (Carrington and Kensley, 1969)

An interesting feature seen in the T2/T3 excavation, as well as in other excavations in the study area, is a prominent lamination standing in slight relief (Plate 11.19, arrowed). It resembles a bedding plane, but closer inspection reveals that is actually cross-cut by primary laminae, demonstrating it to be a misleading feature. The "false bedding plane" is probably caused by very slight cementing of grains and is most likely a water-table phenomenon.

Sub-unit 3c: — Overlying the bioturbated horizon capping sub-unit 3b are strongly bioturbated, fine sands (Fig. 11.9: 10,11). *Planolites montanus* burrows are abundant and horizons of *Skolithos* '*mini* occur in places. As shown by lacquer peel, the full extent of activity by the producer of *Planolites montanus* is not recorded as visible burrows ('adelobioturbation'). Despite the strong bioturbation, thin to medium-scale bedding is indicated by wind-etching (Plate 11.20) and vestigial parallel lamination is present (also seen in lacquer peel). Laterally persistent horizons of very-small-scale, ripple trough cross-lamination are common. As in the bioturbated horizon capping the previous sub-unit, the very small, cross-laminated sets are 2-6 cm in length, generally less than ~1 cm thick, with foreset laminae outlined by heavy mineral grains. Southward directions of migration predominate, but oppositely-directed foreset laminae are common. Some cross-cutting thalassinoidean burrows are present, but most of the sporadically-distributed *Thalassinoides* burrows are relatively small-scale, local systems, possibly suggesting penecontemporaneity with the accumulation of the sub-unit. This sub-unit, at the top of Unit 3, is sharply erosively truncated.

UNIT 4

Unit 4 is ~4.0 m thick and is divided into 4 sub-units. Sub-unit 4a (~0.6 m thick) contains a cross-laminated, thick bed, with reactivation surfaces. Sub-unit 4b is low-angle, trough cross-stratified, shelly, coarse sand. with numerous, large bivalve traces in its lower portion. Sub-unit 4c is trough cross-stratified, shelly, coarse sand interbedded with lenses of low-angle parallel-laminated and structureless fine sand. Sub-unit 4d consists of thin to very thin and discontinuous beds of coarse sand interbedded with fine-sandy thin beds.

Sub-unit 4a: — The sharp lower contact is overlain by ~10 cm of cross-stratified, coarse sand. Closely overlying and forming the remainder of the sub-unit is a thick, cross-laminated bed (0.3-0.4 m thick) representing the northward migration of a small, subaqueous dune (Plates 11.22, 11.23). The bed is divided into a series of sets representing increments of migration separated by cross-cutting erosion surfaces (reactivation surfaces) (Figure 11.12, upper panel).

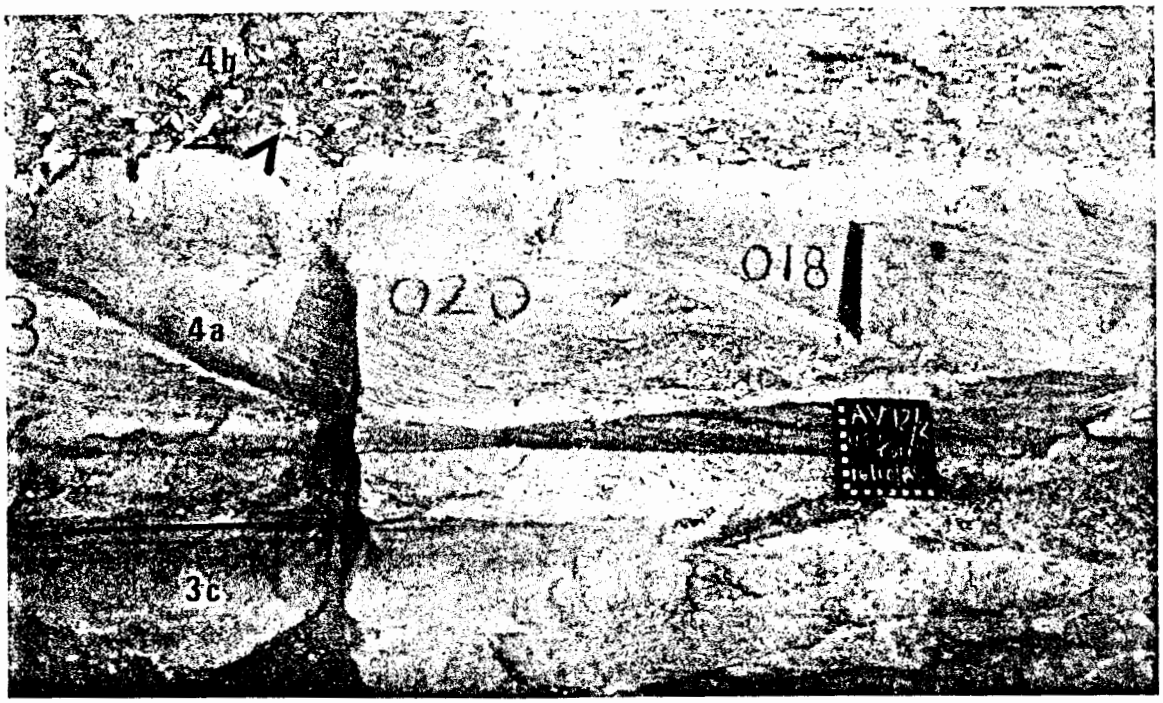

Plate 11.22 Block Section. Sharp contact on Unit 3 overlain by cross-stratified coarse sand and cross-laminated, thick bed with reactivation surfaces (sub-unit 4a). The latter was eroded and overlain by shelly, coarse-grained, amalgamated trough lags (sub-unit 4b). Note *Lutraria* bivalve in life position (arrowed) and *Lutraria* burrows that just penetrate 4a. North is right. Scale in cm.

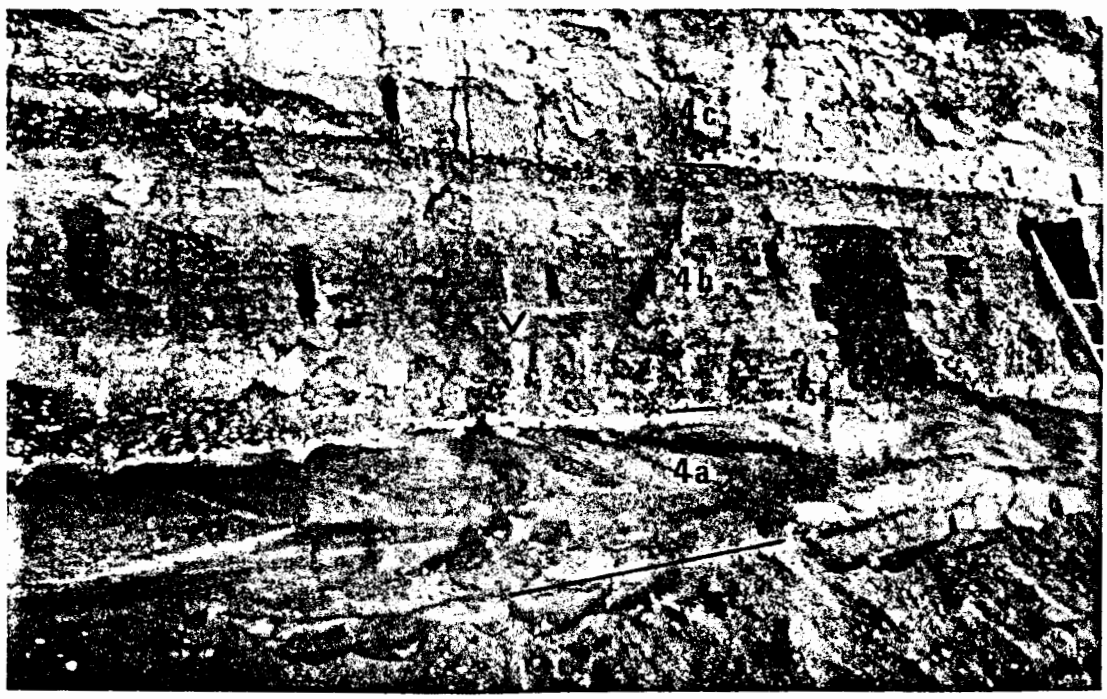

Plate 11.23 Block Section, Unit 4. Abundant *Lutraria* burrows in the lower part of sub-unit 4b (Lutraria bed), with *in situ* specimen arrowed. Sub-unit 4b consists mainly of shelly, coarse trough lags, whilst sub-unit 4c contains a relatively greater proportion of fine-sandy interbeds. Vertical slits in face are sites of palaeocurrent measurements, dark rectangle on right is lacquer peel in progress. North is right. Scale in dm .

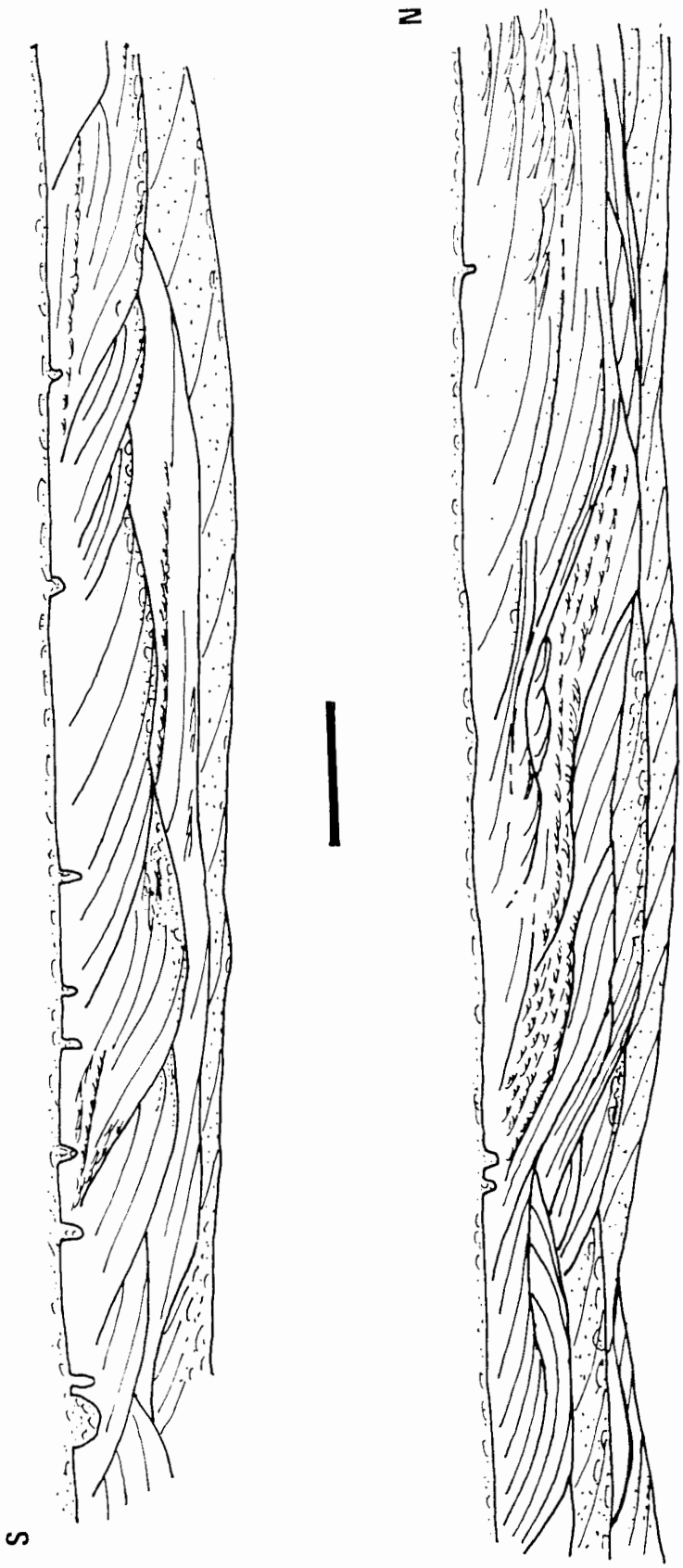

Figure 11.12 Block Section., Unit 4. Field sketch of sub-unit 4a. Scale bar is ~0.5 m.

The bases of the sets are shallowly trough-shaped, so that the underlying bed has a gently-scalloped upper contact. The cross-laminae are alternately rich and poor in finely-comminuted shell. The foresets are sigmoidal, indicating a bedform with a convex, rounded crest. The foresets flatten to tangential, near-concordancy with the trough bases and in some examples curve upwards in parallel with the "downstream" trough limb. Coarse sand and shell fragments are concentrated in the foreset toepoints and the trough, where oppositely-directed (back-flow) ripple cross-laminated sets are sometimes present. In some sets, very-small-scale ripple trough cross-lamination, outlined by heavy mineral grains, is present in the convex, upper foresets, where low-angle discordancies between laminae also occur. A horizontal cut into one example revealed small rib-and-furrow structures with a palaeocurrent azimuth of ~265°, approximately transverse to the main, north-migrating dune. Grain size analyses of samples from near the upper, middle and lower parts of a set illustrate the coarsening down the foresets (Fig. 11.13: 12,13,14). Bioturbation is sporadic, with some small, vertical chevron traces in the lamination and the occasional thalassinoidean burrow.

Laterally northwards the geometry of the bed becomes complex (Fig. 11.12, lower panel), with evidence that erosional episodes became more marked. For a period, accretion of the advancing dune was dominated by deposition in very-small-scale ripples. Subsequently, the cross-strata become increasingly lower angled and disappear laterally as ripple trough cross-lamination becomes dominant (Fig. 11.12, lower panel, right) and the grain-size increases to medium-grained sand (Figure 11.13: 15). The ripple troughs are 10-15 cm in length, 2-5 cm thick and palaeocurrent azimuths are to the north and northeast. The degree of bioturbation increases and some *Skolithos* '*bundles*' burrows extend across the thickness of the sub-unit and are truncated at its upper contact. Still farther north, the ripple trough cross-lamination dies out as shelly, coarse-sandy, low-angle cross-stratified trough-lags appear. Large (5-8 cm in diameter), vertical, unlined burrows, with chevron structure defined by the orientations of shell fragments, become abundant. The large mactrid bivalve, *Lutraria lutraria*, occurs in articulated, life position within some of these traces (Plates 11.22, 11.23, arrowed). Bowl-shaped depressions, interpreted as ray-holes, are common (cf. Plate 10.24).

Sub-unit 4b: — The top of the previous sub-unit is eroded and the erosion surface is laterally-persistent over the exposure (~40 m). It is overlain by shelly, coarse-sandy, low-angle cross-stratified to structureless, amalgamated, trough lags. The lower ~0.4 m of the sub-unit is strongly bioturbated, mainly by numerous, vertical *Lutraria* burrows, some of which just penetrate the top of the underlying sub-unit (Plates 11.22, 11.23). Ray holes are common. In the northern part of the exposure, where sub-unit 4a resembles the overlying 4b, some of the *Lutraria* burrows cross-cut the sharp 4a/4b contact. Within sub-unit 4b, many of the *Lutraria* burrows span the entire thickness of the lower, strongly-bioturbated 0.4 m portion and are truncated along its top. However, examples of *Lutraria* burrows that were truncated during the accumulation of the bioturbated lower portion are also present and some articulated, but horizontal *Lutraria* bivalves represent individuals washed out of their burrows. A few *Lutraria* burrows continue into the overlying, less bioturbated part of the sub-unit.

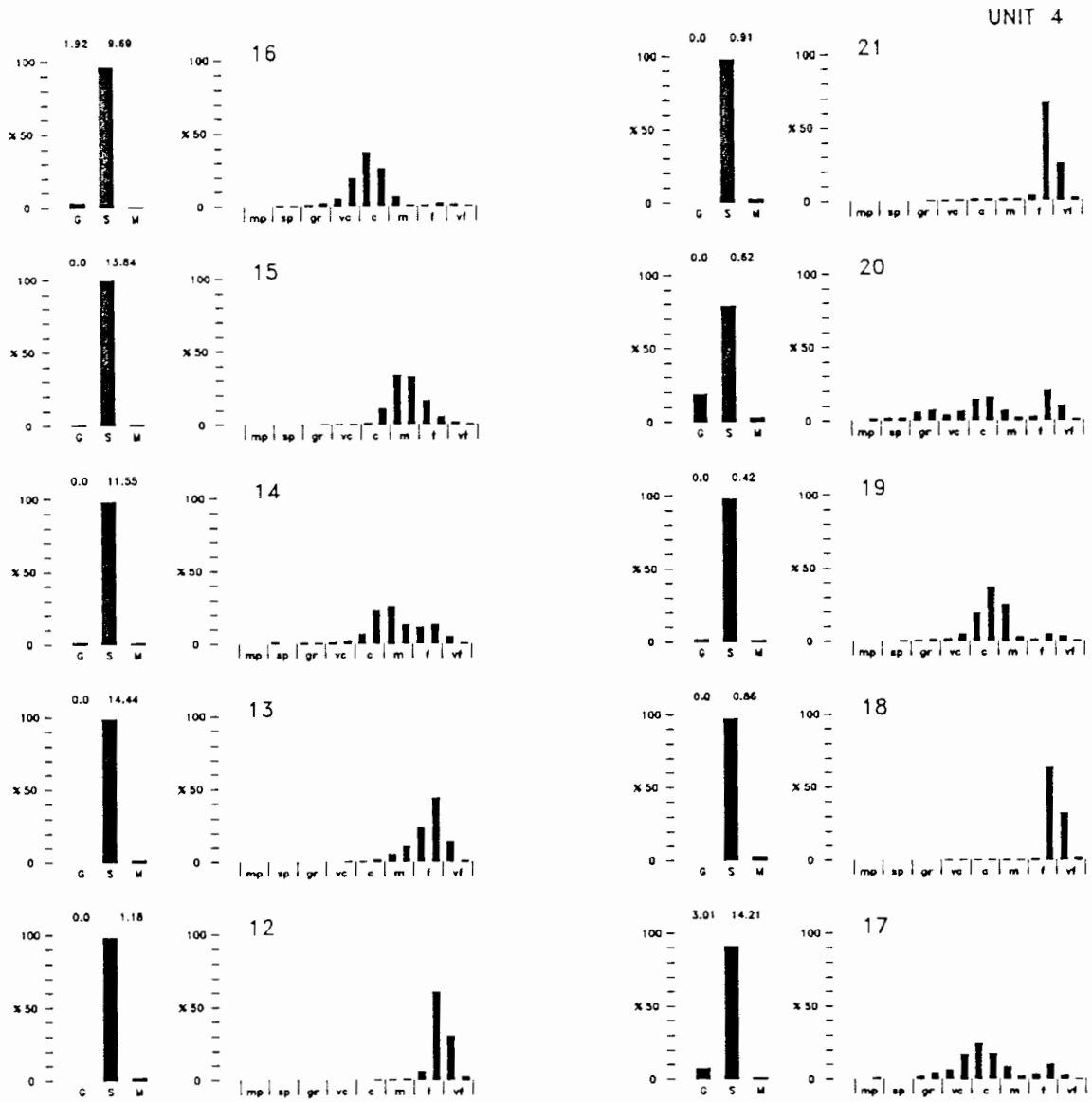

Figure 11.13 Block Section, Unit 4. Grain size analyses ($CaCO_3$ free). Sample positions in Fig. 11.8.

The remainder of sub-unit 4b consists mainly of low-angle, cross-stratified, coarse sand with varying shell content (Fig. 11.13: 16,17). Sets vary from a few cm thick and 1-2 m in length, with very low-angle to indeterminate stratification, to larger cross-stratified beds up to 20 cm thick and several metres in lateral extent. Some sets are noticeably more coarser-grained and shell-rich than others (e.g. Fig. 11.13: 17). Palaeocurrent azimuths are dominantly north and northwestwards, with very few southward azimuths. Thin intercalations of fine sand occur (1-3 cm thick and 1-2 m long) and these are usually structureless. An example of a coarse-sandy, cross-stratified bed showed lateral fining northwards, becoming mainly bioturbated fine sand with *Planolites montanus* burrows and faint, low-angle parallel lamination, with some very-small-scale ripple cross-lamination indicated by distorted heavy mineral cross-laminae. Bioturbation in the bulk of the sub-unit consists of very sporadic, reddened *Thalassinoides* burrows. The top of Sub-unit 4b is marked by a laterally-persistent, sharp surface dipping very gently southwestwards (Plate 11.23).

Sub-unit 4c: — This sub-unit is distinguished by its larger proportion of fine-sandy beds (fL, Fig. 11.13: 18), interbedded with cross-stratified, coarse-sandy, trough lags (Fig. 11.13: 19). The fine-sandy beds are very low-angle, parallel-laminated to structureless and are up to ~20 cm thick and several metres in length. Examples of low-angle, cross-stratified, coarse-sandy beds fining laterally to laminated fine sand are present. Coarse sand laminae and "stringers" are locally present in the fine-sandy beds, as well as heavy-mineral-rich laminae associated with indistinct, very-small-scale ripple trough cross-lamination. Some fine-sandy beds underlying coarse-sandy lags have very irregular, "bumpy" upper contacts, with concavo-convex relief on the scale of a few centimetres, but possible associated burrowing is not readily evident. Bioturbation is medium to strong and consists of local disruption of lamination, as well as many small chevron traces, but visible *Planolites montanus* burrows are sparse. Ray holes are present, but are less common than in sub-unit 4b. Reddened thalassinoidean burrows are very sporadically present.

Sub-unit 4d: — Decalcification and loss of structure distinguish this sub-unit in the uppermost metre of Unit 4. Very thin, lensoid to discontinuous beds of low-angle, cross-stratified to structureless coarse sand are interbedded with laminated to structureless fine sand (Plate 11.24). The coarse horizons (Fig. 11.13: 20) overlie sharp contacts that are very gently scalloped by shallow troughs. The overlying fine sands (Fig. 11.13: 21) locally interfinger with the coarse, basal bed, indicating deposition as coarse-fine couplet beds. Bed contacts become diffuse upwards and the top of Unit 4 is marked by the rapid, complete disappearance of primary structure. Reddened, relatively small *Thalassinoides* burrows (0.5-1.- cm in diameter) are common.

Plate 11.24 Block Section. Thin, discontinuous interbeds of coarse sand. in sub-unit 4d and rapid upward disappearance of primary structure over gradational contact with Unit 5. Dark rectangle is lacquer peel. North is right. Scale in cm/dm.

Faunal notes: — The "*Lutraria* bed" in the lower part of Unit 4 is developed only in the exposures in the southwestern part of the T2/T3 excavation. The main faunal assemblage in Unit 4 is the abraded, *Chamelea krigei*-dominated assemblage observed at the previous sections (15, 3b; 16, 3b), with shells predominantly in convex-up, hydrodynamically-stable orientations. Occasionally, specimens of *C. krigei* are found with both valves in close association. This suggests burial of the articulated, gaping specimen before decay of the hinge ligament. Only one articulated, closed specimen was found that appeared to be in life position (hinge-line subvertical, posterior uppermost). One notable, additional taxon common in this southwestern part of the excavation is a large haliotid (abalone or "perlemoen"). In the exposures of Unit 4 in the southeastern corner of the T2/T3 excavation, the herbivorous gastropods *Oxystele* and *Turbo* become noticeably more common in the eastwards direction. Importantly, where Unit 4 directly overlies (covers) bedrock, *in situ* oysters (*Crassostrea margaritacea*) and brachiopods (*Kraussina rotundata*) are abundant (Plates 11.25, 11.26).

UNIT 5

A unit, ~1.7 m thick, of mainly structureless, fine sand, with scattered coarse grains. The unit is capped by a pedogenic hardpan consisting of pinkish-white, slightly calcareous, mud.

The material overlying the uppermost, diffuse, coarse-sandy horizons of sub-unit 4d is massive fine sand, with scattered coarse grains, and unequivocal marine trace fossils are absent. As at previous sections, a pale, pedogenic mud "hardpan" is developed in the top of the unit.

UNIT 6

A unit, 5-6 m thick, of muddy, brown, thickly-bedded, medium-grained, massive sands. The colour is due to the mud content that occurs as grain coatings and interstitial mud.

Overlying the sharp contact developed on the "hardpan" capping Unit 5 is a thick unit identical to Unit 6 of Section 15.

UNIT 7

Structureless, pale yellow-brown, loose, medium sands, 1-4 m thick, with sparse coarse grains.

The loose, modern sand cover overlying the sharp contact developed on the compact, muddy sands of Unit 6.

Plate 11.25 Oysters (*Crassostrea margaritacea*) encrusting large boulder near the Block section, where Unit 4 directly overlies bedrock. Pen for scale.

Plate 11.26 Brachiopods (*Kraussina rotundata*) nestled in bedrock crevices near the Block section, where Unit 4 directly overlies bedrock. Pen for scale.

CHAPTER 12

DEPOSITIONAL ENVIRONMENTS ON AVONTUUR_A AND THE 50 M PACKAGE

12.1 FACIES DEFINITION

The *in situ*, abraded crusts of phosphorite, underlying the basal gravel facies and adhering to the bedrock, are part of the succession and must feature in its interpretation. The phosphorite is therefore defined as the **eroded phosphorite facies**. It is readily evident from the graphic logs of the sections in the AV T2/T3 excavation (Fig. 12.1) that the marine deposits there consist of three main facies. The **basal gravel facies** is a relatively thin deposit (<1 m thick) overlying bedrock. The lower portion of the marine deposits consists of a 3-4 m thickness of predominantly fine sand, with well-preserved primary structures in the lower portion and abundant bioturbation in the upper portion. A variety of primary structures and ichnofabrics are present, but sections 15 and 16 are representative of the typical facies development around most of the AV T2/T3 exposures. The lower part of the marine sequence as typically developed is defined as the **large-scale, parallel-laminated, to massive, to burrowed fine sand facies**. A sharp, laterally persistent, eroded contact occurs at the top of the **large-scale, parallel-laminated, to massive, to burrowed fine sand facies**. The overlying upper portion of the marine deposits, ~5 m thick, contains abundant, shelly, cross-stratified coarse sand, interbedded with cross-stratified to low-angle, cross-laminated fine-sandy beds. This is defined as the **shelly, cross-stratified coarse and fine sand and low-angle, cross-laminated fine sand facies**.

Primary structures lose definition in the uppermost part of the previous facies. Above a thin gradational interval, the vestigial bedding and marine trace fossils disappear and the sediment is a massive sand, ~2.0 m thick, with a pedogenic mud hardpan developed in its upper part (Plate 11.8). This is defined as a fourth facies, the **massive sand with pedogenic hardpan facies**. Sharply overlying the hardpan is a thick (5-6 m thick), brown unit that contrasts with the underlying, pale-coloured marine sands. This is called the **brown, massive, muddy, medium-grained sand facies**. The **modern, unconsolidated aeolian sand facies** caps the sequence.

In the lower part of the Block Section, a distinctly different suite of facies occur in the lateral equivalent of the **large-scale, parallel-laminated, to massive, to burrowed fine sand facies** (Fig. 12.1). Overlying the basal gravel is a **medium-bedded, small-scale, trough cross-laminated/low-angle parallel-laminated to burrowed fine sand facies** (Unit 2). This is closely overlain by a **swaley cross-stratified fine sand facies** (sub-unit 3b). The previous facies passes up into a **parallel-laminated and very-small scale trough cross-laminated, bioturbated, fine sand facies** (sub-unit 3c).

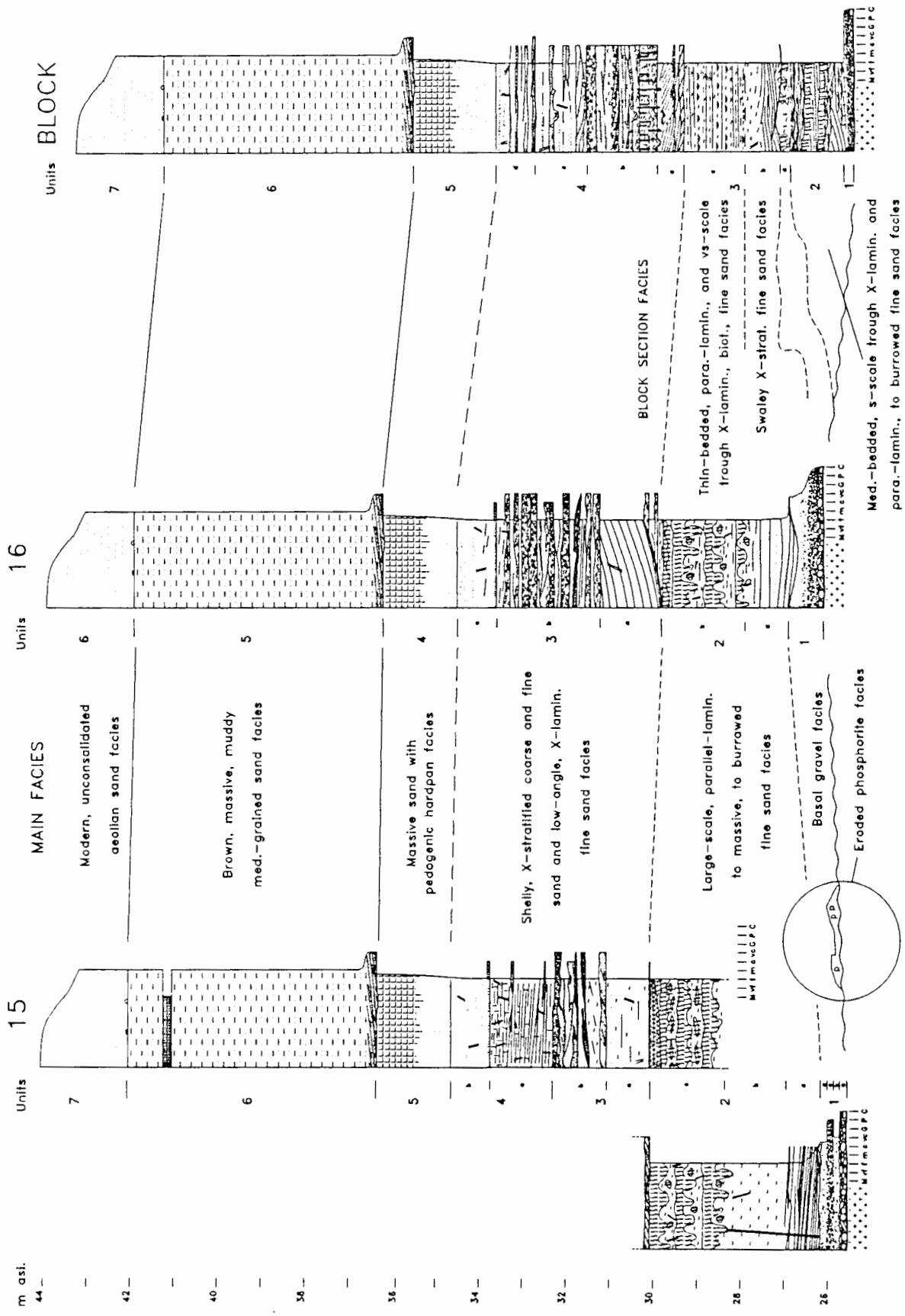

Figure 12.1 Sections from Avontuur-A, T2/T3, with facies defined.

12.2 INTERPRETATION

On a narrow coastal plain with a relatively steep, seaward bedrock gradient, such as is the situation of the study area, it is reasonable to assume that the ancient palaeoshorelines were approximately parallel to the modern coastline and normal to the seaward gradient. However, local bedrock topography will influence the orientations of palaeo-shorelines. Palaeoshoreline orientation may also be estimated from the large-scale strike and dip of the associated deposits (McCubbin, 1982). In the AV T2/T3 excavation, the most prominent bedding surface is the laterally-persistent, generally flat, sharp contact between the **large-scale, parallel-laminated, to massive, to burrowed fine sand facies** and the overlying **shelly, cross-stratified coarse and fine sand and low-angle, cross-laminated fine sand facies** (Fig. 12.1). The elevations of this contact around the excavation were surveyed. The depositional strike is ~340° (NNW-SSE) and dips shallowly at ~1° to the WSW. The depositional strike is parallel to the general coastline orientation, suggesting that local topography did not significantly influence the strike of the palaeoshoreline around the AV T2/T3 area.

The Eroded Phosphorite Facies

The abraded crusts of phosphorite can be interpreted as the remnants of a phosphorite bed that has been extensively eroded, producing the phosphorite clasts in the marine gravels. Their position on the bedrock unconformity may suggest that the erosion took place during the transgression preceding marine deposition in the area. This interpretation implies that the phosphorite was deposited during a sea-level fluctuation preceding that which gave rise to the overlying deposits. In this case the phosphorite is stratigraphically separate from the overlying marine deposits. More extensive, *in situ* phosphorite is preserved in the embayment formed by the main bedrock ridge (Zone 4A, Fig. 9.1). This is described in the next chapter (Chapter 13) and sheds additional light on the context of phosphorite deposition, providing evidence for an alternative interpretation.

The Basal Gravel Facies

The gravels basal to marine sequences and overlying unconformities or erosion surfaces are often interpreted as transgressive lag deposits (e.g. Clifton, 1981). These are residual deposits abandoned on the transgressed surface as the shoreline advanced landward. The shoaling waves drive most of the bedload sediment landwards, leaving behind large clasts and sediment caught in topographic traps. As the transgression proceeds, these deposits may not be covered by further deposition and then become relict and palimpsest sediments on the shelf seaward of the shoreface (Swift *et al.*, 1971). The transgressive lags described by Clifton (1981) are preserved beneath relatively deep-water deposits of the shoreface-offshore transition. They are thin (<30 cm) conglomerates consisting of scattered pebbles in a sandy or muddy matrix, but vary from cobble and boulder beds to granule beds. They are mainly normally graded and the sandy matrix is increasingly muddy towards the top (Clifton, 1981). The interpretation of the basal gravel facies will initially focus on the basal gravel as exemplified at Sections 15 and 16. As the basal gravel overlies a transgressed unconformity, a reasonable working hypothesis would be that it is a transgressive lag.

The basal gravel bed underlying sections 15 and 16 is (overall) normally graded to an upper portion composed of very coarse sand. The coarse sand is cross-stratified and relatively large, near-symmetric, rounded-crest, ripple bedforms have developed on the top of the bed (Fig. 11.4; Plate 11.11). Leckie (1988) has reviewed the characteristics and origin of large ripples formed on coarse-grained sediment in modern and ancient, nearshore to shelf environments (coarse-grained ripples). The wave-formed, coarse-grained ripples (CGR) occur on sharp-based beds that are often graded and structureless, except for imbrication of clasts. When internal stratification is present, it is usually defined by finer-sand laminae and includes: undulatory lower-bounding surfaces; tangentially-based foreset laminae; oppositely-bundled foresets forming chevron structures; a feathering-out of individual coarse laminae from the crest into a fine-sandy trough; sets of unidirectional cross-bedding.

It is clear that the CGR stratification depicted in Fig. 11.4 conforms to this description. The feathering out of coarse laminae from ripple crests into the fine-sandy troughs is well-illustrated by sets 2, 3 and 6 (Fig. 11.4). This is the result of turbulent forces being greatest at the ripple crest, where coarse sediment concentrates, while the finer sediment accumulates in the trough (Leckie, 1988). The CGR at Section 16, with crest spacing of ~2.0-2.2 m and amplitude of 15-20 cm, have ripple indices (length/height) of 10-15. This is typical of the ripple indices of ancient examples presented in Leckie (1988). The ripple symmetry index of an example at Section 16 is 1.14 (horizontal length of stoss side/horizontal length of lee side). The slight landward asymmetry is suggestive of net onshore transport. Similarly, dominantly onshore bedform migration is indicated by the CGR at Section 15 (Fig 11.4).

On the inner shelf south of Alexander Bay (Fig. 3.1), side-scan sonar records reveal abundant CGR in coast-perpendicular strips (De Decker, 1987). The CGR occur down to ~25 m depth, but are more common in less than 15 m depth. Crest spacings vary from 1.0 to 3.0 m and the crests parallel the shoreline. Similarly, the data compilation in Leckie (1988) shows that modern CGR are common in shoreface settings and on "relict" sediments on the inner shelf, but rare occurrences range as deep as 160 m.. The ripple crests are parallel to the shoreline and therefore examples of ancient CGR are useful in estimating palaeoshoreline orientations. The crest orientation of the CGR basal to Section 16 (Plate 11.11) is ~340°, lending additional credence to the inferred strike of the palaeoshoreline (Fig. 12.2). Most modern occurrences of CGR are interpreted to be the product of high-amplitude, long-period storm waves (swell). Although CGR occurs in "relict" sediments in deep water, the bedforms are palimpsest features active during storms for only a portion of the year (Leckie, 1988). Ancient examples of CGR are noted in association with transgressed surfaces as palimpsest features, in upper and lower-shoreface deposits and in the finer-grained offshore transition (Leckie 1988). Notably, CGR occur very commonly in lateral and vertical association with hummocky cross-stratified fine sands (Leckie, 1988)

The undulating, large ripple-forms capping the basal gravel at section 15 and 16 and interfingering with the overlying sand indicate active bedform development immediately prior to and/or during

deposition of the overlying fine sands (Fig. 11.4; Plate 11.11). The latter includes laminae and lenses of very coarse sand, indicating active transport of CGR sediment in a closely associated environment.

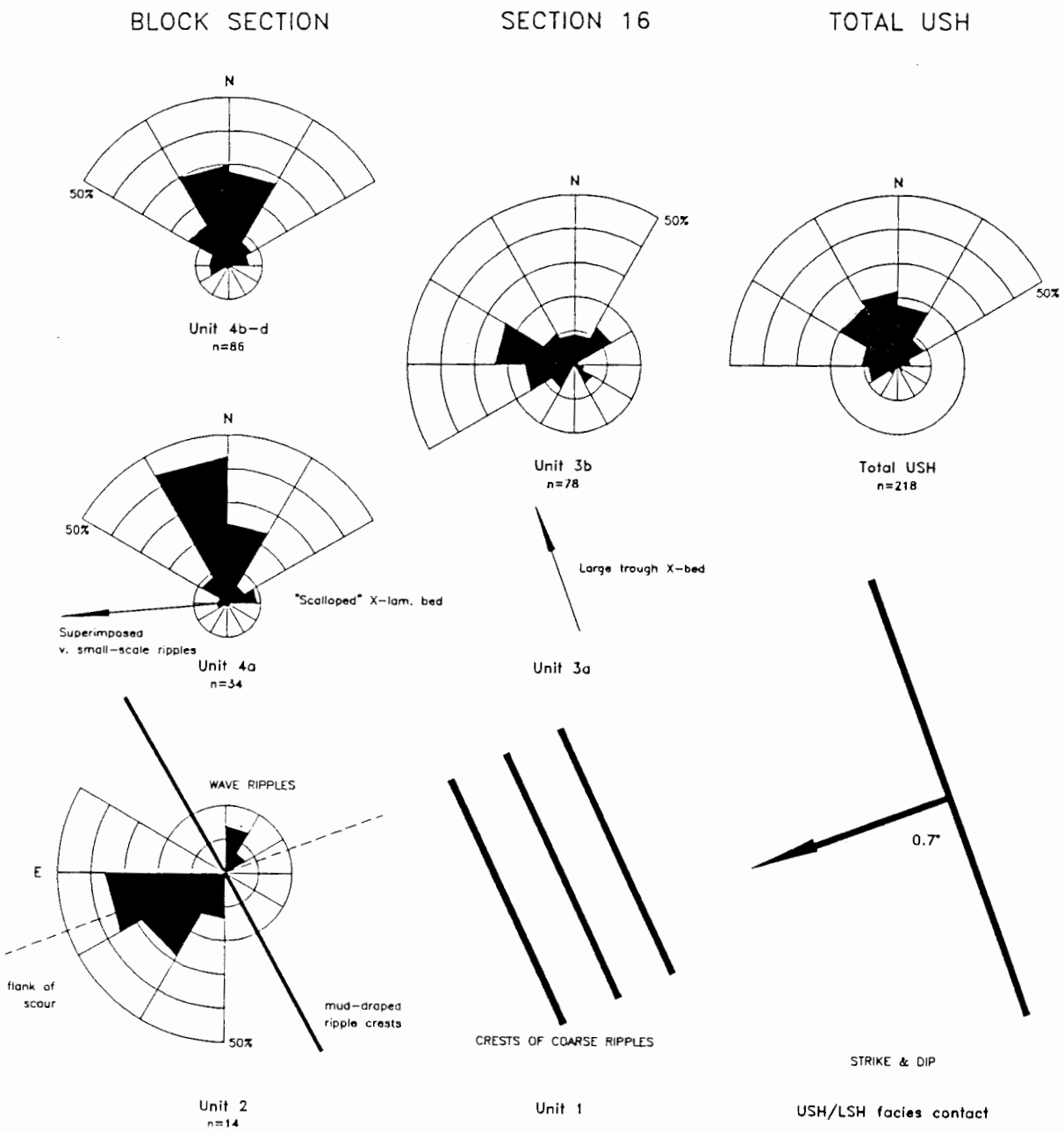

Figure 12.2 Palaeoshoreline indicators and palaeocurrent azimuths in AV T2/T3.

This basal gravel cannot be accurately interpreted as a relict transgressive lag as it is apparently extensively reworked. For similar reasons, interpretation of the CGR as a palimpsest feature on a "relict" transgressive lag is not accurate. If the basal gravel bed were submerged to offshore palaeodepths at some time, the sediment below the periodically reworked upper portion would exhibit bioturbation and the introduction of fine-grained sediment, including mud, from the ambient, low-energy environment. The basal gravel at section 15 does consist of two upward-fining sequences (Plate 11.1), of which the lower (1a+b) is structureless and burrow-mottled with patches of loose, fine sand. Nevertheless, the bed does not exhibit convincing evidence that it has been submerged, uncovered by further sedimentation, at depths greater than those of the shoreface. Furthermore, without being specific about the environments, the covering marine sediments are, overall, a coarsening-up sequence suggestive of shallowing. The fact of capping terrestrial sediments and the present-day land surface means that the contact separating transgressive and regressive deposits is close by. For a transgressive lag, the above all imply a position near the transgressive maximum of its associated sea-level cycle. Such a position would be within the range of reworking and deposition by storms. It is clear that the interpretation of the basal gravel must include consideration of the overlying facies. The context of the basal gravel will therefore be discussed further, after interpretation of the overlying facies. The occurrence of CGR, coupled with the lack of evidence for relatively deep-water, offshore-transition sediments and processes, has served to place the base of the marine sequence at shoreface palaeodepths.

The Large-scale, Parallel-laminated, to Massive, to Burrowed Fine sand Facies

The prime characteristic of this facies is its fining-upward aspect imparted by the upward disappearance of coarse sand and primary structures, whilst bioturbation and the addition of mud increase upward (Plates 11.2, 11.11). These features are suggestive of decreasing energy and rates of deposition. As such, they could be regarded as evidence of deepening. This would imply that the contact separating transgressive from regressive deposits must be above this facies. As the overlying facies is a coarse grained, noticeably higher-energy deposit, the contact may be the laterally-persistent, sharp surface at its base (Fig. 12.1). Stratigraphically, this implies a transgressive, fine-sandy unit overlain by a regressive, coarse-sandy unit.

A major feature of this facies is at odds with the hypothesis that deepening accounts for the upwardly declining energy levels. The bedding everywhere dips at a low, but noticeable, angle in the inferred seaward direction and downlaps onto the underlying basal gravel (Plates 11.2, 11.3, 11.11). Locally, at an atypical location (Block Section), steeper and more obvious lateral accretion surfaces "cross-cut" the major part of the facies (Fig. 11.11, Plates 11.20, 11.21). The consistent, low-angle dip of bedding must reflect successive surfaces during accumulation of the sediment. This implies that the upper, bioturbated part of the facies was high up the palaeoslope and therefore in water more shallow than the lower, laminated part of the facies. The facies is an upward-shallowing sequence and therefore represents progradation and regression.

Interestingly, the **large-scale, parallel-laminated, to massive, to burrowed fine sand facies** resembles a very thick, shoreface storm sequence, especially if considered together with the interfingering **basal gravel facies**. The shoreface sediments described by Kumar and Sanders (1976), from off Long Island, New York, exhibited vertical sequences consisting of a coarse basal lag, a thick interval of laminated sand and a capping of bioturbated sediment. The middle interval of laminated sand lacks pebbles, shell and heavy mineral laminae and is not at all bioturbated. They inferred scour of the shoreface of up to 2 m depth during storms. The maximum thicknesses of the storm-sequence sub-units they recorded result in a storm sequence up to 2.8 m in thickness. This of the same scale of thickness as the **large-scale, parallel-laminated, to massive, to burrowed fine sand facies.**

However, interpretation of the **large-scale, parallel-laminated, to massive, to burrowed fine sand facies** as a storm sequence resulting from a single storm is clearly untenable with the lateral extent of the facies and the aforementioned evidence of progradation. Rather, the facies represents the record of processes acting over the prograding shoreface slope such that the end result resembles a storm sequence. These processes involved the preferential preservation of unbioturbated, laminated sands at the sequence base in deeper water, whilst in shallower water the record is dominated by post-depositional colonization of the substratum by benthic infauna. In terms of the processes indicated by Kumar and Sanders (1976), it can be proposed that the lower, unbioturbated and laminated part of the facies is the record of very intense storms, when the shoreface was deeply eroded and large quantities of sand were put into suspension. This sand was redeposited under flat-bed conditions as the storm waned, forming a thick bed exceeding 1 m in thickness. Subsequent bioturbation during fairweather conditions did not penetrate the lower ~1 m of the thick storm bed. The bioturbated capping would be removed by the next storm. The upwards increase in bioturbation in the facies (Plate 11.11) implies that progressively less material was eroded in the shallower shoreface, with the record of the shallower shoreface increasingly reflecting accretion during fairweather conditions.

The storm sequences from off New York described by Kumar and Sanders (1976) were deposited in depths of 5 to 21 m. The coast is not of very high wave-energy and the sequences therefore represent processes in the lower shoreface (e.g. McCubbin, 1982). It is therefore suggested that the **large-scale, parallel-laminated, to massive, to burrowed fine sand facies** is a lower-shoreface deposit. As will be shown, this interpretation is supported by the nature of the overlying facies. The precise long-term mechanisms by which this facies came to preserve fairweather deposits preferentially in its upper part are not clear and require further investigation. However, the facies is progradational and therefore must preferentially record the processes of lower-shoreface accretion under a net sediment supply. Initial progradation involves the outward and up-building of the lowermost "toe" of the lower shoreface by the offshore transport of sediment during the more intense storms. In the uppermost lower shoreface, accretion could be by the onshore return, under shoaling waves during post-storm recovery, of some of the sand previously moved offshore from it, together with some offshore, but "new" sediment previously sequestered in the upper shoreface and foreshore.

The processes of shallow-marine, storm-sequence sedimentation have received considerable attention since the landmark paper of Kumar and Sanders (1976), particularly in the context of the contentions regarding the origin of hummocky cross-stratification (Duke *et al.*, 1991). Storm sequence models have become more elaborate (e.g. Duke *et al.*, 1991, Cheel and Leckie, 1992), but the essential processes are similar to those outlined by Kumar and Sanders (1976). The idealized sequences for coarse-grained, proximal and fine-grained, distal storm deposits, as formulated by Cheel and Leckie (1992), are presented in Fig. 12.3. As the storm waxes, increasing wave energy erodes the shoreface, putting sand into suspension and concentrating coarse bedload. Towards and at storm peak, a net offshore combined-flow from coastal set-up is established and the mobilized sediment is transported down the shoreface. Coarse sediment is deposited proximally, to form a basal gravel, whilst fine sand is carried farther offshore, depositing in upper-regime, laminated beds. As the storm wanes, the offshore flow diminishes and oscillatory flow becomes dominant. In the proximal setting, onshore-asymmetric oscillation reworks the top of the gravel bed, forming CGR, which is covered by sand transported shorewards, producing the overlying, laminated sand bed. In the more distal location, hummocky cross-stratification (HCS) forms under symmetric oscillatory flow by deposition from dense suspension. The sequences are capped by wave ripples formed as conditions return to normal. In the cases of particularly intense storms when the locales of storm deposition are farther offshore than usual, or muddy shelves, or in a transgressive regime, the storm sequence will be overlain by shelf muds.

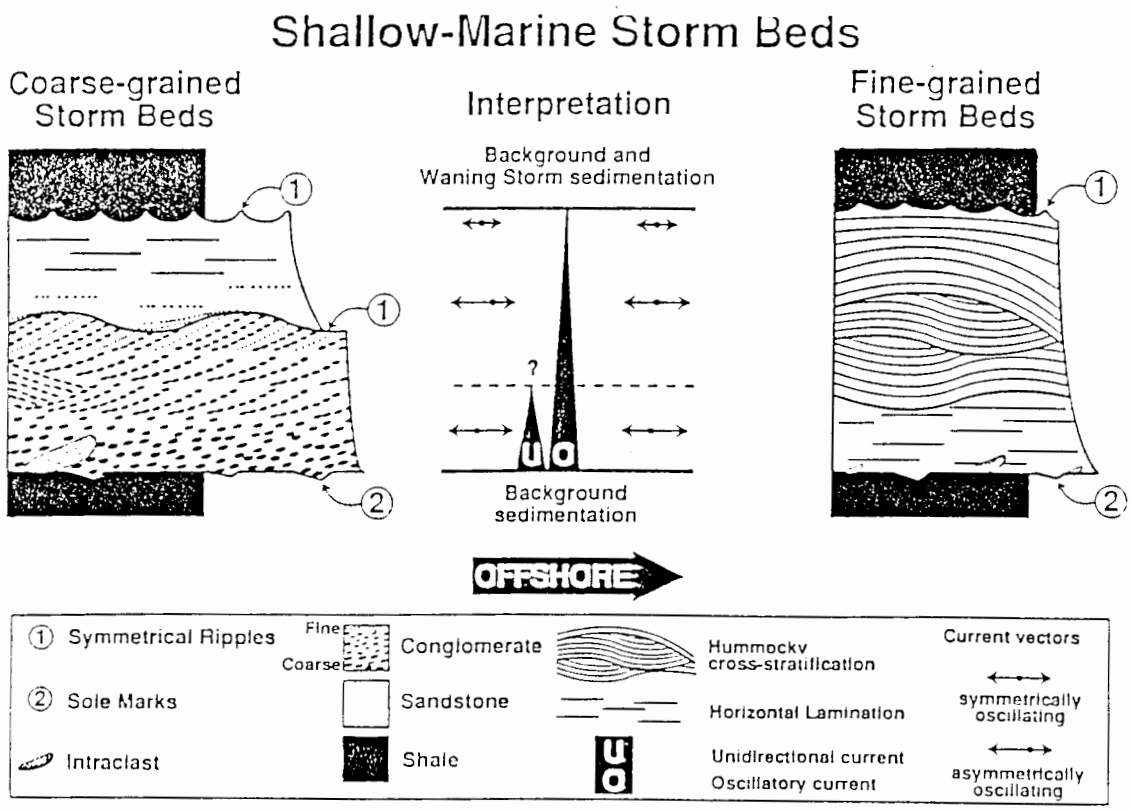

Fig. 12.3 Model of shallow-marine storm deposition. From Cheel and Leckie (1992).

The main features of the **basal gravel facies** with CGR and the overlying, parallel-laminated sub-facies of the **large-scale, parallel-laminated, to massive, to burrowed fine sand facies,** as observed at sections 15 and 16, correspond well with the elements of the coarse-grained storm sequence model of Cheel and Leckie (1992). The CGR have been discussed above. The coarse sand lenses in the overlying fine sands (Plate 11.3) show evidence of onshore (upslope) movement where cross-stratified, or where they are "swept out" in the onshore direction. This is consistent with storm-wane onshore transport of the coarse sand fraction. It is not being suggested that the basal portion of the lower shoreface as preserved at sections 15 and 16 represents a single storm sequence. The basal gravel at Section 15 is clearly an amalgamated unit (Plate 11.1) and more cryptic amalgamation of separate storm deposits is certain to be present in the overlying, fine sands. The development of CGR on the tops of basal gravels and as "gravel wave trains" interbedded with laminated fine sand occurs widely in the base of the marine sequence in the extensive Avontuur-A exposures examined by the writer. The upward diminishing in the development of "gravel wave trains" is consistent with the suggestion that the deposits of progressively less intense storms are preserved upwards in the lower-shoreface deposits.

An important difference between the idealized storm sequence and its analogues in the Avontuur deposits is that the laminated fine sands overlying CGR downlap onto the interfingering CGR at relatively steep angles (e.g. Fig. 11.4), imparting the impression of a fine-sandy, subaqueous dune advancing offshore onto gravel ripples. This may be an excellent example of the selective transport of the coarse and fine sand fractions under shoaling waves, with the coarse particles moving landward under the powerful onshore stroke, whilst the fine-sandy slope represents the advancing front of fine sand moving seaward under the weaker, but more prolonged, offshore stroke (Komar, 1976). The steepening of the lamination shown in Plate 11.3 is also suggestive of offshore transport of fine sand. It is considered likely that most of the laminated fine sand overlying CGR in the Avontuur-A exposures represents offshore transport. Notably, locally developed in the laminated sand interval at the base of the marine sequences in AV T2/T3 are isolated sets of swaley cross-stratification (SCS). Only a few sets are present (e.g. 2 or 3 swales and a hummock) and they are sharply overlain by parallel-laminated fine sand. Isolated, truncated *Granularia-Palaeophycus* burrow clumps are often present in the SCS sand below the overlying sharp contact. These occurrences suggest the local preservation of deposits of lesser storms, when sequences resembling the more distal sequences (Fig. 12.3) were deposited in shallower depths. This further illustrates the more composite and amalgamated record of storm deposition in the study area.

In the unbioturbated, laminated fine sands overlying the basal gravel, the presence of undulatory bedding planes and lateral thickening and thinning of the so-called parallel lamination has been noted (e.g. Plates 11.3, 11.11). This lamination resembles the type recently described from shallow-marine deposits by Arnott (1993), who proposes that it be named "quasi-planar" lamination. Quasi-planar laminated beds are interpreted to be deposited under high-energy, combined-flow conditions with a net offshore transport direction (Arnott, 1993). The thicknesses of beds ranges from a few cm to several dm and most consist of a single lamina-set representing a single storm event. Where not

removed by subsequent erosion, a capping wave-rippled and bioturbated interval is present. The setting of quasi-laminated bedding is interpreted as the lower shoreface to shallow shelf (Arnott, 1993).

More detailed comparisons between the features of storm-deposited fine sands described by Cheel and Leckie (1992) and Arnott (1993) and those of the study area should involve grain-fabric studies (cf. Cheel, 1991; Cheel and Leckie, 1992; Arnot, 1993). Notwithstanding, it can be proposed with confidence that the basal gravel and immediately-overlying unbioturbated sands are genetically related and represent the deposits of the more intense storms, laid down in the lower shoreface. Moreover, on the basis of the high-energy environment, with amalgamation of storm deposition, these are proximal lower-shoreface deposits. The basal gravels, as exemplified at sections 15 and 16, probably consist mainly of material transported from the upper shoreface seaward to the lower shoreface. Any gravel initially at the site of deposition would have been reworked during the storm events, rendering it unrecognizable as a pre-existing lag. Only boulders resting directly on bedrock, or gravel embedded in bedrock fissures, may qualify as the elements of a transgressive lag. The **basal gravel facies** is therefore included as a storm deposit of the lower shoreface and is not regarded separately as a transgressive lag.

The interpretation of the remainder of the **large-scale, parallel-laminated, to massive, to burrowed fine sand facies** mainly involves consideration of the trace fossils. The strong *Granularia-Palaeophycus* bioturbation in the uppermost part of the facies can reasonably be regarded as representing a shallow-tier ichnocoenosis or palaeocommunity, although the burrowing is locally quite penetrative and extends downwards from the main, shallow horizon as the pendant burrow clumps (Plate 11.4). Similarly, the *Skolithos* '*bundles*' horizons (Plate 11.5) clearly represent a shallow-infaunal palaeocommunity. Although these burrows are mainly preserved in the uppermost part of the lower-shoreface deposits in AV T2/3 exposures, they would have been present to greater depths across the lower shoreface at particular times. This is shown for the *Granularia-Palaeophycus* burrows in Plate 11.11. Similarly, *Skolithos* '*bundles*' burrows may occur over most of the thickness of variations of lower-shoreface facies present in other excavations on Avontuur-A. The massive, *Planolites montanus*-burrowed, middle part of the subfacies developed at Section 15 (Plate 11.2) could be interpreted as the result of preservation of a deeper tier of bioturbation than the *Granularia-Palaeophycus*-burrowed subfacies. However, the occurrence of *Planolites*-burrowed zones parallel with the foresets of subaqueous dunes, presumably formed during brief periods of stalled migration, suggests that it is the burrow of a shallow-tier, opportunistic, deposit feeder. Thus the massive, *Planolites*-burrowed subfacies of the lower shoreface may represent intermediate rates of deposition, rather than the preferential preservation of the lower portions of beds. Lacquer peels reveal vestigial parallel-lamination, apparently in thin beds, with some very-small-scale trough cross-lamination. The vestigial laminae of muddy sand associated with the *Granularia-Palaeophycus* ichnocoenosis confirm that the top of the lower shoreface was deposited in fairweather conditions. It is possible that a significant portion of the mud might have been "captured" by the activities of the burrow dwellers by extraction from the water column and conversion to pellets (Bromley, 1990).

THE MEDIUM-BEDDED, SMALL-SCALE, TROUGH CROSS-LAMINATED/LOW-ANGLE PARALLEL-LAMINATED TO BURROWED FINE SAND FACIES

This facies occurs exclusively in Unit 2 of the Block Section (Fig. 12.1). The basic facies character is of erosively-based, parallel-laminated and cross-laminated beds with bioturbated tops (Plate 11.17, Fig. 11.10). These resemble the relatively thin (<0.5 m) beds that have been interpreted as individual storm sequences (Howard, 1972; Bourgeois, 1980; Howard and Reineck, 1981). Sub-unit 1 in Fig. 11.10 consists of two such sequences that were subsequently deeply eroded. Sub-units 2 and 3 together form another sequence, but the swaley interbed in 3 suggests the possibility of amalgamation. Sub-unit 4 is a sequence. Sub-unit 5 includes a sequence terminating in a muddy drape that was not significantly eroded prior to the resumption of deposition. The trough cross-lamination represents 3-dimensional ripples which resemble the bundled, unidirectional wave-ripple lamination described by de Raaf *et al.* (1977). Notably, the wave-ripple lamination is mainly directed into the SW quadrant (Fig. 12.2, Unit 2).

The wave-ripple azimuths indicate strong offshore transport and the facies is therefore interpreted to have been deposited under offshore-directed, combined-flow, storm-generated currents. It is possible that the trough-based wave ripples may be the sinuous-crested type noted by Arnott (1993) and similarly interpreted. Wavey lamination tends to occur near the tops of mud-draped sequences and may have originated from relatively high flow strengths combined with high sand loads. Prior to the deposition of capping mud drapes, straight-crested wave ripples formed, with crestal orientations parallel to the palaeoshoreline (Fig. 12.2, Unit 2), but the internal lamination indicates that net offshore transport was still operating during storm wane. The preservation of the mud drapes must be attributed to a relatively short interval of time intervening before they were overlain by subsequent deposits, otherwise they would have been mixed and disrupted by *Granularia-Palaeophycus* burrowing. This might suggest storm sequences formed during the same storm season. The wave-rippled sediment contains slightly, but noticeably, more very fine sand and mud (actually coarse silt) than most other samples of fine-grained sand from the marine deposits (Fig. 11.9).

In view of the relatively low-energy environment implied by small ripples in fine to very fine sand and mud drapes, the combined-flow, offshore transport indicated and the relatively thin nature of inferred storm-sequence beds, the **medium-bedded, small-scale, trough cross-laminated/low-angle parallel-laminated to burrowed fine sand facies** is considered to represent the most distal, lower-shoreface deposits preserved in the marine sequence in the AV T2/T3 excavation. The important feature of this facies is that it is only preserved in a small area and has a markedly eroded, high-relief upper contact. In view of the depositional processes already outlined for the basal gravel and lower part of the lower shoreface that have general application, it can be concluded that this facies was more extensive, but has been eroded everywhere else during storms and replaced by more proximal shoreface deposits. It is likely that this "patch" of distal lower-shoreface deposit at the Block Section location has been preserved due to its position against the landward flank of a bedrock ridge (Fig. 11.1). Although the small "reef" to landward may have afforded some protection from offshore storm

currents, the much larger ridge to the immediate seaward probably constrained the lowering of offshore storm currents onto the deposits against its flank. Notably, the down-cutting associated with the closely-overlying **swaley cross-stratified fine sand facies** is most marked opposite a saddle in the flanking bedrock ridge (Fig. 11.1), where a high-angle scour is preserved (Plate 11.21). Over the ~1 m of the scour edge exposed by digging into the face, the edge has an orientation perpendicular to the palaeoshoreline (Fig. 12.2).

The eroded, distal lower-shoreface deposit is overlain by a nearly structureless, bioturbated, fine sand (sub-unit 3a), with truncated *Granularia-Palaeophycus* burrow clumps within and at the top of the bed. Accordingly, sub-unit 3a is an amalgamated and bioturbated record of storm deposition, probably deposited at depths intermediate to the underlying distal facies and the proximal deposits of sections 15 and 16. The basal gravel underlying the eroded, distal lower-shoreface deposit must also have been deposited at similar or deeper depths.

The basal gravel facies: — The basal gravel underlying the distal lower-shoreface deposit is thin and lacked a very-coarse-sandy capping with CGR. It is either a storm gravel deposited distally by intense storms, or a transgressive lag, or some combination of these origins. It post-dates the **eroded phosphorite facies**. Because it underlies a distal shoreface deposit very near proximal, CGR-type, lower-shoreface storm gravel (sections 15 and 16), it is slightly older than the proximal basal gravel.

The cobble and boulder gravel in the southern part of the AV T2/T3 excavation (Plate 11.16) post-dates the **eroded phosphorite facies** and is not overlain by the wave-rippled, distal lower-shoreface sands, but by laminated, proximal, lower-shoreface fine sands. It is inversely graded, with a capping "armour" of tabular and discoidal cobbles and boulders. This was produced by the very-high-energy deposition of large clasts on top of a pebble gravel, or by strong winnowing of finer gravel from a previously thicker bed. Notably, the presence of white, calcareous crusts on upper clast surfaces was recorded, but these were unfortunately not sampled. The presence of white crusts can be confirmed from Plate 11.16 (e.g. on dark clast subjacent to survey staff). The crusts are probably calcareous algae. Such epibenthic encrustation suggests that the basal gravel was exposed for a period. This is expected as the armoured bed was last in the proximal lower shoreface, where it would have been regularly swept of overlying fine sand before final burial beneath the prograding sand wedge. The upward-coarsening, armoured character, lack of muddy matrix and setting in the proximal lower shoreface suggest that the basal gravel is unlikely to be a true transgressive lag as it must have been reworked or perhaps entirely deposited during storms. Notably, where imbrication can be seen in Plate 11.16 (e.g. below right-hand end of survey staff), the clasts dip towards the upper right corner of the photograph, which is towards the palaeoshoreline. This is consistent with deposition by a seaward current. The transport and deposition of clasts the size of small boulders during offshore storm flows may be regarded with some disbelief. Evidence from the next excavation to be described (Zone 4A, Chapter 13) further supports the interpretation of the basal gravels as lower-shoreface storm deposits, rather than as transgressive lags.

THE SWALEY CROSS-STRATIFIED FINE SAND FACIES

This facies occurs in sub-unit 3b in the Block Section (Figure 12.1). At the immediate section site occur a series of sharp-based, wide troughs, with near-concordant internal lamination and "offshoots" that form a hummock over the adjacent swale. The presence of such swaley cross-stratification (SCS) (Leckie and Walker, 1982) as a few isolated sets in places in the lower part of proximal lower-shoreface deposits has been noted above. At the Block Section, the SCS forms a slightly more laterally-persistent facies. The SCS grades and thickens laterally into the infill of large, erosional scour cut into the underlying deposits. The infill exhibits a laterally accreting aspect with a depositional style that is clearly related to that of the adjacent SCS (Fig. 11.11). Deposition was preceded by marked erosion that locally produced a high-angle, overhanging scour in the underlying deposits (Fig. 11.11, Plate 11.21). The deep scour must have been filled immediately, forestalling imminent collapse of the overhanging scour wall. Pebbles and shells were swept into the troughs of scours, in places accumulating incrementally at the bases of accreting slopes.. Isolated large cobbles are locally present in the scours, with mean diameters of 10-15 cm. Isolated pebbles and shells, including large oyster shells (*Crassostrea*), occur in places on the barnacle-plate-rich, thick laminae of the facies. These features point to a high-energy environment with closely temporally-associated erosion and redeposition.

Swaley cross stratification is closely related to hummocky cross-stratification (HCS) and may be a more amalgamated version of HCS formed in shallower water (Leckie and Walker, 1982; Walker *et al.*, 1983; Dott and Bourgeois, 1983; Leithold and Bourgeoise, 1984). Duke *et al.* (1991) have presented evidence that HCS forms in practically pure oscillatory flow and rapidly becomes "anisotropic" or migrating with the superimposition of a weak, unidirectional flow. A direct comparison with more consistently-developed SCS/HCS bedding and storm sequences is not being drawn here. Nevertheless, there is a striking similarity in the SCS/HCS type of deposition and the **swaley cross-stratified fine sand facies** and it is therefore suggested that this facies at the Block Section was deposited under strongly-oscillatory, combined-flow conditions. In this case, relatively distal shoreface environments are not indicated. The facies situation is part of the general, proximal lower-shoreface progradation down the Avontuur-A bedrock slope.

As in the preservation of the eroded remnant of underlying, distal lower-shoreface deposits, the influences of local bedrock topography probably account for the development of this atypically-preserved facies. The situation of the Block Section in a corner of a basin (Fig. 11.1), against a bedrock ridge, with a larger bedrock "reef" to seaward, very likely resulted in locally complex wave action and storm flows. Together with changes in the local orientation of the lower-shoreface slope that would have occurred as it progradationally lapped around bedrock complexities, this has resulted in localized variations of facies vertical sequence. Deposition of this facies is envisaged to have occurred when the locale was in an "offshore" breaker zone formed during storms over bedrock reefs to the seaward of the open-coast, breaker and surf zone.

The sorted bulk sample of the fauna deposited in the scours of the **swaley cross-stratified fine sand facies** confirms that the high diversity seen in the field is due to the high proportion of vagile, epifaunal gastropods. Small, worn *Crassostrea* shells form a significant portion of the fauna. Other rocky-shore representatives are common, such as limpets, mussels, barnacles and brachiopods. Many of the mytilids and brachiopods are articulated juveniles. Clusters of detached juvenile barnacles, attached around their rims, are intact, indicating short transport paths. This confirms the "swept in" nature of the shell deposit, rather than a lag origin. Representatives from the sandy shore are minor, but include articulated specimens. The high-diversity, mainly epifaunal nature of the assemblage is consistent with the shell being mainly swept in from off nearby rocky environments such as reefs, with some exhumed infauna also contributing to the assemblage. Notably, the robust bivalve *Chamelea krigei*, very abundant in the cross-stratified, coarse sands of the upper marine section, is absent in the assemblage.

The Parallel-laminated and very-small scale Trough cross-laminated, Bioturbated, Fine sand Facies

At the Block Section, intensely *Granularia-Palaeophycus*-burrowed, muddy horizons are not developed in the uppermost part of the lower-shoreface deposits (sub-unit 3c). Instead, 10-15 cm thick beds of parallel-laminated sand and wave-rippled, fine sand are strongly bioturbated, evidently by *Planolites montanus* and other infauna that have left few definite burrows. In one part of the exposure where the bioturbation is less, the beds are seen to overlie sharp lower contacts and have bioturbated upper portions (Plate 10.14). The upper portions of the beds usually have very-small-scale wave-ripple lamination, indicated by wispy heavy-mineral laminae. *Skolithos 'mini'* horizons mark the upper contacts of beds and *Trichichnus* and chevron traces cross-cut beds between bioturbated horizons. These beds appear to be small-scale versions of the "parallel-to-bioturbated" storm sequences described by Howard (1972) and Howard and Reineck (1981). They reflect the nature of deposition in the uppermost part of the lower shoreface of these marine sections, but generally the evidence of individual sequences is blurred by expansion of the upper, bioturbated divisions of beds. This reflects a relatively slow rate of accumulation and the preservation of less-bioturbated beds such as at the Block Section implies a locally more rapid sedimentation rate.

The Shelly, Cross-stratified Coarse and Fine sand and Low-angle, Cross-laminated Fine sand Facies

At any particular locality, a sharp, laterally-persistent, eroded contact is basal to this facies. The coarse sand in the marine deposits has mainly been deposited in this facies. In contrast with the gently seaward-dipping, flat seabed indicated for the underlying, lower-shoreface deposits, the abundant cross-stratification in this facies indicates an irregular seabed characterized by migrating bedforms. In the shoreface environment, the coarsest sediment is driven onshore by the strong, short, landward stroke of shoaling-wave, oscillatory currents (Komar , 1976). Coarse-grained, lunate megaripples migrate shoreward from the breaker zone (Clifton *et al.*, 1971). Bars, troughs and rip

channels form in the breaker and surf zone (upper shoreface) over a wide range of wave conditions and migrate and erode with changing wave conditions (Short, 1984). Wave-approach at an angle to the shoreline generates longshore currents that drive bedforms along longshore troughs and feed into rip channels where bedforms migrate offshore (Hunter *et al.*, 1979). Accordingly, the **shelly, cross-stratified coarse and fine sands and low-angle, cross-laminated fine sand facies** is identified as the most shallow-marine environment represented in the sections and to be the deposits of the upper shoreface.

The composition and taphonomy of the faunal assemblage in this facies is consistent with deposition in the breaker and surf zone. The assemblage is dominated by a single species, *Chamelea krigei*, a venerid bivalve with an orbicular, concentrically coarsely-ribbed, robust shell and shallow pallial sinus. This species mainly occurs in an abraded, disarticulated, convex-up state, but well-preserved valves are present and rare examples with matching, associated valves are found. Although extinct, *Chamelea krigei* is identical in its basic functional morphology to the extant venerid *Venus verrucosa*. Indeed, a closely related species, *Venus* cf. *V. verrucosa* is common, but not abundant, in the same assemblage and occurs in a similar proportion of taphonomic states. It can only be distinguished from *C. krigei* by individual examination and from the extant *V. verrucosa* by ribbing detail. This bivalve design is functional in the shallow-infaunal, shifting-substratum habitat. *Chamelea krigei* inhabited the subtidal environment, in the shifting bedforms, and was not swept in from the shallower, intertidal environment. Its shells attain the highest concentrations in low-angle, cross-stratified to structureless, coarse-sandy beds that represent the amalgamation of lags formed in troughs.

Abraded oyster (*Crassostrea*) and brachiopod fragments and valves are also very abundant. Notably, these taxa are found *in situ* on bedrock and large boulders that were buried beneath this facies. (Plates 11.25, 11.26). *In situ Crassostrea* are very rarely encountered beneath the lower-shoreface deposits in AV T2/T3 (one observation only). This is consistent with the subtidal, upper-shoreface habitat of *Crassostrea margaritacea*. The diversity of the upper-shoreface assemblage is low relative to the assemblage associated with the **swaley cross-stratified fine sand facies** and is mainly due to a small number of herbivorous, rocky-shore inhabitants such as limpets (Patellidae, Fissurellidae), abalone (Haliotis), *Turbo*, *Oxystele* and the main predators, *Spinucella* and *Cabestana* (equivalent to *Nucella* and *Argobuccinum* in the modern shore). These taxa in the abraded fauna are considered to be para-autochthonous and derived from the intertidal and sub-tidal rocky substrata of the palaeoshoreline

Hunter *et al.* (1979) predicted that laterally-persistent, eroded contacts should be produced during the progradation of a barred upper shoreface. This is formed by erosion in rip channels and should be overlain by coarse, rip-channel deposits with seaward-orientated cross-bedding. Clifton (1981) has documented these features in Miocene shoreline deposits of California and inferred a barred coastline. In contrast, progradation of the non-barred upper shoreface would produce a more interfingering contact with lower-shoreface deposits and less of a grain-size discontinuity (Hunter *et al.*, 1979). The laterally-persistent, sharp contact between fine-sandy, lower-shoreface deposits and coarse, upper-

shoreface deposits in the AV T2/T3 exposures is therefore suggestive of a barred upper shoreface. However, cross-bedding in the immediately overlying coarse sands does not have a noticeable offshore commonality of palaeocurrent azimuths, nor is the bedding scale noticeably different from the remainder of the facies. Like the cross-bedding in the remainder of the facies, that generally overlying the basal contact exhibits mainly northward azimuths, with both on- and offshore-directed cross-bedding also present locally.

At Section 16, a large, deep trough occurs in the base of the upper-shoreface deposits (Plate 11.12, sub-unit 3a). The trough was eroded into cross-stratified sands deposited earlier in the lower part of the upper shoreface. A large subaqueous dune migrated down the trough and symmetrically infilled it. The associated palaeocurrent azimuth is parallel to the general trend of the palaeoshoreline (Fig. 12.2, sub-unit 3a). At Section 15, a thick, fine-sandy bed (sub-unit 3a) occurs in the base of the upper-shoreface deposits. Although exposure was poor, the thick bed is not laterally persistent and *Skolithos* 'bundles' burrows are associated with its base (Plate 11.5). It is possible that this bed may also be the infill of a large trough similar to that at Section 16. Unfortunately, the internal structure of the bed is obscure. The large trough-infill at Section 16 and inferred at Section 15 are isolated features "embedded" in the upper-shoreface deposits and are not regularly developed around the exposures in the excavation. The situation of sections 15 and 16 opposite the "opening" of the AV T2/T3 basin to the west (Fig. 11.1) may explain their formation. The high bedrock rimming the basin in the west would have been submerged reefs in upper-shoreface palaeodepths. Storm-generated bottom flow would have been constrained to leave the basin over the saddle in the west (Fig. 11.1). The location and orientation of rip channels would have been influenced by the topographic constraints on seaward flow. The troughs cut into earlier upper-shoreface progradation are tentatively interpreted as rip channels. Interestingly, the cutting of the troughs and their filling are separated in time. The inferred trough at Section 15, with the *Skolithos* 'bundles' burrows in its base (Plate 11.5), remained inactive for a period, accumulating muddy sediment before being infilled. At Section 16, muddy laminae and very-small-scale ripples were deposited in the trough base, in the vanguard of the migrating dune. This indicates relatively quiescent deposition, protected in the deep trough from the main flow driving the dune. Thus the troughs do not seem to have been filled immediately after their erosion by rapid deposition during storm wane, but were relatively persistent features.

At the Block Section, the sharp, basal contact of the facies is overlain by cross-bedding directed to the NE and E. The thick cross-laminated bed at the base of the facies (sub-unit 4a) may be an example of scalloped cross-bedding (Fig. 11.12). Scalloped cross-bedding is interpreted to result from the migration of smaller bedforms along the lee slopes and troughs of the main bedform, transverse to main direction of migration (Rubin, 1987). In the example discussed by Rubin (1987), the main bedform was interpreted as a bar flanking a rip channel, with the subsidiary bedforms representing the migration of dunes seawards in the rip channel. In the example from the study area, the palaeocurrent azimuths measured within upper parts of scallops are mainly parallel to the general palaeoshoreline trend (Fig. 12.1, sub-unit 4a). This represents the migration direction of the main bedform under the influence of an alongshore current. A palaeocurrent azimuth due west was

measured in the coarse-grained, "upturned," lower right part of a scallop (Fig. 11.12). The very-small-scale ripples on the upper parts of foresets of some sets also migrated due west (Fig. 12.2, sub-unit 4a). Thus the superimposed bedforms in the shelly, coarse-grained trough of the main bedform were probably migrating westwards. Although not consistently developed laterally, it is considered likely that an element of bedform superimposition was involved on the production of a part of this bed, but fluctuating flow conditions are implied by the very-small-scale ripples overlying erosive surfaces within scallops. The scalloped part of sub-unit 4a is considered to represent the longshore migration of a bar-like, positive-relief feature formed in the outer upper shoreface. Laterally northwards, the migration increments of the bar became more complex (Fig. 11.12) before it apparently "died-away" into an area of wave-rippled sand accumulation.

The deposition of beds in couplets consisting of a lower, coarse-grained part, often with small-scale CGR with wavelengths of 0.5-1.0 m, overlain and locally interfingering with a fine-sandy upper portion, is characteristic of this facies (Fig. 11.5). This indicates that the coarse-grained portions are trough lags between fine-sandy bedforms. The coarse sand was initially deposited on the lower foresets of the migrating bedforms, with subsequent erosion of the bedform producing CGR and a sharp, contact on the top of the coarse sand in the trough. Renewed migration of the bedform then covers the CGR. The amalgamation of trough lags is a major characteristic of this facies. Thin interbeds of low-angle, parallel-laminated fine sands may be equivalent to the outer planar facies of Clifton *et al.* (1971) that is present under the surf bore and on the seaward slopes of bars (Hunter *et al.* (1979). The thick unit with gently seaward-dipping parallel lamination in Section 15 (sub-unit 4a) (Plates 11.6, 11.7) resembles swash stratification of the foreshore environment. However, this interpretation is inconsistent with the cross-stratification of deposits laterally at the same elevation. This local development of a thick, plane-laminated bed in the upper shoreface is considered due to a lack of coarse sand for bedform development (Clifton. 1988). Consequently, deposition took place in the outer planar facies mode. As a whole, fine-sandy beds become more common upwards in the facies.

At the Block Section, the palaeocurrent azimuths of both fine-sandy and coarse-grained cross-beds are mainly alongshore and obliquely onshore, with minor shore-normal, offshore and onshore azimuths (Fig. 12.2, Unit 4b-d). In contrast, palaeocurrent azimuths at Section 16 are dominated by obliquely offshore transport, with a secondary obliquely onshore mode (Fig. 12.2, Unit 3b). Whilst both fine and coarse-sandy beds contribute to the offshore mode, the onshore mode mainly reflects the transport of coarse sand. There is probably a bias in the palaeocurrent azimuths stemming from the orientations of the exposures, due to transport directions parallel to the exposure being more readily discerned (the Block Section exposure is approximately shore-parallel, Section 16 exposure is shore-normal). The combination of the palaeocurrent measurements, together with additional measurements made around the excavation (Fig. 12.2, Total USH), shows mainly alongshore transport, varying through obliquely offshore to obliquely onshore in the longshore direction, with minor shore-normal, on- and offshore, transport. This is consistent with the effective waves approaching the shore obliquely from the south, as they do at present.

The strongly longshore-directed cross-bedding present over most of the exposures argues that the upper shoreface would have been of a general oblique bar-rip channel type, but relatively thicker units with onshore cross-stratification that may represent the lower parts of bars, as predicted by Hunter *et al.* (1979), are not a feature of this progradational record. The abundant shelly, trough lags suggest a very amalgamated record of upper shoreface sedimentation. The greater abundance of fine-sandy beds in the upper part of this facies in places, that probably reflects increasing preservation of the outer planar facies, may partly incorporate the lower, seaward slopes of bars. A coarse subfacies at the top of the upper-shoreface deposits, that may have represented the inner rough facies of (Clifton et al. (1979) (toe-of-beach gravel), is not noticeably developed. It will be shown below that the pedogenic profile overlying the upper-shoreface deposits was not developed in foreshore deposits, which are absent.

THE MASSIVE SAND WITH PEDOGENIC HARDPAN FACIES

The basal contact of this facies appears gradational and represents a change from underlying, decalcified marine sand with trace fossils and vestigial primary structure, to massive sand with a slightly darker hue (Plates 11.8, 11.24). Although apparently gradational, at the sections this boundary is quite clearly defined within about a 20 cm interval. Scrutiny of this contact in the AV T2/T3 excavation and in other excavations on Avontuur-A reveals that a diffuse horizon of coarse sand commonly occurs at the base of the facies. The occasional isolated pebble, sometimes angular, occurs along this level. More importantly, very thinly-scattered fragments of bone, mainly tortoise in origin, also occur in places. A mandible of a rhinoceros was found in the contact horizon. Although rare, entire tortoise skeletons are found within the **massive sand with pedogenic hardpan *facies***. The most impressive example is shown in Plate 12.1. In Plate 12.1, note that the **massive sand with pedogenic hardpan facies** is compact and overhangs the softer marine sand with trace fossils, the contact between the two occurring along the edge of the overhang. The presence of terrestrial vertebrates on the basal contact and within the facies clearly indicates that the facies does not represent a pedogenic profile developed in the top of the marine sands. Rather, a cryptic contact separates this facies from the underlying marine sands. Accordingly, the **massive sand with pedogenic hardpan facies** is interpreted as reworked marine sand. The reworking probably took place under aeolian conditions, but sedimentary structures are lacking and have presumably been destroyed by subsequent soil-profile development and root-stirring. The grain-size analyses from this facies (Fig. 11.3: 10,11,12,13) show an increase of medium-grained sand in the uppermost part. Deposition of medium-grained sand characterizes the overlying aeolian deposits of the **brown, massive, muddy, medium-grained sand facies**. As a significant thickness of upper-shoreface sediment is present in AV T2/T3, the deflation involved mainly the foreshore deposits that can be assumed to have overlain the upper-shoreface deposits. Importantly, where the cryptic contact is present, the lack of concentrations of pebbles and cobbles on the top of the deflated marine deposits suggests that such coarse material was absent in the uppermost part of the marine sequence. This suggests that deposits of a wide, fine-sandy foreshore completed the marine section.

Although the presence of a unit of reworked marine sand above a cryptic contact has general application to the Avontuur-A exposures and the contact can in places be traced for several tens of metres, it is emphasized that the contact cannot be recognized everywhere. Moreover, at certain locales it appears that the marine sediments extend into the pedogenic profile associated with the facies. For instance, in Plate 12.2 from the northeastern corner of the AV T2/T3 excavation, it can be seen that relict columns of coarse-grained, upper-shoreface sediment are present in the decalcified pedogenic profile. Here a unit of reworked sand is either very thin or not present. This observation implies that the cryptic contact underlying the reworked sand has a low-relief topography. It is likely that the occasional pebble and the bones accumulated mainly in the wide topographic hollows.

The Brown, Massive, Muddy, Medium-grained sand Facies

The sharp contact basal to this facies, on the surface of the pedogenic hardpan developed in the previous facies (Plate 11.9), implies that a significant hiatus probably intervened between the pedogenesis in the **massive sand with pedogenic hardpan facies** and renewed erosion and deposition. At Section 15 in the lowermost ~0.4 m of the facies (Plate 11.9), the thin, discontinuous laminae of coarse sand interbedded with medium-grained sand strongly resemble the sedimentary characteristics of aeolian sand sheet deposition (Ahlbrandt and Fryberger, 1982). Within the facies, large-scale, tangential-based cross-bedding in thick, tabular beds indicates deposition by northwards-

Plate 12.1 Large tortoise (?*Geochelone* sp.) in the reworked marine sand capping the marine deposits. The soft, primary marine sands are recessed, indicating the approximate position of the contact.

Plate 12.2 Relict columns of shelly, upper-shoreface sand in the decalcified pedogenic profile. Tool is 42 cm long.

migrating aeolian dunes (Plate 12.3), indicating dominant southerly wind as at present. However, for the most part of the facies, sedimentary structures have been obscured by the development of intergranular, brown mud, inferred to be pedogenic in origin. Subtle colour variation of the pedogenic mud, on the scale of thick bedding (Plate 11.10), suggests a succession of superimposed soil profiles. Distinct muddy beds are present in the facies. These are thin (<0.5 m) relative to their lateral extent (10-50 m) and thin to disappearance laterally. These muddy beds are the most readily-discerned palaeosurfaces in the facies. They are interpreted to represent the deposition, in local, shallow, topographic lows, of pedogenic mud washed out of the sands by sheetwash. The formation of muddy ponds occurs in the present-day, after rainfall in hollows in the modern sand-sheet surface.

Accordingly, the **brown, massive, muddy, medium-grained sand facies** is interpreted to be mainly the deposits of aeolian dunes and sand sheets, with local sheetwash deposition. The position of muddy pond deposits in the lower portion of the facies implies "early" development of pedogenic mud. The facies probably accumulated mainly during periods of arid climate, with pedogenic processes operating during wetter periods.

THE MODERN, UNCONSOLIDATED AEOLIAN SAND FACIES

The modern topography of vegetated linear dunes, separated by sand sheets, attests to aeolian deposition in the geologically-recent past. Wind ripples with coarse-grained crests form where

vegetation is disturbed. The stabilization by vegetation indicates that incipient pedogenic processes are acting at present. The similarity in the grain-size distribution of the modern sand sheet and the sand of the underlying facies (Fig. 11.6) supports the interpretation that the latter was deposited by similar processes.

Plate 12.3 Faint large-scale aeolian (dune) cross-bedding in the brown, massive, muddy, medium-grained sand facies. North is left. Large trowel is ~30 cm long.

12.3 SUMMARY AND STRATIGRAPHIC IMPLICATIONS

The interpretation of the AV T2/T3 exposures unequivocally establishes that the marine deposits were laid down the proximal shoreface environment (Fig. 12.4). The occurrence of upper-shoreface deposits overlying lower-shoreface deposits establishes that the marine deposits represent progradation of the shoreline during a regression. The setting of the marine basal gravels in the proximal lower shoreface reveals that they are not transgressive lags, but are proximal marine, storm-deposited beds. The facies deposited at the greatest palaeodepth is a small erosional remnant of distal lower-shoreface facies preserved only because of protecting bedrock topography. In general, erosion in the proximal lower shoreface during intense storms has swept away pre-existing, deeper-water facies in the vanguard of the prograding shoreface wedge.

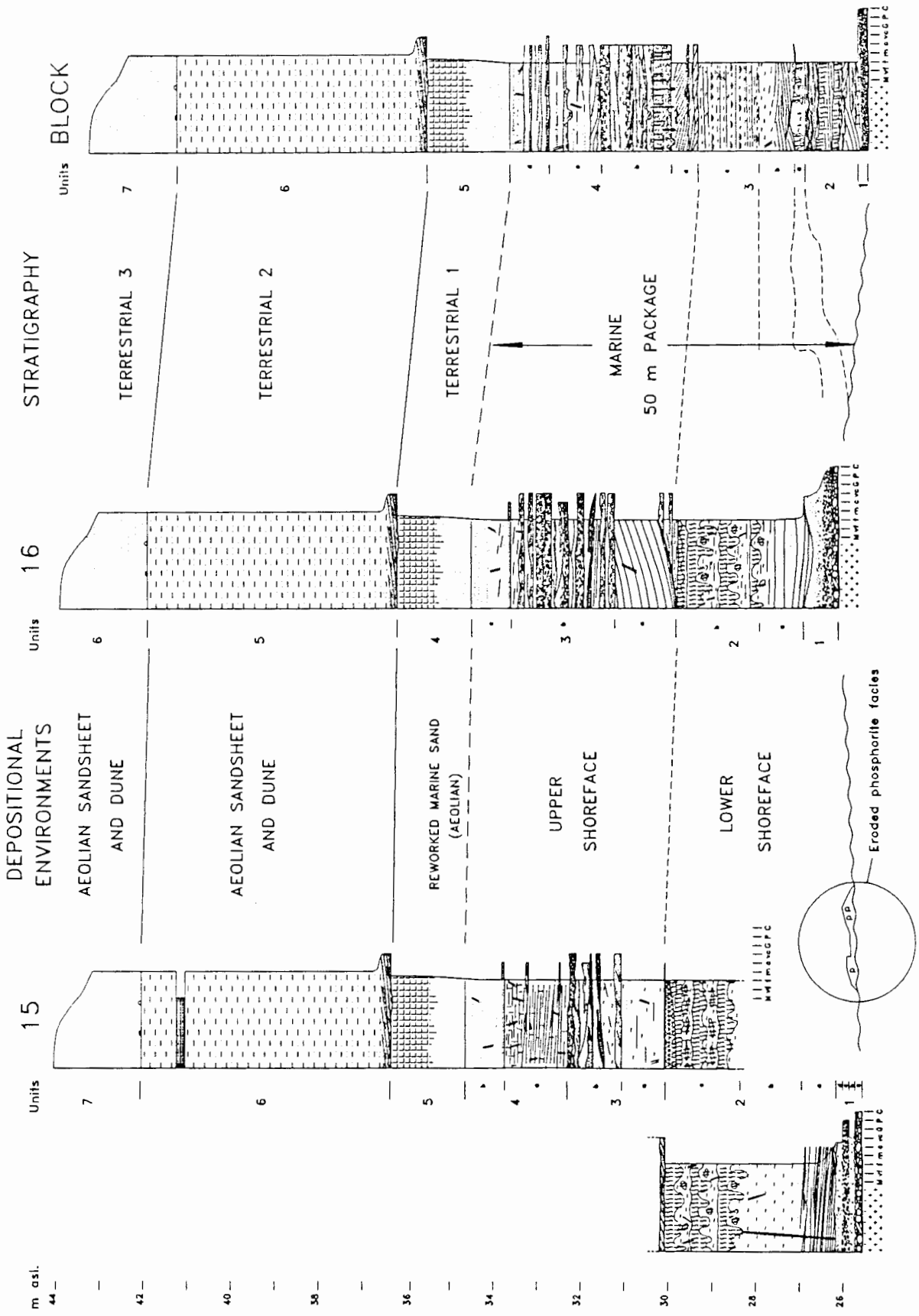

Fig. 12.4 Depositional environments and stratigraphy in AV T2/T3.

The extensive exposures in other excavations on Avontuur-A also consist of proximal shoreface deposits. Similarly, the basal gravels are revealed as proximal, lower-shoreface storm-gravels. The marine deposits at all exposures on Avontuur-A relate to a single regression and therefore form a single stratigraphic unit of formation status (Fig. 12.4). Where shells are preserved, the main shell beds were deposited in the lower shoreface during storms. The shell beds therefore "sample" the fauna generally available from intertidal to lower-shoreface depths. Although moderately diverse, the storm shell-bed faunas form a single biostratigraphic assemblage. The presence of *Donax haughtoni* Carrington and Kensley, 1969, in the Avontuur-A exposures, enables the regressive formation to be identified with their "45-50 m Transgression complex" (Carrington and Kensley, 1969). The "transgressive complex" must now be regarded as a regressive unit. The "45-50 m" elevations refer to the maximum altitude that the transgression associated with the marine deposits attained (Carrington and Kensley, 1969). Accordingly, the "45-50 m" regressive deposits should extend seawards from the transgressive maximum around 45-50 m asl. In the study area, the altitude of the transgressive maximum cannot be confirmed, as extensive exposures are not present at those elevations. The highest-elevation exposure in the study area is a small trench on the Ryskop part of Avontuur-A at ~50 m asl (Fig. 9.1). Within the shallow trench in the pedogenic profile, large, tabular boulders appear to have been deposited on the face of a prograding foreshore closely overlying the bedrock (Plate 12.4). It is reasonable to assume that this foreshore is related to the extensive regressive deposits farther down-dip. The apparent foreshore deposit at ~50 m asl. is consistent with a transgressive maximum near that elevation, but it cannot be proved as the actual transgressive maximum. In order to establish the altitude of the transgressive maximum unequivocally, it is required to locate the landward limit of the regressive foreshore deposits where they overlie older, truncated deposits, preferably terrestrial in origin.

It is necessary rename the "45-50 m Transgression complex" of Carrington and Kensley (1969), in order to reflect the new observations. This has been done (Pether, 1986a) and the name "50 m Package" is now in use for this regressive marine formation (Fig. 12.4). *Donax haughtoni* remains the prime zone fossil of the formation and the 50 m asl. maximum altitude of the associated sea-level cycle is still primarily dependent on the observations of Carrington and Kensley (1969).

After seaward progradation of the 50 m Package palaeoshoreline, aeolian processes reworked the top of the marine sequence, destroying its upper portion and redepositing a thin unit of reworked marine sand that was subsequently subject to pedogenesis. At the AV T2/T3 locality, the intertidal, foreshore deposits were mainly removed. At all the other localities within the bedrock embayments to the north and east of AV T2/T3 on Avontuur-A, the deflation of the top of the marine sequence has been more severe and the upper-shoreface facies has also been extensively removed, except for traces of its lower part in places. The unit of reworked marine sand and its associated pedogenic profile represents the initial terrestrial unit overlying the 50 m Package (Fig. 12.4, Terrestrial 1).

The erosion of the upper part of the marine sequence has removed the contact between the swash cross-stratified foreshore and the cross-stratified upper shoreface. This foils the accurate estimation

of sea-level elevation when the palaeoshoreline passed over the AV T2/T3 area. Assuming that the observations made on the high-energy coast of Oregon are applicable (Clifton *et al.*, 1971; Hunter *et al.*, 1979), the palaeodepth of the lower contact of the upper shoreface facies would have been about 4 to 6 m.

It seems reasonable to suggest that sea-level was at ~36 m asl. when the palaeoshoreline prograded over the AV T2/T3 area. From the palaeoshoreline at ~50 m asl., sea-level dropped about 10 m for every ~1 km of progradation.

The main period of terrestrial deposition on Avontuur-A is represented by the **brown, massive, muddy, medium-grained sand facies** (Fig. 12.4, Terrestrial 2). This an amalgamated record of aeolian sand sheet and dune deposition, with some small-scale aqueous deposition and punctuated by periods of pedogenesis that "weld" the record into an apparently nearly-homogeneous unit. The **modern, unconsolidated aeolian sand facies** (Fig. 212.4, Terrestrial 3) is the youngest potential addition to the top of unit Terrestrial 2.

The **eroded phosphorite facies** is unaccounted for in the stratigraphy of the Avontuur-A exposures. The phosphorite is an important focus in the next excavation to be described (Zone 4A).

Plate 12.4 Exposure at ~50 m asl. in a small trench on Ryskop, showing imbricate, large, tabular boulders probably deposited on the foreshore. Person for scale.

CHAPTER 13

THE ZONE 4A EXPOSURES AND CONTEXT OF PHOSPHORITE DEPOSITION

13.1 SETTING

The Zone 4A excavation is on Hondeklip and is situated well within the deep, south-facing embayment produced by the ancient fluvial channel and the associated bedrock ridge that forms its seaward flank (Fig. 13.1). Having established in the preceding chapter that the deposits overlying the Avontuur-A bedrock gradient represent a prograding, regressive palaeoshoreline during a falling sea-level, it is useful now to view the setting of 50 m Package deposition in terms of the interactions of the falling sea-level, the processes of shoreline progradation and the bedrock topography.

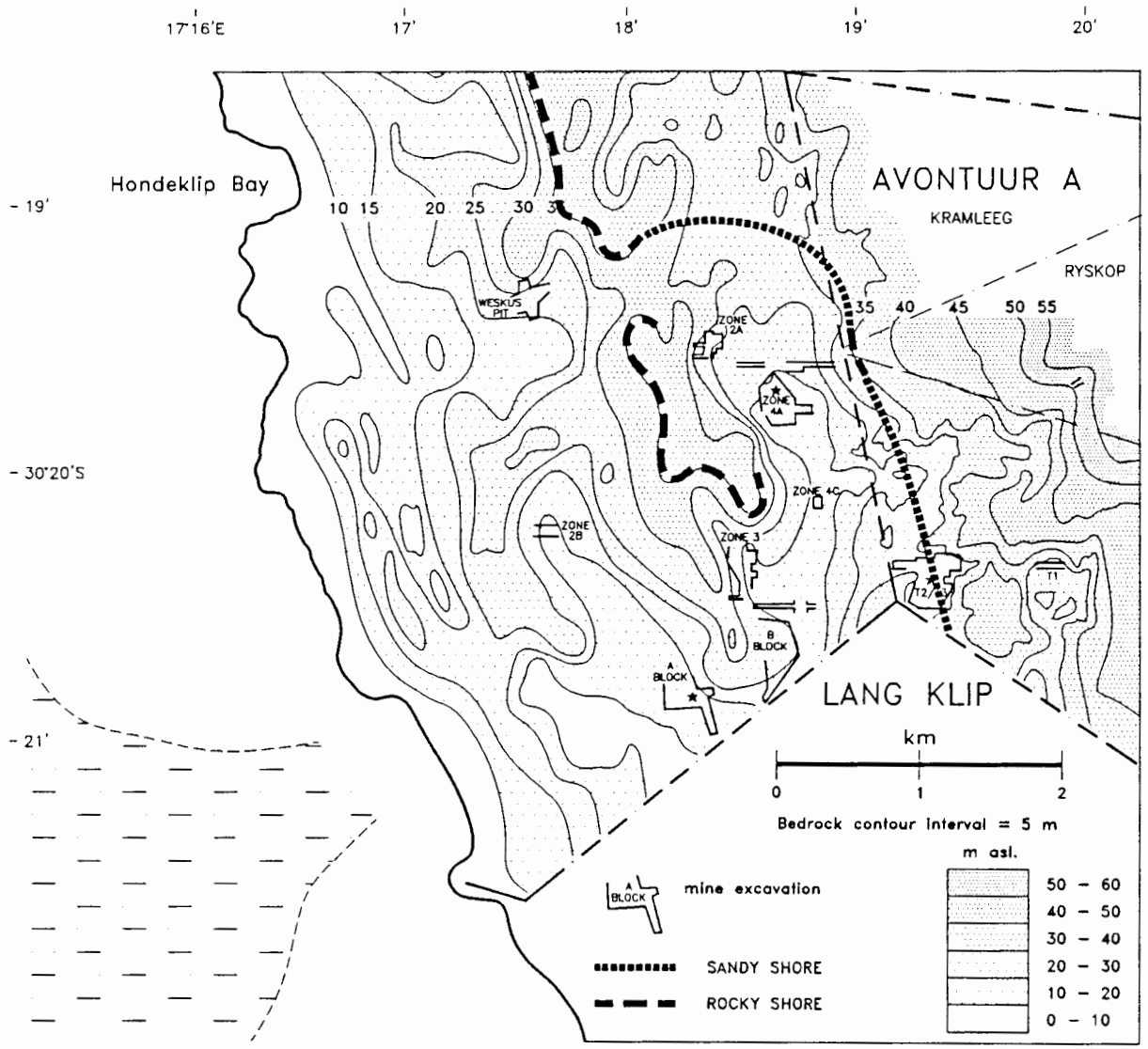

Figure 13.1 Simple palaeogeography at the time when the main bedrock ridge was just emergent.

At the time when the 50 m Package palaeoshoreline was situated at ~50 m asl., the main bedrock ridge would have been a large, offshore reef with its crest in ~15 m water depth. Storm wave activity would have regularly swept its crest free of sediment and the reef-crest environment could be viewed as an offshore "hardground" at this stage. As sea-level dropped from 50 m asl., the shallowing bedrock ridge would have increasingly functioned as a barrier to incoming wave energy. The prograding shoreline to the east of the ridge on Avontuur-A would have undergone a progressive decrease in incident wave energy. By the time the palaeoshoreline was at ~36 m asl. over the AV T2/T3 locality, the main bedrock ridge would have been just emergent and a "new," rocky palaeoshoreline on the seaward flank of the emerging headland would have been in the process of being established (Fig. 13.1). By this stage, the Zone 4A locality can be expected to have an initial regressional record consisting of lower-shoreface storm deposition.

13.2 SECTION 5

Section 5 (Fig. 13.2) is situated in the centre of the Zone 4A excavation and overlies groundwater-saturated, deeply-weathered, green (~5Y 4/3), micaceous, finely foliated gneissic bedrock. After exposure the weathered bedrock effloresces yellow sulphates and this is due to the oxidation of finely-disseminated pyrite in the micaceous clay. Thin "laminae" of fine-grained pyrite are present in jointing planes, along with carbon. The initial, conglomeratic part of the section (units 1-3) was described from a N-S orientated exposure beside a sump cut into bedrock. The remainder of the section was described on a north-facing, E-W orientated face ~10 m to the south.

UNIT 1

A bed of phosphorite rock, ~1.0 m thick. Two sub-units are present. Sub-unit 1a is a an olive-grey, muddy, cemented phosphatic rock with abundant shell moulds and with scattered, matrix-supported, rounded, quartz pebbles, granules and coarse sand. Sub-unit 1b is a dark-brown (chocolate-brown), sandy (quartzose) phosphorite rock containing quartz cobbles and pebbles and the moulds of shell fragments. Distinctive invertebrate and vertebrate faunas are associated with the unit.

Sub-unit 1a: — The lower contact is flat and sharp on the weathered bedrock and has a small-scale relief of a few cm (Plate 13.1). The sub-unit is 0.4-0.7 m thick, the variation in thickness due to the undulating upper contact. Overlying the lower contact is a cemented "rind," 1-3 cm thick, of yellow-brown (10YR 5/8), ferruginous material with sparse quartz granules and coarse sand and mica. The latter suggests that this is a horizon of mixed weathered bedrock and deposited sand. Overlying the rind is a 10-20 cm thickness of light yellow-brown (2.5Y 6/4), soft mud. Sparsely scattered in the mud are Fe-oxide-coated, rounded, small, quartz pebbles, together with matrix-supported coarse sand grains and granules. Above the soft horizon the sandy mud bed is cemented, but crumbly, and is olive-grey (~5Y 6/2), with abundant shell moulds and matrix-supported, rounded, small to medium-size, quartz pebbles, with scattered quartz granules and coarse sand. Notably, small, rounded, chocolate-brown phosphorite pebbles are very sparsely scattered in the sub-unit.

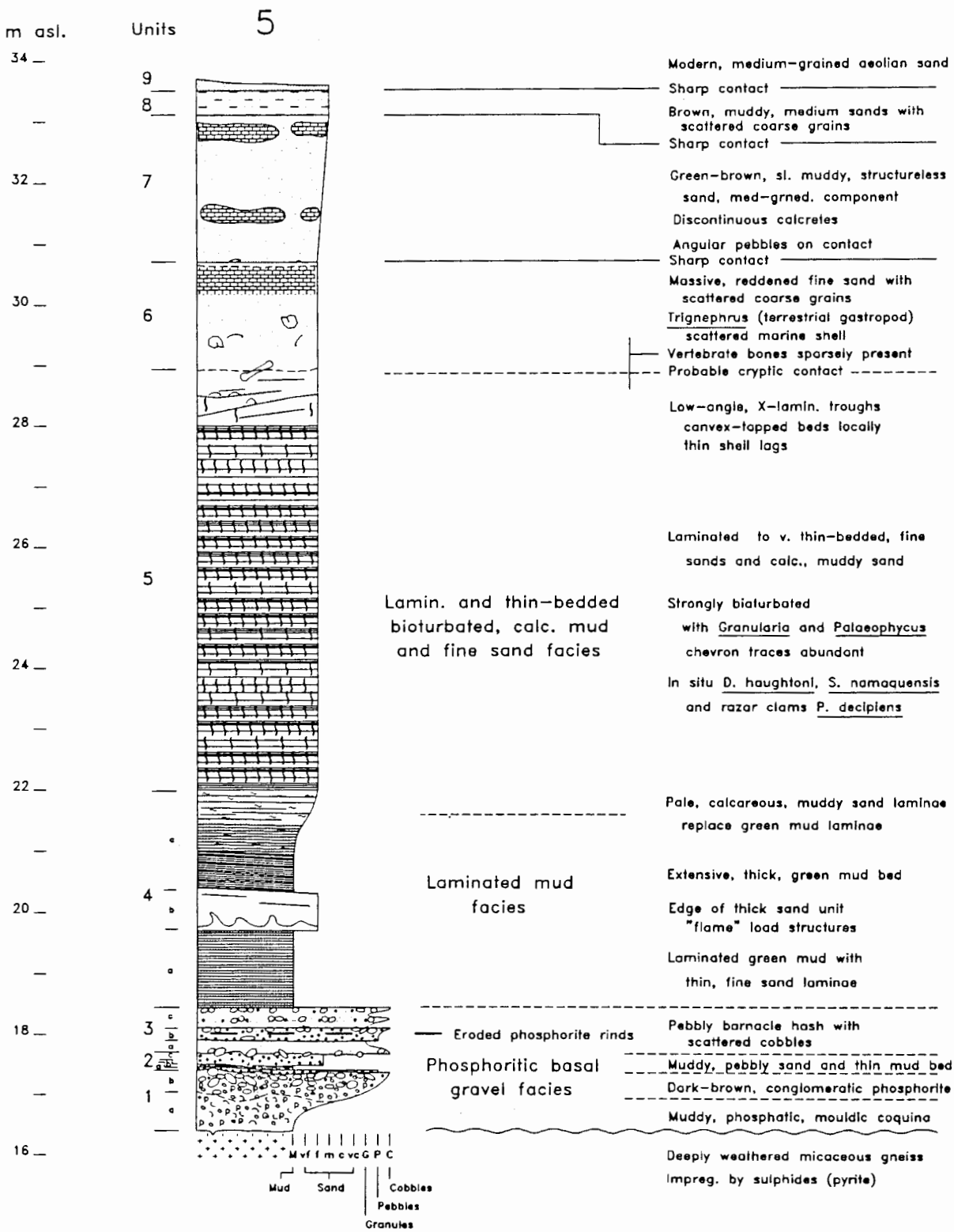

Figure 13.2 Section 5, graphic log.

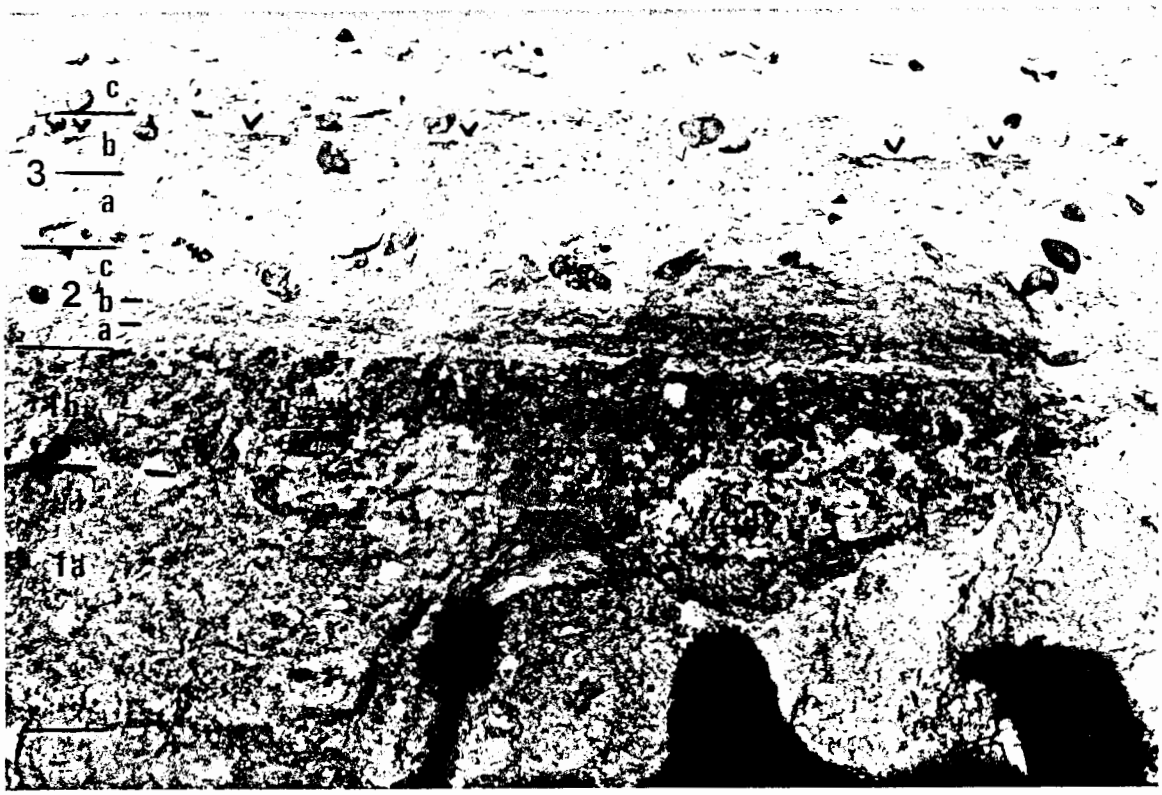

Plate 13.1 Section 5, units 1, 2 and 3. Phosphorite rinds in sub-unit 3b arrowed. North is left. Scale in cm.

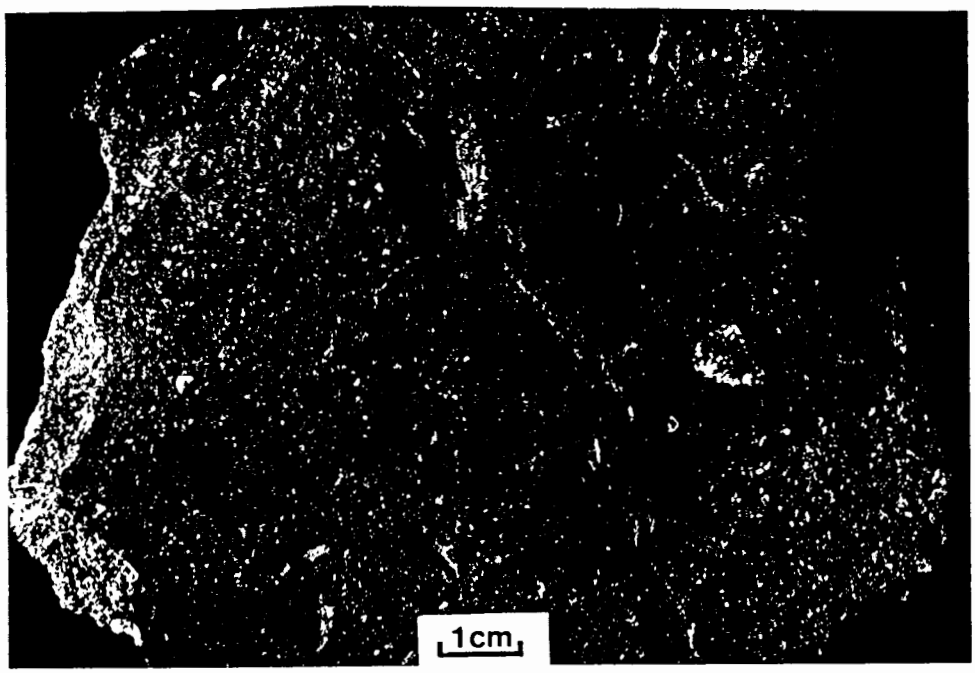

Plate 13.2 Section 5, sub-unit 1. Eroded top of the dark-brown phosphorite. Note truncated shell casts and protruding pebbles.

Sub-unit 1b: — The contact between sub-unit 1a and sub-unit 1b is undulating and defined by an abrupt colour and textural change to dark, chocolate-brown (7.5YR 4/2) phosphorite (Plate 13.1) of the type broadly distributed as clasts throughout the study area and also present as abraded, *in situ* crusts on bedrock and large boulders in every excavation. An erosive contact between the two sub-units cannot be identified with precision and it seems to have been obscured by brown-coloured phosphatization of the uppermost few cm of sub-unit 1a. However, an erosive contact is indicated by the larger quartz clasts included in sub-unit 1b. Sub-unit 1b contains sub-angular to rounded, quartz cobbles and small to large pebbles, whereas scattered small pebbles occur in sub-unit 1a. The clasts are mainly supported in the phosphorite matrix, but clast-supported cobble and pebble clusters are locally present. The dark-brown, sandy phosphorite irregularly fills the interstices between clasts. In places, interstices are filled with non-phosphatic, sandy mud and appear to represent simple infiltration of such material into the open interstices. The sand in the phosphorite is poorly sorted, with scattered rounded granules and coarse sand grains. Fe-oxide staining is pervasive on quartz clasts and in cracks in the phosphorite.

The shell content, like that in the underlying bed (sub-unit 1a), is mainly mouldic, but the moulds are of fragmented shell, while those in the underlying bed are noticeably of many more, relatively intact shells. The moulds of small barnacle fragments are ubiquitous and many of the moulds contain vestigial traces of degraded shell. The irregular moulds of the small barnacle fragments impart a coarse porosity to the phosphorite material. The "density" of the phosphorite material is very variable. Different generations of phosphorite deposition are apparent by the crude, irregular layering of phosphorite with differing sand and mouldic shell-fragment content. However, in other places the phosphorite material appears more developed and denser without crude layering, as if by downward penetration. The dense phosphorite is best developed at the top of the bed (Plate 13.2). Plate 13.2 illustrates the variable porosity and density of the phosphorite. The infillings of shell moulds tend to be "more pure" (non-porous and non-sandy) than the surrounding phosphorite. Some phosphorite-filled shell moulds have vestigial shell structure, indicating that replacement processes may have been active, as well as apparent deposition. The chocolate-brown phosphorite has an eroded upper surface on which the truncated phosphorite infills of shells can be distinguished . Quartz clasts project from the surface and on some granules, slight bevels produced by abrasion can be seen. A fortuitous break in a specimen of phosphorite reveals the presence of a smoothed, eroded surface within the bed, a few cm below its eroded top.

A large, vertical thin section from the chocolate-brown phosphorite bed clearly illustrates the successive generations of phosphorite deposition (Plates 13.3, 13.4). The X-ray fluorescence analyses of phosphatic sediments are presented in Table 13.1. Sub-unit 1a, has a surprisingly high P_2O_5 content of ~30%, a high carbonate (CaO) content and a low SiO_2 content reflecting its muddy, micritic nature and low siliciclastic content (Table 13.1, col. 1). The dark-brown phosphorite from Zone 4A (sub-unit 1b) and the eroded, dark-brown phosphorite crust from AV T2/T3 are very similar in composition (Table 13.1, cols. 2 and 3). The dark-brown phosphorite is poorer in carbonate and phosphate than the pale, muddy, mouldic coquina, but it has a greater siliciclastic content.

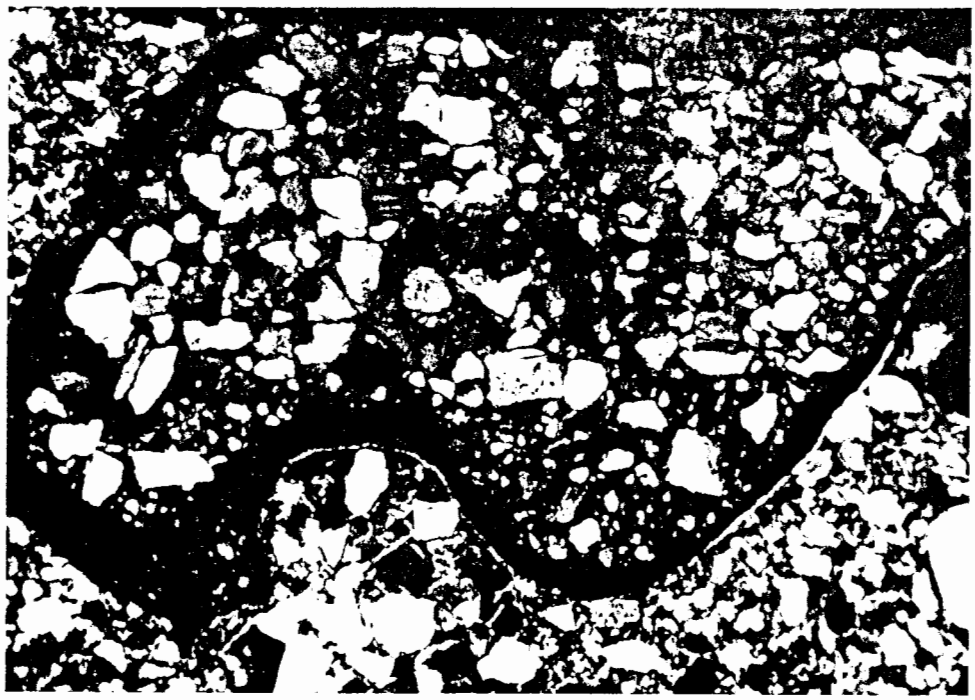

Plate 13.3 Section 5, sub-unit 1b. Vertical thin section showing two generations of phosphorite deposition. XPL, field of view is 2.5 mm.

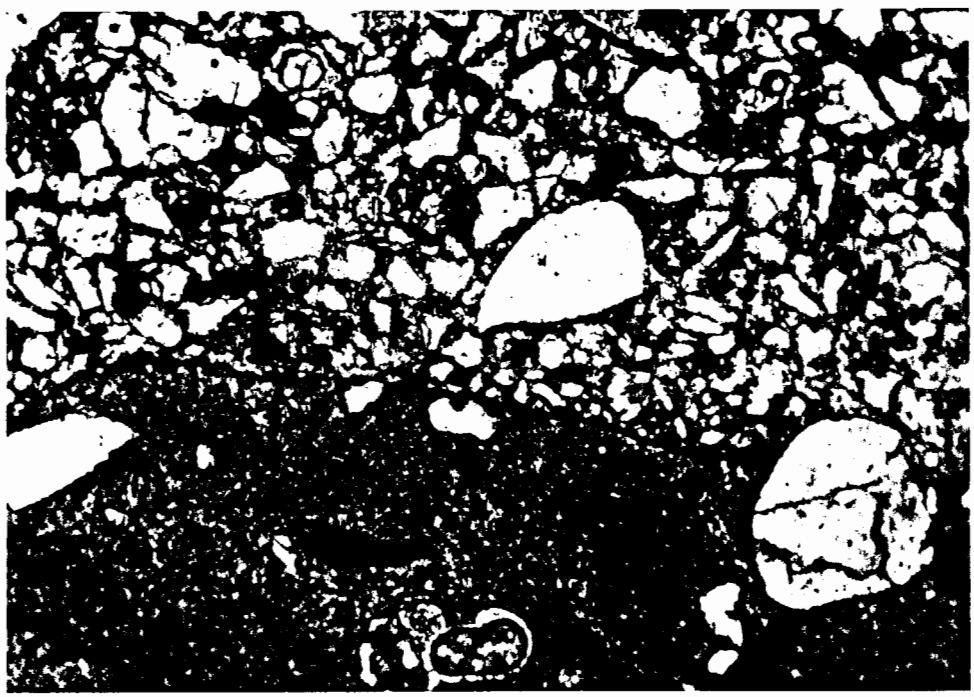

Plate 13.4 Section 5, sub-unit 1b. Vertical thin section showing two generations of phosphorite deposition. The earlier, grain-poor phosphorite may have been eroded (protruding grain on right). PPL, field of view is 2.5 mm.

Faunal notes: — The best-preserved shells in the mainly mouldic coquina of sub-unit 1a are abraded *Crassostrea* and brachiopod valves. Although only moulds of most of the shelly fauna in sub-unit 1a are available, a distinct assemblage differing from that normally observed in shoreface deposits can be discerned. Moulds of coral of the genus *Schizoculina* are a striking feature. These are moulds of broken branches, 1-2 cm in diameter and several cm in length. The unusual taxa include the bivalves *Glycymeris* and *Isognomon.* The internal casts of an unidentified, small tellinid bivalve, *Macoma* sp., are very common and occur in an articulated condition . Among the gastropods, moulds of *Turritella* are noticeable. Moulds of a small, delicate tusk-shell (scaphopod), *Dentalium* sp., occur.

Table 13.1 XRF analyses of phosphatic sediments from Zone 4A (1, 2) and AV T2/T3. (3).

	1	2	3
	olive-grey	dark brown	dark-brown
SiO_2	8.33	30.77	39.09
TiO_2	0.12	0.37	0.14
Al_2O_3	2.26	2.95	3.08
Fe_2O_3	2.64	4.37	1.52
MnO	0.16	0.08	0.03
MgO	0.5	0.72	0.36
CaO	46.83	31.16	29.32
Na_2O	0.57	0.95	0.77
K_2O	0.58	1.08	1.17
P_2O_5	30.31	18.76	19.29
H_2O-	0.83	0.96	0.49
LOI	6.27	7.95	4.81

The common occurrence of dark-brown, bone pebbles in the basal marine gravels has been noted. In Zone 4A the phosphate-mineralized bone clasts are most abundant. These are found embedded in sub-unit 1b, but much rolled bone also occurs in the overlying gravels of units 2 and 3. Both marine and terrestrial vertebrates are represented. Cobble- to small-boulder-size vertebrae and rib fragments of large cetaceans (whales) are the most common bones. Large (up to ~20 cm long), peg-like teeth (cf. sperm whales) are common and obviously come from an extinct species. The distinctive, curled earbones of whales are also found, as well as occasional skull fragments. Some examples of the vertebrae and teeth do not seem to have undergone much abrasion. Shark teeth, including the teeth of the giant Mio-Pliocene shark, *Carcharodon megalodon*, are more abundant than elsewhere in the

study area. A variety of other presumed fish teeth occur and include the curious pharyngeal grinding plates of an extinct wrasse, *Labrodon*, described from the Eocene of Bogenfels (Böhm, 1926).

The terrestrial vertebrate fossils are dominated by the molar and tusk fragments of extinct, primitive proboscideans (elephants) of the family Gomphotheridae. Next in abundance are teeth and limb bones of rhinoceros. One tooth has been identified by Dr. Q.B. Hendey as the extinct rhino *Ceratotherium praecox.* Teeth of the ancestral horse, *Hipparion*, have been found. The bones also include unidentifiable bovid bones (buffaloes, antelopes) and a possible palaeotragine (extinct giraffid). Rarer finds include "fin" bones of seals. A carnassial tooth of a creodont (primitive carnivore) was found. The limb bone of a giant ostrich, remarkably larger than that of the extant species (*Struthio* sp.), was also found.

UNIT 2

A unit, ~0.3 m thick, consisting of three sub-units. Sub-unit 2a is a thin, sandy and pebbly bed capped by a phosphorite lamination. Sub-unit 2b is a thin, burrowed, mud bed. Sub-unit 2c is a slightly-muddy, fine-sandy bed with scattered pebbles.

Sub-unit 2a: — Overlying the eroded top of the phosphorite bed is a partly matrix-supported, thin bed (3-8 cm thick) of rounded, small and medium-size quartz pebbles, rounded quartz granules and very coarse sand in a matrix of green, muddy fine sand. Irregularly-shaped phosphorite clasts with rounded edges are sparsely scattered in the bed. Laterally the bed becomes shell-rich, but the shells are mainly the right (upper) valves of *Crassostrea* and brachiopod valves. The valves are in convex-up orientation. The top of the bed is draped by a lamina of dark-brown phosphorite, 1-5 mm thick.

Sub-unit 2b: — An olive-green (5Y 4/4), thin bed of mud, 4-8 cm thick, which is strongly bioturbated by unlined burrows, ~0.5 cm in diameter, that are filled with yellow fine sand. In all respects the burrows resemble *Planolite montanus*, but the contrast between the burrow fills and the host sediment is marked, as if the burrow-filling sand was piped down from above. This bed was eroded, producing a relief of ~1 cm and unroofing the *Planolites* burrows.

Sub-unit 2c: — Overlying the sharp contact is a slightly muddy, fine-to medium sandy bed with finely-comminuted shell and scattered, well-rounded, small quartz pebbles and coarse sand. The pebbles are slightly more abundant in the lower part of the bed. An isolated, tabular cobble overlies the lower contact. The top of the bed is eroded and the contact is very irregular, with relief of up to 10 cm (Plate 13.1).

UNIT 3

A thick bed (~0.6-0.8 m thick), mainly of fragmented shell of barnacle origin (barnacle hash), with pebbles and scattered cobbles. Three sub-units are defined, with the central sub-unit being more pebbly than the underlying and overlying sub-units. Eroded remnants of a dark-brown phosphorite rind occur in the central sub-unit.

Sub-unit 3a: — Scattered along the irregular contact are rounded, tabular and discoidal, small cobbles and large pebbles of quartz and local rock, together with irregularly-shaped cobbles and pebbles of phosphorite (Plate 13.1). Some clasts straddle the contact and appear to have been driven into it. An indication of imbrication is present and involves the isolated clasts straddling the contact. These exhibit dips in a northerly direction. Several tabular to discoidal cobbles in the remainder of the unit exhibit similar dips varying through NW to NE. Overlying the contact is a bed, ~20 cm thick, of sandy shell hash consisting mainly of barnacle fragments, with scattered small, quartz pebbles. A subtle horizon of pebbles and granules in the middle of the bed indicates amalgamation.

Sub-unit 3b: — Overlying an indistinct contact is a bed, ~20 cm thick, of clast-supported, rounded granules to small pebbles, with scattered large pebbles and cobbles, in a barnacle hash matrix. The bed has an upward-coarsening aspect due to the cobbles being more common in the upper portion (Plate 13.1). However, isolated islands of dark-brown phosphorite occur along a horizon in the middle of the bed (Plate 13.1). Their tops are identical to the eroded top of the Unit 1 phosphorite, but the slight bevelling of protruding granules is not observed. Shell fragments in the phosphorite rinds are noticeably dissolved. This feature indicates that sub-unit 3b is also an amalgamated bed. The phosphorite rinds are present laterally in Unit 3, as revealed through the disturbed surface of the bed. There are up to three rinds in vertical succession, foming more extensive slabs than evident at the section site, but these could not be traced laterally.

Sub-unit 3c: — Sharply overlying the previous sub-unit, this ~30 cm thick bed is distinguished by being a less sandy and more well-sorted "purer" barnacle hash than the underlying beds (Plate 13.1). Small pebbles and granules are scattered in the sub-unit. Large pebbles and cobbles occur along a horizon as isolated clasts and small clusters.

UNIT 4

A thick unit (~3.5 m thick) consisting mainly of green, laminated mud and fine sand. A thick bed of structureless, fine sand occurs (sub-unit 4b). Sandy laminae become dominant upwards, defining a coarsening-up trend.

Sub-unit 4a: — Overlying the upper barnacle hash is interlaminated green mud and fine sand (10Y 6/2) forming a 1.2 m thick bed. The fine sand laminae are 1-2 mm thick, separated by muddy laminae 1-10 mm thick. No macrofossils or trace fossils are present.

Sub-unit 4b: — A bed of fine sand (fL), ~0.7 m thick, overlying a sharp contact. It is structureless except for faint *Planolites montanus* mottling. Traced laterally, this sub-unit is seen to be the thin edge of a laterally-extensive, large sand body that thickens eastwards to ~1.8 m ~150 m to the east of the section. Flame structures are common at intervals all along its base. Thin to medium bedding, with faint lamination, is conformable with the broadly convex top of the sand body.

Sub-unit 4c: — Overlying the fine sand bed is a thick (~0.6 m), laminated, green mud bed. It is thickest at Section 5 and along the south wall of the Zone 4A excavation and is laterally continuous around the excavation, providing an important marker horizon. Its elevation rises to the northeast as an increasing thickness of underlying, older sediments is present between it and the basal gravels. Gradationally overlying the mud is inter-laminated fine sand and mud, with moderate bioturbation as sand-filled *Planolites* burrows. The fine-sandy laminae become thicker and more abundant upwards, the green mud laminae "die away" and the uppermost 0.5 m of the sub-unit is mainly slightly muddy, fine sand in which pale, calcareous mud laminae appear.

UNIT 5

A thick unit (~6.5 m thick), consisting of laminated to thin-bedded fine sands and calcareous, sandy mud. Bioturbation is strong.

Unit 5 is distinguished by laminae to thin beds of green, fine sand interbedded with pale, muddy, calcareous laminae (Plate 13.5). Leaching of carbonate occurred preferentially in the fine-sandy beds. Thin, diffuse horizons of comminuted shell occur in places. Bioturbation is strong, extensively distorting the lamination. The burrows are mainly *Palaeophycus tubularis*, *P. 'annulatus'* and *Granularia*, but the formation of dense burrow-clumps, as at AV T2/T3, is not a feature. Small mud pellets (*Tibikoia*) are abundant in the calcareous laminae. Chevron traces are common. *Planolites 'threads'* occurs, but not abundantly. Scattered *Thalassinoides 'multiplex'* systems occur.

Shell fragments occur very sparsely and are mainly of rocky shore taxa (*Crassostrea*, patellids, fissurellids, *Turbo*). *In situ* (life position), juvenile *Donax haughtoni* and *Standella namaquensis* bivalves occur sparsely along horizons. The razor clam, *Phaxas decipiens*, is quite common scattered about in the unit (*in situ*) and a prominent horizon of *in situ* specimens is present (Plate 13.5).

Upwards in the unit, fine-sandy deposition becomes increasingly dominant and muddy, calcareous lamination less prominent. Low-angle cross-lamination fills wide, shallow troughs (~4-6 m long, 10-30 cm thick) and thin layers of shell fragments are more prominent. At the section site, a convex-topped, bar-like bed is present (Plate 13.6). The top of the unit is a gradational contact, but is defined by a rapid colour change to reddened, structureless sediment of a pedogenic profile.

Faunal notes: — As on Avontuur-A, a feature of the transition from marine sediments to the pedogenic profile is the occurrence of vertebrate bones. Although widely scattered and sparse, the bones are noticeably more abundant than on Avontuur-A and occur near the top of the sequence from Zone 12A to Zone 4C (Fig. 13.1). They are also better preserved (less fragmentary) and a clear association with an obscure erosive contact is not present. The bone finds seem to occur in a "zone" about the pedogenic transition. However, when slightly below the main level of the transition, with marine sediments laterally present at the same elevation, at no site could unequivocal marine trace fossils be found intimately between the bones. This suggests an association with a palaeosurface

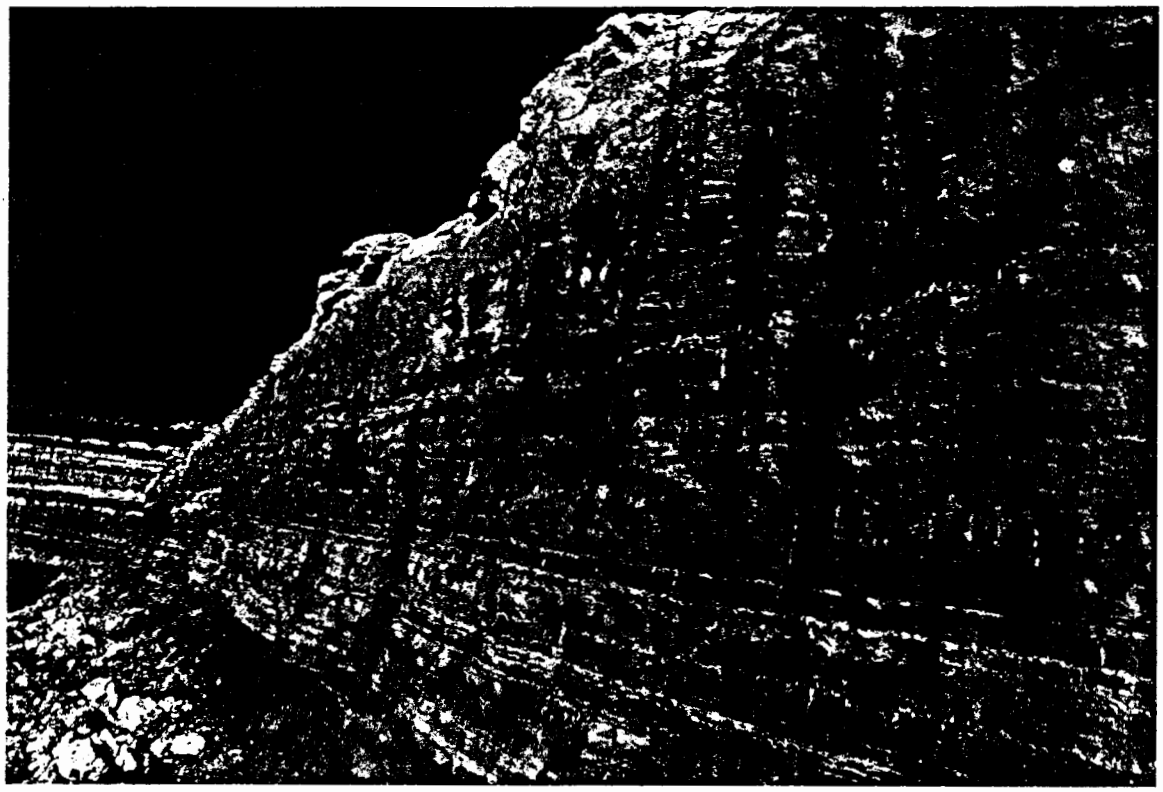

Plate 13.5 Section 5, Unit 5. Laminated to thinly-bedded, bioturbated fine sands and muddy, calcareous sands. Horizon of *in situ* razor clams (*Phaxas decipiens*) arrowed. View is eastwards.

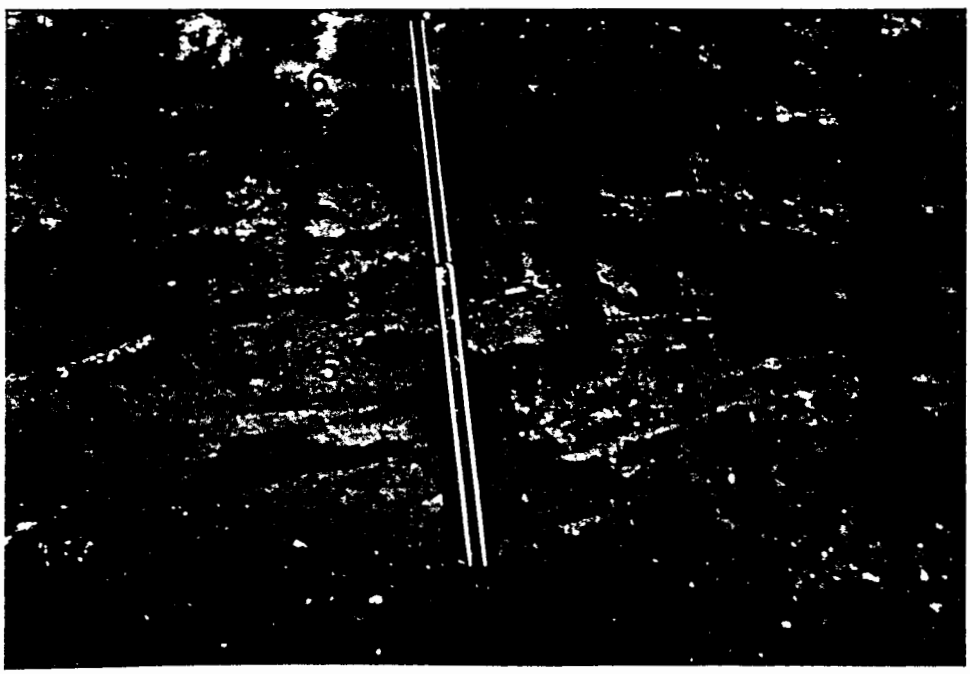

Plate 13.6 Section 5, showing contact between units 5 and 6. North is right. Survey staff for scale.

that is even more cryptic than that on Avontuur-A. The bones also occur in greater concentrations compared with the scattered nature of occurrence on Avontuur-A. The most spectacular bone find is shown in Plate 13.7. This find could be excavated from above, due to its occurrence just below a bench in the excavation. A more typical find is shown in Plate 13.8. Many of the bones show tooth punctures attributable to hyaenas and accumulation in hyaena lairs is the probable origin of the more marked bone concentrations (G. Avery, personal communication, 1984).

It is emphasized that these bones are quite different in preservation from the mineralized and petrified, dark-brown, generally abraded, "bone pebble and cobble" assemblage found associated with basal gravels and phosphorite in the base of the sequence. They are pale, soft and friable and can only be collected by careful exposure and the application of consolidants.

The assemblage consists mainly of post-cranial material and is dominated by the limb bones of bovids, mainly antelopes. Among the cranial material is an undescribed gazelle, *Gazella* sp, possibly ancestral to the springbok (*Antidorcas*), and the steenbok, *Raphicerus*. Limbs and teeth of *Equus* (zebra) are common. Carnivores are well-represented and include the jackal (*Canis mesomelas*), an extinct hyaena, *Hyaena hyaena* cf. *makapania*, and an unidentified felid. Other taxa represented are ostrich (*Struthio*) and tortoises (*Chersina* sp.).

UNIT 6

A reddened pedogenic profile with calcareous nodules and a crudely-laminar calcrete.

The reddened sand is mainly fine-grained (fL), with sparsely-scattered grains of rounded, coarse sand. Juvenile *Crassostrea* shells and shells of the terrestrial gastropod *Trigonephrus* are scattered in the compact, structureless sediment. A crudely-laminar calcrete occurs near the top and is closely overlain by a sharp, erosive contact.

UNIT 7

Green-brown structureless, slightly muddy sand with calcrete horizons.

Angular pebbles occur sparsely along the lower contact. The green-brown sediment is noticeably more medium-grained than the underlying sands and has sparsely-scattered grains of rounded, coarse sand. The slight mud content is probably pedogenic in origin. Two dense calcretes occur in the unit and their sharp boundaries and discontinuous, slab-like aspect hint at possible dissolution at some stage.

UNIT 8

Medium-grained, structureless sand with scattered coarse grains and an intergranular mud content.

A unit, 0.4 m thick, of aeolian sand with pedogenic mud. The contact with the underlying unit is sharp.

Plate 13.7 Accumulation of bones (*Equus* and bovids) in the top of marine sequence just south of Zone 4A. Scale in cm.

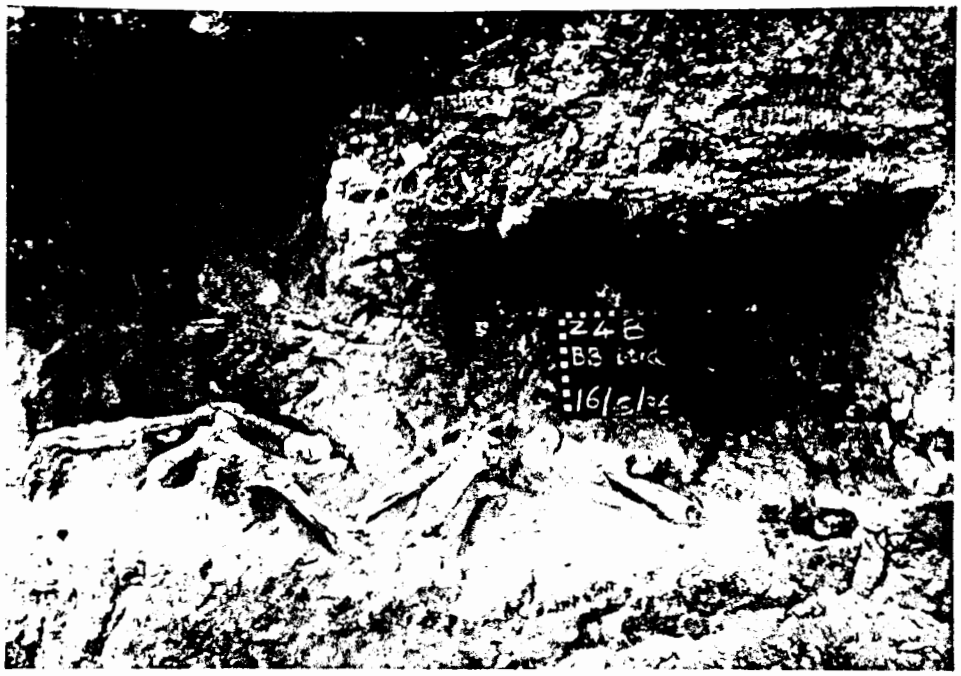

Plate 13.8 Bones on cryptic palaeosurface in the pedogenic profile. Site just south of Zone 4A. Scale in cm.

UNIT 9

The *modern, unconsolidated aeolian sand facies.*

The modern aeolian sands are very thin at this locality.

13.3 THE SEDIMENTARY GEOMETRY OF ZONE 4A

The sections measured in Zone 4A are basically similar and the differences that are present relate to the broader sedimentary geometry of the infilling of the embayment. The basal phosphorite and overlying gravels (Section 5, units 1, 2 and 3) also exhibit important lateral changes. A series of "mini-sections" through the basal gravels were measured in exposures provided by grade-testing trenches made prior to mining. The location of the transects is shown in Fig. 13.4. These lateral variations and the overall geometry of the Z4A excavation are summarised schematically in Figs. 13.3 and 13.4.

LATERAL VARIATION OF THE BASAL GRAVELS

The N-S transect lies along a N-S channel in the bedrock that is ~1.5 m lower than the elevation of the bedrock to the immediate east. The W-E transect proceeds from the bedrock low, onto the higher bedrock to the east (Figs. 13.3, 13.4). Northwards from the site of Section 5 (Fig. 13.3, lower panel left), the cemented, muddy mouldic coquina (sub-unit 1a) disappears and the concentration of quartz pebbles increases. From halfway along the N-S transect, sub-unit 1a is a clast-supported, sub-angular to rounded, quartz pebble gravel with a soft, muddy matrix. However, the muddy matrix is similar in hue to the mouldic coquina, being pale green to pale brown. Darker green, micaceous matrix in the lowermost part shows the mixing-in of decomposed bedrock. Notably, irrregularly-shaped clasts of dark-brown phosphorite occur at the base, along with bone pebbles.

The dark-brown phosphorite interstitial to sub-unit 1b also disappears northwards (Fig. 13.3, lower panel) and in its place is pale, muddy matrix like that in the underlying bed. Halfway along the N-S transect, sub-unit 1b is clast-supported and the only dark-brown phosphorite that can be recognized is a thin crust on the top of the bed. This is absent farther north. The sub-unit maintains its character as a cobble gravel capping Unit 1, but other than the disparity of clast sizes, the contrast between the sub-units seen at the section site has disappeared. Traced east out of the bedrock low (Fig. 13.3, upper panel), the two sub-units become indistinguishable, the clast size rapidly dwindles to small pebbles, becomes matrix-supported and in the east the unit becomes a muddy, mouldic coquina like that at Section 5.

From Section 5 along the transects, the muddy unit (Unit 2) maintains its character as a structureless, slightly muddy, sandy bed with scattered small pebbles. The eroded, laminated mud near its base (sub-unit 2b) is only present at the section site. Unit 2 thins and pinches out along the X-Y transect (Fig. 13.3, upper panel). Just before pinch-out interlaminae of mud appear. Due east of Section 5

(not on a transect), Unit 3 directly overlies the phosphorite top of Unit 1.and Unit 2 has also pinched out. Unit 2 is confined to the bedrock depression.

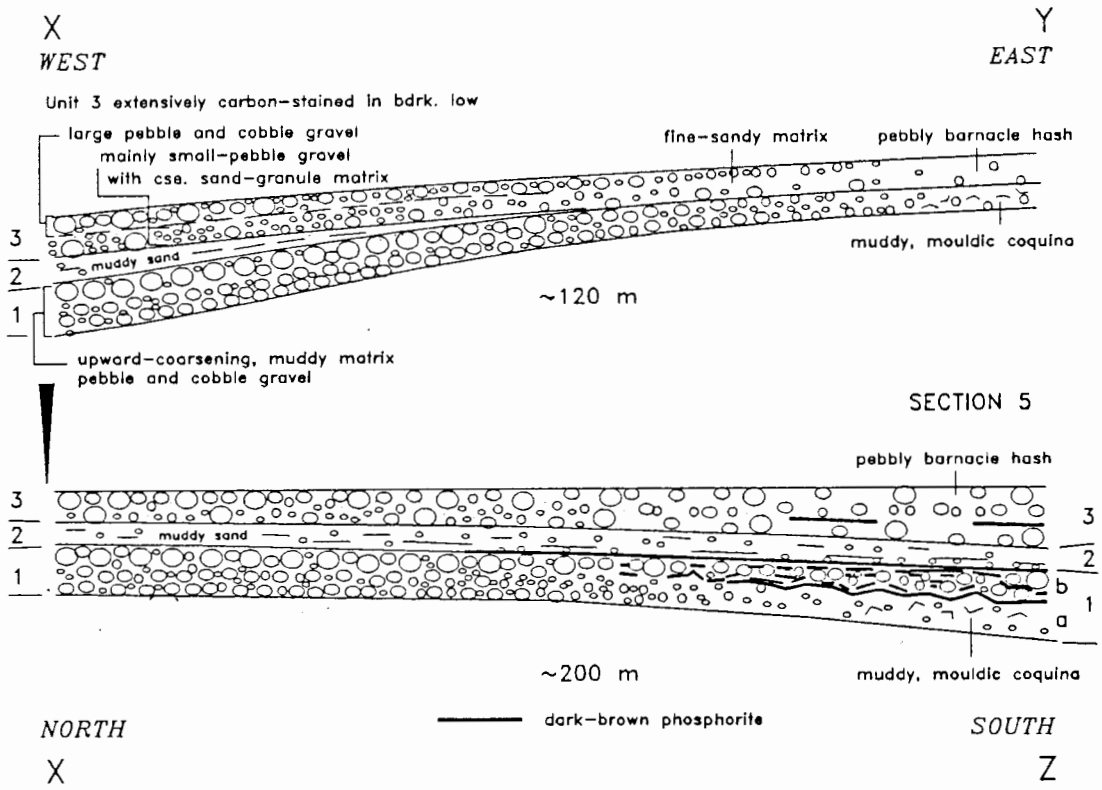

Figure 13.3 Zone 4A. Lateral variations of units 1-3. Locations of sections in Fig. 13.4.

Northwards from Section 5, the phosphorite rinds in Unit 3 are no longer found (Fig. 13.3, lower panel). The bulk of the unit changes gradationally from a barnacle hash to a very-coarse-sandy, well-rounded, granule and small pebble gravel and a well-defined, capping cobble bed is developed. The basal contact, with isolated and clustered pebbles and cobbles, maintains its character throughout the transects. Eastwards from the bedrock depression (Fig. 13.3, upper panel), the unit thins only slightly as it laps onto higher bedrock, but the bulk of the unit becomes increasingly sandy and clast-size decreases, until in the east it is a barnacle hash with scattered pebbles. In the area around point X, Unit 3 is extensively carbon-stained.

GEOMETRY OF THE EMBAYMENT FILL

At Section 5, in the northwestern corner of the excavation, a thick unit of laminated mud (Unit 4) overlies the barnacle hash (Unit 3) (Fig. 13.2) (Plate 13.9) and mud deposition was interrupted by the deposition of the thick, lenticular body of fine sand (sub-unit 4b). In contrast, in the northeastern corner of the excavation, the barnacle hash of Unit 3 is overlain by interbedded fine sand and thin gravels basal to a thick unit of structureless, fine sand (Plate 13.10). This unit thins westwards (along the northern wall) and southwards (along the eastern wall) and is clearly a wedge of sand that prograded into the embayment at Zone 4A (Fig. 13.4), but did not reach the Section 5 site. This progradational sand wedge is called Unit PW

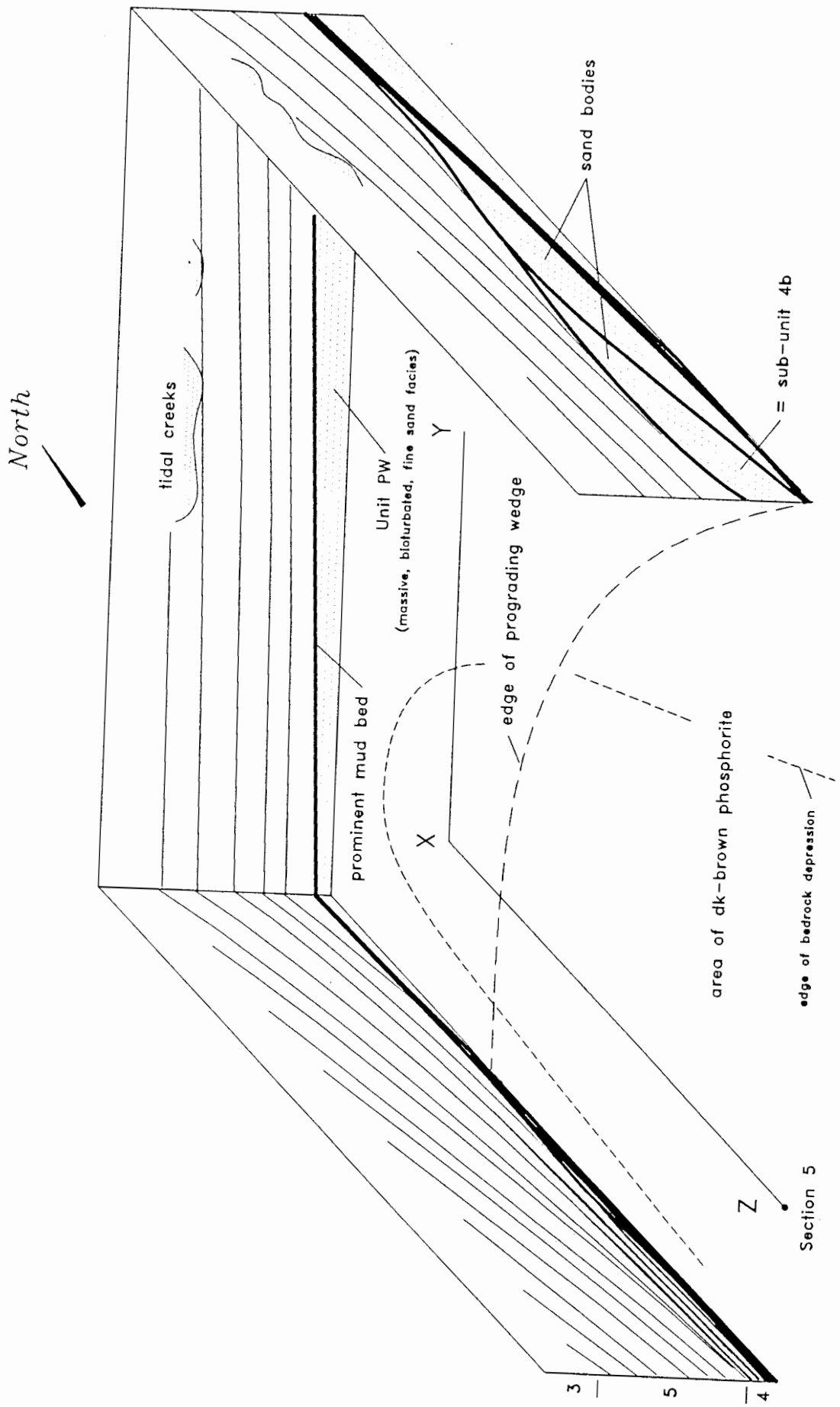

Figure 13.4 Schematic sedimentary geometry of Zone 4A.

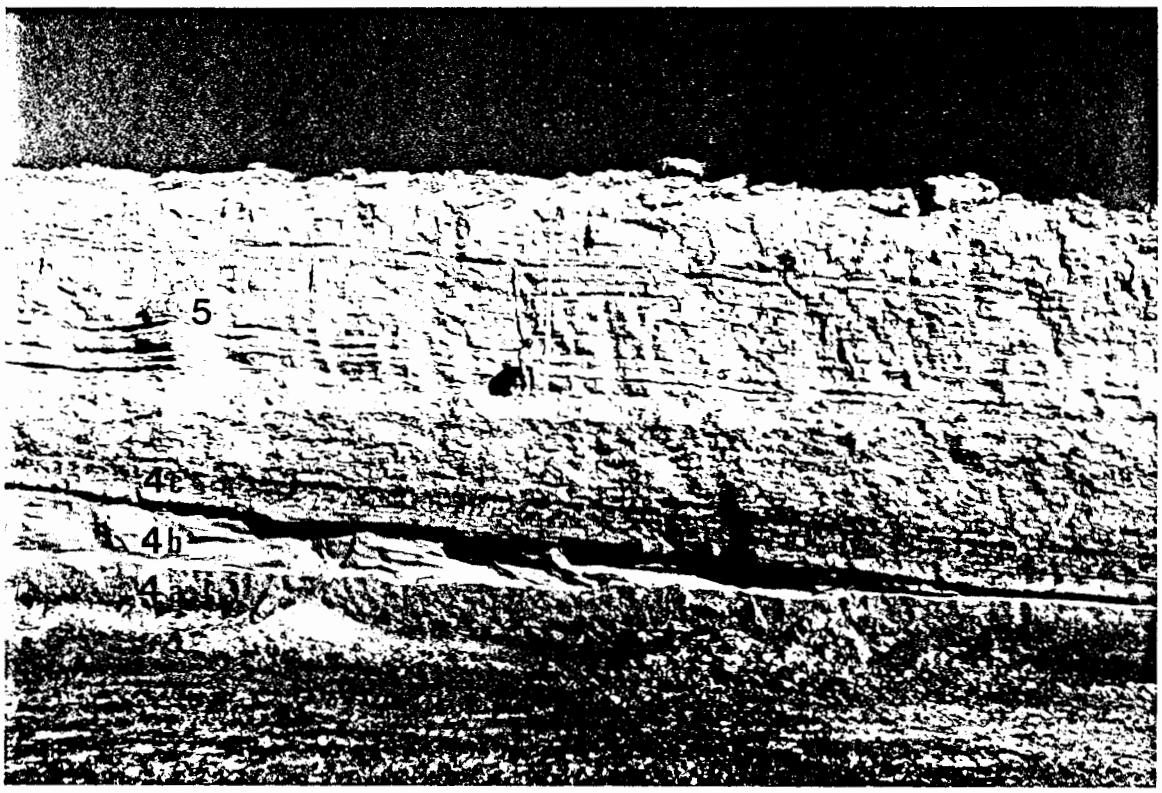

Plate 13.9 Zone 4A, south face, showing thinning edge of lenticular sand body (sub-unit 4b) and overlying, thick mud bed (sub-unit 4c). West is right. Person with survey staff for scale.

Plate 13.10 Zone 4A, northeastern corner, showing Unit PW thinning into embayment. Person for scale.

The structureless nature of Unit PW indicates total bioturbation. The main depositional features are horizons of transported *Crassostrea* shells. Most of these show little abrasion and occur as mutually-attached clusters. Many closed examples, with their upper valves in position, are present. One closed example was still unfilled with sand. The disarticulated, but closely associated, bones of a whale were found in the basal part of Unit PW (Plate 13.11). The mandible of a dolphin was also found in the unit. Progradation of the sand wedge ceased and it was overlain by an inter-laminated mud and fine sand bed that is laterally continuous around the excavation and thickens down the depositional slope towards Section 5.

Around most of the excavation, the mud unit (≈Unit 4) is overlain by the rather uniform facies of laminated and burrowed calcareous mud and fine sand represented in Section 5 by Unit 5. However, along the eastern wall, the mud unit is "split" by the deposition of a large, lenticular body of fine sand (Fig. 13.4). The sand body is flat-based, with a broadly convex top and the bedding shows vertical accretion. Other than the occasional laminae of calcareous mud and faintly-defined low-angle lamination, there is little structure present in the sand body. Load structures occur along the base. After deposition of the sand body, mud deposition resumed, but was interrupted by the deposition of a second, major sand body overlapping the first. Similarly, mud deposition resumed after its formation. This second body can be traced to Section 5, where its thin edge is represented by sub-unit 4b (Plate 13.9). The sand bodies are elongate in approximately the W-E direction.

The sand bodies interbedded with the mud unit clearly show that deposition of the mud unit is strongly diachronous. The origin of the mud unit is best revealed along the western wall of the excavation, where the bedding in Unit 5 dips gently to the south, but slightly steeper than elsewhere (Fig. 13.4). Individual thin beds in Unit 5 can be traced for some distance downdip as they flatten gradually, become more muddy and lap tangentially onto the mud unit, adding another lamina-set to the latter. Thus the main infilling of the embayment locale of Zone 4A took place in a manner analogous to Gilbertian deltaic deposition. The laminated to thinly bedded Unit 5 represents the "foresets," whilst Unit 4 is made up of the muddy "bottomsets" deposited at depth.

The remaining feature of the Zone 4A exposures is the occurrence of the lower parts of erosional channels at a high level in Unit 5 (Fig. 13.4). The bottoms of the channels are filled with coarse sand, shells and barnacle hash. The channel infills fine upwards rapidly and their flanks are then obscure. The fills also fine laterally, so that only one flank is outlined by grain-size contrast (Plate 13.12). Proximity to the pedogenic profile results in obscurity of the upper parts of the channels. Undulating contacts overlain by the the coarse-sandy channel-bottom deposits attest to the lateral migration of the channels.

Plate 13.11 Zone 4A, northeast. Associated bones of a whale in the base of Unit PW. Scale in dm/cm.

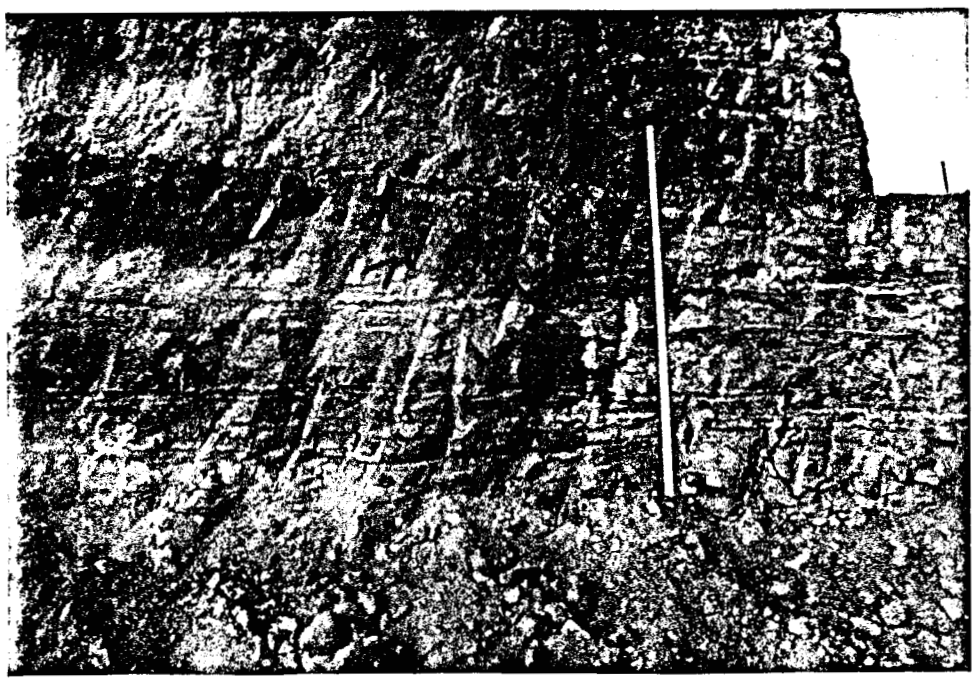

Plate 13.12. Zone 4A, east face. Channel (arrowed) cut into top of Unit 5 and filled with coarse sand and barnacle shell. 4 m staff for scale.

13.4 DEPOSITIONAL ENVIRONMENTS OF ZONE 4A

FACIES DEFINITION

Four facies accommodate most of the marine deposits in Zone 4A (Fig. 13.2). The upper, terrrestrial portion of the section is not discussed in detail. Separate phosphorite facies and basal gravel facies cannot be defined at this site in Zone 4A as the phosphorite is clearly intimately related to the history of the basal gravel. Units 2 and 3 of the basal gravel both have a phosphorite content, albeit minor. Moreover, the interpretations of units 1 and 3 are strongly linked. A **phosphoritic basal gravel facies** is therefore indicated and includes units 1 to 3. Unit PW is a **massive, bioturbated, fine sand facies**. Unit 4 is the **laminated mud facies**. The large, lenticular, sand bodies interbedded with the laminated muds (represented by sub-unit 4b at the section site) are a distinct facies, but these more locally-developed features are not discussed separately. Unit 5 is a **laminated and thinly bedded, bioturbated, calcareous mud and fine sand facies**.

THE PHOSPHORITIC BASAL GRAVEL FACIES

The phosphatic, slightly pebbly, muddy, mouldic coquina: — The initial environment for which evidence is preserved in Zone 4A was probably anoxic to some degree, as suggested by the pyrite- and organic carbon impregnation of the decomposed bedrock. As shown in Fig. 13.3, the mouldic coquina (sub-unit 1a) apparently represents the laterally-fining part of high-energy, conglomerate deposition. The lateral variation of sub-unit 1a is marked and occurs on the scale of a few tens of metres. A similar scale of variation in the overlying Unit 3, which is better exposed than the basal, muddy conglomerate, lends credence to the rapid lateral variation observed in sub-unit 1a. If it is contrarily assumed that the muddy, mouldic coquina was deposited separately from the laterally-adjacent conglomerate, the presence of scattered small pebbles and large shells in the bed remain to indicate relatively high-energy deposition. The concentration of the shell moulds in sub-unit 1a at Section 5 shows that the bed was deposited as a coarsely-shelly coquina. The coquina had an open framework which was subsequently infiltrated by the deposition of mud. This indicates that the coquina was deposited in an environment where the ambient levels of energy were low. The mud was mainly calcareous and was subsequently phosphatized, as shown by the XRF analysis (Table 13.1, col.1).

Although the fauna in the bed is mouldic, a considerable portion of the moulds are readily recognizable. An important component of the fauna is the valves of oysters (*Crassostrea*). These are identified by the relatively large size and "thickness" of the mould, which often contains shell matter. The flat, right valves are mainly seen. This qualitative observation is reliable to the extent that the larger, cup-shaped, left (attached) valves, with their chambered umbos, are also readily recognizable in mould or "semi-mould" form. Numerous plates of barnacles, identified by the casts of their internal canals, can be seen in every hand-specimen fragment of the mouldic bed. Many of these are large plates (~0.5-2.0 cm), consistent with the coarse-shelly nature of the coquina. Kraussinid brachiopod moulds are also readily identified by their shape and ribbing and are abundant. Parallels may be

drawn with the closely overlying sub-unit 2a, which contains shell that consists practically exclusively of the flat, upper valves of *Crassostrea* and flat brachiopod (*Kraussina*) valves. Although not a barnacle hash like Unit 3, sub-unit 1a was nevertheless very rich in barnacle shell.

Oysters, barnacles and brachiopods are abundant and ubiquitous in the shell beds of the shoreface deposits that comprise practically all of the marine sediments of the study area. Despite their abundance in the mouldic coquina, it is immediately clear from the moulds that an assemblage quite different from the shoreface assemblages is present. The unique fauna must be accounted for in the interpretation of the depositional environment. The small, delicate scaphopods (tusk-shells), *Dentalium* sp., indicate a low-energy environment. Most scaphopods live offshore (Kilburn and Rippey, 1982). The *Turritella* moulds resemble the extant species, *T. declivis*, which inhabits the present-day shelf, but not the shoreface. *Glycymeris* species are characteristic of coarse substrata in current-swept conditions and are more typical of shallow-shelf settings, rather than shoreface environments (Thomas, 1975). The abundant moulds of a tellinid, *Macoma* sp., in an articulated condition, indicate a proximal source for that taxon. The tellinids are mainly deposit-feeders and are characteristic of fine-grained substrata in relatively low-energy conditions (Kilburn and Rippey, 1982), in embayments and from lower shoreface to offshore depths. *Isognomon* is found in abundance, sometimes articulated, at one other locality in the study area (A Block). Importantly, it occurs beneath lower shoreface basal gravel, in a sandy-mud bed with small pebbles and scattered larger clasts. Broken branches of the coral, *Schizoculina fissipara*, are present in the same bed and are common in sub-unit 1a, but are very rare in shoreface assemblages. *In situ Schizoculina* was found in Zone 12 and at one locality on Avontuur, but these occurrences are of the encrusting form, rather than ramose. The branching form of the coral may have grown at depths below frequent-storm wave-base.

The environmental interpretation of the mouldic coquina fauna is considerably aided by the recovery of a very similar assemblage from mining exposures at Koingnaas, ~15 km to the north of the study area (Fig. 4.1). The assemblage came from a sandy mud bed overlying bedrock, but underlying 50 m Package lower-shoreface deposits (Plate 13.13). This assemblage contributed several new species to the 50 m Package fauna. Importantly, all the unique faunal elements of the mouldic coquina are present (*Glycymeris*, *Isognomon*, *Turritella declivis*, *Dentalium* and abundant broken branches of *Schizoculina*). Additional deep-water taxa are present (*Tugali*, *Ringicula*). Similarly, abraded *Crassostrea*, brachiopods and barnacles are present.

It is concluded that the phosphatic, muddy, mouldic coquina in Zone 4A represents relatively high-energy deposition in a setting offshore of the shoreface, where deposition of mud normally takes place. The unique elements of the fauna are regarded as para-autochthonous and derived by erosion associated with the depositional event. They are the inhabitants of the distal lower shoreface and offshore transition that are seldom transported to shallow water and are therefore not normally found in shoreface assemblages. The worn oysters are the main allochthonous component of the fauna and were derived by erosion in the shoreface, with subsequent offshore transport of mainly the light, flat

valves. Accordingly, the phosphatic, muddy, mouldic coquina is interpreted as a storm deposit. It represents distal deposition offshore by a very intense storm.

The presence of phosphorite clasts in the mouldic coquina, as well as in the base of its apparent lateral equivalent a short distance away, shows that dark-brown phosphorite and bone pebbles were available from the onset of deposition in Zone 4A.

Plate 13.13 Koingnaas. Muddy, distal lower-shoreface, storm-deposited gravels. Offshore transition assemblage collected from base of sequence behind tool. West is right. Tool is 42 cm long.

The quartzose sandy and conglomeratic, dark-brown phosphorite: — The dark-brown phosphorite (sub-unit 1b) probably overlies an erosive contact on the underlying sub-unit 1a. This is suggested by the undulating lower boundary of the phosphorite material and the large pebbles and cobbles included in the bed. The layering within the bed is obscure and its main feature is upward-coarsening evident in the cobbles in the upper portion of the bed. However, an amalgamated unit is implied by the crudely-defined, successive generations of phosphorite. Direct parallels can be drawn between this bed and the overlying Unit 3. At the Section site, both beds have high barnacle fragment content, with cobbles distributed rather than clast-supported. Both beds exhibit a rapid lateral coarsening northwards from the section site (Fig. 13.3, Z-X). Whilst sub-unit 1b becomes clast-supported, Unit 3 becomes a small-pebble gravel with a capping cobble bed. Both beds fine rapidly eastwards onto higher bedrock (Fig. 13.3, X-Z). In the case of Unit 3, primary bedding indicates three period of deposition of pebbly barnacle hash (sub-units a-c), but the eroded phosphorite rind within sub-unit 3b indicates additional depositional events (assuming that the phosphorite was deposited in an intervening, inactive period). Additional phosphorite rinds occur in Unit 3. Both beds therefore contain evidence of multiple episodes of phosphorite deposition.

As Unit 3 accumulated during at least four, and possibly as many as six, distinct depositional events, it is remarkable that a characteristic, relatively short-range lateral variation was maintained throughout the accumulation of the entire unit. There is an upward-coarsening trend, best seen in the northwest (Fig. 13.3, X), where a capping cobble layer was deposited. The muddy Unit 1 was deposited in a more distal location than Unit 3 and it is therefore reasonable to assume that it is a similarly amalgamated unit, possibly more so than Unit 3. If this is the case, then it also exhibits a continuity in the lateral variation of successive additions, but with a more marked upward-coarsening trend.

The parallels between units 1 and 3 further include the locale of preserved phosphorite. The *in situ* phosphorite in both beds is only found in the southern part of Zone 4A. In the case of Unit 3, this could have arisen from the higher energy in the north implied by the lateral variation of the clast size i.e. the thin phosphorite rinds in the north were eroded. This explanation could also apply to Unit 1b. An alternative suggestion would be that the present distribution of phosphorite reflects its preferred site of deposition. This seems less likely because of the eroded tops of phosphorite rinds in Unit 3 and the strongly eroded top of Unit 1. Furthermore, remnant phosphorite occurs in excavation, including Zone 12 on the flanks of the bedrock ridge (Fig. 13.1), where *in situ* phosphorite occurs at ~30 masl. The fact that the wedge that prograded into Zone 4A (Unit PW) pinches out apparently at the edge of preserved, *in situ* phosphorite (Fig. 13.4) is therefore regarded as somewhat of a "red herring." The edge Unit PW was probably not in that location during the deposition of Unit 1b and was probably still approaching during the deposition of Unit 3.

Sub-unit 1b and Unit 3 are interpreted as storm-deposited conglomerates and coquinas. The muddy matrix of sub-unit 1b indicates deposition in a distal location, in the offshore transition. Like sub-unit 1a, it must therefore also represent deposition by particularly intense storms. The coarser nature of 1b relative to 1a probably reflects a less distal location. Unit 3 was deposited more proximally, closer to the edge of the prograding shoreface wedge. The lower energy involved in its deposition relative to Unit 1 is explicable by the overall decreasing energy levels behind the main bedrock ridge, as sea-level dropped. Similarly, its upward-coarsening reflects the approaching shoreline. Unit 2, the muddy, pebbly sand, reflects more minor storm deposition.

The qualitatively-noted tendency for flat clasts in Unit 3 to dip to the NW through to the NE suggests that the depositional currents probably flowed from those directions. The clasts that straddle the lower contact of the unit could have achieved that condition by scouring at the upcurrent end of the clast, with it subsequently tipping into the scour. Inspection of the bedrock contours intuitively suggests that seaward bottom flow, generated by coastal set-up against shorelines on Avontuur-A, would have been constrained to exit the embayment southwards along the landward flank of the main bedrock ridge. During the period when sea-level was relatively high over the study area and the palaeoshorelines were situated over Avontuur-A , the Zone 4A locale, against the steepest part of the bedrock ridge, was probably regularly current-swept. The deposition of the phosphorite took place mainly in the low sedimentation-rate environment, some distance offshore from the higher rates of sedimentary activity closer to the prograding shoreface wedge. The pyrite and carbon impregnation of the decomposed

bedrock and the carbon in Unit 3 indicate accumulation of organic matter in the embayment. The deposition of phosphorite occurred in an environment where calcite and aragonite were dissolved. The phosphorite rinds in Unit 3 reflect the final seaward retreat of the phosphorite-forming environment from the Zone 4A area.

As sketched at the beginning of this chapter, the crest of the main bedrock ridge would have been an offshore, non-depositional "hardground" during the transgressive maximum of the 50 m Package. Evidence that the ridge was more than a "gneiss hardground" is the presence of remnant phosphorite on the ridge flanks at ~30 m asl. (Zone 12, Fig. 13.1). Clavate borings (*Gastrochaenolites lapidicus* Kelly and Bromley, 1984) occur in the foliated gneiss. These are lined with typical dark-brown phosphorite in laminae conformable with the shape of the boring (Plate 13.14). This could be interpreted as an originally calcareous lining, produced by the boring bivalve, that has been replaced by phosphorite. However, immediately adjacent is another boring with a passive phosphorite-fill blocking the boring in a meniscoid fashion. A pebble was then lodged in the boring, followed by further phosphorite deposition lining the boring, the surface of which bears a bioglyph of vertical, scratch-like traces. This boring-fill is clear evidence for the deposition of the phosphorite as a mud. In another example, phosphorite and shell evidently filled a hole in the bedrock (Plate 13.15). The phosphorite is chaotically laminated and a burrow is present in the phosphorite. The feature is regarded as a burrow rather than a boring because it bears a well-defined bioglyph of vertical grooves similar to those made by crustaceans on their burrow walls. In contrast, the bioglyphs of boring bivalves are concentric due to the rotation of the shell (Kelley and Bromley, 1984). The chaotic lamination may be the result of collapse of the phosphorite into the hole, but the activity of the burrowing animal may also have contributed. Some of the lamination in the phosphorite is parallel to the burrow wall. It therefore appears that abandoned bivalve borings were reoccupied by crustaceans that actively plastered phosphorite mud onto the boring walls. Phosphorite infillings of holes in the gneiss were also burrowed.

A cobble gravel. ~0.4 m thick, overlies the bored bedrock. Dark-brown phosphorite is present in the interstices of the clasts. The bed is overlain by a coarser cobble bed with a sandy matrix and abundant clasts of phosphorite. Thus any phosphorite draping the basal cobble bed would have been eroded during the deposition of the overlying bed. The phosphorite hardground on the ridge crest would have been eroded as sea-level dropped from the transgressive maximum. Similarly, the phosphorite deposited on the bedrock on Avontuur-A was eroded in the vanguard of the approaching shoreline. There is therefore no requirement to postulate that the phosphorite clasts present in the base of Unit 1 in Zone 4A are derived from the deposits of the preceding sea-level cycle.

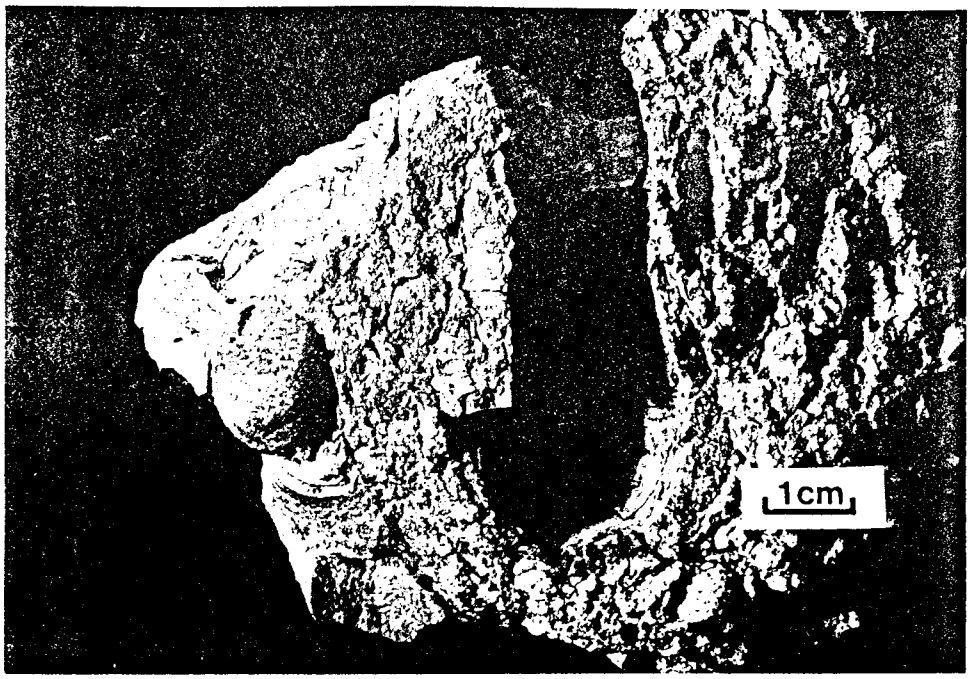

Plate 13.14 Clavate borings into foliated gneiss, with phosphorite linings and fillings.

Plate 13.15 Portion of phosphorite infilling of cavity in gneiss. Note chaotic lamination of phosphorite and bioglyph of vertical stratches in apparent burrow. Scale same as previous plate.

The Massive, Bioturbated, Fine sand Facies

This facies is developed in the sediment wedge that laps into the Zone 4A locality, Unit PW. The total bioturbation reflects an environment where erosion and redeposition were not marked. Thin pebble gravels occur in the base of the facies and horizons of large oyster shells (*Crassostrea*) occur in the lower portion of the facies. These occurrences represent the highest-energy deposition in the facies. The facies is overlain by several metres of shallow-marine sediments and therefore cannot be of very shallow origin. The highest energy deposition is preserved in the lower part of the facies, consistent with lower-shoreface facies architecture as observed at AV T2/T3. The regressive context, sedimentary geometry, fine-sandy, but not muddy, texture, poorly developed basal gravel and total bioturbation all point to a low-energy analogue of lower-shoreface deposition. This facies is regarded as the lower shoreface wedge of the low wave-energy shoreline that prograded into the protected embayment forming as the main bedrock ridge became emergent.

The *Crassostrea* shells in the lower portion of the facies occur in mutually-attached clusters of elongated individuals, indicating competition for space such as in a dense colony. Their articulated condition suggests that they were plucked during storms from the fringes of an oyster bed based on accumulated shells and only transported down the shoreface. The whale (Plate 13.11), which may only have been a shark-scavenged, partial carcass, was deposited on the floor of the embayment, possibly against the foot of the shoreface wedge. Together with the dolphin remains, its presence is consistent with an embayment still mainly open to the sea

The Laminated Mud Facies

The progradation of the low-energy, open-marine, bay margin was arrested and the sediment wedge was overlain by the laminated muds of this facies (Unit 4, a, c) (Fig. 13.4). This represents a dramatic shift in the depositional regime of the embayment to markedly lower energy levels. The deposition of the laminated muds reflects the end of an open-marine embayment in the lee of the bedrock ridge. The relationship of the laminated muds to the sedimentary geometry of Zone 4A has been outlined. The mud was deposited at the bases of successive gentle slopes into a body of water several metres in depth (Figs. 13.2, 13.4). Deposition on the slopes leading down to the laminated muds gave rise to the next facies.

The Laminated and Thinly bedded, Bioturbated, Calcareous Mud and Fine sand Facies

The geometry of this facies (Unit 5) reflects the steady infilling and shrinking of a basin. The environment was of low energy, as attested by the strong bioturbation and small depositional increments of fine sand separated by finely-laminated, burrowed, calcareous mud. The uniformity of this facies over its thickness indicates similar conditions over most of the sloping floor of the basin. This suggests a well-ventilated water column. A thin-shelled razor clam, *Phaxas decipiens*, is the most abundant taxon. This species inhabits soft substrata down to depths of 100 m on the open coast (Kilburn and Rippey, 1982). The preference for a low-energy habitat is consistent with its

occurrence in this facies and it also suggests normal marine salinity. Estuarine taxa are not present. Rocky shore species occur sparsely in thin shell layers.

This facies is interpreted as the infilling of a low-energy embayment. This embayment could be vizualized as a deep marine lagoon, partially open to the sea. The "cutting-off" of the embayment from open-coast conditions was due to the continued emergence of the bedrock ridge, with development of a barrier-beach in the south, across the mouth of the embayment in the area between Zone 3 and B Block (Fig. 13.1). In a sense, the bay/deep lagoon was a "hole" in the prograding shoreline caused by the "progradational jump" controlled by the emergence of the bedrck ridge. The absence of estuarine taxa and essentially marine nature of the bay-infill suggests that the bay was well-connected to the sea via active tidal channels. Tidal inlet facies are recognized in Zone 3. The **laminated mud facies** was deposited in the deepest part of the bay. The large, lenticular, sand bodies embedded in the laminated mud indicate locally higher rates of fine-sand deposition, forming large, dune-like features on the bay floor. They may be broadly analogous to flood-tidal deltas. The lack of significant mud and the bedding conformable with the convex tops suggests rapid accumulation and vertical rather than lateral accretion. They probably reflect enhanced input of sand into the quiet embayment and stronger circulation.

The coarse-sandy channel deposits eroded in the top of this facies are suggested to be tidal creeks (Fig. 13.4). This implies that deposits of the intertidal environment were at the level where the pedogenic profile (Unit 6) is now present. Although the fossil bones found around the base of the pedogenic profile may be indicating an erosional palaeosurface, as on Avontuur-A , they occur close to the intertidal level in the section, where terrestrial vertebrate fossils might be expected. It is therefore possible that some of the bones found in the Zone 4a area may be contemporaneous with the 50 m Package lagoon.

13.5 SUMMARY AND STRATIGRAPHIC IMPLICATIONS

Despite their very different appearance, the mouldic coquina (sub-unit 1a), the quartzose-conglomeratic phosphorite (sub-unit 1b) and the locally-phosphoritic barnacle hash basal to the 50 m Package possess strong sedimentological similarities. They can all be interpreted as storm deposits. The main differences are due to distal vs proximal depositional sites, with mud infiltration, phosphatization, phosphorite deposition and shell dissolution characterizing the deeper, distal environment. Furthermore, the marine sequence at Zone 4A (Fig. 13.5), including the phosphorite deposition, is entirely sensible in terms of regressive progradation during falling sea-level and the effects of the emergence of the main bedrock ridge. The emerging bedrock ridge reduced the wave-energy incident on the prograding shoreline to the east. The distal storm deposits were thereby protected from erosion as the shoreline approached and depths decreased. The progradation of the low-energy shoreface into the embayment ceased when the ridge was fully emergent, and the embayment subsequently became a low-energy bay environment analogous to a deep lagoon.

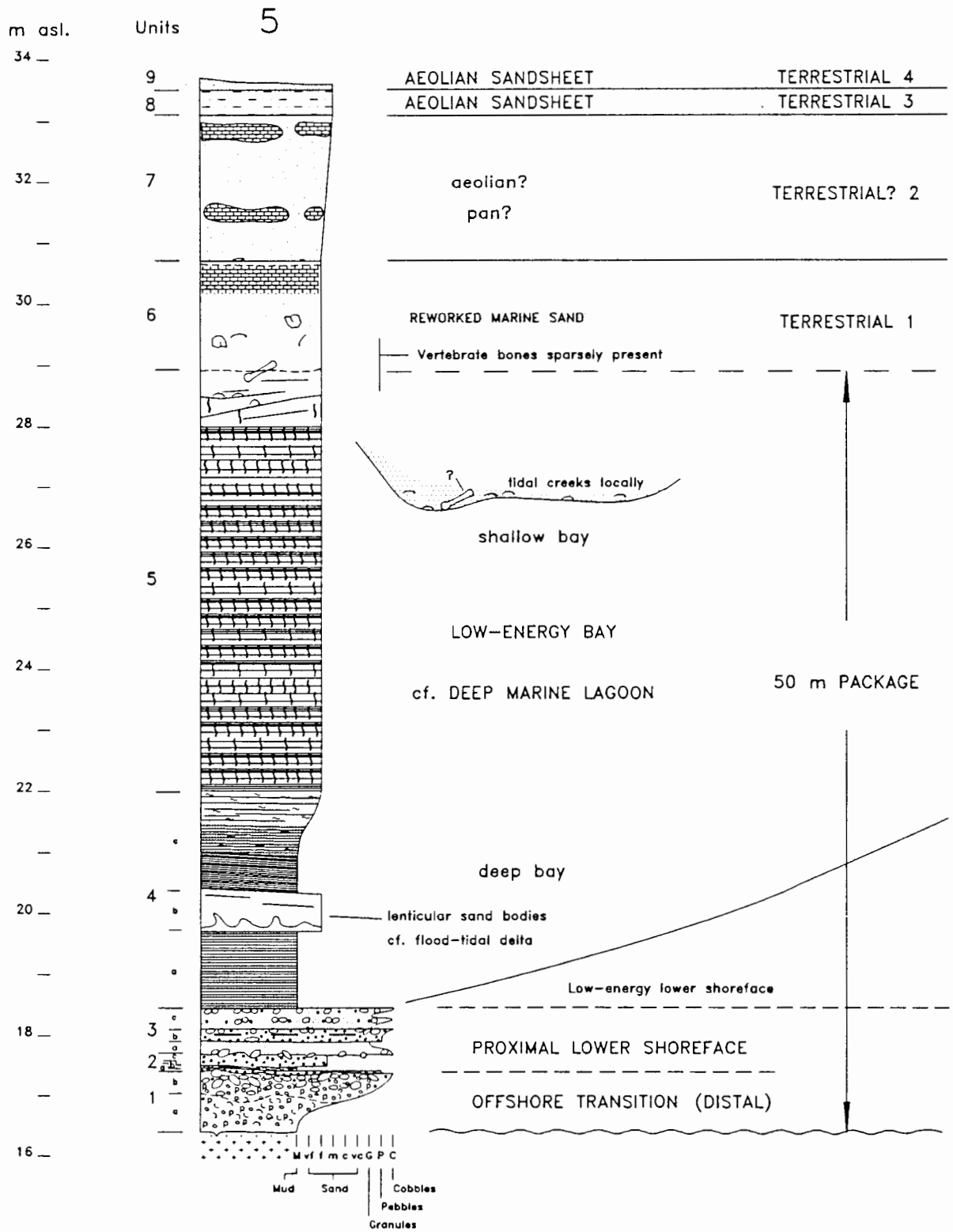

Figure 13.5 Section 5. Depositional environments and stratigraphy.

In terms of the preceding interpretation, any *a priori* stratigraphic significance attached to the phosphorite bed and its eroded top falls away. The phosphorite, including its clasts of earlier phosphorite, can more parsimoniously be regarded as part of a single regressive sedimentary package. The occurrence of *Donax haughtoni* in Zone 4A confirms that the marine sequence is the 50 m Package. The strong faunal contrast between the phosphatic, mouldic coquina underlying the phosphorite and the assemblages typically found in the 50 m Package is due to environmental differences, rather than temporal changes in the fauna due to adaptation and extinction.

Four terrestrial units can be recognized. Terrestrial 1 represents reworked marine sand and a pedogenic profile and is the equivalent of Terrestrial 1 on Avontuur-A. Unit Terrestrial 2 is unusually green in colour and probably represents a combination of aeolian deposition and ephemeral pan development. Notably, the present land surface in the Zone 4A area is a wide topographic low. Terrestrial 3 resembles Terrestrial 2 as on Avontuur-A. Terrestrial 4 represents present-day depositional processes.

CHAPTER 14

THE A BLOCK EXPOSURES AND THE 30 M PACKAGE

14.1 SETTING

The A Block excavation is located seaward of the main bedrock ridge (Fig. 14.1), to the immediate west of the termination of the ridge in the south. A low bedrock gradient extends seawards from the site, which would have been fully exposed to open-coast conditions. The lower part of the marine sequence in A Block records the continued progradation of the 50 m Package farther seaward of the barrier that developed across the embayment defined by the bedrock ridge. The main part of the marine sequence no longer represents 50 m Package deposits.

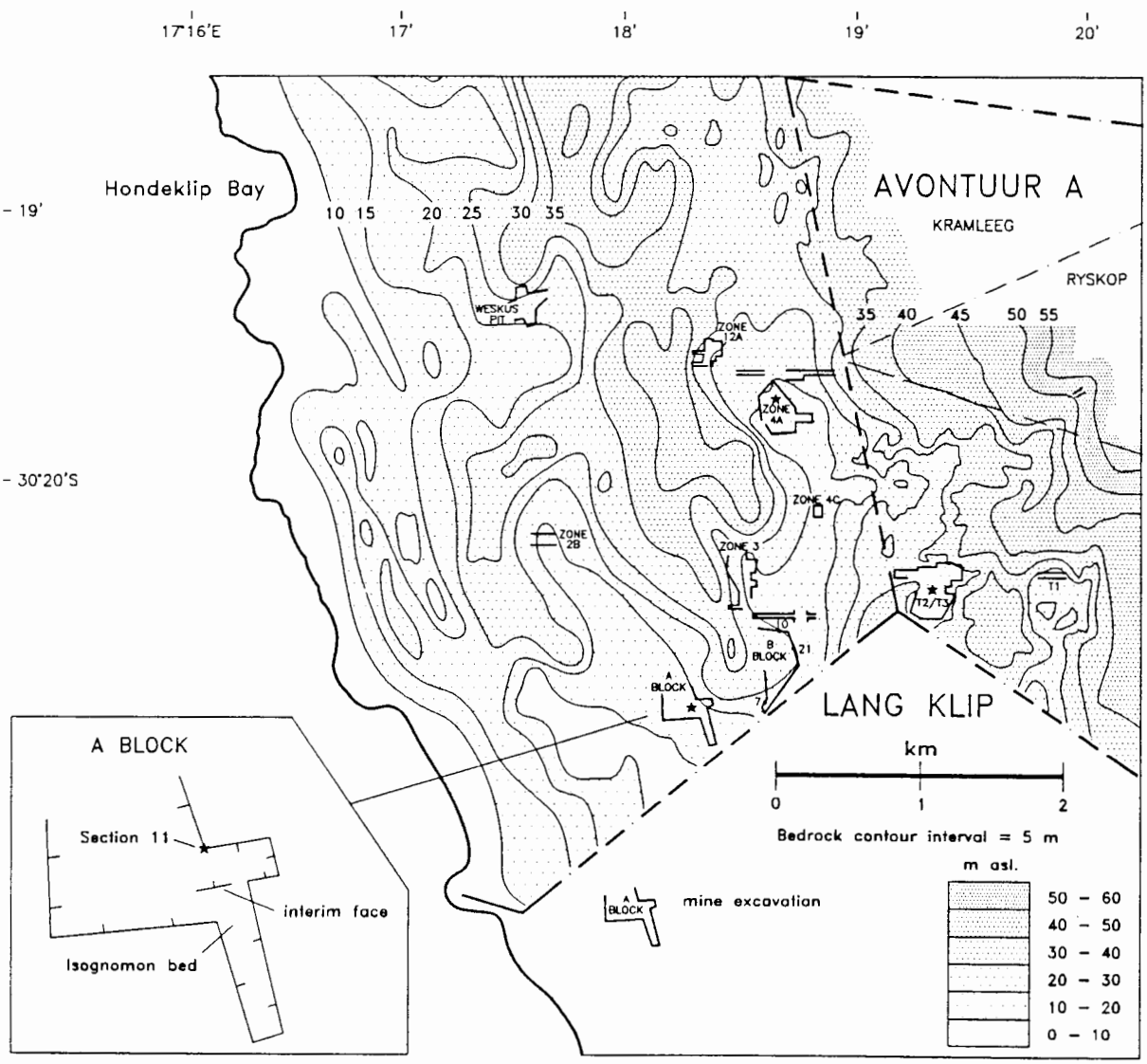

Figure 14.1 Location map, with inset showing position of Section 11 on corner in A Block. The positions of sections from B Block shown in Fig. 14.4 are indicated.

14.2 SECTION 11

Section 11 (Fig. 14.2) is situated on the eastern wall of the A Block excavation (Fig. 14.1), on the corner of a trench extension farther to the east. A section (Section 1) was measured on the south wall of A Block. This section is not presented in detail, but the features of the south wall will be described and contrasted with those in Section 11.

UNIT 1

Unit 1 is the basal kaolinitic deposit that has been described and interpreted in Chapter 5.

UNIT NS

A bed of yellow, muddy, poorly-sorted sand, ~30 cm thick, with sparsely scattered, small pebbles. Its notable feature is the occurrence of many valves, some articulated, of the large, heavy bivalve, Isognomon gariesensis.

Unit NS (Plate 14.1) occurs slightly to the south of the immediate section site. It was not available for inspection at the time the section was measured. The unit is labelled NS. It sharply overlies kaolinitic basal deposits and has an irregular top overlain by a very-coarse-sandy bed with cobbles and pebbles which is the basal gravel of the marine sequence. Washing of the muddy sediment to recover the fauna revealed that more angular pebbles of local rock are present than are usually found in the marine gravels. In addition to *Isognomon*, abraded and broken valves of oysters, mainly relatively small specimens, are abundant in the assemblage. Worn brachiopod valves and large barnacle plates are also major constituents. Unusual faunal elements are relatively large echinoid spines, 2-3 mm in diameter, but very few echinoid plates occur. Small species are a feature and several "new" species of very small (<1 cm) bivalves and gastropods occur. The assemblage includes an unidentified, small mactrid, not previously encountered, and an unidentified tellinid cf. *Macoma*. The material is crushed, but examples in articulated condition could be seen.

UNIT 2

A basal gravel, ~0.5 m thick, of clast-supported pebbles and very coarse sand, overlying cobbles and small boulders.

At the section site, the sharp contact on kaolinitic, sandy clay is overlain by a clast-supported, small to large-pebble gravel with cobbles and small boulders in the lower portion of the bed. The matrix is coarse sand to granule-size grains, with infiltrated fine sand. Clasts of phosphorite are present.

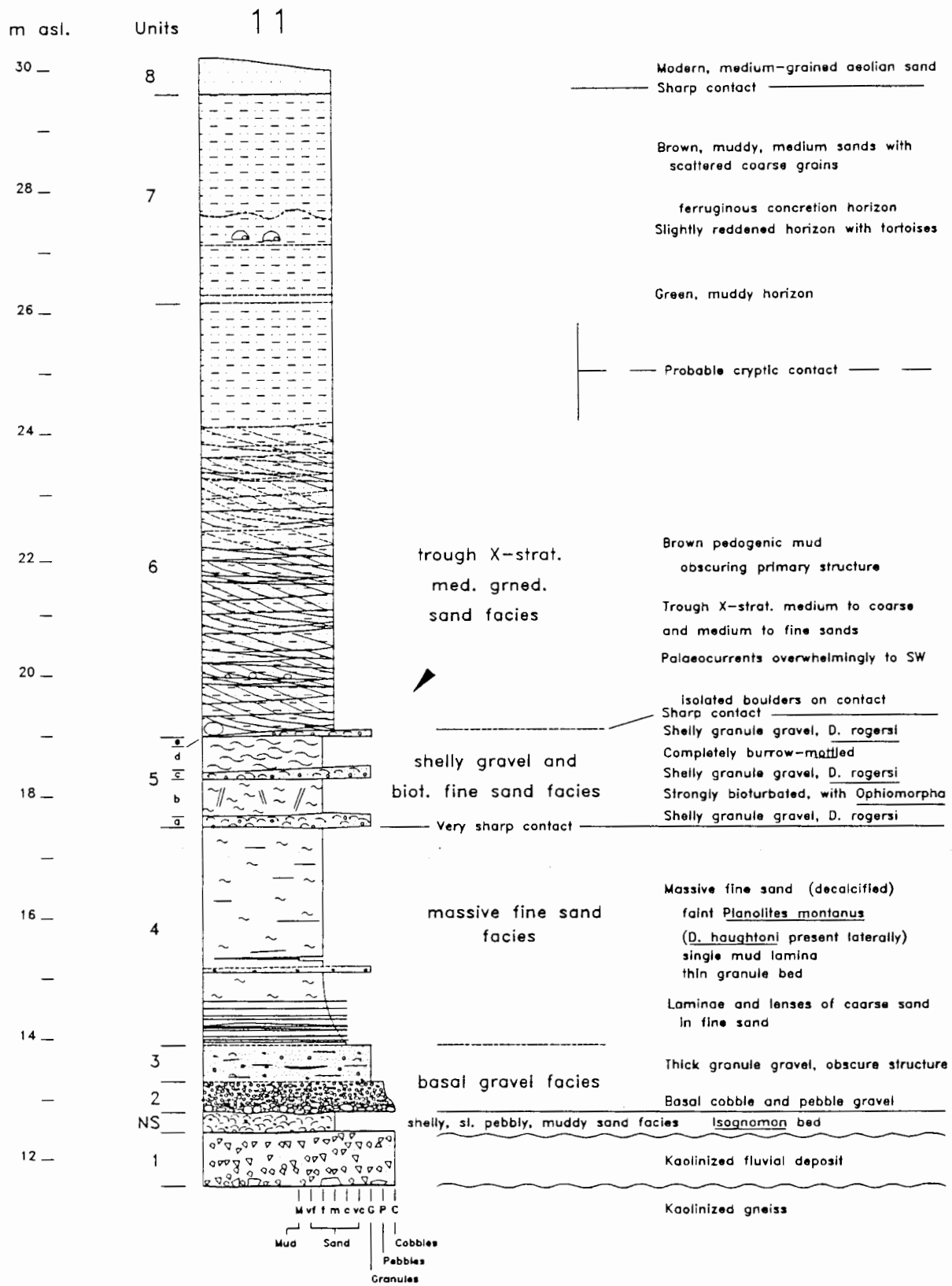

Figure 14.2 Section 11, graphic log and facies. Unit NS, although not at the immediate section site, is included beneath the section.

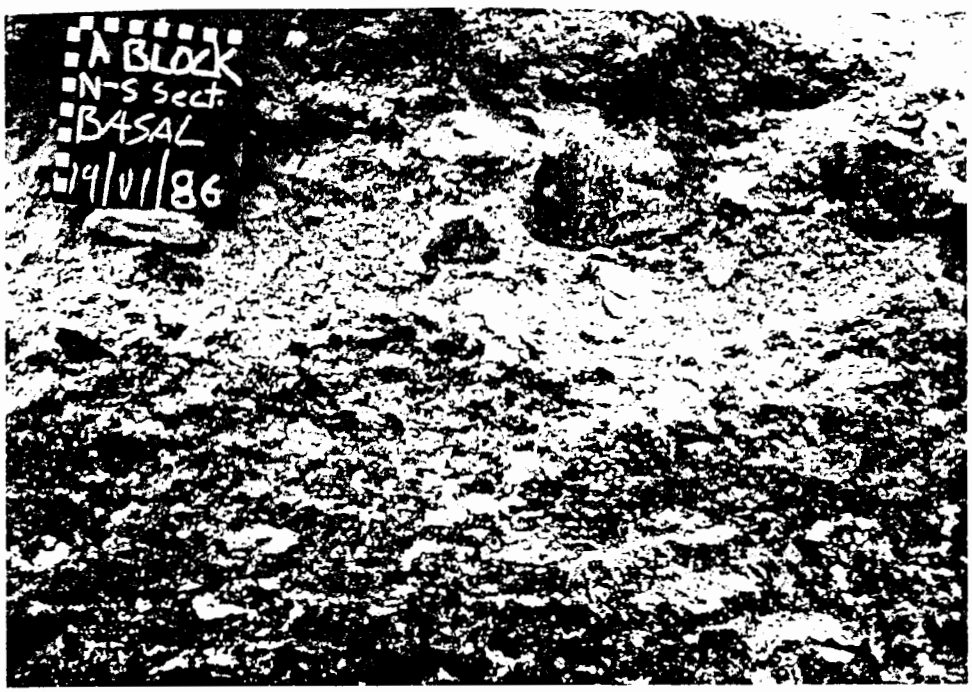

Plate 14.1 A Block. Base of marine sequence showing muddy *Isognomon* coquina underlying 50 m Package basal gravel. Scale in cm.

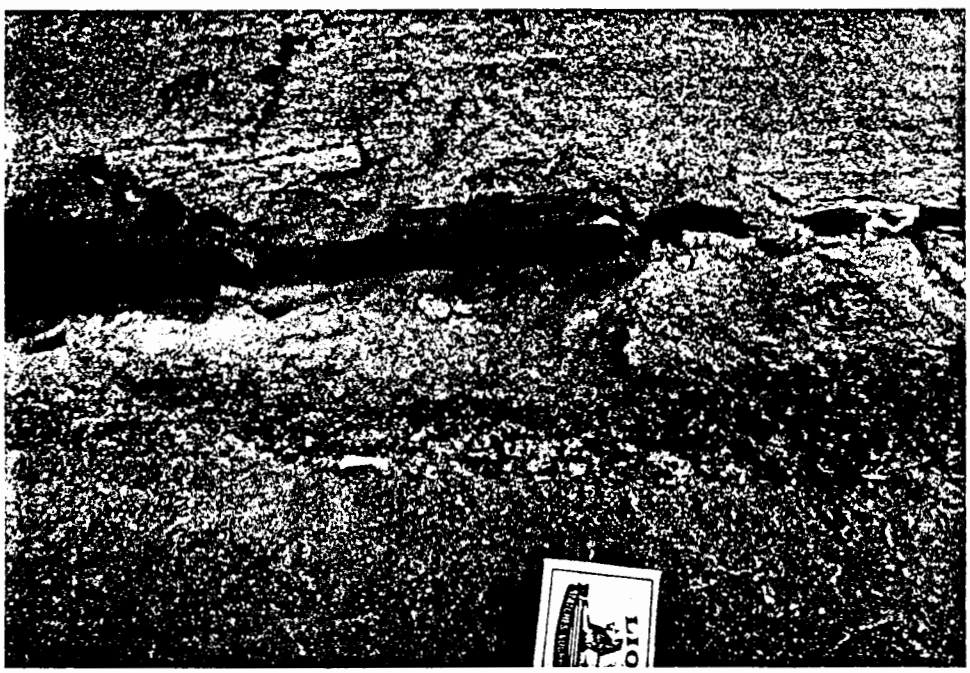

Plate 14.2 Section 11, Unit 4. Thin granule gravel and thick mud lamina in nearly structureless, bioturbated fine sand. Matchbox is 3.5 cm wide.

UNIT 3

Well-rounded, very coarse sand to granule gravel, ~0.6 m thick, with sparsely scattered, small to medium pebbles.

The lower contact is defined by an abrupt decrease in the clast size. The granule gravel is clast-supported, with interstitial fine sand. Abraded *Crassostrea* valves are sparsely present and are the flat, upper valves. Indistinct sub-horizontal stratification is present and a thin lense of fine sand is trough-shaped, 30 cm in length and 7 cm thick. Burrow mottles defined by concentrations of fine sand are sparsely present.

UNIT 4

Mainly massive, fine (fL), green sand, ~3.5 m thick.

Gradationally overlying Unit 3 are thin, gently west-dipping, lenses and laminae of coarse sand interbedded with fine, pale green (~5Y 7/2) sand. *Planolites 'spaghetti'* burrows are present in the fine sands and occur sporadically in the lower 1.5 m of the unit.. The coarse sands disappear upwards, but ~1.2 m from the base of the unit is a thin bed of granule gravel. This is closely overlain by a thick, single lamination (1-1.5 cm thick) of hard, green mud with no visible sand content. Its top is formed into small, convex "mounds " separated by sharp, V-shaped indentations (Plate 14.2). The mud lamination pinches out over ~2 m. Vestiges of low-angle lamination are present in the surrounding fine sand. The remainder of the unit is massive sand in which horizontal lamination to very thin bedding can be very faintly discerned. The only other visible features are the burrow mottles of *Planolites montanus*. Shell fragments and comminuted shell are absent. The top of the unit is a very sharp, slightly undulating contact with overlying, shelly, granule to small-pebble gravel.

In the middle of this unit in the south wall of A Block is a laterally-extensive, small-pebble gravel bed 0.3-0.5 m thick (Plate 14.3). The shell content consists nearly exclusively of the scattered, flat, upper (right) valves of *Crassostrea*. The bed has undulating upper and lower contacts and is crudely stratified, consisting of overlapping, thinner beds ~10 cm thick and one to several metres in extent. In many places the internal beds are separated by thin troughs of fine sand. Some fine-sandy intercalations drape the locally-convex tops of the gravel layers. These features indicate that the bedding of the gravel represents deposition in coarse-grained ripples (CGR).

Only *Crassostrea* and unidentifiable shell fragments could be found in units 2 to 4, until more recent extensions of the excavation revealed a bed containing *Donax haughtoni* . A whale rib was found in the unit. It bears deep scores that are attributable to biting by sharks (Q.B. Hendey, personal communication). The mandible of an extinct seal, *Homiphoca capensis*, was also found in the unit.

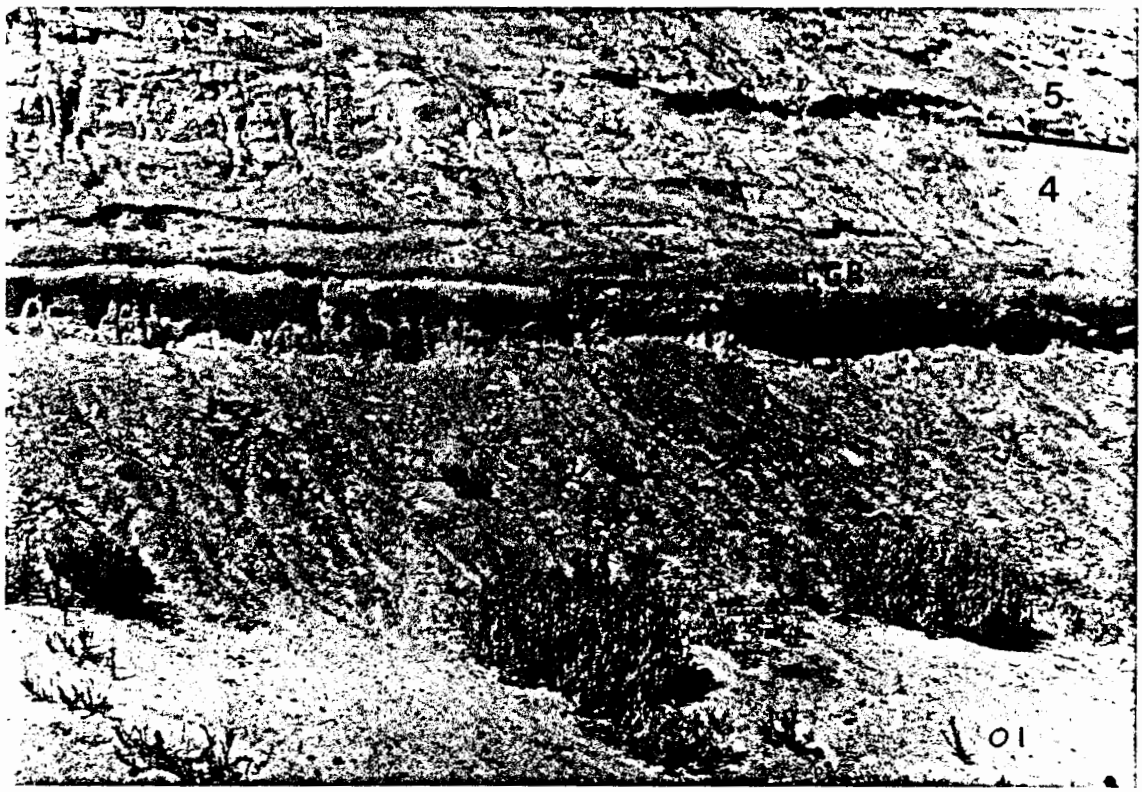

Plate 14.3 A Block, south face. Lateral equivalent of Unit 4 of Section 11, showing granule-gravel bed (CGR) interpreted as storm-deposited and wave-reworked, with formation of coarse-grained ripples.

Plate 14.4 Section 11. Sharp contact between units 4 and 5. Sub-unit 5a gravel contains *Donax rogersi*. Scale bar is 10 cm.

UNIT 5

Three shelly, very coarse sand to granule gravels are separated by two bioturbated, fine-sandy beds and form a unit, ~1.4 m thick, with five sub-units.

Sub-unit 5a: — The underlying, sharp contact of this ~20 cm thick, shelly, fine gravel is particularly sharp, (Plate 14.4), with no evidence of cross-cutting bioturbation. The granule gravel is clast-supported and the abundant, worn, shell fragments are sub-horizontal, indicating low-angle, cross-stratification. Convex fragments and shells are convex-up. *Crassostrea* fragments and right (flat) valves are abundant in the abraded assemblage. Barnacle plates comprise most of the finer fraction of shell fragments. The fine sand interstitial to the granule gravel is rich in finely-comminuted shell, in which fine echinoid spines are particularly noticeable. This comminuted-shell content contrasts with the underlying fine sands, which lack fine shell debris. A small whale tooth was found (unphosphatized). Phosphorite clasts are present as small pebbles and granules, but are not abundant. Laterally, both northwards and eastwards from the corner section site over ~20 m, the bed thins, becomes finer-grained (coarse sandy) and pinches out.

Fragments of a large, thick-shelled, robust bivalve are very numerous in sub-unit 5a and the umbonal fragments are readily identified as *Donax.* Relatively intact valves of the *Donax* occur and confirm that it is the extinct *Donax rogersi* Haughton, 1926. A large fissurellid (key-hole limpet), the extinct *Fissurella glarea*, is also present.

Sub-unit 5b: — A fine (fL) sand bed, ~0.6 m thick, pale green in hue (~5Y 7/2), with abundant, fine echinoid spines and nearly totally bioturbated (Plate 14.5). Coarse grains are scattered in the bed, as well as sparse, small shell fragments. *Planolites 'spaghetti'* is abundant. Vestigial thin bedding is present as diffuse horizons richer in dark heavy minerals. Large burrows are present and are *Ophiomorpha borneensis.* Some thin (~1 cm diam.), small, reddened, thalassinoidean burrows are present. Laterally northwards, heavy-mineral lamination is well-developed in the bed and outlines numerous chevron traces (Plate 14.6).

Sub-unit 5c: — Identical to sub-unit 5a, but with larger shell fragments. Similar to sub-unit 5a, the bed thins and dies away laterally to both the north and east of the section site, but more rapidly (Plate 14.6).

Sub-unit 5d: — ~40 cm of fine sand (fL), more yellow in hue than 5b (~5Y 7/8), but totally bioturbated, with only burrow mottling visible.

Sub-unit 5e: — 10-15 cm of very coarse sand and shell fragments capping the unit.. The bed pinches out laterally more rapidly than the underlying, coarse sub-units (Plate 14.6) and near its pinch-out appears effectively as a lens in the base of the overlying unit. Nevertheless, at the section site, its shell content and coarse-sandy to granule-gravel grain size prompt its inclusion with the underlying beds which it resembles. The immediately overlying sediment of Unit 6 lacks shell and is medium to coarse grained.

Plate 14.5 Section 11, Unit 5b, showing very strong bioturbation, with *Ophiomorpha* burrows and *Planolites* '*spaghetti*'. Pen for scale.

Plate 14.6 Section 11. Just north of section site. Sharp contact on Unit 4 overlain by Unit 5. Note numerous chevron traces in heavy-mineral lamination of sub-unit 5b, pinching out of sub-unit 5c, very strong bioturbation in sub-unit 5d and sharp contact with Unit 6. North is left. Geological hammer for scale.

Additional notes: — In contrast to the rapid northward and eastward (landward) pinching-out of the shelly, granule gravel beds of Unit 5, the lateral extension of the same beds southwestwards is dramatic. The identical unit with the three shelly beds could be readily identified in the opposite wall of the eastern trench and could be traced on the south wall of A Block (Plate 14.7). The thin, shelly, granule-gravel beds of Unit 5 (sub-units a,c e) are actually remarkably laterally extensive in the seaward direction, well exceeding ~250 m in lateral extent.

On the south wall, where a section was measured, the contact between units 4 and 5 is also markedly well-defined, with high-angle scours and sharp relief.(Plate 14.8). The three shelly, fine-gravel beds all exhibit undulatory upper and lower contacts, crude cross-stratification and locally contain thin troughs of bioturbated fine sand. They all contain *Donax rogersi* (e.g. Plate 14.8). The intervening fine-sandy beds are strongly bioturbated and *Ophiomorpha borneensis* is common. Notably, the gravel beds have the same stratification features as the small-pebble gravel bed interbedded in the underlying Unit 4. They are therefore also regarded as the deposits of migrating coarse-grained ripples.

As outlined by its "marker" gravels and well-defined upper and lower contacts, Unit 5 exhibits a distinct wedge geometry. From the section site, the unit thins landwards down the exposure in the trench extending to the east (Fig. 14.1). On the south wall of A Block to the southwest of the section site, the trio of "marker gravels" are in the lower portion of a unit that is now twice its thickness at the section site. The bed overlying the correlate of sub-unit 5e consists of strongly bioturbated, fine sand, with abundant *Ophiomorpha borneensis* burrows (i.e. it represents the same facies as sandy sub-units 5b and 5d). Unit 5 is thus a seaward-thickening wedge.

UNIT 6

A very thick unit (~7 m thick), of trough cross-stratified, fine to medium and medium to coarse sands. The sand is brown due to grain-coatings of pedogenic mud.

The lower contact of this unit on the bioturbated and burrowed, fine sands of sub-unit 5d is sharp (Plate 14.6). The contact consists of the erosive bases of overlying trough cross-beds and is therefore undulatory. The contact is not necessarily precisely marked by grain-size contrast or colour contrast. For instance, to the east of the section site, some isolated boulders occur on the contact (Plate 14.9), which otherwise is not obvious. The mobilization and redeposition of fine sand underlying the unit tends to obscure its lower contact.

The unit is slightly muddy, yellow-brown-coloured (~10YR 6/6) and medium-grained and superficially resembles the **brown, massive, medium-grained sand facies** overlying the marine sequence on Avontuur-A (Fig. 12.1). Similarly, the brown colouration is due to a pedogenic mud content of 5-15%. However, this unit exhibits high-angle, trough cross-stratification. The troughs vary from ~1 m to several metres in length and are 5-30 cm thick. Both planar and tangential foresets occur. Larger-scale bedding organization is difficult to unravel laterally, due to the profusion of troughs and the

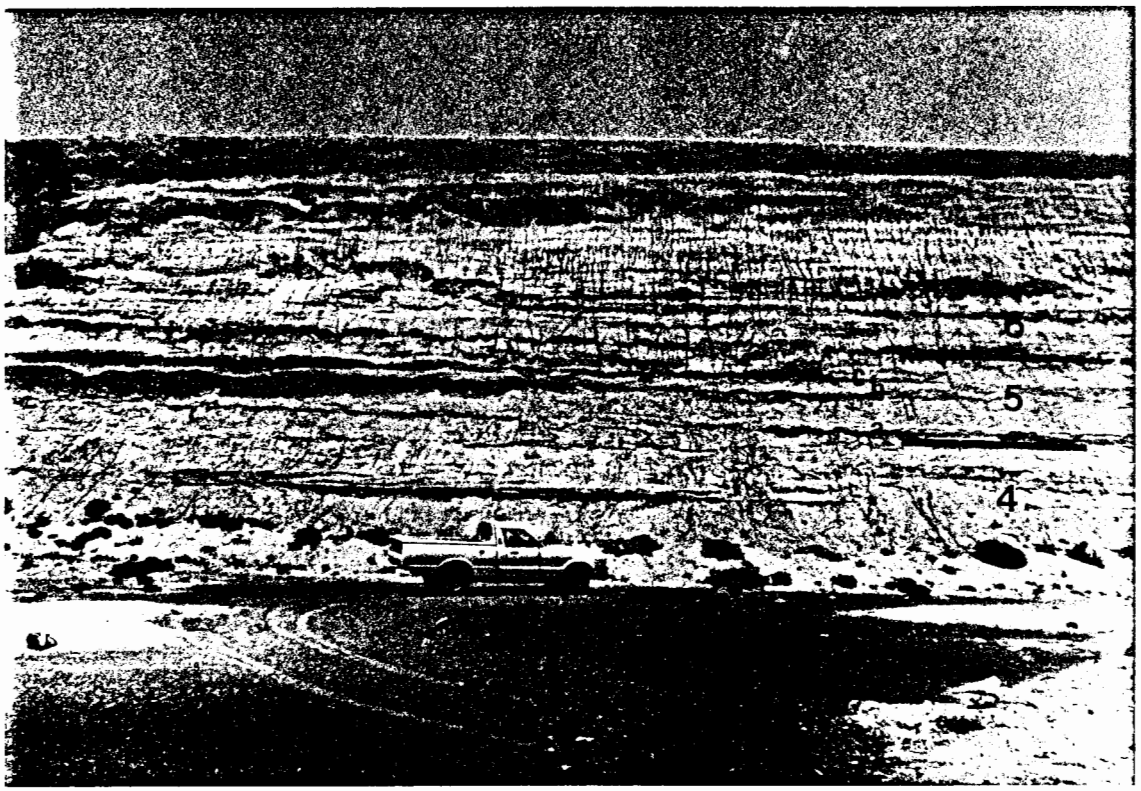

Plate 14.7 A Block, south face. Equivalent of units 4, 5 and 6 of Section 11. Note much thicker Unit 5 and laterally-persistent, undulating, granule gravels. West is right.

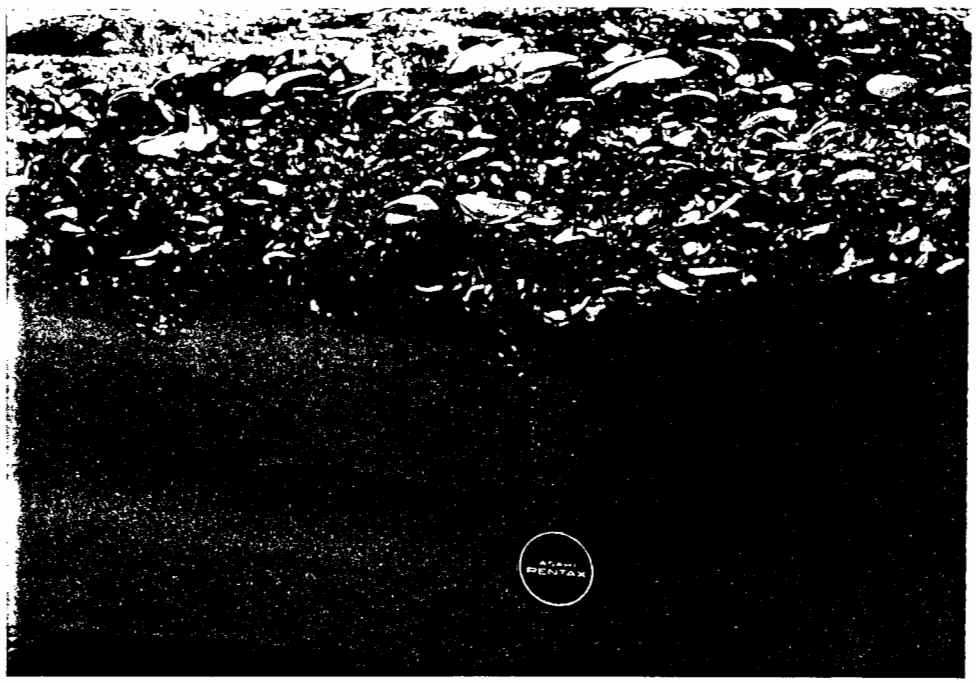

Plate 14.8 A Block, south face. Sharp contact between Unit 4 and Unit 5 with *D. rogersi.* Note convex-up orientations in the (swell) wave reworked top. West is right. Lens cap is 5 cm in diameter.

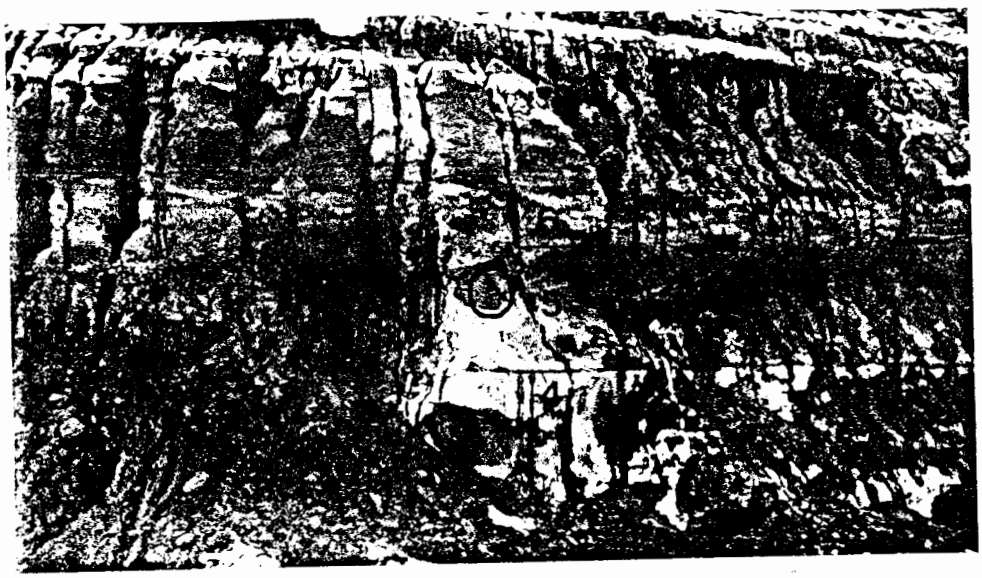

Plate 14.9 Section 11, Lateral variation eastwards. Granule gravel sub-units in Unit 5 have pinched out and Unit 5 is thinning eastwards. Isolated boulders on lower contact of Unit 6 arrowed. East is right. Geological hammer (circled) for scale.

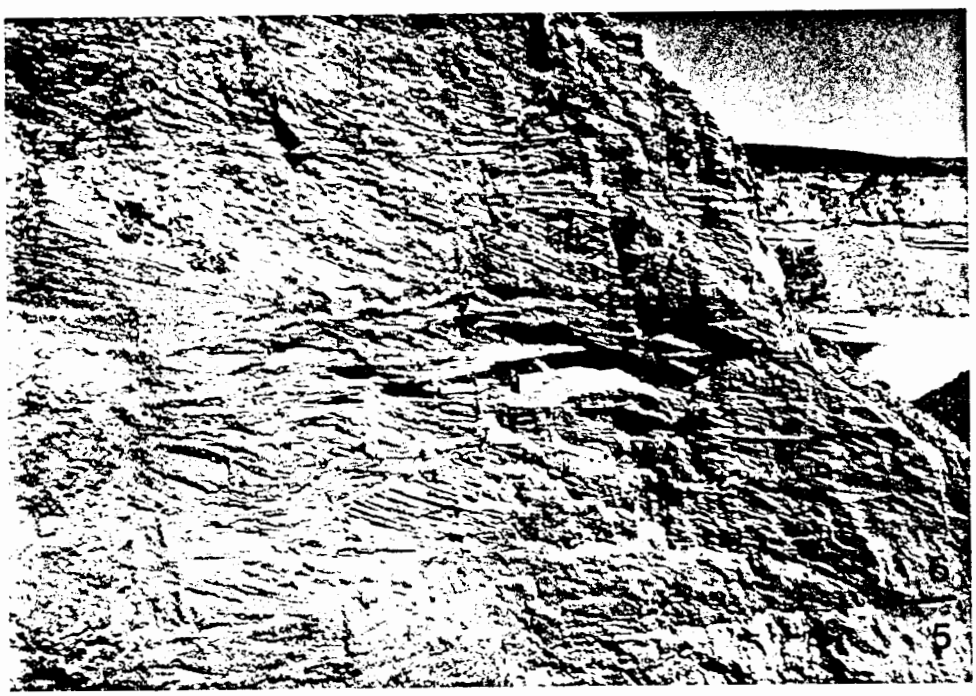

Plate 14.10 Section 11, Unit 6. Trough cross-stratification (megaripples) with palaeocurrent azimuths to the west and southwest. West is right. Matchbox (centre) is 5 cm long.

obscuring pedogenic mud. However, thick bedding (30-100 cm thick) is indicated by the more persistent bedding planes that could be observed. Isolated pebbles and cobbles occur on some bedding planes. The palaeocurrent azimuths at Section 11 are overwhelmingly offshore to the southwest (Plate 14.10). The sand is mainly medium-grained, but grain-size analyses of the unit show the modal size shifting about the medium size class, sometimes slightly coarser (cL) and sometimes slightly finer (fU). Except for mottle-like disturbances of cross-stratification, trace fossils are apparently absent. Sedimentary structure in the upper part of the unit is obscure and its upper contact is therefore poorly defined.

UNIT 7

Mainly muddy, brown, massive, medium-grained sand, ~3.0 m thick.

An olive-green (5Y 6/4), muddy sand, ~10 cm thick, marks the base of the unit. It is overlain by structureless, brown, muddy, medium-grained sand with scattered coarse grains. Two tortoise skeletons occur together in a slightly reddish zone, the top of which is marked by an undulating horizon of Fe-oxide concretions. Just below the surface of the unit are thin, vertical veins of pale, pink pedogenic mud (7.5Y 8/2) resembling the pedogenic hardpan found on Avontuur-A.

UNIT 8

Modern aeolian sand sheet.

14.3 DEPOSITIONAL ENVIRONMENTS OF A BLOCK

FACIES DEFINITION

Unit NS near the section site is very distinct as a **shelly, slightly pebbly, muddy sand facies**. Units 2 and 3 together comprise the **basal gravel facies** (Fig. 14.2). A mainly **massive fine sand facies** is defined by Unit 4. Unit 5 is a **shelly, granule gravel and interbedded, bioturbated, fine sand facies**. The pedogenic mud content of Unit 5 is ignored and it is a **trough cross-stratified, medium-grained sand facies**.

THE SHELLY, SLIGHTLY PEBBLY, MUDDY SAND FACIES

This facies is only locally present and has been eroded away elsewhere. Scattered, worn specimens of *Isognomon* occur in the overlying basal gravel in A Block and in the southwestern part of B Block (Fig. 14.1). Although in this case *Isognomon* dominates the assemblage, the mixed fauna of abraded, shallow-water taxa and well-preserved, delicate, minimally-transported, unusual taxa, together with the muddy nature of the bed, are clear similarities in common with the mouldic coquina in Zone 4A and the muddy shell unit on Koingnaas. The facies is therefore interpreted as a distal storm deposit laid down as an "*Isognomon* coquina" in the transition to the offshore. Similarly, the *Isognomon* and other articulated bivalves and well-preserved, small taxa are para-autochthonous, whilst the

Crassostrea fragments and probably most of the abraded brachiopod shells are the swept-in, allochthonous components of the assemblage.

THE BASAL GRAVEL FACIES

The upward-fining character of the basal gravel at Section 11, with coarse-sandy lenses and laminae in the immediately overlying fine sands, strongly resembles the basal gravel facies of sections 15 and 16 on Avontuur-A (and at most other sections on Avontuur-A). Accordingly, it is interpreted as a typical proximal lower-shoreface, storm-deposited and wave-reworked basal gravel.

THE MASSIVE FINE SAND FACIES

The gradational lower contact of Unit 4 with the coarse-sandy top of the basal gravel, interbedded, gently seaward-dipping, thin lenses and laminae in the lower portion of the facies, very strong bioturbation and loss of primary structure associated with *Planolites montanus* burrow mottles ('adelobioturbation'), but presence of vestigial thin lamination, are all features typical of the lower to middle portion of the lower-shoreface fine sands seen on Avontuur-A. Accordingly, the facies is regarded as a proximal, lower-shoreface deposit. The gravel bed in the middle of the facies on the south wall of A Block, with the features produced by migration of CGR, is interpreted as a storm deposit reworked by wave action (swell) in the lower shoreface. The single, thick lamination of green mud (Plate 14.2) indicates that a period of very low-energy occurred. This is consistent with the relatively deep shoreface environment inferred, but normally the evidence of such quiet deposition is later eroded in this (lower) part of the lower shoreface.

THE SHELLY, GRANULE GRAVEL AND INTERBEDDED, BIOTURBATED, FINE SAND FACIES.

The main feature of the granule gravel beds of this facies (Unit 5, a,c,e) is their considerable lateral extent in relation to their thinness. All three gravel beds pinch out rapidly in the vicinity of the section site, but extend to the south and west as prominent "gravel-sheet marker beds" (Plate 14.7). The stratification of the gravel beds is identical to that of the equally extensive gravel bed in the underlying Unit 4 (Plate 14.7). Accordingly, the shelly granule-gravel beds are also interpreted as storm-deposited and wave-reworked gravel sheets.

The main indication of the mode of deposition of the interbedded, strongly to completely bioturbated, fine sands is the heavy-mineral lamination in sub-unit 5b (Plate 14.6). The lamination (together with the bioturbation), indicates small depositional increments. The concentration of heavy minerals suggests comparatively low-energy flow (e.g. 20-40 cm/s) sufficient to entrain the quartz grains, but not the black ore grains. It is possible that the heavy mineral grains were pre-concentrated in small wave ripples (as is seen in the fine sands in the upper part of the lower-shoreface facies on Avontuur-A), with subsequent increasing flow washing out the ripples and further concentrating the heavy minerals. The bioturbated, fine-sandy beds in this facies are therefore interpreted as fairweather deposits, relative to the storm-deposited gravel interbeds.

The interbedding of storm-deposited and wave-reworked gravel sheets with relatively thick, strongly bioturbated, fine sands is suggestive of deposition in the lower shoreface, rather than in the upper shoreface.

The interesting fact that all three gravel beds (sub-units 5a-c) pinch out in approximately the same location can be intuitively explained in relation to the bedrock topography (Fig. 14.1). The position of the palaeoshoreline during deposition of the storm-deposited beds must have been to the landward of A Block. It is suggested that the palaeoshoreline abutted the "nose" of the bedrock ridge, which formed a headland on the northern side of a sandy, curving shoreline. During storm activity with Southern Ocean swell from the southwest, rip-channel migration would have been northwards, but would have been constrained by the rocky headland. The preferential location of rip channels against the headland would have resulted in relatively greater volumes of storm-entrained gravels accumulating in the lower shoreface at this location. The headland controlled the northern edge of the storm-deposited gravel sheets with some precision. Notably, the CGR bed in Unit 4 in the southern wall of A Block also pinches out northwards, as it is not present at the section site. However, in view of the above, it would be unsurprising if the thin, granule-gravel bed at ~1.2 m from the base of Unit 4 (Plate 14.2) is the edge of the CGR bed.

THE TROUGH CROSS-STRATIFIED, MEDIUM-GRAINED SAND FACIES

The lower contact of this facies developed in Unit 6 is sharp, but locally interfingering where the underlying fine sands appear to have been redeposited in the base of the facies. Isolated boulders on the contact attest to very high-energy conditions. The trough cross-stratification, with foresets both angular and tangential to set lower contacts, resembles the megaripple cross-stratification illustrated by Clifton *et al.* (1971) and Hunter *et al.* (1979). Accordingly this facies is interpreted as the deposits of the upper shoreface. The sharp lower contact overlain by seaward-directed cross-stratification (Plate 14.10) is as predicted by Hunter *et al.* (1979) for oblique-barred shorelines and is also predicted from the interpretation of the underlying facies.

The absence of shells in the facies is considered to be due to dissolution associated with the pedogenesis to which the sediment has been subjected. The facies disappears as the unit rapidly becomes structureless ~5 m from its base. A coarse horizon near the top that could be a candidate for a toe-of-beach gravel was not observed. As on Avontuur-A, a precise estimation of the associated sea-level is therefore not possible. The top of Unit 6 was taken at the first bedding feature to appear, namely a structureless, thin (10 cm), green bed of muddy sand. This appears to correspond on the south wall with a thicker (~30 cm), green clay bed that was deposited in a wide, shallow depression. The thin, green, mud seemingly overlies the last, clearly discernible, trough cross-stratification too closely (~2 m) for it to be interpreted as ponding in the backbeach environment. It is therefore interpreted as a terrestrial feature such as a shallow pan. The presence of tortoise carapaces ~1 m above the "green pan" confirms that the remainder of the section represents terrestrial deposition, probably as aeolian sand sheets.

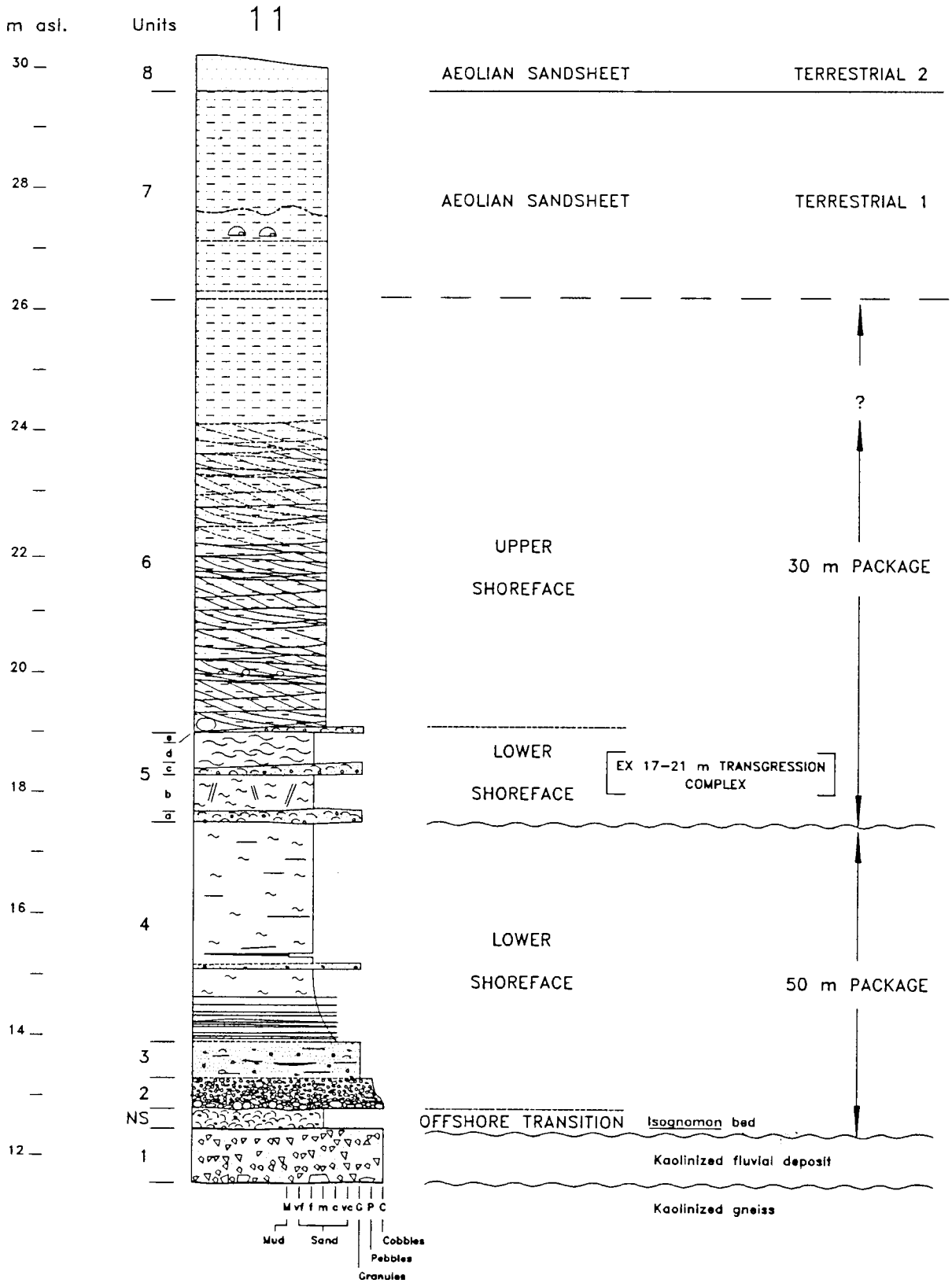

Figure 14.3 Section 11, depositional environments and stratigraphy.

14.4 SUMMARY AND STRATIGRAPHIC IMPLICATIONS

A thin, eroded remnant of muddy, shelly deposit (Unit NS), an *Isognomon* coquina representing deep-water storm deposits of the offshore transition, occurs beneath a proximal, storm-deposited and swell-reworked gravel (Fig. 14.3). This gravel is basal to lower-shoreface, storm-deposited, fine, bioturbated sands (units 2-4). A prominent granule-gravel unit in the lower-shoreface fine sands is also a storm-deposited and swell-reworked, CGR bed. The presence of the zone fossil *Donax haughtoni* Carrington and Kensley, 1969, in this sequence (Unit 4) indicates that it is 50 m Package sediment. The upward-shallowing sequence represents the continued regressional progradation of the 50 m Package seaward of the bedrock ridge.

A markedly sharp contact is developed on the top of the 50 m Package sediments. It is overlain by a wedge-shaped unit (Unit 5) that thickens seaward at the expense of the underlying 50 m Package deposits. The granule gravels in this unit are also storm-deposited and swell-reworked, CGR beds. They are interbedded and overlain by strongly bioturbated, fine sands with relict lamination. The unit is also interpreted as proximal lower-shoreface deposition. Indeed, at the most landward exposure east of the section, the unit is only ~1 m thick and is overlain by a >5 m thickness of trough cross-stratified, medium-grained sands representing the upper-shoreface environment (Unit 6).

The fauna in the CGR gravels of Unit 5 contains *Donax rogersi*, an extinct species of biostratigraphic importance that was noted by Carrington and Kensley (1969). *Donax rogersi* was recorded by Carrington and Kensley (1969) from their "17-21 m Transgression Complex" (Table 3.1). As *D. rogersi* was not ever found together with *D. haughtoni*, they suggested that *D. rogersi* may have evolved from *D. haughtoni*, developing a more robust, heavy shell as an adaptation to the more energetic environment implied by the coarse sediments of the "17-21 m Transgression Complex."

The particularly clear-cut contact on top of the *D. haughtoni*-bearing Unit 4, beneath the *D. rogersi*-bearing Unit 5, supports Carrington and Kensley's (1969) findings that the two *Donax* species occur in stratigraphically separate formations. The contrast in the preservation of shell across the contact also indicates that a significant hiatus occurs across the contact. While the 50 m Package fine sand of Unit 4 is devoid of finely-comminuted, carbonate sand, the 30 m Package sand immediately above the contact contains much fine shell debris such as benthic foraminifera and small echinoid spines.

Clearly, the *D. rogersi*-bearing Unit 5 is Carrington and Kensley's "17-21 m Transgression Complex" and actually occurs between those elevations (Fig. 14.2) in the study area. It is now shown to have been deposited in the lower shoreface and to be overlain by thick, cross-stratified, upper-shoreface deposits, establishing that the "17-21 m Transgression Complex" is actually the lower part of a larger regressive, progradational sequence. The coarse-grained nature attributed to the "17-21 m Transgression Complex" stems from the presence of storm-deposited, lower shoreface gravels. The fact that the lower shoreface wedge pinches out just landward of Section 11, and is absent in B Block, ~ 50 m to the east, shows that Section 11 is situated some relatively short distance seaward of the transgressive maximum from which the regressional sequence prograded. The "17-21 m

Transgression Complex" is thus identified as the "transgressive maximum of the lower shoreface environment" of a sea-level at a higher elevation.

It can also be concluded that pedogenic processes in the relatively coarse-grained, upper-shoreface deposits, with dissolution of shell and development of brown, obscuring mud, has probably caused them to go unrecognized as shallow-marine deposits.

Detailed observations and faunal sampling have been carried out in the B Block and Zone 3 excavations (Fig. 14.1) to the landward of Section 11 in A Block. This has enabled the precise tracing of the disconformity between 50 m Package deposits (with *D. haughtoni*) and those of the overlying, now expanded "17-21 m Transgression Complex" (with *D. rogersi*) (Fig. 14.4). The disconformity is marked by overlying pebbles and cobbles and by the contrast in the preservation of carbonate, if below the pedogenic profile (Plate 14.11). In the southwestern part of B Block, the disconformity is at 22 m asl. It is overlain by upper shoreface deposits in which *D. rogersi* occurs in living position. In the northern end of B Block, the disconformity is at 29 m asl., but is overlain by only ~1 m thickness of recognizable marine sediment, coarse-grained and cross-stratified. In Zone 3, the disconformity is present only in the southwestern part of the excavation, where it commences at 27 masl. (Plate 14.12) and can be traced by a line of pebbles in the brown pedogenic profile up to ~30 m asl. In the southwestern corner of Zone 3, the presence of beds with *D. rogersi* immediately overlying beds with *D. haughtoni* confirms the continuity of the disconformity (Plate 14.13).

Thus the zone fossil, *D. rogersi*, occurs in a regressive, progradational package that extends seawards from a transgressive maximum at approximately 30 m asl. The presence of a transgressive maximum palaeoshoreline at ~30 m asl. confirms another observation reported in Carrington and Kensley (1969), namely the existence of a "29-34 m Beach" (Table 3.1) in the coastal-plain stratigraphic sequence. From the "29-34 m Beach," Carrington and Kensley described an extinct species of keyhole limpet, *Fissurella glarea*. This species occurs abundantly in the "17-21 m" deposits that are now established as extending seawards from ~30 m asl. It is not found in the 50 m Package. Thus it can confidently be concluded that the "29-34 m Beach" and "17-21 m Transgression Complex" are part of the same progradational formation. This package of regressive deposits is now called the 30 m Package (Pether, 1986a).

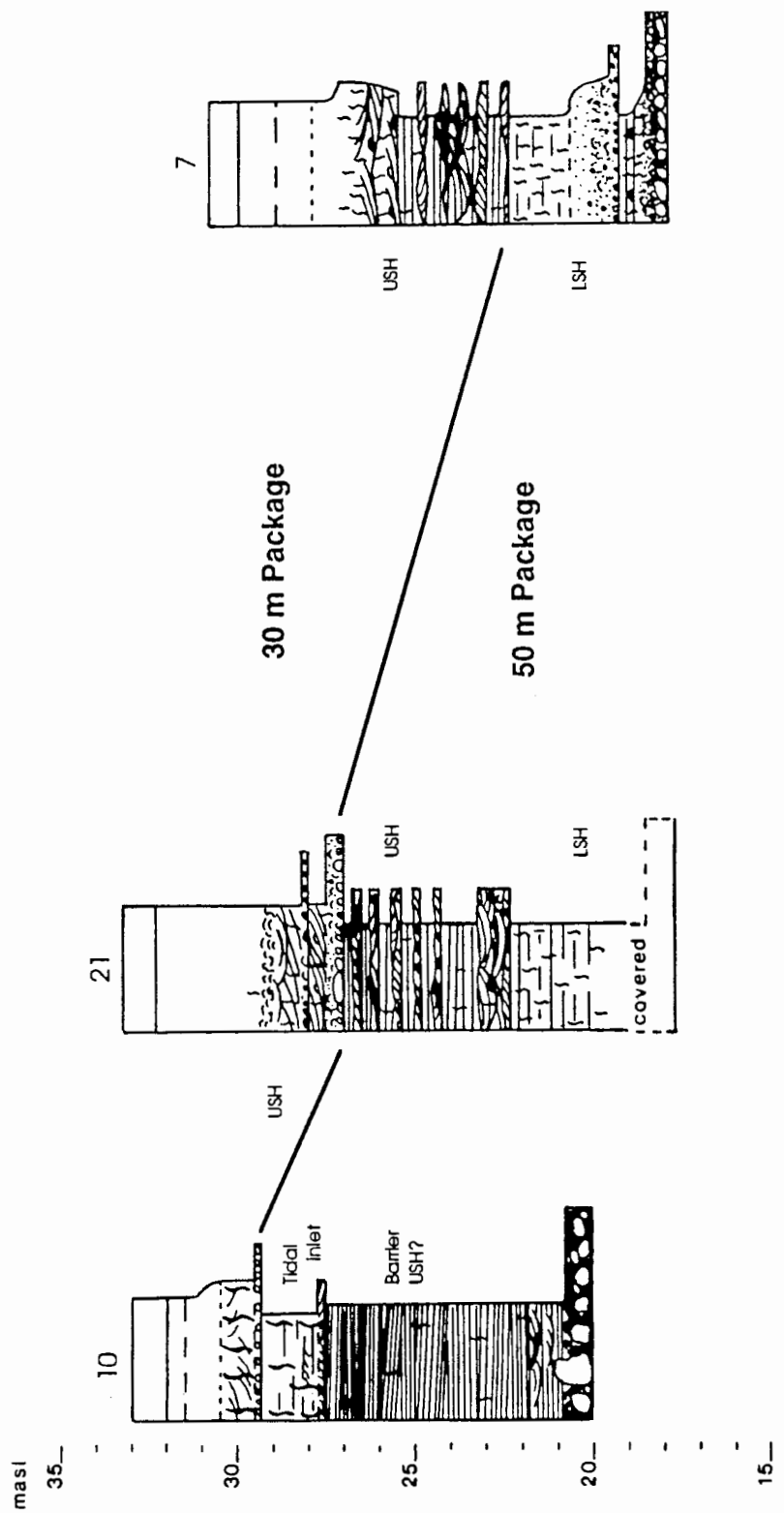

Figure 14.4 Sedimentary geometry in B Block. Section 7 in the southwestern part of B Block. Section 10 is at the northern wall of B Block and Section 21 at an intermediate position on the east wall.

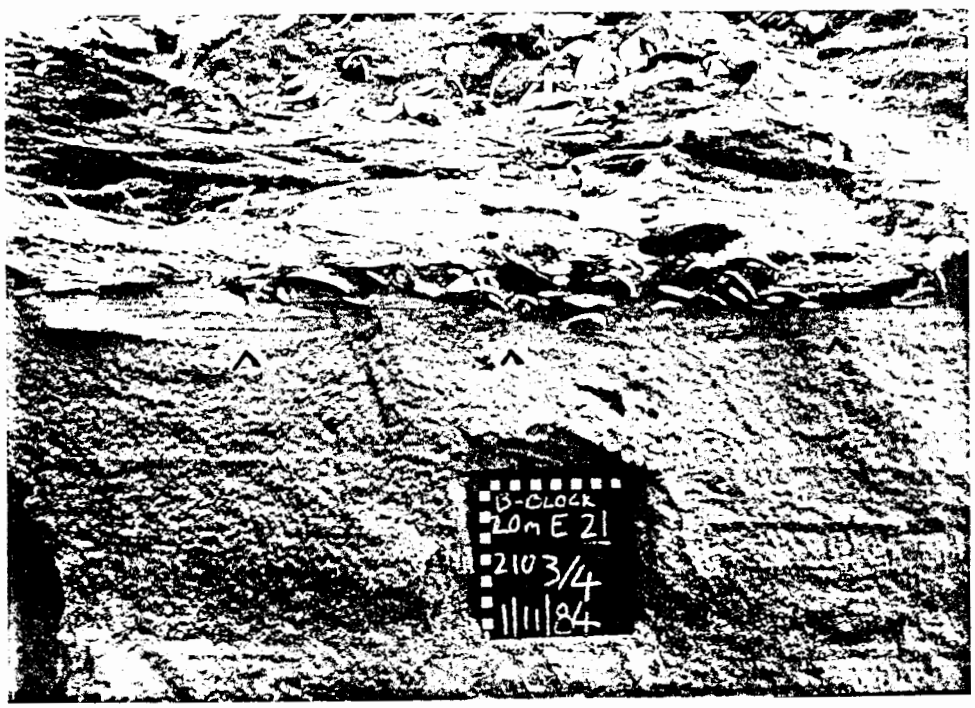

Plate 14.11 B Block, east face Contact (arrowed) between underlying, decalcified, 50 m Package upper-shoreface sands and shelly, coarse sands of 30 m Package (with comminuted shell content). Pebbles and shell slightly above actual contact. (Section 21). North is left. Scale in cm.

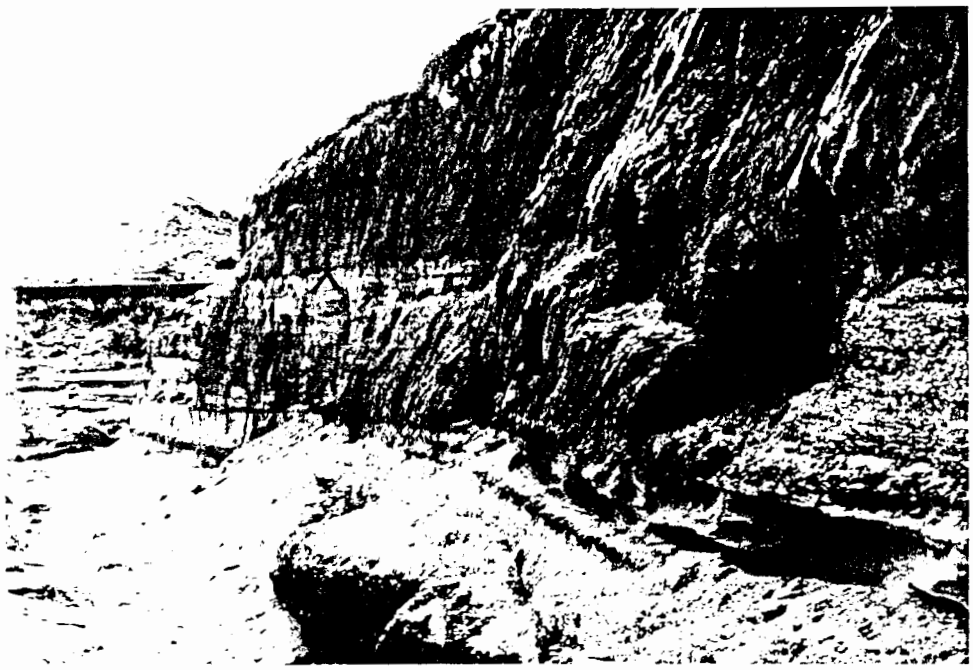

Plate 14.12 Zone 3, trench in southwestern corner, south face, looking east. Lower contact of 30 m Package (arrowed), overlain by granule gravel and scattered cobbles. Note that pedogenic processes have imparted a massive appearance to the 30 m Package, whilst the 50 m package sediments below are clearly bedded. Scale bar is ~1 m long.

Plate 14.13 Zone 3, west end of southwestern trench, south face. Lower contact of 30 m Package (arrowed). Shell bed below includes *D. haughtoni*, shells behind person are *D. rogersi*.

CHAPTER 15

THE PALAEONTOLOGY AND AGE OF THE MARINE DEPOSITS

15.1 INTRODUCTION

The rich shell beds in the study area have facilitated considerable improvement in the knowledge of the fossil mollusc fauna of the west coast of southern Africa. In many cases, shells could simply be picked up or scratched out with all the enjoyment of collection. In others, painstaking care under trying conditions was required. A vital contribution to the molluscan fauna came from beyond the immediate study area, from the distal lower-shoreface, muddy bed on Koingnaas, to which attention was directed by the geologists of De Beers Namaqualand Mines Division. The results of searches for the scarce vertebrate material in the study area have produced a small, unspectacular assemblage, but the purpose of achieving some age constraints has been realized. Ironically, the most important find was not unearthed during the searches of and excavations into the walls of the excavations, but was found on a Zone 4A overburden dump by the hawk-eyed mine geologist, Mike Mittelmeyer, to whom this study owes the major age constraint for the deposits.

New species of molluscs collected during the initial stages of this study are described in Kensley and Pether (1986), in which the writer provided the geological context and B. Kensley (National Museum of Natural History, Smithsonian Institution, Washington D.C.) described the taxa and analysed the fauna, with some contributions from the writer. Brachiopods were passed on for study to C. H. C Brunton (British Museum of Natural History, London) and N. Hiller, (Rhodes University, Grahamstown, South Africa), the results of which are published in Brunton and Hiller (1990). Samples of sediment containing benthic foraminifera were passed to I. K. McMillan (consulting) who has kindly provided the writer with a detailed list of taxa and his analysis. S. Cairns (National Museum of Natural History, Smithsonian Institution, Washington D.C.) identified the fossil coral. The vertebrate material was identified by Q. B. Hendey (formerly South African Museum, presently Durban Museum). The writer has carried out an initial investigation of the fossil barnacles, resulting in the description of a new species. The main findings of these contributions are included here.

15.2 THE INVERTEBRATES

The Molluscs

The molluscan fauna from the study area includes 92 species, 15 taxa identified to generic level and several unidentified, very small taxa. The data in Table 15.1 show that a more diverse fauna (78 species) was recovered from 50 m Package deposits, whilst 48 species were found in the 30 m Package. This is probably due to most of the shelly exposures in the area being in the 50 m Package and wider sampling is required to examine the apparent diversity contrast. About half of the fauna is extinct. Approximately 50% of the 50 m Package taxa are extinct and 40% of the

30 m Package taxa. Slightly more than one third of the fauna is common to both stratigraphic units and 11 extinct taxa occur in both units.

Table 15.1 General data of the Mollusca from the study area.

Distribution in stratigraphic units	**50 m P**	**30 m P**	**TOTAL**
Total no. of species	78	48	92
Total no. of extinct species	37	19	45
Lyellian percentage (percentage extant)	53%	60%	51%
No. of warm-water taxa	14	12	20
No. of species common to both 50 and 30 m packages	34		
No. of extinct species in common	11		
No. of warm-water species in common	7		
Zoogeographic affinities			
No. of species extant on east and west coasts	27		
No. of species extant on east coast only	11		
No. of species with West-African-Mediterranean affinities	9		

A significant number of warm-water taxa occur in the assemblage. Chief among these is the oyster, *Crassostrea margaritacea*, which is abundant in both the 50 and 30 m packages. Moreover, the presence of *in situ* oysters on boulders in the 30 m Package shows that they lived at that time, rather than the robust oyster shells having been reworked from 50 m Package deposits. A cooler temperature regime during 30 m Package times therefore seems implausible on the available evidence (Kensley and Pether, 1986).

The samples of fauna from the periods represented by the 50 and 30 m packages is too small and from too local an area to form the basis of detailed palaeobiogeographic conclusions. The faunas undoubtedly have a context in the general late Tertiary cooling trend. However, samples of comparable size of earlier faunas (e.g. Miocene) are not available for comparison. It can be noted

that the assemblage in the shoreline deposits that succeed the 30 m Package is overwhelmingly modern (personal observations). This suggests considerable extinction and speciation subsequent to 30 m Package times.

Of primary biostratigraphic importance is that this study has confirmed Carrington and Kensley's (1969) findings on the value of *Donax haughtoni* and *Donax rogersi* as zone fossils, now for the 50 m Package and 30 m Package, respectively. Furthermore, the several species of extinct taxa that have been found in only one of the units are potential candidates as additional zone fossils (Tables 15.2, 15.3). Thus, where the *Donax* species are absent in an assemblage, there is an improved probability that the stratigraphic unit to which the shelly bed belongs can be identified.

Table 15.2 List of extinct species (†) found only in the 50 m Package.

GASTROPODA

†*Cabestana casus* Kensley and Pether, 1986

†*Burnupena aestus* Kensley and Pether, 1986

†*Calliostoma depressa* Carrington and Kensley, 1969

†*Calyptraea viridarena* Carrington and Kensley, 1969

†*Clanculus lutosus* Kensley and Pether, 1986

†*Crepidula deprima* Kensley and Pether, 1986

†*Drillia tempestae* Kensley and Pether, 1986

†*Fasciolaria dinglei* Kensley and Pether, 1986

†*Haliotis saldanhae* Kensley, 1972

†*Patella hoffmani* Kensley and Pether, 1986

†*Pseudoliva lutulenta* Kensley and Pether, 1986

†*Terebra canisaxi* Kensley and Pether, 1986

†*Trophon carringtoni* Kensley and Pether, 1986

BIVALVIA

†*Chamelea krigei* Haughton, 1926

†*Donax haughtoni* Carrington and Kensley, 1969

†*Glycymeris fulleri* Kensley and Pether, 1986

†*Notocallista schwarzi* (Newton, 1913)

BRACHIOPODA

†*Kraussina lata* Haughton, 1932

†*Kraussina laevicostata* Brunton and Hiller, 1990

†*Kraussina cuneata* Brunton and Hiller, 1990

CIRRIPEDIA

†*Notomegabalanus kenslyi* Pether, 1990

Table 15.3 List of extinct species found only in the 30 m Package.

GASTROPODA

†*Burnupena rogersi* Kensley and Pether, 1986

†*Fissurella glarea* Carrington and Kensley, 1969

†*Ocenebra petrocyon* Kensley and Pether, 1986

†*Thais arenae* Kensley and Pether, 1986

BIVALVIA

†*Cardita unica* Kensley and Pether, 1986

†*Donax rogersi* Haughton, 1926

The probability of being able to recognize a 50 m Package assemblage is markedly improved (Table 15.2). The amount of taxa unique to the 30 m Package is markedly less, but *Donax rogersi* is usually abundant (sandy shores) and *Fissurella glarea* (rocky shores) is very common in the 30 m Package. The recognition of 30 m Package deposits also involves the presence of the species listed in tables 15.3 and 15.4, but the absence of those in Table 15.2.

Table 15.4 List of extinct species found in both the 50 m Package and the 30 m Package.

GASTROPODA

†*Calyptraea kilburni* Kensley and Pether, 1986

†*Clanculus murrayi* Carrington and Kensley, 1969

†*Epitonium lycocephalum* Kensley and Pether, 1986

†*Fissurella robusta* Sowerby, 1892

†*Melapium hawthornei* Kensley and Pether, 1986

†*Namamurex odontostoma* Carrington and Kensley, 1969

†*Spinucella praecingulata* (Haughton, 1932)

†*Ocenebra bonaccorsii* Carrington and Kensley, 1969

†*Patella hendeyi* Kensley and Pether, 1986

BIVALVIA

†*Carditella calipsamma* Carrington and Kensley, 1969

†*Cuna aquaedulcensis* Kensley, 1977

†*Dosinia sicarinus* Kensley and Pether, 1986

†*Isognomon gariesensis* Kensley and Pether, 1986

†*Petricola prava* Kilburn Tankard, 1975

†*Standella namaquensis* Carrington and Kensley, 1969

BRACHIOPODA

†*Kraussina rotundata* Brunton and Hiller, 1990

†*Cancellothyris platys platys* Brunton and Hiller, 1990

The taxa found only in the muddy, distal, lower-shoreface to offshore deposits form a distinct assemblage potentially useful for recognizing these deposits.

Table 15.5 Species that are associated with muddy, distal deposits.

GASTROPODA

†*Bolma anoropha* Kensley and Pether, 1986

†*Clanculus lutosus* Kensley and Pether, 1986

†*Melapium hawthornei* Kensley and Pether, 1986

†*Pseudoliva lutulenta* Kensley and Pether, 1986

Ringicula turtoni Bartsch, 1915

Tugali barnardi (Tomlin, 1932)

Turritella declivis Adams and Reeve, 1848

BIVALVIA

†*Glycymeris fulleri* Kensley and Pether, 1986

†*Isognomon gariesensis* Kensley and Pether, 1986

Melliteryx capensis (Sowerby, 1889)

†*Notocallista schwarzi* (Newton, 1913)

Nuculana bicuspidata (Gould, 1845)

SCAPHOPODA

Dentalium sp.

BRACHIOPODA

†*Kraussina laevicostata* Brunton and Hiller, 1990

?†*Kraussina cuneata* Brunton and Hiller, 1990

†*Cancellothyris platys petalos* Brunton and Hiller, 1990

It is emphasized that, although based on a large collection, the collection is very local in provenance. The "zone fossil candidates" must be tested by the recovery of additional large assemblages from other areas, preferably where independent indications of their stratigraphic provenance exist, such as depositional environments (palaeodepths) of the shelly bed and its position in the larger-scale progradational geometry of the coastal plain. The elevation of an occurrence of shell, by itself, is an unreliable basis for inferring the stratigraphic context of a shell bed. This is implicit in the progradational nature of the record: deposits of a particular sea-level cycle may be preserved at any elevation below the transgressive maximum, if the subsequent transgression did not completely erode the record of the previous regression.

The fauna preceding that of the 50 m Package is unknown and thus the lower stratigraphic limits of the extinct species in the 50 m Package are undetermined.

Illustrations of many of the extinct taxa from the study area are provided in Appendix A. The faunal list is provided in Appendix B.

THE BRACHIOPODS

The brachiopods from the study area are mainly of the genus *Kraussina* which is endemic to southern Africa. The kraussinids from the study area are the oldest fossils of the genus (Brunton and Hiller,1990). The extant *K. rubra* occurs in both packages and three new, extinct species are present. *Kraussina lata*, described by Haughton (1932) from the "basal grits" at De Punt, is redescribed and a neotype established (Brunton and Hiller,1990). The occurrence of the genus *Cancellothyris* establishes a link with the Australian region. The source of the abundant, resinous, phosphatic, shell fragments in the 50 m Package is the inarticulate brachiopod identified by Brunton and Hiller (1990) as *Pelagodiscus* sp. At present *Pelagodiscus* lives in bathyal to abyssal depths, apparently migrating there during relatively recent geological history. The oldest record of the genus is tentatively lower Miocene, with Plio-Pleistocene occurrence in the Crag deposits of England (Brunton and Hiller, 1990).

Importantly, the extinct brachiopods are of potential biostratigraphic usefulness. *Kraussina lata* and *K. laevicostata* are recorded from only the 50 m Package (Table 15.2). *Kraussina rotundata* is the most common species and occurs in both packages (Table 15.4). *Kraussina laevicostata* and a large, wide subspecies of *Cancellothyris platys* (*C. platys petalos*) may have palaeoenvironmental utility, as they were found in the muddy, offshore-transition deposit on Koingnaas (Table 15.5) (Brunton and Hiller, 1990). The list of brachiopods is included in Appendix B.

THE BENTHIC FORAMINIFERA

The benthic foraminiferal assemblages in 6 samples from the study area (4 from the 50 m Package and 2 from the 30 m Package) all indicate a littoral or just sub-littoral environment that was well-oxygenated and turbulent, with a minimal influence of fresh-water discharge from rivers. On the basis of the local biostratigraphic ranges of taxa, an earliest Pleistocene age (latest Tiglian-earliest Eburonian) is indicated for all the samples (I. K. McMillan personal communication, 1994). The list of benthic foraminifera is provided in Appendix C.

15.3 THE VERTEBRATES

The vertebrates fossils from the study area form three, distinct assemblages. The oldest vertebrate remains are the dark-brown, phosphate-mineralized (petrified) bones and teeth that occur in the base of the sequence (the basal, petrified, mixed assemblage). A second, small assemblage is found within the sediments of the 50 m Package (the 50 m Package marine assemblage). The third assemblage mainly overlies the marine sequence (the capping, terrestrial assemblage).

The Basal, Petrified, Mixed Assemblage

The bulk of this material is broadly distributed as unidentifiable bone pebbles and worn shark teeth, mainly in the basal gravels. It is only in Zone 4A, in direct association with the preserved phosphoritic basal gravel, that more intact bones and teeth fossils are found. The small assemblage is a mixed marine and terrestrial fauna (Table 5.5), in which the marine component is dominant. The shark teeth, ray tooth plates and a variety of other smaller, presumed fish teeth are the most abundant component. The shark teeth will be examined in the near future by L. Compagno (South African Museum). The most spectacular remains are the "cobbles and boulders" of whale vertebrae and unusually-large teeth of what is presumed to be very large, predatory whales.

Table 15.6 The remanié fauna on the coastal plain unconformity.

MARINE

CHONDRICHTHYES

SELACHII

numerous shark teeth including rare specimens of *Carcharodon megalodon.*

BATOIDEA

tooth plates of rays.

OSTEICHTHYES

variety of presumed fish teeth, including pharyngeal tooth plates of extinct wrasse *Labrodon.*

MAMMALIA

CETACEA (whales)

numerous unidentifiable vertebral and rib fragments, "earbones" and unusually large teeth.

PINNIPEDIA

flipper bone of a seal (rare).

TERRESTRIAL

AVES

STRUTHIONIFORMES

Struthio sp., very large tarso-metatarsus.

MAMMALIA

CARNIVORA

tooth of a creodont (primitive hyaena).

PROBOSCIDEA

Gomphotheriidae (teeth and "ivory"of extinct relatives of elephants).

PERISSODACTYLA

Rhinocerotidae teeth of *Ceratotherium praecox*, ancestor of the white rhino.

ARTIODACTYLA

Equidae teeth of *Hipparion* (ancestral horse).

Bovidae teeth and limb bones.

Giraffidae tooth of possible palaeotragine.

The terrestrial component is dominated by the molars and tusk fragments of extinct, elephant-like gomphotheres. The giant ostrich is particularly interesting and it is tempting to speculate that it may represent the bird responsible for the unusual eggs reported by Corbett (1989) from the Miocene Rooilepel Sandstone of southern Namibia (Fig. 3.1).

The mixed, marine and terrestrial fauna has a Mio-Pliocene aspect and its age cannot be accurately constrained (Q. B. Hendey, personal communication). The preservation of some recognizable elements of this fauna in Zone 4A, when it has been reduced to a gravel everywhere else, is related to the deep bedrock embayment formed by the ancient fluvial channel. From the nature of the 50 m Package infill of Zone 4A, it is clear how the remains of marine vertebrates and shed shark teeth deposited in the shelf environment, at the height of the 50 m Package transgression, would have been protected from subsequent destruction during the regression. The emergence of the bedrock ridge caused low-energy, embayment-fill deposits to be deposited on the distal storm deposits that enclose the bones (Fig. 13.. Without the protection of the seaward-flanking bedrock ridge, a high-wave-energy shoreface would have prograded over Zone 4A, sweeping the shelf fossil record away.

During periods of low sea-level in the middle and late Miocene, the bedrock channel would have been re-occupied by fluvial systems. As transgressing sea-levels approached the bedrock ridge from the west, the area well behind the bedrock ridge would also have been protected. Temporary back-barrier environments would probably have developed before final inundation under relatively low-energy wave-conditions. With deepening to lower-shoreface depths and increasing wave energy, the terrestrial deposits enclosing the land mammals would have been winnowed, concentrating the bones as a transgressive lag. Thus some of the terrestrial remains deposited behind the bedrock ridge when it was a fluvial or paralic environment would have been preserved in the immediate area, which then became a shallow shelf and the depositional site of marine fauna. Once the bedrock channel was extant, these processes would have been repeated over successive sea-level cycles. Flushing of the channel by fluvial erosion during regressions would be the most likely means by which the bone accumulation in the area could be destroyed.

The dark-brown, phosphate-mineralized (petrified) bones and teeth in the base of the marine sequence in the study area are therefore a remanié fauna, both contributed to and subtracted from over a number of sea-level fluctuations.

THE 50 M PACKAGE MARINE ASSEMBLAGE

A second, very small assemblage consists of marine vertebrate material that is contemporaneous with the deposition of the 50 m Package. These bones were found unequivocally enclosed in the 50 m Package. They do not exhibit mineralization and are pale and brittle. The extinct seal *Homiphoca capensis* is described from early Pliocene deposits of the Varswater Formation at Langebaanweg, where its remains occur in abundance and represent individuals varying in age from very young to very old. It is therefore the local coastal seal during Pliocene times (Hendey, 1981a). As is evident from the limited fauna, bones other than those of whales are very scarce within lower

shoreface deposits. A portion of a whale's rib cage occurred at Section 15 on Avontuur-A (Chapter 11) and the most interesting whale find was in Zone 4A, within Unit PW (Plate 13.11).

Table 15.7 Vertebrate fossils contemporaneous with the 50 m Package.

OSTEICHTHYES		
	fish teeth.	
MAMMALIA		
CETACEA		
	Whale vertebra, ribs, "earbones" and rare skull fragments.	
	Delphinidae	mandible and skull fragments.
PINNIPEDIA		
	Phocidae	*Homiphoca capensis* mandible.
AVES		
	Spheniscidae	*Spheniscus* sp.

The Capping Terrestrial Assemblage

The third assemblage of vertebrates from the study area consists of the skeletal material collected at the top of the marine sections, where the bones occur in the transition between marine sediments and the pedogenic profile. This is the largest terrestrial vertebrate assemblage recovered (Appendix D) and is dominated by bovid limb bones. These occurrences were first noticed in the Zone 4A area, where the bones are most abundant (Plates 13.7, 13.8). Initially it was thought that the bones were deposited in an intertidal flat environment that represented the final marine-related deposition of the 50 m Package. They were therefore thought to be contemporaneous with the 50 m Package. The subsequent discovery, on Avontuur-A, that occurrences of scattered bone are associated with a cryptic deflation surface on top of the marine deposits, necessitated a re-evaluation.

Notably, the Zone 4A area is at present topographically lower than the surroundings. This condition probably also applied in the past. The low area would have been a site of shallow pan development during wetter climatic periods. As such, it might have been a watering place for animals and a site of carnivore predation, ultimately causing a greater concentration of vertebrate bones superimposed on the 50 m Package infill and perhaps "leaked" into it in places. However, since the shallowest levels of 50 m Package deposition occurred approximately at the same elevation, the possibility that some of the bones from the Zone 4A area may be contemporaneous with the 50 m Package cannot be entirely discarded.

The initial age constraint from this assemblage was the occurrence of *Equus capensis* (extinct Cape horse) (Pether, 1986a). Subsequently, the jaw of the extinct Mio-Pliocene pig *Nyanzachoerus* was found on the overburden dump adjacent to Zone 4A by mine geologist M. Mittelmeyer, where overburden stripped from extensions to Zone 4A had been deposited. The jaw was still partially

enclosed in matrix, which consisted of barnacle-plate-rich, coarse sand. The enclosing sediment was identical to that comprising the lensoid fills of erosional channels in the upper part of the sequence of Zone 4A. These features are interpreted as tidal creeks (Chapter 13). It is probable that the jaw came from this context. Notwithstanding the uncertainty as to the precise provenance of the *Nyanzachoerus* jaw, it is certainly closely associated with the 50 m Package.

15.4 THE AGE OF THE MARINE DEPOSITS

At an earlier stage in this study, when it was thought that the capping terrestrial vertebrate assemblage in the Zone 4 A area was contemporaneous with the 50 m Package, the presence of *Equus* indicated an age for the 50 m Package younger than the ~2 Ma dispersal of the horse in Africa (Pether, 1986a). The presence of *Nyanzachoerus* now indicates that the 50 m Package must be older than ~2.5 Ma, when *Nyanzachoerus* appears to have become extinct (Cooke, 1984).

The marine deposits at high elevation on the Namaqualand coastal plain, to the east of the area (the "75-90 m Transgression Complex" of Carrington and Kensley, 1969),), have been correlated by Hendey, (1981a,b) with the early Pliocene Varswater Formation and sea-level cycle TP1 of Vail and Hardenbol (1979). This correlation is accepted here and, following Hendey (1981a) these deposits have been renamed the 90 m Package in Pether (1986a). It is reasonable to assume that the 90 m Package was laid down, like the 50 m Package, during regression. Consequently, the 50 m Package cannot correlate with the regression from the early Pliocene high sea-level and must relate to the subsequent sea-level cycle. Accordingly, the 50 m Package must be between ~4 and ~2.5 myr old. The South Atlantic passive margin, relatively stable tectonic setting of the study area, together with the primarily glacio-eustatic control of sea-level in the latest Tertiary, permits the use of global curves of sea-level history. It is proposed that the 50 m Package may correlate with the regression from the middle Pliocene sea-level high at ~3 Ma, at the boundary of 3rd order cycles 3.6 and 3.7 (Haq *et al.*, 1987). The presence in the 50 m Package of the Langebaanian seal, *Homiphoca capensis*, is consistent with this age. The 30 m Package is correlated with the subsequent, 3rd order cycle regression (3.7/3.8 boundary), 1.6-2.0 Ma in the late Pliocene.

The occurrence of *Equus* in the capping terrestrial assemblage provides a maximum age of ~2 Ma for the deposition of the terrestrial sediment on the eroded top of the 50 m Package.

These ages for the 50 m and 30 m packages conflict with the single age indicated for both packages in terms of the benthic foraminiferal biostratigraphy developed by I. K. McMillan. A single age around the Plio-Pleistocene boundary is incompatible with the faunal contrast in the molluscan assemblages from the packages and the field evidence that the 50 m Package sands were decalcified prior to the 30 m Package transgression. It is also incompatible with the presence of *Nyanzachoerus* in the 50 m Package, which became extinct ~2.5 Ma. However, the benthic foraminifera from the muddy, distal 50 m Package bed on Koingnaas indicate a middle Pliocene age in terms of the biostratigraphic scheme (McMillan, 1993), compatible with the vertebrate evidence from the study area. Thus it

seems that the shallow-water benthic foraminiferal assemblages lack adequate age resolution, but the biochronology is correct for the deeper-water assemblage.

CHAPTER 16

CONCLUDING DISCUSSION

16.1 BRIEF SUMMARY OF COASTAL-PLAIN HISTORY

The topography of the gneiss bedrock in study area reveals the presence of a large channel. The location of the channel was influenced by a resistant dolerite dyke and a closely adjacent, brecciated fault. The faulting is parallel to the regional tectonic "grain" and is probably a very old feature, last active during late Jurassic/early Cretaceous continental break-up. The location of the fault influenced the emplacement of a dolerite dyke around this time. The bedrock along the channel is deeply weathered and kaolinized. The oldest sedimentary deposit preserved is associated with the development of this bedrock topography. This basal deposit consists of a remnant patch of kaolinitic, quartz gravels and sands in which bedding and decomposed boulders can be discerned. Petrographic and SEM study reveals the presence of feldspar and authigenic kaolinite. Most notably, the heavy mineral content includes diamonds. Plant fragments are sparsely present and from nearby the study area, where thicker, equivalent, deposits occur, a pollen assemblage was obtained. It is clear that the deposit was originally a high-energy, fluvial arkose laid down in the base of the channel. Subsequently, both it and the bedrock were kaolinized during a major period of weathering.

Large boulders of silcrete are closely spatially associated with the kaolinitic basal deposit. Field and petrographic evidence shows that the silcrete is indurated, kaolinitic basal deposit. Petrographically and geochemically the silcrete conforms with weathering-profile silcretes on the coastal plain of the southern Cape (Summerfield, 1983). The formation of the silcrete is therefore related to the period of weathering that kaolinized the fluvial deposits and underlying gneiss.

Preliminary analysis of the pollen from the basal kaolinitic deposit indicates an assemblage derived from yellowwood (*Podocarpus*) and ironwood (*Olea*) forest. The ironwood pollen, together with the minor presence presence of Asteraceae ("daisies"), indicates an age for the deposit not older than Oligocene.

It is suggested that the gross topography was developed by fluvial erosion during the major Oligocene regression (Siesser and Dingle, 1981). Arkosic gravels and sands infilling the channel were subsequently kaolinized and locally silicified together with the underlying gneiss, under humid conditions with abundant vegetation and poor drainage. A late Oligocene and early Miocene age is suggested for these events. During the subsequent history of the area, the channel was exhumed and the diamond content of the basal kaolinitic deposits redistributed. Although the topography would have been modified, the effects of mid-Tertiary incision persisted as an important antecedent control on marine deposition in the area.

The study area would have been affected by a middle Miocene transgression and the middle to Late Miocene regression, but deposits of this age have evidently not been preserved on the Namaqualand coastal plain. The oldest marine deposits are those of the 90 m Package, between 75 to 90 m asl. to the immediate east of the study area. On the basis of the record at Langebaanweg and global sea-level history, the 90 m Package is early Pliocene in age. These high-elevation deposits are better exposed north of Kleinzee and at Alexander Bay.

The oldest marine deposits in the study area, an alloformation called the 50 m Package, was laid down by shoreline progradation during a regression from at least 50 m asl. The 50 m Package overlies bedrock or eroded kaolinitic basal deposits and underlying, older marine deposits are not present in the study area. However, on the landward side of the main bedrock ridge flanking the ancient Oligocene channel, conditions were favourable for the preservation of a remanié accumulation of the phosphatized bones of land and sea mammals from earlier times. Some of the elements in the fauna may be as old as middle to late Miocene, whilst others may have been left in the wake of the transgression that immediately preceded the 50 m Package regression. The presence of an extinct pig, *Nyanzachoerus*, in the 50 m Package, indicates that it is older than ~2.5 Ma. The 50 m Package may have been deposited during the regression from a middle Pliocene high sea-level about 3 Ma.

Subsequently, the high-lying 50 m Package overlying the relatively steeper bedrock gradient on Avontuur-A was severely eroded, with the removal of its foreshore and most of its upper-shoreface deposits. Consequently, the thicknesses of 50 m Package deposits preserved in local basins and embayments are lower shoreface deposits. The overlying aeolian deposits cover remains of *Equus* and must therefore be younger than ~2 Ma. Within the bedrock channel, a nearly-complete vertical sequence of 50 m Package environments is preserved. Between the time of its deposition and the next transgression, the 50 m Package was subjected to decalcification.

Possibly about 1 myr after deposition of the 50 m Package, the next transgression reached ~30 m asl. The 30 m shoreline abutted the seaward flank of the bedrock ridge and would have eroded most of the 50 m Package deposits seaward of the bedrock ridge. However, the transgression "overrode" 50 m Package deposits filling the area of low bedrock west of the nose of the bedrock ridge. Another progradational wedge built out seawards from the 30 m asl. transgressive maximum, forming the regressional 30 m Package alloformation. Subsequent terrestrial (aeolian) erosion of the top of the 30 m Package mainly affected its foreshore deposits. Thick upper-shoreface deposits are present in the 30 m Package and in places the trough cross-bedding is only 1-2 m beneath the present land surface. Pedogenesis produced an obscuring, intergranular mud content and destroyed the shell content, causing the 30 m Package upper-shoreface facies to superficially resemble terrestrial deposits. The 30 m Package extends to near the present-day shoreline, where it is overlain by regressive foreshore deposits relating to an ?early Pleistocene high sea-level that reached ~10 m asl.

Both the 50 and 30 m packages contain a molluscan fauna that indicates temperatures considerably warmer than those that presently wash the upwelling-dominated coast. Despite evidence for

Benguela upwelling since ~10 Ma in the late Miocene, with Pliocene intensification (Siesser, 1978), the Pliocene coast of Namaqualand was clearly not affected by upwelling as it is experienced at present. Modern molluscan faunas appear after the 30 m Package, apparently in the early Pleistocene. An early hypothesis to explain the warmer seas along Namaqualand was that warm water from the Agulhas Current had easier access to the west coast when the low-lying land between the Cape Peninsula and mainland (Cape Flats) was a shallow strait (Haughton, 1932). A modern version of the Agulhas-water hypothesis could invoke a reduced intensity of atmospheric circulation during times of warm Pliocene interglacial climate. Reduced intensity of the trades would reduce upwelling along the west coast. Reduced trades over the Indian Ocean would reduce the transport in the Agulhas Current, enhancing its tendency to round Africa, rather than to retroflect to the south. These conditions are invoked to explain the presence of warm-water molluscs on the Namaqualand coast during the last deglaciation (Pether, 1994). They may be an analogue for interglacial conditions in the Pliocene.

16.2 SEDIMENTOLOGICAL ASPECTS

The two formations that make up the major portion of the coastal-plain marine record, the 50 m Package and the 30 m Package, were laid down as classic regressive sequences during shoreline progradation seawards from their transgressive maxima. Knowing that the coastal-plain record conforms to this model considerably aids in the interpretation of the local details of the record. This is well-illustrated by Zone 4A in the study area, where the emergence of the bedrock ridge resulted in very different deposits in close proximity, which could only be understood in the progradational framework. High-energy, but distal storm deposits were succeeded by low-energy, proximal deposits, due to ridge emergence reducing the exposure of the shoreline to the east (landwards) to open-coast wave-energy. Low-energy, lower-shoreface sediments therefore lapped into the channel. When the bedrock ridge became fully-emergent, the shoreline was established on its seaward flank and the channel at Zone 4A became the locality of low-energy, bay-infill.

In terms of the idealized model of shoreline progradation, each regressive package would extend seawards from the transgressive maximum as a seaward-thickening wedge incorporating successively deeper environments in its base (e.g. the 30 m Package at A Block). Furthermore, a shallow-marine, progradational package must be subject to the same large-scale controls that produce the record of the continental margin. In terms of sequence stratigraphy, the 50 and 30 m packages are "mini" highstand systems tracts, each comprising only one parasequence. Their sedimentary geometry is the result of the interaction between the rate of sea-level change and sediment supply. However, due to their much shorter depositional time scale, subsidence is not a factor. Instead, bedrock gradient with respect to sea-level and sediment supply is important. In reality, the overall bedrock gradient and detailed relief vary within and between areas, creating bays, headlands, local basins, reefs and terraces in the progradational setting. This bedrock topography mainly influences the range of facies developed e.g. high-energy sequences in exposed coastal settings, lower-energy sequences in

protected embayments, localities of enhanced seaward storm transport and deposition of gravel. The proximity of a particular "coastal compartment" to the locations of fluvial input will also influence the lithology e.g. conglomeratic vs. sandy shorelines.

An important general conclusion is that true transgressive lags are absent beneath the marine deposits. The basal gravels in the study area were swept from the upper shoreface and foreshore in increments into the lower shoreface. The gravels in the proximal environment were then regularly reworked under swell, until they were finally buried beneath the prograding shoreface wedge. Probably only sediment sequestered in crevices in the bedrock, large boulders and isolated clasts represent material last mobile during transgression. Where the muddy, deepest-water facies are preserved, they do not overlie lags, but rest directly on bedrock or a thin gravel with locally-derived, angular bedrock material. The distally-deposited gravels and shell were infiltrated by mud. In the 50 m Package, widespread phosphorite deposition occurred in the offshore environment. Erosion during intervening storms produced phosphorite clasts that show multiple generations of deposition. Erosion of the offshore phosphorite increased in frequency and intensity as sea-level fell from the transgressive maximum and the prograding shoreface approached, eventually destroying most of the offshore facies, except for coarsening-upward remnants preserved in localized circumstances, such as in the case of Zone 4A.

These storm-deposited gravels are clearly diamondiferous, but the depths in which they were deposited may not be generally appreciated. Traditionally, the concentration of diamonds is regarded as an upper shoreface process. In the study area, the lower shoreface gravels filling the areas of low bedrock (and their diamond content) were removed from the upper shoreface. With a knowledge of the bedrock topography and the palaeodepths in the overlying marine sediments, the depths at which large areas of bedrock were finally buried can be established. For instance, sea-level was maintained well above bedrock during the progradation of both the 50m and 30m Packages; thus only the highest bedrock was covered by foreshore (intertidal) deposits. However, surf-zones would have locally intersected the flanks of bedrock highs. Although the thicker, lower-shoreface gravels are generally mined, it is possible that economic opportunities may exist in the thin gravels on the bedrock flanking the bedrock lows.

In Zone 4a, the basal gravels exhibited a persistent aspect of lateral variation, despite deposition at different depths and different energy levels. In A Block, a control on storm-gravel distribution by a northern headland seemed to have operated. These features suggest that the distribution of gravels could be predicted to a degree. There can be no doubt that a clearer perception of the depositional palaeodepth of various gravels and coarse sands will result in improved ore prediction.

16.3 STRATIGRAPHIC CONCLUSIONS

The main stratigraphic conclusions emerging from this work is that Carrington and Kensley's (1969) units are recognized, but are now placed in their correct environmental context. The "17-21 m

Transgression Complex" and "29-34 m Beach" together comprise a single regressive package, the 30 m Package. Carrington and Kensley's recognition of *Donax haughtoni* and *D. rogersi* as zone fossils is confirmed.

Phosphoritic beds and muddy units in the base of the marine deposits, usually preserved in bedrock depressions, are referred to as "E-stage" among mine geologists on west coast diamond mines. The "E-stage" terminology stems from Haughton's (1932) oldest biostratigraphic zone, "Zone E." Carrington and Kensley's (1969) Pliocene "fossiliferous phosphatic siltstones" (Table 3.1) are very likely these "E-stage" beds. "E-stage" has been discussed by (Tankard, 1966, 1975a,b) and Hendey (1981a, 1981b) and is subdivided into lower, middle and upper stages. Various correlations have been proposed for these parts of "E-stage." These will not be reviewed in detail here, but mainly involve correlation with perceived Miocene units (e.g. the "Saldanha Formation") and the early Pliocene Varswater Formation. In the study area, the phosphatic mouldic coquina and phosphoritic quartzose gravel in Zone 4A would be regarded as "E-stage" beds. Previously, the writer has also correlated these beds with the early Pliocene 90 m Package, deposited during the sea-level cycle preceding the 50 m Package (e.g. Kensley and Pether, 1986; Pether, 1986a).

Thus an important result of this study is the recognition that these units represent distal storm deposition in the 50 m Package, with phosphatization and phosphorite deposition being superimposed upon the storm deposits in the offshore environment. The eroded top of the phosphorite is not an unconformity, but an intraformational erosion surface developed by regression and falling sea-level, bringing the offshore beds into the erosive shoreface environment. Similarly the *Isognomon* bed in A Block (Unit NS) would have been considered as an "E-stage" sub-unit. From the sequence-stratigraphic point of view, these beds have no status separate from the overlying shoreface deposits as all were laid down during the same regression.

As regards the biostratigraphic status of "E-stage," Haughton erected "Zone E" on the basis of the section described by Reuning (1931) at De Punt (Fig. 3.1). Here a small assemblage was contained in "basal grits" perceived to be underlying a correlate of the Eocene or older, Pomona quartzite (silcrete) of southern Namibia. This is the type locality of the brachiopod *Kraussina lata* Haughton, 1932. "Zone E" and "Zone of *Kraussina lata*" are synonymous. The apparent considerable age of "Zone E" can now be shown as false. The kraussinids are a relatively recent evolutionary development and, in fact, the oldest kraussinids known are those from the study area. Their inferred ancestors are in the Miocene (Brunton and Hiller,1990). The patellid from the "basal grits" in the South African Museum collections has been identified as *Cellana capensis*. The genus *Cellana* extends from the Miocene. The small scallop in the collection is *Chlamys tincta*, an extant species. Thus the type locality of "Zone E" or "E stage" has no biostratigraphic validity.

The stratigraphy of the Namaqualand coastal plains is simplified by the merging of "E-stage" with the 50 m Package. However, the possibility of remnants of older sediments being present beneath a progradational package cannot be entirely discarded. The probability of them being present can be

evaluated in terms of the proximality of the shoreface deposits generally overlying the basal contact. However, the "burden of proof" is now reversed in the sense that it has to be shown that lithological and fossil assemblage contrasts are not merely a reflection of a deeper environment and that the contact separating the under- and overlying deposits is not an intraformational, lower shoreface erosion surface. This shift from lithostratigraphy to a genetic, sequence stratigraphy necessitates that the progradational packages be regarded as alloformations.

The "Old Beach" of Davies (1973), extending north from Walvis Bay, Namibia, at elevations between 9-25 m asl., corresponds to the 30 m Package because these deposits contain the zone fossils *Donax rogersi* and *Fissurella glarea*. Near Walvis Bay, the 30 m Package *Donax rogersi* has been found below 30 m asl. in thin, residual, marine gravels (the Rooikop gravels). However, marine gravels extend to a transgressive maximum at ~50 m asl. where they overlap aeolian material (J.D. Ward and J. Pether, unpublished observations), indicating the likely presence of the 50 m Package in the Central Namib. Murray *et al.* (1970) have already correlated the "Upper Terrace" (D, E and F beaches) of southern Namibia with the "17-21m Complex" (30 m Package) in Namaqualand. The 50 m Package is evidently not well-preserved in Namibia. However, marine gravels up to 60 m asl. in northern Namibia (Hallam, 1964) may include this formation. Near Bogenfels (Torbogenbucht), Beetz (1926) recorded a raised beach at 40 m asl. (Haughton, 1932). Hallam (1964) mentioned "vestigial gravels" at 30-35 m asl., above the F, E, D set of deposits and Stocken (1978) also mentioned the possibility of older gravels being present.

De Villiers and Söhnge (1959) noted important aspects of the sedimentary geometry at Alexander Bay. Notably, Upper Terrace gravel beds project beyond the edge of the cliff separating this terrace from the Middle Terrace, and are thus younger than the underlying deposits on the Middle Terrace. Furthermore, they noted an unconformity in the Middle Terrace deposits. They concluded that the Upper Terrace is younger than the Middle Terrace and imply that deposits on the Middle Terrace were laid down during different sea-level stages. Thus, though the bedrock topography (terraces) at Alexander Bay corresponds generally with the sea-level history deduced at Hondeklip, this correspondence must necessarily be viewed with suspicion. The geometry noted by De Villiers and Söhnge (1959) can be explained by the cliffs and terraces simply being overlain by progradational packages. Limited biostratigraphic data from the terraces just north of Port Nolloth (Gresse, 1988) suggests that deposits on the Upper Terrace at ~60 m asl. correlate with the 50 m Package, or are older. The deposits on the Middle Terrace at ~35 m asl. contain 3 taxa confined to the 50 m Package at Hondeklip and, considering the elevation, probably represent that alloformation. However, the same 3 taxa were also sampled from deposits on the Lower Terrace.

On the basis of elevation, the 50 m Package should occur on the Upper Terrace (30-60 m asl.). The geometry noted by De Villiers and Söhnge (1959), together with evidence for its occurrence on the Middle Terrace, suggests that it does. Similarly, the 30 m Package should occur on the Middle Terrace, but must be locally underlain by 50 m Package deposits (e.g. the unconformity in the Middle

Terrace deposits noted by De Villiers and Söhnge (1959). The 50 m Package may apparently even extend onto the Lower Terrace in places.

South of the study area, to the north of the Olifants River in the De Punt area, *D. haughtoni* occurs in truncated deposits overlying the bedrock sea-cliffs, indicating that it is the 50 m Package that overlies the planed bedrock at ~27 m asl. *Donax rogersi* is found in the spoil of prospecting pits in the lower-lying coastal plain farther north, as well as in cliff exposures to the south of the Olifants River (Fig. 3.1). Thus the 30 m Package can be recognized over ~1500 km of the southern African west coast.

The firm establishment, on the basis of sedimentary geometry, of a 30 m asl. transgressive maximum, is an important advance for coastal-plain stratigraphy. The importance of fixing such maxima is that they are the most reliable feature for testing subsequent differential uplift along the margin periphery. The maxima at about 50 m asl. and about 90 m asl. require further investigation. This is increasingly difficult for the older, higher packages, due to the more residual nature of the marine sedimentary record. Nevertheless, the depositional rather than the erosional record must be regarded as the most reliable indicator of palaeodepths, because cliffs and terraces on bedrock are subject to more equivocal interpretations. They reflect stillstands, are influenced by bedrock lithology and are locally rather than regionally developed. In addition, they can be inherited from previous transgressions, can be subsequently enhanced and need not form at the sea-level maxima. Thus all cliffs and terraces must be placed in their correct geological context by examination of the depositional environments and geometry of the overlying marine sediments.

REFERENCES

Ahlbrandt, T.S. and Fryberger, S.G. 1982. Eolian deposits. In: In: Scholle, P.A. and Spearing, D. (eds.), Sandstone Depositional Environments. *Memoirs of the American Association of Petroleum Geologists* **31**: 11-47.

Allen, J.R.L. 1982. Sedimentary structures: their character and physical basis. *Developments in Sedimentology* **30B**. Amsterdam, Elsevier.

Alpers, C.N. and Brimhall, G.H. 1988. Middle Miocene climatic change in the Atacama Desert, northern Chile: evidence from supergene mineralization at La Escondida. *Bulletin of the Geological Society of America* **100**: 1640-1656.

Arnot, R.W.C. 1993. Quasi-planar-laminated sandstone beds of the Lower Cretaceous Bootlegger Member, north-central Montana: evidence of combined-flow sedimentation. *Journal of Sedimentary Petrology* **63**: 488-494.

Beetz, P.R.W. 1926. Die Tertiärablagerungen der Küstennamib. In: Kaiser, E. (ed.), *Die Diamantenwüste Südwestafricas,* Band **2**: 1-54. Berlin: Dietrich Reimer (Ernst Vosen).

Birch, G.F. 1975. Sediments on the continental margin off the west coast of South Africa. *Bulletin of the Joint Geological Survey/University of Cape Town Marine Geoscience Unit* **6**: 1-142.

Birch, G.F., Day, R.W. and Du Plessis, A. 1991. Nearshore Quaternary sediments on the west coast of southern Africa. *Bulletin of the Geological Survey of South Africa* **101**: 1-14.

Birch, G.F., Rogers, J. and Bremner, J.M. 1986. Texture and compostion of surficial sediments of the continental margin of the republics of South Africa, Transkei and Ciskei. *Maps, Geological Survey of South Africa Marine Geoscience Series* **3** (Sheets 1-4).

Böhm, J. 1926. Über tertiäre Versteinerungen von den Bogenfelser Diamantfeldern. In: Kaiser, E. (ed.), *Die Diamantenwüste Südwestafricas,* Band **2**: 55-87. Berlin: Dietrich Reimer (Ernst Vosen).

Bouma, A.H. 1969. *Methods for the Study of Sedimentary Structures.* New York: Wiley-Interscience.

Bourgeois, J. 1980. A transgressive shelf sequence exhibiting hummocky cross-stratification: the Cape Sebastian Sandstone (Upper Cretaceous), southwestern Oregon. *Journal of Sedimentary Petrology* **50**: 681-702.

Bourgeois, J. and Leithhold, E.L. 1984. Wave-worked conglomerates - depositional processes and criteria for recognition. In: Koster, E.H. and Steele, R.J. (eds.), Sedimentology of Gravels and Conglomerates. *Memoir of the Canadian Society of Petroleum Geologists* **10**: 331-343.

Bremner, J.M. 1981. Sediments on the continental margin off South West Africa between latitudes 17° and 25° South. *Bulletin of the Joint Geological Survey/University of Cape Town Marine Geoscience Unit* **10**: 1-233.

Bremner, J.M., Rogers, J. and Birch, G.F. 1986. Surficial sediments of the continental margin of South West Africa (Namibia). *Maps, Geological Survey of South West Africa (Namibia) Marine Geoscience Series* (Sheets 1-4).

Bremner, J.M., Rogers, J. and Willis, J.P. 1990. Sedimentological aspects of the 1988 Orange River floods. *Transactions of the Royal Society of South Africa* **47** (3): 247-294.

Bromley, R.G. 1990. *Trace Fossils: biology and taphonomy.* London: Unwin Hyman.

Bromley, R.G. and Frey, R.W. 1974. Redescription of the trace fossil *Gyrolithes* and taxonomic evaluation of *Thalassinoides, Ophiomorpha* and *Spongeliomorpha. Bulletin of the Geological Society of Denmark* **23**: 311-335.

Brunton, C.H.C. and Hiller, N. 1990. Late Cainozoic brachiopods from the coast of Namaqualand, South Africa. *Palaeontology* **33**: 313-342.

Carrington, A.J. and Kensley, B. F. 1969. Pleistocene molluscs from the Namaqualand coast. *Annals of the South African Museum* **52** (9): 189-223.

Chapman, P. and Shannon, L.V. 1985. The Benguela Ecosystem Part II. Chemistry and related processes. In: Barnes, M. (ed.), *Oceanography and Marine Biology. An Annual Review* **23**: 183-251. Aberdeen: University Press.

Cheel, R.J. 1991. Grain fabric in hummocky cross-stratified storm beds: genetic implications. *Journal of Sedimentary Petrology* **61**: 102-110.

Cheel, R.J. and Leckie, D. 1992. Coarse-grained storm beds of the Upper Cretaceous Chungo Member (Wapiabi Formation), southern Alberta, Canada. *Journal of Sedimentary Petrology* **62**: 933-945.

Clifton, H.E., Hunter, R.E. and Phillips, R.L. 1971. Depositional structures and processes in the non-barred, high-energy nearshore. *Journal of Sedimentary Petrology* **41**: 651-670.

Clifton, H.E. 1973. Pebble segregation and bed lenticularity in wave-worked versus alluvial gravel. *Sedimentology* **20**: 173-187.

Clifton, H.E. 1981. Progradational sequences in Miocene shoreline deposits, southeastern Caliente Range, California. *Journal of Sedimentary Petrology* **51**: 165-184.

Clifton, H.E. 1988. Sedimentologic approaches to paleobathymetry, with applications to the Merced Formation of Central California. *Palaios* **3**: 507-522.

Clifton, H.E. and Dingler, J.R. 1984. Wave-formed structures and paleoenvironmental reconstruction. *Marine Geology* **60**: 165-198.

Clifton, H.E. and Thompson, J.K. 1978. *Macaronichnus segregatis*: a feeding structure of shallow marine polychaetes. *Journal of Sedimentary Petrology* **48** (4): 1293-1302.

Coetzee, J.A. 1978. Climatic and biological changes in south-western Africa during the late Cainozoic. *Palaeoecology of Africa* **10**: 13-29.

Coetzee, J.A. 1981. A palynological record of very primitive angiosperms in Tertiary deposits of the south-western Cape Province, South Africa. *South African Journal of Science* **77**: 341-343.

Coetzee, J.A. 1986. Palynological evidence for major vegetation and climatic change in the Miocene and Pliocene of the south-western Cape. *South African Journal of Science* **82**: 71-72.

Coetzee, J.A. and Rogers, J. 1982. Palynological and lithological evidence for the Miocene palaeoenvironment in the Saldanha region (South Africa). *Palaeogeography, Palaeoclimatology, Palaeoecology* **39**: 71-85.

Coetzee, J.A., Scholtz, A. and Deacon, H.J. 1983. Palynological studies and vegetation history of the Fynbos. In: Deacon, H.J., Hendey, Q.B. and Lambrechts, J.J.N. (eds.), *Fynbos palaeoecology: a preliminary synthesis*. South African National Scientific Programmes Report No.**75**: 156-173.

Cooke, H.B.S. 1984. Horses, elephants and pigs as clues in the African later Cainozoic. In: Vogel, J.C. (ed.), *Late Cainozoic Palaeoclimates of the Southern Hemisphere*. Rotterdam, A.A. Balkema: 473-482.

Corbett, I.B. 1989. The sedimentology of diamondiferous deflation deposits within the Sperrgebiet, Namibia. *Unpublished Ph.D. thesis, University of Cape Town.*

Curran, H.A. 1976. A trace fossil brood structure of probable callianassid origin. *Journal of Paleontology* **50** (2): 249-259.

D'Alessandro, A. and Bromley, R.G. 1987. Meniscate trace fossils and the *Muensteria–Taenidium* problem. *Palaeontology* **30** (4): 743-763.

Davies, J.L. 1964. A morphogenetic approach to world shorelines. *Zeitschrift für Geomorphology* **8**: 127-142.

Davies, O. 1973. Pleistocene shorelines in the western Cape and South West Africa. *Annals of the Natal Museum* **21** (3): 719-765.

Day, R.W. 1987. False Bay dolerites. *Annals of the Geological Survey of South Africa* **21**: 1-7.

DeCelles, P.G. 1987. Variable preservation of middle Tertiary, coarse-grained, nearshore to outer-shelf storm deposits in southern California. *Journal of Sedimentary Petrology* **57**: 250-264.

De Decker, R.H. 1987. The geological setting of diamondiferous deposits on the inner shelf between the Orange River and Wreck Point, Namaqualand. *Bulletin of the Geological Survey of South Africa* 86: 1-99.

De Decker, R.H. 1988. The wave regime on the inner shelf of the Orange River and its implications for sediment transport. *South African Journal of Geology* **91**: 358-371.

De Villiers, J. and Söhnge, P.G. 1959. Geology of the Richtersveld. *Memoir of the Geological Survey of South Africa* 48: 1-295.

De Wit, M.C.J. 1990. Palaeoenvironmental interpretation of Tertiary sediments at Bosluispan, Namaqualand. *Palaeoecology of Africa* **21**: 101-118.

Dingle, R.V. 1971. Tertiary sedimentary history of the continental shelf off southern Cape Province, South Africa. *Transactions of the Geological Society of South Africa* **74**: 173-185.

Dingle, R.V. 1973. The geology of the continental shelf between Lüderitz and Cape Town, (Southwest Africa) with special reference to Tertiary strata. *Journal of the Geological Society of London* **129**: 337-363.

Dingle, R.V. 1980a. Sedimentary basins on the continental margins of Southern Africa. An assessement of their hydrocarbon potential. *Erdol und Kohle-Erdgas-Petrochemie vereinigt mit Brennstoff-Chemie* 33 (10): 457-463.

Dingle, R.V. 1980b. Large allochthonous sediment masses and their role in the construction of the continental slope and rise off southwestern Africa. *Marine Geology* **37**: 333-354.

Dingle, R.V. 1992/93. Structural and sedimentary development of the continental margin off southwestern Africa. *Communications of the Geological Survey of Namibia* 8: 35-43.

Dingle, R.V. and Hendey, Q.B. 1984. Late Mesozoic and Tertiary sediment supply to the eastern Cape Basin (SE Atlantic) and palaeo-drainage systems in southwestern Africa. *Marine Geology* **56**: 13-26.

Dingle, R.V. and Nelson, G. 1993. Sea-bottom temperature, salinity and dissolved oxygen on the continental margin off south-western Africa. *South African Journal of Marine Science* **13**: 33-49.

Dingle, R.V. and Siesser, W.G. 1977. Geology of the continental margin between Walvis Bay and Ponta do Ouro. *Map, Geological Survey of South Africa Marine Geoscience Series* **2** (map and explanatory notes).

Dingle, R.V., Siesser, W.G. and Newton, A.R. 1983. *Mesozoic and Tertiary Geology of Southern Africa.* Rotterdam: A.A. Balkema.

Dingle, R.V., Birch, G.F., Bremner, J.M., De Decker, R.H., Du Plessis, A., Engelbrecht, J.C., Fincham, M.J., Fitton, T., Flemming, B.W., Gentle, R.I., Goodlad, S.W., Martin, A.K., Mills, E.G., Moir, G.J., Parker, R.J., Robson, S.H., Rogers, J., Salmon, D.A., Siesser, W.G., Simpson, E.S.W., Summerhayes, C.P., Westall, F., Winter, A. and Woodborne, M.W. 1987. Deep-sea sedimentary environments around southern Africa (South-East Atlantic and South-West Indian Oceans). *Annals of the South African Museum* **98** (1): 1-27.

Dott., R.H. Jr. and Bourgeois, J. 1982. Hummocky stratification: significance of its variable bedding sequences. *Bulletin of the Geological Society of America* **93**: 663-680.

Dott., R.H. Jr. and Bourgeois, J. 1983. Hummocky stratification: significance of its variable bedding sequences: discussion and reply. *Bulletin of the Geological Society of America* **94**: 1249-1251.

Droser, M.L. and Bottjer, D.J. 1989. Ichnofabric of sandstones deposited in high-energy nearshore environments: measurement and utilization. *Palaios* **4**: 598-604.

Duke, W.L., Arnott, R.W.C. and Cheel, R.J. 1991. Shelf sandstones and hummocky cross-stratification: new insights on a stormy debate. *Geology* **19**: 625-628.

Duncan, A.R., Erlank, A.J. and Betton, P.J. 1984. Appendix 1: Analytical techniques and database descriptions. *Special Publication of the Geological Society of South Africa* **13**: 389-395.

Du Plessis, A. and Glass, J.G. 1991. The Geology of False Bay. *Transactions of the Royal Society of South Africa* **47**: 495-517.

Dupré, W.R. 1984. Reconstruction of paleo-wave conditions during the late Pleistocene from marine terrace deposits, Monterey Bay, California. *Marine Geology* **60**: 435-454.

Du Toit, A.L. 1954. *The Geology of South Africa* (3rd Edition). Edinburgh: Oliver & Boyd.

Elliott, T. 1986. Siliciclastic Shorelines. In: Reading, H.G. (ed.), *Sedimentary Environments and Facies* (2nd Edition): 155-188. Oxford, Blackwell Scientific Publications.

Flemming, B.W. 1977. Depositional processes in Saldanha Bay and Langebaan Lagoon. *Bulletin of the Joint Geological Survey/University of Cape Town Marine Geoscience Unit* **8**: 1-215.

Forbes, V.S. and Rourke, J. 1980. *Paterson's Cape Travels, 1777 to 1779.* Johannesburg: The Brenthurst Press.

Frakes, L.A. 1979. *Climates through Geologic Time.* Amsterdam: Elsevier.

Frankel, J.J. and Kent, L.E. 1938. Grahamstown surface quartzites. *Transactions of the Geological Society of South Africa* **40**: 1-42.

Frankel, J.J. 1952. Silcrete near Albertinia, Cape Province. *South African Journal of Science* **49**: 173-182.

Frey, R.W. 1970. Trace fossils of Fort Hays Limestone Member of Niobrara Chalk (Upper Cretaceous), west-central Texas. *University of Kansas Paleontological Contributions, Article* **53** (Cretaceous 2): 1-41.

Frey, R.W., Curran, H.A. and Pemberton, S.G. 1984. Tracemaking activities of crabs and their environmental significance: the ichnogenus *Psilonichnus*. *Journal of Paleontology* **58** (2): 333-350.

Frey, R.W. and Howard, J.D. 1985. Trace fossils from the Panther Member, Star Point Formation (Upper Cretaceous), Coal Creek Canyon, Utah. *Journal of Paleontology* **59** (2): 370-404.

Frey, R.W. and Howard, J.D. 1990. Trace fossils and depositional sequences in a clastic shelf setting, Upper Cretaceous of Utah. *Journal of Paleontology* **64** (5): 803-820.

Frey, R.W., Howard, J.D. and Pryor, W.A. 1978. *Ophiomorpha*: its morphologic, taxonomic, and environmental significance. *Palaeogeography, Palaeoclimatology, Palaeoecology* **23**: 199-229.

Fürsich, F.T. 1981. Invertebrate trace fossils from the Upper Jurassic of Portugal. *Comunicacões dos serviços geológicos de Portugal* **67**: 153-168.

Gao, G. and Land, L.S. 1991. Nodular chert from the Arbuckle Group, Slick Hills, SW Oklahoma: a combined field, petrographic and isotopic study. *Sedimentology* **38**: 857-870.

Gautier, A.M. and von Pechman, E. 1984. Mineral separation by centrifugation with heavy liquids - improvement of a method. *Schwiezerische Mineralogische und Petrographische Mitteilungen* **64**: 459-464.

Glass, J. 1977. Deep weathering of the southwestern Cape Granite and Malmesbury Group: palaeoclimatic implications. *Technical Report of the Joint Geological Survey/University of Cape Town Marine Geology Programme* **9**: 118-135.

Gordon, A.L. 1985. Indian-Atlantic transfer of thermocline water at the Agulhas Retroflection. *Science* **227**: 1030-1033.

Gresse, P.G. 1988. Washover boulder fans and reworked phosphorite in the Alexander Bay Formation. *South African Journal of Geology* **91** (3): 391-398.

Hallam, C.D. 1964. The geology of the coastal diamond deposits of southern Africa (1959). In: Haughton, S.H. (ed.), *The Geology of some Ore Deposits in southern Africa.* Vol. 2: 671-728. Johannesburg: Geological Society of South Africa.

Häntzschel, W. 1975. Trace fossils and problematica. In: Teichert, C. (ed.), *Treatise on Invertebrate Paleontology.* Part **W**, suppl. 1, 269 pp. Boulder, Colorado and Lawrence, Kansas. Geological Society of America and University of Kansas Press.

Haq, B.U., Hardenbol, J. and Vail, P.R. 1987. Chronology of fluctuating sea levels since the Triassic. *Science* **235**: 1156-1167.

Harmse, J.T. and Swanevelder, C.J. 1987. Spatial variation in the granulometric properties of Sandveld aeolianites. *Annals of the Geological Survey of South Africa* **21**: 51-58.

Hartnady, C.J.H. and Rogers, J. 1990. The scenery and geology of the Cape Peninsula. *Guidebook Geocongress '90 Geological Society of South Africa* **M1**: 1-67.

Haughton, S.H. 1926. On some new mollusca from Tertiary beds in the west of the Cape Province. *Transactions of the Royal Society of South Africa* **13**: 159-162.

Haughton, S.H. 1928. The palaeontology of the Namaqualand coastal deposits. In: Wagner, P.A. and Merensky, H. 1928. The diamond deposits on the coast of Little Namaqualand. *Transactions of the Geological Society of South Africa* **31**: 1-41.

Haughton, S.H. 1932. The Late Tertiary and Recent deposits of the west coast of South Africa. *Transactions of the Geological Society of South Africa* **34**: 19-58.

Hendey, Q.B. 1978. Preliminary report on the Miocene vertebrates from Arrisdrift, South West Africa. *Annals of the South African Museum* 76: 1-41.

Hendey, Q.B. 1981a. Palaeoecology of the Late Tertiary fossil occurrences in "E" Quarry, Langebaanweg, South Africa, and a re-interpretation of their context. *Annals of the South African Museum* **84**: 1-104.

Hendey, Q.B. 1981b. Geological succession at Langebaanweg, Cape Province, and global events of the Late Tertiary. *South African Journal of Science* **77**: 33-38.

Hendey, Q.B. 1983a. Cenozoic geology and palaeogeography of the Fynbos region. In: Deacon, H.J., Hendey, Q.B. and Lambrechts, J.J.N. (eds), *Fynbos palaeoecology: a preliminary synthesis.* South African National Scientific Programmes Report No. **75**: 35-60.

Hendey, Q.B. 1983b. Palaeontology and palaeoecology of the Fynbos region: an introduction. In: Deacon, H.J., Hendey, Q.B. and Lambrechts, J.J.N. (eds.), *Fynbos palaeoecology: a preliminary synthesis.* South African National Scientific Programmes Report No. **75**: 87-99.

Hendey, Q.B. 1983c. Palaeoenvironmental implications of the Late Tertiary vertebrate fauna of the Fynbos region. In: Deacon, H.J., Hendey, Q.B. and Lambrechts, J.J.N. (eds.), *Fynbos palaeoecology: a preliminary synthesis.* South African National Scientific Programmes Report No. **75**: 100-115.

Hendey, Q.B. 1984. Southern African late Tertiary vertebrates. In: Klein, R.G. (ed.), *Southern African Prehistory and Paleoenvironments*: 81-106. Rotterdam, A.A. Balkema.

Hendey, Q.B. and Dingle, R.V. 1990. Onshore sedimentary phosphate deposits in south-western Africa. In: Burnett, W. C. and Riggs, S.R. (eds.), *Phosphate Deposits of the World*, Vol. **2**: 200-206. Cambridge: Cambridge University Press.

Heron, S.D., Jr., Moslow, T.F., Berelson, W.M., Herbert,J.R., Steele, G.A., III, and Susman, K.R. 1984. Holocene sedimentation of a wave-dominated barrier-island shoreline: Cape Lookout, North Carolina. *Marine Geology* **60**: 413-434.

Heward, A.P. 1981. A review of wave-dominated clastic shoreline deposits. *Earth-Science Reviews* **17**: 223-276.

Hopwood, A.T. 1929. New and little known mammals from the Miocene of Africa. *American Museum Novitates* **344**: 1-9.

Howard, J.D. 1972. Trace fossils as criteria for recognizing shorelines in the stratigraphic record. In: Rigby, J.K. and Hamblin, W.M. (eds.), Recognition of ancient sedimentary environments. *Special Publication of the Society of Economic Paleontologists and Mineralogists* **16**: 215-225.

Howard J.D. and Frey, R.W. 1975. Estuaries of the Georgia coast, U.S.A.: sedimentology and biology. II. Regional animal-sediment characteristics of Georgia estuaries. *Senckenbergiana Maritima* **7**: 33-103.

Howard J.D. and Frey, R.W. 1984. Characteristic trace fossils in nearshore to offshore sequences, Upper Cretaceous of east-central Utah. *Canadian Journal of Earth Sciences* **21**: 200-219.

Howard J.D. and Frey, R.W. 1985. Physical and biogenic aspects of backbarrier sedimentary sequences, Georgia coast, U.S.A. *Marine Geology* **63**: 77-127.

Howard, J.D., Mayou, T.V. and Heard, R.W. 1977. Biogenic structures formed by rays. *Journal of Sedimentary Petrology* **47**: 339-346.

Howard, J.D. and Reineck, H-E. 1981. Depositional facies of high-energy beach-to-offshore sequence: comparison with low-energy sequence. *Bulletin of the American Association of Petroleum Geologists* **65**: 807-830.

Hunter, R.E., Clifton, H.E. and Phillips, R.E. 1979. Depositional processes, sedimentary structures and predicted vertical sequences in barred nearshore systems, southern Oregon coast. *Journal of Sedimentary Petrology* **49**: 711-726.

Ingram, R.L. 1954. Terminology for the thickness of stratification and parting units iin sedimentary rocks. *Bulletin of the Geological Society of America* **65**: 937-938.

Jack, A.M. 1980. The geology of western Namaqualand. *Bulletin of the Chamber of Mines Precambrian Research Unit* **29**: 1-173. University of Cape Town: Department of Geology.

Johnsson, M.J. 1990. Overlooked sedimentary particles from tropical weathering environments. *Geology* **18**: 107-110.

Jones, J.B. and Segnit, E.R. 1971. The nature of opal. I. Nomenclature and constituent phases. *Journal of the Geological Society of Australia* **18**: 57-68.

Joubert, P., Marais, J.A.H., Van Aswegen, G. and Van der Merwe, S.W. 1980. Okiep Group. In: Kent, L.E. (comp.), Stratigraphy of South Africa. Part 1. Lithostratigraphy of the Republic of South Africa, South West Africa/Namibia and the Republics of Bophuthatswana, Transkei and Venda. SACS. (South African Commitee for Stratigraphy), *Handbook of the Geological Survey of South Africa* **8**: 275-281.

Jury, M.R. 1985a. Case studies of alongshore variations in wind-driven upwelling in the southern Benguela region. In: Shannon, L.V. (ed.), *South African Ocean Colour and Upwelling Experiment*: 29-46. Cape Town: Sea Fisheries Research Institute.

Jury, M.R. 1985b. Air temperature gradients along the western Cape coast during southerly winds. *South African Journal of Science* **81**: 17-20.

Jury, M.R. and Taunton-Clark, J. 1986. Wind-driven upwelling off the Namaqualand coast of South Africa in spring, 1980. *South African Journal of Marine Science* **4**: 103-110.

Kaiser, E. (ed.). 1926. *Die Diamantenwüste Südwestafrikas.* Band 1 and 2. Berlin: Dietrich Reimer (Ernst Vosen).

Kamola, D.L. 1984. Trace fossils from marginal-marine facies of the Spring Canyon Member., Blackhawk Formation (Upper Cretaceous), east-central Utah. *Journal of Paleontology* **58** (2): 529-541.

Kamstra, F. 1985. Environmental features of the southern Benguela with special reference to the wind stress. In: Shannon, L.V. (ed.), *South African Ocean Colour and Upwelling Experiment*: 13-27. Cape Town: Sea Fisheries Research Institute.

Kelly, S.R.A. and Bromley, R.G. 1984. Ichnological nomenclature of clavate borings. *Palaeontology* **27**: 793-807.

Kennedy, W.J. 1967. Burrows and surface traces from the Lower Chalk of southern England. *Bulletin of the British Museum (Natural History)*, Geology **15**: 127-167.

Kensley, B. and Pether, J. 1986. Late Tertiary and Early Quaternary fossil Mollusca of the Hondeklip, area, Cape Province, South Africa. *Annals of the South African Museum* **97** (6): 141-225.

Kent, L.E. and Davies, O. 1980. Tertiary and Quaternary Periods. In: Kent, L.E. (comp.), Stratigraphy of South Africa. Part 1. Lithostratigraphy of the Republic of South Africa, South West Africa/Namibia and the Republics of Bophuthatswana, Transkei and Venda. SACS. (South African Commitee for Stratigraphy), *Handbook of the Geological Survey of South Africa* **8**: 603-628.

Keyser, U. 1972. The occurrence of diamonds along the coast between the Orange River, estuary and the Port Nolloth Reserve. *Bulletin of the Geological Survey of South Africa* **54**: 1-23.

Keyser, U. 1976. Namaqaland river deposits. In: Coetzee, C.B. (ed.), Mineral resources of the Republic of South Africa. *Handbook of the Geological Survey of South Africa* **7**: 25-27.

Khalaf, F.I. 1988. Petrography and diagenesis of silcrete from Kuwait, Arabian Gulf. *Journal of Sedimentary Petrology* **58**: 1014-1022.

Kilburn, R.N. and Rippey, E. 1982. *Sea shells of Southern Africa.* Johannesburg: MacMillan South Africa.

Komar, P.D. 1976. *Beach processes and sedimentation.* Englewood Cliffs, New Jersey: Prentice-Hall Inc.

Korn, H. and Martin, H. 1951. The seismicity of South-West Africa. *Transactions of the Geological Society of South Africa* **54**: 85-88.

Krige, A.V. 1927. An examination of the Tertiary and Quaternary changes of sea-level in South Africa, with special stress on the evidence in favour of a Recent world-wide sinking of ocean-level. *Annals of the University of Stellenbosch* **5** (A) (1): 1-81.

Kukal, Z. (ed.). 1990. The Rate of Geological Processes. *Earth Science Reviews* **28** (1-3): 1-284.

Kumar, N. and Sanders, J.E. 1976. Characteristics of shoreface storm deposits: modern and ancient examples. *Journal of Sedimentary Petrology* **46**: 145-162.

Lamplugh, G.W. 1902. Calcrete. *Geological Magazine* **9**: 575.

Leckie, D. 1988. Wave-formed, coarse-grained ripples and their relationship to hummocky cross-stratification. *Journal of Sedimentary Petrology* **58**: 607-622.

Leckie, D. and Walker, R.G. 1982. Storm- and tide-dominated shorelines in Cretaceous Moosebar-Lower Gates interval — outcrop equivalents of deep basin gas trap in western Canada. *Bulletin of the American Association of Petroleum Geologists* **66**: 138-157.

Leithold, E.L. and Bourgeois, J. 1984. Characteristics of coarse-grained sequences deposited in nearshore, wave-dominated environments — examples from the Miocene of south-west Oregon. *Sedimentology* **31**: 749-775.

Logan, R.F. 1972. The geographical divisions of the deserts of South West Africa. *Mitteilungen der Basler Afrika Bibliographien* **4-6**: 46-65.

Longiaru, S. 1987. Visual comparators for estimating the degree of sorting from plane and thin section. *Journal of Sedimentary Petrology* **57**: 791-794.

Lutjeharms, J.R.E. and Meeuwis, J.M. 1987. The extent and variability of South-East Atlantic upwelling. In: Payne, A.I.L., Gulland, J.A. and Brink, K.H. (eds.), The Benguela and Comparable Ecosystems. *South African Journal of Marine Science* **5**: 51-62.

Marais, J.A.H. and Joubert, P. 1980. Little Namaqualand Suite. In: Kent, L.E. (comp.), Stratigraphy of South Africa. Part 1. Lithostratigraphy of the Republic of South Africa, South West Africa/Namibia and the Republics of Bophuthatswana, Transkei and Venda. SACS. (South African Commitee for Stratigraphy), *Handbook of the Geological Survey of South Africa* **8**: 294-304.

McCubbin, D.G. 1982. Barrier-island and strand-plain facies. In: Scholle, P.A. and Spearing, D. (eds.), Sandstone Depositional Environments. *Memoirs of the American Association of Petroleum Geologists* **31**: 247-279.

McFarlane, M.J. 1983. Laterites. In: Goudie, A.S. and Pye, K. (eds.), *Chemical Sediments and Geomorphology: Precipitates and Residua in the Near-Surface Environment*. 7-59. London: Academic Press.

McMillan, I.K. 1986. Cainozoic planktonic and larger foraminifera distributions around Southern Africa and their implications for past changes of oceanic water temperatures. *South African Journal of Science* 82: 66-69.

McMillan, I.K. 1993. Foraminiferal biostratigraphy, sequence stratigraphy and interpreted chronostratigraphy of marine Quaternary sedimentation on the South African continental shelf. *South African Journal of Science* 89: 83-89.

Meeuwis, J.M. and Lutjeharms, J.R.E. 1990. Surface thermal characteristics of the Angola-Benguela front. *South African Journal of Marine Science* 9: 261-279.

Meyer, R. and Pena Dos Reis, R.B. 1985. Paleosols and alunite silcretes in continental Cenozoic of western Portugal. *Journal of Sedimentary Petrology* **55** (1): 76-85.

Miller, D.E., Yates, R.J., Parkinton, J.E. and Vogel, J.C. 1993. Radiocarbon-dated evidence relating to a mid-Holocene relative high sea-level on the south-western Cape coast, South Africa. *South African Journal of Science* **89**: 35-44.

Moslow, T.F. and Tye. R.S. 1985. Recognition and characterization of Holocene tidal inlet sequences. *Marine Geology* **63**: 129-151.

Mountain, E.D. 1952. The origin of silcrete. *South African Journal of Science* **48**: 201-204.

Muller, J. 1981. Fossil pollen records of extant angiosperms. *The Botanical Review* **47**:1-142.

Murata, K.J. and Norman, M.B. 1976. An index of crystallinity for quartz. *American Journal of Science* **276**: 1120-1130.

Murray, L.G., Joynt, R.H., O'Shea, D.O'C., Foster, R.W. and Kleinjan, L. 1970. The geological environment of some diamond deposits off the coast of South West Africa. In: Delaney, F.M. (ed.), *The Geology of the East Atlantic Continental Margin.* Reports of the Institute of Geological Sciences **70** (16): 119-141.

Nelson, G. and Hutchings, L. 1983. The Benguela Upwelling Area. *Progress in Oceanography* **12**: 333-356.

O'Shea, D. O'C. 1971. An outline of the inshore submarine geology of southern S.W.A and Namaqualand. *Unpublished M.Sc thesis. University of Cape Town.*

Parker, R.J. 1971. The petrography and major element geochemistry of phosphorite nodule deposits on the Agulhas Bank, South Africa. *Bulletin of the South African National Commitee for Oceanographic Research, Marine Geology Programme* **2**: 1-94.

Parker, R.J. and Siesser, W.G. 1972. Petrology and origin of some phosphorites from the South African continental margin. *Journal of Sedimentary Petrology* **42**: 434-440.

Partridge, T.C. and Maud, R.R. 1987. Geomorphic evolution of South Africa since the Mezozoic. *South African Journal of Geology* **90**: 179-208.

Partridge, T.C. and Maud, R.R. 1989. The end–Cretaceous event: New evidence from the southern hemisphere. *South African Journal of Science* **85**: 428-430.

Pemberton, S.G. and Frey, R.W. 1982. Trace fossil nomenclature and the *Planolites-Palaeophycus* dilemma. *Journal of Paleontology* **56** (4): 843-881.

Pemberton, S.G. and Jones, B. 1988. Ichnology of the Pleistocene Ironshore Formation, Grand Cayman Island, British West Indies. *Journal of Paleontology* **62** (4): 495-505.

Pervesler, P. and Dworschak, P.C. 1985. Burrows of *Jaxea nocturna* Nardo in the Gulf of Trieste. *Senckenbergiana Maritima* **17**: 33-53.

Pether, J. 1983. The Lithostratigraphy of Hondeklip Bay: A Reconnaissance. *Unpublished B.Sc. Honours Project. University of Cape Town.*

Pether, J. 1986a. Late Tertiary and Early Quaternary marine deposits of the Namaqualand coast, Cape Province: new perspectives. *South African Journal of Science* **82**: 464-470.

Pether, J. 1986b. The Late Tertiary and Early Quaternary marine deposits of the coast of Namaqualand, Cape Province. *Institute of Coastal Research, University of Port Elizabeth, Report No.* **12**: 50-60.

Pether, J. 1986c. Fossil molluscs from Hondeklipbaai. *Fourth Conference of the Palaeontological Society of South Africa*, 22-25 September, 1986. Abstract, 1p.

Pether, J. 1987. Shallow marine deposition in the Pliocene of Namaqualand. *Handbook of the Sixth National Oceanographic Symposium*, 6-10 July, 1987. Abstract **B 27**, 1p.

Pether, J. 1990. A new *Austromegabalanus* (Cirripedia, Balanidae) from the Pliocene of Namaqualand, Cape Province, South Africa. *Annals of the South African Museum* **99** (1): 1-13.

Pether, J. 1994. Molluscan evidence for enhanced deglacial advection of Agulhas water in the Benguela Current, off southwestern Africa. *Palaeogeography, Palaeoclimatology, Palaeoecology* **111**: 99-117.

Pettijohn, F.J. 1975. *Sedimentary Rocks* (3rd Edition). New York: Harper and Row.

Pickford. M. 1981. Preliminary Miocene mammalian biostratigraphy for western Kenya. *Journal of Human Evolution* **10**: 73-97

Pickford. M. 1987. Miocene Suidae from Arris Drift, South West Africa/Namibia. *Annals of the South African Museum* **97**: 283-295.

Pickerill, R.K. 1989. *Compaginatichnus*: a new ichnogenus from Ordovician flysch of eastern Canada. *Journal of Paleontology* **63** (6): 913-919.

Powers, M.C. 1953. A new roundness scale for sedimentary particles. *Journal of Sedimentary Petrology* **23**: 117-119.

Preston-Whyte, R.A., Diab, R.D. and Tyson, P.D. 1977. Towards an inversion climatology for southern Africa. Part II: non-surface inversions in the lower atmosphere. *South African Geographical Journal* **59**: 47-59.

Raaf, J.F.M. de, Boersma, J.R. and van Gelder, A. 1977. Wave-generated structures and sequences from a shallow-marine succession, Lower Carboniferous, County Cork, Ireland. *Sedimentology* **24**: 451-483.

Raper, P.E. and Boucher M. (eds.) 1988. *Robert Jacob Gordon, Cape Travels, 1777 to 1786.* Vol.2. Johannesburg: The Brenthurst Press.

Reid, D.L., Erlank, A.J. and Rex, D.C. 1991. Age and correlation of the False Bay dolerite swarm, south-western Cape, Cape Province. South African Journal of Geology 94: 155-158.

Reineck, H.-E. and Singh, I.B. 1973. *Depositional Sedimentary Environments.* Berlin: Springer-Verlag.

Reuning, E. 1931. The Pomona-quartzite and oyster-horizon on the west coast north of the mouth of the Oliphants River, Cape Province. *Transactions of the Royal Society of South Africa* **19**: 205-214.

Robinson, G.D. 1980. Possible quartz synthesis during weathering of quartz-free mafic rock, Jasper County, Georgia. *Journal of Sedimentary Petrology* **50**: 193-203.

Rogers, A.W. 1904. Geological survey of parts of the division of Piquetberg, Clanwilliam and Van Rhyn's Dorp. *Annual Report of the Geological Commission 1903*, Cape of Good Hope, Department of Agriculture: 141-167.

Rogers, A.W. 1905. *An Introduction to the Geology of the Cape Colony.* London: Longmans, Green and Co.

Rogers, A.W. 1911. Geological survey of parts of the Van Rhyn's Dorp and Namaqualand Divisions. *Sixteenth Annual Report of the Geological Commission 1911*, Cape of Good Hope, Department of Mines: 9-84.

Rogers, J. 1977. Sedimentation on the continental margin off the Orange River and the Namib Desert. *Bulletin of the Joint Geological Survey/University of Cape Town Marine Geoscience Unit* **7**: 1-162.

Rogers, J. 1980. First report on the Cenozoic sediments between Cape Town and Elands, Bay. *Geological Survey of South Africa Open File* **136**.

Rogers, J. 1982. Lithostratigraphy of Cenozoic sediments between Cape Town and Eland's Bay. *Palaeocology of Africa* **15**: 121-137.

Rogers, J. 1983. Lithostratigraphy of Cenozoic sediments on the coastal plain between Cape Town and Saldanha Bay. *Technical Report of the Joint Geological Survey/University of Cape Town Marine Geoscience Unit* **14**: 87-103.

Rogers, J. and Bremner, J.M. 1991. The Benguela Ecosystem. Part VII. Marine-geological aspects. In: Barnes, M. (ed.), *Oceangraphy and Marine Biology. An Annual Review* **29**: 1-85. Aberdeen: University Press.

Rogers, J., Pether, J., Molyneux, R., Hill, R.S., Kilham, J.L.C., Cooper, G. and Corbett, I. 1990. Cenozoic geology and mineral deposits along the west coast of South Africa and the Sperrgebiet. *Guidebook Geocongress '90 Geological Society of South Africa*, **PR1**: 1-111.

Ross, G.M. and Chiarenzelli, J.R. 1985. Paleoclimatic significance of widespread Proterozoic silcretes in the Bear and Churchill provinces of the northwestern Canadian shield. *Journal of Sedimentary Petrology* 55 (2): 196-204.

Rossouw, J. 1984. Review of existing wave data, wave climate and design waves for South African and South West African (Namibian) coastal waters. *Report of the South African Council for Scientific and Industrial Research* **T/SEA 8401**: 1-66.

Rubin, D.M. 1987. Formation of scalloped cross-bedding without unsteady flows. *Journal of Sedimentary Petrology* **57**: 39-45.

SACS (South African Commitee for Stratigraphy). 1980. Stratigraphy of South Africa. Part 1. Lithostratigraphy of the Republic of South Africa, South West Africa/Namibia and the Republics of Bophuthatswana, Transkei and Venda. Kent, L.E. (comp.), *Handbook of the Geological Survey of South Africa* **8**.

Schulze, B.R. 1972. South Africa. In: Griffiths, J.F. (ed.), Climates of Africa. *World Survey of Climatology* **10**: 501-566. Amsterdam: Elsevier.

Schumann, E.H. and Perrins, L-A. 1982. Tidal and inertial currents around South Africa. *Proceedings of the 18th Coastal Engineering Conference, ASCE, Cape Town, South Africa*, November **14-19**, 1982.

Scrutton, R.A. and Dingle, R.V. 1974. Basement control over sedimentation on the continental margin west of southern Africa. *Transactions of the Geological Society of South Africa* **77**: 253-260.

Shackleton, N.J. and Kennet, J.P. 1975. Paleotemperature history of the Cenozoic and the initiation of Antarctic glaciation: oxygen and carbon isotope analyses in DSDP sites 277, 279 and 281. In: Kennet, J.P. *et al.* (eds.), *Initial reports of the Deep Sea Drilling Project* **29**:743-755.

Shannon, L.V. 1985. The Benguela Ecosystem. Part I. Evolution of the Benguela, physical features and processes. In: Barnes, M. (ed.), *Oceangraphy and Marine Biology. An Annual Review* **23**: 105-182. Aberdeen: University Press.

Shannon, L.V. 1988. Ocean climate changes and variability from a South African perspective. In: Macdonald, I.A.W. and Crawford, R.J.M. (eds.), Long-term data series relating to southern Africa's renewable natural resources. *South Africa National Scientific Programmes Report No.* **157**: 415-424.

Shannon, L.V. and Agenbag, J.J. 1987. Notes on the recent warming in the southeast Atlantic and possible implications for the fisheries of the region. *Collection of scientific papers of the International Community of Southeast Atlantic Fisheries* **14**: 243-248.

Shannon, L.V., Agenbag, J.J., Walker, N.D. and Lutjeharms, J.R.E. 1990. A major perturbation in the Agulhas retroflection area in 1986. *Deep-Sea Research* **37** (3): 493-512.

Shannon, L.V. and Anderson, F.P. 1982. Applications of satellite ocean colour imagery in the study of the Benguela Current system. *South African Journal of Photogrammetry, Remote Sensing and Cartography* **13** (3): 153-169.

Shannon, L.V., Boyd, A.J., Brundrit, G.B. and Taunton-Clark, J. 1986. On the existence of an El Niño-type phenomenon in the Benguela System. *Journal of Marine Research* **44**: 495-520.

Shannon, L.V. and Chapman, P. 1983. Suggested mechanism for the chronic pollution by oil of beaches east of Cape Agulhas, South Africa. *South African Journal of Marine Science* **1**: 231-244.

Shannon, L.V., Agenbag, J.J. and Buys, M.E.L. 1987. Large- and mesoscale features of the Angola-Benguela front. In: Payne, A.I.L., Gulland, J.A. and Brink, K.H. (eds.), The Benguela and Comparable Ecosystems. *South African Journal of Marine Science* **5**: 11-34.

Shannon, L.V., Lutjeharms, J.R.E. and Agenbag, J.J. 1989b. Episodic input of Subantarctic water into the Benguela region. *South African Journal of Science* **85**: 317-322.

Shannon, L.V., Seely, M.K. and Ward, J.D. 1989a. Proceedings of the Namib-Benguela Interactions Workshop. Gobabeb, Namibia, 28 to 30 November 1988. *Occasional Report No.* **41**, *Ecosystems Programmes*, FRD, Pretoria.

Shillington, F.A., Brundrit, G.B. and Lutjeharms, J.R.E. 1990. The coastal current circulation during the Orange River flood. *Transactions of the Royal Society of South Africa* **47** (3): 307-330.

Short, A.D. 1984. Beach and nearshore facies: southeast Australia. *Marine Geology* **60**: 261-282.

Siesser, W.G. 1978. Aridification of the Namib Desert: evidence from oceanic cores. In: Van Zinderen Bakker, E.M. (ed.), *Antarctic glacial history and world palaeoenvironments*. Rotterdam: Balkema: 105-113.

Siesser, W.G. and Dingle, R.V. 1981. Tertiary sea-level movements around southern Africa. *Journal of Geology* **89**: 83-96.

Siesser, W.G. and Salmon, D. 1979. Eocene marine sediments in the Sperrgebiet, South West Africa. *Annals of the South African Museum* **79** (2): 9-34.

Simpson, S. 1975. Classification of trace fossils. In: Frey, R.W. (ed.), *The Study of Trace Fossils*: 39-54. New York: Springer-Verlag.

Singer, A. 1980. The paleoclimatic interpretation of clay minerals in soils and weathering profiles. *Earth Science Reviews*, **15**: 303-326.

Smale, D. 1978. Silcretes and associated silica diagenesis in southern Africa and Australia. In: Langford-Smith, T. (ed.), *Silcrete in Australia*: 261-279. Department of Geography, University of New England.

Smith, A.G., Hurley, A.M. and Briden, J.C. 1981. *Phanerozoic paleocontinental world maps*. Cambridge: Cambridge University Press.

Stocken, C.G. 1978. A review of the later Mesozoic and Cenozoic deposits of the Sperrgebiet. *Unpublished report, Consolidated Diamond Mines of Namibia*, for SACS, 1980.

Stromer, E. 1931. Reste süsswasser-und land-bewohnender Wirbeltiere aus den Diamantfeldern Klein-Namaqualandes (Südwes-Afrika). *Sitzungsberichte Bayerische Akademie der Wissenschaften* **1931**: 17-47.

Summerfield, M.A. 1981. *The nature and occurrence of silcrete, southern Cape Province, South Africa*. Research Paper **28**: 1-36. School of Geography, University of Oxford,

Summerfield, M.A. 1982. Distribution, nature and probable genesis of silcrete in arid and semi-arid southern Africa. In: Yaalon. D.H. (ed.), *Aridic Soils and Geomorphic Processes*. Catena, Supplement **1**: 37-65.

Summerfield, M.A. 1983a. Petrography and diagenesis of silcrete from the Kalahari Basin and Cape coastal zone, southern Africa. *Journal of Sedimentary Petrology* **53**: 895-909.

Summerfield, M.A. 1983b. Silcrete as a palaeoclimatic indicator: evidence from southern Africa. *Palaeogeography, Palaeoclimatology, Palaeoecology* **41**: 65-79.

Summerfield, M.A. 1983c. Geochemistry of weathering profile silcretes, southern Cape Province, South Africa. In: Wilson, R.C.L. (ed.), *Residual Deposits: Surface Related Weathering Products and Materials*. Geological Society of London Special Publication 11: 167-178.

Summerfield, M.A. 1983d. Silcrete. In: Goudie, A.S. and Pye, K. (eds.), *Chemical Sediments and Geomorphology: Precipitates and Residua in the Near-Surface Environment*. 59-91. London: Academic Press.

Tankard, A.J. 1966. The Namaqualand Coastal Deposits with special reference to the area between the Groen and Buffels rivers. *Unpublished B.Sc Project. University of Natal.*

Tankard, A.J. 1974a. Petrology and origin of the phosphorite and aluminium phosphate rock of the Langebaanweg-Saldanha area, south-western Cape Province. *Annals of the South African Museum* 65: 217-249.

Tankard, A.J. 1975a. The late Cenozoic History and Palaeoenvironments of the coastal margin of the south-western Cape Province. *Unpublished Ph.D. thesis. Rhodes University, Grahamstown.*

Tankard, A.J. 1975b. The marine Neogene Saldanha Formation. *Transactions of the Geological Society of South Africa* 7: 257-264.

Tankard, A.J. and Rogers, J. 1978. Late Cenozoic palaeoenvironments on the west coast of southern Africa. *Journal of Biogeography* **5**: 319-337.

Taunton-Clark, J. 1985. The formation, growth and decay of upwelling tongues on response to the mesoscale wind field during summer. In: Shannon, L.V. (ed.), *South African Ocean Colour and Upwelling Experiment*. 47-61. Cape Town: Sea Fisheries Research Institute.

Terry R.D. and Chilingar, G.V. 1955. Summary of "Concerning some additional aids in studying sedimentary formations" by M.S. Shvetsov. *Journal of Sedimentary Petrology* **25**: 229-234.

Thiry, M. and Millot, G. 1987. Mineralogical forms of silica and their sequence of formation in silcretes. *Journal of Sedimentary Petrology* **57** (2): 343-352.

Thomas, R.D. 1975. Functional morphology, ecology and evolutionary conservatism in the Glycymerididae (Bivalvia). *Palaeontology* **18**: 217-254.

Vail P.R and Hardenbol, J. 1979. Sea-level changes during the Tertiary. *Oceanus* **22**: 71-79.

Van Heerden, I.L. 1986. Fluvial sedimentation in the ebb-dominated Orange Estuary. *South African Journal of Science* **82**: 141-147.

Visser, H.N. and Toerien, D.K. 1971. Die geologie van die gebied tussen Vredendal en Elandsbaai. *Explanation of sheets* **3118C** *(Doring Bay) and* **3218A** *(Lambert's Bay).* Geological Survey of South Africa.

Visser, D.J.L., Johnson, M.R., Walraven, F., Theron, J.N., Toerien, D.K., Malherbe, S.J., Wolmarans, L.G., Brandl, G., Hine, S.S., Coertze, F.J. and Smit, P.J. 1984. *Geological Map of the Republics of South Africa, Transkei, Bophuthatswana, Venda and Ciskei and the Kingdoms of Lesotho and Swaziland.* Geological Survey of South Africa. The Government Printer, Pretoria.

Vossler, S.M. and Pemberton, S.G. *Skolithos* in the Upper Cretaceous Cardium Formation: an ichnofossil example of opportunistic ecology. *Lethaia* **21**: 351-362.

Wagner, P.A. and Merensky, H. 1928. The diamond deposits on the coast of Little Namaqualand. *Transactions of the Geological Society of South Africa* **31**: 1-41.

Walker, N.D. and Gillooly, J.F. 1984b. Spatial and temporal behaviour of sea-surface temperatures in the South Atlantic. *South African Journal of Science* **80**: 97-100.

Walker, N., Taunton-Clark, J. and Pugh, J. 1984a. Sea temperatures off the South African west coast as indicators of Benguela warm events. *South African Journal of Science* **80**: 72-77.

Walker, R.G., Duke, W.L. and Leckie, D.A. 1983. Hummocky stratification: significance of its variable bedding sequences: discussion and reply. *Bulletin of the Geological Society of America* **94**: 1245-1249.

Ward, J.D. 1987. The Cenozoic succession in the Kuiseb valley, Central Namib Desert. *Memoir of the Geological Survey of South West Africa/Namibia* **9**.

Ward, J.D. and Corbett, I.B. 1990. Towards an age for the Namib. In: Seely, M.K. (ed.), Namib ecology: 25 years of Namib research. *Monograph of the Transvaal Museum* 7: 17-26.

Ward, J.D., Seely, M.K. and Lancaster, N. 1983. On the antiquity of the Namib. *South African Journal of Science* **79**: 175-183.

Wentworth, C.K. 1922. A scale of grade and class terms for clastic sediments. *Journal of Geology* 30: 377-392.

Williams, L.A. and Crerar, D.A. 1985. Silica diagenesis II. General Mechanisms. *Journal of Sedimentary Petrology* **55** (3): 312-321.

Williams, L.A., Parks, G.A. and Crerar, D.A. 1985. Silica diagenesis I. Solubility controls. *Journal of Sedimentary Petrology* **55** (3): 301-311.

Woodborne, M.W. 1987. Acoustic stratigraphy and bedrock morphology of the Namaqualand inner shelf immediately north of the Buffels River Mouth, Kleinzee (Diamond Concession Area No. 4). *Technical Report of the Joint Geological Survey/University of Cape Town Marine Geoscience Unit* **17**: 51-60.

Wopfner, H. 1978. Silcretes in northern South Australia and adjacent regions. In: Langford-Smith, T. (ed.), *Silcrete in Australia*: 93-141. Department of Geography, University of New England.

Wright, L.D. and Coleman, J.M. 1973. Variations in morphology of major river deltas as functions of ocean wave and river discharge. *Bulletin of the American Association of Petroleum Geologists* **57**: 370-398.

Yates, R.J., Miller, D.E., Halkett, D.J., Manhire, A.H. and Parkington, J.E. 1986. A late mid-Holocene high sea-level: a preliminary report on geoarchaeology at Elands Bay, western Cape Province, South Africa. *South African Journal of Science* **82**: 164-165.

APPENDIX A

ILLUSTRATIONS OF EXTINCT INVERTEBRATE MACROFOSSILS

FROM THE NAMAQUALAND COASTAL PLAIN

ALL SCALE BARS ARE 1 CM

UNLESS OTHERWISE STATED

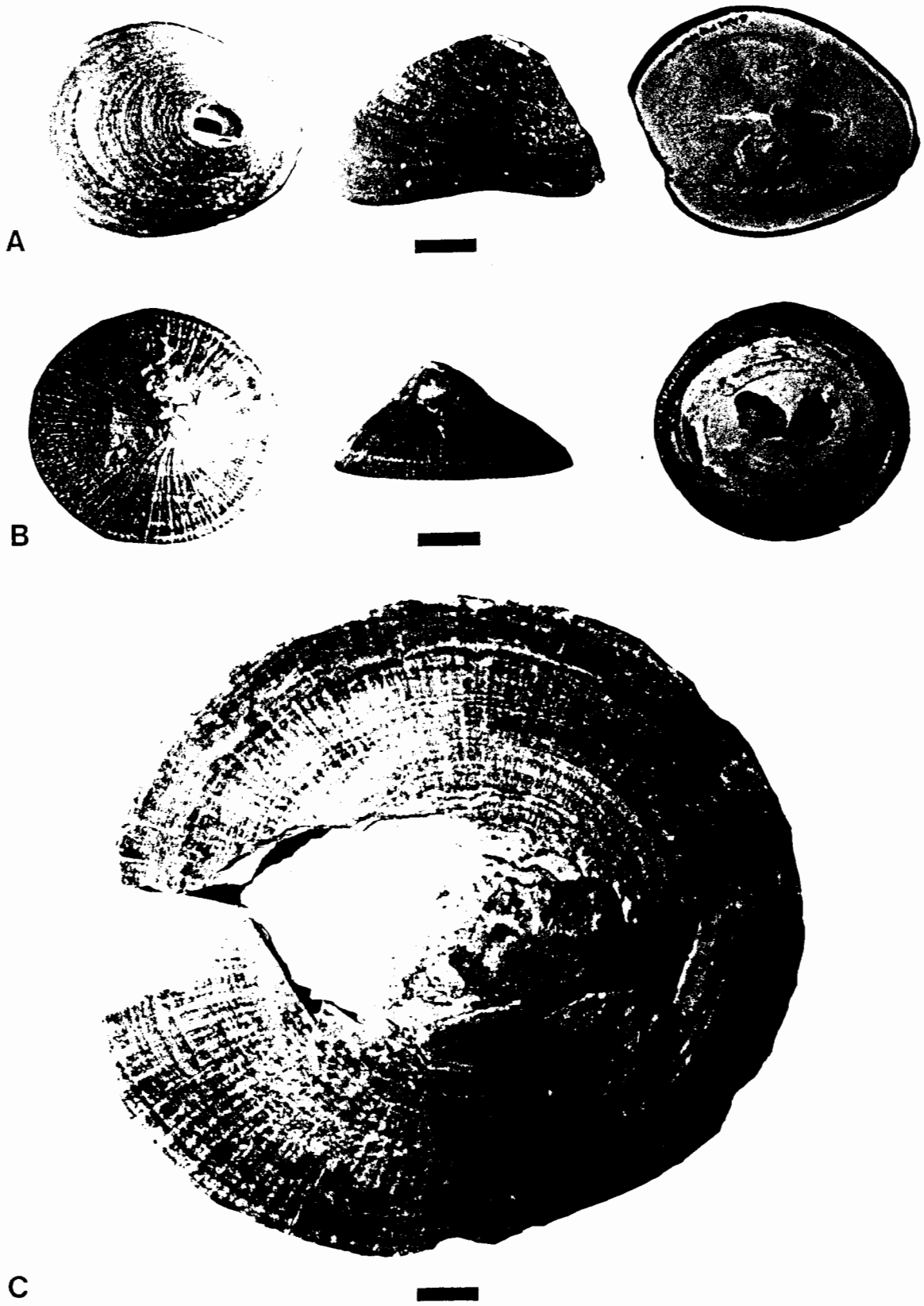

Plate A1 **A.** *Fissurella robusta.* **B.** *Patella hoffmani.* **C.** *Patella hendeyi.*

Plate A2 **A.** *Patella hendeyi.* **B.** *Patella hendeyi.*

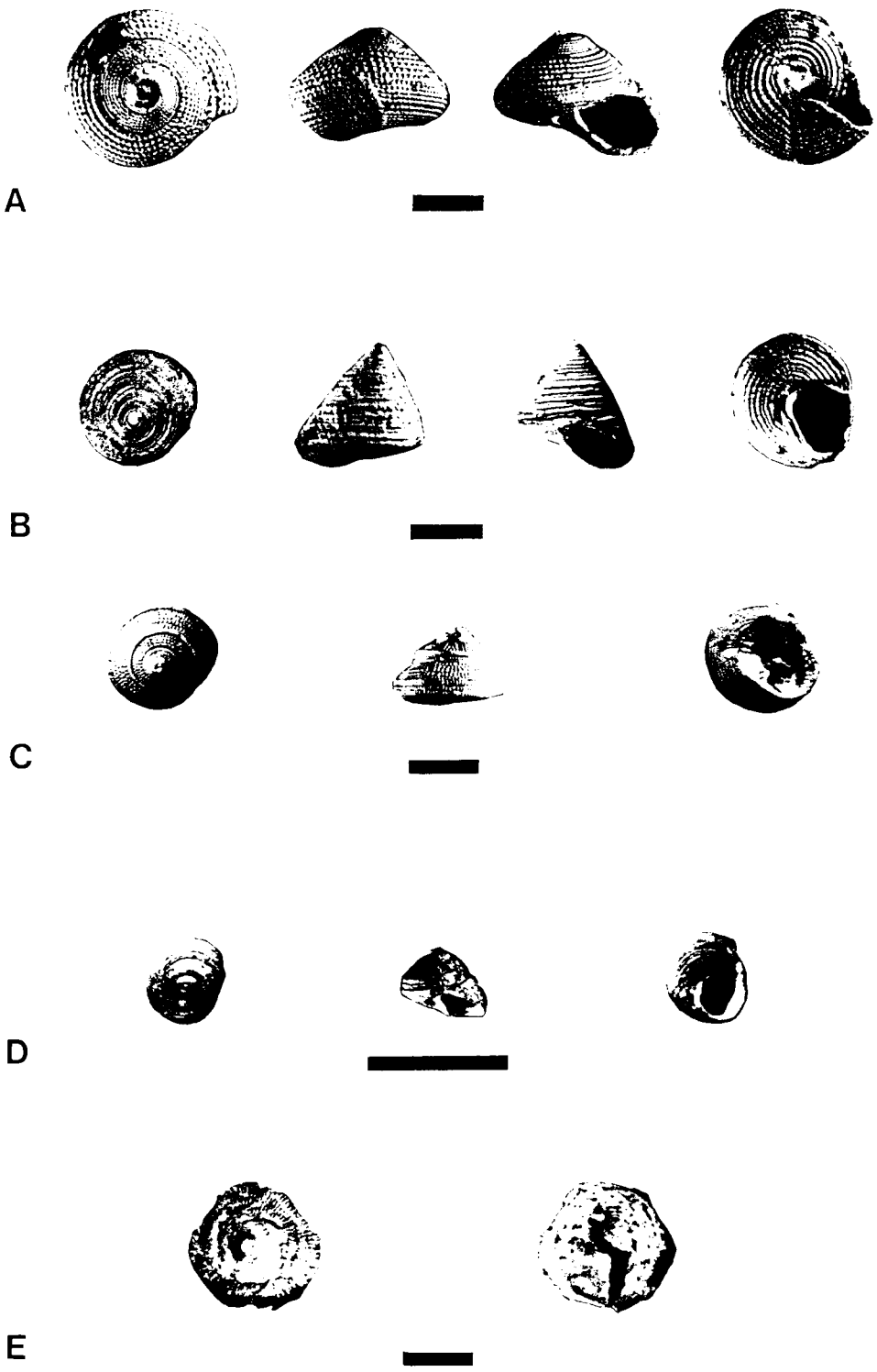

Plate A3 **A.** *Calliostoma depressa.* **B.** *Cantharidus (Jujubinus) striatus.* **C.** *Clanculus murrayi.* **D.** *Gibbula zonata patula.* **E.** *Calyptraea kilburni.*

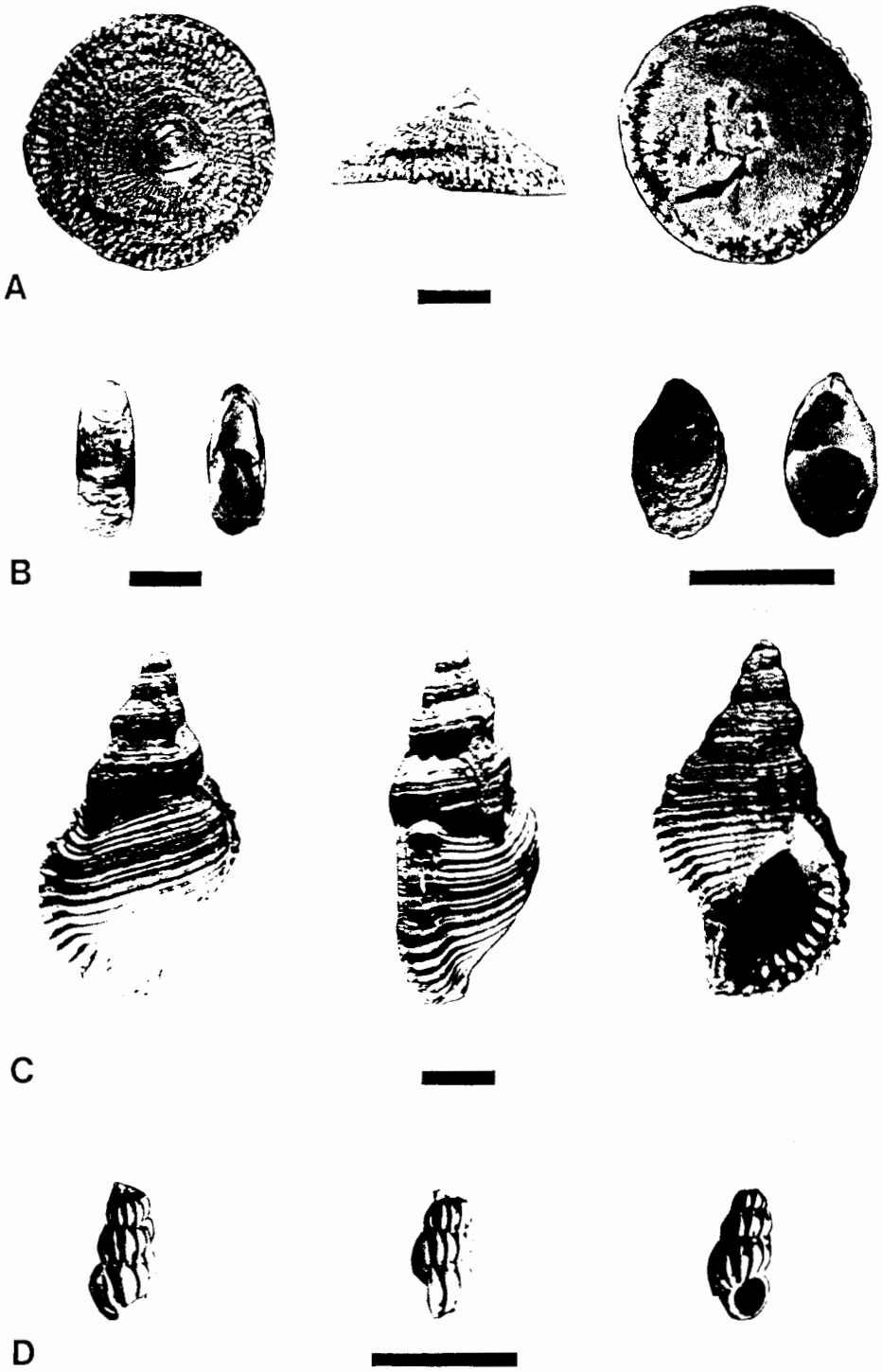

Plate A4 **A.** *Calyptraea viridarena.* **B.** *Crepidula deprima.* **C.** *Cabestana casus.* **D.** *Epitonium lycocephalum.*

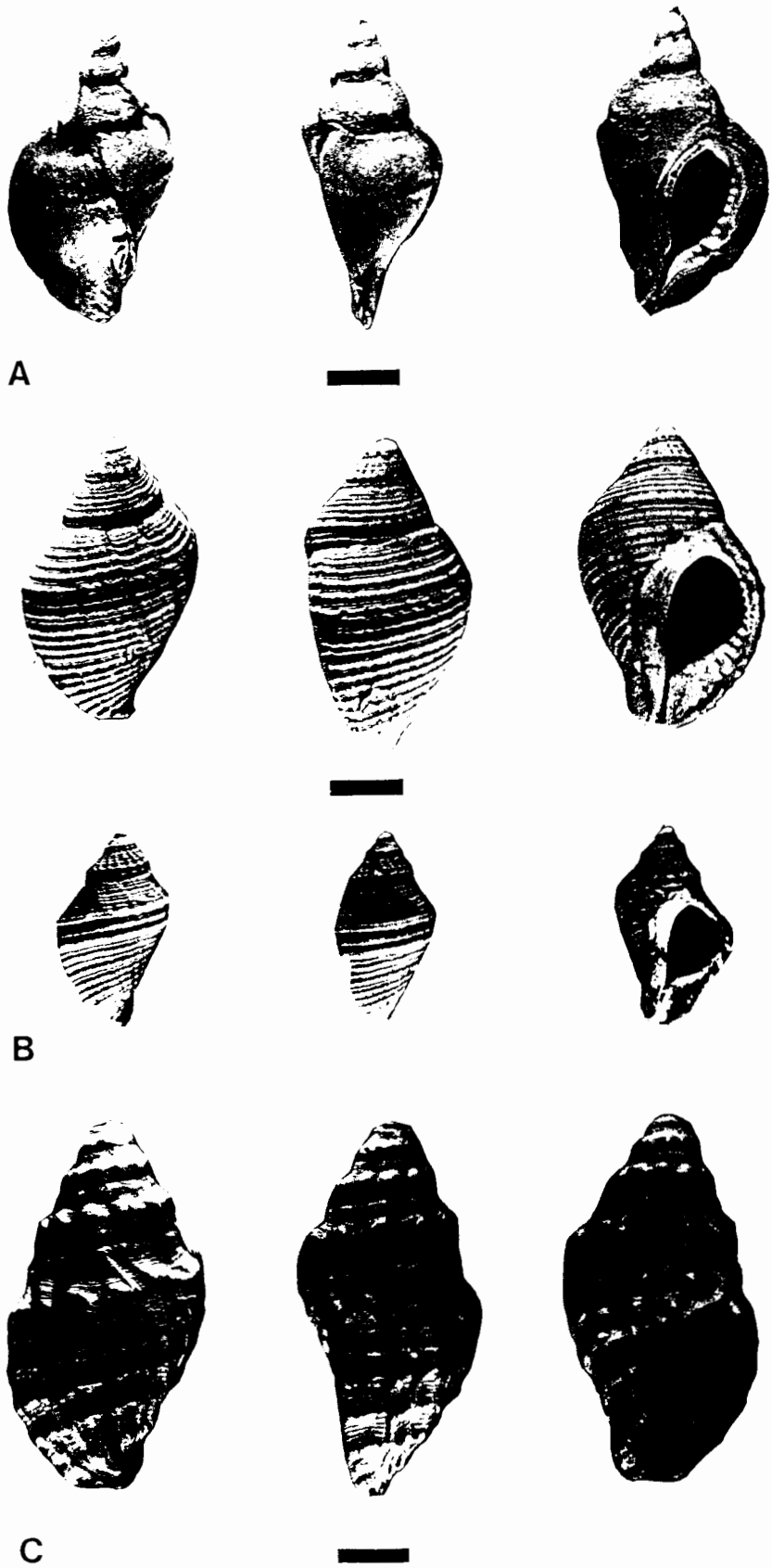

Plate A5 **A.** *Namamurex odontostoma.* **B.** *Spinucella praecingulata.* **C.** *Thais arenae.*

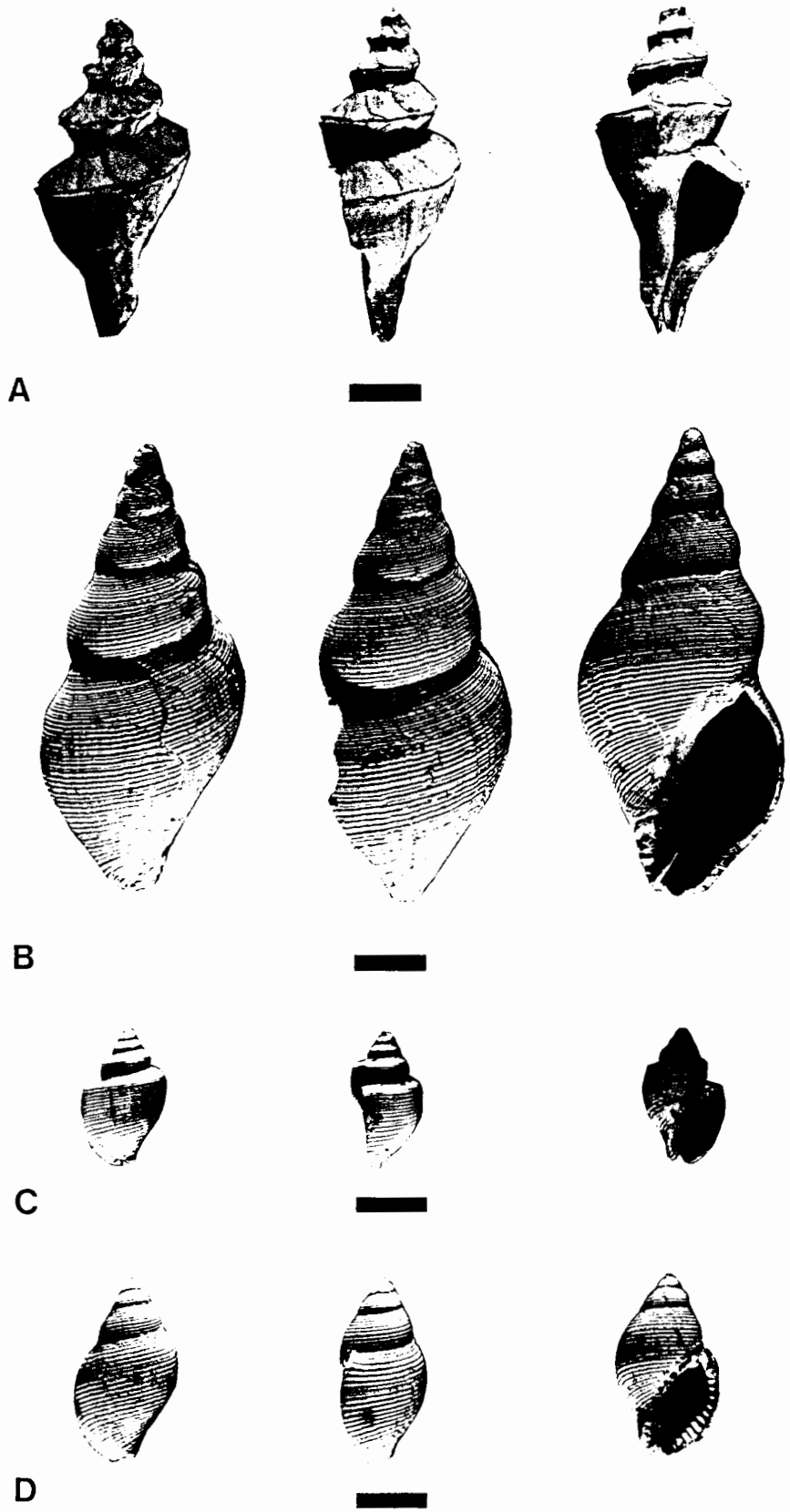

Plate A6 **A.** *Trophon carringtoni.* **B.** *Burnupena aestus.* **C.** *Burnupena rogersi.* **D.** *Triumphis dilemma.*

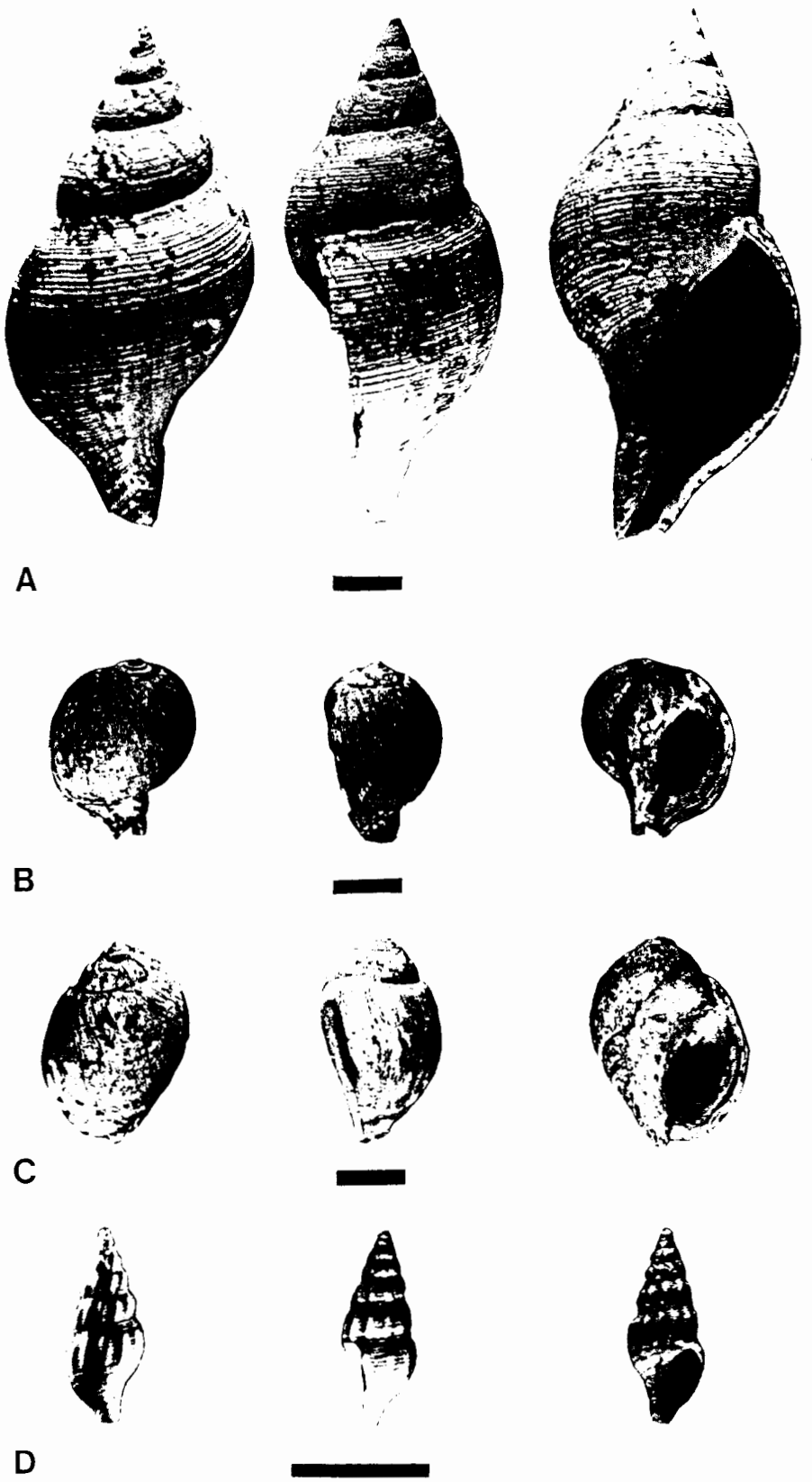

Plate A7 **A.** *Fasciolaria dinglei.* **B.** *Melapium hawthorni.* **C.** *Pseudoliva lutulenta.* **D.** *Drillia tempestae.*

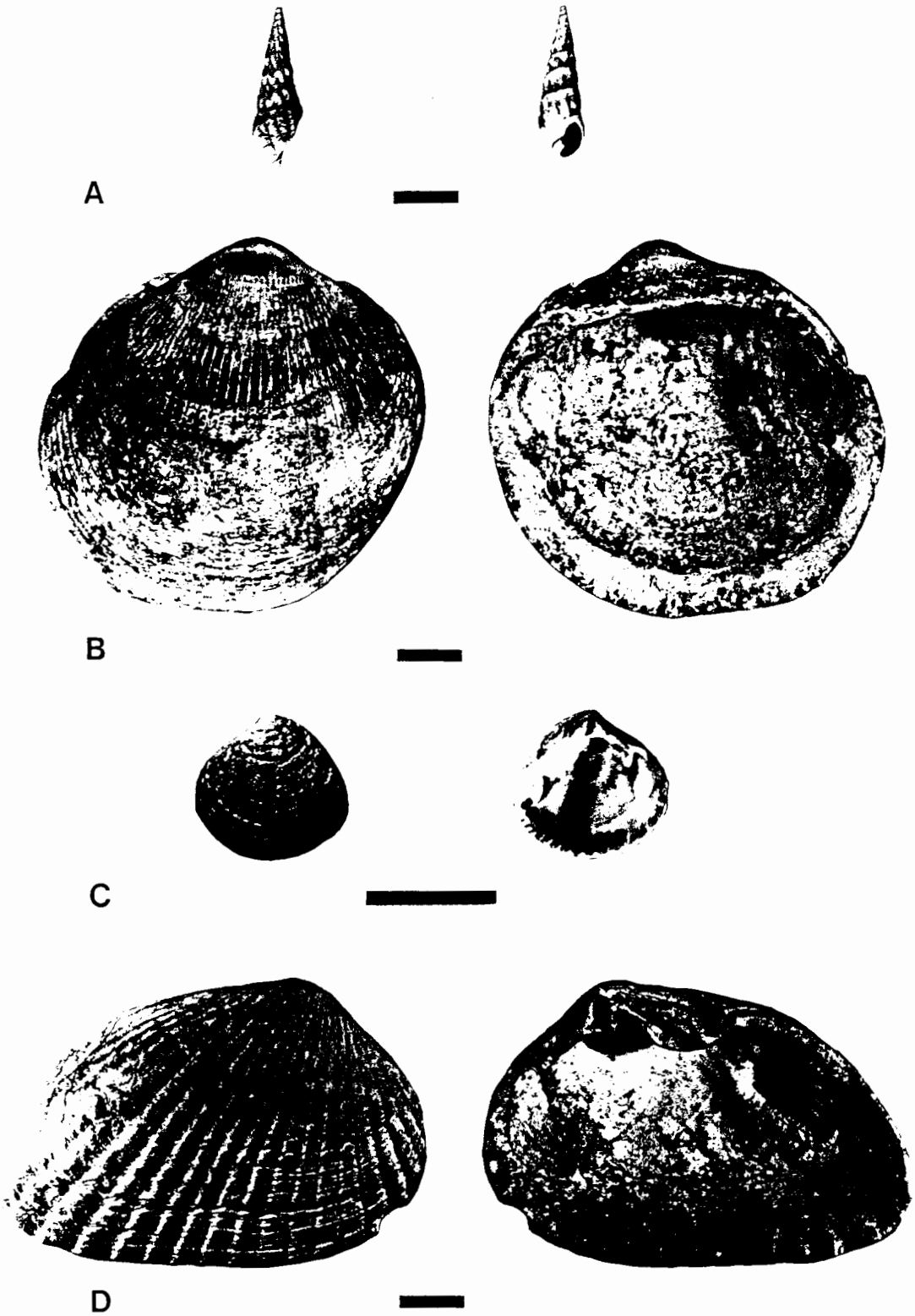

Plate A8 **A.** *Terebra canisaxi.* **B.** *Glycymeris fulleri.* **C.** *Cardita unica.* **D.** *Carditella calipsamma.*

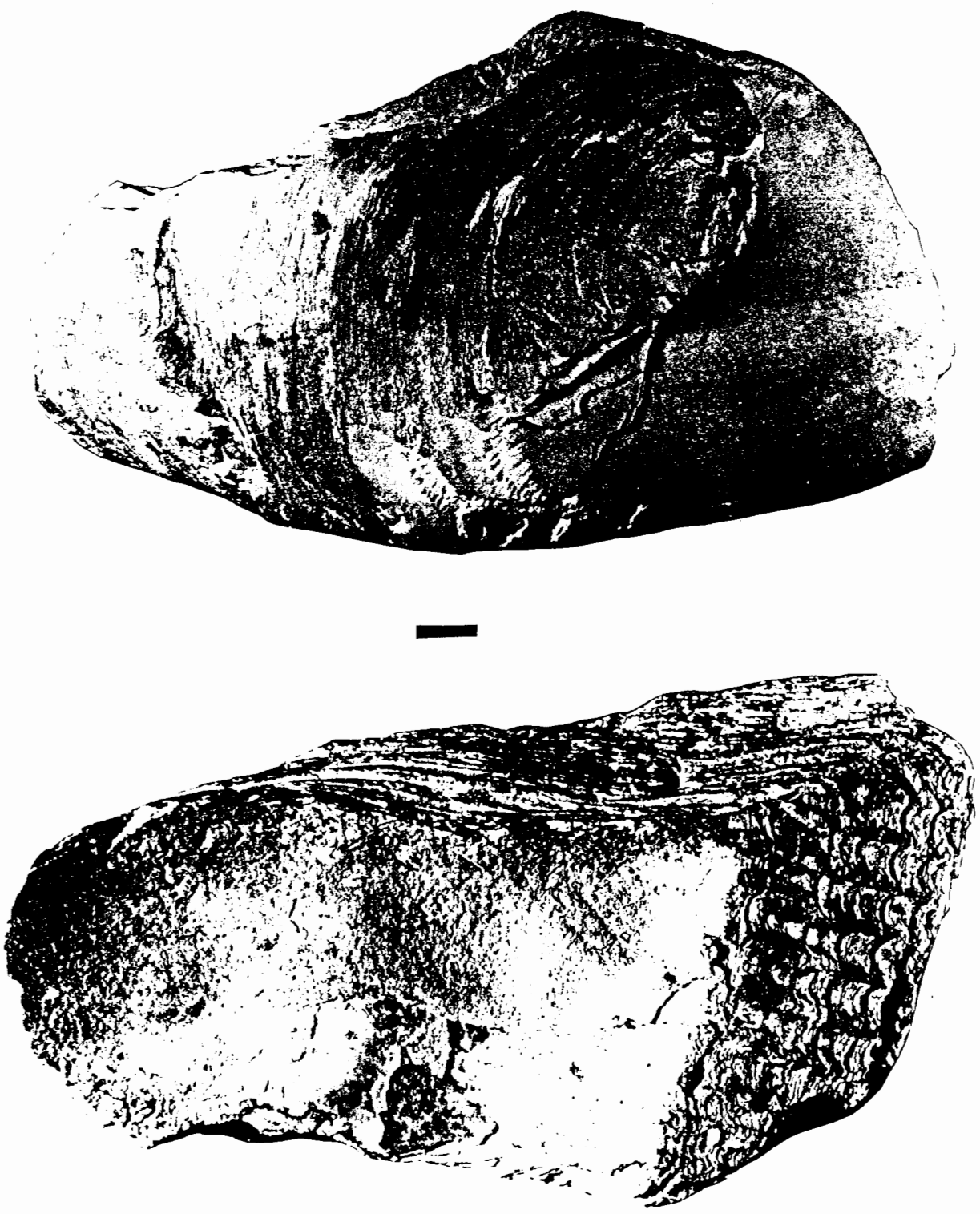

A

Plate A9 A. *Isognomon gariesensis.*

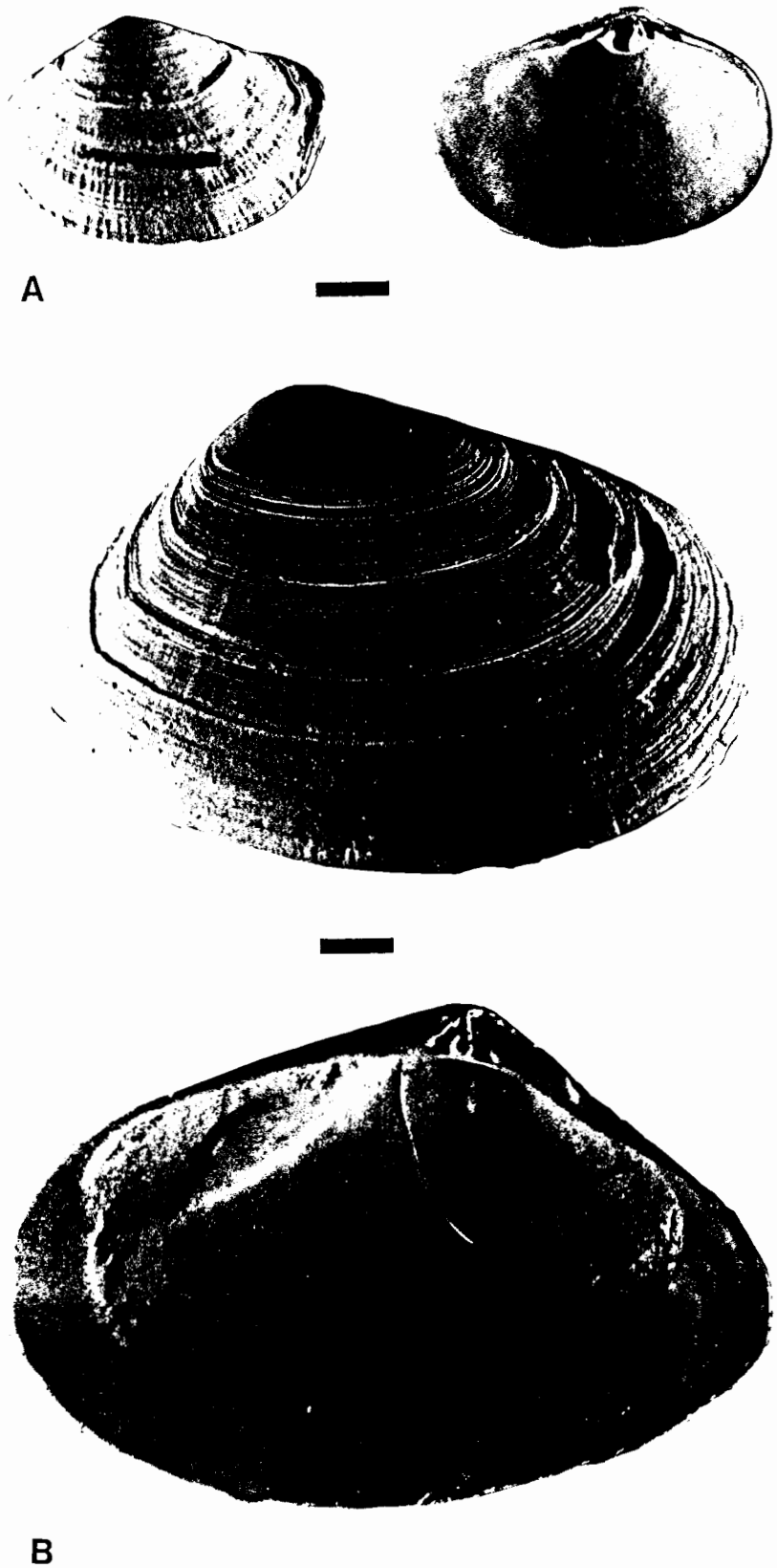

Plate A10 **A.** *Standella namaquensis.* **B.** *Donax haughtoni.*

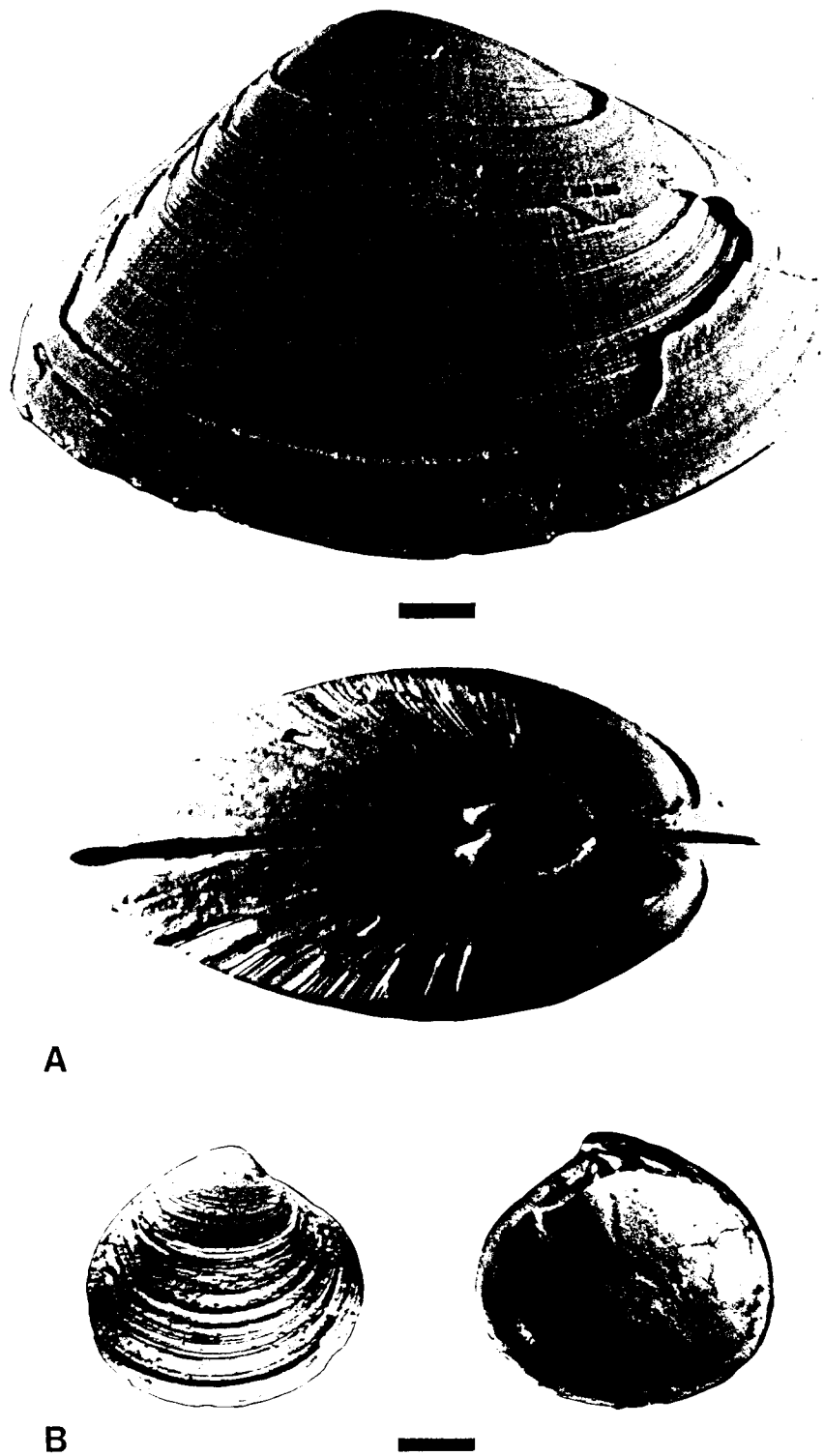

Plate A11 **A.** *Donax rogersi.* **B.** *Chamelea krigei.*

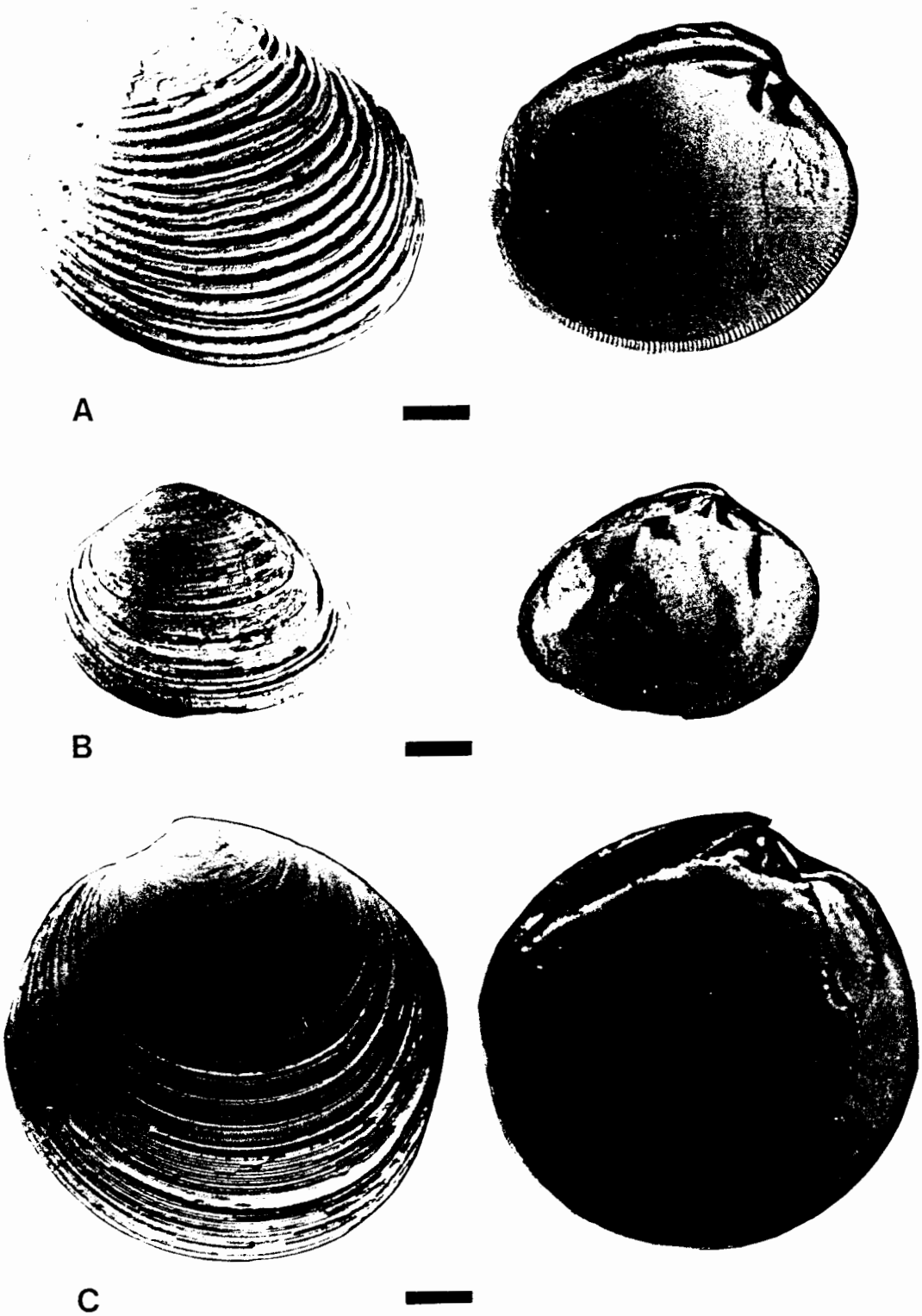

Plate A12 **A.** *Venus verrucosa.* **B.** *Notocallista schwarzi.* **C.** *Dosinia sicarisinus.*

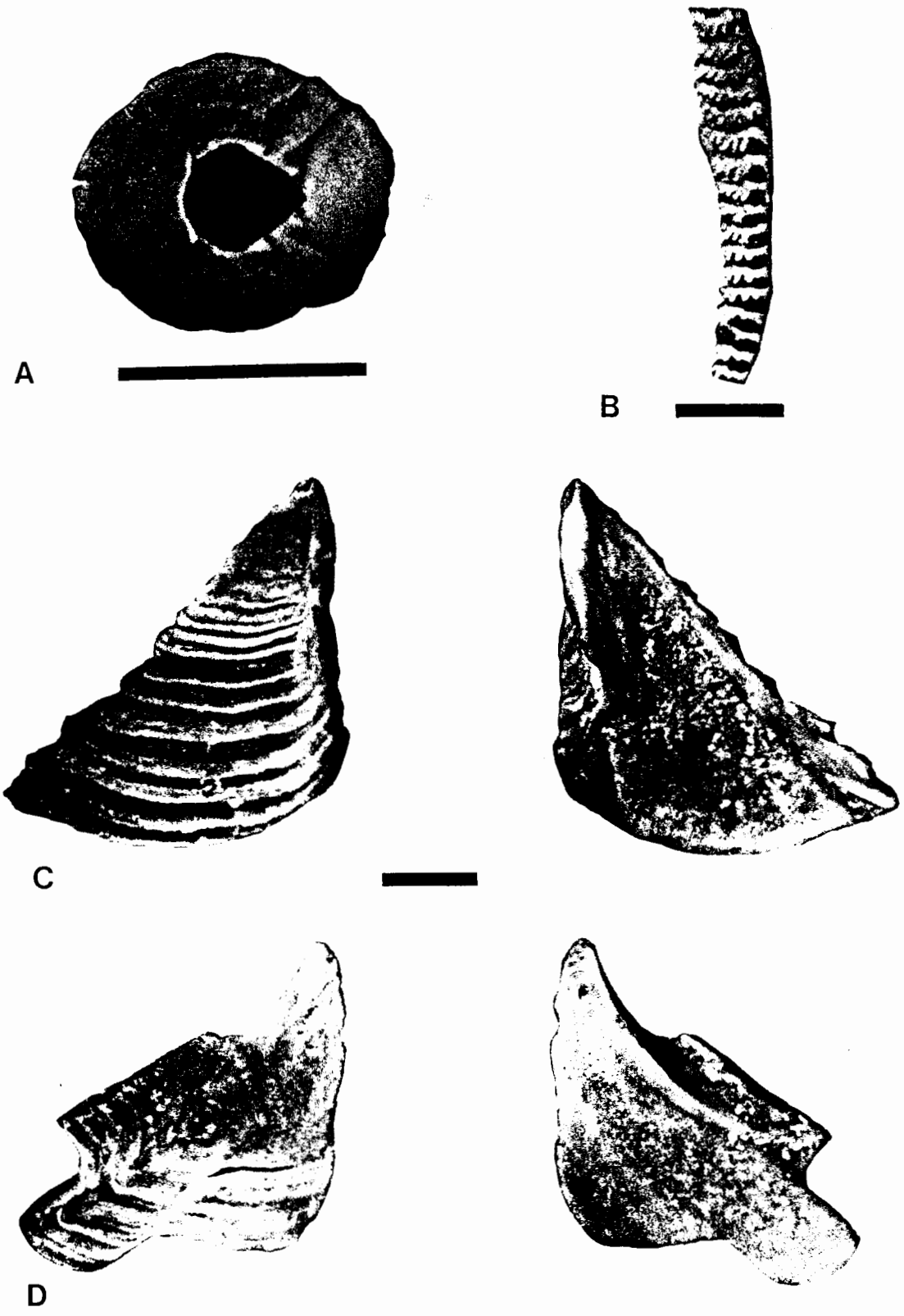

Plate A13 *Notomegabalanus kensleyi.* **A.** Top view. Scale bar is 1 cm. **B.** Edge of wall plate, showing downward-pointing denticles. Scale bar is 1 mm. **C–D.** Opercular plates of aperture. **C.** External and internal views of scutum. Scale bar is 1 mm. **D.** External and internal views of tergum. Scale bar is 1 mm.

APPENDIX B LIST OF INVERTEBRATE MACROFOSSILS

MOLLUSCA

CLASS GASTROPODA

SUBCLASS PROSOBRANCHIA

ORDER ARCHAEOGASTROPODA

FAMILY HALIOTIDAE

†*Haliotis saldanhae* Kensley, 1972

FAMILY FISSURELLIDAE

Amblychilepas scutellum (Gmelin, 1791)

Diodora elevata (Dunker, 1846)

†*Fissurella glarea* Carrington and Kensley, 1969

†*Fissurella robusta* Sowerby, 1892

Fissurellidea aperta (Sowerby, 1825)

Tugali barnardi (Tomlin, 1932)

FAMILY PATELLIDAE

Helcion sp.

Patella argenvillei Krauss, 1848

Patella barbara Linnaeus, 1758

Patella granatina Linnaeus, 1758

†*Patella hendeyi* Kensley and Pether, 1986

†*Patella hoffmani* Kensley and Pether, 1986

Patella miniata Born, 1778

Patella sp.

FAMILY TROCHIDAE

†*Calliostoma depressa* Carrington and Kensley, 1969

Cantharidus (Jujubinus) striatus (Linnaeus, 1758)

†*Clanculus lutosus* Kensley and Pether, 1986

†*Clanculus murrayi* Carrington and Kensley, 1969

Gibbula zonata patula Kensley and Pether, 1986

Oxystele sinensis (Gmelin, 1791)

FAMILY PHASIANELLIDAE

Tricolia capensis (Dunker, 1846)

FAMILY TURBINIDAE

Turbo cidaris Gmelin, 1791

†*Bolma anoropha* Kensley and Pether, 1986

ORDER MESOGASTROPODA

FAMILY LITTORINIDAE

Littorina sp.

FAMILY VERMETIDAE

Vermetus sp.

Turritella carinifera Lamarck, 1822

Turritella declivis Adams and Reeve, 1848

FAMILY MELANELLIDAE

Melanella sp.

FAMILY CREPIDULIDAE

Calyptraea helicoidea Sowerby, 1883

†*Calyptraea kilburni* Kensley and Pether, 1986

†*Calyptraea viridarena* Carrington and Kensley, 1969

Crepidula porcellana Lamarck, 1801

†*Crepidula deprima* Kensley and Pether, 1986

FAMILY TRIVIIDAE

†*Hespererato oppenheimeri* Carrington and Kensley, 1969

FAMILY NATICIDAE

Natica cf. *adansoni* Blainville, 1824

Sinum concavum (Lamarck, 1822)

FAMILY CYMATIIDAE

†Cabestana *casus* (Kensley and Pether, 1986). (previously as *Argobuccinum*).

ORDER HETEROGASTROPODA

FAMILY EPITONIIDAE

†*Epitonium lycocephalum* Kensley and Pether, 1986

ORDER NEOGASTROPODA

FAMILY MURICIDAE

†*Ocenebra bonaccorsii* Carrington and Kensley, 1969

Ocenebra purpuroides (Reeve, 1845)

†*Ocenebra petrocyon* Kensley and Pether, 1986

†*Thais arenae* Kensley and Pether, 1986

Nucella dubia (Krauss, 1848)

†*Spinucella praecingulata* (Haughton, 1932). (previously as *Purpura*, *Nucella*).

†*Namamurex odontostoma* Carrington and Kensley, 1969

†*Trophon carringtoni* Kensley and Pether, 1986

FAMILY BUCCINIDAE

Afrocominella capensis (Dunker in Philippi, 1844)

†*Burnupena aestus* Kensley and Pether, 1986

Burnupena papyracea (Bruguière, 1789)

†*Burnupena rogersi* Kensley and Pether, 1986

†*Triumphis dilemma* Kilburn and Tankard, 1975

FAMILY NASSARIIDAE

Bullia annulata (Lamarck, 1816)

Bullia digitalis (Dillwyn, 1817)

Bullia laevissima (Gmelin, 1791)

Nassarius kochianus (Dunker, 1846)

†*Nassarius litorafontis* Carrington and Kensley, 1969

FAMILY FASCIOLARIIDAE

†*Fasciolaria dinglei* Kensley and Pether, 1986

Fusus faurei Barnard, 1959

FAMILY OLIVIDAE

†*Melapium hawthornei* Kensley and Pether, 1986

†*Pseudoliva lutulenta* Kensley and Pether, 1986

FAMILY MARGINELLIDAE

Marginella sp.

FAMILY TURRIDAE

†*Drillia tempestae* Kensley and Pether, 1986

†*Turris nigrovitta* Carrington and Kensley, 1969

FAMILY TEREBRIDAE

†*Terebra canisaxi* Kensley and Pether, 1986

FAMILY CONIDAE

Conus mozambicus Hwass in Bruguière,1789

SUBCLASS OPISTHOBRANCHIA

ORDER CEPHALASPIDEA

FAMILY RINGICULINAE

Ringicula turtoni Bartsch, 1915

FAMILY CYLICHNIDAE

Cylichna tubulosa Gould, 1859

CLASS BIVALVIA

SUBCLASS PROTOBRANCHIA

ORDER NUCULOIDA

FAMILY NUCULANIDAE

Nuculana bicuspidata (Gould, 1845)

SUBCLASS AUTOBRANCHIA

ORDER ARCOIDA

FAMILY GLYCYMERIDAE

†*Glycymeris fulleri* Kensley and Pether, 1986

FAMILY ARCIDAE

Arca avellana Lamarck, 1819

†*Arca halmyrus* Carrington and Kensley, 1969

Arca noae Linnaeus, 1758

ORDER MYTILOIDA

FAMILY MYTILIDAE

Aulacomya ater (Molina, 1782)

Choromytilus meridionalis (Krauss, 1848)

Perna perna (Linnaeus, 1758)

ORDER PTERIODA

FAMILY ISOGNOMONIDAE

†*Isognomon gariesensis* Kensley and Pether, 1986

ORDER OSTREOIDA

FAMILY OSTREIDAE

Crassostrea margaritacea (Lamarck, 1819)

†*Ostrea* cf. *subradiosa* Böhm and Weisfermel, 1913

FAMILY PECTINIDAE

Chlamys sp.

Hinnites sp.

ORDER VENEROIDA

FAMILY LASAEIDAE

Melliteryx capensis (Sowerby, 1889)

FAMILY CARDITIDAE

†*Cardita unica* Kensley and Pether, 1986

†*Carditella calipsamma* Carrington and Kensley, 1969

FAMILY CONDYLOCARDIINAE

†*Cuna aquaedulcensis* Kensley, 1977

FAMILY CARDIIDAE

Cardium sp.

FAMILY MACTRIDAE

†*Mactra* cf *dernbergi* Böhm and Weisfermel,1913

Scissodesma spengleri (Linnaeus,1767)

Lutraria sp.

†*Standella namaquensis* Carrington and Kensley, 1969

FAMILY CULTELLIDAE

Phaxas decipiens (Smith, 1904)

FAMILY TELLINIDAE

Tellina ponsonbyi (Sowerby, 1889)

Tellina trilatera Gmelin, 1791

†*Gastrana fibrosa* Kilburn and Tankard, 1975

†*Gastrana rostrata* Carrington and Kensley, 1969

Gastrana sp.

Leporimetis hanleyi (Dunker, 1853)

FAMILY DONACIDAE

†*Donax haughtoni* Carrington and Kensley, 1969

†*Donax rogersi* Haughton, 1926

FAMILY SEMELIDAE

Theora sp.

FAMILY VENERIDAE

Venus cf. *verrucosa* Linnaeus, 1758

†*Dosinia sicarinus* Kensley and Pether, 1986

Tivela cf. *compressa* (Sowerby, 1851)

†*Chamelea krigei* Haughton, 1926

†*Notocallista schwarzi* (Newton, 1913)

FAMILY PETRICOLIDAE

†*Petricola prava* Kilburn and Tankard, 1975

ORDER MYOIDA

FAMILY CORBULIDAE

Corbula palaegialus (Carrington and Kensley, 1969)

FAMILY HIATELLIDAE

?*Hiatella* sp.

FAMILY PHOLADIDAE

Barnea truncata (Say, 1822)

CLASS POLYPLACOPHORA

ORDER NEOLORICATA

FAMILY ISCHNOCHITONIDAE

Chaetopleura pertusa

cf. *Dinoplax* sp.

FAMILY CHITONIDAE

cf. *Chiton* sp.

CLASS SCAPHOPODA

FAMILY DENTALIIDAE

Dentalium sp.

BRACHIOPODA

CLASS INARTICULATA

FAMILY DISCINIDAE

Pelagodiscus sp.

CLASS ARTICULATA

FAMILY KRAUSSINIDAE

Kraussina rubra (Pallas, 1766)

†*Kraussina lata* Haughton, 1932

†*Kraussina rotundata* Brunton and Hiller, 1990

†*Kraussina laevicostata* Brunton and Hiller, 1990

†*Kraussina cuneata* Brunton and Hiller, 1990

FAMILY CANCELLOTHYRIDIDAE

†*Cancellothyris platys platys* Brunton and Hiller, 1990

†*Cancellothyris platys petalos* Brunton and Hiller, 1990

OTHER INVERTEBRATES

ANTHOZOA (CORAL)

Schizoculina fissipara (Milne Edwards and Haime)

BRYOZOA

Undet. (several taxa).

POLYCHAETA (WORMS)

Undet. calcareous worm tubes.

CIRRIPEDIA (BARNACLES)

FAMILY BALANIDAE

Austromegabalanus (Notomegabalanus) kensleyi Pether, 1990

Austromegabalanus (Austromegabalanus) sp.

Megabalanus sp.

Balanus sp.

DECAPODA (CRABS)

Undet. crab claws.

APPENDIX C LIST OF BENTHIC FORAMINIFERA

Ammonia sp.

?Ammonia sp

Bolivina cf. *pseudoplicata* Heron-Allen and Earland

?Bolivina sp.

Brizalina sp.

?Buliminoides sp.

Cibicides sp.

Cibicidoides sp.

?Discorbis sp.

Elphidium advenum (Cushman)

Elphidium sp. 1

Elphidium sp. 2

Elphidium sp.1 (Asano)

Elphidium sp.2 (Asano)

?Eponides sp.

Fissurina cf. *lucida* (Williamson)

Fissurina cf. *marginata* (Walker and Boys)

Fissurina sp.

Globigerina bulloides D 'Orbigny

Globigerina quinqueloba Natland

Globigerina cf. *calida* Parker

Globorotalia cf. *hirsuta* (D 'Orbigny)

Globulina sp.

?Globulina sp.

Hanzawaia sp.

Haynesina cf. *germanica* (Ehrenberg)

Lagena cf. *laevis* (Montagu)

Lagena cf. *perlucida* (Montagu)

Lagena sp.

Lobatula lobatula (Walker and Jacob)

Marginulina sp.

"Medocia" sp. (=*Discorbis "algoaensis"* - undescribed species)

Nonion boueanus (D'Orbigny)

Nonionella sp.

Oolina squamosulcata (Heron-Allen and Earland)

Orbulina universa D'Orbigny

Oolina cf. *austroatlantica* (McMillan thesis)

Oolina cf. sp. A

Oolina cf. *squamosa* (Montagu)

Oolina sp. A

Oolina sp. (Smooth)

?Oolina sp. (Hispid ornament)

?Oolina sp.(Hispid)

Pararotalia nipponica (Asano)

?Planorbulina sp.

?Planorbulinella sp.

Planularia sp.

Planulinoides biconcavus (Jones and Parker)

Pseudononion cf. *chiliensis* (Cushman and Kellett)

Pyrgo sp.

Quinqueloculina sp.

Rosalina cf. *globularis*

Rosalina cf. *globularis* D 'Orbigny

Stainforthia cf. *schreibersiana* (Czjzek)

Triloculina sp.

Uvigerina sp.

Vaginulina sp. (Fat)

APPENDIX D LIST OF FOSSIL VERTEBRATES

P = PHOSPHATIC PETRIFIED BONE

CLASS CHONDRICHTHYES

ORDER SELACHI

cf. *Carcharodon megalodon*	Tooth **P**
Gen. and spp not det.	Numerous teeth **P**

ORDER BATOIDEA(rays)

Gen. and spp not det.	Various tooth plates **P**

CLASS OSTEICHTHYES

Labrodon sp.	Numerous teeth **P**
Gen. and spp not det.	Teeth, vertebrae, otoliths

CLASS REPTILIA

ORDER CHELONIA

Chersina sp.	Several
?Geochelone sp.	

CLASS AVES

ORDER STRUTHIONIFORMES

Family Struthionidae

Struthio sp.	Large **P**
Struthio sp.	Long bones

Family Spheniscidae

Spheniscus sp.

Gen. and spp not det.

CLASS MAMMALIA

ORDER CARNIVORA

Gen. and spp not det.	Numerous post cranial bones
Gen. and spp not det.	Metatarsal and tooth

Family Phocidae	
Homiphoca capensis	Mandible
Gen. and spp not det.	Phalanges **P**
Family Hyaenidae	
Hyaena hyaena	Cranial and post cranial
Creodont	Carnassial **P**
Family Felidae	
?Felid	Scapula
ORDER PROBOSCIDAE	
Family Gomphotheriidae	
Gen. and spp not det.	Teeth fragments and phosphatized ivory **P**
ORDER PERISSODACTYLA	
Family Equidae	
Hipparion	Teeth **P**
Equus capensis	Teeth and post cranial
Family Rhinocerotidae	
Ceratotherium praecox	Tooth **P**
Gen. and spp not det.	Teeth and post cranial bones
ORDER ARTIODACTYLA	
Family Suidae	
Nyanzachoerus kanamensis	
Family Giraffidae	
?Palaeotragine	**P**
Family Bovidae	
Gazelle	Cranial and post cranial
?Raphicerus	Mandible fragment
Gen. and spp not det.	Numerous post cranial bones
ORDER CETACEA	
Gen. and spp not det.	Teeth, vertebrae and rib fragments **P**
Gen. and spp not det	

CLASS DELPHINIDAE

Dolphin	Mandible & skull fragments